

Copyright
by
Stewart Andrew Vaculik
2008

**The Dissertation Committee for Stewart Andrew Vaculik Certifies that this is
the approved version of the following dissertation:**

**A FRAMEWORK FOR ELECTROMECHANICAL ACTUATOR
DESIGN**

Committee:

Delbert Tesar, Supervisor

Carolyn Seepersad

Richard Hooper

Richard Crawford

Elmira Popova

S.V. Sreenivasan

**A FRAMEWORK FOR ELECTROMECHANICAL ACTUATOR
DESIGN**

by

Stewart Andrew Vaculik, B.S.M.E; M.S.E.

Dissertation

Presented to the Faculty of the Graduate School of

The University of Texas at Austin

in Partial Fulfillment

of the Requirements

for the Degree of

Doctor of Philosophy

The University of Texas at Austin

May 2008

Acknowledgements

I would like to thank Dr. Tesar for his guidance throughout the process of researching and writing of this report. I would also like to express my gratitude to my dissertation committee members for agreeing to serve, reading my dissertation, and providing valuable feedback during my proposal and defense presentations. I am grateful for the assistance of Pradeepkumar Ashok, a fellow graduate student who discussed many of my research ideas with me and provided helpful suggestions. I would like to thank my parents for encouraging me to attend college and for their continuing support of my graduate education. Most of all, I would like to thank my wife, Jennifer, for her support during my entire graduate study and for helping me to compile this document. This work was supported by the Office of Naval Research (Grant N00014-06-1-0213).

A Framework for Electromechanical Actuator Design

Publication No. _____

Stewart Andrew Vaculik, Ph.D

The University of Texas at Austin, 2008

Supervisor: Delbert Tesar

Electromechanical actuators are becoming an increasingly popular alternative to traditional hydraulic actuators for ship, aircraft, vehicle suspension, robotic, and other applications. These actuators generally include an electric motor, gear train, bearings, shafts, sensors, seals, and a controller integrated into a single housing. This integration provides the advantages of a single shaft, fewer bearings, and ultimately, reduced weight and volume.

Research has shown that the motor and gear train are the most critical, performance-limiting components in an actuator, and *balancing the performance parameters* (torque, weight, inertia, torque density, and responsiveness) among them is not trivial. The Robotics Research Group currently addresses this task by using intuitive rules of thumb and the designers' experience, and this often requires multiple design iterations between the motor and gear train. In this regard, this research will provide preliminary guidelines for choosing the gear ratios and relative sizes of the motor and gear train when integrating a switched reluctance motor (SRM) with three different gear trains (hypocyclic gear train (HGT), star gear train coupled with a parallel eccentric gear

train (Star+PEGT), and star compound gear train coupled with a parallel eccentric gear train (Star Compound+PEGT)) in the preliminary design stage.

Research has also shown that there are cost benefits to developing actuator product families to meet the needs of a particular application domain. In this regard, *scaling rules* for the SRM, HGT, PEGT, and integrated actuators built from them (with diameters ranging from 6 to 50 inches and gear ratios from 100 to 450) will be developed. These scaling rules describe how the performance parameters vary as the size (diameter and aspect ratio) is varied and are useful for quickly sizing motor, gear train, and actuator designs. These scaling rules are useful for two purposes: 1) learning the relationships between the performance and dominant design parameters and 2) obtaining intermediate sizes not previously considered. The rules will be simple enough for designers to learn and use to make intelligent design parameter choices (purpose 1) but will also have sufficient accuracy for obtaining intermediate designs (purpose 2). The scaling rules are summarized in a series of three-dimensional design maps, with an emphasis on the development of visual decision-making tools.

This research also formulates an actuator design procedure that incorporates the two central concepts of this research, balancing parameters and scaling, and this procedure is embedded within computational (MatLab) and solid modeling (SolidWorks) software programs. In addition to developing rules for scaling and balancing parameters, the procedure was also used for the following purposes. First, direct drive and geared actuators were compared in terms of their torque density and responsiveness to determine which alternative is superior for different gear ratio, diameter, and load inertia combinations. Second, alternative minimum sets of actuators were developed for an illustrative application, and the anticipated performance losses due to using common parameters among the sets were quantified.

Table of Contents

Chapter 1	Introduction.....	1
1.1	Overview.....	1
1.2	Motivation.....	2
1.3	Integrating Motors and Gear Trains.....	2
1.4	Scope.....	3
1.5	Research Goals.....	4
1.6	Design Rule Preview.....	7
1.7	Chapter Overview	9
Chapter 2	Literature Review.....	14
2.1	Literature Review Summary.....	15
2.2	Electromechanical Actuators	22
2.2.1	Electromechanical vs. Hydraulic Actuators.....	22
2.2.2	RRG Actuator Research.....	27
2.2.3	Off-the-Shelf Actuators	28
2.2.4	EMA Literature Summary	30
2.3	Gear Train Design.....	31
2.3.1	Gear Train Design Literature Summary	41
2.4	Integrating Motors and Gear Trains.....	41
2.4.1	Designing for Inertial Loads	42
2.4.2	Integrating Motor and Gear Train Literature Summary	51
2.5	Scaling.....	54
2.5.1	Scaling Literature Summary	60
2.6	Product Family Design	62
2.6.1	Product Family Design Literature Summary	68
2.7	Regression, Metamodeling, and Response Surface Methodology.....	70
2.7.1	Regression.....	70
2.7.1.1	Least Squares.....	74
2.7.1.2	Assessing Model Validity (Error Metrics).....	74

2.7.1.3	Use of Regression Techniques in the Current Research	75
2.7.1.4	Least Squares Assumptions and Inference	77
2.7.2	Metamodeling	77
2.7.2.1	Model Choices	78
2.7.3	Response Surface Methodology (RSM)	79
2.7.4	Justification for Use of Regression, Metamodeling, and RSM Techniques	83
2.7.5	Regression, Metamodeling, and RSM Literature Summary	85
2.8	Design Space Visualization (Graphical User Interface Development)	86
2.8.1	Robotics Research Group (RRG) Decision-Making Framework	86
2.8.2	Graphical Engineering Design Interfaces	88
2.8.3	Features of Visual Decision-Making Support Systems	91
2.8.3.1	Visualizing Multiple Objectives	93
2.8.3.2	Uncertainty in the Design Process	94
2.8.4	Design Space Visualization Literature Summary	95
2.9	Patents	96
2.9.1	Electromechanical Actuator Patents	97
2.9.2	Gear Trains	102
2.9.3	Product Family (Line) Design	105
2.9.4	Patent Literature Summary	105
2.10	Summary	106
Chapter 3	Parametric Models	107
3.1	Definitions	108
3.2	Preliminary and Detailed Design Stages	109
3.3	Fundamental Design Parameters	113
3.4	General Performance Parameter Computations	116
3.4.1	Inertia Computations	117
3.5	General Geartrain Parametric Model	118
3.5.1	Bending Stress in Gear Teeth	119
3.5.2	Effect of Diametral Pitch on Torque Capacity	122

3.5.3	Contact Stress in Gear Teeth.....	123
3.5.4	Pitch Line and Sliding Velocities	124
3.5.5	Effect of Contact Ratio on Torque Capacity.....	125
3.5.6	Gear Rim Thickness and Tooth Height	128
3.5.7	Gear Bore Diameter	129
3.5.8	Gear Rim Diameter	130
3.6	Chapter Roadmap.....	130
3.7	Switched Reluctance Motor (SRM).....	130
3.7.1	Key SRM Design Parameters	134
3.7.2	Air Gap.....	136
3.7.3	Stator Geometry	136
3.7.4	Rotor Geometry	137
3.7.5	Winding Parameters.....	138
3.7.6	Length Parameters	140
3.7.7	Torque	140
3.7.8	Weight and Inertia.....	141
3.7.8.1	Back Iron.....	141
3.7.8.2	Poles	141
3.7.8.3	Motor Shaft	142
3.7.8.4	Motor Shell.....	142
3.7.9	Total Motor Weight and Inertia	142
3.8	Gear Trains.....	143
3.9	Hypocyclic Gear Train (HGT).....	143
3.9.1	Key HGT Design Parameters.....	147
3.9.2	Eccentricity and Gear Ratio	149
3.9.3	Geometry Relationships.....	151
3.9.4	Balancing Mass Model	154
3.9.5	Weight and Inertia Computations	154
3.9.6	Total Weight	154
3.9.7	Total Inertia.....	155

3.10	Parallel Eccentric Gear Train (PEGT)	155
3.10.1	Key PEGT Design Parameters.....	160
3.10.2	1 st Stage Geometry and Gear Ratio.....	163
3.10.3	PEGT Eccentricity and Gear Ratio	165
3.10.4	Geometry Relationships.....	166
3.10.5	Weight and Inertia Computations	169
3.10.6	Total Weight	169
3.10.7	Total Inertia.....	169
3.11	SRM+HGT.....	170
3.12	SRM+PEGT.....	171
3.13	Gear Ratio Ranges	173
3.14	Bearing Design and Selection Issues	174
3.14.1	Bearing Life	174
3.14.2	Bearing Friction (Approximation).....	176
3.14.3	Bearing Friction	177
3.14.4	Friction Power Loss	177
3.15	Speed and Life Limits.....	178
3.15.1	Motors	178
3.15.2	Gear Trains.....	178
3.15.3	Bearings	179
3.16	Summary.....	181
Chapter 4	Actuator Design Procedures	182
4.1	High Level Actuator Design Development Process	182
4.2	Current Actuator Design Procedure.....	184
4.3	Proposed Actuator Design Procedure	186
4.3.1	Actuator Design Procedure Tasks.....	188
4.3.2	Motor Design Procedure	192
4.3.3	Gear Train Design Procedure.....	195
4.3.3.1	Internal Design Parameters	198
4.3.3.2	Constants and Fixed Parameters	199

4.3.4	Actuator Design Procedure (Textual Description)	200
4.4	Computational Tool	203
4.5	Summary	204
Chapter 5	Scaling Rules and Design Maps	205
5.1	Representation.....	206
5.1.1	Three-Dimensional Surfaces (Design Maps).....	207
5.1.2	Low Order Polynomial Scaling Rules	208
5.1.3	Two-Dimensional Plots	210
5.1.4	Simple Power Law Scaling Rules.....	211
5.1.5	Summary of Representations	212
5.2	Component Scaling Rules.....	213
5.2.1	SRM Scaling Rules	213
5.2.2	HGT Scaling Rules	223
5.2.3	PEGT Scaling Rules (1 st Stage Star Gear Train)	237
5.2.3.1	Bearing-Limited PEGT Designs	238
5.2.3.2	Strategies for Balancing the Bearing and Gear-Tooth Limited Torque Capacities in the PEGT.....	246
5.2.3.3	Gear Tooth-Limited PEGT Designs.....	250
5.2.4	PEGT Scaling Rules (1 st Stage Star Compound Gear Train) ...	261
5.2.5	Notes on the Gear Train Scaling Rules.....	271
5.2.5.1	Torque Capacity Modification	271
5.2.5.2	Choosing the Diametral Pitch	273
5.2.5.3	Relationship Between Bending and Contact Stresses	273
5.3	Comparisons Between the HGT and the Star+PEGT Alternatives ...	275
5.4	Comparisons Between the Star and Star Compound 1 st Stage PEGT Alternatives	280
5.5	Actuator Design Maps and Scaling Rules	282
5.6	Discussion of Results.....	283
5.6.1	3-D Maps and Polynomial Scaling Rules	283
5.6.2	2-D Maps and Power-Law Scaling Rules	284
5.6.3	Curve-Fitting Errors.....	284

5.6.4	Diameter and Aspect Ratio Parameters	285
5.6.5	Torque, Weight, and Inertia	285
5.6.6	Torque Density and Responsiveness	286
5.7	Using the Design Maps and Scaling Rules	287
5.8	Summary	288
Chapter 6	Balancing Parameters.....	289
6.1	Need for Balancing Parameters	290
6.2	Key Actuator Design Parameter Choices	291
6.2.1	Choice of Gear Ratio	293
6.2.2	Choice of Gear Train Aspect Ratio.....	293
6.2.3	Choice of Motor Aspect Ratio	293
6.2.4	Choice of Overall Aspect Ratio	294
6.2.5	Choice of Motor to Overall Length Ratio (K_l)	294
6.2.6	Choice of Motor to Gear Train Diameter Ratio (K_d).....	294
6.2.7	Importance of These Design Parameters	296
6.3	Types of Balance.....	296
6.3.1	Balance Between the Motor and Gear Train-Limited Torque Capacities	297
6.3.2	Balance Between the Weight/Inertia of the Motor and Gear Train	299
6.3.3	Balance Between the Tooth-Limited and Bearing-Limited Torque Capacity in the PEGT	300
6.3.4	Balancing Bearing Life Between Multiple Bearings	300
6.4	Balancing Parameters Examples.....	301
6.5	Example 1: Balancing the Motor and Gear-Tooth Limited Torque Capacities	303
6.5.1	SRM+HGT	304
6.5.2	SRM+Star+PEGT	311
6.5.3	SRM+Star Compound+PEGT	319
6.5.4	Comparisons Between the SRM+HGT and SRM+Star+PEGT Alternatives	325

6.5.5	Comparisons Between the Star and Star Compound 1 st Stage PEGT Alternatives	328
6.6	Example 2: Effect of Gear Ratio on Balance Between Weight/Inertia in the Motor and Gear Train	330
6.6.1	SRM+HGT.....	331
6.6.2	SRM+Star+PEGT (Effect of Variation of 1 st Stage Gear Ratio).....	340
6.6.2.1	Background	340
6.6.2.2	Results	341
6.6.3	SRM+Star Compound+PEGT (Effect of Variation of 1 st Stage Gear Ratio).....	349
6.7	Discussion of Results.....	356
6.7.1	Diameter, Gear Ratio, and Aspect Ratio Parameters.....	356
6.7.2	Balancing Motor and Gear Tooth Limited Torque Capacities	357
6.7.3	Distribution of Weight and Inertia.....	357
6.7.4	Torque Density.....	358
6.7.5	Responsiveness	358
6.7.6	Power-Law Scaling Rules.....	359
6.7.7	Design Parameter Ranges	359
6.8	Summary	360
Chapter 7	Comparisons Between Direct Drive and Geared Actuators	361
7.1	Responsiveness Relationships	362
7.1.1	Geared System Responsiveness.....	364
7.1.2	Direct Drive System Responsiveness	366
7.2	Off-The-Shelf Component Characteristics and Comparisons	366
7.2.1	Off-The-Shelf Motor Characteristics.....	366
7.2.2	Comparisons of Direct Drive and Geared Systems Using Off-the-Shelf Components.....	370
7.2.2.1	Comparing Systems of the Same Size	372
7.2.2.2	Comparing Systems of the Same Torque Capacity.....	375
7.2.3	Off-the-Shelf Comparison Summary	378
7.3	Comparisons Based on the SRM, HGT, and PEGT	379

7.3.1	Example 1: Comparing Systems of the Same Size	380
7.3.1.1	SRM (Direct Drive Reference Designs).....	381
7.3.1.2	SRM (Direct Drive) vs. SRM+HGT (Geared).....	383
7.3.1.3	SRM (Direct Drive) vs. SRM+Star+PEGT (Geared)	392
7.3.1.4	SRM (Direct Drive) vs. SRM+Star Compound+PEGT (Geared)	400
7.3.1.5	Example 1 Discussion of Results	408
7.3.2	Example 2: Comparing Systems of the Same Torque Capacity	411
7.3.2.1	SRM (Direct Drive) vs. SRM+HGT (Geared).....	412
7.3.2.2	SRM (Direct Drive) vs. SRM+Star+PEGT (Geared)	419
7.3.2.3	SRM (Direct Drive) vs. SRM+Star Compound+PEGT (Geared)	425
7.3.2.4	Example 2 Discussion of Results	431
7.4	Other Geared System Considerations	432
7.5	Effect of Output Speed on Responsiveness	433
7.6	Summary	434
Chapter 8	Development of a Minimum Set of Actuators	435
8.1	Need for a Minimum Set.....	436
8.2	Minimum Set Literature.....	437
8.3	Minimum Set Criteria	441
8.4	Low Cost Minimum Set Features	443
8.4.1	Common Motor Diameters	444
8.4.2	Variable 1 st Stage Gear Ratio.....	445
8.4.3	Common Gear Train Diameters.....	448
8.4.4	Moving from 3 to 6 Crankshafts.....	448
8.4.5	Materials	449
8.5	Example 1: Alternative Minimum Sets.....	449
8.5.1	Reference Set of Actuator Designs	450
8.5.2	Alternative Minimum Sets.....	453
8.5.2.1	Choice of Common Motor Diameters.....	454
8.5.2.2	Minimum Sets 1-5(Fixed 1 st Stage Gear Ratio).....	455

8.5.2.3	Minimum Sets 6-10 (Variable 1 st Stage Gear Ratios)	460
8.5.3	Minimum Sets 1-10: Summary and Additional Results	467
8.6	Example 2: Reducing the Number of Actuators in a Set	473
8.6.1	Reference Set of Actuators	474
8.6.2	A Potential Reduced Set of Actuators	476
8.6.3	Other Potential Reduced Sets of Actuators	479
8.7	Minimum Set Development Procedure	484
8.8	Inversion of the Product Development Process	484
8.9	Summary	486
Chapter 9	Summary and Recommendations	488
9.1	Overview	488
9.1.1	Integrating Motors and Gear Trains	489
9.1.2	Motivation	489
9.1.3	Scope	490
9.1.4	Research Goals	490
9.2	Chapter Roadmap	492
9.3	Background and Parametric Model Development	492
9.3.1	Literature Review (Chapter 2)	492
9.3.2	Parametric Model Development (Chapter 3)	497
9.3.2.1	Preliminary and Detailed Design Stages	497
9.3.2.2	Motor and Gear Trains Considered	499
9.3.2.3	Basic Design and Performance Parameters	501
9.3.2.4	Torque, Weight, and Inertia Computations	503
9.3.3	Actuator Design Procedures (Chapter 4)	505
9.3.3.1	Proposed Actuator Design Procedure	505
9.3.3.2	Motor Design Procedure	507
9.3.3.3	Gear Train Design Procedure	509
9.4	Summary of Key Results	511
9.4.1	Scaling Rules and Design Maps (Chapter 5)	511
9.4.1.1	HGT Scaling Rules and Design Maps	512

9.4.1.2	Torque and Speed Relationship in the PEGT.....	514
9.4.1.3	Relationship Between Bending and Contact Stresses	516
9.4.1.4	Comparisons Between the HGT and the Star+PEGT Alternatives	517
9.4.1.5	Key Results from Chapter 5	519
9.4.2	Balancing Parameters (Chapter 6)	521
9.4.2.1	Actuator Design Parameter Choices for Balancing Parameters	521
9.4.2.2	Types of Balance.....	522
9.4.2.3	Balancing the Motor and Gear Train Torque Capacities in the SRM+Star+PEGT Actuator	523
9.4.2.4	Comparisons Between the SRM+HGT and SRM+Star+PEGT Alternatives.....	527
9.4.2.5	Balancing the Weight and Inertia in the SRM+HGT Actuator.....	529
9.4.2.6	Key Results from Chapter 6	534
9.4.3	Comparison of Direct Drive and Geared Actuators (Chapter 7)	536
9.4.3.1	Responsiveness Relationships.....	537
9.4.3.2	Comparison Assumptions	540
9.4.3.3	Comparing Geared and Direct Drive Systems of the Same Size.....	541
9.4.3.4	Key Results from Chapter 7	548
9.4.4	Minimum Set Development (Chapter 8).....	550
9.4.4.1	Low Cost Minimum Set Features	550
9.4.4.2	Reference Set of Designs	554
9.4.4.3	Choice of Common Motor Diameters	554
9.4.4.4	Minimum Set 3 (Fixed 1 st Stage Gear Ratio).....	555
9.4.4.5	Minimum Set 8 (Variable 1 st Stage Gear Ratios).....	558
9.4.4.6	Minimum Sets 1-10 Summary and Additional Results	561
9.4.4.7	Potential Reduced Sets of Actuators	562
9.5	Recommendations.....	565
9.5.1	Model Development and System Comparisons	565

9.5.2	Actuator Design Procedure	566
9.5.3	Component Scaling Rules.....	566
9.5.4	Balancing Parameters.....	567
9.5.5	Designing for High Torque Density	567
9.5.6	Designing for High Responsiveness	568
9.5.7	Gear Ratio Choice.....	568
9.5.8	Motor Speed Choices.....	569
9.5.9	Distribution of Weight and Inertia.....	569
9.5.10	Choosing Between Direct Drive and Geared Systems	570
9.5.11	Minimum Set	571
9.6	Contributions.....	572
9.7	Future Work.....	573
9.7.1	Actuator Design Process.....	574
9.7.2	Knowledge Base for EMA Design	574
9.7.3	Uncertainty in the Parameters.....	575
9.7.4	Other Metamodels (Curve-Fitting) Approaches	576
9.7.5	Torque to Inertia Ratio/Responsiveness	576
9.7.6	Star Compound Gear Trains	577
9.7.7	Bearing Load Capacity	577
9.7.8	Minimum Set	578
9.7.9	Parameter Reduction.....	579
	Appendices.....	581
	Appendix A1: Computational and Solid Modeling Tools	582
A1.1	SRM	584
A1.2	HGT	585
A1.3	PEGT (with Star and Star Compound 1 st Stage Alternatives)	587
A1.4	SRM+HGT.....	590
A1.5	SRM+PEGT (with Star and Star Compound 1 st Stage Alternatives)	590
A1.6	General Computation Files	591

Appendix A2: Link Between Matlab and SolidWorks	593
Appendix A3: HGT Balancing Mass Computations	596
A3.1 Balancing Mass Geometry	597
A3.2 Cross-Sectional Area of Balancing Mass.....	599
A3.3 Balancing Mass Weight	600
A3.4 Center of Mass	600
A3.5 Balance of Forces.....	601
A3.6 Balance of Moments	603
A3.7 Balancing Weight and Inertia	604
Appendix A4: AGMA Bending Stress J-Factor	605
Glossary	608
Acronyms.....	609
References.....	610
Electromechanical Actuators	610
Gear Train Design.....	613
Motor Design	614
Switched Reluctance Motor (SRM) Design	614
Balancing Motor and Gear Train	615
Scaling.....	616
Product Family Design	617
Regression Analysis.....	619
Metamodels and Response Surface Methodology.....	619
Design Space Visualization	621
Patents.....	622
Solution Techniques: Optimization and Multi-Objective Design	622
Solution Techniques: Solving Polynomial Systems of Equations.....	623

List of Tables

Table 2.1: Summary of Key References and Their Relevance to the Current Research	15
Table 2.2: Literature Review Findings and This Research’s Contributions (Based on All of the Papers Listed in the References Section)	19
Table 2.3: Suggested Gear Train Type for Different Actuator Types (Classes), from Gloria and Tesar [2004]	20
Table 2.4: Summary of RRG Research on Integrated Actuator Design	28
Table 2.5: Suggested Gear Train Types for a Range of Gear Ratios.....	32
Table 2.6: System and Tooth Level Design Parameters for the Hypocyclic Gear Train	35
Table 2.7: Suggested Optimum Gear Ratios for Inertial Loads.....	53
Table 2.8: Scale-Based Product Family Design Methods (*Same aircraft family, **Same electric motor family, “P” indicates preset common and scaling parameters).....	67
Table 2.9: Representative Set of Actuator Design and Performance Parameter Data	71
Table 2.10: Tabular Results of Torque (in-lbf) as a Function of Diameter and Aspect Ratio.....	82
Table 3.1: Fundamental Design and Performance Parameters and Performance Metrics	114
Table 3.2: Percentage of Total Gear Tooth Load (s) as a Function of Contact Ratio	126
Table 3.3: SRM Design Parameters Classified by Component (for generating reference design).....	131

Table 3.4: SRM Parameters (Discussed in this section).....	133
Table 3.5: SRM Assumptions	135
Table 3.6: Summary of SRM Design and Performance Parameter Relationships	135
Table 3.7: AWG Conductor Diameters and Safe Current Limits	139
Table 3.8: HGT Design Parameters Classified by Component (for generating reference design).....	145
Table 3.9: HGT Parameters (Discussed in this section)	146
Table 3.10: HGT Assumptions	148
Table 3.11: Summary of HGT Design and Performance Parameter Relationships	149
Table 3.12: PEGT Design Parameters Classified by Component (for generating reference design).....	157
Table 3.13: PEGT Parameters (Discussed in this section)	159
Table 3.14: PEGT Assumptions	161
Table 3.15: Summary of PEGT Design and Performance Parameter Relationships	162
Table 3.16: SRM+HGT Design Parameters Classified by Component (for generating reference design).....	171
Table 3.17: SRM+PEGT Design Parameters Classified by Component (for generating reference design).....	173
Table 4.1: Proposed Actuator Design Procedure Tasks.....	189
Table 4.2: Different Methods Used to Formulate the Objective Function	191
Table 4.3: Standard Actuator Design and Performance Parameter Data Summary	192
Table 4.4: SRM Constants and Fixed Parameters	194
Table 4.5: Illustration of Searching Winding Parameter to Maximize SRM Torque	195
Table 4.6: Illustration of Searching Gear Tooth Parameters to Meet Target Gear Ratio in the HGT	198

Table 4.7: Suggested Proportions for the HGT and PEGT Internal Design Parameters	199
Table 4.8: Constants/Fixed Parameters for the HGT and PEGT	200
Table 5.1: Scaling Rule Representations and Their Relative Benefits (“1” means the best and “5” means the worst)	213
Table 5.2: SRM Assumptions	214
Table 5.3: SRM Design and Performance Parameter Data.....	219
Table 5.4: SRM Design Map Coefficients, n_i $(P_p = n_0 + n_1 D_m + n_2 A_m + n_3 D_m A_m + n_4 D_m^2 + n_5 A_m^2 + n_6 D_m A_m^2 + n_7 D_m^2 A_m + n_8 D_m^3 + n_9 A_m^3)$	219
Table 5.5: SRM Error Metrics	220
Table 5.6: SRM Power-Law Scaling Rules $(P_p = k D_m^b = k D_m^{b-1} L_m)$	223
Table 5.7: HGT and PEGT Constants and Fixed Parameters	225
Table 5.8: Suggested Proportions for the HGT Internal Design Parameters	225
Table 5.9: HGT Design and Performance Parameter Data.....	231
Table 5.10: HGT Design Map Coefficients, n_i $(P_p = n_0 + n_1 D_g + n_2 A_g + n_3 D_g A_g + n_4 D_g^2 + n_5 A_g^2 + n_6 D_g A_g^2 + n_7 D_g^2 A_g + n_8 D_g^3 + n_9 A_g^3)$	232
Table 5.11: HGT Error Metrics	232
Table 5.12: HGT Power-Law Scaling Rules $(P_p = k D_g^b = k D_g^{b-1} L_g)$	236
Table 5.13: HGT Bearing Load Capacity Requirements (lbf).....	237
Table 5.14: PEGT Design Parameters and Assumptions	239
Table 5.15: PEGT Design and Performance Parameter Summary	240
Table 5.16: Effect of Output Speed on PEGT Torque Capacity (fixed bearing life and load capacity)	244

Table 5.17: Comparison of Bearing and Tooth-Limited Load Capacities of the PEGT	246
Table 5.18: Suggested Proportions for the PEGT Internal Design Parameters ...	252
Table 5.19: Star+PEGT Design and Performance Parameter Data	256
Table 5.20: Star+PEGT Design Map Coefficients, n_i $(P_p = n_0 + n_1 D_g + n_2 A_g + n_3 D_g A_g + n_4 D_g^2 + n_5 A_g^2 + n_6 D_g A_g^2 + n_7 D_g^2 A_g + n_8 D_g^3 + n_9 A_g^3)$	256
Table 5.21: Star+PEGT Error Metrics	256
Table 5.22: Star+PEGT Power-Law Scaling Rules $(P_p = k D_g^b = k D_g^{b-1} L_g)$	260
Table 5.23: Star+PEGT Bearing Load Capacity Requirements (lbf)	261
Table 5.24: Star Compound+PEGT Design and Performance Parameter Data...	266
Table 5.25: Star Compound+PEGT Design Map Coefficients, n_i $(P_p = n_0 + n_1 D_g + n_2 A_g + n_3 D_g A_g + n_4 D_g^2 + n_5 A_g^2 + n_6 D_g A_g^2 + n_7 D_g^2 A_g + n_8 D_g^3 + n_9 A_g^3)$	267
Table 5.26: Star Compound+PEGT Error Metrics	267
Table 5.27: Star Compound+PEGT Power-Law Scaling Rules $(P_p = k D_g^b = k D_g^{b-1} L_g)$	270
Table 5.28: Star Compound+PEGT Bearing Load Capacity Requirements (lbf)	271
Table 5.29: Relative Values of the Bending and Contact Stresses in the HGT...	274
Table 5.30: Comparison Between the HGT and the Star+PEGT (Gear-Tooth Limited Torque Capacities for both gear trains)	276
Table 5.31: Comparison Between the Star Compound and Star 1 st Stage Gear Train Options for the PEGT	281
Table 6.1: SRM Design Assumptions.....	302
Table 6.2: Gear Train Design Constant Parameters and Assumptions.....	302

Table 6.3: Actuator Parameter Choices for Example 1 (SRM+HGT).....	304
Table 6.4: SRM+HGT Design and Performance Parameter Data	304
Table 6.5: SRM+HGT Power-Law Scaling Rules $(P_p = kD_g^b)$	307
Table 6.6: Distribution of Weight and Inertia (as a % of the total) in the Motor and Gear Train as a Function of Diameter (for the SRM+HGT Actuator)	308
Table 6.7: Variation of Basic Design Parameters as a Function of Diameter (for the SRM+HGT Actuator)	310
Table 6.8: SRM+HGT Bearing Load Capacity Requirements (lbf).....	311
Table 6.9: Actuator Parameter Choices for Example 1 (SRM+Star+PEGT)	311
Table 6.10: SRM+Star+PEGT Design and Performance Parameter Data.....	312
Table 6.11: SRM+Star+PEGT Power-Law Scaling Rules $(P_p = kD_g^b)$	314
Table 6.12: Distribution of Weight and Inertia (as a % of the total) in the Motor and Gear Train as a Function of Diameter (for the SRM+Star+PEGT Actuator)	315
Table 6.13: Variation of Basic Design Parameters as a Function of Diameter (for the SRM+Star+PEGT Actuator).....	318
Table 6.14: SRM+Star+PEGT Bearing Load Capacity Requirements.....	318
Table 6.15: Actuator Parameter Choices for Example 1 (SRM+Star Compound+PEGT)	319
Table 6.16: SRM+Star Compound+PEGT Design and Performance Parameter Data	319
Table 6.17: SRM+Star Compound+PEGT Power-Law Scaling Rules $(P_p = kD_g^b)$	322
Table 6.18: Distribution of Weight and Inertia (as a % of the total) in the Motor and Gear Train as a Function of Diameter (for the SRM+Star Compound+PEGT Actuator)	322

Table 6.19: Variation of Basic Design Parameters as a Function of Diameter (for the SRM+Star Compound+PEGT Actuator)	325
Table 6.20: SRM+Star Compound+PEGT Bearing Load Capacity Requirements	325
Table 6.21: Comparison Between the SRM+HGT and the SRM+Star+PEGT (Gear-Tooth Limited Torque Capacities for both gear trains)	326
Table 6.22: Comparison Between the Star Compound and Star 1 st Stage Gear Train Options for the PEGT	329
Table 6.23: Actuator Design Parameter Choices for Example 2 (SRM+HGT) ..	332
Table 6.24: SRM+HGT Design and Performance Parameter Data	332
Table 6.25: Percentage Change of the SRM+HGT Performance Parameters as the Gear Ratio is Varied from 100 to 400 for Different Diameters	335
Table 6.26: Distribution of Weight and Inertia (as a % of the total) in the Motor and Gear Train as a Function of Diameter and Gear Ratio (for the SRM+HGT Actuator)	337
Table 6.27: Variation of Basic Design Parameters as a Function of Diameter and Gear Ratio (for the SRM+HGT Actuator).....	339
Table 6.28: Motor, Bearing, and Gear-Tooth Limited Torque Capacities for a recent PEGT Prototype Effort	340
Table 6.29: Actuator Design Parameter Choices for Example 2 (SRM+Star+PEGT)	342
Table 6.30: SRM+Star+PEGT Design and Performance Parameter Data.....	342
Table 6.31: Percentage Change of the SRM+Star+PEGT Performance Parameters as the Gear Ratio is Varied from 100 to 175 for Different Diameters	345

Table 6.32: Distribution of Weight and Inertia (as a % of the total) in the Motor and Gear Train as a Function of Diameter and Gear Ratio (for the SRM+Star+PEGT actuator)	346
Table 6.33: Variation of Basic Design Parameters as a Function of Diameter and Gear Ratio (for the SRM+Star+PEGT actuator)	348
Table 6.34: Actuator Design Parameter Choices for Example 2 (SRM+Star Compound+PEGT)	349
Table 6.35: SRM+Star Compound+PEGT Design and Performance Parameter Data	350
Table 6.36: Percentage Change of the SRM+Star Compound+PEGT Performance Parameters as the Gear Ratio is Varied from 150 to 450 for Different Diameters	352
Table 6.37: Distribution of Weight and Inertia (as a % of the total) in the Motor and Gear Train as a Function of Diameter and Gear Ratio (for the SRM+Star Compound+PEGT actuator)	354
Table 6.38: Variation of Basic Design Parameters as a Function of Diameter and Gear Ratio (for the SRM+Star Compound+PEGT actuator).....	356
Table 7.1: Motor, Gear Train, and Load Parameters	363
Table 7.2: Direct Drive System (Kollmorgen QT-9704 Motor) Design and Performance Parameter Data Used for Comparison with Geared Systems (K=0).....	372
Table 7.3: Geared System (Emoteq 7000 Series Motor + Nabtesco RV-320E Gear Train) Design and Performance Parameter Data (K=0)	373

Table 7.4: Direct Drive System (Kollmorgen T-10020 Motor) Design and Performance Parameter Data Used for Comparison with Geared Systems (K=0).....	375
Table 7.5: Geared System (Emoteq 3000 Series Motor + Nabtesco RV-6E Gear Train) Design and Performance Parameter Data (K=0)	376
Table 7.6: SRM Design Constant Parameters and Assumptions	379
Table 7.7: HGT and PEGT Constant Parameters and Assumptions.....	380
Table 7.8: Gear Ratios for Geared Systems.....	381
Table 7.9: Direct Drive (SRM) Design and Performance Parameter Data Used for Comparison with Different Geared Systems (K=0).....	382
Table 7.10: Direct Drive (SRM) Responsiveness (rad/sec^2) as a Function of K.....	382
Table 7.11: SRM+HGT Design and Performance Parameter Data (K=0).....	384
Table 7.12: Comparison of Torque Density Between the Geared (SRM+HGT) and Direct Drive (SRM) Systems	385
Table 7.13: Geared (SRM+HGT) Output Responsiveness Benefit Ratio as a Function of Diameter and K (Gear ratio = 100 to 1)	389
Table 7.14: Geared (SRM+HGT) Input Responsiveness Benefit Ratio as a Function of Diameter and K (Gear ratio = 100 to 1)	390
Table 7.15: Distribution of Inertia in the Motor, Gear Train, and Load as a Function of Diameter and Gear Ratio (All inertia values are reflected to the output.)	391
Table 7.16: SRM+Star+PEGT Design and Performance Parameter Data (K=0).....	393
Table 7.17: Comparison of Torque Density Between the Geared (SRM+Star+PEGT) and Direct Drive (SRM) Systems	394

Table 7.18: Geared (SRM+Star+PEGT) Output Responsiveness Benefit Ratio as a Function of Diameter and K (Gear ratio = 100 to 1)	397
Table 7.19: Geared (SRM+Star+PEGT) Input Responsiveness Benefit Ratio as a Function of Diameter and K (Gear ratio = 100 to 1)	398
Table 7.20: Distribution of Inertia in the Motor, Gear Train, and Load as a Function of Diameter and Gear Ratio (All inertia values are reflected to the output.)	399
Table 7.21: SRM+Star Compound+PEGT Design and Performance Parameter Data (K=0).....	401
Table 7.22: Comparison of Torque Density Between the Geared (SRM+Star Compound+PEGT) and Direct Drive (SRM) Systems	402
Table 7.23: Geared (SRM+Star Compound+PEGT) Output Responsiveness Benefit Ratio as a Function of Diameter and K (Gear ratio = 100 to 1)	405
Table 7.24: Geared (SRM+Star Compound+PEGT) Input Responsiveness Benefit Ratio as a Function of Diameter and K (Gear ratio = 100 to 1)	406
Table 7.25: Distribution of Inertia in the Motor, Gear Train, and Load as a Function of Diameter and Gear Ratio (All inertia values are reflected to the output.)	407
Table 7.26: Gear Ratios for Geared Systems.....	411
Table 7.27: Direct Drive (SRM) Design and Performance Parameter Data Used for Comparison with Different Geared Systems (K=0).....	412
Table 7.28: Direct Drive (SRM) Responsiveness (rad/sec^2) as a Function of K.	413
Table 7.29: SRM+HGT Design and Performance Parameter Data (K=0)	413
Table 7.30: Comparison of Torque Density Between the Geared (SRM+HGT) and Direct Drive (SRM) Systems	414

Table 7.31: Geared (SRM+HGT) Output Responsiveness Benefit Ratio as a Function of Torque Capacity and K.....	418
Table 7.32: Distribution of Inertia in the Motor, Gear Train, and Load as a Function of Torque Capacity (All inertia values are reflected to the output.)	419
Table 7.33: Direct Drive (SRM) Design and Performance Parameter Data Used for Comparison with Different Geared Systems (K=0).....	420
Table 7.34: Direct Drive (SRM) Responsiveness (rad/sec ²) as a Function of K.	420
Table 7.35: SRM+Star+PEGT Design and Performance Parameter Data (K=0)	421
Table 7.36: Comparison of Torque Density Between the Geared (SRM+Star+PEGT) and Direct Drive (SRM) Systems	422
Table 7.37: Geared (SRM+Star+PEGT) Output Responsiveness Benefit Ratio as a Function of Torque Capacity and K.....	424
Table 7.38: Distribution of Inertia in the Motor, Gear Train, and Load as a Function of Torque Capacity (All inertia values are reflected to the output.)	425
Table 7.39: Direct Drive (SRM) Design and Performance Parameter Data Used for Comparison with Different Geared Systems (K=0).....	426
Table 7.40: Direct Drive (SRM) Responsiveness (rad/sec ²) as a Function of K.	426
Table 7.41: SRM+Star Compound+PEGT Design and Performance Parameter Data (K=0).....	427
Table 7.42: Comparison of Torque Density Between the Geared (SRM+Star Compound+PEGT) and Direct Drive (SRM) Systems	427
Table 7.43: Geared (SRM+Star Compound+PEGT) Output Responsiveness Benefit Ratio as a Function of Torque Capacity and K.....	430

Table 7.44: Distribution of Inertia in the Motor, Gear Train, and Load as a Function of Diameter and Gear Ratio (All inertia values are reflected to the output.)	430
Table 8.1: Actuator Torque Requirements.....	450
Table 8.2: Design Parameters for Reference Set	451
Table 8.3: Design and Performance Parameters for the Reference Set (12 distinct motor diameters and fixed gear ratio and aspect ratio).....	453
Table 8.4: SRM Design and Performance Parameters for the Reference Set (12 distinct motor diameters and 12 motors total)	453
Table 8.5: Common Motor Diameter Choices for Minimum Set Alternatives 1-5.....	455
Table 8.6: Gear Train Design Parameters for Minimum Sets 1-5	455
Table 8.7: Design and Performance Parameters for Minimum Set #3 (3 distinct motor diameters and fixed gear ratio)	456
Table 8.8: SRM Design and Performance Parameters for Minimum Set #3 (3 distinct motor diameters and 12 motors total)	457
Table 8.9: Tabular Comparison of the Performance Parameters Between Minimum Set #3 and the Reference Set	458
Table 8.10: Minimum Set Options 1-5, Based Upon the Number of Distinct Motor Sizes (common motor diameters for each noted in bold)	460
Table 8.11: Gear Train Design Parameters for Minimum Sets 6-10	462
Table 8.12: Design and Performance Parameters for Minimum Set #8 (3 distinct motor diameters and variable gear ratio)	463
Table 8.13: SRM Design and Performance Parameters for Minimum Set #8 (3 distinct motor diameters and 3 motors total)	463

Table 8.14: Tabular Comparison of the Performance Parameters Between Minimum Set #8 and the Reference Set	464
Table 8.15: Minimum Set Options 6-10, Based Upon the Number of Distinct Motor Sizes (common motor diameters for each noted in bold)	467
Table 8.16: Total Number of Distinct Motor Diameters and Distinct Motor Sizes Required for Each Minimum Set	468
Table 8.17: Tabular Summary of the Average Percent Change in the Performance Parameters for the Different Minimum Set Alternatives	469
Table 8.18: Motor Aspect Ratio Range for Minimum Sets 1-5 (Fixed Gear Ratio of 140)	473
Table 8.19: Motor Aspect Ratio Range for Minimum Sets 6-10 (Variable Gear Ratios)	473
Table 8.20: Design and Performance Parameters for Minimum Set #6 (reference designs for this section)	475
Table 8.21: SRM Design and Performance Parameters for Minimum Set #6 (reference designs for this section)	475
Table 8.22: Design and Performance Parameters for a Potential Reduced Set of Actuators	477
Table 8.23: Tabular Comparison of the Performance Parameters Between Reduced Set and the Reference Set	478
Table 8.24: Reduced Minimum Sets and Criteria Values for Each	480
Table 9.1: Summary of Key References and Their Relevance to the Current Research	494
Table 9.2: Literature Review Findings and This Research's Contributions (Based on All of the Papers Listed in the References Section)	497

Table 9.3: Fundamental Design and Performance Parameters	502
Table 9.4: Summary of PEGT Design and Performance Parameter Relationships	504
Table 9.5: Input and Output Information (Parameters) for the Actuator Design Procedure Tasks	507
Table 9.6: SRM Constants and Fixed Parameters	508
Table 9.7: Suggested Proportions for the HGT and PEGT Internal Design Parameters	510
Table 9.8: Constants/Fixed Parameters for the HGT and PEGT	511
Table 9.9: HGT Power-Law Scaling Rules ($P_p = kD_g^b = kD_g^{b-1}L_g$)	513
Table 9.10: Comparison of Bearing and Tooth-Limited Torque Capacities of the PEGT.....	516
Table 9.11: Relative Values of the Bending and Contact Stresses in the HGT...	517
Table 9.12: Individual Motor and Gear Train Power-Law Scaling Rules ($P_p = kD^b = kD^{b-1}L$)	520
Table 9.13: Key Actuator Design Parameter Choices	522
Table 9.14: Types of Balance Between the Motor and Gear Train	523
Table 9.15: SRM+Star+PEGT Power-Law Scaling Rules ($P_p = kD_g^b$)	526
Table 9.16: Percentage Change of the SRM+HGT Performance Parameters as the Gear Ratio is Varied from 100 to 400 for Different Diameters	531
Table 9.17: Distribution of Weight and Inertia (as a % of the total) in the Motor and Gear Train as a Function of Diameter and Gear Ratio (for the SRM+HGT Actuator)	533
Table 9.18: Actuator Power-Law Scaling Rules ($P_p = kD^b$)	534
Table 9.19: Motor, Gear Train, and Load Parameters	538

Table 9.20: Direct Drive (SRM) Design and Performance Parameter Data Used for Comparison with Different Geared Systems (K=0).....	542
Table 9.21: Direct Drive (SRM) Responsiveness (rad/sec ²) as a Function of K.	542
Table 9.22: SRM+HGT Design and Performance Parameter Data (K=0).....	543
Table 9.23: Geared (SRM+HGT) Output Responsiveness Benefit Ratio as a Function of Diameter and K (Gear ratio = 100 to 1)	547
Table 9.24: Summary of Alternative Minimum Sets and Relative Commonality and Cost Assessments (Set number references come directly from Chapter 8.)	552
Table 9.25: Actuator Torque Requirements.....	553
Table 9.26: Design and Performance Parameters for the Reference Set (12 distinct motor diameters and fixed gear ratio and aspect ratio).....	554
Table 9.27: Common Motor Diameter Choices for Minimum Set Alternatives 1-5555	
Table 9.28: Design and Performance Parameters for Minimum Set #3 (3 distinct motor diameters and fixed gear ratio).....	556
Table 9.29: Tabular Comparison of the Performance Parameters Between Minimum Set #3 and the Reference Set	557
Table 9.30: Design and Performance Parameters for Minimum Set #8 (3 distinct motor diameters and variable gear ratio)	559
Table 9.31: SRM Design and Performance Parameters for Minimum Set #8 (3 distinct motor diameters and 3 motors total)	559
Table 9.32: Tabular Summary of the Average Percent Change in the Performance Parameters for the Different Minimum Set Alternatives.....	561
Table 9.33: Reduced Minimum Sets and Criteria Values for Each.....	563

Table A.1: SRM Design Parameters Classified by Component (for generating reference design).....	584
Table A.2: MatLab Files for Stand-Alone (Direct Drive) SRM Designs without an SRM (Section 3.7)	585
Table A.3: HGT Design Parameters Classified by Component (for generating reference design).....	586
Table A.4: MatLab Files for Stand-Alone HGT Designs without an SRM (Section 3.9)	586
Table A.5: PEGT Design Parameters Classified by Component (for generating reference design).....	588
Table A.6: MatLab Files for Stand-Alone PEGT Designs without an SRM (Section 3.10)	589
Table A.7: MatLab Files for SRM+HGT Actuator (Section 3.11).....	590
Table A.8: MatLab Files for SRM+Star+PEGT and SRM+Star Compound+PEGT Actuator Designs (Section 3.12)	591
Table A.9: MatLab Files for General Computations	592
Table A.10: Balancing Mass Parameters	598
Table A.11: Bending Stress Relationships for Different Load Conditions and Tooth Height to Width Ratios	607

List of Figures

Figure 1.1: Electromechanical Actuator [Tesar et al., March 2004]	1
Figure 1.2: Actuator with Two Stage Gear Train (Ship Rudder Control Application)	6
Figure 1.3: Actuator with Two Stage Gear Train (Aircraft Control Surface Application) [Kendrick and Tesar, 2006]	6
Figure 1.4: Scaled Set of Surgical Manipulator Actuators (Diameters: 2,3,4,5,7,10 inches).....	6
Figure 1.5: Torque as a Function of Gear Mesh Diameter and Aspect Ratio (A) for the Hypocyclic Gear Train.....	7
Figure 1.6: SRM Scaling Rule (Design Map) of Torque vs. Diameter and Aspect Ratio.....	8
Figure 2.1: Electromechanical Actuator Design Process, from Gloria and Tesar [2004].....	21
Figure 2.2: EMA for Aircraft Flight Control Surfaces, from Howe [2000]	24
Figure 2.3: Suggested EMA to Replace Hydraulic Actuator for the Space Shuttle, from Collamore and Lister [1990]	25
Figure 2.4: Thrust Vector Control Actuator, from Kittock [1993]	26
Figure 2.5: HD Systems Electromechanical Actuator [2007]	29
Figure 2.6: Nabtesco Electromechanical Actuator [2008].....	29
Figure 2.7: Bonfiglioli Gearmotor [2007]	30
Figure 2.8: Nuttall Gearmotor [2007].....	30
Figure 2.9: Sumitomo Gearmotor [2007]	30
Figure 2.10: Standard External and Internal Spur Gear Meshes, from Savage, Coy, and Townsend [1982]	33

Figure 2.11: Two-Dimensional Design Space Relating Number of Teeth and Diametral Pitch, with Limiting Stress Constraints Indicated, from Savage, Coy, and Townsend [1982]	34
Figure 2.12: HGT Design Procedure, from Park and Tesar [2005].....	36
Figure 2.13: Gear Train Weight as a Function of Tooth Numbers and Gear Ratio for Spur and Planetary Gear Trains, from Roos and Spiegelberg [2004]	38
Figure 2.14: Gear Train Inertia as a Function of Tooth Numbers and Gear Ratio for Spur and Planetary Gear Trains, from Roos and Spiegelberg [2004]	39
Figure 2.15: Multi-Stage Gear Train Design Process Flow Chart, from Bai, Chong, and Kubo [2003]	40
Figure 2.16: Normalized Move Time (t_f/β) as a Function of Motor (α) and Gear Train (γ) Dimensionless Ratios (Refer to Table 2.7 for a complete description of these parameters.), from Chiang [1990]	44
Figure 2.17: Normalized Stall Power as a Function of Normalized Move Time τ_s and Inertia Ratio η (a function of gear ratio), from Meier and Raider [1976]	45
Figure 2.18: Maximum Motor Torque Required (M_{max}) as a Function of Motor Speed (ω_c) and Gear Ratio (z) (with fixed motor and load inertia), from Shuxing and Ping [1997]	47
Figure 2.19: Motor Safe Operation Area (SOAR) as a Function of Gear Ratio and Motor Speed (Shaded region is considered optimal for minimizing losses.), from Brierley, Colyer, and Trzynadlowski [1989]	48
Figure 2.20: Normalized Acceleration (a) as a Function of Normalized Gear Ratio (i) (Normalization with respect to optimum values), from Saner [2004]	49

Figure 2.21: Determination of Scaling Rules from Experimental Data, from Mendez and Ordonez [2003]	56
Figure 2.22: Robust Concept Exploration Method (Example Product Family Design Method), from Simpson et. al. [1996].....	62
Figure 2.23: Scale-Based Product Family (Scaling parameter t), from Fellini et al. [2005].....	64
Figure 2.24: Module-Based Product Family (Shared modules m_2 between 1 st 2 products), from Fellini et al. [2005].....	64
Figure 2.25: Conditional Distribution of y given x , from Cook and Weisberg [1999]	72
Figure 2.26: Metamodeling Techniques Overview, from Simpson et al. [2001] ..	78
Figure 2.27: a) Full Factorial, b) Fractional Factorial, and c) Central Composite Experimental Designs for a Problem with 3 Factors and 2 Levels for Each Factor, from Simpson et al. [2001]	80
Figure 2.28: SRM Scaling Rule (Design Map) of Torque vs. Diameter and Aspect Ratio (with x and y axes mapped to a -1 to 1 scale)	82
Figure 2.29: Prediction of Performance Parameters at Intermediate Values of Diameter Using Previous Design Information.....	84
Figure 2.30: Representative Actuator Performance Map, from Ashok and Tesar [2007].....	87
Figure 2.31: Graphical User Interface for Design, from Simpson et al., [2007] ...	89
Figure 2.32: Radar Chart Used to Simultaneously Display Multiple Objectives, from Hanne and Trinkaus [2003]	93
Figure 2.33: Parallel Coordinates Plot Used to Simultaneously Display Multiple Objectives, from Messac and Chen [2000].....	94

Figure 2.34: Representative 3-D Design Maps to be Used in a Future Visual Actuator Design Environment (with x and y axes mapped to a -1 to 1 scale).	96
Figure 2.35: Electromechanical Actuator from Patent 6,791,219, from Eric and Gary [2004].....	98
Figure 2.36: Electromechanical Actuator from Patent 5,041,748, from Huber [1991]	99
Figure 2.37: Electromechanical Actuator from Patent 6,095,293, from Brundrett et al. [2000].....	100
Figure 2.38: Electromechanical Actuator from Patent 6,736,233, from Beishline et al. [2004].....	101
Figure 2.39: Gear Train from Patent 4,386,540, from Skaggs [1983].....	103
Figure 2.40: Gear Train from Patent 6,661,139, from Moskob [2003]	104
Figure 3.1: Detailed Actuator Design Including an SRM and HGT.....	109
Figure 3.2: Detailed Actuator Design Including an SRM and PEGT	110
Figure 3.3: Preliminary Actuator Design Including an SRM and HGT	111
Figure 3.4: Preliminary Actuator Design Including an SRM and PEGT	112
Figure 3.5: Preliminary and Detailed Actuator Design Stages (“Y” indicates Yes and “N” indicates No).....	113
Figure 3.6: Forces on a Typical Gear Tooth.....	119
Figure 3.7: Nominal Load Condition (3 teeth in contact).....	125
Figure 3.8: Peak Load Condition (5 teeth in contact).....	126
Figure 3.9: Estimate of Load Sharing Factor for Nominal and Peak Loading Conditions	127
Figure 3.10: Gear Rim Shown on HGT Wobble Gear.....	128
Figure 3.11: SRM Reference Design	131

Figure 3.12: SRM Rotor	134
Figure 3.13: SRM Stator	134
Figure 3.14: Air Gap Distance	136
Figure 3.15: HGT Reference Design	144
Figure 3.16: HGT Gear Mesh Detail	146
Figure 3.17: Wobble Gear (Teeth not shown)	146
Figure 3.18: Eccentricity (e) of the HGT	150
Figure 3.19: HGT Overall Length and Diameter Parameters	152
Figure 3.20: Balancing Mass Geometry	154
Figure 3.21: Actuator Shaft with 2 Balancing Masses Attached	154
Figure 3.22: Star+PEGT Reference Design.....	156
Figure 3.23: Star Compound+PEGT Reference Design.....	156
Figure 3.24: Star Gear Train (1 st Stage) for PEGT	157
Figure 3.25: Star Compound Gear Train (1 st Stage) for PEGT	158
Figure 3.26: PEGT Gear Mesh Detail.....	160
Figure 3.27: Typical PE Gear	160
Figure 3.28: 1 st Stage Star Gear Train for PEGT with Labeled Gear Sizes.....	164
Figure 3.29: 1 st Stage Star Compound Gear Train for PEGT with Labeled Gear Sizes	164
Figure 3.30: Eccentricity (e) of the PEGT	165
Figure 3.31: PEGT Overall Length and Diameter Parameters	166
Figure 3.32: SRM+HGT Reference Design	170
Figure 3.33: SRM+Star+PEGT Reference Design	172
Figure 3.34: SRM+Star Compound+PEGT Reference Design	172

Figure 3.35: Maximum Bearing Linear Speeds for Different Lubrication Methods, from Timken [2004].....	180
Figure 4.1: High Level Actuator Development Process	183
Figure 4.2: Current RRG Actuator Design Procedure	185
Figure 4.3: Proposed Actuator Design Procedure (D_p -design parameter, P_p - performance parameters)	187
Figure 4.4: SRM Reference Design	193
Figure 4.5: HGT Reference Design	196
Figure 4.6: PEGT Reference Design	196
Figure 4.7: SRM+HGT Reference Design	201
Figure 4.8: SRM+PEGT Reference Design.....	201
Figure 5.1: Three-Dimensional Representation of a Scaling Rule (Design Map)	208
Figure 5.2: Two-Dimensional Representation of a Scaling Rule	211
Figure 5.3: SRM Reference Design	214
Figure 5.4: SRM Torque Design Map	215
Figure 5.5: SRM Weight Design Map	216
Figure 5.6: SRM Inertia Design Map	217
Figure 5.7: SRM Torque Density Design Map.....	217
Figure 5.8: SRM Responsiveness Design Map.....	218
Figure 5.9: SRM Torque Design Map (2-D)	220
Figure 5.10: SRM Weight Design Map (2-D)	221
Figure 5.11: SRM Inertia Design Map (2-D).....	221
Figure 5.12: SRM Torque Density Design Map (2-D)	222
Figure 5.13: SRM Responsiveness Design Map (2-D).....	222
Figure 5.14: HGT Reference Design	224

Figure 5.15: HGT Torque Design Map.....	228
Figure 5.16: HGT Weight Design Map	229
Figure 5.17: HGT Inertia Design Map.....	229
Figure 5.18: HGT Torque Density Design Map	230
Figure 5.19: HGT Input Responsiveness Design Map	230
Figure 5.20: HGT Output Responsiveness Design Map.....	231
Figure 5.21: HGT Torque Design Map (2-D).....	232
Figure 5.22: HGT Weight Design Map (2-D)	233
Figure 5.23: HGT Inertia Design Map (2-D).....	233
Figure 5.24: HGT Torque Density Design Map (2-D)	234
Figure 5.25: HGT Input Responsiveness Design Map (2-D)	234
Figure 5.26: HGT Output Responsiveness Design Map (2-D).....	235
Figure 5.27: PEGT Design (Reference Geometry for Bearing-Limited PEGT Design, Diameter = 11 inches).....	238
Figure 5.28: SKF Cylindrical Roller Bearings Selected for PE Gear (cage that retains rollers not shown)	241
Figure 5.29: PEGT Torque Scaling Rule (Diameters 5-12 inches) $(T = 0.006\mathcal{D}_g^{2.93} = 0.006\mathcal{D}_g^{1.93}L_g)$	241
Figure 5.30: PEGT Torque Scaling Rule (Diameters 18-48 inches) $(T = 0.005\mathcal{D}_g^{2.99} = 0.005\mathcal{D}_g^{1.99}L_g)$	242
Figure 5.31: Effect of Output Speed on PEGT Torque Capacity	244
Figure 5.32: Strategies for Increasing the PEGT Bearing-Limited Load Capacity	247
Figure 5.33: Bearing-Limited Torque Capacity as a Function of Center Distance for the PEGT (based on the 11 inch diameter prototype design, with fixed bearing load capacity and gear mesh dimensions).....	248

Figure 5.34: Star+PEGT Reference Design.....	251
Figure 5.35: Star+PEGT Torque Design Map	253
Figure 5.36: Star+PEGT Weight Design Map	253
Figure 5.37: Star+PEGT Inertia Design Map	254
Figure 5.38: Star+PEGT Torque Density Design Map.....	254
Figure 5.39: Star+PEGT Input Responsiveness Design Map.....	255
Figure 5.40: Star+PEGT Output Responsiveness Design Map	255
Figure 5.41: Star+PEGT Torque Design Map (2-D)	257
Figure 5.42: Star+PEGT Weight Design Map (2-D).....	257
Figure 5.43: Star+PEGT Inertia Design Map (2-D)	258
Figure 5.44: Star+PEGT Torque Density Design Map (2-D).....	258
Figure 5.45: Star+PEGT Input Responsiveness Design Map (2-D).....	259
Figure 5.46: Star+PEGT Output Responsiveness Design Map (2-D)	259
Figure 5.47: Star Compound+PEGT Reference Design	262
Figure 5.48: Star Compound+PEGT Torque Design Map	263
Figure 5.49: Star Compound+PEGT Weight Design Map	264
Figure 5.50: Star Compound+PEGT Inertia Design Map	264
Figure 5.51: Star Compound+PEGT Torque Density Design Map.....	265
Figure 5.52: Star Compound+PEGT Input Responsiveness Design Map	265
Figure 5.53: Star Compound+PEGT Output Responsiveness Design Map	266
Figure 5.54: Star Compound+PEGT Torque Design Map (2-D)	267
Figure 5.55: Star Compound+PEGT Weight Design Map (2-D)	268
Figure 5.56: Star Compound+PEGT Inertia Design Map (2-D)	268
Figure 5.57: Star Compound+PEGT Torque Density Design Map (2-D).....	269
Figure 5.58: Star Compound+PEGT Input Responsiveness Design Map (2-D)	269

Figure 5.59: Star Compound+PEGT Output Responsiveness Design Map (2-D)	270
Figure 5.60: Percent Difference Between the Performance Parameters of the HGT and Star+PEGT Alternatives (Only average values of the percent difference are plotted for each performance parameter.)	276
Figure 5.61: Percent Difference Between the Performance Parameters of the Star Compound+PEGT and Star+PEGT Alternatives (Only average values of the percent difference are plotted for each performance parameter.)	281
Figure 6.1: SRM+HGT Reference Design Illustrating Important Design Parameter Choices	292
Figure 6.2: SRM+Star+PEGT Reference Design Illustrating Important Design Parameter Choices	292
Figure 6.3: SRM+HGT Design (with Inside Stator and Outside Rotor)	298
Figure 6.4: SRM+HGT Torque as a Function of Diameter	305
Figure 6.5: SRM+HGT Weight as a Function of Diameter	305
Figure 6.6: SRM+HGT Torque Density as a Function of Diameter	306
Figure 6.7: SRM+HGT Output Responsiveness as a Function of Diameter	306
Figure 6.8: Percentage of Weight in the Motor and Gear Train as a Function of Diameter (for the SRM+HGT Actuator)	308
Figure 6.9: Percentage of Inertia in the Motor and Gear Train as a Function of Diameter (for the SRM+HGT Actuator)	309
Figure 6.10: Variation of K_d , K_t , and A_g as a Function of Diameter (for the SRM+HGT Actuator)	310
Figure 6.11: SRM+Star+PEGT Torque as a Function of Diameter	312
Figure 6.12: SRM+Star+PEGT Weight as a Function of Diameter	313

Figure 6.13: SRM+Star+PEGT Torque Density as a Function of Diameter	313
Figure 6.14: SRM+Star+PEGT Output Responsiveness as a Function of Diameter	314
Figure 6.15: Percentage of Weight in the Motor and Gear Train as a Function of Diameter (for the SRM+Star+PEGT Actuator)	316
Figure 6.16: Percentage of Inertia in the Motor and Gear Train as a Function of Diameter (for the SRM+Star+PEGT Actuator)	316
Figure 6.17: Variation of K_d , K_l , and A_g as a Function of Diameter (for the SRM+Star+PEGT Actuator)	317
Figure 6.18: SRM+Star Compound+PEGT Torque as a Function of Diameter..	320
Figure 6.19: SRM+Star Compound+PEGT Weight as a Function of Diameter .	320
Figure 6.20: SRM+Star Compound+PEGT Torque Density as a Function of Diameter	321
Figure 6.21: SRM+Star Compound+PEGT Output Responsiveness as a Function of Diameter.....	321
Figure 6.22: Percentage of Weight in the Motor and Gear Train as a Function of Diameter (for the SRM+Star Compound+PEGT Actuator)	323
Figure 6.23: Percentage of Inertia in the Motor and Gear Train as a Function of Diameter (for the SRM+Star Compound+PEGT Actuator)	323
Figure 6.24: Variation of K_d , K_l , and A_g as a Function of Diameter (for the SRM+Star Compound+PEGT Actuator)	324
Figure 6.25: Percent Difference Between the Performance Parameters of the SRM+HGT and SRM+Star+PEGT Alternatives (Only average values of the percent difference are plotted for each performance parameter.)	326

Figure 6.26: Percent Difference Between the Performance Parameters of the SRM+Star Compound+PEGT and SRM+Star+PEGT Alternatives (Only average values of the percent difference are plotted for each performance parameter.).....	329
Figure 6.27: SRM+HGT Weight as a Function of Gear Ratio and Diameter.....	333
Figure 6.28: SRM+HGT Torque Density as a Function of Gear Ratio and Diameter	333
Figure 6.29: SRM+HGT Output Responsiveness as a Function of Gear Ratio and Diameter.....	334
Figure 6.30: Percentage Change of the SRM+HGT Performance Parameters as the Gear Ratio is Varied from 100 to 400 (Only average values of the percentage change are plotted for each performance parameter.) ..	336
Figure 6.31: Percentage of Weight in the Motor and Gear Train as a Function of Gear Ratio for the Overall Diameter of 12 inches (for the SRM+HGT Actuator)	337
Figure 6.32: Percentage of Inertia in the Motor and Gear Train as a Function of Gear Ratio for the Overall Diameter of 12 inches (for the SRM+HGT Actuator)	338
Figure 6.33: Variation of K_d and A_m as a Function of Gear Ratio (8 inch diameter SRM+HGT actuator)	339
Figure 6.34: SRM+Star+PEGT Weight as a Function of Gear Ratio and Diameter	343
Figure 6.35: SRM+Star+PEGT Torque Density as a Function of Gear Ratio and Diameter.....	343
Figure 6.36: SRM+Star+PEGT Output Responsiveness as a Function of Gear Ratio and Diameter	344

Figure 6.37: Percentage Change of the SRM+Star+PEGT Performance Parameters as the Gear Ratio is Varied from 100 to 175 (Only average values of the percentage change are plotted for each performance parameter.) ..	345
Figure 6.38: Percentage of Weight in the Motor and Gear Train as a Function of Gear Ratio for the Overall Diameter of 12 inches (for the SRM+Star+PEGT actuator)	347
Figure 6.39: Percentage of Inertia in the Motor and Gear Train as a Function of Gear Ratio for the Overall Diameter of 12 inches (for the SRM+Star+PEGT actuator)	347
Figure 6.40: Variation of K_d and A_m as a Function of Gear Ratio (8 inch diameter SRM+Star+PEGT actuator)	348
Figure 6.41: SRM+Star Compound+PEGT Weight as a Function of Gear Ratio and Diameter	350
Figure 6.42: SRM+Star Compound+PEGT Torque Density as a Function of Gear Ratio and Diameter	351
Figure 6.43: SRM+Star Compound+PEGT Output Responsiveness as a Function of Gear Ratio and Diameter	351
Figure 6.44: Percentage Change of the SRM+Star Compound+PEGT Performance Parameters as the Gear Ratio is Varied from 150 to 450 (Only average values of the percentage change are plotted for each performance parameter.)	353
Figure 6.45: Percentage of Weight in the Motor and Gear Train as a Function of Gear Ratio for the Overall Diameter of 12 inches (for the SRM+Star Compound+PEGT actuator)	354

Figure 6.46: Percentage of Inertia in the Motor and Gear Train as a Function of Gear Ratio for the Overall Diameter of 12 inches (for the SRM+Star Compound+PEGT actuator)	355
Figure 6.47: Variation of K_d and A_m as a Function of Gear Ratio (8 inch diameter SRM+Star Compound+PEGT actuator)	355
Figure 7.1: Responsiveness as a Function of Diameter for Emoteq Brushless DC Motors-High Torque Series ($R_d = 8170D_m^{-1.53}$)	367
Figure 7.2: Torque Density as a Function of Diameter for Emoteq Brushless DC Motors-High Torque Series ($T_w = 0.127D_m$)	368
Figure 7.3: Responsiveness as a Function of Diameter for Emoteq Brushless DC Motors-Megaflux Thin Ring Series ($R_d = 7456D_m^{-1.79}$)	368
Figure 7.4: Torque Density as a Function of Diameter for Emoteq Brushless DC Motors-Megaflux Thin Ring Series ($T_w = 0.203D_m$)	369
Figure 7.5: Torque Density as a Function of Diameter for Rocky Mountain Technologies SRM ($T_w = 0.028D_m$)	370
Figure 7.6: Illustration of Geared and Direct Drive Systems of the Same Size (The geared system will always have a larger torque capacity.).....	371
Figure 7.7: Illustration of Geared and Direct Drive Systems of the Same Torque Capacity (The geared system will always be smaller than the direct drive system.)	372
Figure 7.8: Comparison of Torque Density Between the Geared and Direct Drive Systems	374
Figure 7.9: Geared and Direct Drive Output Responsiveness as a Function of K and Gear Ratio	375

Figure 7.10: Comparison of Torque Density Between the Geared and Direct Drive Systems	376
Figure 7.11: Geared and Direct Drive Output Responsiveness as a Function of K and Gear Ratio	378
Figure 7.12: Comparison of Torque Density Between the Geared (SRM+HGT) and Direct Drive (SRM) Systems (Geared torque densities are an average for the 4 different gear ratio choices for each diameter.)	385
Figure 7.13: SRM+HGT Output Responsiveness as a Function of Diameter and Gear Ratio (practically independent of K).....	386
Figure 7.14: SRM+HGT Input Responsiveness as a Function of Diameter and Gear Ratio (practically independent of K).....	387
Figure 7.15: Geared (SRM+HGT) Output Responsiveness as a Function of Diameter and Gear Ratio (practically independent of K)	387
Figure 7.16: Geared (SRM+HGT) and Direct Drive (SRM) Output Responsiveness as a Function of K and Gear Ratio (for diameter = 10 inches)	389
Figure 7.17: Geared (SRM+HGT) and Direct Drive (SRM) Input Responsiveness as a Function of K and Gear Ratio (for diameter = 10 inches)	390
Figure 7.18: Percentage of Inertia in the Motor, Gear Train, and Load as a Function of Gear Ratio for the Overall Diameter of 10 inches (for the SRM+HGT actuator)	392
Figure 7.19: Comparison of Torque Density Between the Geared (SRM+Star+PEGT) and Direct Drive (SRM) Systems	393
Figure 7.20: SRM+Star+PEGT Output Responsiveness as a Function of Diameter and Gear Ratio (practically independent of K).....	394

Figure 7.21: SRM+Star+PEGT Input Responsiveness as a Function of Diameter and Gear Ratio (practically independent of K).....	395
Figure 7.22: Geared (SRM+Star+PEGT) Output Responsiveness as a Function of Diameter and Gear Ratio (practically independent of K)	395
Figure 7.23: Geared (SRM+ Star+PEGT) and Direct Drive (SRM) Output Responsiveness as a Function of K and Gear Ratio (for diameter = 10 inches)	397
Figure 7.24: Geared (SRM+Star+PEGT) and Direct Drive (SRM) Input Responsiveness as a Function of K and Gear Ratio (for diameter = 10 inches)	398
Figure 7.25: Percentage of Inertia in the Motor, Gear Train, and Load as a Function of Gear Ratio for the Overall Diameter of 10 inches (for the SRM+Star+PEGT actuator)	400
Figure 7.26: Comparison of Torque Density Between the Geared (SRM+Star Compound+PEGT) and Direct Drive (SRM) Systems	401
Figure 7.27: SRM+Star Compound+PEGT Output Responsiveness as a Function of Diameter and Gear Ratio (practically independent of K)	402
Figure 7.28: SRM+Star Compound+PEGT Input Responsiveness as a Function of Diameter and Gear Ratio (practically independent of K)	403
Figure 7.29: Geared (SRM+Star Compound+PEGT) Output Responsiveness as a Function of Diameter and Gear Ratio (practically independent of K).....	403
Figure 7.30: Geared (SRM+Star Compound+PEGT) and Direct Drive (SRM) Output Responsiveness as a Function of K and Gear Ratio (for diameter = 10 inches)	404

Figure 7.31: Geared (SRM+Star Compound+PEGT) and Direct Drive (SRM) Input Responsiveness as a Function of K and Gear Ratio (for diameter = 10 inches).....	405
Figure 7.32: Percentage of Inertia in the Motor, Gear Train, and Load as a Function of Gear Ratio for the Overall Diameter of 10 inches (for the SRM+Star Compound+PEGT actuator)	408
Figure 7.33: Comparison of Torque Density Between the Geared (SRM+HGT) and Direct Drive (SRM) Systems	414
Figure 7.34: Geared (SRM+HGT) Output Responsiveness as a Function of Actuator Weight and Load to Motor Inertia Ratio K (Load Inertia, $I_l = KI_{ref} = KWR^2$).....	415
Figure 7.35: Geared (SRM+HGT) and Direct Drive (SRM) Output Responsiveness as a Function of K (for lower range of K and highest torque value)...	416
Figure 7.36: Geared (SRM+HGT) and Direct Drive (SRM) Output Responsiveness as a Function of K (for full range of K and highest torque value)	417
Figure 7.37: Percentage of Inertia in the Motor, Gear Train, and Load as a Function of Torque Capacity (for the SRM+HEGT actuator)	419
Figure 7.38: Comparison of Torque Density Between the Geared (SRM+Star+PEGT) and Direct Drive (SRM) Systems	421
Figure 7.39: Geared (SRM+Star+PEGT) and Direct Drive (SRM) Output Responsiveness as a Function of K (for lower range of K and highest torque value)	423
Figure 7.40: Geared (SRM+Star+PEGT) and Direct Drive (SRM) Output Responsiveness as a Function of K (for full range of K and highest torque value)	423

Figure 7.41: Percentage of Inertia in the Motor, Gear Train, and Load as a Function of Torque Capacity (for the SRM+Star+PEGT actuator)	425
Figure 7.42: Comparison of Torque Density Between the Geared (SRM+Star Compound+PEGT) and Direct Drive (SRM) Systems	427
Figure 7.43: Geared (SRM+Star Compound+PEGT) and Direct Drive (SRM) Output Responsiveness as a Function of K and Gear Ratio (for lower range of K and highest torque value)	428
Figure 7.44: Geared (SRM+Star Compound+PEGT) and Direct Drive (SRM) Output Responsiveness as a Function of K and Gear Ratio (for full range of K and highest torque value)	429
Figure 7.45: Percentage of Inertia in the Motor, Gear Train, and Load as a Function of Torque Capacity (for the SRM+Star Compound+PEGT actuator)	431
Figure 8.1: Illustration of Reducing the Size of a Family of Products to the Point Where Two Products are Merged into One [Fellini, Kokkolaras, and Papalambros, 2003]	437
Figure 8.2: Example Results for the CDM, Illustrating the Performance Loss Due to the Sharing of Parameters Between Product Designs in a Family ..	439
Figure 8.3: Number of Products (P) vs. Performance Loss (δ) due to Sharing Parameters Among Products in a Family	440
Figure 8.4: SRM+Star+PEGT Actuator	444
Figure 8.5: Illustration of Motor and Gear Train Size Variation as the Gear Train (Actuator) Torque Capacity is Increased (constant motor diameter and variable motor length)	445
Figure 8.6: Star Gear Train (1 st Stage) for PEGT	446

Figure 8.7: Illustration of Motor and Gear Train Size Variation as the Gear Train Torque Capacity is Increased (constant motor diameter and length)	447
Figure 8.8: Star Compound Gear Train (1 st Stage) for PEGT with 6 Crankshafts	449
Figure 8.9: Illustration of Motor and Gear Train Size Variation as the Gear Train (Actuator) Torque Capacity is Increased (variable motor diameter and length)	452
Figure 8.10: Graphical Comparison of the Performance Parameters Between Minimum Set #3 and the Reference Set (Average values from the entire set of actuators are plotted for each performance parameter.)	459
Figure 8.11: Graphical Comparison of the Performance Parameters Between Minimum Set #8 and the Reference Set (Average values from the entire set of actuators are plotted for each performance parameter.)	465
Figure 8.12: Weight Percent Difference Between the Minimum Set Alternatives and the Reference Set (Average values are plotted for each minimum set alternative.)	470
Figure 8.13: Inertia Percent Difference Between the Minimum Set Alternatives and the Reference Set	471
Figure 8.14: Torque Density Percent Difference Between the Minimum Set Alternatives and the Reference Set	471
Figure 8.15: Output Responsiveness Percent Difference Between the Minimum Set Alternatives and the Reference Set	472
Figure 8.16: Graphical Comparison of the Performance Parameters Between the Reduced Set and the Reference Set (Average values from the entire set of actuators are plotted for each performance parameter.)	478
Figure 8.17: Weight Penalty (lbf) as a Function of Number of Actuators in the Set	481

Figure 8.18: Percent Increase in Weight (%) as a Function of Number of Actuators in the Set.....	482
Figure 8.19: Percent Increase in Weight (%) as a Function of Number of Motor Designs in the Set.....	483
Figure 9.1: Electromechanical Actuator [Tesar et al., March 2004]	488
Figure 9.2: Actuator with Two Stage Gear Train (Ship Rudder Control Application)	491
Figure 9.3: Scaled Set of Surgical Manipulator Actuators (Diameters: 2, 3, 4, 5, 7, and 10 inches)	492
Figure 9.4: Detailed Actuator Design Including an SRM and HGT.....	498
Figure 9.5: Preliminary Actuator Design Including an SRM and HGT	498
Figure 9.6: SRM Reference Design.....	500
Figure 9.7: HGT Reference Design	500
Figure 9.8: Star+PEGT Reference Design.....	501
Figure 9.9: Illustration of Motor and Gear Train Design Parameters.....	502
Figure 9.10: Proposed Actuator Design Procedure (D_p -design parameter, P_p -performance parameters)	506
Figure 9.11: HGT Torque Design Map.....	512
Figure 9.12: HGT Torque Design Map (2-D).....	513
Figure 9.13: Effect of Output Speed on PEGT Torque Capacity	514
Figure 9.14: Percent Difference Between the Performance Parameters of the HGT and Star+PEGT Alternatives (Only average values of the percent difference are plotted for each performance parameter.)	518
Figure 9.15: SRM+Star+PEGT Torque as a Function of Diameter	524
Figure 9.16: SRM+Star+PEGT Weight as a Function of Diameter	525

Figure 9.17: SRM+Star+PEGT Torque Density as a Function of Diameter	525
Figure 9.18: SRM+Star+PEGT Output Responsiveness as a Function of Diameter	526
Figure 9.19: Percentage of Weight in the Motor and Gear Train as a Function of Diameter for the SRM+Star+PEGT Actuator.....	527
Figure 9.20: Percentage of Inertia in the Motor and Gear Train as a Function of Diameter for the SRM+Star+PEGT Actuator.....	527
Figure 9.21: Percent Difference Between the Performance Parameters of the SRM+HGT and SRM+Star+PEGT Alternatives (Only average values of the percent difference are plotted for each performance parameter.)	528
Figure 9.22: SRM+HGT Weight as a Function of Gear Ratio and Diameter.....	529
Figure 9.23: SRM+HGT Torque Density as a Function of Gear Ratio and Diameter	530
Figure 9.24: SRM+HGT Output Responsiveness as a Function of Gear Ratio and Diameter.....	530
Figure 9.25: Percentage Change of the SRM+HGT Performance Parameters as the Gear Ratio is Varied from 100 to 400 (Only average values of the percentage change are plotted for each performance parameter.) ..	532
Figure 9.26: Percentage of Weight in the Motor and Gear Train as a Function of Gear Ratio for the Overall Diameter of 12 inches (for the SRM+HGT Actuator)	533
Figure 9.27: Percentage of Inertia in the Motor and Gear Train as a Function of Gear Ratio for the Overall Diameter of 12 inches (for the SRM+HGT Actuator)	534
Figure 9.28: Illustration of Geared and Direct Drive Systems of the Same Size (The geared system will always have a larger torque capacity.).....	540

Figure 9.29: Illustration of Geared and Direct Drive Systems of the Same Torque Capacity (The geared system will always be smaller than the direct drive system.)541

Figure 9.30: Comparison of Torque Density Between the Geared (SRM+HGT) and Direct Drive (SRM) Systems (Geared torque densities are an average for the 4 different gear ratio choices for each diameter.)544

Figure 9.31: SRM+HGT Output Responsiveness as a Function of Diameter and Gear Ratio (practically independent of K).....545

Figure 9.32: Geared (SRM+HGT) Output Responsiveness as a Function of Diameter and Gear Ratio (practically independent of K)545

Figure 9.33: Geared (SRM+HGT) and Direct Drive (SRM) Output Responsiveness as a Function of K and Gear Ratio (for diameter = 10 inches)546

Figure 9.34: 3-D Plot of Geared (SRM+HGT) and Direct Drive (SRM) Output Responsiveness as a Function of K and Gear Ratio (for diameter = 10 inches)547

Figure 9.35: Percentage of Inertia in the Motor, Gear Train, and Load as a Function of Gear Ratio for the Overall Diameter of 10 inches (for the SRM+HGT Actuator)548

Figure 9.36: SRM+Star+PEGT Actuator Suggested for the Minimum Set Alternatives551

Figure 9.37: Graphical Comparison of the Performance Parameters Between Minimum Set #3 and the Reference Set (Average values from the entire set of actuators are plotted for each performance parameter.)558

Figure 9.38: Graphical Comparison of the Performance Parameters Between Minimum Set #8 and the Reference Set (Average values from the entire set of actuators are plotted for each performance parameter.).....	560
Figure 9.39: Weight Percent Difference Between the Minimum Set Alternatives and the Reference Set	562
Figure 9.40: Weight Penalty (lbf) as a Function of Number of Actuators in the Set	564
Figure 9.41: Percent Increase in Weight (%) as a Function of Number of Actuators in the Set.....	564
Figure A.1: SRM Reference Design	584
Figure A.2: HGT Reference Design	585
Figure A.3: Star+PEGT Reference Design.....	587
Figure A.4: Star Compound+PEGT Reference Design	587
Figure A.5: Actuator Design Information Flow Between MatLab-Excel-SolidWorks	593
Figure A.6: SolidWorks Design Table in Microsoft Excel for the HGT Wobble Gear	594
Figure A.7: HGT Shaft Geometry	597
Figure A.8: Balancing Mass Geometry	598
Figure A.9: Shaft with Balancing Masses Attached.....	598
Figure A.10: Balancing Geometry.....	599
Figure A.11: Wobble Gear and Weights of 3 Individual Sections	599
Figure A.12: HGT Balancing Free-Body Diagram.....	601
Figure A.13: Relevant HGT Geometry Dimensions for Balancing Relationships	602
Figure A.14: Modeling a Gear Tooth as a Beam with Applied Load F Near the Pitch Circle.....	605

Chapter 1 Introduction

1.1 OVERVIEW

One of the Robotics Research Group (RRG) missions is to design an array of Electromechanical Actuators (EMA), which, because of their distinctive features, forms a complete architecture of actuators that are useful as building blocks for intelligent open architecture machines. To fulfill this mission, the RRG is developing a science of design for intelligent mechanical systems, which include EMA as one of the key elements. Currently, the RRG focuses on designing EMA for a wide variety of applications including vehicle drive wheels, aircraft control surfaces, submarine control surfaces, robotic manipulators, and many others. An example of a fully integrated actuator previously designed by the RRG for a manipulator shoulder is shown in Figure 1.1, where the locations of some of the basic components are labeled.

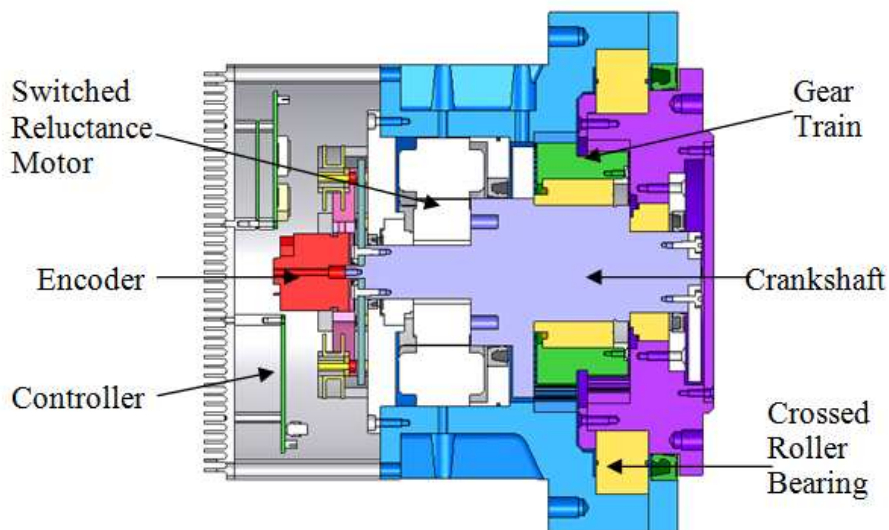


Figure 1.1: Electromechanical Actuator [Tesar et al., March 2004]

1.2 MOTIVATION

The EMA within the scope of this research include an electric motor, gear train, bearings, shafts, sensors, seals, and a controller in a single, integrated housing (Figure 1.1). Based upon the development of conceptual and prototype actuator designs for many different applications, experience has shown that the motor and gear train are the most critical, performance-providing (or limiting) actuator components. The EMA design process currently used by the RRG is based on intuitive rules of thumb and the experience of the designers and often requires multiple design iterations between the motor and gear train. This research aims to improve this limited process by studying the fundamental design problem of coupling an electric motor to a gear train and proposing an actuator design framework to manage it. The proposed framework will decrease the amount of time and effort required to obtain a preliminary, balanced actuator design. There is also a desire to develop scaled sets of actuators (i.e., product lines or families) and understand how the performance of an actuator changes as the basic dimensions are varied. The outcome of this research will be fundamental design rules useful for coupling a motor and gear train and scaling rules that can be used to rapidly develop scaled actuator designs. This research builds upon a preliminary research effort by the same authors that dealt with many of the same actuator design issues [Vaculik and Tesar, 2004].

1.3 INTEGRATING MOTORS AND GEAR TRAINS

The integration of motor and gear train in a single housing allows for high torque and power density in a minimum weight/volume envelope and a reduced number of parts. However, this integration presents the challenge of balancing the parameters between the motor and gear train to achieve the overall performance objectives of the actuator. In this report, *balancing parameters* will be defined as the allocation of torque, weight, inertia,

torque density (torque to weight ratio), and responsiveness (torque to inertia ratio) between the motor and gear train and specifically determining the actuator design parameters (gear ratio, motor size/inertia, motor speed, and other geometric dimensions of the motor and gear train) that achieve the desired allocation. For example, after a specific actuator type has been chosen for an application, RRG designers often meet and use their past experience and intuition to suggest a value for the gear ratio between the motor and the gear train. Then, as time progresses, the gear ratio choice and other design parameter choices are revisited until a final design is achieved. Common issues faced are that the design parameters that achieve optimum motor performance are not optimum for the gear train (and vice versa) and one component limits actuator performance more than the other. These types of design trade-offs must be resolved, preferably by a formal analytical procedure.

1.4 SCOPE

This research will focus on the preliminary design of rotary¹ electromechanical actuators of the type shown in Figure 1.1. Only the gear train and motor will be considered in detail because these are typically the components that dictate the performance capabilities and limits of an actuator. One motor (the switched reluctance motor (SRM)) and three different gear train types (hypocyclic gear train (HGT), star 1st stage gear train coupled with the parallel eccentric gear train (Star+PEGT), and star compound 1st stage gear train coupled with the parallel eccentric gear train (Star Compound+PEGT)) will be considered. The SRM and three gear train types will be discussed in detail in Chapter 3. In general, designing/selecting other actuator

¹This choice is based on the reality that all hydraulic systems were removed from industrial robots by 1980, all linear actuators were removed by 1990, such that today, this cost effective system is durable enough to last 90,000 hours in a high duty cycle task.

components (housings, shafts, bearings, seals, sensors, etc.) after preliminary motor and gear train designs have been developed should not limit performance below that of the motor or gear train. While both operational/control (voltage, current, duty cycle, turn-on and turn-off angles, etc.) and design parameters (diameters, lengths, numbers of teeth, and other geometric parameters) can be used to improve actuator performance², only the effect of design parameters will be considered here. Finally, this research focuses on fully understanding the actuator design problem (careful choice of design parameter inputs, standard assumptions, component modeling equations, etc.) in the preliminary stages of design before resorting to model reduction and iterative solution techniques.

1.5 RESEARCH GOALS

This research fits within the context of RRG's high level (long-term) actuator development objectives, summarized as follows:

- maximize actuator performance,
- enable/improve human choice of design parameters to achieve target performance,
- minimize weight and development cost, and
- develop minimum sets of actuators for each selected application domain.

To make progress on these high level objectives, the specific goals of the present research are to:

1. balance parameters between the motor and gear train for a single-stage actuator configuration (SRM+HGT),

² This improvement in performance can be achieved through the use of performance maps and envelopes [Ashok and Tesar, 2007].

2. balance parameters between the motor and gear train for two two-stage actuator configurations (SRM+Star+PEGT, and SRM+Star Compound+PEGT),
3. generate sets of scaled motors, gear trains, and actuators and develop scaling rules that accurately represent the effect of design parameter choices on actuator performance (for the three different motor-gear train combinations listed in goals 1 and 2), and
4. determine a minimum set of actuators based on the standard SRM+Star+PEGT actuator combination for an illustrative application.

Considering Goal 1, Figure 1.1 illustrates an actuator with a single stage gear train. Single stage gear trains are generally used for moderate output torque and speed requirements and where a minimum number of parts are desirable. For Goal 2, Figure 1.2 and Figure 1.3 display recent RRG actuator designs that utilize two stage gear trains, each with a first stage star compound gear train (SCGT). Two stage gear trains are useful in applications where relatively high torques, low output speeds (or high gear ratios) are required and when minimizing the effect of load inertia on motor responsiveness is critical. Quantitative examples illustrating the need to balance parameters for single and two-stage gear trains are provided in Chapter 6. Considering Goal 3, Figure 1.4 displays a family of 6 scaled actuators designed for a surgical manipulator application with diameters ranging from 2 to 10 inches and a common aspect ratio (i.e., ratio of overall length to diameter). Figure 1.5 illustrates how the torque capacity scales with the gear mesh diameter and aspect ratio for the gear train types shown in Figure 1.1 and Figure 1.4. Scaling rules for the motor and gear trains within the scope of this research will be provided in Chapter 5.

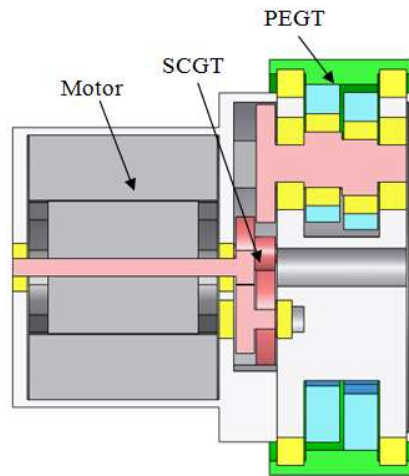


Figure 1.2: Actuator with Two Stage Gear Train (Ship Rudder Control Application)

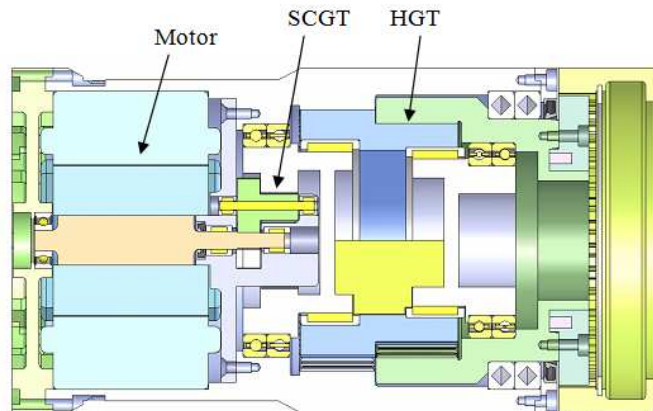


Figure 1.3: Actuator with Two Stage Gear Train (Aircraft Control Surface Application) [Kendrick and Tesar, 2006]

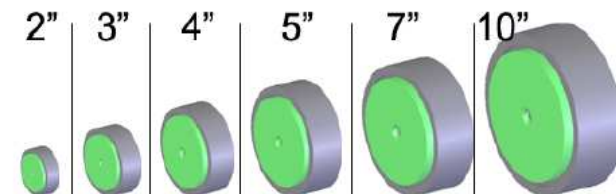


Figure 1.4: Scaled Set of Surgical Manipulator Actuators (Diameters: 2,3,4,5,7,10 inches)

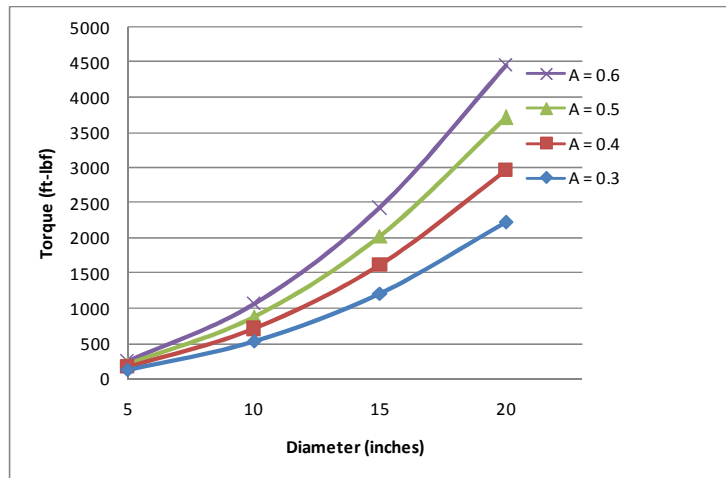


Figure 1.5: Torque as a Function of Gear Mesh Diameter and Aspect Ratio (A) for the Hypocyclic Gear Train

Each family (e.g., a scaled set) of actuators may then be subdivided into a minimum set (Goal 4) to satisfy the broadest range of performance objectives for a given application domain. This concept of a minimum set of actuators will be discussed in further detail in Chapter 8.

When these research goals are achieved, the actuator designer will have the framework and tools necessary to design individual actuators and to design sets (or families) of actuators based on the SRM and three gear train types under consideration.

1.6 DESIGN RULE PREVIEW

Embedded in each of the specific research goals outlined above is the focus on providing the actuator designer with increased knowledge of how design parameter choices affect the basic actuator performance parameters (torque, weight, inertia, torque density, and responsiveness) and how to make design parameter choices in the presence of competing objectives. To enable and maximize human choice of design parameters when balancing and scaling the actuator, there will be an emphasis on providing visual

representations (e.g., two and three-dimensional plots, solid models) to the designer. Figure 1.6 provides a representative scaling rule that provides a visual tool for understanding how the torque capacity of the SRM varies as a function of its overall diameter and aspect ratio (i.e., stack length (L) divided by overall diameter (D)). The term “design map” will also be used to describe the surface shown in Figure 1.6. This representative design map is a preview of one of the common representations used to present the results of this research, and the reader is encouraged to keep this graphic in mind when reading through the text. The key results for scaling (Chapter 5), balancing parameters (Chapter 6), and minimum set development (Chapter 8) will be summarized in the form of two and three-dimensional design maps and look-up tables.

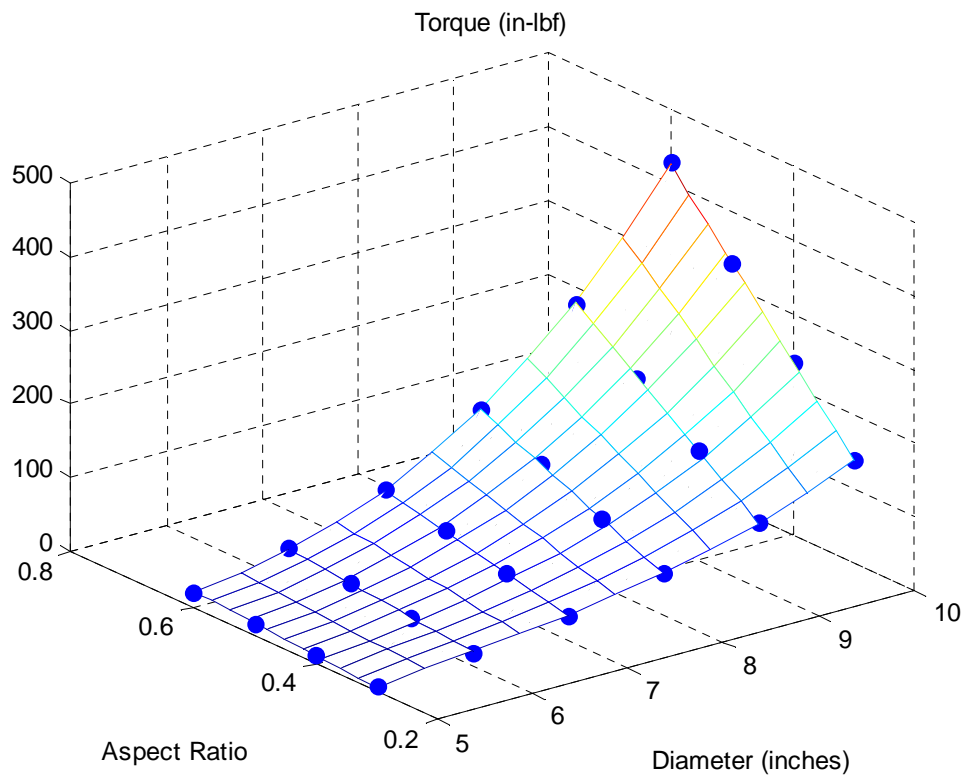


Figure 1.6: SRM Scaling Rule (Design Map) of Torque vs. Diameter and Aspect Ratio

An important relationship between the present research and other ongoing research at RRG should be noted. The present research will develop *design maps* useful for *designing* actuators, where the designer must choose parameters including diameter, length, numbers of teeth, motor air gap, and other geometric parameters. An analogous, parallel visualization effort at RRG in developing (*operational*) *performance maps* useful for *operating* actuators has reached a level of maturity and has been documented in a recent publication [Ashok and Tesar, 2007]. In actuator operation, the human operator often chooses adjustable parameters such as voltage, duty cycle, and motor turn-on and turn-off angles. The mathematical framework developed for actuator operation by Ashok and Tesar is directly applicable for actuator design in this work, and this point will be discussed in further detail in Chapter 2 (Section 2.8.1) and Chapter 9 (Section 9.7).

The parametric models, design rules/maps, solid models, etc. documented in this research should provide an integral part of the future development of a visual decision support system (i.e., software) for EMA actuator design. Future researchers will use the present results as the data (information) for the decision support system. The exercising of the analytical actuator parametric model (Chapter 3) to obtain the actuator design data for the actuator design maps is analogous to running a test on a physical test bed to obtain the actuator operational data for the actuator performance maps.

1.7 CHAPTER OVERVIEW

This chapter has provided some preliminary background to understand the electromechanical actuator design problem, and has presented the motivation, scope, and goals of the current research.

Chapter 2 will provide a literature review that addresses the following key topics: comparison of electromechanical actuator designs, balancing motor and gear train,

scaling, and product family design. In each of these areas, a summary of the findings and contributions of this research effort will be discussed. A discussion of regression, metamodeling, and Response Surface Methodology (RSM) techniques will also be included because they are being used to represent the design rules/maps. An overview of design space visualization techniques will illustrate the importance of providing visual decision-making tools to a designer. Other background topics that will be briefly discussed include the following: comparison of electromechanical and hydraulic actuators, gear train design, and relevant patents. These topics provide the reader with additional insight into the electromechanical actuator design problem.

Chapter 3 will develop the parametric models for the SRM and the three gear train types (HGT, Star+PEGT, and Star Compound+PEGT) being considered in this research. In general, the parametric models will be built upon the models of past RRG researchers and will be augmented where necessary. A discussion of the most fundamental design parameter choices for these motor and gear train types will also be presented. Because the gear ratio is arguably the most fundamental design parameter choice for a gear train, the standard gear ratio ranges suggested for each gear train type will be discussed. The physical phenomena that limit the speed and life of motors, gear trains, and bearings will also be briefly discussed. These sections should provide guidance to future actuator designers when choosing gear ratios and operating speeds.

Chapters 4, 5, 6, and 7 provide the core contribution of this research to the RRG and the design community as a whole. Chapter 4 will present the current RRG actuator design procedure and then proposes a new, augmented procedure. The features of both the current and proposed design procedures will be discussed, with an emphasis on the advantages of the proposed procedure (visualization to enhance the designer's ability to manage major objectives such as performance levels, torque capacity, parametric

balance, etc.). A brief description of each of the embedded design tasks will be discussed. Because the procedure was embedded in the computational software MatLab, a brief discussion of this implementation will be provided. Each step of the design procedure includes graphical tools (plots of design rules, look-up tables, solid models, etc.) that can guide the designer's decisions.

Chapter 5 will define scaling rules as analytical relationships between performance parameters and design parameters that are based on a relatively small number of carefully chosen motor, gear train, and/or actuator designs. Scaling rules will be represented in simple power-law form, the standard low-order polynomial form used in RSM, two-dimensional plots, and three-dimensional surfaces (design maps). The scaling rules will be developed using the regression techniques in Chapter 2 in conjunction with the actuator design procedure in Chapter 4. Because each scaling rule will involve pre-specified design and performance parameters ranges, justification for these ranges will be provided. Collectively, the scaling rules to be provided can be considered a database from which a designer can select the appropriate rules based on a specific application and/or the specific design and performance parameters of interest for a given application domain. Since scaling rules will then be available for three different gear train types, objective comparisons will be made between them in terms of the basic performance parameters of interest: torque capacity, weight, inertia, torque density, and responsiveness.

Chapter 6 will define the concept of balancing parameters in the context of the actuator design problem. Specifically, this chapter will provide quantitative guidelines (in the form of plots of design rules and solid models) for choosing fundamental motor parameters (aspect ratio, diameter, and speed) and gear train parameters (reduction ratio, aspect ratio, and diameter) to balance the performance parameters between the motor and

gear train. Different levels of balance between a motor and a gear train will be considered, including: 1) balance between gear tooth-limited and motor-limited torque capacity (essential), 2) balance between the weight/inertia of the motor and gear train (not essential but highly desirable), and 3) balance between the tooth-limited and bearing-limited torque capacity in the parallel eccentric gear train (desirable but not always possible). Detailed examples for the first two levels of balance will be provided.

Chapter 7 will use the actuator design procedure of Chapter 4 to answer the question: “Why use a gear train?”, by making multiple comparisons between direct drive and geared actuators. One comparison will involve off-the-shelf motors and gear trains, and the rest will be based on the motor and gear train parametric models presented in Chapter 3. The results will illustrate the fundamental trade-off between torque density and responsiveness encountered when choosing between direct drive and geared systems. Suggestions regarding when to use a gear train (based on torque density and responsiveness requirements) will be provided based on the results of the comparisons. To parallel the analytical argument for using a gear train, other practical considerations involved when using a gear train including backlash/lost motion, increased complexity, and increased number of parts/bearings will be briefly discussed. Gear tooth level design work is an ongoing concentration at RRG and involves an in-depth study of tooth stresses, geometry, deformation, and tolerances.

Chapter 8 will define the concept of a minimum set of actuators and develop criteria with which to determine if a set of actuators is a minimum set for a given application. The concept will be illustrated with an example in which alternative minimum sets of actuators based on the standard SRM+Star+PEGT combination will be developed for an example set of torque requirements.

Chapter 9 will summarize the key results, recommendations, and contributions of this research and will also recommend the future work needed to build upon this research. An important area of future work discussed will be the application of the actuator design framework developed in the present research (parametric models (Chapter 3); actuator design procedures, computational software, and solid modeling tools (Chapter 4); and design maps and rules for scaling (Chapter 5) and balancing parameters (Chapter 6)) to other gear train types. In particular, the computational procedures described in Chapter 4 should be extended into a more formal design process, in which the design maps and rules developed here become an integral part.

Chapter 2 Literature Review

The literature review will begin with a review of electromechanical actuator designs for aircraft and space applications, where the benefits of electromechanical actuators over traditional hydraulic actuators are well documented. Then, electromechanical actuator designs from the academic community and from industry will be briefly reviewed. Literature on gear train design will be discussed to provide the necessary background for designing the three gear trains considered in this research. The next section will emphasize the problem of coupling an electric motor to a gear train. Scaling literature will be reviewed because the development of scaling rules for motors, one and two-stage gear trains, and actuators is a key contribution of this research. Product family design methods (to produce the minimal set for a given application domain) will be discussed because of their emphasis on scaling and because the design procedures proposed in this research are similar in form and content. This chapter outlines the specific contribution of this research in each of these areas.

A discussion of regression, metamodeling, and Response Surface Methodology (RSM) techniques will also be included because these techniques are being used to represent the design rules/maps of Chapters 5, 6, and 7. An overview of design space visualization techniques and related literature will outline the features of an effective visual decision-making environment or user interface. Finally, a brief review of the patent literature on most of the topics listed above is provided to identify inventions that embody them. The topics listed in this paragraph are included to help the reader understand how to use these techniques and to provide the reader with key references, but this research will not make a specific contribution in these topics.

2.1 LITERATURE REVIEW SUMMARY

This section provides two summary tables that serve as a roadmap for this chapter. Table 2.1 provides a listing of the most important literature for this research and is classified by topic. Table 2.2 provides a summary of the findings and this research's specific contributions for each of the primary topics: electromechanical actuator design, balancing motors and gear trains, scaling, product family design, and design space visualization. For a more detailed look at each of these topics and results from specific references, the reader can read through the entire chapter.

Table 2.1: Summary of Key References and Their Relevance to the Current Research

Author (Topic)	Description	Relevance
Ashok and Tesar [2002] (Motor Design)	<ul style="list-style-type: none"> • A comprehensive study on the switched reluctance motor (SRM) • Detailed analytical model, with different SRM configurations noted • Design procedure for computing internal motor design parameters 	<ul style="list-style-type: none"> • Employ their standard outside stator, inside rotor SRM model directly in this research
Park and Tesar [2005] (Gear Trains)	<ul style="list-style-type: none"> • A comprehensive study on the hypocyclic gear train (HGT) • Partitioning design and performance parameters into the system level and the tooth level • Detailed analytical model and design procedure 	<ul style="list-style-type: none"> • Employ their gear train model directly in this research • HGT model also useful for the PEGT because both have circular arc teeth
Sigwald and Tesar [2008] (Gear Trains)	<ul style="list-style-type: none"> • A geometric study on the parallel eccentric gear train (PEGT) • Derivation of crankshaft bearing forces as a function of gear mesh forces • Determination of maximum gear ratio (approximately 35 to 1) to avoid interference 	<ul style="list-style-type: none"> • Employ their gear train model directly in this research • Utilize crankshaft bearing force expressions to determine other bearing forces • Use maximum gear ratio and other parametric guidelines
Roos and Spiegelberg [2004] (Gear Trains)	<ul style="list-style-type: none"> • Comparison of gear train size, weight, and inertia of simple spur and planetary gear trains given the same materials, gear ratio, and set of constraints • Graphical solution process used to illustrate the benefits of planetary gears 	<ul style="list-style-type: none"> • Use of three-dimensional surfaces as a design aid • Models formulated for objective comparison between different gear train types

Table 2.1: Summary of Key References and Their Relevance to the Current Research
(Continued)

Author (Topic)	Description	Relevance
Bai, Chong, and Kubo [2003] (Gear Trains)	<ul style="list-style-type: none"> • Partitioning of preliminary gear train design into dimensional and configuration design • 4-step procedure to automate the preliminary design of multi-stage gear trains 	<ul style="list-style-type: none"> • Illustrates that gear ratio choice is not trivial and guided search algorithms can be helpful • One of only a few references on multi-stage gear trains
Chiang [1990] (Balancing Motor and Gear Train)	<ul style="list-style-type: none"> • Derivation of expression for the move time of a disk drive system as a function of the gear ratio; motor power, time constant, and inertia; and load inertia • Design objective was to achieve minimum move time by careful choice of these parameters 	<ul style="list-style-type: none"> • Suggests that optimum gear ratio differs for low and high power (speed) motors • Normalization and use of dimensionless parameters simplifies the design process and interpretation of results
Meier and Raider [1976] (Balancing Motor and Gear Train)	<ul style="list-style-type: none"> • Derivation of expression for the motor power required as a function of move time and inertia ratio, where the inertia ratio is defined as the motor inertia divided by the total inertia • Design objective was to minimize the motor power required by choice of the inertia ratio and gear ratio 	<ul style="list-style-type: none"> • Suggests that optimum gear ratio differs when different motor power metrics (rated, peak, and average) are considered • Similar approach and use of graphical results when compared to Chiang
Tal and Kahne [1973] (Balancing Motor and Gear Train)	<ul style="list-style-type: none"> • Identification of the critical problem in incremental (start-stop) motion system design as overheating of the motor • Design objective was to minimize the motor temperature by selection of the motor size and gear ratio 	<ul style="list-style-type: none"> • Suggests that the optimum gear ratio differs when different load types (inertial and torque) are dominant • Use of dimensionless, equivalent motor and load parameters
Mendez and Ordonez [2003] (Scaling Rules)	<ul style="list-style-type: none"> • Algorithm combines linear regression and dimensional analysis to obtain scaling laws (rules) in power form from a set of existing data • Algorithm seeks to uncover the simplest scaling rules that still provide a user-specified error level 	<ul style="list-style-type: none"> • Importance of a balance between simplicity and accuracy when fitting • Scaling rules obtained in only one form and for simple systems with a few design parameters
Simpson [2004] (Product Family Design)	<ul style="list-style-type: none"> • Survey paper on product family design methods and associated computational tools • Classification of product families/methods into module and scale-based • Summary of optimization approaches used to solve product family design problems 	<ul style="list-style-type: none"> • Scale-based product families are analogous to the scaled sets of actuators sought here • Classification of product family development efforts using multiple criteria (common parameter specification, # of objectives, # of problem stages, solution algorithm, etc.)

Table 2.1: Summary of Key References and Their Relevance to the Current Research
(Continued)

Author (Topic)	Description	Relevance
Simpson et. al. [1996] (Product Family Design)	<ul style="list-style-type: none"> • Presentation of the Robust Concept Exploration Method (RCEM), useful for designing product families • Method includes experimental design and model fitting techniques to reduce computational expense 	<ul style="list-style-type: none"> • One of the few comprehensive methods for developing product families • No scaling rules developed
Fellini et. al. [2005] (Product Family Design)	<ul style="list-style-type: none"> • Method to design families of products and control the anticipated performance losses • Illustrates trade-off between maximizing commonality and minimizing performance losses • Only method found that allows designers to pre-specify acceptable performance losses 	<ul style="list-style-type: none"> • One of the few comprehensive methods for developing product families • Method applicable for module and scale-based families • No scaling rules developed
Fellini, Kokkolaras, and Papalambros [2003] (Product Family Design, Minimum Set)	<ul style="list-style-type: none"> • Product portfolio reduction method used to reduce the number of products in a family and measure performance losses. • Extends commonality among products in a family to the point where two products merge 	<ul style="list-style-type: none"> • Only literature found on the minimum set concept • A starting point for developing problem formulation, minimum set objectives, and solution algorithms for reducing the size of a family
Cook and Weisberg [1999] (Regression Analysis)	<ul style="list-style-type: none"> • Overview of regression techniques for fitting data • Description of least squares estimation • Summary of assumptions necessary for doing statistical inference 	<ul style="list-style-type: none"> • Utilize regression techniques to fit the actuator design data with low-order polynomials
Simpson et. al. [2001] (Metamodeling)	<ul style="list-style-type: none"> • Survey paper on the use of metamodeling in engineering design • Metamodeling can be used to reduce computational expense if accuracy can be sacrificed. • Identifies the two critical steps of choosing an experimental design and choosing a model-fitting technique 	<ul style="list-style-type: none"> • Discussed pitfalls to avoid when apply metamodeling techniques to deterministic models • Suggested the best experimental design and model-fitting techniques based on ease of use, number of parameters, and model type
Myers and Montgomery [1995] (RSM Techniques)	<ul style="list-style-type: none"> • Overview of experimental design, model choice, and model fitting techniques used in RSM 	<ul style="list-style-type: none"> • Utilize full factorial experimental designs and regression models to curve-fit the actuator design data • Response surfaces become the sought-after design maps

Table 2.1: Summary of Key References and Their Relevance to the Current Research
(Continued)

Author (Topic)	Description	Relevance
Ashok and Tesar [2007] (Design Space Visualization)	<ul style="list-style-type: none"> • Proposed math-based visualization framework for multi-input, multi-output systems • Provided literature review on design space visualization techniques • Computation of norms from performance maps and decision surfaces 	<ul style="list-style-type: none"> • Reviewed same literature and summarized suggested features of a visual decision-making environment • Illustrate how the math tools can be applied directly to the actuator design maps
Waskow and Tesar [1996] (Model Reduction)	<ul style="list-style-type: none"> • Reviewed the methods used to reduce and solve polynomial systems of equations often encountered in designing mechanical systems • Applied a resultant elimination technique to some example problems 	<ul style="list-style-type: none"> • Suggested which methods are most useful for reducing and solving polynomial equations • Applied these methods to a manipulator design problem
Gloria and Tesar [2004] (Model Reduction)	<ul style="list-style-type: none"> • Used Groebner bases to solve the same problem solved by Waskow and Tesar and illustrated how it required less simplifying assumptions • Applied Groebner bases to an example motor/gear train design problem and uncovered design insights gained from the reduced model 	<ul style="list-style-type: none"> • Identified implementation challenges when increasing the number of parameters • Identified the need to deal with complex coefficients, large number of equations sometimes generated, and impact of term ordering

Table 2.2: Literature Review Findings and This Research’s Contributions (Based on All of the Papers Listed in the References Section)

Topic	Findings	Contributions
Electromechanical Actuators (Industrial and Patent Literature)	<ul style="list-style-type: none"> •Limited off-the-shelf availability •Custom designs •Key parameters: torque, weight, compactness, frequency response 	<ul style="list-style-type: none"> •Formalize the RRG actuator design procedure to move closer to standardization. •Integrate motor and gear train for compact designs. •Include torque to inertia ratio (responsiveness) as a preliminary frequency response metric.
Balancing Motor and Gear Train	<ul style="list-style-type: none"> •Identified critical parameters: gear ratio, motor speed, motor size for motor/gear train integration •Emphasis on inertial loads and maximizing acceleration •Graphical results for optimum parameter values 	<ul style="list-style-type: none"> •Provide guidelines for choosing critical parameters for single and two-stage gear trains. •Include inertial and torque loads. •Generate graphical results (design maps) for decision-making.
Scaling	<ul style="list-style-type: none"> •Scaling rules developed for scale-model testing and for learning. •Rules developed for simple systems. •Determination of scaling limits, constant parameters 	<ul style="list-style-type: none"> •Develop scaling procedure for the more complex actuator model, and use it to obtain scaled sets of actuators and the corresponding scaling rules (design maps). •Determine suitable constant and scaling parameters for the considered motors and gear trains.
Product Family Design	<ul style="list-style-type: none"> •Tools available to design actuator families •No scaling rules developed •Performance losses due to commonality illustrated •Little guidance for reducing family size (obtaining a minimum set) 	<ul style="list-style-type: none"> •Develop scaling rules for existing and future actuator product families. •Use scaling rules for both learning and obtaining intermediate designs. •Determine a minimum set of actuators for a selected application.
Design Space Visualization	<ul style="list-style-type: none"> •Discovered the parallel between the RRG’s current operational visualization framework and future design visualization framework •Identified features of an effective visual design decision-making environment 	<ul style="list-style-type: none"> •Develop design maps with the aim to use them in a future visual actuator design environment. •Illustrate that RRG’s math tools can be used with the developed design maps. •Embody the identified features in the design maps.

This electromechanical actuator design research fits into the overall scope of the EMAA (Electro-Mechanical Actuator Architecture, Tesar [2000-2007]). In the EMAA, there are ten classes of actuators, which are described in terms of their performance parameter requirements (high rigidity, fault tolerant, high torque, etc.). Each of the ten classes of actuators satisfies the requirements for a given application domain (aircraft, ships, automobile, manufacturing cells, etc.). Prior research at the RRG [Gloria and Tesar, 2004] studied the motor-gear train coupling issues between the SRM and the star, star compound, and hypocyclic gear trains and made two important contributions to the EMA literature. First, the authors developed parametric models for these actuator

components and proposed the best geartrain type that met a given class’s performance parameter requirement(s) (Table 2.3). In the table, “Hypo” refers to the hypocyclic gear train, “Compound” refers to a star compound gear train, and “Combo” refers to a star compound gear train coupled with a hypocyclic gear train, making it a two-stage gear train in the context of this research. Their suggestions were based on rules of thumb and the RRG’s experience in actuator design at the time of publishing.

Table 2.3: Suggested Gear Train Type for Different Actuator Types (Classes), from Gloria and Tesar [2004]

		Performance Parameters						
Actuator Type	Gear Train Type	Reduction Ratio	Power	Torque	Weight	Inertia	Stiffness	Efficiency
Very High Torque	Combo	High	Med	High	Med	Low	High	Med
Very Rugged	Hypo	Med	Low	Med	Med	Med	High	Med
Very Quiet	Hypo	Med	Low	Med	Med	Med	High	Med
High Accuracy	Hypo	High	Med	Med	Med	Med	High	Med
Extreme Low Weight	Combo	High	High	Med	Low	Low	Med	Med
High Efficiency	Hypo	Med	Low	Low	Med	Med	Med	High
Responsive	Combo	High	Med	Med	Med	Low	Med	Med
Simplicity	Compound	Low	Med	Low	High	Low	Low	Low

Second, they also propose the use of the formal, symbolic algebraic reduction technique of Grobner bases to solve the non-linear parametric model governing an actuator design. These and other related techniques objectively reduce the number of unknown parameters and equations in a coupled set of equations. The authors’ primary

contributions are summarized in the actuator design process that they structured and utilized (Figure 2.1).

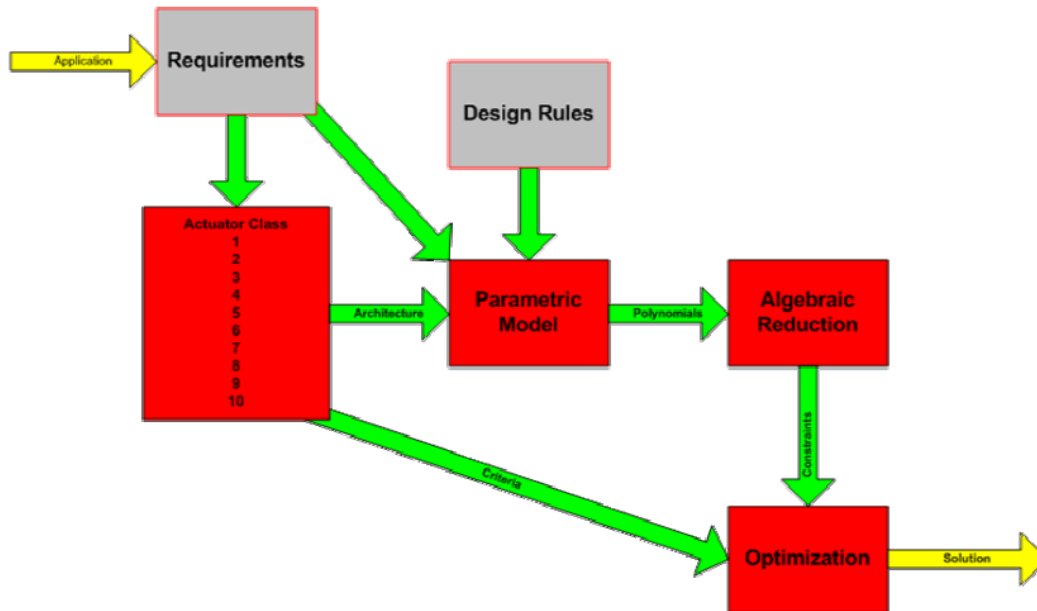


Figure 2.1: Electromechanical Actuator Design Process, from Gloria and Tesar [2004]

The primary limitation of the authors' approach was that it yielded results that were not useful for large numbers of equations and variables. In their context, not useful meant that the resulting reduced model did not improve the designer's ability to gain additional insights not available from the original (not reduced) model³.

This research will propose an alternative approach (see Section 3.9 and 4.3.3) to solve the multiple, non-linear, coupled sets of equations that govern the actuator design problem. This approach consists of the computation of the internal motor and gear train parameters from the overall/external design parameters given as inputs by the designer. Mathematically, enough equations are added to a set (or enough unknown parameters are

³ This approach may still have value in individual component (motor or gear train) design problems where fewer variables are faced at one time.

specified by the designer) so that a system with n equations and n unknown parameters is achieved and is solvable. This approach also involves the design of a small set of motors, gear trains, and actuators and the embedding of their design and performance parameter information in the form of two and three-dimensional design maps (see Chapters 5 and 6). These maps (i.e., visual representations of the actuator design process) will serve as a tool that can help a novice designer learn how parametric choices affect actuator performance (termed “design insights” by Gloria and Tesar). Gloria and Tesar did not evaluate (in great detail) their approach on its ability for the designer to learn more about parameter choices in the actuator.

2.2 ELECTROMECHANICAL ACTUATORS

2.2.1 Electromechanical vs. Hydraulic Actuators

Swingle and Edge [1981] present the results of a study advocating the replacement of hydraulic actuators with electromechanical actuators on a space shuttle, with emphasis on an aerosurface application. According to the authors, EMAs exhibit the following advantages over their hydraulic alternatives: weight reduction, higher energy efficiency, easier maintenance, easier testing (no ground hydraulic system required), and a cleaner vehicle. The EMA exhibits higher energy efficiency because it spends much less energy during low/no-load conditions than the equivalent hydraulic system. No hydraulic fluid or complex valve and piping system is required for EMAs because power transmission is accomplished via wiring. Howe [2000] surveys the development of electromechanical actuators for a variety of applications being pursued by his research group. In particular, the replacement of hydraulic actuators for aircraft flight control surfaces with EMAs is discussed, with an emphasis on the power density and fault tolerant advantages of EMAs (Figure 2.2). Other authors have made similar

comparisons between hydraulic and electromechanical actuators (refer to “Electromechanical Actuator” heading in the References section for a complete list), noting the following characteristics for hydraulic actuators: potential for contamination, low temperature incompatibility, high maintenance costs, extensive ground support, auxiliary equipment required (pumps, compressors, accumulators, valves, etc.), potential for leaks, difficulty in system servicing (pump, reservoir, filters, etc. required on test cart), and low reliability. Electromechanical actuators have the following additional advantages over their hydraulic alternatives: no potential for leaks, ruggedness, and simple installation. The primary reason for replacement of hydraulic actuators with EMAs appears to be an EMA’s potential for weight reduction and improved durability.

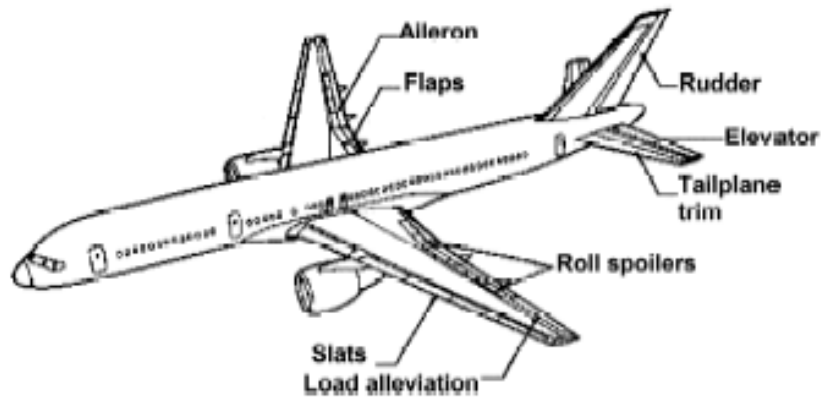


Fig. 1. Potential aircraft flight control surfaces controllable by EHAs/EMAs.

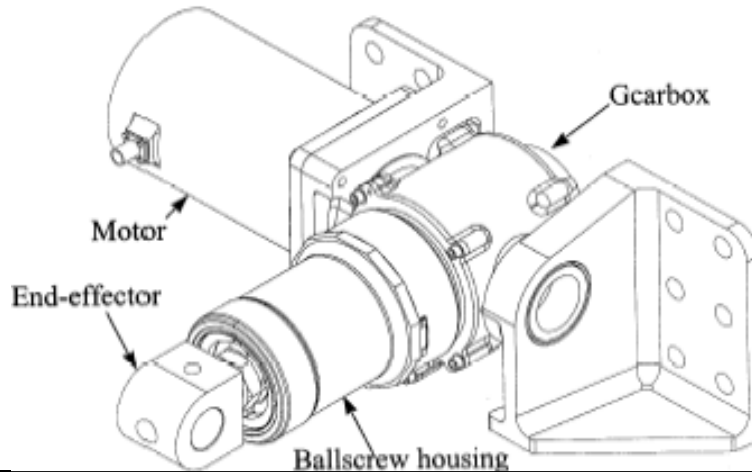


Figure 2.2: EMA for Aircraft Flight Control Surfaces, from Howe [2000]

In each of the following references, an electromechanical actuator was designed to replace a hydraulic actuator, and the primary dimensions and performance specifications of the actuators were provided. Bozzola [1985] describes the design of actuators used to index the rotor (linear) and fold the blades (rotary) in a helicopter. Both actuators consist of a complex arrangement of rotary motors, simple gear trains, differentials, and linear actuators. Collamore and Lister [1990] present the design of an

EMA for the advanced launch system propellant control effectors on a space shuttle. The actuator consists of a two brushless DC motors (for fault tolerance), a harmonic gear train, and integrated electronics (Figure 2.3). Chun and Brunson [1987] provide an overview of transmission options for space manipulator actuators, including the advantages and disadvantages of the following: direct drive systems, harmonic drives, spur gears, torque tubes, and cycloidal speed reducers. The features of the spur gear systems cited include compactness, stiffness governed by tooth shape, backdrivability proportional to the inverse of the gear ratio, and reduced backlash and friction by preloading. The authors also assert the following important conclusion: *gear weight and motor inertia are dominant for high gear ratio designs and motor weight and gear inertia are dominant for low gear ratio designs.*

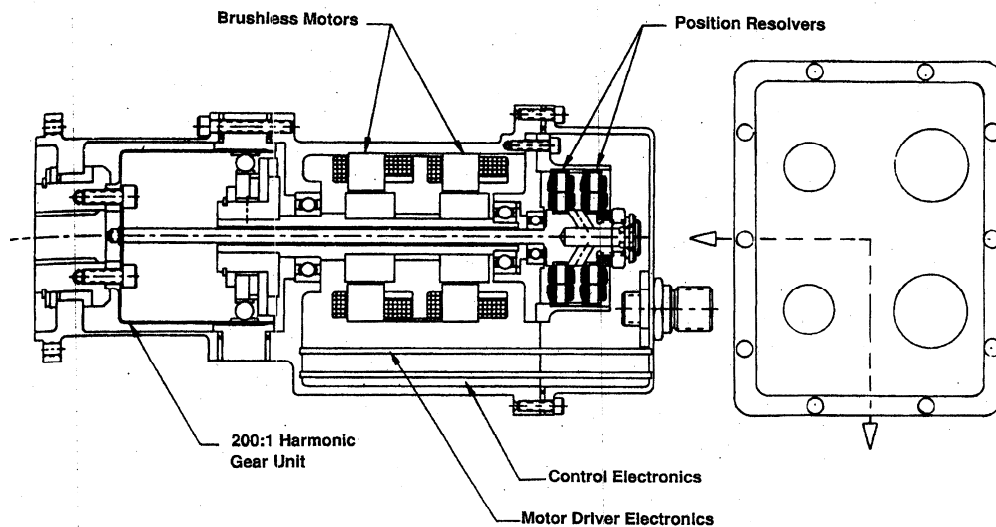


Figure 1. Electromechanical Actuator For ALS Propellant Control Effectors

Figure 2.3: Suggested EMA to Replace Hydraulic Actuator for the Space Shuttle, from Collamore and Lister [1990]

Kittock [1993] details the design of a thrust vector control actuator for rocket engines. The actuator consists of a brushless DC motor, simple spur gear train, and a ball

screw to convert rotary to linear motion (Figure 2.4). Zubkow [1992] presents the design of two thrust vector control actuators. One actuator consists of a brushless DC motor and a roller screw, and the other consists of a brushless DC motor, gear train, and a ball screw. Smith [1984] covers the design of a Boeing 727 upper rudder actuator that consists of a brushless DC motor, planetary gear train, roller screw, and electronic controller.

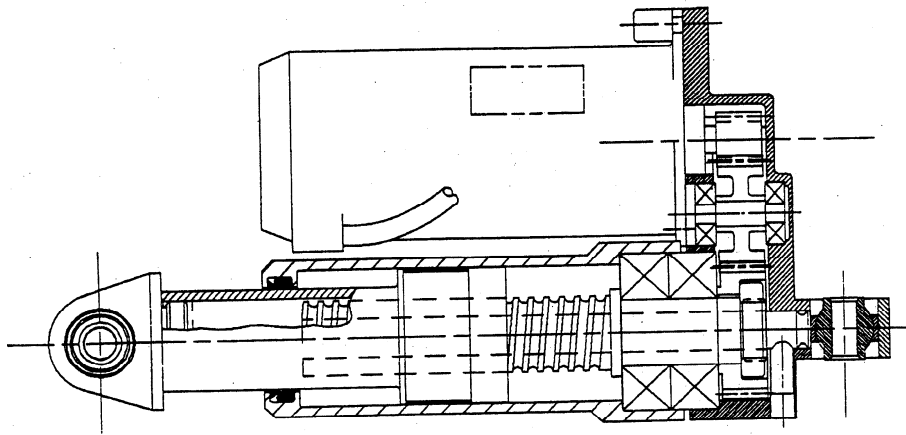


Figure 2.4: Thrust Vector Control Actuator, from Kittock [1993]

The EMA designs described in the research efforts above illustrate that electromechanical actuators are being considered in a wide variety of applications and that the designs are as varied as the applications themselves. The EMAs do exhibit the following general similarities:

- integration of motor and gear train into a compact and lightweight package,
- emphasis on torque, weight, compactness as key performance parameters,
- emphasis on frequency response (more than expected),

- importance of high strength magnet properties in motor design and selection,
- reliance on advances in materials to maintain the EMA benefit over hydraulic systems, and
- the need for linear motions (many actuators use ball or roller screws to convert rotary to linear motion.).

Many of these points (with the exception of 3 and 6) are embodied in current RRG and industry actuator designs. However, the literature suggests that the frequency response of an actuator should be added to the list of the actuator performance parameters currently being considered [Collamore and Lister, 1990; Kittock, 1993; and Zubkow, 1992]. The torque to inertia ratio is a simple metric that has been used to compare the acceleration (responsiveness) of different motor designs [West and Leonard, 1955 and Krishnan, 1987], and it will be used in this research as a starting point to begin to describe actuator frequency response. Where adequate performance specifications and dimensioned drawings have been provided, these actuators (though somewhat dated) are suitable for a comparative analysis with the actuators developed in this research.

2.2.2 RRG Actuator Research

The RRG is developing different classes of actuators to meet the requirements of a variety of applications and to begin to populate the electromechanical actuator design architecture [Tesar, 2000-2007]. The RRG has been working on electromechanical actuator design for 30 years, and Table 2.4 lists the reports (along with student authors) that have been completed since 1985 on the topic of fully integrated actuator design. The current research is only the fourth work that includes both an electric motor and gear train. The works by Grupinski [1996] and Wiese [1997] were research efforts aimed at

delivering a prototype. The work by Gloria [2004] is the only RRG research effort that considers both the electric motor and gear train and aims to improve the current design process by the studying motor and gear train coupling problem. The current research builds primarily upon the work of Gloria and also integrates the works on switched reluctance motors [Ashok and Tesar, 2002], hypocyclic gear trains [Park and Tesar, 2005 and Kendrick and Tesar, 2006] and parallel eccentric gear train [Sigwald and Tesar, 2008 and Tesar et al., 2008].

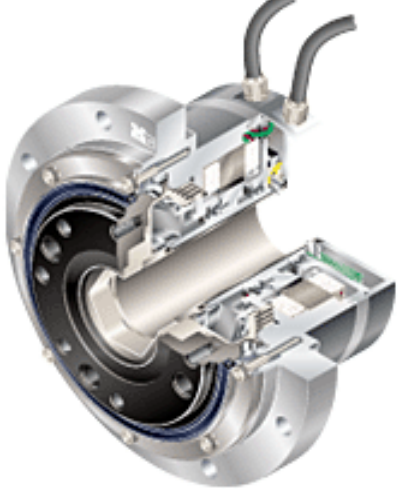
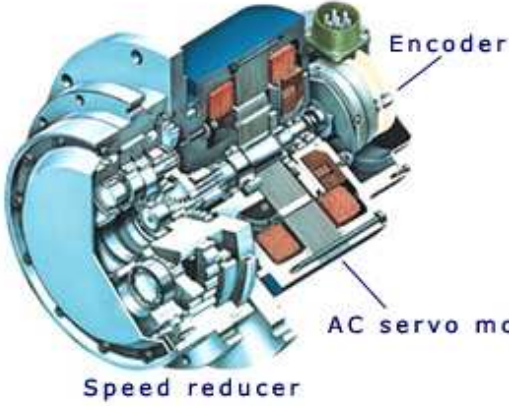
Table 2.4: Summary of RRG Research on Integrated Actuator Design

Title (Year)	Student Author	Description
Design of Low Cost Robotic Actuators for a Modular, Reconfigurable Six-Degree of Freedom Robotic Manipulator (1996)	S. Grupinski	Design and fabrication of two sizes of modular, compact actuator designs, which include a motor, gear train, position sensor, and joint bearing
Low Cost Actuator Design for Modular Robots (1997)	G. Wiese	Design of a low-cost electromechanical actuator and its internal wiring
Architectural Design of a Precision Linear Actuator Module	D. Black	Development of a linear electromechanical actuator architecture and design of a spectrum of high performance linear actuators
Parametric Modeling and Design Synthesis for Electromechanical Actuators (2004)	C. Gloria	Development of a design process for electromechanical actuators, which includes the actuator architecture, a parametric model, and the algebraic model reduction technique of Groebner Bases

2.2.3 Off-the-Shelf Actuators




Electromechanical actuators of the type addressed in this research fall under the industrial category of integrated motor/controller/gear drives, and the following

companies were found to offer these types of products: Moog Inc., Duff-Norton Inc., Parker-Hannafin Corp., Astromec, Danaher, Sumitomo, Nabtesco, and HD Systems. Two companies, HD Systems (Figure 2.5) and Nabtesco (Figure 2.6) provide detailed documentation on the design of electromechanical actuators that can be considered similar to the actuators in the present research. These actuators include integrated motor and gear train designs in the same housing and have the same cylindrical geometry commonly used in RRG actuators. Because design and performance parameter information is available for these actuators, they are suitable for direct comparison with the actuators to be developed during this research.

	
<p>Figure 2.5: HD Systems Electromechanical Actuator [2007]</p>	<p>Figure 2.6: Nabtesco Electromechanical Actuator [2008]</p>

Industry also offers “gear motors”, which include a motor and gear train design that are not contained in a single housing. While many different varieties of these actuators are available, “concentric” gear motors (shown in Figure 2.7-Figure 2.9) are the type most similar to the actuators of the current research. These gear motors are not as suitable for comparison with RRG EMAs. However, these designs do illustrate that the

manufacturer is addressing the motor and gear train coupling problem so that the end user can expect improved performance (e.g., reduced weight, less parts) when compared to individual motors, couplings, and gear trains (where each component is designed or selected separately).

		
<p>Figure 2.7: Bonfiglioli Gearmotor [2007]</p>	<p>Figure 2.8: Nuttall Gearmotor [2007]</p>	<p>Figure 2.9: Sumitomo Gearmotor [2007]</p>

2.2.4 EMA Literature Summary

After reviewing the actuator design literature from the academic and industrial communities, it is obvious that integrated electromechanical actuators are not widespread, standard off-the-shelf products like the individual electric motors and gear trains of which they are made. Many researchers have expressed this sentiment. According to Haskew and Schinstock [1998], “EMA design and development is not yet a mature technology.” According to Howe [2000], “many actuator types are currently emerging with varying operational characteristics (hydraulic, electric, etc.), displacements (rotary or linear), speeds of response, positional accuracies, and duty cycles.” Also, many electromechanical actuator designs are custom designs, in contrast to standard electric motor designs [Bolton, 1994]. Further evidence that electromechanical actuators are not a standard, mature technology is that current researchers are still defining the problem [Messine et al., 1998 and Fitani et al., 2004]. If researchers are still defining the problem,

then developing this standard is still in the future, and this research works toward establishing this standard.

In addition, there are only a small number of companies that manufacture electromechanical actuators, and of the companies that do make them, the number, type, and layout of the actuator components varies significantly. This variation is also evident in the EMA designs from the research community described above. Thus, if a customer purchases actuators of the same size from different companies, the operating characteristics and performance capabilities will likely be different. More research on motor design, gear train design, the actuator design process itself, and integrating motors and gear trains is needed so that actuators can become standard commercially-available products that are utilized in many applications. *This research will provide contributions on the latter two topics: 1) improving the current EMA design process to move closer to standardization (Chapter 4) and 2) the motor-gear train integration problem (Chapter 6).*

2.3 GEAR TRAIN DESIGN

This section reviews background literature on gear trains that is necessary to understand and design the gear train types considered in this research: hypocyclic gear train [Park and Tesar, 2005 and Kendrick and Tesar, 2006] and star/star compound coupled with the parallel eccentric gear train [Tesar et al., 2008]. Modeling equations and solid models of these gear trains will be detailed in Chapter 3.

Townsend [1991] provides a comprehensive text on gear train design that includes the following relevant issues: a detailed discussion of low pressure angle gearing, internal gears, important performance parameters, choosing among different gear train types, and epicyclic gear trains. The discussion on internal gearing highlights the challenges, primarily interference, associated with the small tooth number differences

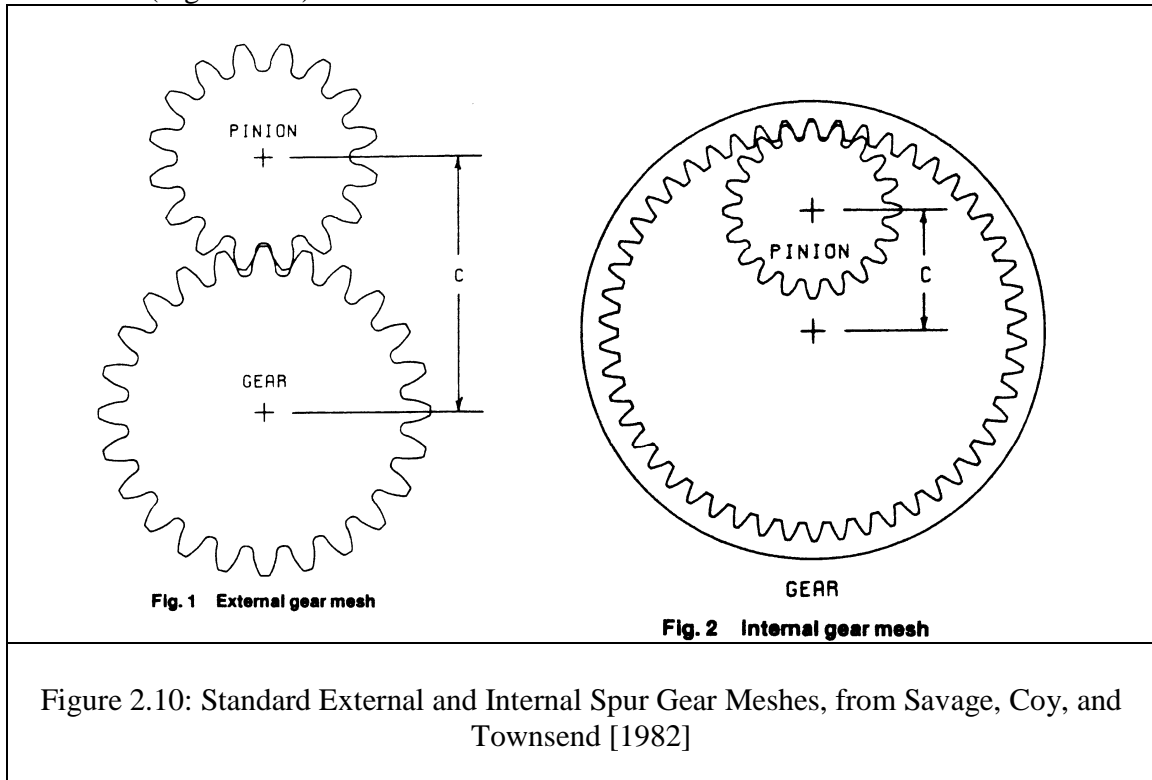
(i.e., mating gears of almost the same size) employed in the hypocyclic and parallel eccentric gear trains of this research. The author provides recommendations regarding the proper gear train type for a given target gear ratio (Table 2.5), which will be used as a model to generate similar results for the gear trains considered here. The table contains gear trains that are most relevant to the current research. The gear ratios and assembly constraints of various epicyclic and star compound gear trains were also derived and will be used directly in this research. The performance parameters of efficiency and power loss are derived as functions of the design parameters and could be used in this research as additional metrics to compare gear train designs if necessary.

Table 2.5: Suggested Gear Train Types for a Range of Gear Ratios

Gear Ratio Range	Suggested Gear Train Type	Number of Gears in the Gear Train
Up to 5:1	Single reduction spur	2
	Simple planetary	3
Up to 100:1	Fixed differential	5
	Harmonic drive	2

Savage, Coy, and Townsend [1982] provide guidelines to determine the optimum tooth number combinations to achieve compact external and internal gear arrangements using involute teeth (Figure 2.10). To use the analytical model derived by these researchers to develop gear train designs, the designer must provide desired design parameter values for gear ratio, torque capacity, material strengths, pressure angle, and aspect ratio (common, independent choices made by gear train designers), and the tooth numbers and diametral pitches can then be calculated with the objective of minimizing the center distance of the gear set. The center distance of the gear train is used as a the measure of compactness. Constraints considered include bending fatigue, contact fatigue, and interference and are written as functions of only the tooth number and

diametral pitch after some simplifying assumptions are applied. A two-dimensional design space with these two free design parameters was then generated, and when the constraint lines were plotted in the space, the acceptable (feasible) design region was identified (Figure 2.11).



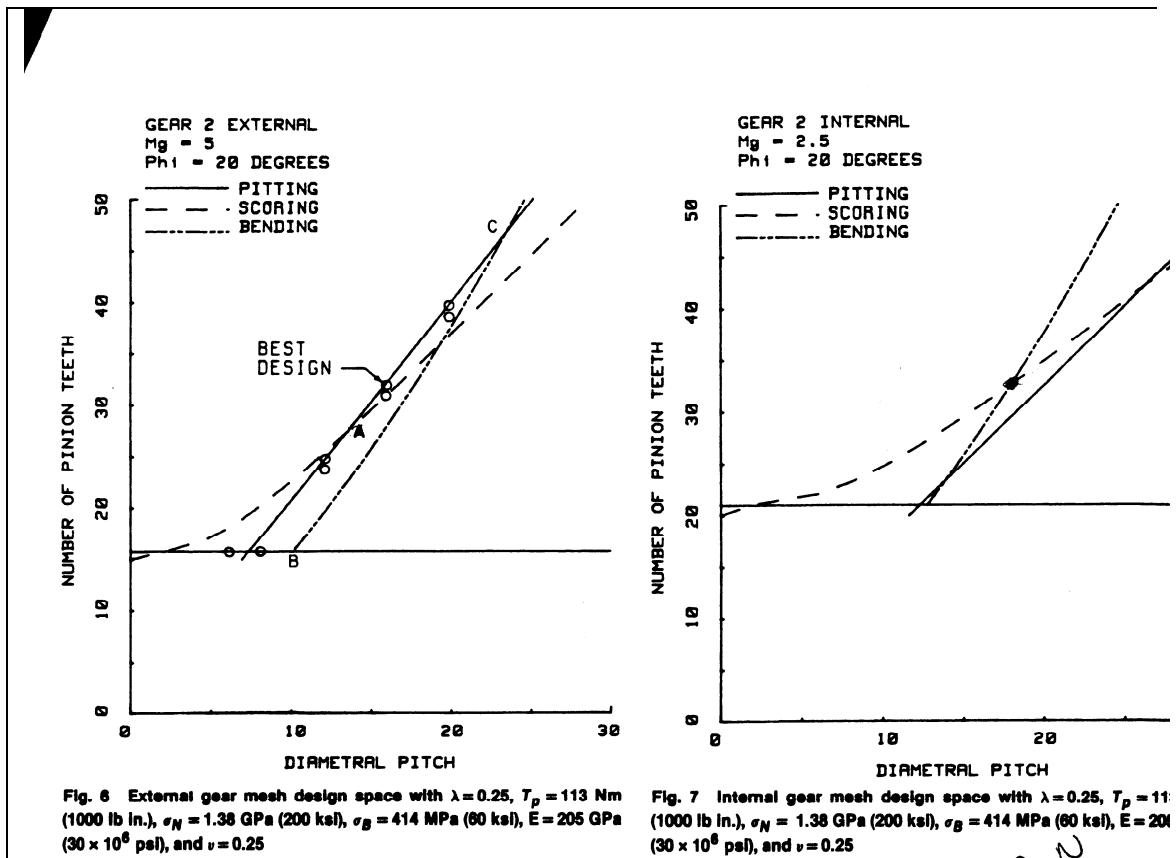


Figure 2.11: Two-Dimensional Design Space Relating Number of Teeth and Diametral Pitch, with Limiting Stress Constraints Indicated, from Savage, Coy, and Townsend [1982]

The approach applied by these authors applies equally well to the gear trains considered in this research, with the exception that the circular arc tooth profile replaces the standard involute profile considered by the authors. One limitation of the involute profile is that only a limited set of diametral pitches are available based on established American Gear Manufacturers Association (AGMA) manufacturing practices [Norton, 2000]. For the circular arc profile, however, any diametral pitch can be achieved because there is currently no standard (restrictive) tooling to generate the teeth. Because of this fact, many more tooth number combinations are available to achieve a given gear ratio

target when using circular arc teeth. The authors attempt to achieve balance in the design by ensuring that the safety factors for the bending and contact stresses are similar. This concept of “balancing” parameters will be discussed in greater detail in this report in Chapter 6 and will be extended to the balance between a motor and a gear train and include torque capacity, weight, inertia, and other parameters.

Park and Tesar [2005] completed a comprehensive study on the hypocyclic gear train, which employs the circular arc tooth profile. The authors partitioned the gear train design problem into the system level and the tooth level and provided justification for which design and performance parameters should be considered in each level (Table 2.6). The system level parameters include those that are most often considered in the preliminary stages of design, and many rules of thumb relating these parameters are available for standard involute teeth [see Norton, 2000 or many other machine design textbooks]. While this research was done for the hypocyclic gear train, it is also relevant for the parallel eccentric gear train because both gear trains employ circular arc gear teeth and involve similar relative motion in an internal gear mesh. The authors also provided a detailed analytical model relating the performance parameters of the gear train to the system level design parameters and formulated a design procedure to compute these parameters (Figure 2.12). Steps 1 and 2 of this procedure will be performed in this research.

Table 2.6: System and Tooth Level Design Parameters for the Hypocyclic Gear Train

System Level	Tooth Level (Circular Arc Teeth)
Pitch diameter	Pressure angle
Eccentricity	Tooth height
Number of teeth	Tooth thickness
Face width	Various radii

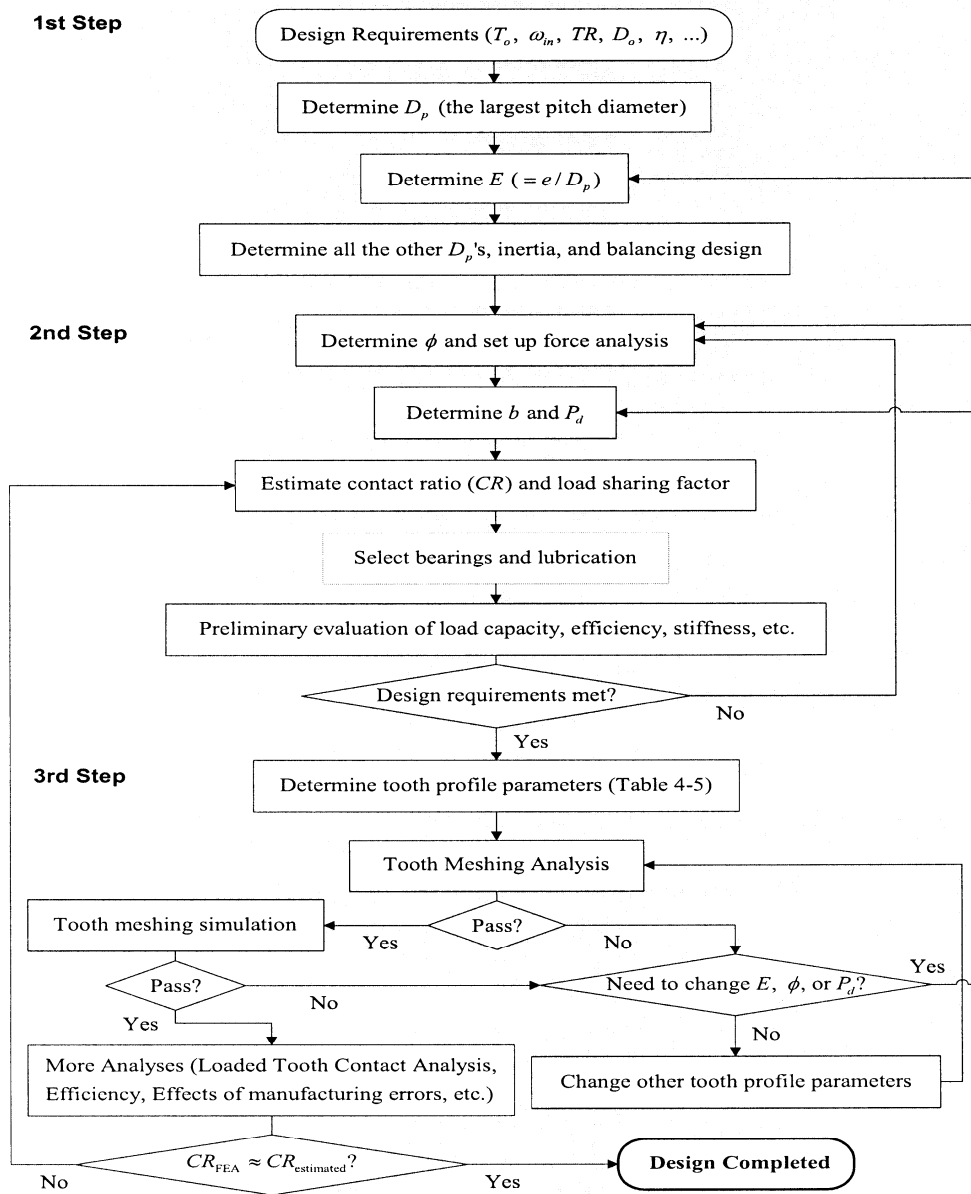


Figure 2.12: HGT Design Procedure, from Park and Tesar [2005]

The current research will focus on the system level design problem, using the assumptions necessary from the tooth level (regarding contact ratios, minimum and maximum tooth number differences for mating gears, and minimum eccentricity) in order

to be able to generate gear train designs. In particular, a contact ratio of 3 (same as the number of teeth in mesh) and a minimum tooth number difference of 3 will be used to generate the gear train designs for Chapters 5-8. As deeper understanding of the tooth level design and performance parameter relationships are developed, they can be incorporated into this research. The identification of the critical design parameters for the system level gear train design problem by Park and Tesar was very useful in the current research for identifying the corresponding design parameters for the gear trains and motors being considered here. Also, many of modeling equations documented by the authors will be used directly in this research.

Roos and Spiegelberg [2004] make a comparison of simple spur and planetary gear trains given the same materials, gear ratio, and set of constraints. Because their work uses a similar approach to gear train design as this research (see Section 4.3.3), it will be reviewed in detail. Detailed parametric models that expressed the gear train size, weight, and inertia as a function of gear ratio, center distances, ring gear radius, and face width were derived. Using the same set of assumptions for the two different gear train types allowed for a fair comparison between them for a given set of target performance parameters (Figure 2.13 and Figure 2.14). The solution procedure used to arrive at results was graphical and subjective in that arbitrary choices of some design parameters were made in order to arrive at a solvable set of equations. The primary results of this effort were as follows:

- Contact stress limits the minimum sizes of the gears in most cases for both spur and planetary gear trains.
- Bending stress is only limiting for very hard steels, which have relatively high contact strength.

- Bending stress only needs to be calculated for the smaller gear in a mesh because it will always have the higher stress.
- Required size, weight, and inertia are less for planetary gear trains than simple spur gear pairs for the same level of performance.

This was one of the few works that could provide a baseline for comparison of results. It also illustrated the value of plotting three-dimensional design surfaces that show how design parameter choices (gear ratio, center distances, ring gear radius, and face width) affect the performance parameters (gear size, weight, and inertia).

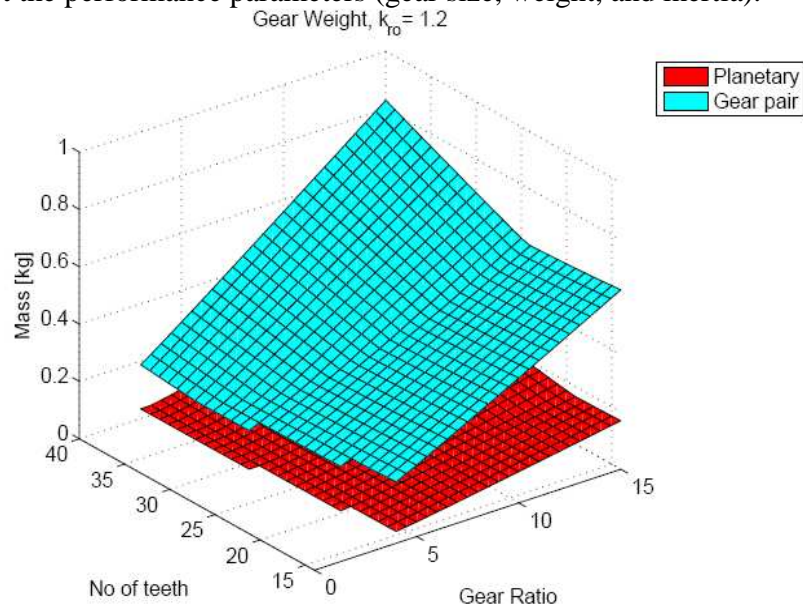


Figure 2.13: Gear Train Weight as a Function of Tooth Numbers and Gear Ratio for Spur and Planetary Gear Trains, from Roos and Spiegelberg [2004]

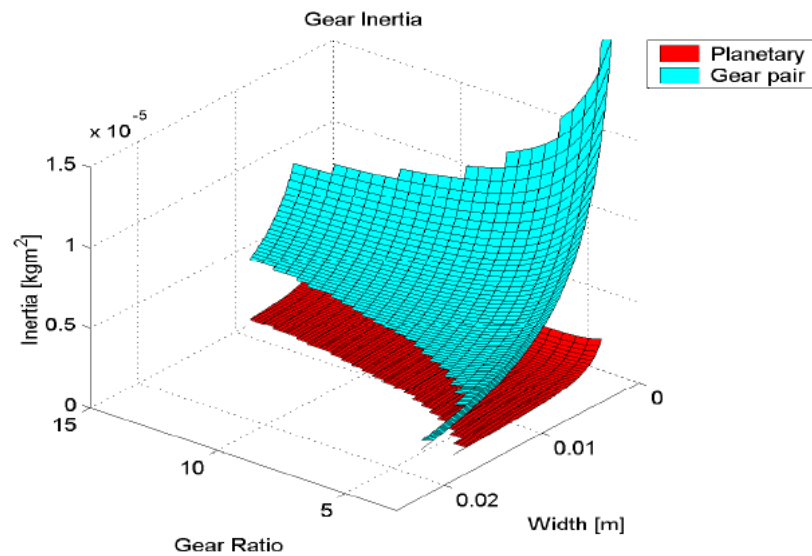


Figure 2.14: Gear Train Inertia as a Function of Tooth Numbers and Gear Ratio for Spur and Planetary Gear Trains, from Roos and Spiegelberg [2004]

Bai, Chong, and Kubo [2003] partition preliminary gear train design into dimensional design and configuration design. They provide the following 4-step procedure (Figure 2.15) to automate the preliminary design of multi-stage gear drives.

1. Determine number of stages and types of gears.
2. Determine gear ratios/number of teeth using one of two methods to split the ratios among the stages (random search method or simulated annealing).
3. Perform dimensional design using generate and test (exhaustive search) method.
4. Perform configuration design using simulated annealing.

This procedure is similar to the RRG approach used to develop gear train designs (see Section 4.3.3) and to the approach to be followed in this research. In the RRG approach, “configuration design” is usually handled in step 1 via user input. The

designer provides numerical values for the performance parameters (power, overall gear ratio, and speed), and the algorithm determines the design parameters (number of teeth, diametral pitch, and face width) that minimize the gear train volume subject to meeting center distance and interference constraints. This work provides a good reference for designing a multi-stage gear train, a task which will be extended to address the research goal for two stage gear trains. It organizes the design parameters so that parameters are dealt with in certain steps of the procedure, which is necessary to maintain control of the design and so that a human decision maker can balance competing objectives. The overall objective of minimizing gear box volume is an example of one of the many objectives the designer might be seeking for given actuator design. Also, the different methods used to split the overall gear ratio into the gear ratios for the individual stages reveal that this task is not trivial and certainly affects the overall performance of the design.

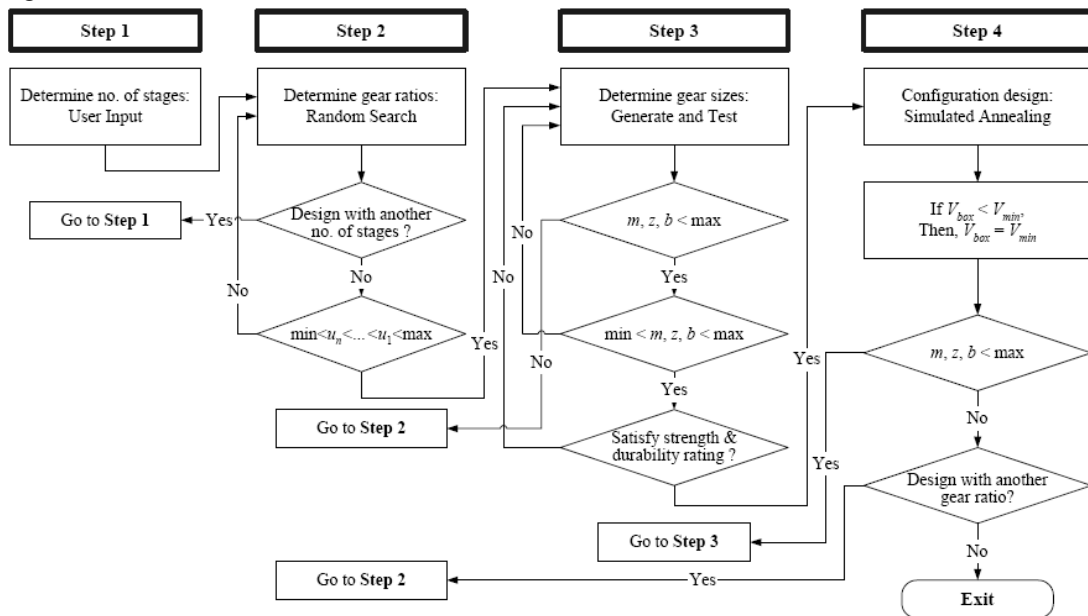


Figure 2.15: Multi-Stage Gear Train Design Process Flow Chart, from Bai, Chong, and Kubo [2003]

2.3.1 Gear Train Design Literature Summary

The last two references [Roos and Spiegelberg, 2004 and Bai, Chong, and Kubo, 2003] are useful for the current research because they provide a means to compare gear trains of different types and an automated procedure to design multi-stage gear trains, respectively. These authors prioritized the design and performance parameters, constraints, and objectives. This research will formulate a design procedure similar in form to that of Bai, Chong, and Kubo [2004] and past RRG researchers [Park and Tesar, 2005 and Kendrick and Tesar, 2006] (Chapter 4) and provide comparisons between single stage and two stage gear trains similar in form to those of Roos and Spiegelberg [2003] (Chapter 5).

2.4 INTEGRATING MOTORS AND GEAR TRAINS

Integrating a motor and gear train is a fundamental design problem that must be solved to design the electromechanical actuators of this research. Despite its importance for actuators and other electromechanical systems, there is not much recent literature available on the topic. This section reviews literature that includes both the motor and the gear train and discusses how to effectively integrate them to maximize performance. Each work was reviewed for the key principles and design approaches that could aid in improving the current actuator design process.

The fundamental governing equation of an integrated motor and gear train system can be written as:

$$T_m - T_f - T_{loss} - \frac{T_l}{g} = \left(I_m + \frac{I_g}{g^2} + \frac{I_l}{g^2} \right) \alpha \quad \text{Eqn. 1}$$

where the parameters are:

$$T_m = \text{motor torque}$$

T_f = friction torque

T_{loss} = motor iron/copper losses

T_l = load torque

g = gear ratio

I_m = motor inertia

I_g = gear train inertia (reflected to the load)

I_l = load inertia

α = acceleration

For the purposes of this discussion, the friction loads (T_f) and motor iron and copper losses (T_{loss}) can be neglected. Then, this equation can be solved for the motor torque as:

$$T_m = \left(I_m + \frac{I_g}{g^2} + \frac{I_l}{g^2} \right) \alpha + \frac{T_l}{g} \quad \text{Eqn. 2}$$

This form of the equation is useful because it expresses the motor torque required to overcome inertial (acceleration) and external loads, with the dominant load term depending on the particular application. For example, high acceleration (responsiveness) is required in systems that must change speed rapidly in a short amount of time and in positioning applications where a system must move from point to point very quickly. The first term in the equation dominates for these systems. For systems with low speeds, high output torques, and/or stationary loads, the second term dominates. For systems with relatively high motor, gear train, and bearing speeds, the friction torque and motor loss terms (omitted from the equation) can sometimes be significant.

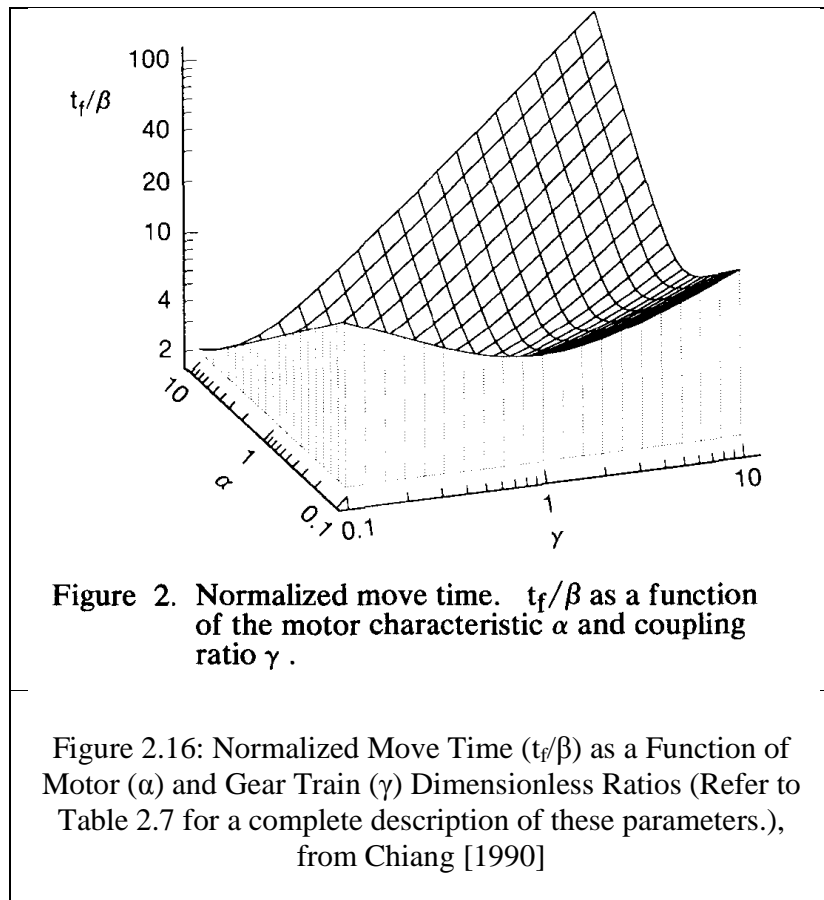
2.4.1 Designing for Inertial Loads

This section reviews literature that provides guidance in designing for inertial loads and reveals that the gear ratio is a fundamental design parameter in coupling a

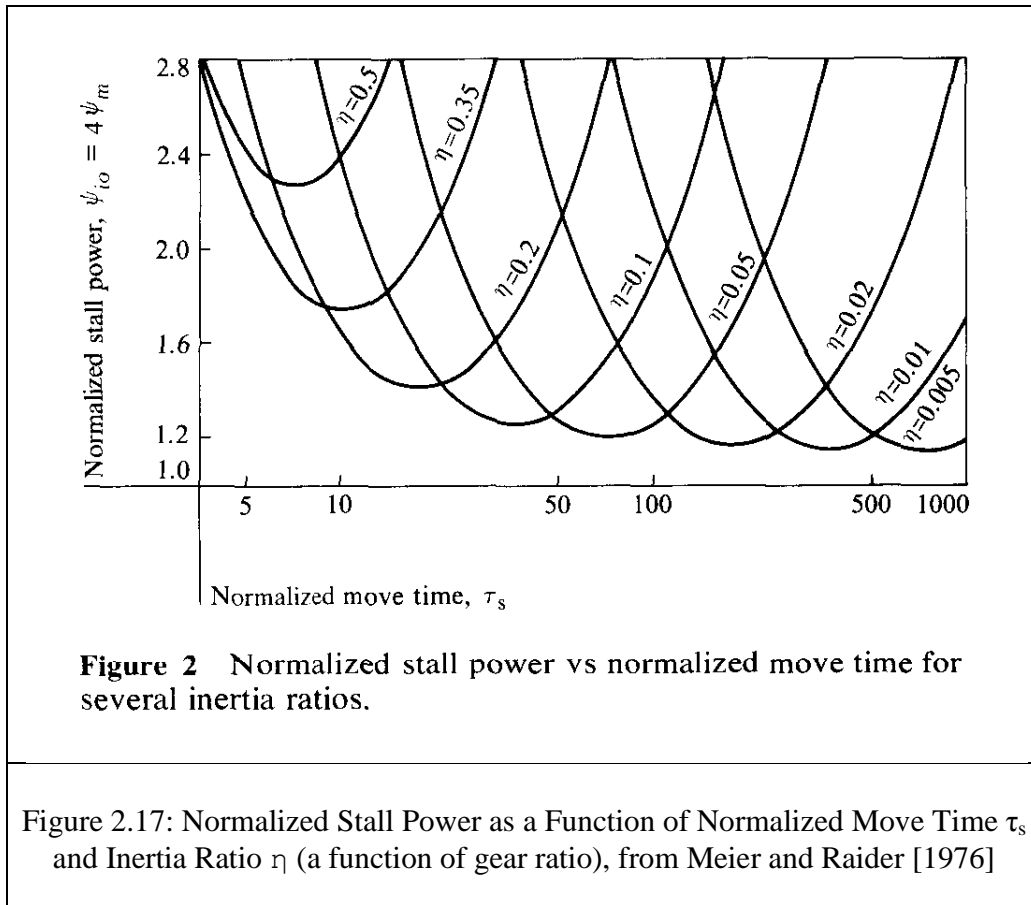
motor with a gear train for these types of loads. Most of the references cited below begin with the basic governing equation shown above.

West and Leonard [1955] suggest that achieving maximum acceleration of the load is a common goal in motor-gear train systems. The authors derive the optimum gear ratio ($g_{\text{optimum}} = \sqrt{I_l/I_m}$) that maximizes acceleration for a fixed motor torque (or minimizes the required motor torque for a fixed motor acceleration). This optimum gear ratio illustrates the principle of matched inertias (sometimes called inertia matching) that is commonly discussed in this area of the literature. The authors suggest that the ratio of motor torque squared to motor inertia (T_m^2/I_m) is a criterion that must be maximized when designing or selecting motors for maximum acceleration. The criterion provides an immediate determination of the feasibility of a given motor for this particular objective.

Chiang [1990] begins with the fundamental governing equation above and derives an expression for the move time of a disk drive system as a function of the gear ratio; motor power, time constant, and inertia; and load inertia (Figure 2.16). The design objective was to achieve minimum move time by careful choice of the parameters listed. The authors formulate a motor selection procedure based on their move time analysis. Like West and Leonard [1955], the authors derive an identical expression for the optimum gear ratio but assert that it is only applicable for relatively low power (speed) motors. The authors also present another optimum gear ratio that is suitable for higher power motors. Key principles taken from this work include the normalization of all the parameters involved and the suggestion that gear train and load parameters (inertias, speeds, etc.) be well understood before attempting to design the motor.



Meier and Raider [1976] derive an expression for the motor power required as a function of move time (τ_s) and inertia ratio (η), where the inertia ratio is defined as the motor inertia divided by the total inertia (Figure 2.17). Their approach and the parameters they consider closely parallel that of Chiang [1990]. For a given move time, their results allow the determination of the inertia ratio and gear ratio that minimizes the motor power required. The authors determine that these optimum ratios are different when optimizing different motor power parameters: rated motor power, peak input power, or average input power. Like other authors, normalization of parameters is also done, and the significance of the motor time constant is discussed.



Ohm [2007] states that “the choice of motor and gear train is very important in servo system design because non-optimal selection can lead to poor performance and increased costs,” and “there is no straightforward procedure for servo system component (motor, gear train, power supply, etc.) selection.” The author asserts that inertial torque is often the most significant torque requirement and friction and damping torques can be neglected. Thus, the suggested calculation of acceleration capabilities using only inertial loads (as in Eqn. 2) has some validity. As a rule of thumb, *the authors suggest selecting the gear ratio so that the maximum desired load speed corresponds to 50% of the maximum motor speed* because this ensures that nearly continuous motor stall torque is available at the maximum load speed.

Fussell and Taft [1995] outline a procedure to select brushless dc motors and the gear ratio given the load torque and speed characteristics. *The authors suggest selecting the gear ratio so that the maximum desired load speed corresponds to 75% to 80% of the maximum motor speed.* According to these authors, gear trains should be used for systems with the following characteristics: high output torque and low output speed, high load inertia and low move times, and when matching the peak power points of the motor and the load.

Bullock [2000] recommends speed matching as the first step in sizing a motor and gear train combination (i.e., an actuator) for a given application. *He suggests selecting the gear ratio so that the maximum desired load speed corresponds to the motor's rated speed.* Four reasons to maximize the gear ratio are discussed, with the primary reason being the reduction in reflected load (and gear train) inertia. Like other authors, the author recommends that the reflected load inertia be equal to the motor inertia, but that mismatches of 4 to 1 can be tolerated without a loss of bandwidth (a measure of frequency response).

Shuxing and Ping [1997] discuss parametric design of EMAs, beginning with Eqn. 2 and describe the fundamental task in actuator design as matching the load torque and speed requirements with the available torque and speed characteristics of the actuator. They also provide guidelines for choosing the gear ratio and operating speed to minimize the torque required by the motor (Figure 2.18). One limitation asserted by the authors is that gear ratios are usually less than 10 to 1, which makes their work applicable to only the lower ratio gear trains considered in this research (i.e., the parallel eccentric gear train with only a small reduction in the 1st stage). There does not appear to be a particular reason the authors' consider gear ratios less than 10 to 1 to be the most common.

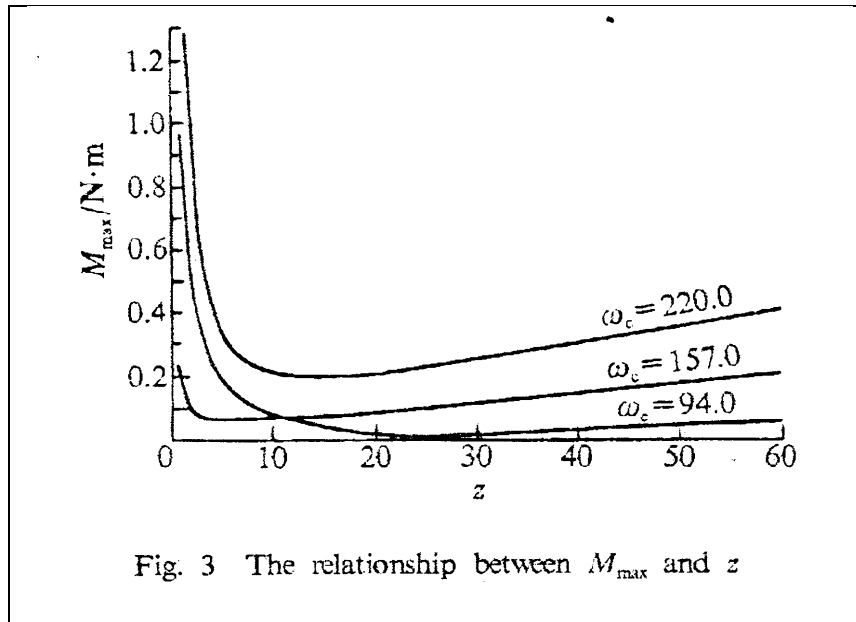


Figure 2.18: Maximum Motor Torque Required (M_{\max}) as a Function of Motor Speed (ω_c) and Gear Ratio (z) (with fixed motor and load inertia), from Shuxing and Ping [1997]

Tal and Kahne [1973] identify the critical problem in incremental (start-stop) motion system design as overheating of the motor. Unlike the above works that attempt to maximize acceleration, the authors provide guidelines for minimizing the motor temperature by selection of the motor size and gear ratio. Similar to other works, an equivalent load parameter (including torque, inertia, move time and distance) and an equivalent motor parameter (line resistance, thermal resistance, inertia, torque constant) are developed. The primary conclusion is that if acceleration torque dominates (i.e., responsiveness is the most critical requirement), the gear ratio should be chosen to match motor and reflected load inertia exactly. If the load torque dominates, the magnitude of the equivalent load parameter determines the required gear ratio.

Brierley, Colyer, and Trzynadlowski [1989] formulate the selection of motor and gear train to minimize energy consumption (losses) as a non-linear constrained

optimization problem. The reduction of the problem to only three design parameters (gear ratio, maximum motor speed, and move time) allowed a graphical solution process. The authors select a desired move time and then plot the constraints (maximum motor speed, motor current, armature voltage, and allowable move time) on a two-dimensional plot of gear ratio and motor speed to define a safe operation area (Figure 2.19). Then, the designer can graphically make parametric choices to minimize losses.

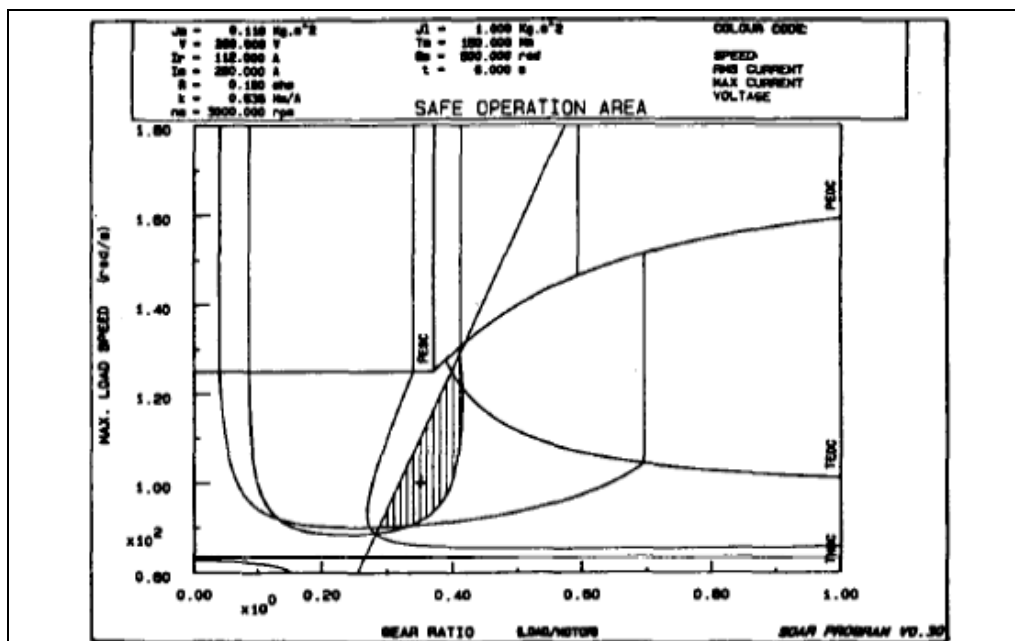


Fig. 4. Exemplary "SOAR" plot.

Figure 2.19: Motor Safe Operation Area (SOAR) as a Function of Gear Ratio and Motor Speed (Shaded region is considered optimal for minimizing losses.), from Brierley, Colyer, and Trzynadlowski [1989]

Saner [2004] derives expressions for the optimum gear ratio for two different actuator types: 1) actuators with a linear characteristic (maximum torque inversely proportional to speed) and 2) thermally limited actuators, with velocity independent maximum torque but with a limited RMS current. The gear ratio is chosen to maximize

peak acceleration for type 1 actuators and to maximize RMS acceleration for type 2 actuators. The authors suggest that gear ratios lower than the computed optimums should be avoided because of a sharp decrease in acceleration (Figure 2.20).

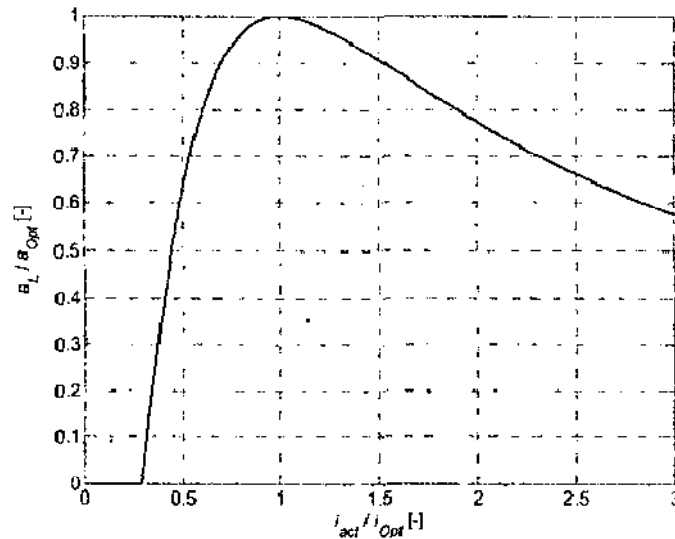


Fig. 4. Qualitative behavior of the maximal acceleration of the load depending on the scaled gear ratio i . It can be seen that a gear ratio lower than i_{Opt} results in a swifter decrease of a_t than a ratio higher than i_{Opt} .

Figure 2.20: Normalized Acceleration (a) as a Function of Normalized Gear Ratio (i) (Normalization with respect to optimum values), from Saner [2004]

Hamel and Widner [1998] develop an optimal gear shifting strategy for robotic actuators. While variable ratio gear trains are not in the scope of this research, the authors' results are related. According to the authors, to achieve desired joint motion and acceleration, the gear ratio and motor speeds should vary during a given motion trajectory and that the gear ratio tends toward a value that allows a motor to operate at a speed where it provides peak power. However, in many common robotic tasks (pick and place, painting, cutting, welding, etc.), the speed and gear ratio changes occur mainly when the

joint is either beginning or finishing the task. Thus, for most of the task motion, the optimal speed and gear ratio are fixed values. This provides some justification for the constant gear ratio actuators developed in this research. Variable gear ratio gear trains are particularly useful for vehicle drive wheel applications, in which multiple gear train output speeds are required to achieve different vehicle speeds.

Lee [2007] notes that the torque to inertia ratio of a motor is a good measure of responsiveness, and that brushless dc motors have significantly higher torque to inertia ratios than brushed dc or induction motors. The author recommends that the motor inertia be made as small as possible with a lower stability limit of 20-25% of the load inertia. Systems where the reflected load inertia is equal to the motor inertia (i.e., matched inertias) consume the minimum amount of power and have the highest bandwidth. Combining these two statements, *the suggested motor inertia as a function of load inertia is $0.2I_l < I_m < I_l$.*

Armstrong [1998] discusses the effects of changing the gear ratio based on the size of the motor inertia relative to the load inertia. If the load inertia is relatively large compared to motor inertia, increasing the gear ratio is beneficial. This is because it reduces the torque required to accelerate the (large) load inertia by the square of the gear ratio while only decreasing the motor torque linearly with the ratio. The net effect is that less torque is needed to achieve the same level of acceleration. If load inertia is relatively small compared to motor inertia (e.g., when using the HGT or other gear trains with relatively high gear ratios), increasing the gear ratio is not beneficial because it will have a minimal effect on the total inertia (sum of motor and load inertias), while still decreasing the motor torque by the ratio (i.e., law of diminishing returns). The net effect is that more torque is needed to achieve the same level of acceleration, so the designer

may not be able to find a suitable motor or may need to choose a larger motor to meet the increased torque requirement and pay the cost of the increased inertia.

2.4.2 Integrating Motor and Gear Train Literature Summary

The important results and guidelines from the above literature are as follows.

- Design and/or characterize the load torque, speed, and inertia characteristics before attempting motor design or selection.
- The gear ratio is the most important parameter for achieving balance between a motor and the gear train.
- Qualitative and quantitative guidelines are provided for selecting the optimum gear ratio, relationship between motor and output speed, and the size of the motor.
- In addition to considering overall design objectives, the gear ratio should also be selected to obtain a suitable relationship between maximum motor speed and maximum output speed.
- Motor size selection is typically easier after the selection of the gear ratio.
- The gear train inertia is usually insignificant compared to the load inertia. (However, for the higher gear ratio and higher load capacity gear trains considered in this research, gear train inertias can be of similar magnitude or much larger than the load inertia.)
- Inclusion of more motor parameters (such as motor power, winding resistance, torque constant, time constant, etc.) than those considered here may be necessary to verify the motor and gear train parameter choices.
- Maximizing motor power and minimizing motor losses and winding temperatures are other common design objectives.

- Normalization of parameters and use of dimensionless parameters allow easier interpretation of results and provide more physical insight.

Table 2.7 summarizes the analytical solutions for optimum gear ratios derived by some of the above authors. These gear ratio results along with the suggestions for the relationship between maximum output speed and rated motor speed (from Ohm [2007], Fussel and Taft [1995], and Bullock [2000]) will be used as benchmarks for the actuator designs to be developed in this report. Actuators designed using the guidelines from different research efforts will obviously result in different performance results. One of the aims of this research is to provide similar guidelines for the different motor and gear train combinations considered in this research. This literature on designing for inertial loads reinforced some of the conclusions from the EMA literature summarized above. Specifically, the frequency response (or responsiveness) of an actuator should be added to the list of the critical actuator performance parameters, and a suggested starting point is to use the torque to inertia ratio.

Table 2.7: Suggested Optimum Gear Ratios for Inertial Loads

Authors	Optimum Gear Ratio	Parameter Descriptions
West and Leonard	$g_{opt} = \sqrt{\frac{I_L}{I_M}}$	I_L = Load inertia I_M = Motor inertia
Chiang	$g_{opt} = \gamma \sqrt{\frac{I_L}{I_M}} \text{ (in general)}$ $g_{opt} = \sqrt{\frac{I_L}{I_M}} \text{ (for small } P_o)$ <p>where</p> $\gamma = \frac{1.3182}{\alpha}, \alpha = \sqrt{\frac{\beta}{\tau_m}}$ $\beta = \left(\frac{I_L \theta_L^2}{P_o} \right)^{1/3}, \tau_m = \frac{I_M R}{K^2}$	γ = Inertia ratio I_L = Load inertia I_M = Motor inertia α = dimensionless variable β = Equivalent load parameter τ_m = Motor time constant (no load) θ_L = Output load displacement P_o = Motor power at stall R = Motor coil resistance K = Motor torque constant
Tal and Kahne	$g_{opt}^2 = \frac{I_L}{I_M} (1 + \alpha)^{1/2}$ <p>where</p> $\alpha = \frac{T_L \tau^4}{12 I_L^2 \theta_L^2}$	I_L = Load inertia I_M = Motor inertia α = Equivalent load parameter T_L = Output load torque τ = Move time θ_L = Output load displacement

The current research will consider these quantitative results for their relevance to the current actuators. Much of the literature focused on balancing the motor and gear train parameters for systems with dominant inertial loads (i.e., acceleration (responsiveness)). However, little guidance for systems with dominant external torque loads was provided. *The major contribution of this research will be the development of quantitative guidelines for balancing motor and gear train designs for both types of loads (see Chapters 6 for external torque load and Chapter 7 for inertial loads). These guidelines will include strategies for choosing gear ratio, motor size, and motor speed for both one and two-stage gear trains.* To develop useful scaling rules and to start working

towards a minimum set of actuators, the design problem of integrating the motor and gear train within the actuator must be studied first so that the designer can control the parameters of each actuator in a set. In many application domains, the requirements will dictate that many common assumptions, parameters settings, performance parameters, etc. be common for every actuator design in a set (that meet the application's requirements).

Before concluding this section, the reader should note the use of two and three-dimensional plots (Figure 2.16-Figure 2.20) to help the designer visualize the motor-gear train integration problem and aid in the decision-making process of choosing the design parameters. A more detailed discussion of design space visualization tools is provided in Section 2.8 of this chapter.

2.5 SCALING

Mendez and Ordonez [2003] present an algorithm that obtains scaling laws (rules) in power form from a set of existing data (Figure 2.21). The algorithm combines linear regression analysis and dimensional analysis and seeks to uncover the simplest scaling rules that still provide a user-specified error level. These two analyses are commonly used in isolation to develop models based on experimental data. While dimensional analysis is well-suited to determining a dimensionally correct model, it does not suggest that the model obtained is the most accurate. The authors use linear regression techniques to achieve the needed accuracy by minimizing the least-squares error between the data points and the fitted model. Dimensional analysis is used to obtain a ranking of the most significant parameters in the problem. The user input to the algorithm consists of a set of experimental data and a matrix of units in the form commonly used for dimensional analysis. The “simplest” scaling rules are obtained by attempting to remove

independent parameters and round exponents without significantly increasing the least squares error. The authors note the importance of the balance between the simplicity and accuracy of the fitted models. The most accurate model contains all of the parameters and has the minimum least squares error, while the simplest model has the fewest parameters and the maximum least squares error. The user must select a model that balances these two conflicting objectives by specifying a tolerance level on the errors.

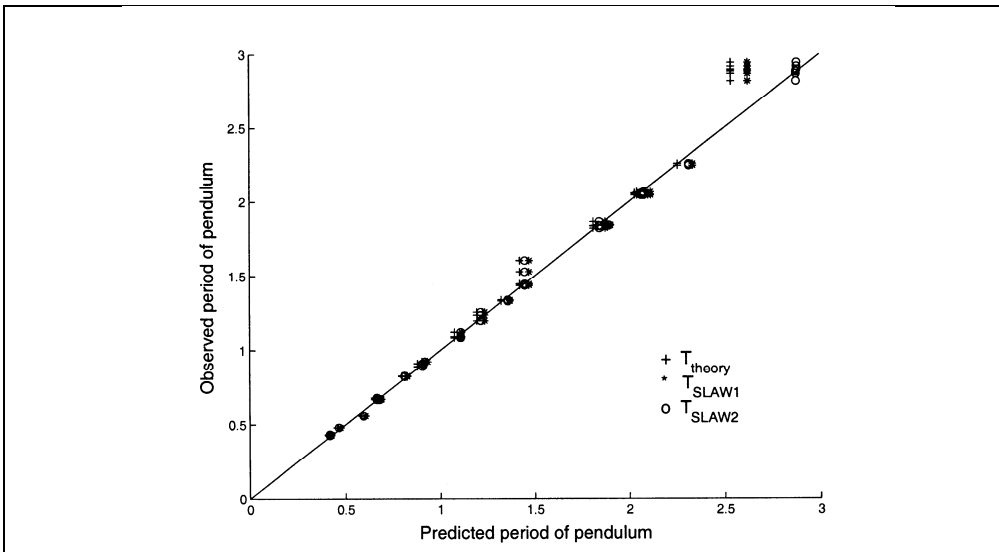


Figure 3: Different scaling laws for the period of a pendulum.

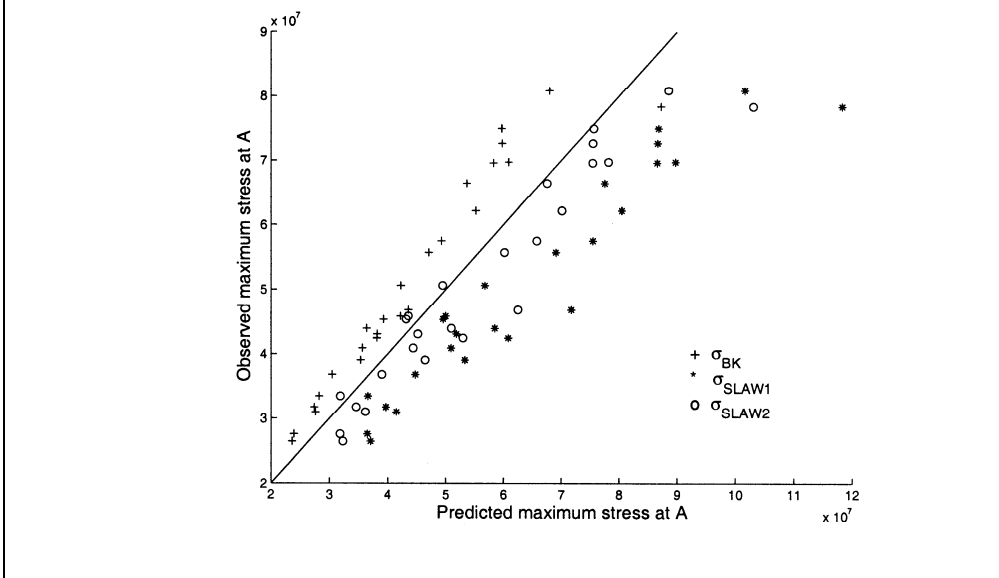


Figure 6: Different scaling laws for maximum stress at A.

Figure 2.21: Determination of Scaling Rules from Experimental Data, from Mendez and Ordonez [2003]

This work provided a guide for the development of scaling rules from existing design parameter data, a fundamental task in this research. The proposed algorithm is

well-suited for direct application to a carefully developed set of actuator parameter data and could be used to obtain actuator scaling rules. However, the authors only discuss the use of a simple power law form for the scaling rules and apply linear regression techniques. It is believed that the scaling rules obtained in this research would be better described by polynomials obtained with linear regression techniques. This polynomial form is a common form used for data obtained from computer experiments [Simpson et. al., 2001]. While the author's work may be somewhat limited to systems that can only be described by a power law, their overall approach and philosophy used to develop scaling rules provides important background for the current research.

Cheng and Cheng [1999] use the standard approach of dimensional analysis to develop scaling rules that describe the optimum size of an indenter for material hardness testing. From this work, the basic steps needed to obtain scaling rules using dimensional analysis are as follows: 1) choose a set of independent dimensions, 2) express each parameter (both dependent and independent) in terms of the independent dimensions, 3) apply dimensional analysis to determine the relevant dimensionless groups, and 4) run a set of experiments (FEA, numerical simulation, or physical experiments) to uncover the relationship between the sets of dimensionless groups. An additional step of fitting the calculated data with an appropriate function can also be performed. The authors use the units of modulus of elasticity and displacement as fundamental dimensions rather than using the more common units of mass, length, and time [Fox and McDonald, 1998]. In this work, the authors were more interested in the particular physical phenomenon being studied than scaling rule development, so the authors used simple linear and power function scaling rules to fit the results obtained from FEA.

Another effort develops scaling rules for a flexible kinetic sculpture used for entertainment purposes [Gooch and Raine, 2000]. The design of the sculpture was based

on the desired static and dynamic behavior using basic solid mechanics theory. As in most scaling efforts, the choice of which parameters to hold constant and which to vary when scaling up and down had to be made. In this case, the author chose to design for similar buckling stability for each of the different sculpture sizes. The authors discovered that a scaling limit was reached due to the applied material stresses reaching the yield stress for the given material, despite satisfying the buckling stability criterion.

The approach used by these authors to develop scaling relationships between different sizes of a system is very common in the literature and is illustrated here. Consider an example where the objective is to design two cantilever beams of different sizes that have the same deflection. The deflection (y) can be written as a function of the applied load (F), length (L), modulus of elasticity (E), and area moment of inertia (I).

$$y = \frac{FL^3}{3EI} \quad \text{Eqn. 3}$$

If the deflection is to be held constant between the two different sizes of beams (denoted by subscripts 1 and 2), the following series of equations holds.

$$\begin{aligned} y_1 &= y_2 \\ \frac{F_1 L_1^3}{3E_1 I_1} &= \frac{F_2 L_2^3}{3E_2 I_2} \\ \frac{F_1 L_1^3}{E_1 I_1} &= \frac{F_2 L_2^3}{E_2 I_2} \end{aligned} \quad \text{Eqn. 4}$$

Equal deflection can then be assured by making parameter choices that satisfy the last equation. If the parameter of interest is the applied load on beam 2 (F_2), the last equation gives the following.

$$F_2 = F_1 \left(\frac{L_1}{L_2} \right)^3 \left(\frac{E_2}{E_1} \right) \left(\frac{I_2}{I_1} \right)$$

Eqn. 5

OR

$$F_2 = F_1 (\Delta L)^3 (\Delta E) (\Delta I)$$

The final equation determines the applied load on beam 2 given the known changes in geometry (L and I) and material (E). The reader here should recognize that this approach works well for simple equations with only a single term but is more difficult when the dependent parameter is a complex, multi-term, nonlinear function of the design parameters, as in the actuator design model to be detailed in Chapter 3.

Pasini, Smith, and Burgess [2003] use different scaling factors for the height and width dimensions to optimize the bending stiffness of a cantilever beam structure. The authors use basic equations from the theory of solid mechanics, and their use of different scaling factors for different components and dimensions is also critical for electromechanical actuator design. These authors and others [Liang, Xie, and Steven, 1999] suggest formulating the (dimensional) parametric model being used in terms of normalized, dimensionless scaling factors (ϕ) that are ratios of a parameter in a scaled design (x_s) to the same parameter in another unscaled, baseline design (x_b).

$$\phi = \frac{x_s}{x_b}$$

Eqn. 6

Advantages of this approach include the following: 1) the parameters considered are dimensionless, so difficulties with different units can be avoided, and 2) the dimensionless parameters typically vary over smaller ranges relative to their original dimensional values.

Nakajima, Ogawa, and Fujimasa [1989] discuss the physical limits of scaling down stirling engines for actuators. Geometrical scale analysis and simulation were used

to determine how the performance parameters changed as design parameters were reduced. The authors note that the influence of various physical phenomena on performance change as the overall engine size is reduced, and a similar argument can be made for any actuator component design. If possible, this research will attempt to identify physical limits of scaling an actuator.

2.5.1 Scaling Literature Summary

For the present research, *scaling* will be defined as resizing a given actuator design to meet a different set of numerical performance requirements (torque, weight, etc.). Changing scale, therefore, can be thought of as changing the basic size or weight of the design while maintaining the same arrangement of components.

Given this definition, a number of important points from the literature can be discussed in the context of this research. Many of the above works discuss scaling limitations and attempt to determine which parameter or physical phenomenon limits the design as we scale up and down. In the context of this research, bending and contact stresses dictate the scaling limits for gear train design⁴. Another designer choice discussed by the authors is which design and performance parameters should be held constant as a system is being scaled. Stress limits for gear teeth and magnetic flux density for electric motors are natural choices for the actuators sizes (approximately 5-50 inches in diameter) being considered in this research. Related questions are which parameters should be included, can be omitted, and are most significant for the system being considered. RRG experience in actuator design suggested that the overall diameter, length, and gear ratio are some of the most critical parameters in the actuator (see Section 3.3). Lastly, many of the above researches deal with relatively simple equations when

⁴ Note that velocity also directly affects the contact stresses (durability) in the gear train, especially in terms of its bearings.

compared to the models that will be common in this research, and it is therefore difficult to apply their approaches directly.

Scaling rules, to be introduced in detail in Chapter 5, will be defined as analytical relationships among the design and performance parameters of a motor, gear train, or actuator. The analytical relationships developed by many of the authors (such as those in Mendez and Ordonez [2003]) can be considered scaling rules according to the current definition. Similar to the scaling rules found in the literature, this research will attempt to find scaling rules that can be used 1) to interpolate accurately between existing data points (which often requires more complex equations) and 2) as a learning tool for less experienced actuator designers (which requires simpler rules). The latter use of the rules was not emphasized much in the literature, and this research will tailor the rules to balance these two uses. Finally, it is important to note that no quantitative comparison is possible between the current and past research because the systems being considered are different, but the overall philosophies and approaches used by the various authors provided valuable background.

This research will develop simple scaling rules for torque, weight, inertia, torque to inertia ratio (responsiveness), and torque to weight ratio (torque density) and how they vary as a function of overall diameters, lengths, and aspect ratios for the motor, gear train, and overall actuator. These initial scaling rules will be similar in complexity to the example in this section and will not include many of the internal dimensions of the actuator components in order to keep the rules simple. *The major contributions of this research in the area of scaling are that it 1) introduces a step-by-step procedure to scale motors, gear trains, and actuators (Chapter 4) and 2) provides a method to generate scaling rules useful for understanding (learning) the design-performance parameter relationships and obtaining intermediate designs accurately (Chapter 5).*

2.6 PRODUCT FAMILY DESIGN

Designing sets of actuators with similar features and parameters can be classified as “product family” or “product platform” design according to the literature, and the next section of the literature review will be devoted to this area. Much of this section has been adapted from a previous research project completed by the author [Vaculik and Tesar, 2005]. Both the previous research project and the current research share the common objective of developing families (or sets) of actuators for target application domains, so the reader should benefit greatly from reviewing this section. The RRG is currently developing actuator product families for some of the following applications: battlefield, anti-terrorism, space, surgery, educational, precision, and human rehabilitation. This was the only area of the literature in which well-developed methods (model development, solution techniques, step-by-step procedures, choosing scaling factors, etc. as shown in Figure 2.22) were available for developing scaled sets of actuators and actuator components.

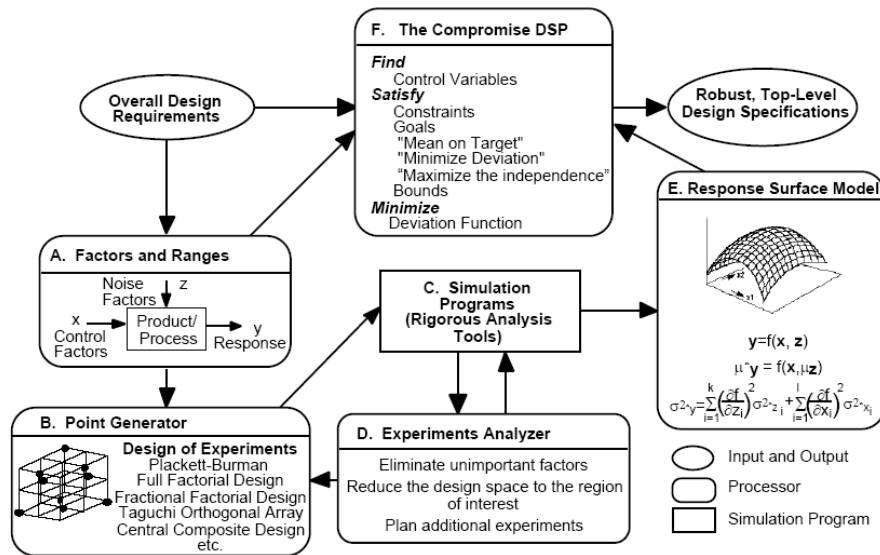
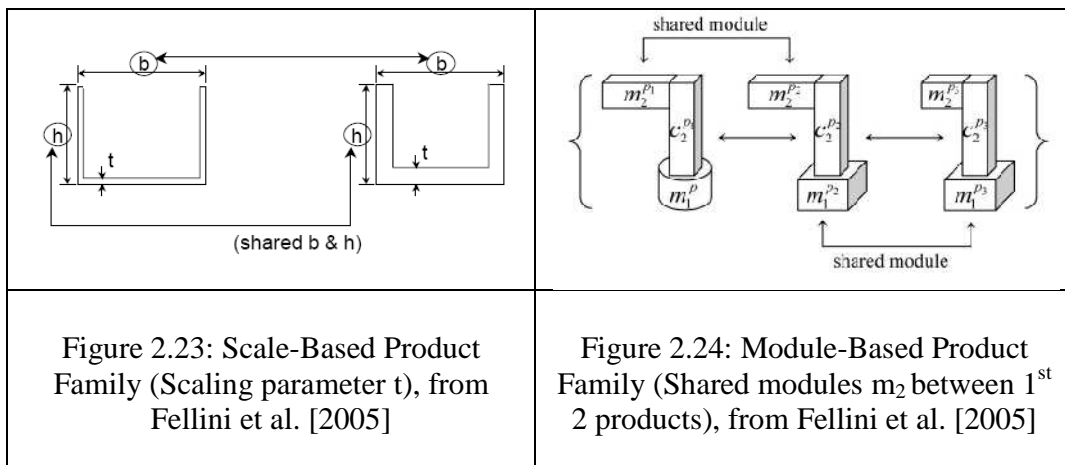


Figure 2.22: Robust Concept Exploration Method (Example Product Family Design Method), from Simpson et. al. [1996]

Research has shown that the development of product families allows companies to meet the requirements of a wide variety of market niches [Simpson, 2004]. A survey of the literature reveals that existing product family design methods could be used to develop an electromechanical actuator family and explore the anticipated performance trade-offs. Product family design involves the simultaneous development of a common product platform and a family of distinct products that share the platform [Simpson, 2004]. By definition, multiple products in the family share a set of common parameters (*e.g.*, dimensions, materials, interfaces, components), and these parameters comprise the “common” platform. The products in the family are differentiated by allowing “scaling” parameters (in a scale-based family, Figure 2.23) or the set of components (in a module-based family, Figure 2.24) to vary to meet a set of distinct requirements. A product family is said to have a high level of “commonality” if many parameters are shared among the products in the family. For example, a family of electric motors has been developed [Simpson, Maier, and Mistree, 2001], and only the stack length and current are allowed to vary to meet a range of output torque requirements, while the number of turns, wiring cross-sectional areas, and other geometric dimensions are identical for every product in the family and form the common platform. The major advantages of the product family design approach (compared to single product designs) are decreased manufacturing and inventory costs and reduced time to market for future generations of products [Simpson, 2004 and Simpson, Maier, and Mistree, 2001].



The success of a product family is highly dependent on the choice of the common platform, and the literature addresses this important issue. A key trade-off in product family design is *achieving commonality* among the products in a family (which can reduce cost) while *meeting the distinct performance* requirements of each individual product in the family [Seepersad, Mistree, and Allen, 2002; D'Souza and Simpson, 2003; and Messac, Martinez, and Simpson, 2002]. In many cases, optimizing each product in a family for performance will require the sacrifice of common components, dimensions, and orientations (i.e., commonality) among the entire family. This research will assume that there are cost benefits to reducing the family size, but no effort will be made to analytically model these costs because of the difficulty of this aspect of the design task in the preliminary stages of design. Nonetheless, a reduced family size (i.e., a minimum set) implies the ability to certify the performance and to minimize replacement spares or to reduce the cost of refreshment to prevent obsolescence.

Many different product family design methods have been developed, and these can be classified in a number of ways. First, product family design methods have been employed at different stages of the design process. Some methods are applicable in the early stages of design when defining the architecture of a product, while others are

applicable when the architecture is well defined and dimensioning the form or determining the best selection of components is of interest [Simpson, Seepersad, and Mistree, 2001; Fellini et. al., 2005; and Seepersad, Mistree, and Allen, 2002]. This research project focuses on the latter methods because the architecture of the actuator family sought is well defined in RRG Electro-mechanical Actuator Architecture (EMAA) [Tesar, 2000-2007]. Second, the overall approaches used in product family design can be classified as top-down and bottom-up [Simpson, 2004 and Simpson, Maier, and Mistree, 2001]. The top-down approach involves an up-front decision to design a product platform and its derivative products and does not utilize existing product designs extensively while the bottom-up approach involves redesigning and consolidating a set of existing products. Top-down approaches avoid the costly redesign of existing products, and, if done efficiently, can reduce the need to perform bottom-up design. The benefit of bottom-up approaches is that much design knowledge and experience from the product development process for an existing set of products is available, while its primary drawback is that investments in the development of the individual, unrelated products have already been made and cannot be recovered. This research project focuses on the top-down approach primarily because a limited number of existing actuator designs is available and to reduce prototype development costs. Third, restricting the focus to top-down approaches, methods can be classified based upon those that are suitable for developing module-based product families and those that can be used to develop scale-based product families.

This research focuses on scale-based product families because the set of components in each actuator in the family sought is limited in variability, and the ability to scale an existing actuator design is an important research question for the RRG at this time. Table 2.8 (adapted from Vaculik and Tesar [2005]) provides a listing of the scale-

based product family methods and information about the product families developed. The names of the methods have been abbreviated for brevity since they are not central to the current discussion (refer to the work noted above and the References section of this report for authors and more details). Proceeding across the top row, the table details the number of products in each family, number of design parameters for the product, number of problem stages, and the number of problems and parameters solved in each stage. The following discussion highlights some of the important distinctions among the various methods.

Table 2.8: Scale-Based Product Family Design Methods (*Same aircraft family, **Same electric motor family, “P” indicates preset common and scaling parameters)

Method	# Products per Family	# Design Parameters per Product	# Problem Stages	Stage 1 # Optimization Problems,# Parameters	Stage 2 # Optimization Problems,# Parameters
RCEM*	3	8	1	1,36	
GABM*	3	14	1P	1,28	
PVTEM*	4(3*)	15(6*)	1P	1,21(20*)	
PPCEM (CDSP)**	10	8	2P	1,13	10,6
PPCEM (PP)**	10	8	1P	1,26	-
PPCEM (PP,PFPE)**			2	1,40	10,2
VBPDMD**	10	8	2	1,46	10,4
PA**	10	8	2P	1,9	10,2
			2P	1,12	10,2
			1P	1,28	-
PPD	2	4	1P	1,7	
CDM	2(3)	24	2	1,48(72)	1,24<n<48(72)
SPVM	2	66	2		1,14
PRM	3	8	2	1,22	1,12

The two primary tasks in product family design are designing the platform and designing the individual products around the platform [Nayak, Chen, and Simpson, 2002; Messac, Martinez, and Simpson, 2002; and Gonzales-Zugasti et al., 2000]. In the context of this research, the actuator product platform has been pre-defined in the RRG electromechanical actuator architecture [Tesar, 2000-2007], and the individual products (actuators) in each family can be designed by using the actuator design procedure to be discussed in Chapter 4. Referring to the 4th column of Table 2.8, authors have approached the product family design problem in different ways: as a two-stage problem [Nayak, Chen, and Simpson, 2002 and D’Souza and Simpson, 2003] and as a single-stage problem [Messac, Martinez, and Simpson, 2002]. In the two-stage approach, the first stage involves developing the common product platform around which the individual

products in the family will be based. The second stage then instantiates the individual products in the family. In the single-stage approach, the product platform and the individual products are designed simultaneously in one solution run. A key issue in product family design (also evident in the scaling literature) is the decision of which parameters are common (termed common or platform parameters) and which are variable (scaling variables) among the products in a family [Nayak, Chen, and Simpson, 2002; Messac, Martinez, and Simpson, 2002; and Gonzales-Zugasti et al., 2000]. Earlier works by these authors simply select the common and scaling parameters based on experience and past literature (designated by a “P” in the 4th column of Table 2.8), while some of the above referenced works utilize optimization or other objective techniques to determine these parameters, which is obviously more desirable. The impact of choosing different sets of common parameters in an actuator family on performance was investigated in a past research effort [Vaculik and Tesar, 2005] and will be further investigated further in Chapter 8.

Much of the reviewed product family design literature that was used to design a specific product family implemented some form of optimization, such as goal programming, physical programming, or genetic algorithms. Because designing sets of scaled actuators can be considered product family design and the use of optimization and other problem-solving tools is well suited for product family design, the use of these tools to design actuators should be considered in future research.

2.6.1 Product Family Design Literature Summary

Many of the product family design methods identified (like the actuator design procedure detailed in Chapter 4) can be used to develop scaled sets (i.e., families) of actuators. A step in this direction was taken in a past research effort by using the existing

methods to develop multiple families of actuators [Vaculik and Tesar, 2005]. The literature revealed the following critical issues in product family design: the specification of the product platform, the design of the individual products in a family, the basic design trade-offs, and the designation of common and scaling parameters. The following important observations from this literature focus primarily on the features and steps of the most applicable methods instead of the (less important) numerical results that describe the product families obtained. All of the methods require the designer to provide design variable ranges, desired performance parameters, and a constrained product family optimization problem (i.e., an analytical model for design), so these aspects of the methods will not be discussed further. Some distinguishing factors among the methods are the choice of problem formulation (optimization vs. sets of polynomial equations), number of stages (essentially the number of optimization problems to solve), selection of common parameters and scaling parameters (preset by the designer or determined by the method), and the designer's weighting of preferences (when multiple, competing objectives are involved). All of these issues are addressed in the proposed actuator design procedure in Chapter 4.

The literature is lacking in two respects with regard to the current research. First, none of the current methods studied the development of scaling rules based on the product families obtained. Though many of the authors used regression and response surface methodology (RSM) techniques in their product family development, the only results presented were the values of the discrete design and performance parameter data. The data for developing graphical design rules/maps was available, but no researchers suggested their development. Second, only one method was found that addressed the problem of reducing the size of a family (i.e., obtaining a minimum set for a target application as listed in the goals in Section 1.5 of Chapter 1) [Fellini, Kokkolaras, and

Papalambros, 2003]. *In this regard, this research will make two important contributions: 1) development of scaling rules based on a scaled sets of motors, gear trains, and actuators (Chapters 5 and 6) and 2) the determination of a minimum set of actuators for a given application domain (Chapter 8).*

2.7 REGRESSION, METAMODELING, AND RESPONSE SURFACE METHODOLOGY

This section will begin with an overview of regression analysis. Many texts on regression are available, but the terminology and presentation below was taken mainly from Cook and Weisberg [1999]. Then, the concepts of metamodeling and response surface methodology (RSM), the most commonly used metamodeling technique, will be described. Then, the justification for using regression, metamodeling, and RSM techniques in this research will be provided.

The reader should note here that the present research is not making a contribution (or extension) in these areas but is simply using them as tools to represent the actuator design maps/rules (in the form of two and three dimensional surfaces) to be detailed in Chapters 5 and 6. Each of these tools can be considered to be in a mature state of development based on wealth of literature available in each area and the fact that they are used by researchers in many different fields, even those outside of engineering.

2.7.1 Regression

From a mathematical point of view, the design parameter (diameter, length, aspect ratio, gear ratio, etc.) and performance parameter (torque, weight, inertia, etc.) information available from a set of actuator designs is simply a set of data (Table 2.9). While plots of the data are useful for visualizing results, it is often useful to fit the data with a surface that can be represented mathematically. Then, the surface and the mathematical representation become useful tools for understanding how the design

parameters can be modified to achieve the desired performance parameter outcomes. Regression analysis is commonly used for curve and surface fitting of data, and it will be briefly discussed in this section.

Table 2.9: Representative Set of Actuator Design and Performance Parameter Data

Diameter (inches)	Aspect Ratio	Torque (ft-lbf)	Weight (lbf)	Inertia (lbm-in⁴)	Torque Density (ft-lbf/lbf)	Responsiveness (ft-lbf/lbm-in⁴)
5	0.75	2561	15	0.5	171	5336
10	0.75	20420	117	11.8	175	1737
15	0.75	68737	390	87.5	176	785
5	1.00	3415	20	0.6	170	5315
10	1.00	27227	156	15.7	175	1736
15	1.00	91650	520	116.7	176	785
5	1.25	4269	25	0.8	170	5282
10	1.25	34034	195	19.6	174	1735
15	1.25	114560	651	145.9	176	785

In regression terminology, the (dependent) performance parameters are commonly known as responses (usually denoted by the variable y), and the (independent) design parameters are commonly known as predictors (usually denoted by the variable x).

Using these definitions, regression is defined as studying the conditional distribution of y given x . For each value of x , y can be considered to have a distribution, as shown in Figure 2.25. Regression techniques are used to fit the data with a function (often called a model) that passes through the mean of each distribution, and the resulting curve (or surface) through the means can be used to predict values of y for specific values of x .

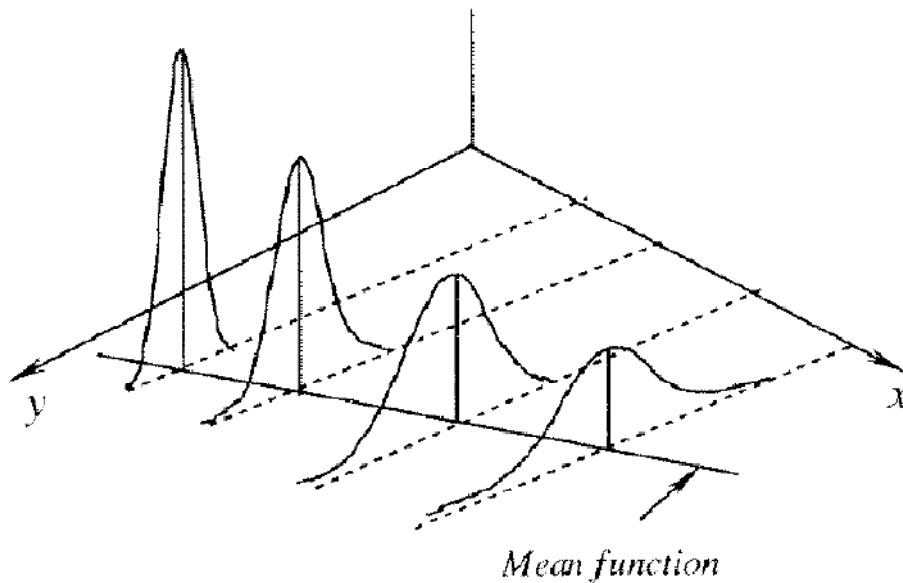


Figure 2.25: Conditional Distribution of y given x , from Cook and Weisberg [1999]

In the context of the actuator design problem, regression techniques will be used to study how the basic performance parameters of the actuator, the y parameters, vary as a function of the design parameters, the x parameters. The primary difference between the data sets commonly used in regression analysis and the current research is that the current data sets are deterministic and have zero variance.

Before defining the most common regression models used in practice, some nomenclature must be defined. Consider the general case where there are p predictors of interest, x_1, x_2, \dots, x_p , the response is denoted by y , and a set of data with n independent observations of the predictors and response are available from measurement or calculation. From the predictors, terms are created, and the terms are used to build regression models. When fitting data with the commonly used low-order polynomials, the terms can be as follows:

- the predictors themselves (x_1, x_2, \dots), which are commonly called main effects;

- transformations of the predictors ($x_1^2, x_2^2, \text{etc.}$); or
- products of predictors and transformations of predictors ($x_1x_2, x_1^2x_2, \text{etc.}$), which are commonly called interactions.

For example, a quadratic polynomial model with a single predictor x and response y can be written as follows.

$$\hat{y} = n_0 + n_1x + n_2x^2 \quad \text{Eqn. 7}$$

In this equation, \hat{y} denotes the fitted values (because y is reserved for the original data points), and the terms u are as follows.

$$u_0 = 1, u_1 = x, u_2 = x^2$$

A linear polynomial model with two predictors, x_1 and x_2 , can be written as follows.

$$\hat{y} = n_0 + n_1x_1 + n_2x_2 + n_3x_1x_2 \quad \text{Eqn. 8}$$

In this equation, the terms are as follows.

$$u_0 = 1, u_1 = x_1, u_2 = x_2, u_3 = x_1x_2$$

Finally, the two most common models to be used in this research will be the full quadratic and full cubic polynomial models with two predictors, given by the following.

$$\hat{y} = n_0 + n_1x_1 + n_2x_2 + n_3x_1^2 + n_4x_2^2 + n_5x_1x_2 \quad \text{Eqn. 9}$$

$$\hat{y} = n_0 + n_1x_1 + n_2x_2 + n_3x_1^2 + n_4x_2^2 + n_5x_1^3 + n_6x_2^3 + n_7x_1x_2 + n_8x_1^2x_2 + n_9x_1x_2^2 \quad \text{Eqn. 10}$$

Any of the above example linear regression models can be summarized compactly in matrix notation.

$$\hat{y} = \mathbf{n}^T \mathbf{u} \quad \text{Eqn. 11}$$

where

$$\hat{y} = (y_1 \ y_2 \ \dots \ y_n)^T$$

$$\mathbf{x} = (x_1 \ x_2 \ \dots \ x_p)^T$$

$$\mathbf{n} = (n_0 \ n_1 \ \dots \ n_{k-1})^T$$

$$\mathbf{u} = (u_0 \ u_1 \ \dots \ u_{k-1})^T$$

In this general model, there are p predictors (denoted by \mathbf{x}), k terms (denoted by \mathbf{u} with coefficients \mathbf{n}), and n independent observations (i.e., the data points, denoted by \mathbf{y}).

2.7.1.1 *Least Squares*

The least squares technique is commonly used to estimate the coefficients \mathbf{n} by minimizing the sum of the squared differences between the fitted values $\hat{\mathbf{y}}$ and the actual data values \mathbf{y} . The function to be minimized is called the residual sum of squares (RSS), and is given by the following.

$$RSS = \sum_{i=1}^n (\hat{y}_i - y_i)^2 \quad \text{Eqn. 12}$$

When \hat{y}_i is substituted into RSS, the values of the coefficients that minimize RSS are called the least squares estimates of the coefficients. Algorithms for computing least squares estimates of the coefficients in low-order polynomials are available in MatLab and many other computational software programs. These algorithms will be used directly in this research. In order for a unique solution of the least squares problem to exist, the number of terms should be less than or equal to the number of observations (data points), meaning $k \leq n$.

Because regression is being used mainly as a tool for visualization in this research, the above brief summary is sufficient to understand how to obtain the coefficients and generate the two and three dimensional design maps.

2.7.1.2 *Assessing Model Validity (Error Metrics)*

To assess how well the hypothesized regression model fits the data (i.e., the quality of the fit), a number of error metrics will be used. Many of these metrics are a function of the error (distance) between the fitted value and the data point, defined as follows.

$$e_i = \hat{y}_i - y_i \quad \text{Eqn. 13}$$

Some of these metrics are the average error (E_{avg}), maximum error (E_{max}), and root mean square error (RMSE). [Wang and Shan, 2007 and Jin, Chen, and Simpson, 2001].

$$E_{avg} = \frac{\sum_{i=1}^n e_i}{n} \quad \text{Eqn. 14}$$

$$E_{max} = \text{maximum}(e_1, e_2, \dots, e_n) \quad \text{Eqn. 15}$$

$$RMSE = \sqrt{\frac{\sum_{i=1}^n e_i^2}{n}} \quad \text{Eqn. 16}$$

Though the correlation coefficient (usually termed R^2) is often used in standard regression analyses, it has little relevance in the current research because the data sets are deterministic and therefore have zero variance. Future research that incorporates uncertainty into the design maps and the design process will allow the use of this common statistical metric.

2.7.1.3 Use of Regression Techniques in the Current Research

The focus of this research is on laying a foundation for the representation of actuator data with visual 3-D design maps, and it is important at this stage to simply find a model that fits the data reasonably well. For the purposes of this research, the models obtained should be useful for quickly estimating the performance parameters from a design map to within approximately 10% accuracy (that is, within 10% of the value anticipated from a detailed analysis). This level of accuracy is sufficient for the preliminary stages of design, which is the stage of the design process that is the focus of this research.

There will be less of a focus on finding the “best” model (minimizing the number of terms in the regression model, comparing alternative models via hypothesis tests, etc.). These model-building tasks can in general be performed using standard regression tools, but they will offer very little benefit to the user viewing the design maps in this research.

Furthermore, because the current data sets being fitted in this research have zero variance, there is no statistical basis for some of these techniques and thus they cannot be done here. For all of these reasons, simple visual assessments of how well the model fits the data and the standard error metrics defined above will be used to obtain curve and surface fits that are useful for quickly obtaining reasonably accurate predictions of actuator performance.

The following is a set of general guidelines that will be considered when developing regression models.

- The simplest model that describes the data is the best model because more terms require more computation (inversion of larger matrices when using least squares estimation) to obtain the coefficients.
- If theory or analytical models are available, that information should be used when selecting the terms in the model.
- Always plot the data and visually assess how well the regression model fits the data before looking at the relevant statistical metrics.
- Logarithms are useful transformations when there is a large range in the values of the data points. A common rule of thumb about transforming using logarithms is to use them when the ratio between the largest and smallest values of a variable have a ratio of greater than 10.
- Interpolation using regression models is generally acceptable and is one of the most common uses of regression techniques.
- Extrapolation, predicting beyond the ranges of the data used to fit the model, is generally not advisable unless there is strong evidence to support it.

2.7.1.4 Least Squares Assumptions and Inference

The are four standard assumptions used when computing the least squares coefficient estimates are:

- a linear mean function (linear in the coefficients as shown in Eqn. 11),
- constant conditional variance,
- normality of conditional distributions, and
- independence of observations (depends on data collection procedure).

The data that is being fitted via least squares must satisfy these assumptions in order to do inference based on the data. Common inference techniques involve computation of confidence intervals, prediction intervals, and hypothesis testing. As stated previously, the focus of the present research is mainly on obtaining a model that fits the data reasonably well and regression is being used mainly as a visualization tool. Thus, there is currently no need for doing inference, but future researchers should consider their inclusion.

2.7.2 Metamodeling

Metamodeling is the process of fitting a set of data with a model that can be represented by a mathematical expression. The prefix “meta” is attached to the word modeling because the data itself typically comes either from an analytical model or finite element model rather than a real physical system. Thus, a metamodel can be thought of as a model of a model and is also sometime called a surrogate model.

The metamodeling process has been described (Figure 2.26) as a three step process.

1. Choose an experimental design.
2. Choose a model to fit the data.
3. Fit the model to the observed data.

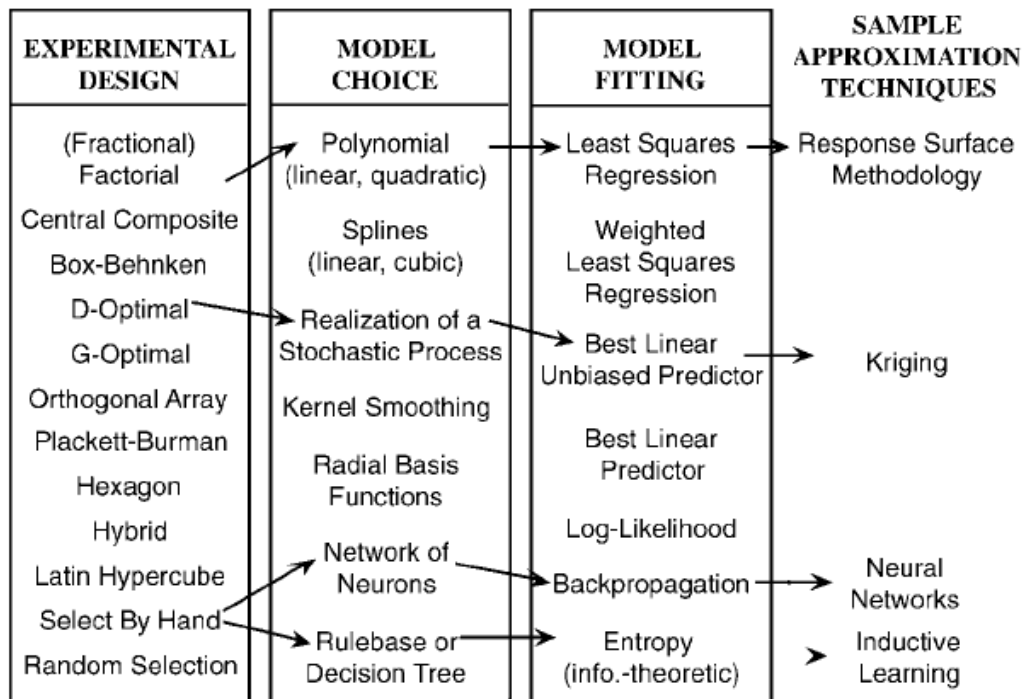


Figure 2.26: Metamodeling Techniques Overview, from Simpson et al. [2001]

2.7.2.1 Model Choices

The most common model choices for engineering design problems have been identified by numerous researchers.

- Response Surface Methodology (RSM) [Myers and Montgomery, 1995]
- Kriging [Martin and Simpson, 2005; Sacks et al., 1989; and Welch et al., 1992]
- Radial Basis Functions (RBF) [Mullur and Messac, 2005 and Hussain, Barton, and Joshi, 2002]
- Multivariate Adaptive Regression Splines (MARS) [Friedman, 1991]
- Support Vector Regression (SVR) [Clarke, Griebisch, and Simpson, 2005]
- Artificial Neural Networks (ANN) [Rumelhart, Widrow, and Lehr, 1994]

- Bayesian techniques [Currin et al., 1991; Pacheco, Amon, and Finger, 2003; Osio and Amon, 1996]

Simpson et al. [2001] provide one of the most recent and comprehensive survey papers on metamodeling in engineering design. According to different researchers [Barton, 1998 and Simpson et al., 2001] and also judging by the wealth of literature in the area, RSM is by far the most common metamodeling approach, and it is based on fitting data with the low-order polynomial regression models discussed in the previous Section 2.7.1. The other techniques listed are considered promising alternatives to RSM but are still very much in the research and development stage in relation to the engineering design process. RSM has the following advantages over the other techniques: transparency (ease of determining significant factors directly from coefficients), simplicity (ease of implementation, no arbitrary designer choices), computational efficiency, and suitability for fitting non-linear data sets [Jin, Chen, and Simpson, 2001].

2.7.3 Response Surface Methodology (RSM)

RSM techniques typically use 1st, 2nd, or 3rd order polynomials to fit data sets and were originally developed as a means to find the parameter values that result in optimum response in a chemical experiment [Box and Wilson, 1951]. There have been numerous RSM review papers published over the years, which have revealed that RSM is also useful for prediction (i.e., interpolation) and uncovering (i.e., learning) the underlying functional relationships of the phenomenon being studied [Hill and Hunter, 1966; Mead and Pike, 1975; Myers, Khuri, and Carter, 1989; Carley, Kamneva, and Reminga, 2004].

Common experimental designs (also known as sampling methods) that are used in RSM implementations include: full factorial, fractional factorial, central composite (CCD), Latin hypercube, and Box-Behnken. The full factorial design is sometimes called

a uniform design because it simply involves an evenly spaced grid of points. Figure 2.27 illustrates some of these representative experimental designs for problems with the three variables X1, X2, and X3. The bold points in the figures are the values at which data points are evaluated via a physical experiment, finite element analysis, and/or computer simulation. In this research, analytical models of the motors and gear trains embedded in a computer simulation environment will be used to generate the data. The “experimental” verbiage originates from the early uses of RSM techniques for physical experiments in chemistry and related fields, but the same basic principles apply to computer experiments or any function evaluation.

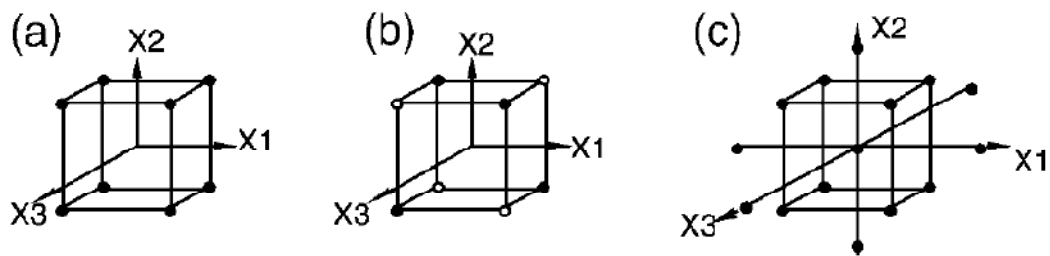


Figure 2.27: a) Full Factorial, b) Fractional Factorial, and c) Central Composite Experimental Designs for a Problem with 3 Factors and 2 Levels for Each Factor, from Simpson et al. [2001]

The design parameters/variables/predictors in the experimental design context are commonly termed factors, and the values of the design parameters are called levels. The number of data points (n) that need to be evaluated for a full factorial design with m levels and p factors is given by the following expression.

$$n = m^p \quad \text{Eqn. 17}$$

Thus, the full factorial design with 3 factors and 2 levels in Figure 2.27 requires 8 data points. From this expression, it is obvious that increasing the number of

parameters/factors in the problem exponentially increases the number of function evaluations required.

In many physical and computer experiments, computing the values of the responses is computationally expensive, and the overall objective when choosing an experimental design is to obtain the maximum amount of information with the minimum amount of computational effort (which usually translates into a small number of data points). For this reason, the fractional factorial, central composite, latin hypercube, and other experimental designs were formulated as alternatives to the full factorial design. Each of the former designs has fewer points than the full factorial design when considering the same number of factors. The current research will use full factorial designs for the generation of all the design maps because the present analytical models run very fast with the current computer processor speeds.

Figure 2.28 is a representative response (or decision) surface for torque (\hat{T}) as a function of the two factors (or design parameters) diameter (D) and aspect ratio (A). The experimental design was a full factorial with 4 levels and 2 factors, resulting in a total of $4^2=16$ data points. In this map, the design parameters have been mapped to a -1 to 1 scale. This type of transformation and/or normalization is commonly done in RSM implementations in order to eliminate the effect that different magnitudes of the parameters can have on the resulting regression equation and the surface fitted to the data. The raw data (with the original, unmapped values for the diameter and aspect ratio parameters) for the plot is given in Table 2.10.

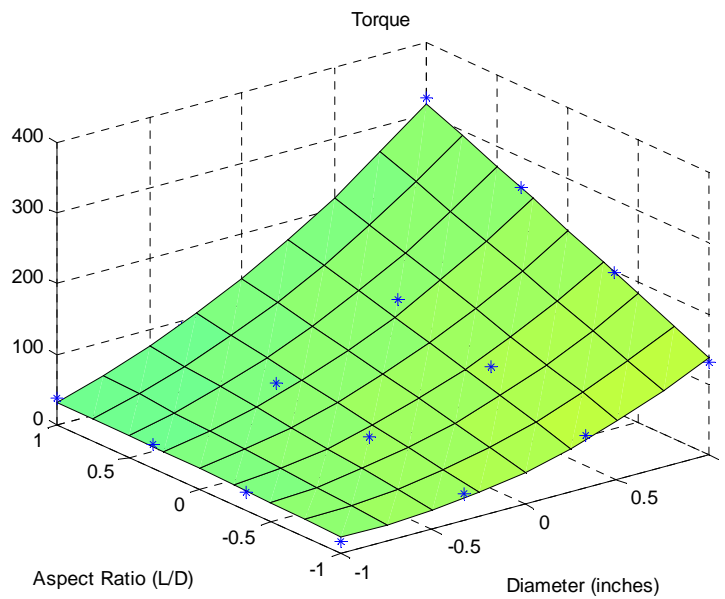


Figure 2.28: SRM Scaling Rule (Design Map) of Torque vs. Diameter and Aspect Ratio (with x and y axes mapped to a -1 to 1 scale)

The surface can be represented mathematically by the following 3rd order polynomial equation.

$$\hat{T} = 93.0226 + 92.7598D + 35.2879A + 35.3496D^2 + -1.1222A^2 + 42.0727D^3 + 5.6791A^3 + 1.4623Dx_2 + 16.6828D^2A + 1.012DA^2 \quad \text{Eqn. 18}$$

Table 2.10: Tabular Results of Torque (in-lbf) as a Function of Diameter and Aspect Ratio

Torque (in-lbf)		Aspect Ratio			
		0.3	0.4	0.5	0.6
Diameter (inches)	5	17	26	33	39
	6	39	58	74	90
	7	75	111	145	178
	8	131	196	257	323

2.7.4 Justification for Use of Regression, Metamodeling, and RSM Techniques

The use of regression, metamodeling, and response surface methodology techniques in the present research can be justified for a few reasons.

First, metamodeling is commonly used to reduce the computational effort associated with solving complex analyses based on analytical models, differential equations, and/or finite element models. It is often simpler to work with the metamodel (identify trends, make design parameter decisions, etc.) than the original, more complex model. The tasks that will benefit from metamodeling in this research include the following: searching gear tooth numbers to satisfy a desired gear ratio, searching wire sizes and numbers of turns for the SRM, and efficiently predicting gear train load capacity as a function of geometry. More details on these design tasks will be provided in Chapter 4, Section 4.3.

Second, it is useful for quickly scaling existing motor, gear train, and actuator design information to obtain a ballpark estimate of performance without doing detailed analyses. In the context of this research, scaling can be defined as being able to predict the performance parameters of actuators for values of the design parameters that have not yet been considered. This idea is illustrated graphically in Figure 2.29, in which the highlighted points are the results of detailed actuator design efforts, and the goal is to quickly and accurately predict torque capacity at intermediate values of the diameter.

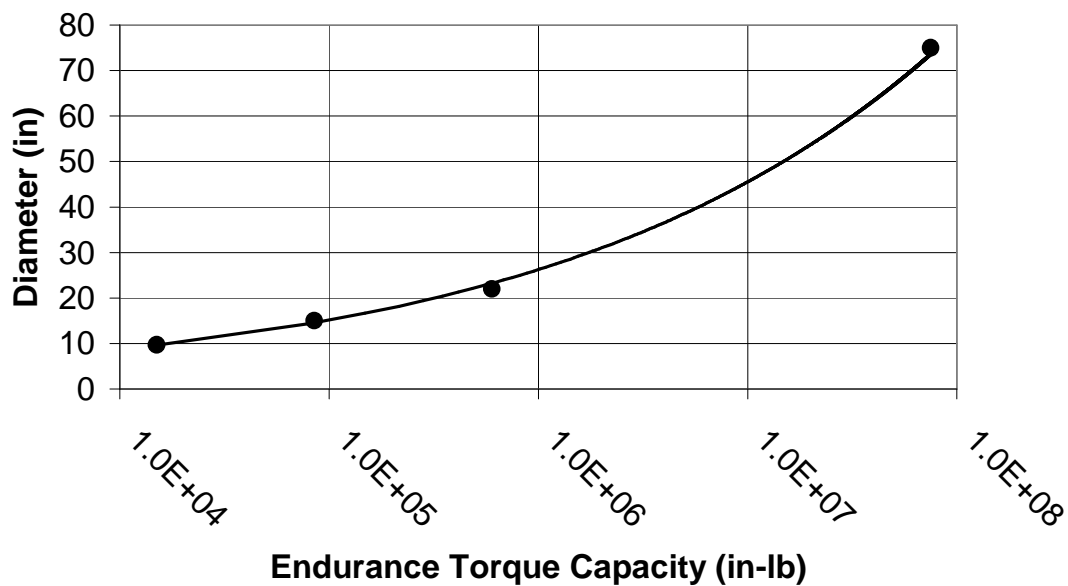


Figure 2.29: Prediction of Performance Parameters at Intermediate Values of Diameter Using Previous Design Information

The goal of the scaling efforts in this research will be efficient generation of approximate torque, weight, inertia, torque density, and responsiveness, information for sets of motor, gear train, and actuator designs (without the need to commence a detailed design effort or form a multi-person team). The basic scenario in which the scaling rules (to be illustrated in detail in Chapter 5) are useful can be described as follows. Suppose that a set of available actuator designs exist, a customer requests an intermediate size that has not been previously considered, and the actuator designer would like to be able to respond quickly and decide whether to pursue a detailed design. In order to respond to the customer, the RRG could put together a team and generate actuator design performance information, but this often requires valuable time and effort. The expertise currently exists but it is inefficient to continuously apply the same expertise to similar actuator design efforts. Alternatively, the proposed scaling rules/maps can be used to

quickly generate approximate performance for an actuator size so that the designer can make a judgment about whether or not to pursue a detailed design. This frees up the designer and other team members to work on the more challenging problems. The scaling rules of Chapter 5 will attempt to succinctly summarize the current expertise that is commonly used by RRG motor and gear train designers.

Third and finally, the use of metamodeling techniques provides a means for designer learning. Viewing the metamodels of the more complex actuator models, the designer can learn the underlying functional relationships, identify significant factors, and gain knowledge of the dominant design parameters for a particular component. The process of learning and then using the gained knowledge to make a decision in the design process has been termed visual design steering by some researchers [Winer and Bloebaum, 1999].

2.7.5 Regression, Metamodeling, and RSM Literature Summary

This section has provided a brief overview of regression, metamodeling, and RSM techniques. The treatment is sufficient for the reader to understand how to use standard regression and RSM techniques to fit the actuator design data with low-order polynomials (also known as response surfaces). A review of the literature has shown that the use of these techniques to represent the proposed design rules is justified by their use in similar applications in the literature. The three different representations of the results (3-D response surface (Figure 2.28), polynomial equation, and tabular summary (Table 2.10)) suggested above will each be useful to the designer, and it is expected that the 3-D response surface will be the most useful for a potential future visual actuator design software. Chapters 5 and 6 will use these three representations and the three error metrics defined in Section 2.7.1.2 to summarize a set of accurate design rules for the SRM, HGT,

PEGT, and integrated actuators. These preliminary rules should become invaluable tools for future motor, gear train, and actuators designers. In closing this section, the reader is referred to the following references [Jin, Chen, and Simpson, 2001; Mullur and Messac, 2005; Mullur and Messac, 2006, Simpson, Lin, and Chen, 2001; and Hussain, Barton, and Joshi, 2002]. In each of these papers, the authors provide excellent examples for comparing the different metamodeling approaches (listed in Section 2.7.2.1) for real data sets, and they also provide useful graphical and tabular summaries of results.

2.8 DESIGN SPACE VISUALIZATION (GRAPHICAL USER INTERFACE DEVELOPMENT)

This research initially proposed to use two and three-dimensional plots of design information (termed design rules and design maps throughout this report) to aid the designer in making parameter choices to achieve a desired performance. This emphasis lead to the study of literature discussing design space visualization and decision-making tools. This section will review some of the key references in this area. The reader here should note that this research is not making a specific contribution to this body of literature. It is simply using it as a model (and a collection of lessons learned) for the development of a future visual actuator design decision support system.

2.8.1 Robotics Research Group (RRG) Decision-Making Framework

Ashok and Tesar [2007] provide a visualization framework that allow a user to create a visual decision making interface for any multi-input multi-output (MIMO) system. The authors provide an extensive literature review of visualization techniques for MIMO systems and assert that there is no method available that shows one how to create a visual decision making interface for a MIMO starting from the modeling stage. The framework is discussed in the context of the operation of an electromechanical actuator, but the ideas can easily be extended to the current actuator design research. In

both operation and design, a human decision maker must make intelligent choices of the operational (or design) parameters in order to optimize (manage) the performance parameters of the system. The framework includes the following: Bayesian causal network modeling of the system of interest, representative decision scenarios, tools to obtain performance maps (Figure 2.30) and decision surfaces, and computation of norms (single number values) useful for making quick decisions. The authors illustrate that their framework can account for the anticipated non-linearities and uncertainties in MIMO systems and highlight them to the operator (or designer). The envisioned future decision making framework for actuator design will be very similar in content and detail when compared to the current framework for actuator operation. The primary exception is that the actuator analytical models used to generate the design maps are currently deterministic, while the Bayesian causal models used to generate actuator operational performance maps are inherently probabilistic. However, almost all of the tools to create decision surfaces and norms for actuator operation can be applied directly in the future actuator design decision making framework.

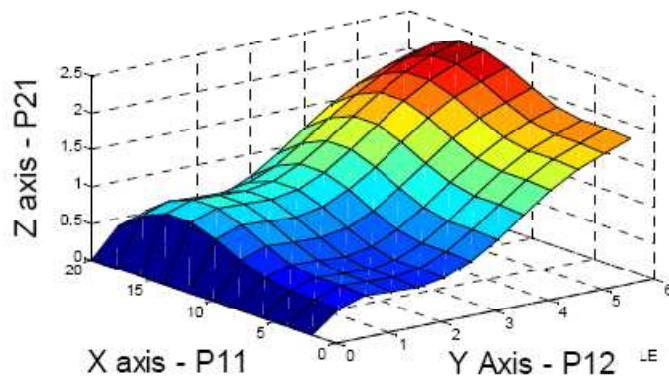


Figure 2.30: Representative Actuator Performance Map, from Ashok and Tesar [2007]

The ultimate goal of the current RRG decision-making framework is to allow intelligent operation of an actuator (or any system in general). Intelligence can be described as the ability to reconfigure available resources to adapt to varying task requirements. This intelligence should enable a smaller minimum set of actuators because it can effectively bridge larger gaps in performance capabilities between standard size actuators. Thus, instead of designing a new actuator size to meet a new (previously not considered) actuator requirement, intelligence may allow an existing actuator size to meet the requirement without any changes in the geometry (scaling) of the actuator.

2.8.2 Graphical Engineering Design Interfaces

Simpson, et al. [2007] describe 4 engineering design problems (I-beam, desk lamp, aircraft wing, and job shop manufacturing system) and corresponding graphical user interfaces for each (Figure 2.31). The objective of the paper was to share the design interfaces with the engineering design community and also to share their insights with other researchers who are developing tools to support design space visualization.

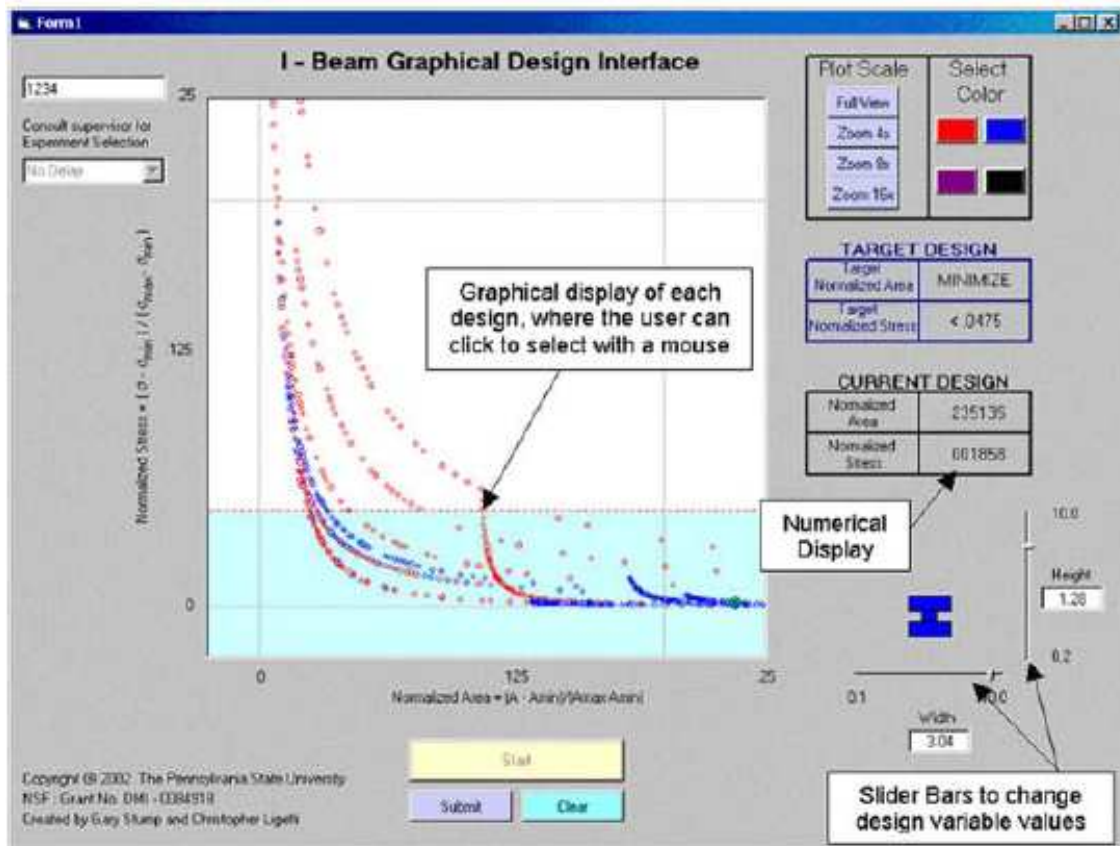


Figure 2.31: Graphical User Interface for Design, from Simpson et al., [2007]

Since a long-term goal of the present research is to lay the foundation for a future actuator design visualization tool, the following insights from this reference are very relevant. The authors' literature review highlighted the three requirements for an effective design interface: it must be 1) integrative, 2) visual, and 3) fast (provide real-time feedback to user inputs). These features are evident in the authors' design interfaces presented in the work. The authors assert that using metamodels for computations in graphical user interfaces is preferable to using the original, often computationally intensive analysis (FEA, physical testing etc.) if the "fast" requirement is to be achieved. In this context, metamodels are simple mathematical approximations of the generally

more complex models used for detailed design and analysis. In the current actuator design research, each design map can be mathematically represented by a low-order polynomial equation (for example), and these approximate equations meet the definition of a metamodel as it is used by these particular authors. A specific example from this research is the design map for gear train torque as a function of diameter and aspect ratio (recall Figure 1.5 in Chapter 1), which is generated from the AGMA standards for gear teeth stresses. The design map is a simpler, metamodel-based representation of the original AGMA stress equations. The natural issue that arises when using metamodels is trying to achieve fast computations with the approximate metamodels that are by definition less accurate than the original analysis models. The basic features of the authors' developed graphical design interfaces include: slider bars to control design parameter inputs, a dimensioned drawing of the system being designed, numerical and graphical displays of objective function and constraint values, and the ability to respond to user inputs in real-time (Figure 2.31). The designer has the ability to change the input design parameters at any time and view the resulting values of the performance parameters, giving the designer the ability to "steer" the solution process based on his/her own expertise. Though beyond the scope of the current research, the authors' use the design interfaces to conduct experiments that measure the effect of response delay (e.g., slow computations or less than immediate feedback to the user) and other features of the interfaces on design efficiency (task completion time) and effectiveness (percent error). When a future visual actuator design user interface is developed, interested readers are encouraged to consult the work of Simpson et al. [2007] for assessing its value and determining how to improve upon any shortcomings. In conclusion, the authors' write, "*we have just scratched the surface of a very large, complex, and challenging problem,*

namely, how to develop effective user interfaces to support engineering design and decision-making.”

2.8.3 Features of Visual Decision-Making Support Systems

The two important works summarized above give the reader a snapshot of the literature on the design space visualization and available decision-making tools. To limit the scope of this section, only literature that dealt with decision-making in general terms (i.e., not applied to a specific system or component) was reviewed for this research. This was done because the current research focus was on understanding the key parts of a decision-making support system, and how application-specific actuator knowledge could be incorporated into a visual environment. Some of the literature focused on the combination of visualization in an optimization setting [Winer and Bloebaum, 1999; Simionescu and Beale, 2004; Messac and Chen, 2000; Eddy and Lewis, 2002], and others focused on visualization environment without a specific problem representation in mind [Hanne and Trinkaus, 2005; Dillon, Talbot, and Hillis, 2005; Andrienko and Andrienko, 2001]. Because formal optimization techniques will not be used in this research, this distinction is not critical here but may be so for future RRG actuator design researchers.

Referring primarily to the work of Dillon, Talbot, and Hillis [2005] and also to the referenced works in the above paragraph, a listing of the key features of a successful decision support system was compiled and can be summarized as follows.

- Do not overload the user with irrelevant information. Creating an easy-to-use interface is more important than including every conceivable feature.
- All of the information shown in different displays, windows, or tabs should be linked such that choices made in one display are reflected in other displays.

- High-level information (e.g., overall performance metrics) should be available, particularly when non-experts will be viewing the information.
- Low-level information (with more internal details) should be available for experts.
- The user should have the ability to drill down to the lower levels of the problem and be able to view/modify internal parameters and any assumptions when necessary.
- Multiple input and output layers are suggested to help the user prioritize the decision making process.
- The interface should be interactive, allowing user input of independent parameters.
- Display of static information should be included because the user can become confused when there is a large amount of changing information on a display.
- Display of dynamic information is always necessary because conveying this information is often the primary purpose of the interface.
- The interface must be able to display information from multiple, competing objectives.
- The interface must be able to handle uncertain or imprecise information.
- When necessary, color, size, shape, or similar highlighting effects should be used to bring information to the user's attention.

Many of these features are embodied in the visual decision-making interfaces developed by the researchers. Messac and Chen [2000] add the following important qualities for a visualization environment for an optimization process.

- A quick glance at the display should clearly convey to the designer the state of a given design.
- The display environment should provide a history of the iterative process used to arrive at the current state.
- The display should involve some scaling and/or transformation of parameters to eliminate the difficulty of dealing with disparate units and large parameter ranges.

2.8.3.1 *Visualizing Multiple Objectives*

The literature discusses a few options to aid in the simultaneous visualization of multiple, competing objectives. First, Figure 2.32 provides an illustration of the use of a radar graph to simultaneously display multiple objectives. Each of the axes on the plot represents the value of one objective, the point represents the current value, and the arrow represents the desired direction of increase for that objective.

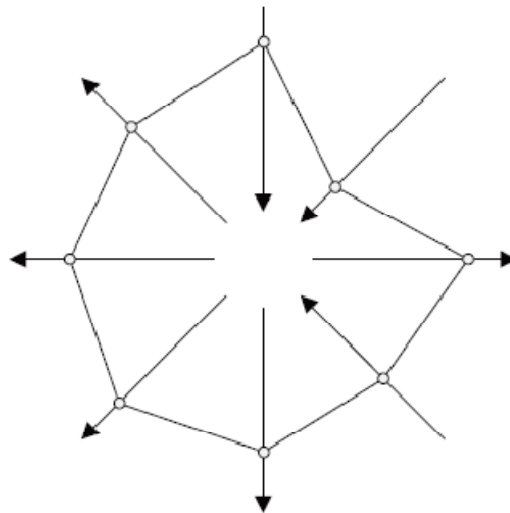


Figure 2.32: Radar Chart Used to Simultaneously Display Multiple Objectives, from Hanne and Trinkaas [2003]

Second, Figure 2.33 provides a parallel coordinates plot that simultaneously displays the values of multiple objectives (4 in this case: thickness, profit, mass, and height). The distance from the bottom of the plot to the intersection on the vertical line for each objective represents its value. Each line that connects the values on the 4 vertical axes represents a specific iteration of the process. One of the distinct differences between a parallel coordinates plot and radar plot is that the former can display the time history of the values of the parameters by showing multiple lines on the same plot. However, these plots can become difficult to interpret as the number of lines increases.

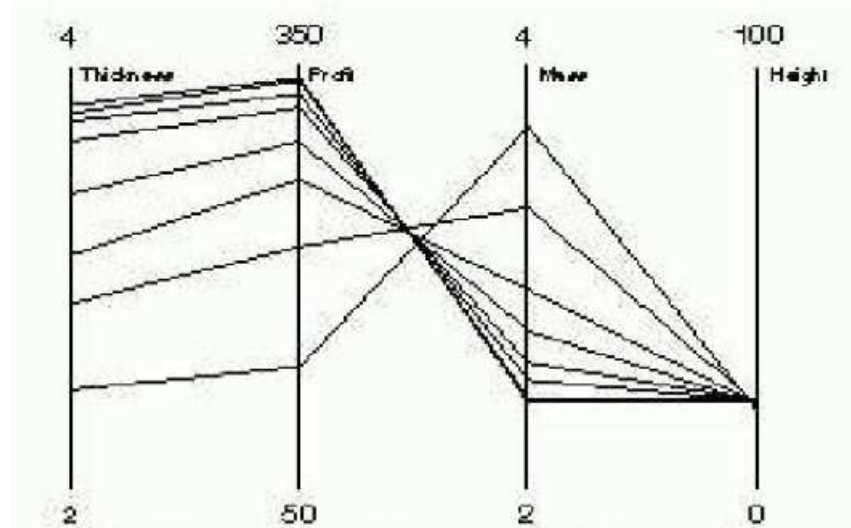


Figure 2.33: Parallel Coordinates Plot Used to Simultaneously Display Multiple Objectives, from Messac and Chen [2000]

If applicable, these two visual representations could be used for the generation of future actuator design maps.

2.8.3.2 *Uncertainty in the Design Process*

Kanukolanu, Lewis, and Winer [2006] propose a visualization method useful for solving multi-objective design problems in which there are coupled systems with

uncertain parameter information (in the design variables, constraints, and objectives) existing between the systems. This work is of interest because one of the important items of future work for this research is the incorporation of uncertainty in the design maps (of Chapters 5 and 6) and the actuator design process (of Chapter 4). Note that uncertainty is inherent in the performance maps and decision-making framework for operation summarized by Ashok and Tesar [2007] because their data is based on uncertain sensor data or nominally accurate physical models.

In the context of this research, one way design parameter uncertainty can exist is when a motor designer develops a motor with limited and uncertain parameter information about the gear train, even though the motor and gear train share common dimensions and are physically coupled in the actuator. The sharing of inputs and outputs between subsystem models (e.g., the motor and gear train in an actuator) is what makes their solution practically difficult and contributes uncertainty. Uncertainty can also exist due to the fact that a maximum of 3 design parameters can be displayed in the design maps at a given instant (Figure 2.28), but there are certainly more parameters that affect the shape of the map. Not including these other parameters and/or making assumptions about them also adds uncertainty.

2.8.4 Design Space Visualization Literature Summary

This research will focus on developing the actuator knowledge base (referred to as “design rules” and “design maps”) necessary to serve as an integral part of a future visual actuator design decision support system. Analytical models for the actuator components (Chapter 3) will be used to obtain the preliminary actuator design information needed to generate the rules. Specifically, this research will present a combination of two-dimensional plots, three-dimensional surfaces (such as those in Figure 2.34), solid

models, and related graphics that designers can use to design motors, gear trains, and integrated actuators. Future work for the current research should incorporate these tools into an intuitive, visual user interface for actuator design. The literature summarized in this section has been useful for identifying the important features of visualization-based design environment, and any future design tools should embody these features.

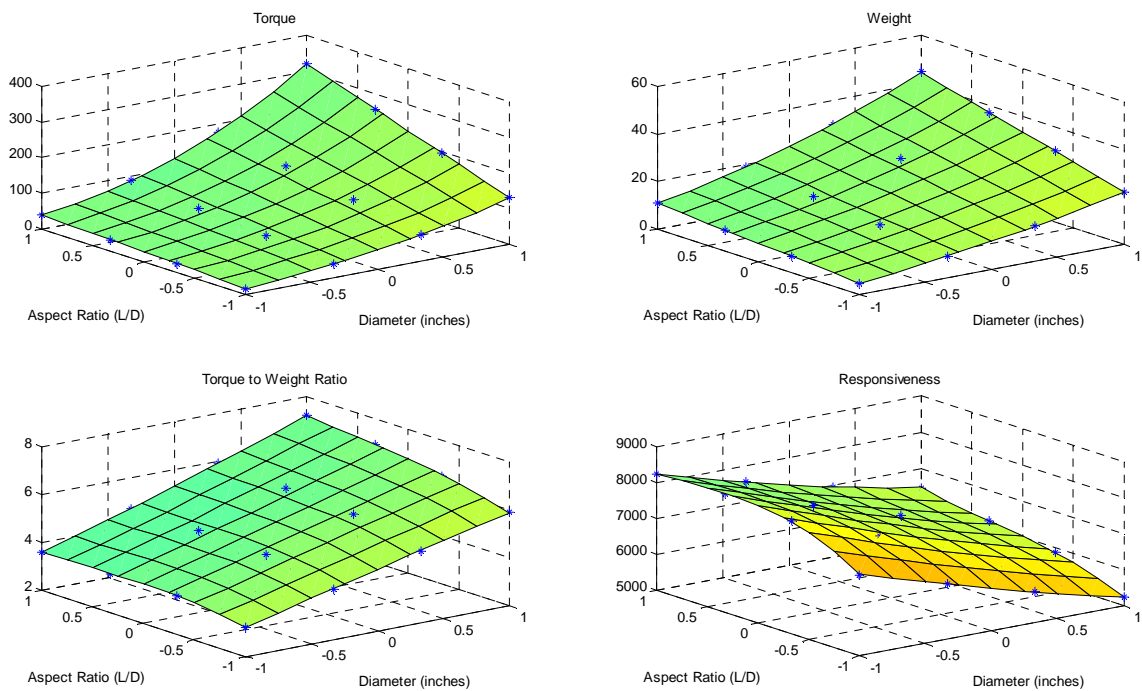


Figure 2.34: Representative 3-D Design Maps to be Used in a Future Visual Actuator Design Environment (with x and y axes mapped to a -1 to 1 scale)

2.9 PATENTS

This section will present a brief review of the patent literature in the following areas: electromechanical actuators, gear trains, and product family (line) design. In particular, a discussion of the key hypocyclic gear train (HGT) and parallel eccentric gear train (PEGT) patents will be provided. While these gear trains have novel features, the focus of this research is on the development of the design rules for these gear trains rather

than improving upon their existing features, and it is hoped that the development process can be applied to other gear trains and machine components.

2.9.1 Electromechanical Actuator Patents

A search for electromechanical actuator patents revealed the following results.

Figure 2.35 is from a patent describing an actuator that includes a brushless DC motor (2), multistage planetary gear train (contained in housing 19), controller (26), and Hall effect sensors (3,7). The emphasis of the invention is on the use of the two “contactless” Hall effect sensors and the developed signal process algorithms to provide both motor commutation signals and output shaft position signals. This patent is representative of many of the other electromechanical actuator patents reviewed in the following ways.

1. The emphasis is on the advances in electronics and control rather than the gear train.
2. The motor and gear train are not integrated into a single housing, as is possible for the hypocyclic gear train.
3. Detailed discussion of the use of a gear train and the associated benefits such as increased torque density is not generally provided.

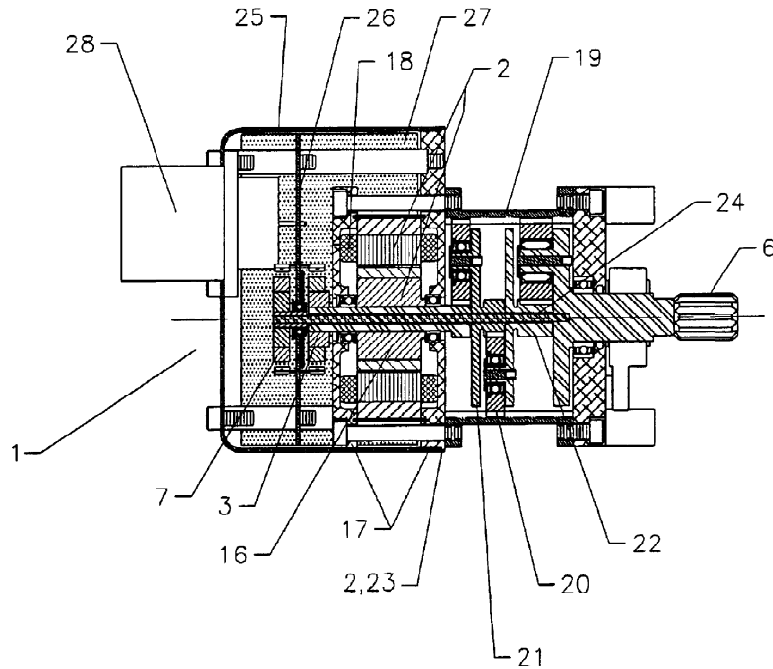


Figure 2.35: Electromechanical Actuator from Patent 6,791,219, from Eric and Gary [2004]

Figure 2.36 is from a patent describing a linear actuator that includes an SRM (16,17) directly driving a ballscrew transmission (19-22). A noteworthy feature of the design is the use of the band clamp 12 to connect the motor housing 11 to the transmission housing 11'.

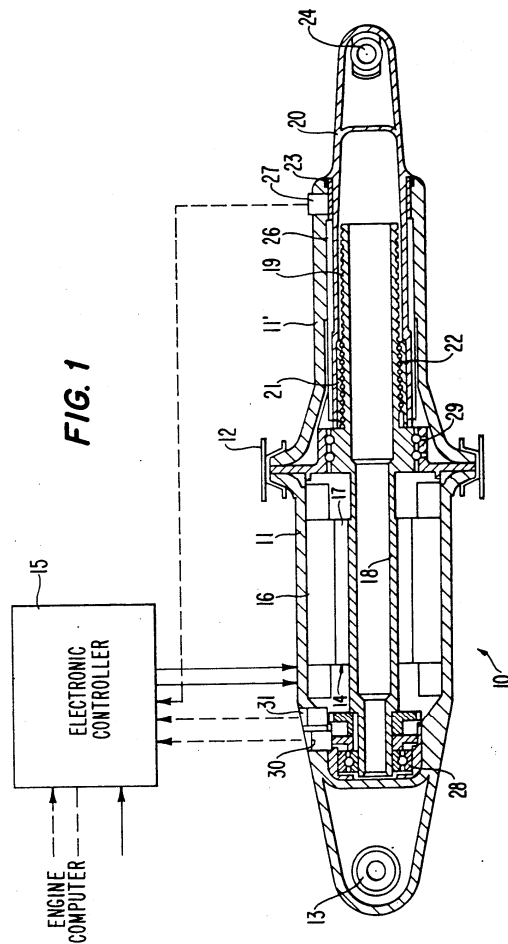


Figure 2.36: Electromechanical Actuator from Patent 5,041,748, from Huber [1991]

Figure 2.37 is from an actuator for an aircraft braking application that includes a motor (50), simple serial gear train (59,60,61), and ballscrew transmission (62,63) for linear output. The author's emphasis is on the ability of the actuator to be quickly and easily replaced for maintenance purposes.

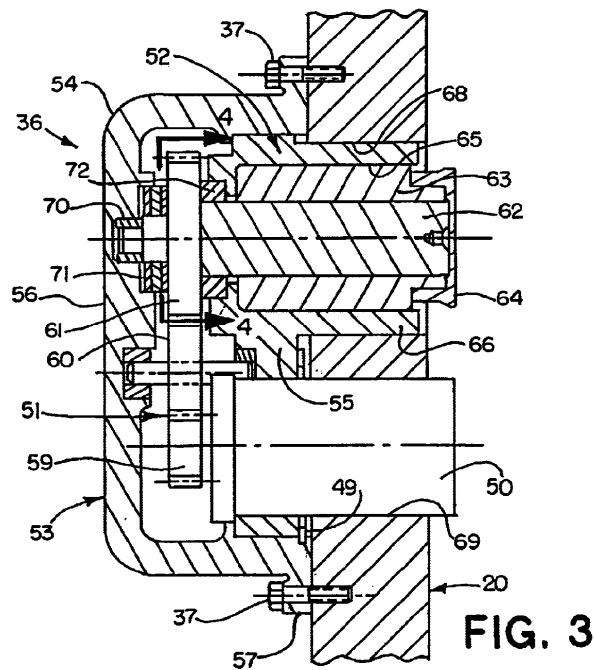


Figure 2.37: Electromechanical Actuator from Patent 6,095,293, from Brundrett et al. [2000]

Figure 2.38 is an actuator composed of a motor (200a) driving a compound gear train (gears 202a, 206a, 208a, 312, and 210a) and its suggested use is for the adjustment of brake, accelerator, and clutch pedals in an automobile. There are three outputs from the gear train, as suggested by the three output ports 109a, 111a, and 113a. The authors discuss various configurations including different options for the gear types and sensors.

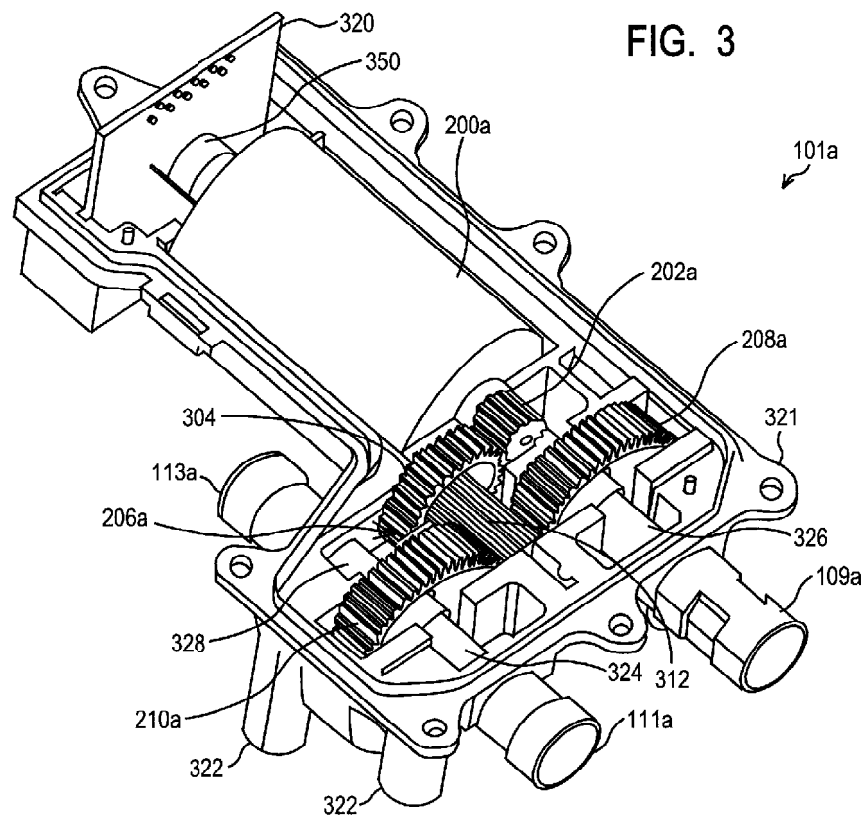


Figure 2.38: Electromechanical Actuator from Patent 6,736,233, from Beishline et al. [2004]

This snapshot of electromechanical actuator patents are representative of the majority reviewed in the following ways.

1. The emphasis is either on the motor/electronics/control aspects or the gear train (or transmission in general) but not both.
2. The motor and gear train are not integrated into a single housing, as is possible for the HGT.

3. Detailed discussion of the use of a gear train and the associated benefits (such as the designer's choice of gear ratio to achieve increased torque density and responsiveness) is generally not provided.
4. There is little or no discussion of integration/balancing of the motor and gear train and how to choose the fundamental coupling parameter (the gear ratio) for optimum performance.
5. Linear actuators are more prevalent in the patent literature (and in the industrial literature) than rotary actuators.
6. "Electromechanical actuators" is often used to refer to a device with only an electric motor and no transmission, with the verbiage based only on the motor's conversion of electrical energy to mechanical energy.

Each of the actuators described in these patents could be replaced by the actuator designs that are the object of this research (composed of SRM with an HGT or PEGT). If performance requirements were available for the actuators described in these patents, quantitative comparisons could be made between them and the actuators of this research.

2.9.2 Gear Trains

While there are thousands of issued patents on specific gear train designs of varying complexities, this section will highlight two patents that described gear trains very similar to the HGT and PEGT, respectively. Understanding of the gear trains described in these patents will greatly improve the reader's understanding of the HGT and PEGT design rules presented in Chapters 5 and 6.

Figure 2.39 provides an image from a patent that describes the benefits and features of the HGT. The authors' note that the relatively low efficiency of worm gears and high part count for epicyclic gear trains were the primary motivations for their

design. The stated benefits of their design include high efficiency (due to low number of gear meshes), low cost production (due to low part count), relatively high gear ratios (due to small tooth number differences), and high torque density (because of the compact arrangement). The reader here is referred to Chapter 2 of Park and Tesar [2005] for a comprehensive review of patent literature relating to the HGT and the use of circular arc gear teeth.

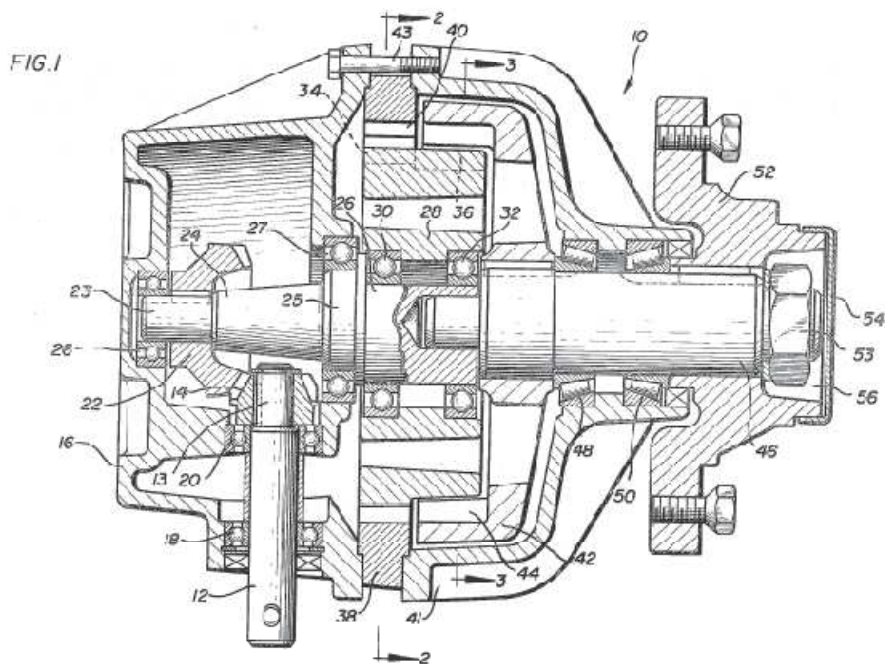


Figure 2.39: Gear Train from Patent 4,386,540, from Skaggs [1983]

Figure 2.40 describes a patent that is identical in functionality to the PEGT described in detail in Sigwald and Tesar [2008], with two key differences. First, the Sigwald and Tesar design consists of a parallel eccentric gear with external teeth and an output gear with internal teeth (see Section 3.10). The design described in this patent consists of a parallel eccentric gear with internal teeth and an output gear with external

teeth. Second, gear train components have been placed inside the motor (3,4), presumably to provide a more compact arrangement. Locating the gear train inside the motor (or vice versa) requires careful control of the design parameters to ensure that the motor-limited torque capacity be balanced with the gear train-limited torque capacity. This concept of balancing parameters between the motor, gear train, and bearings will be discussed in detail in Chapter 7. The reader here is referred to Chapter 2 of Sigwald and Tesar [2007] for a more detailed review of patent literature relating to the PEGT.

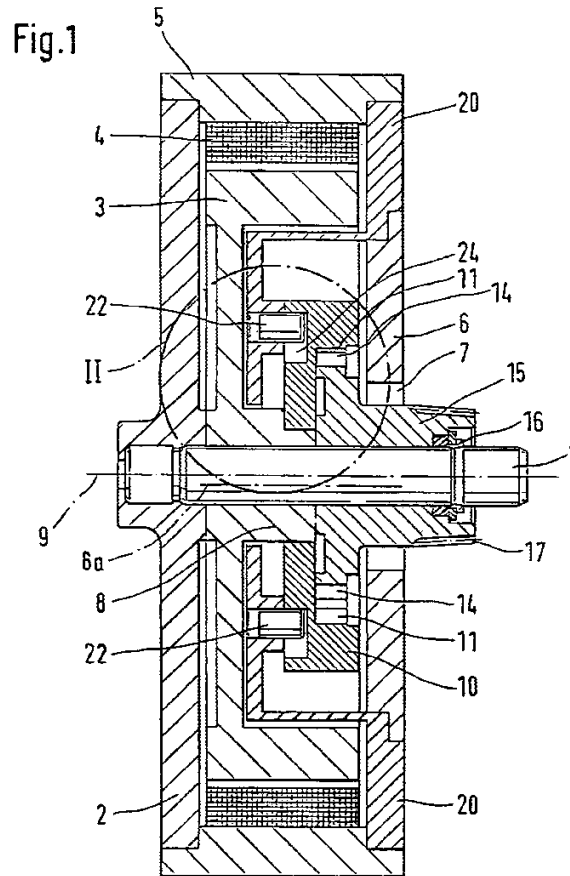


Figure 2.40: Gear Train from Patent 6,661,139, from Moskob [2003]

2.9.3 Product Family (Line) Design

One of the goals of this research is to develop scaling rules for actuator design, with the intention of quickly obtaining product families for target applications. Only a single patent was found on the topic of product families and product lines. Patent# 7,149,662 describes an automated system for comparing a set of user specifications with the performance capabilities of a catalog of optical components. The system attempts to match the user input with the available components and either outputs one of these to the user or outputs designs that bracket the user's desired specifications. The analogous task in this research (to be illustrated in Chapter 5) is to use the design information from existing motor, gear train, and actuator design to quickly estimate the performance an intermediate design. This patent suggests the use of tabular spreadsheets and a look-up table style user interface, but the current research will propose the use of two and three-dimensional design maps in addition to tabular information.

While academic literature relating to the other topics of design space visualization, design rules, visual decision-making tools, etc. was readily available, no patent literature was found on these topics, as expected.

2.9.4 Patent Literature Summary

The important conclusions from the patent literature relevant to the motor, gear train, and actuator designs in the research are similar to the conclusions from the academic and industrial literature search summarized in Section 2.2.4. First, in almost all of the actuator designs found, the motor and gear train are in separate, independent housings. Second, there is little or no discussion on the benefits and trade-offs that are encountered when using a gear train, such as choosing the gear ratio to maximize performance and achieving the optimum motor/gear train combination. The present research addresses these two points by making the following contributions 1) providing

design rules for the SRM+HGT actuator combination (in which both are contained in a single housing) that will allow for efficient generation of sets of actuators (Chapter 5) and 2) providing tools to balance the motor and gear train designs (Chapter 6), and 3) making comparisons between direct drive and geared systems to illustrate the relative benefits of the latter (Chapter 7).

2.10 SUMMARY

The reader here is referred to the two summary tables presented at the beginning of this chapter (Table 2.1 and Table 2.2). These tables serve as a road map for navigating among the various topics discussed. Table 2.1 provided a listing of the most important literature for this research and was classified by topic. Table 2.2 provided a summary of the findings and this research's specific contributions for each of the primary topics: electromechanical actuator design, balancing motor and gear train, scaling, product family design, and design space visualization.

Chapter 3 Parametric Models

This chapter will develop the parametric models for the SRM and the three gear train types (hypocyclic gear train (HGT), star gear train coupled with a parallel eccentric gear train (Star+PEGT), and star compound gear train coupled with a parallel eccentric gear train (Star Compound+PEGT)) being considered in this research. In general, the parametric models will be built upon the models of past RRG researchers and will be augmented where necessary. An important distinction between the preliminary and detailed stages of the actuator design process will be made and will emphasize the focus of this research. A discussion of the most fundamental design parameter choices and performance parameters for these motor and gear train types will also be presented. Because the gear ratio is arguably the most fundamental design parameter choice for a gear train, the standard gear ratio ranges suggested for each gear train type will be discussed. The physical phenomena that limit the speed and life of motors, gear trains, and bearings will also be briefly discussed. These sections should provide guidance to future actuator designers when choosing gear ratios and operating speeds.

The parametric models for the SRM [Ashok and Tesar, 2002] and HGT [Park and Tesar, 2005] have been documented in detail by past researchers. For this reason, the models for these components will be summarized succinctly in a series of graphics and tables. For a more detailed description of many of the modeling equations, the reader is referred to the noted references. The PEGT model will also be summarized in graphical and tabular form. However, since the PEGT is currently at a less mature state of development than the HGT, additional treatment of this gear train is provided in Chapter 5 (Section 5.2.3). The reader is referred to the work of Sigwald and Tesar [2008] for a geometric analysis of the PEGT and a recent report documenting the design of a

prototype based on the PEGT [Tesar et al., 2008]. Finally, though the star (SGT) and star compound gear trains (SCGT) can be used as stand-alone gear trains in some applications, this research will only implement star and star compound gear trains as the 1st stage of the PEGT. Ongoing research at the RRG will develop tools to generate rules for scaling and balancing for the star compound gear train similar to those presented in Chapters 5 and 6 of the present report. The modeling equations provided in this chapter are suitable for direct implementation in a computer software environment and will also serve as a quick reference for motor and gear train designers.

3.1 DEFINITIONS

In parametric design, the three basic types of parameters are design, performance, and intermediate [Donoso and Tesar, 1998]. Design parameters are parameters that the designer can choose independently of others to satisfy the requirements (performance parameters) of a design. Examples of design parameters include the lengths and diameters of the motor, geartrain, and bearings. They can either be geometric or operational parameters and are the inputs to a design analysis process and the output of a design synthesis process. For this research, the design parameters will be limited to the geometry of the actuator.

Performance parameters are parameters that can be written as functions of design parameters and are usually the primary requirements for a design. Examples of performance parameters include the torque, weight, and inertia of the geartrain and motor and the operating life of the bearings. Performance parameters are the output of a design analysis process and the input to a design synthesis process.

Intermediate parameters are a function of the design parameters but are not generally classified as performance parameters. Intermediate parameters are not

independent choices of the designer but are driven by the choice of the governing design parameters. Examples of intermediate parameters include shaft lengths and diameters, motor bore and back iron diameters, gear rim thicknesses, and other dimensions constrained by the design parameters.

3.2 PRELIMINARY AND DETAILED DESIGN STAGES

Before developing the parametric models, a distinction should be made between the preliminary and detailed stages of the actuator design process. Figure 3.1 provides an example of a detailed actuator design that couples an SRM with an HGT, and Figure 3.2 is a similar example for an SRM/PEGT combination.

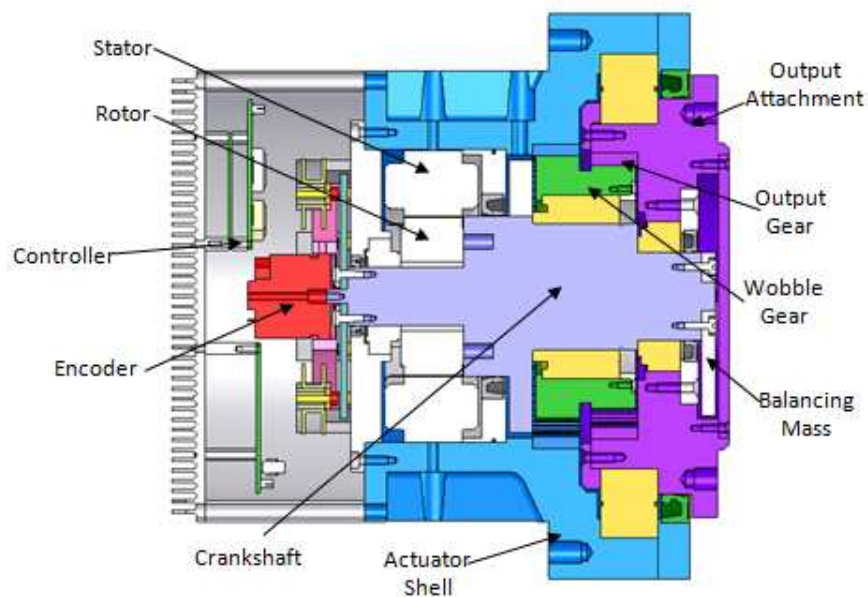


Figure 3.1: Detailed Actuator Design Including an SRM and HGT

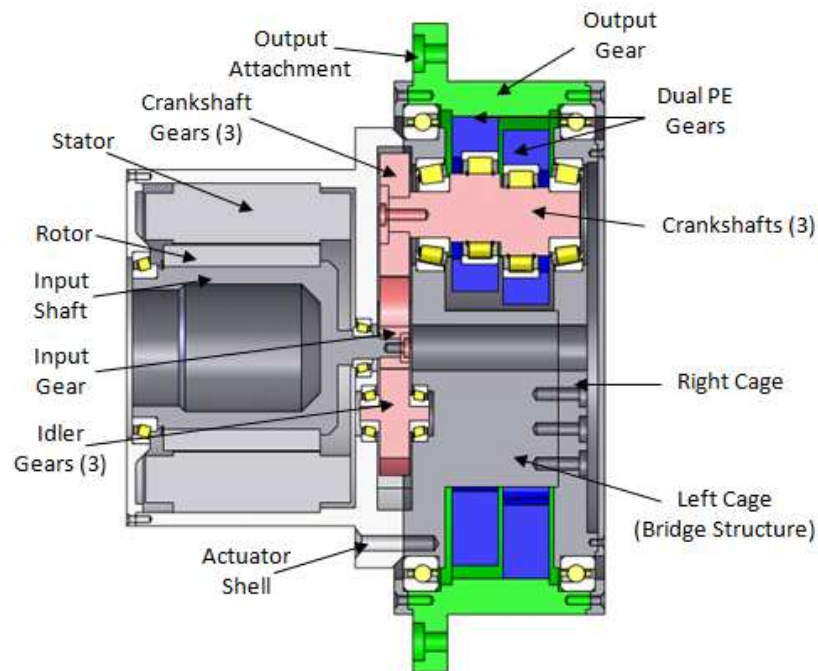


Figure 3.2: Detailed Actuator Design Including an SRM and PEGT

As shown in the figures, the detailed design of an actuator usually involves the following considerations: bearing mounting (snap rings, shoulders, etc.), seals, balancing mass placement (for the HGT), weight reduction, finishing details (chamfers, fillets), assembly modifications, and manufacturability modifications. All of these issues must be dealt with before drawings of the actuator components can be handed over to a manufacturer for production. Experienced designers have these issues in mind when generating a preliminary design even though their design documentation (solid models, specifications, etc.) often does not reflect them.

Figure 3.3 provides an example of a preliminary actuator design that couples an SRM with an HGT, and Figure 3.4 provides a similar example for the SRM/PEGT combination. Developing preliminary designs of this sort does not require the designer to deal with the detailed design issues listed above. Considering these issues during the

preliminary design stage can often complicate the design and decision process, especially for novice designers. Further, it should be noted that many preliminary design tasks are typically independent of the needs of a particular application, while the detailed design tasks are much more application-dependent. For example, during the preliminary design stage, only the high level performance parameters (torque, weight, responsiveness, etc.) and design parameters (overall geometric dimensions, gear ratio, etc.) need to be considered.

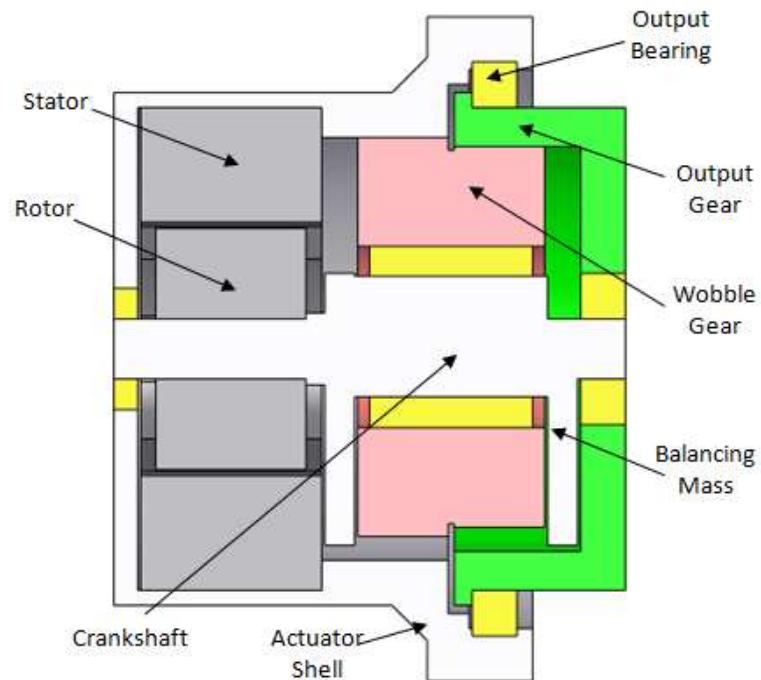


Figure 3.3: Preliminary Actuator Design Including an SRM and HGT

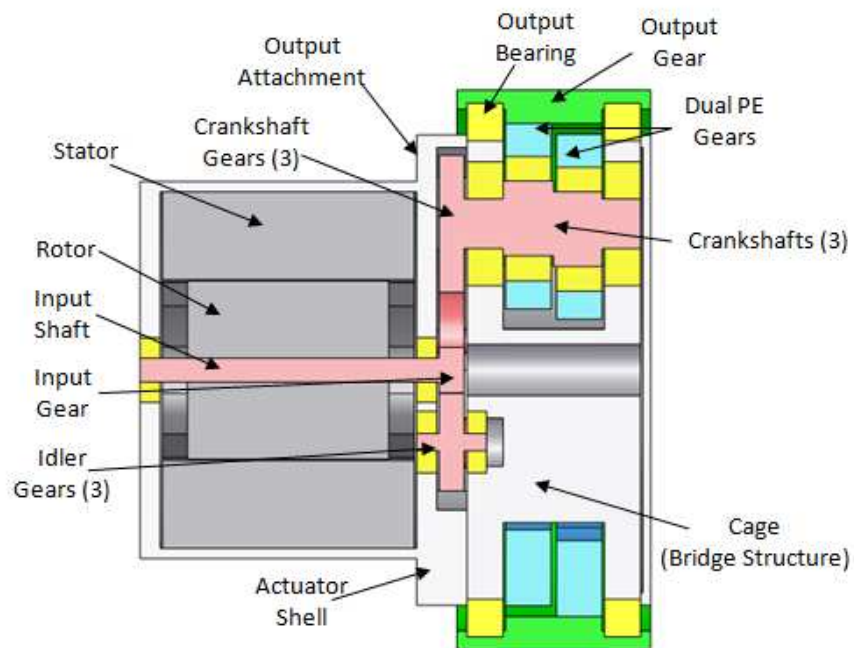


Figure 3.4: Preliminary Actuator Design Including an SRM and PEGT

The parametric models (this chapter), scaling rules, (Chapter 5), rules for balancing parameters (Chapter 6), and the results of Chapters 7 and 8 are useful for the preliminary stages of the actuator design process and provide tools to develop preliminary actuator designs. These preliminary designs will be developed to a sufficient level of detail such that a decision can be made whether or not to pursue a detailed design (Figure 3.5). The RRG's experience in actuator design was embedded into the development of these preliminary actuator designs so that a novice designer can quickly obtain accurate performance parameter information for an actuator design, without detailed consideration of the lower level parameters.

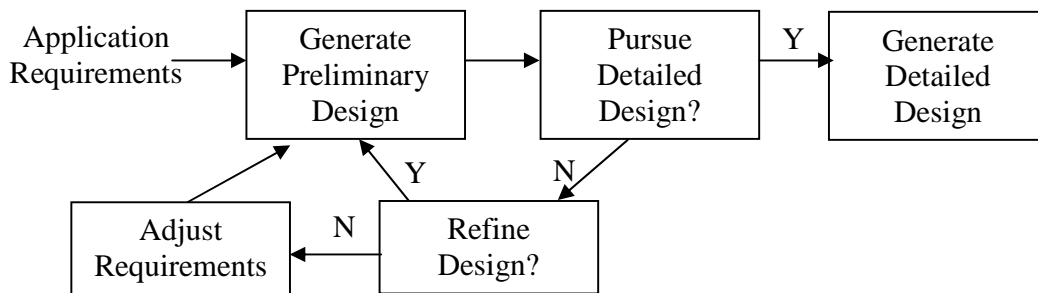


Figure 3.5: Preliminary and Detailed Actuator Design Stages (“Y” indicates Yes and “N” indicates No)

Making this distinction between the preliminary and detailed design stages should aid the movement toward standardization of the RRG actuator designs (Section 2.2.4), allowing proper allocation of priorities and resources toward each.

3.3 FUNDAMENTAL DESIGN PARAMETERS

Table 3.1 lists the fundamental, overall design and performance parameters for the motors and gear trains considered in this research. The design parameters are those that are most often considered and are most relevant during the preliminary stages of design. The performance parameters and metrics are those that can be accurately quantified using an established analytical relationship during the preliminary design stage. Each of these general parameters will be discussed later in this chapter in the context of specific motor and gear train types.

Table 3.1: Fundamental Design and Performance Parameters and Performance Metrics

Design Parameters (D_P)	Performance Parameters (P_P)	Combined Performance Metrics
D _g = gear train diameter L _g = gear train length A _g = gear train aspect ratio D _m = motor diameter L _m = motor length A _m = motor aspect ratio L = overall length A = overall aspect ratio g = gear ratio ω _m =motor speed	T = Torque W = Weight I = Inertia	T _w = Torque to Weight Ratio (Torque Density) R = Torque to Inertia Ratio (Responsiveness/Acceleration)

The gear train diameter (D_g) will be the largest outer diameter of the HGT and PEGT. The motor diameter (D_m) is defined as the largest diameter of the SRM, including the shell. The aspect ratio (A) of an actuator will be defined as the ratio of its overall length to gear train diameter as follows.

$$A = \frac{L}{D_g} = \frac{L_m + L_g}{D_g} \quad \text{Eqn. 19}$$

The aspect ratio of a motor (A_m) or gear train (A_g) will be defined as their length divided by their diameter.

$$A_m = \frac{L_m}{D_m} \quad \text{Eqn. 20}$$

$$A_g = \frac{L_g}{D_g} \quad \text{Eqn. 21}$$

The gear ratio (g) represents a fundamental designer choice for the HGT and PEGT (and any gear train) and can be written as functions of numbers of teeth or pitch diameters of the gears in the train. The gear ratios for the HGT and PEGT will be developed later in this chapter. The motor speed (ω_m) will be defined as the speed that

provides the desired output speed (based on the application) and will be compatible with the computed gear ratio (g).

Other important relationships that are particularly important for controlling the size of the motor relative to the gear train are the ratios of the motor length to overall length (K_l) and motor diameter to gear train diameter (K_d).

$$K_l = \frac{L_m}{L_m + L_g} = \frac{L_m}{L} \quad \text{Eqn. 22}$$

$$K_d = \frac{D_m}{D_g} \quad \text{Eqn. 23}$$

K_l is typically between 0.3 and 0.7 while K_d is typically between 0.5 and 1.0 for the motor-gear train combinations utilized in this research. The exact values of these ratios depend on the choice of the gear ratio between the motor and the gear train. These two parameters will be discussed in greater detail in Section 6.2.

Before proceeding, it is important to make a distinction between the overall, high-level design parameters listed above in Table 3.1 and the internal parameters of the motor and gear train. The remainder of this chapter will mainly focus on these internal parameters and how they can be written as functions of these overall, high-level parameters. Previous researchers at RRG have located and developed standard functional relationships (based on rules of thumb) between these internal parameters and the overall parameters listed above. Ashok and Tesar [2002] have documented these relationships for the SRM and have implemented them in several actuator design efforts, Park and Tesar [2005] have done the same for the HGT, and the current report has done the same for the PEGT. Of these three, the PEGT development is the least mature. Chapter 4 (Section 4.3.3.1) and the computer code used for computation (where the models of this

chapter are embedded, Appendices A and B) will provide full documentation of these internal rules.

3.4 GENERAL PERFORMANCE PARAMETER COMPUTATIONS

Referring back to Table 3.1, weight and inertia are two of the key performance parameters that will be computed for the motor, gear train, and actuator designs in this research. Before getting into the detailed modeling equations in the following sections, a brief note on the computation of weight and inertia is helpful. Most of the motor, gear train, bearing, and actuator components considered in this research are composed of components that are either solid or hollow cylinders, so their volumes (V), weights (W) and inertias (I) can be computed using the following simple equations.

$$V = \frac{\pi(d_o^2 - d_i^2)L}{4} \quad \text{Eqn. 24}$$

$$W = \rho V \quad \text{Eqn. 25}$$

$$I = \frac{W(d_o^2 + d_i^2)}{8} = \frac{\rho\pi(d_o^4 - d_i^4)L}{32} \quad \text{Eqn. 26}$$

The parameters in these expressions are as follows: ρ =material density, d_o =outer diameter, d_i =inner (bore) diameter, and L =length (face width for gear teeth, stack length for motors, etc.).

In most cases, the bearing weight and inertia do not contribute significantly to the overall weight and inertial content of a motor, gear train, or actuator design. When necessary, the volume (V_{bearing}), weight (W_{bearing}), and inertia (I_{bearing}) of a bearing with an inner diameter ID, outer diameter OD, and Width can be computed using the following equations. The k factor is included to account for the fact the bearing is not a solid cylinder and is typically between 70 and 80% for most bearing types.

$$V_{\text{bearing}} = \frac{\pi(OD^2 - ID^2)Width}{4} \quad \text{Eqn. 27}$$

$$W_{bearing} = k\rho V_{bearing} \quad \text{Eqn. 28}$$

$$I_{bearing} = \frac{W_{bearing}(OD^2 + ID^2)}{8} \quad \text{Eqn. 29}$$

The torque to weight ratio or torque density (T_w) and torque to inertia ratio or responsiveness/acceleration (R) can be computed for both the motor and gear train individually or for an integrated actuator as follows.

$$T_w = \frac{T}{W} \left[\frac{ft-lbf}{lbf} \right] \quad \text{Eqn. 30}$$

$$R = \frac{T}{I} \left[\frac{rad}{sec^2} \right] \quad \text{Eqn. 31}$$

The responsiveness will be computed at both the input and output for the motors, gear trains, and actuators in Chapters 5-8 since either may be important for a particular application. Chapter 7 will provide comparisons between direct drive and geared systems based on these two basic ratios. For a fixed output torque, the important issue is how the motor, gear train, and load inertias are affected by different choices of gear ratio.

3.4.1 Inertia Computations

When necessary, the parallel axis theorem will be used to compute inertia (I_p) of a component about an axis that is parallel to its own axis but is offset by a distance r (e.g., the wobble gear in the HGT and the PE gear in the PEGT).

$$I_p = I + Wr^2 \quad \text{Eqn. 32}$$

In this expression, I is the moment of inertia of the component about its own center of mass, and W is the weight of the component.

The output inertia (I_{out}) can be reflected to input (I_{in}) using the following equation, where g is equal to the gear ratio between the input and the output.

$$I_{in} = \frac{I_{out}}{g^2} \quad \text{Eqn. 33}$$

Unless otherwise specified, all gear train inertias in the remainder of this report are the inertias at the input shaft/gear of the gear train. Then, if a motor is coupled with the gear train's input shaft, this gear train inertia can be simply added to the motor inertia. Most gear train manufacturers list the equivalent gear train inertias at the input shaft.

For the purpose of calculating responsiveness of an actuator without specific information about the load inertia and geometry, it is necessary to define a load inertia (I_{load}) that is a multiple of a reasonable reference inertia (I_{ref}).

$$I_{load} = KI_{ref} \quad \text{Eqn. 34}$$

In this report, the reference inertia will be defined as the inertia of the gear train reflected to its input shaft for the systems in Chapters 5, 6, and 8. The reference inertia will be defined as the inertia of a direct drive motor in Chapter 7. The value of K can easily range from 1 to 10,000, and specific values of K will be interpreted in Chapter 7.

For all gear train and motor types, the general design goal is to maximize the torque capacity, torque density, and/or responsiveness while simultaneously minimizing weight and inertia. For the gear train, there is often a desire to achieve as high a gear ratio as possible (to minimize the size of the motor) while still avoiding interference between mating gears. As Chapter 7 will show, torque density and responsiveness are in conflict and are difficult to maximize simultaneously, and one of the two metrics will likely be more critical for a given application.

3.5 GENERAL GEARTRAIN PARAMETRIC MODEL

This section provides general gear train modeling equations that can be used for both the HGT and PEGT. The contact between gear teeth occurs along a line of action, and the radial (W_r), tangential (W_t), and resultant (W) forces are shown in Figure 3.6.

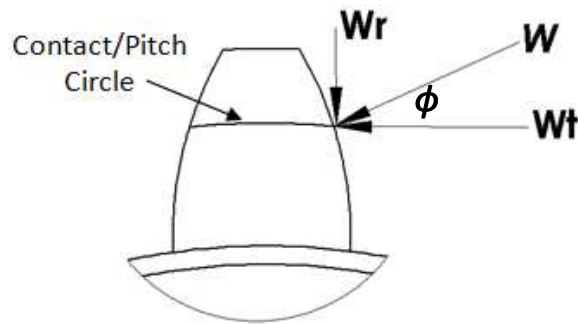


Figure 3.6: Forces on a Typical Gear Tooth

The angle ϕ is the pressure angle, and it is defined as the angle between the line of action (the force vector corresponding to W) and a line tangent to the contact/pitch circle (the force vector corresponding to W_t) at the point of contact. The reaction force between the contacting teeth is the resultant force (W), and it can be divided into its tangential (W_t) and radial components (W_r). The tangential force provides the torque transmission capacity of the geartrain and is the basis for the calculation of the tooth bending and contact stresses detailed below. The tangential forces cause bending of the gear tooth, and stresses result at the root of the tooth. The radial forces can be considered the undesirable byproduct. These radial forces can cause deflection of the gear rim and require the selection of adequate bearings. A constant pressure angle of 25 degrees is commonly used for involute gear teeth and will be used throughout this report until ongoing RRG research in the area of gear tooth interference provides more pressure angle selection guidelines.

3.5.1 Bending Stress in Gear Teeth

Each gear tooth can be modeled as a cantilever beam, with bending stresses resulting at the root of the tooth due to the applied tangential load. These bending stresses (S_b) can be computed as a function of the gear face width (L), diametral pitch

(P_d), and other factors using the standard AGMA approach (taken from Juvinall and Marshek, [2000]).

$$S_b = \frac{W_{t\max} P_d K_v K_s K_o K_m K_b}{LJ} \quad \text{Eqn. 35}$$

The load $W_{t\max}$ is the tangential load on the most heavily-loaded tooth in a gear mesh. The additional parameters in this expression are as follows: J =geometry factor, K_v =velocity factor, K_s =size factor, K_o =overload factor, K_m =load distribution factor, and K_b =rim thickness factor. Note that the face width L is the width of the tooth across the gear blank. The same relationship is used by Park and Tesar for the HGT [2005], and it will be extended here for the PEGT.

The gear train torque capacity (T), tangential load (W_t), and pitch diameter (D) are related by the following equation.

$$T = W_t \frac{D}{2} \quad \text{Eqn. 36}$$

The reader should note the distinction between the load W_t , which is the collective load shared by multiple gear teeth (if more than 1 tooth is in contact), and the load $W_{t\max}$, which is the load on the most heavily-loaded (central) tooth in the gear mesh. An approximate functional relationship between these two loads will be provided in a Section 3.5.5 below.

With the exception of J , K_v , and K_m , the remaining factors will be assumed to be unity for this research. The choice of these factors is not analytically based on geometry but rather on years of testing and standard development by AGMA. Changing the values of these factors could yield changes in torque capacity (and other performance parameters) that are not due to changes in geometry, which is beyond the scope of the present research. This assumption is justified because the remaining factors do not have an analytical description and/or are only discussed in gear design references with respect

to involute gear teeth. The designer is instructed to specify them at his/her discretion based on the needs of the particular application.

The bending stress equation is then reduced to the following.

$$S_b = \frac{W_{t \max} P_d K_m K_v}{LJ} \quad \text{Eqn. 37}$$

The geometry factor J is commonly obtained by referring to AGMA-published look-up tables, but for more efficient calculations, the following analytical expression from [Carroll and Johnson, 1988] may be used.

$$J = \left(1.763 + \frac{17.362}{N_p} + \frac{6.677}{N_g} \right)^{-1} \quad \text{Eqn. 38}$$

In this expression, N_p refers to the number of teeth on the pinion (the smaller gear in a gear mesh pair) and N_g refers to the number of teeth on the gear (the larger gear in a gear mesh pair). The J factor has been introduced by the AGMA to account for the relative shape of the gear teeth (e.g., tooth height to width ratio) and is typically between 0.2 and 0.6. The values of J in standard AGMA look-up tables depend upon the pressure angle, point of load application (tip of tooth or lower), and the numbers of teeth on the mating gears. For a derivation of the physical meaning behind the J factor, refer to Appendix A4.

The velocity factor K_v can be computed using the following expression, where V_p is the pitch line velocity of the gear mesh in units of ft/min.

$$K_v = \sqrt{\frac{78 + \sqrt{V_p}}{78}} \quad \text{Eqn. 39}$$

The velocity factor accounts for the impact loading that can occur between gear teeth at high speeds. Because the sliding velocities in the HGT and PEGT are typically much lower than for standard involute teeth [Park and Tesar, 2005], a new formulation for K_v is suggested.

The load distribution factor K_m is used to account for the increased potential for misalignment of the gear teeth as the face width increases. This factor can vary from 1.0 to 1.8, depending upon the face width and the care in tolerancing the gear teeth and in providing for adequate rigidity in the supporting bearings and structure.

Each gear train torque specification recorded in this report will include the values of these stress modification factors (J, K_v, K_m) used so that future designers can use the results as a baseline for comparison. See Section 5.2.2 for a discussion of the specific values of these factors used for the gear train designs in Chapters 5-8. For reference, Park and Tesar [2005] also provide a discussion of how these modification factors (J, K_v, K_m , etc.) can be adjusted for the circular arc gear teeth utilized in the HGT and PEGT.

3.5.2 Effect of Diametral Pitch on Torque Capacity

The diametral pitch (P_d) is defined as the number of teeth (N) divided by the pitch diameter (D), with lower values designated as coarse and higher values considered fine.

$$P_d = \frac{N}{D} \quad \text{Eqn. 40}$$

The reader should note the dependence of the torque capacity on diametral pitch (P_d) from the previous section. In general, the designer has free choice of the diametral pitch, and this factor has typically been in the range of 5 to 20 for past RRG gear train designs. Lower diametral pitches result in larger teeth, higher torque capacities (i.e., lower stresses for a given geometry), fewer teeth in contact, and in general, more potential for interference, while higher diametral pitches result in the opposite. The designer should pay special attention to the choice of this design parameter based on the specific objectives of the application. Because the torque capacity results of this report are heavily influenced by this choice (see Sections 5.2.5.2 and 5.3), most torque capacity

specifications will have the diametral pitch values and assumptions attached to them for the reader's benefit and to facilitate comparison with future designs.

Instead of the diametral pitch, the circular pitch (p) can be written as a function of the diametral pitch, number of teeth, and pitch diameter as follows.

$$p = \frac{\pi D}{2N} = \frac{\pi}{2P_d} \quad \text{Eqn. 41}$$

The circular pitch is approximately equal to the tooth width at the pitch circle (Figure 3.6), and the factor of 2 in this equation makes the width of the space between the teeth (at the pitch circle) equal to the width of a tooth. In practice, this value must be slightly larger than 2 to allow for adequate clearance and prevention of interference between mating gears.

3.5.3 Contact Stress in Gear Teeth

In addition to the bending stresses described above, contact (Hertzian) stresses occur between gear teeth in contact [Juvinall and Marshek, 2000]. The equation governing these contact stresses (S_c) is:

$$S_c = C_p \sqrt{\frac{W_{t \max} K_o K_v K_s K_m}{DLI}} \quad \text{Eqn. 42}$$

Here, the "K" factors have the same meaning as in the bending stress formulation discussed previously. C_p is the elastic coefficient, and its value depends on the material properties of the gear. When T is measured in-lbf, D and L in inches, and S_c in psi, C_p has a value of 2300 for most steels. I is termed the geometry factor and can be computed as a function of the pressure angle (ϕ) using the following expression.

$$I = \frac{\cos(\phi) \sin(\phi)}{2} \frac{m}{m \pm 1} \quad \text{Eqn. 43}$$

Here, m is velocity ratio between the mating gears and is defined as the ratio of the diameters of the larger and smaller gears in mesh. The denominator is $m+1$ for an

external gear mesh and $m-1$ for an internal gear mesh. The geometry factor accounts for the relative radii of curvature of the teeth on the two mating gears. This factor is typically between 1 and 2 for the internal gear mesh in the HGT and PEGT when these gear trains are used in their normal gear ratio range.

The gear material's contact strength can sometimes limit the torque capacity, but the small tooth number differences between mating gears in the PEGT and HGT usually provide very low contact stresses, and the bending stress dictates the limit on torque capacity. For this reason, all of the gear train torque specifications reported in Chapters 5-8 are based on the loading the teeth up to the bending stress limit rather than the contact stress limit. Ongoing research at the RRG will reveal whether these bending stresses (for peak load capacity) and contact stresses (for durability) can be balanced. Refer to Section 5.2.5.3 for a relative comparison between the bending and contact stresses.

3.5.4 Pitch Line and Sliding Velocities

The following equation describes the pitch line velocity (V_p) of a gear of pitch diameter (D) rotating at a given angular speed (ω_g).

$$V = \frac{D}{2} \omega_g \quad \text{Eqn. 44}$$

As shown in Section 3.5.1 above, one of the correction factors from the AGMA standard for gear teeth bending stress, the velocity factor (K_v), is inversely proportional to this pitch line velocity. High pitch line velocities are undesirable because they increase sliding friction and can lead to torque/power loss and thus poor performance.

The above velocity definition applies to the standards for involute gear teeth and does not directly apply for circular arc gear teeth. In circular arc teeth, the pitch line velocity is not as critical as the relative sliding velocity between the teeth [Juvinal and Marshek, 2000]. Park and Tesar [2005] provide relationships to compute the sliding

velocity in the HGT, which is heavily dependent upon the tooth level parameter choices (including the different radii necessary to define the circular arc). These relationships will not be used directly in this research because the focus in the present research is on the system level parameter choices such as the pitch diameter and number of teeth (see Section 2.3).

3.5.5 Effect of Contact Ratio on Torque Capacity

The PEGT and HGT torque capacities are typically limited by the bending and contact stresses in the gear teeth. Because of the relatively small tooth number differences in the PEGT and HGT gear meshes (and thus, relatively high gear ratios), it is important to determine the approximate number of teeth in contact (known as the contact ratio) before computing the stresses. For involute teeth, standard gear design reference suggests contact ratios between 1 and 2. For the circular arc tooth profile employed in the HGT and PEGT, Park and Tesar [2005] have estimated the number of teeth in contact using finite element analysis (Figure 3.7 and Figure 3.8). Table 3.2 and Figure 3.9 and summarize their key results.

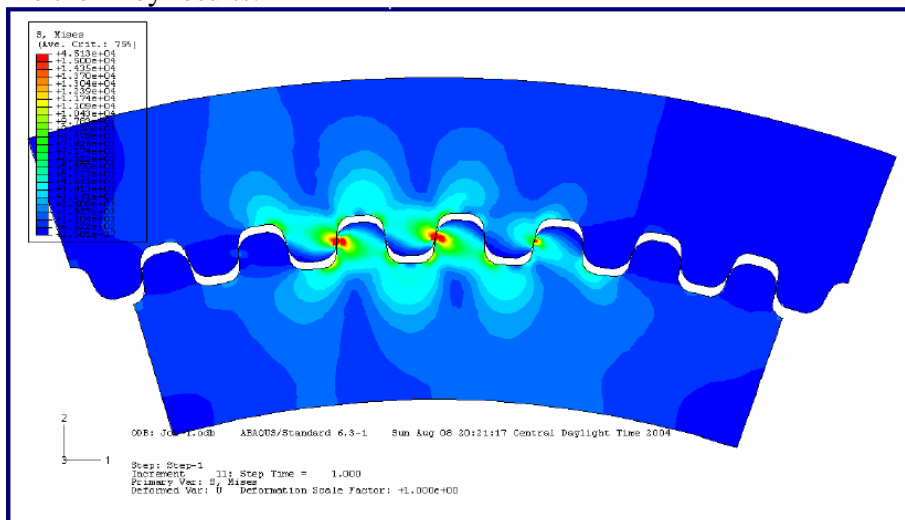


Figure 3.7: Nominal Load Condition (3 teeth in contact)

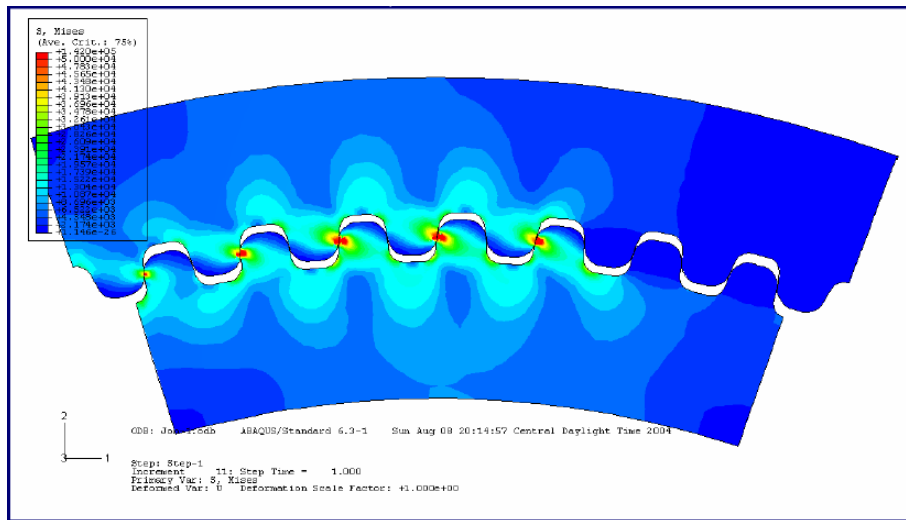


Figure 3.8: Peak Load Condition (5 teeth in contact)

Table 3.2: Percentage of Total Gear Tooth Load (s) as a Function of Contact Ratio

Nominal Load	Contact Ratio	Load Sharing Factor, s (% Total Tangential Load)
1X	3	40
2X	4	35
5X (Peak Condition)	5	27

The load sharing factor (s) is the percentage of the total tangential load taken by the center tooth (i.e., the most heavily-loaded tooth), with the central tooth seeing the largest load.

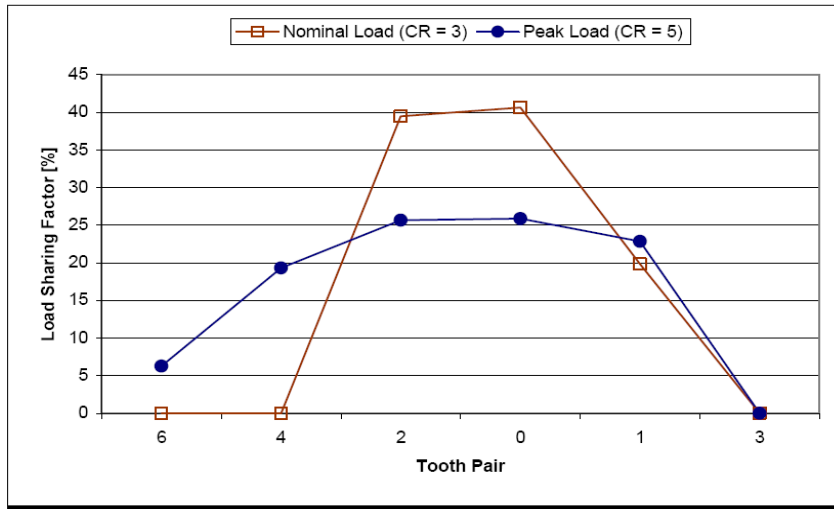


Figure 3.9: Estimate of Load Sharing Factor for Nominal and Peak Loading Conditions

If the load sharing factor (s) can be estimated from the table above or from FEA of the particular gear in question, the maximum tangential load (W_{tmax}) on the most heavily-loaded tooth can be determined as follows.

$$W_{tmax} = sW_t \quad \text{Eqn. 45}$$

The load W_{tmax} is always less than W_t and is the appropriate load to be used is the bending and contact stress relationships in Section 3.5.1. This modification to the standard stress calculations is the primary reason why circular arc are teeth are superior (in terms of load capacity) to involute teeth in the HGT and PEGT geometries.

Note that these loading assumptions are approximate and are subject to continual revision based on FEA results and gear train prototype development. Table 3.2 will be used as the basis of for all of the HGT and PEGT torque capacity calculations in this report. In particular, all of the HGT and PEGT torque capacity values are based on an assumed contact ratio of 3. When better estimates of the contact ratio for a given gear train geometry and tooth specification are available, the results stated in this report need to be updated. While finite element analysis can be used to determine how tooth

deformations affect the contact ratio, the tolerances in the gear tooth dimensions can also play a role, and ongoing research is investigating both of these effects.

3.5.6 Gear Rim Thickness and Tooth Height

The gear rim (Figure 3.10) is the portion of the gear behind the gear teeth that provides resistance to radial deformation.

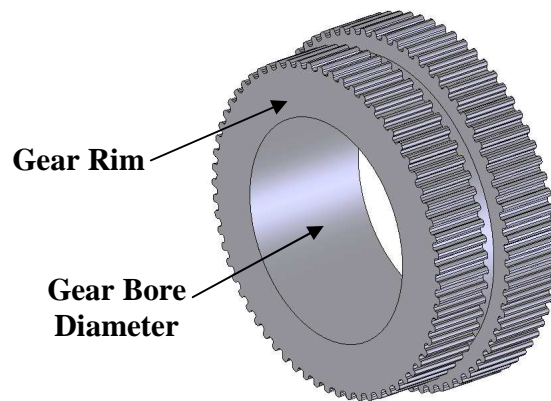


Figure 3.10: Gear Rim Shown on HGT Wobble Gear

The following equation (from the AGMA) gives a minimum value of the gear rim thickness (t) as a function of tooth height (h) to prevent bending stress concentrations.

$$t = 1.2 h \quad \text{Eqn. 46}$$

Because this relationship is based on testing rather than an analytical formulation, it does not need to be satisfied as an equality. The effects of different rim thicknesses on the deflection of a gear can be determined by physical testing of the particular geometry or with FEA software. The tooth heights (h) for standard involute gearing are defined as a function of the diametral pitch (P_d) (or pitch diameter D and number of teeth N) of a gear as follows.

$$h = \frac{2.25}{P_d} = \frac{2.25D}{N} \quad \text{Eqn. 47}$$

The addendum, a , (distance between pitch circle and tip circle) and dedendum, b , (distance between base circle and pitch circle) for involute teeth can also be written as functions of the diametral pitch.

$$a = \frac{1}{P_d} = \frac{D}{N} \quad \text{Eqn. 48}$$

$$b = \frac{1.25}{P_d} = \frac{1.25D}{N} \quad \text{Eqn. 49}$$

For circular arc gear teeth, this relationship does not necessarily hold, and tooth heights are often shorter than standard involute tooth heights to avoid interference and increase bending stiffness (see Appendix A4). However, for the preliminary design focus of this report, this conservative relationship can be used without significant error. As the circular gear geometry is continually refined, tooth height expressions similar in form to the above will be available.

3.5.7 Gear Bore Diameter

Referring to the suggested value for the minimum gear rim thickness above in the previous section, the maximum bore diameter (d_b) of an external gear (such as the wobble gear in Figure 3.10) can be as a function of its pitch diameter (D) and tooth height (h).

$$d_b = D - 3.5h \quad \text{Eqn. 50}$$

The designer may choose to have a smaller bore diameter than given by this equation (and thus a larger rim thickness than the prescribed minimum from the AGMA) to reduce the stress level on the gear or to match the bearing or shaft diameters that interface with the gear. Because circular arc gear teeth are generally shorter than involute gear teeth, this and the relationship in the next section will result in gear bore and rim diameters that are not conservative, so they must be used cautiously. When similar standards are

developed for circular arc teeth, more guidance in choosing these dimensions will be available.

3.5.8 Gear Rim Diameter

The following equation gives the minimum rim diameter (d_{rim}) of an internal gear, given its pitch diameter and tooth height.

$$d_{rim} = D + 3.5h \quad \text{Eqn. 51}$$

Again, this equation can be used as an inequality if the designer chooses to have the rim thickness larger than the prescribed minimum from the AGMA.

3.6 CHAPTER ROADMAP

The remainder of this chapter will discuss the use of the above general design and performance parameter relationships for the following specific systems of interest.

- SRM (stand-alone motor)
- HGT (stand-alone gear train)
- Star+PEGT (stand-alone gear train)
- Star Compound+PEGT (stand-alone gear train)
- SRM+HGT (integrated actuator)
- SRM+Star+PEGT (integrated actuator)
- SRM+Star Compound+PEGT (integrated actuator)

For each of these systems, solid models, dimensioned drawings, and tabular listings of the design and performance parameters will be provided.

3.7 SWITCHED RELUCTANCE MOTOR (SRM)

The SRM is typically coupled with a gear train for most applications being studied by the RRG, but it is useful to have a stand-alone SRM model for considering direct drive systems and for applications in which the motor and gear train are physically

separated. The reference SRM design used for this report is shown in Figure 3.11. Table 3.3 provides a listing of the design parameters (classified by component) that can be used to completely specify the geometry of this reference design (Appendix A1).

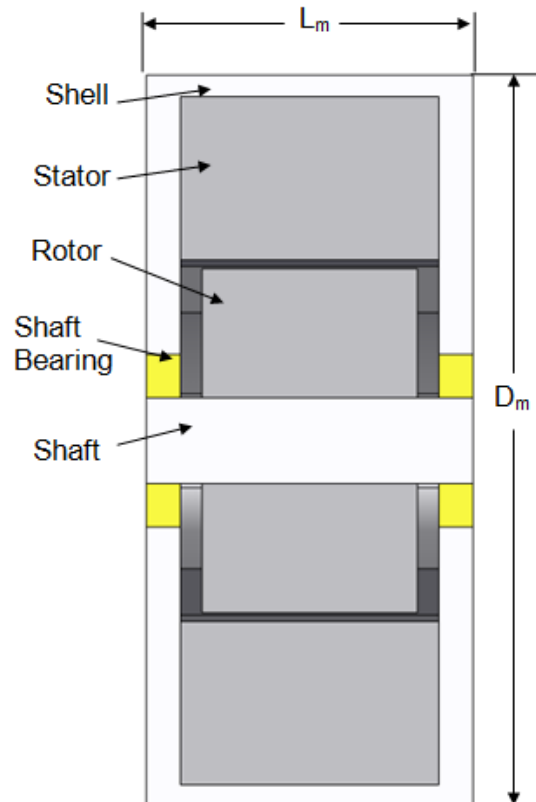


Figure 3.11: SRM Reference Design

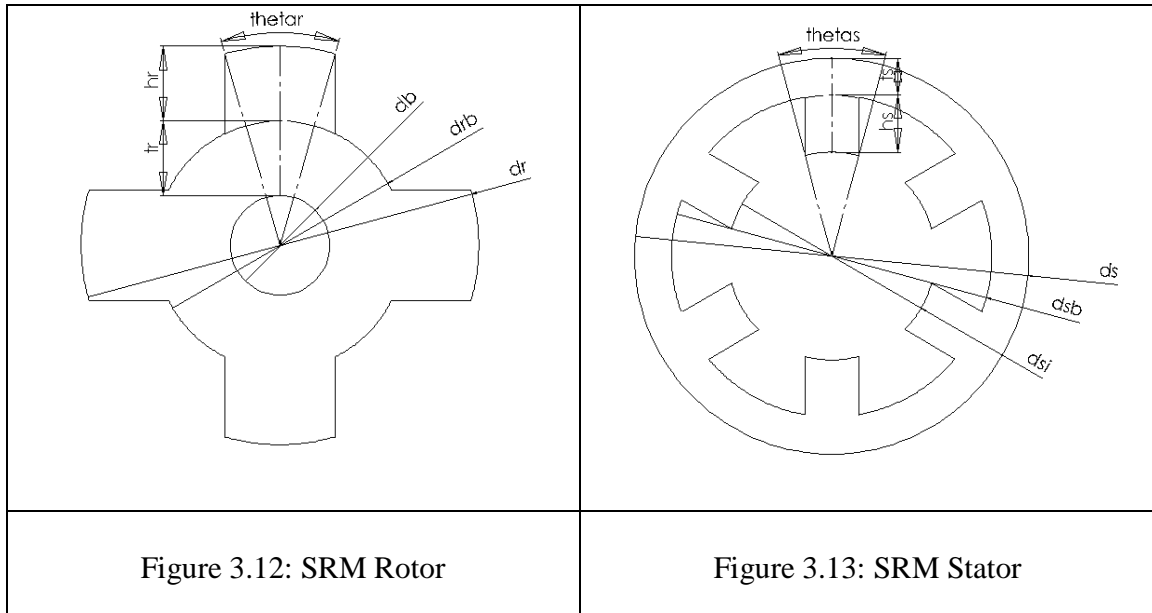
Table 3.3: SRM Design Parameters Classified by Component (for generating reference design)

Component	Design Parameters
Rotor	$d_r, d_{rb}, d_b, \theta_r, t_r, h_r, L_s$
Stator	$d_s, d_{sb}, d_{si}, \theta_s, t_s, h_s, L_m$
Shaft	L_1, d_1
Shaft bearing	ID_shaft_bearing, OD_shaft_bearing, W_shaft_bearing
Shell	$L_{s1}, L_{s2}, L_{s3}, d_{s1}, d_{s2}, d_{s3}, d_{s4}$

The foundation for this model comes from Ashok and Tesar [2002] and other supporting works on SRM design (see “Switched Reluctance Motor Design” heading in the References listed at the end of this report). Figure 3.12 and Figure 3.13 provide dimensioned drawings of the SRM rotor and stator, and Table 3.4 provides a list of the internal design, intermediate, and performance parameters discussed in this section.

Table 3.4: SRM Parameters (Discussed in this section)

Key Internal Design Parameters	Intermediate Parameters	Performance Parameters
d_s Stator outer diameter L Overall stack length ω_m Speed Wiring parameters d_w Diameter I_w Safe current limit Number of poles N_s Stator N_r Rotor Pole angles θ_s Stator θ_r Rotor g Air gap	Diameters d_{sb} Stator back iron d_{si} Stator air gap d_r Rotor air gap d_{rb} Rotor back iron d_{rb} Rotor bore Lengths L_s Stator (w/o windings) L_a Active L_{s1} Shell Back iron thicknesses t_s Stator t_r Rotor Pole heights h_s Stator h_r Rotor Pole widths w_s Stator w_r Rotor Pole center of mass c_s Stator c_r Rotor p Stator pole pitch N Number of turns I_{sat} Saturation current Weights W_{sb} Stator back iron W_{sp} Stator poles W_{rb} Rotor back iron W_{rp} Rotor poles W_{mshaft} Motor shaft W_{mshell} Motor shell Inertias I_{rb} Rotor back iron I_{rp} Rotor poles I_{mshaft} Motor shaft	T_{motor} Torque capacity W_{motor} Weight (total) I_{motor} Inertia (total)



There are a total of 26 design parameters needed to completely describe the geometry of the reference SRM in Figure 3.11. Considering the constraints that come from matching the dimensions of mating components and other common assumptions, the number of independent design parameters is approximately 15 to 20. The designer must choose or search through these remaining independent design parameters to meet a desired set of performance requirements. This relatively large number of parameters is difficult to deal with at one time, and this difficulty usually results in a motor design that meets the requirements but is less than optimal. Overcoming this difficulty is one of the primary motivations for this research and justifies the need for the design rules (Chapters 5 and 6) that illustrate the effect of parameter choices.

3.7.1 Key SRM Design Parameters

All of the intermediate and performance parameters can be written as functions the key internal design parameters listed in Table 3.4. Unless otherwise specified, the

following values (Table 3.5) will be held fixed and can be considered to be the assumptions for all of the SRM designs in this report. The axial clearance noted in the table is a simple approximation used to control the space between mating components and does not significantly affect the performance parameter results.

Table 3.5: SRM Assumptions

Parameter	Value
Number of stator poles	$N_s=6$
Number of rotor poles	$N_r=4$
Stator pole angle	$\theta_s = 30^\circ$
Stator pole angle	$\theta_r = 32^\circ$
Saturation flux density	$B_{sat}=1.56$
Axial clearance	$c = 0.005D_m$
Density	$\rho = 0.284 \text{ lbm/in}^3$

The following sections provide analytical equations to compute the intermediate and performance parameters of the SRM. Table 3.6 contains a summary of the SRM design and performance parameter relationships to be developed in this section. These equations are suitable for direct implementation into a computer environment.

Table 3.6: Summary of SRM Design and Performance Parameter Relationships

Parameter	Equation
Torque	$T_{motor} = 0.9NB_{sat}L_a \frac{d_r}{2} \left(I_w - \frac{I_{sat}}{2} \right)$
Weight	$W_{motor} = W_{sb} + W_{sp} + W_{rb} + W_{rp} + W_{mshaft} + W_{mshell} + W_{bearing}$ $W_{motor_app} = k \frac{\rho \pi l_{s4}^2 L}{4}$
Inertia	$I_{motor} = I_{rb} + I_{rp} + I_{mshaft} + I_{bearing}$

3.7.2 Air Gap

The air gap is the radial distance of the gap between the rotor and stator poles, as shown in Figure 3.14. The following relationship used by Ashok and Tesar [2002] will be used to set the air gap dimensions.

$$g = 0.005L \quad \text{Eqn. 52}$$

The basic principle behind this equation is that the air gap must increase as the axial length L_m increases because tolerance errors are magnified as the length of motor increases. A larger radial air gap must be used to prevent contact between the rotor and stator during operation. If the above relationship results in an air gap of less than 0.01 inches, then the air gap should be set as 0.01 inches. These guidelines are based on manufacturing limits, acoustic noise levels, and torque generation. In general, the choice of air gap for the SRM should be tested using finite element analysis and/or physical testing to ensure that the desired performance is achieved.

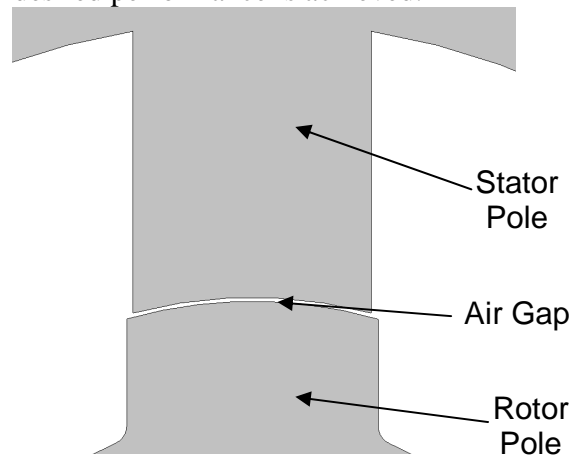


Figure 3.14: Air Gap Distance

3.7.3 Stator Geometry

The stator air gap diameter is given by the following equation.

$$d_{si} = d_r + 2g \quad \text{Eqn. 53}$$

The stator back iron thickness is given by the following equation.

$$t_s = kd_r \sin\left(\frac{\theta_s}{2}\right) \quad \text{Eqn. 54}$$

The factor k has a typical range of 0.5 to 1, where the value of 0.5 gives the smallest back iron thickness and largest pole height (for a fixed d_r). This means more room for windings and thus the highest torque.

The stator back iron diameter is given by the following equation.

$$d_{sb} = d_s - 2t_s \quad \text{Eqn. 55}$$

The stator pole height is given by the following equation.

$$h_s = \frac{d_{sb} - d_{si}}{2} \quad \text{Eqn. 56}$$

The stator pole pitch (i.e., distance between adjacent poles) is given by the following equation.

$$p = \frac{2\pi - N_s \theta_s}{N_s} \quad \text{Eqn. 57}$$

3.7.4 Rotor Geometry

An approximate value for the rotor air gap diameter is given by the following equation.

$$d_r = \frac{d_s}{2} \quad \text{Eqn. 58}$$

An approximate value for the rotor bore diameter is given by the following equation.

$$d_b = \frac{d_r}{2} \quad \text{Eqn. 59}$$

These relationships were formulated by Miller [1993] and discussed in detail by Ashok and Tesar [2002] and can be verified by comparison to off-the-shelf motor designs. Each of the stator and rotor diameters is chosen so that its respective pole height is equal to its back iron height, as shown in Figure 3.12 and Figure 3.13. This choice ensures that the

same flux flow is present in the rotor and stator back irons. Choosing taller poles (for both stator and rotor) compared to a relatively shorter back iron increases the susceptibility of the poles to lateral deformations and the back iron to hoop stresses. Choosing shorter poles and a taller back iron decreases the reluctance (increases the inductance) between the poles and back iron, which can increase the leakage flux that does not follow the desired pole to pole path. For preliminary design, these proposed geometric relationships are sufficient, but a detailed design effort should allow deviation from these simplified relationships.

The rotor back iron thickness is given by the following equation.

$$t_r = kd_r \sin\left(\frac{\theta_r}{2}\right) \quad \text{Eqn. 60}$$

The factor k in this equation has the same interpretation as in the stator back iron thickness expression, and the expressions are also identical.

The rotor back iron diameter is given by the following equation.

$$d_{rb} = d_r + 2t_r \quad \text{Eqn. 61}$$

The rotor pole height is given by the following equation.

$$h_r = \frac{d_r - d_{rb}}{2} \quad \text{Eqn. 62}$$

3.7.5 Winding Parameters

Table 3.7 provides a standard listing of conductor (wire) diameters (d_w) and safe current capacities (I_w). For each SRM designed in this report, an exhaustive search of the wire diameters that maximize the torque capacity (for a fixed stator outer diameter d_s) was performed. More details on the searching process will be provided in Section 4.3.2.

Table 3.7: AWG Conductor Diameters and Safe Current Limits

Size AWG	Conductor Diameter				Single Insulation				Heavy Insulation			Current Limit Amps
	Min.	Nominal		Max.	Min. Inc.	Max. OD		Min. Inc.	Max. OD			
		mm	mm			inches	mm		mm	inches	mm	
8	3.231	3.264	0.1285	3.282				0.084	3.383	0.1332	73	
9	2.878	2.906	0.1144	2.921				0.081	3.02	0.1189	64	
10	2.563	2.588	0.1019	2.601				0.079	2.695	0.1061	55	
11	2.281	2.304	0.0907	2.316				0.076	2.408	0.0948	47	
12	2.032	2.052	0.0808	2.062				0.074	2.151	0.0847	41	
13	1.811	1.829	0.0720	1.839				0.071	1.923	0.0757	35	
14	1.613	1.628	0.0641	1.636	0.041	1.692	0.0666	0.081	1.732	0.0682	32	
15	1.435	1.45	0.0571	1.458	0.038	1.509	0.0594	0.076	1.547	0.0609	28	
16	1.278	1.29	0.0508	1.298	0.036	1.349	0.0531	0.074	1.384	0.0545	22	
17	1.138	1.151	0.0453	1.156	0.036	1.206	0.0475	0.071	1.24	0.0488	19	
18	1.013	1.024	0.0403	1.029	0.033	1.077	0.0424	0.066	1.11	0.0437	16	
19	0.902	0.912	0.0359	0.917	0.03	0.963	0.0379	0.064	0.993	0.0391	14	
20	0.805	0.813	0.0320	0.818	0.03	0.861	0.0339	0.058	0.892	0.0351	11	
21	0.716	0.724	0.0285	0.726	0.028	0.77	0.0303	0.056	0.798	0.0314	9	
22	0.635	0.643	0.0253	0.645	0.028	0.686	0.0270	0.053	0.714	0.0281	7	
23	0.569	0.574	0.0226	0.577	0.025	0.617	0.0243	0.051	0.643	0.0253	4.7	
24	0.505	0.511	0.0201	0.513	0.025	0.551	0.0217	0.048	0.577	0.0227	3.5	
25	0.45	0.455	0.0179	0.457	0.023	0.493	0.0194	0.046	0.516	0.0203	2.7	
26	0.399	0.404	0.0159	0.406	0.023	0.439	0.0173	0.043	0.462	0.0182	2.2	
27	0.358	0.361	0.0142	0.363	0.02	0.396	0.0156	0.041	0.417	0.0164	1.7	
28	0.318	0.32	0.0126	0.323	0.02	0.356	0.0140	0.041	0.373	0.0147	1.4	
29	0.284	0.287	0.0113	0.29	0.018	0.32	0.0126	0.038	0.338	0.0133	1.2	
30	0.251	0.254	0.0100	0.257	0.018	0.284	0.0112	0.036	0.302	0.0119	0.86	
31	0.224	0.226	0.0089	0.229	0.015	0.254	0.0100	0.033	0.274	0.0108	0.7	
32	0.201	0.203	0.0080	0.206	0.015	0.231	0.0091	0.03	0.249	0.0098	0.53	
33	0.178	0.18	0.0071	0.183	0.013	0.206	0.0081	0.028	0.224	0.0088	0.43	
34	0.157	0.16	0.0063	0.163	0.013	0.183	0.0072	0.025	0.198	0.0078	0.33	
35	0.14	0.142	0.0056	0.145	0.01	0.163	0.0064	0.023	0.178	0.0070	0.27	
36	0.124	0.127	0.0050	0.13	0.01	0.147	0.0058	0.02	0.16	0.0063	0.21	
37	0.112	0.114	0.0045	0.117	0.008	0.132	0.0052	0.02	0.145	0.0057	0.17	
38	0.099	0.102	0.0040	0.104	0.008	0.119	0.0047	0.016	0.13	0.0051	0.13	
39	0.086	0.089	0.0035	0.091	0.005	0.104	0.0041	0.015	0.114	0.0045	0.11	

The height on each pole (h) available for windings is given by the following equation.

$$h = kh_s \tag{Eqn. 63}$$

A typical value of the constant k in this expression is 0.85, and physically, this represents the loss in winding space due to the curvature of the stator back iron, presence of insulation, and inability to exactly fill the entire space with windings.

The space between the windings of adjacent poles is given by the following equation.

$$s = kd_w \tag{Eqn. 64}$$

Typical values of the constant k in this expression are between 1 and 5, with higher numbers allowing more space between the windings of adjacent poles and lower numbers providing higher torque capacities.

The width of windings (w) extending beyond the stator length can be computed from the following equation.

$$w = \frac{pd_r}{4} - \frac{s}{2} \quad \text{Eqn. 65}$$

3.7.6 Length Parameters

The axial length of rotor and stator, L_s , (without windings) is given by the following equation.

$$L_s = L - 2w \quad \text{Eqn. 66}$$

The active length (L_a), which is less than the axial length L_s by the lamination stacking factor S_f (typically between 0.8 and 0.9) is given by the following equation.

$$L_a = S_f L_s \quad \text{Eqn. 67}$$

The number of turns (N) is given by the following equation, where P_f is the packing factor (typically is assumed to be about 0.6).

$$N = \frac{8hwP_f S_f}{\pi d_w^2} \quad \text{Eqn. 68}$$

The value given by this expression should be rounded off to the nearest integer to be consistent with motor winding standards.

For the purposes of calculating the weight of the shell outside the motor (L_{s1}), a reasonable shell thickness can be estimated from the overall length.

$$L_{s1} = 0.1L \quad \text{Eqn. 69}$$

3.7.7 Torque

The saturation current (in Amps) is given by the following equation.

$$I_{sat} = \frac{B_{sat} \mathcal{G}}{2\pi N \times 10^{-7}} \quad \text{Eqn. 70}$$

The SRM torque capacity (in Nm) is given by the following equation.

$$T_{motor} = 0.9NB_{sat}L_a \frac{d_r}{2} \left(I_w - \frac{I_{sat}}{2} \right) \quad \text{Eqn. 71}$$

3.7.8 Weight and Inertia

3.7.8.1 Back Iron

The rotor and stator back iron are those portions of the rotor and stator that do not include the poles. The rotor back iron volume, weight, and inertia are given by the following equations.

$$V_{rb} = \frac{\pi(d_{rb}^2 - d_b^2)L_a}{4} \quad \text{Eqn. 72}$$

$$W_{rb} = \rho V \quad \text{Eqn. 73}$$

$$I_{rb} = \frac{W(d_{rb}^2 + d_b^2)}{2} \quad \text{Eqn. 74}$$

The stator back iron volume and weight are given by the following equations.

$$V_{sb} = \frac{\pi(d_s^2 - d_{sb}^2)L}{4} \quad \text{Eqn. 75}$$

$$W_{sb} = \rho V \quad \text{Eqn. 76}$$

3.7.8.2 Poles

The rotor and stator pole widths are given by the following equations.

$$w_r = \frac{d_r}{2} \theta_r \quad \text{Eqn. 77}$$

$$w_s = \frac{d_r}{2} \theta_s \quad \text{Eqn. 78}$$

The rotor and stator pole centers of mass are given by the following equations.

$$c_r = \frac{d_{rb}}{2} + \frac{h_r}{2} \quad \text{Eqn. 79}$$

$$c_s = \frac{d_{si}}{2} + \frac{h_s}{2} \quad \text{Eqn. 80}$$

The rotor and stator pole weights are given by the following equations.

$$W_{rp} = \rho N_r w_r h_r L_s \quad \text{Eqn. 81}$$

$$W_{sp} = \rho N_s w_s h_s L_s \quad \text{Eqn. 82}$$

The rotor pole inertia is given by the following equation.

$$I_{rp} = \frac{W_{rp}(w_r^2 + h_r^2)}{12} + W_{rp}c_r^2 \quad \text{Eqn. 83}$$

3.7.8.3 Motor Shaft

The motor shaft volume, weight, and inertia are given by the following equations.

$$V_{mshaft} = \frac{\pi d_b^2 L_1}{4} \quad \text{Eqn. 84}$$

$$W_{mshaft} = \rho V_{mshaft} \quad \text{Eqn. 85}$$

$$I_{mshaft} = \frac{W_{mshaft} d_b^2}{2} \quad \text{Eqn. 86}$$

3.7.8.4 Motor Shell

The motor shell volume and weight are given by the following equations.

$$V_{mshell} = \frac{\pi \left[(d_{s4}^2 - d_{s1}^2)L_{s1} + (d_{s4}^2 - d_{s2}^2)L_{s2} + (d_{s4}^2 - d_{s3}^2)L_{s3} \right]}{4} \quad \text{Eqn. 87}$$

$$W_{mshell} = \rho V_{mshell} \quad \text{Eqn. 88}$$

3.7.9 Total Motor Weight and Inertia

The weight of the SRM (W_{motor}) can be defined as the sum of all the component weights.

$$W_{motor} = W_{sb} + W_{sp} + W_{rb} + W_{rp} + W_{mshaft} + W_{mshell} + W_{bearing}. \quad \text{Eqn. 89}$$

For a quick estimate of motor weight, knowing only the overall diameter (D_m) and length of the motor (L_m), the following equation can be used.

$$W_{motor_app} = k \frac{\rho \pi D_m^2 L_m}{4} \quad \text{Eqn. 90}$$

Here, k is generally from 70 to 80% for the space between rotor poles and other free space in the motor. This approximate weight calculation is accurate enough to develop preliminary motor designs.

The inertia of the SRM (I_{motor}) is the sum of the inertias of all the rotating parts.

$$I_{motor} = I_{rb} + I_{rp} + I_{mshaft} + I_{bearing} \quad \text{Eqn. 91}$$

The inertia of the bearings ($I_{bearings}$) can also be included in this total inertia, accounting for only the rotating portion of the bearing, but their contribution is typically insignificant compared to rotor and shaft inertias. This inertia limits the acceleration capabilities of the motor. These inertia calculations are sufficiently accurate (to within a few percent) for the purposes of this research. If a solid modeling package is used in conjunction with this design model, exact inertia information is easily calculated with built-in functions.

3.8 GEAR TRAINS

This section will detail the parametric models for the HGT and PEGT. The detailed weight and inertial calculations for the SRM above are meant to serve as a model for the calculation of these parameters for the HGT and PEGT. Since the weight and inertial calculations for these gear trains are analogous to those for the motor and also quite simple, this section only presents summary calculations for these parameters, and the reader is the MatLab computer code for full documentation (Appendix A1).

3.9 HYPOCYCLIC GEAR TRAIN (HGT)

The HGT is typically coupled with a motor for most applications being studied by the RRG, but it is useful to have a stand-alone HGT model for applications in which the motor and gear train are physically separated. The reference HGT design used for this

report is shown in Figure 3.15. Table 3.8 provides a listing of the design parameters (classified by component) that can be used to completely specify the geometry of this reference design (Appendix A1).

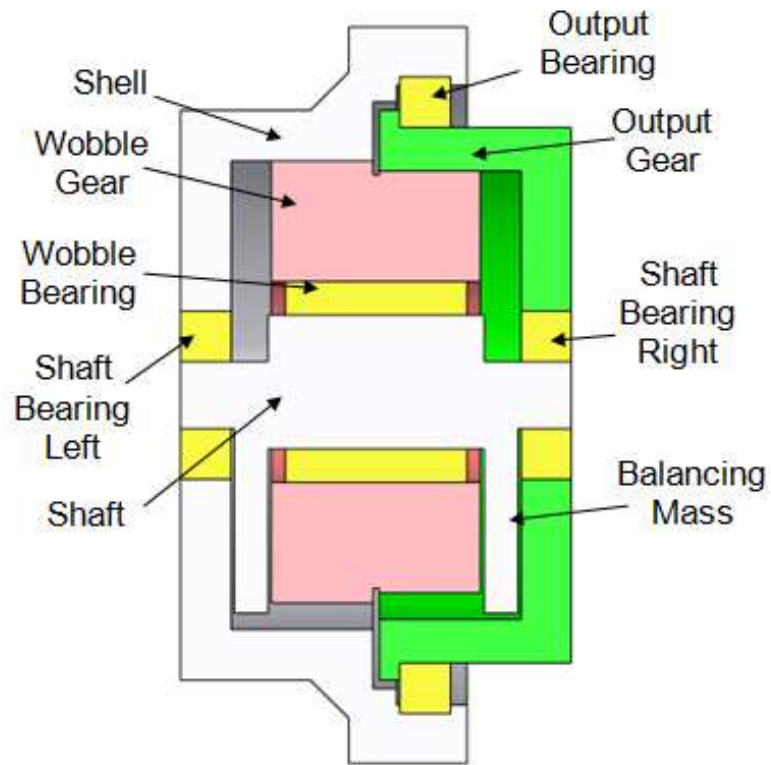


Figure 3.15: HGT Reference Design

The input torque from the motor drives the shaft, on which the wobble gear is mounted eccentrically. The wobble gear meshes with a fixed ring gear in the shell and also meshes with the output gear, which provides the desired output torque and speed from the gear train.

Table 3.8: HGT Design Parameters Classified by Component (for generating reference design)

Component	Design Parameters
Wobble gear	$d_{w1}, d_{w2}, d_{wb}, d_{wo}, L_w$
Output gear	$d_{r2}, L_{o1}, L_{o2}, L_{o3}, d_{o1}, d_{o2}, d_{o3}$
Shaft (including balance masses)	$L_3, L_4, L_5, d_3, d_4, d_5, e, r_{o1}, r_{o2}, w$
Output bearing	ID_output_bearing, OD_output_bearing, W_output_bearing
Wobble bearing	ID_wobble_bearing, OD_wobble_bearing, W_wobble_bearing
Shaft bearing right	ID_shaft_bearing_right, OD_shaft_bearing_right, W_shaft_bearing_right
Shaft bearing left	ID_shaft_bearing_left, OD_shaft_bearing_left, W_shaft_bearing_left
Shell	$d_{r1}, L_{s1}, L_{s3}, L_{s4}, L_{s5}, L_{s6}, L_{s7}, d_{s1}, d_{s4}, d_{s5}, d_{s6}, d_{s7}, d_{s8}, d_{s9}$

The foundation for this model comes from Park and Tesar [2005] and Kendrick and Tesar [2006]. A comprehensive design effort on the hypocyclic gear train was recently completed by Park and Tesar, and Kendrick and Tesar designed an aircraft control surface actuator utilizing this gear train.

Figure 3.16 illustrates how the wobble gear meshes with fixed internal gear that is an integral part of the HGT shell, and Figure 3.17 displays the wobble gear. Table 3.9 lists the internal design, intermediate, and performance parameters discussed in this section. These are considered system level design parameters by Park and Tesar and are sufficient to generate solid models and begin detailed tooth level design (Section 2.3). The tooth level design parameters (circular arc radii, tooth width, tooth thickness, etc.) will not be considered in this research and are being studied by another RRG team member.

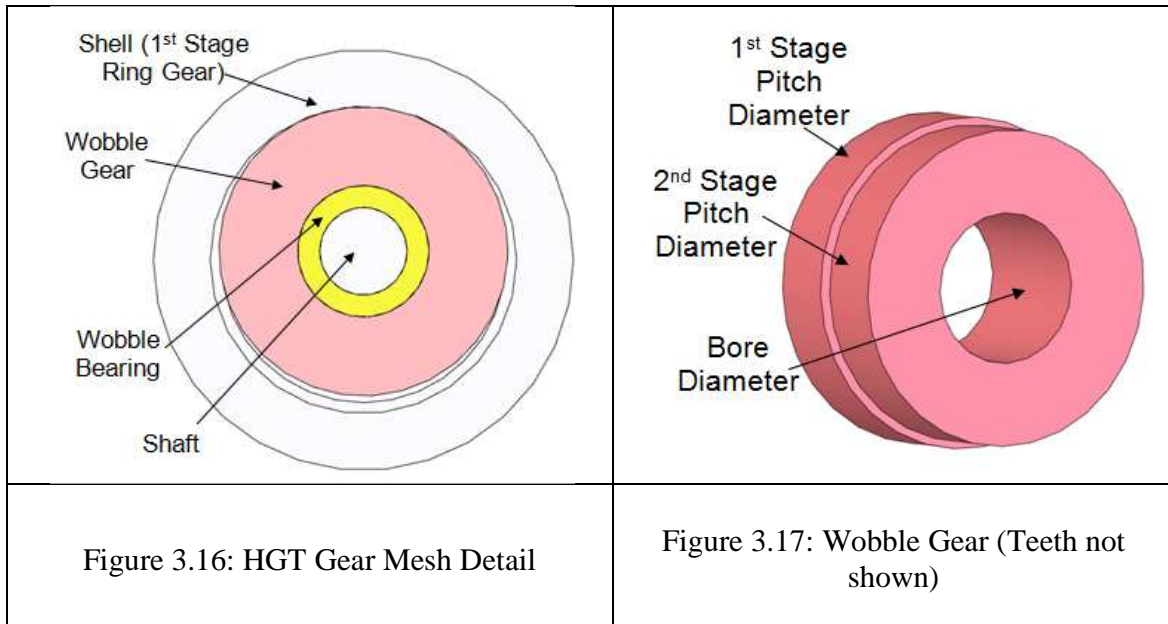


Table 3.9: HGT Parameters (Discussed in this section)

Key Internal Design Parameters	Intermediate Parameters	Performance Parameters
Pitch diameters d_{r1} 1 st stage ring d_{r2} 2 nd stage ring d_{w1} 1 st stage wobble d_{w2} 2 nd stage wobble e Eccentricity L_w One face width L_g Total width/length A Aspect ratio Diametral pitch P_{d_min} Minimum P_{d_max} Maximum Numbers of teeth N_{r1} 1 st stage ring N_{r2} 2 nd stage ring N_{w1} 1 st stage wobble N_{w2} 2 nd stage wobble g Gear ratio ϕ Pressure angle S_b Bending strength S_c Contact strength	d_{wb} wobble gear bore diameter Rim diameters d_{ro1} 1 st stage rim d_{ro2} 2 nd stage rim Weights W_w wobble gear W_{es} eccentric shaft W_o output gear W_{sh} shell $W_{bm1,bm2}$ balancing masses $W_{bearings}$ bearings Inertias I_w wobble gear I_{es} eccentric shaft I_o output gear $I_{bm1,bm2}$ balancing masses $I_{bearings}$ bearings	T_{hgt} Torque capacity W_{hgt} Weight (total) I_{hgt} Inertia (total)

There are a total of 48 design parameters needed to completely describe the geometry of the reference HGT in Figure 3.15. Considering the constraints that come from matching the dimensions of mating components and some other common assumptions (e.g., two balancing masses have the same width, two gear stages have the same face width), the number of independent design parameters is approximately 25 to 30. The designer must choose or search through these remaining independent design parameters to meet a desired set of performance requirements. This relatively large number of parameters is difficult to deal with at one time, and this difficulty usually results in a gear train design that meets the requirements but is less than optimal. Overcoming this difficulty is one of the primary motivations for this research and justifies the need for the design rules (Chapters 5 and 6) that illustrate the effect of parameter choices.

3.9.1 Key HGT Design Parameters

All of the intermediate and performance parameters can be written as functions of the key internal design parameters listed in Table 3.9. Unless otherwise specified, the following values (Table 3.10) will be held fixed and can be considered to be the assumptions for all of the HGT designs in this report. The axial clearance noted in the table is a simple approximation used to control the space between mating components (and also used to give the help the designer understand which components are fixed and which rotate in the HGT) and does not significantly affect the performance parameter results.

Table 3.10: HGT Assumptions

Parameter	Value
Pressure angle	$\phi=25^\circ$
Minimum tooth number difference	$N_{\min}=3$
Number of teeth in contact	3 (nominal load condition)
Efficiency	100%
Axial clearance	$c = 0.005D_g$
Diametral pitch range	$5 < P_d < 25$
Bending strength	$S_b=100$ ksi
Contact strength	$S_c=250$ ksi
Density	$\rho = 0.284$ lbm/in ³
Velocity Factor (K_v)	1.1
Load Distribution Factor (K_m)	1.3
Geometry Factor (J)	0.5
Output Speed (rpm)	1
Bearing Life	5000 hours

The following sections provide analytical equations to compute the intermediate and performance parameters of the HGT. As a preview, Table 3.11 details the gear ratio, torque, weight, and inertia written as functions of the design and intermediate parameters. Torque to weight (T_w) and torque to inertia (R) ratios can be obtained as ratios of these basic parameters. The torque capacity of the gear train is in general based on the gear that experiences the largest bending and contact stresses. In the HGT, the 2nd stage wobble gear is generally used to compute the torque capacity from the gear pitch diameter (d_{r2}) and face width (L_w) using the equation below. The weight and inertia terms contributed by the balancing masses can become quite complex if the two balancing masses commonly used have different radii and widths. However, if some of the dimensions are assumed to be equal for the two masses, the weight and inertia equations can be greatly simplified. It should be noted that the balancing weight is not

generally significant compared to the weight of other HGT components, but the balancing inertia can be significant.

Table 3.11: Summary of HGT Design and Performance Parameter Relationships

Parameter	Equation
Gear Ratio	$g = \frac{N_{w1}N_{r2}}{N_{w2}N_{r1} - N_{w1}N_{r2}} = \frac{d_{w1}d_{r2}}{d_{w2}d_{r1} - d_{w1}d_{r2}}$
Torque	$T_{hgt} = \frac{S_b d_{r2} L_w J}{2P_d K_v K_s K_o K_m K_b S} \text{ (bending stress-limited)}$
Weight	$W_{hgt} = W_w + W_{es} + W_o + W_{sh} + W_{bm1} + W_{bm2} + W_{bearing}$ $W_{hgt_app} = k \frac{\rho \pi D_g^2 L_g}{4}$
Inertia	$I_{hgt} = I_{es} + \frac{I_w}{g_1^2} + W_w e^2 + \frac{I_o}{g^2} + I_{bm1} + I_{bm2} + I_{bearings}$

3.9.2 Eccentricity and Gear Ratio

The eccentricity (e), defined graphically in Figure 3.18 as the distance between the wobble gear centerline and actuator centerline, is a key design parameter in the HGT. It determines the achievable gear ratio of the system and also affects the geometry of the shaft, bearings, balancing masses, and shell.

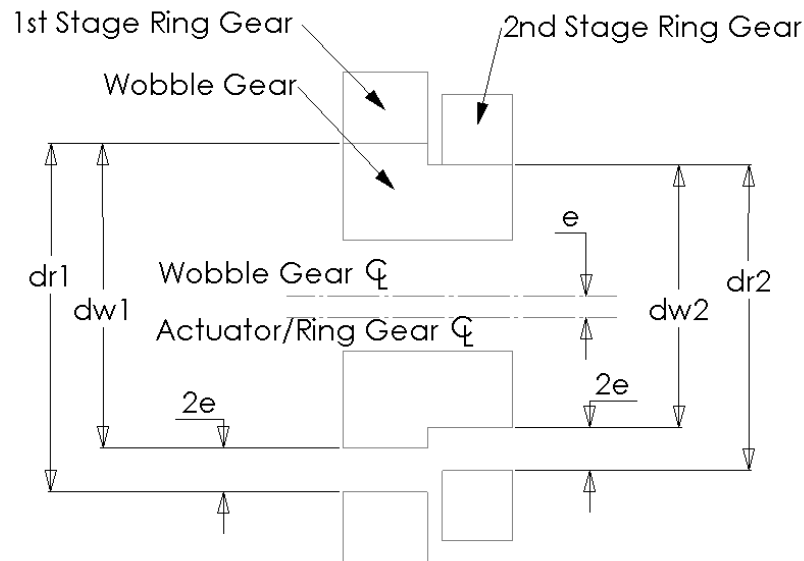


Figure 3.18: Eccentricity (e) of the HGT

The following relationships must hold for the gears in the HGT to mesh properly and perform as designed.

$$\begin{aligned}
 2e &= d_{r1} - d_{w1} \\
 2e &= d_{r2} - d_{w2}
 \end{aligned}
 \tag{Eqn. 92}$$

These equations must be satisfied as equalities when designing the HGT. From the force analysis documented in Vaculik and Tesar [2004], it is clear that decreasing the eccentricity increases the input force available to the gear train for a given motor input torque, which increases the output torque of the gear train. However, for very small eccentricities, gear mesh efficiency is sacrificed, the pitch diameters of the wobble gear are almost identical to those of their respective ring gears, and this can lead to interference, tolerance, and deformation concerns.

For prototyping purposes, it is important to compare the magnitude of the eccentricity to the tooth height and tolerance values for the gear teeth, bearings, and other machined components. A recent HGT prototype effort had a tooth height equal to

approximately one half of the eccentricity, and this resulted in significant tolerance errors in the location of the eccentric relative to the gear train centerline.

The gear ratio between the wobble gear and 1st stage ring gear is

$$g_1 = \frac{d_{w1}}{2e} \quad \text{Eqn. 93}$$

The overall gear ratio between the input shaft and output (2nd stage) ring gear is given by the following equation.

$$g = \frac{d_{w1}d_{r2}}{d_{w2}d_{r1} - d_{w1}d_{r2}} = \frac{N_{w1}N_{r2}}{N_{w2}N_{r1} - N_{w1}N_{r2}} \quad \text{Eqn. 94}$$

The recommended minimum tooth number differences between the wobble gear and 1st stage ($N_{r1} - N_{w1}$) or 2nd stage ($N_{r2} - N_{w2}$) ring gears is generally assumed to be 2 or 3. Current and future research on interference issues in the HGT may support or modify this assumption. These gear ratio and tooth number difference constraints were implemented in a computational environment (Appendix A1) to efficiently identify and search among all of the tooth number combinations that satisfy a desired gear ratio.

At this point, it is important to revisit the diametral pitch parameter (P_d) introduced in Section 3.5.2. When the designer is trying to maximize the gear ratio for a given diameter (d_{r2}) constraint, larger tooth numbers are often required to increase the product in the numerator of the gear ratio expression, and this results in relatively higher diametral pitches (i.e., narrower teeth).

3.9.3 Geometry Relationships

Figure 3.19 displays the overall length (L_g) and diameter (D_g) parameters of the reference HGT design.

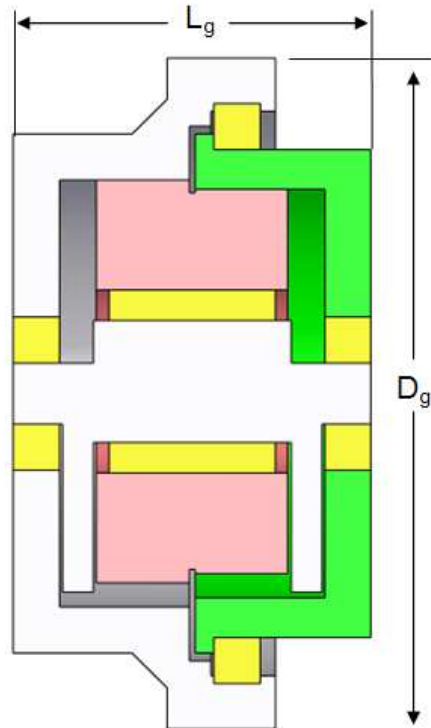


Figure 3.19: HGT Overall Length and Diameter Parameters

Given the overall diameter D_g , the 2nd stage ring gear diameter can be computed from the following equation.

$$d_{r2} = kD_g \quad \text{Eqn. 95}$$

The factor k in this equation is typically between 0.65 and 0.75 for the standard HGT design (in which the output bearing is directly over the output gear mesh as in Figure 3.15) and typically between 0.75 and 0.85 for an HGT design in which the output bearing is moved to the right of the output gear mesh to obtain a more cylindrical design (refer to the Kendrick and Tesar [2006] design, shown in Chapter 1, Figure 1.3). These proportions are chosen in order to maximize the torque capacity of the gear train while trying to ensure adequate space for the output bearing.

Following the development in the general gear train modeling Sections 3.5.6-3.5.8, the minimum ring gear outer (rim) diameters to prevent deformation are given by the following equations.

$$d_{ro1} = k \left(d_{r1} + \frac{7.9}{P_d} \right)$$

$$d_{ro2} = k \left(d_{r2} + \frac{7.9}{P_d} \right)$$

Eqn. 96

The diameter d_{ro1} is a reference dimensions that can be used to determine the outer diameter of the shell, while d_{ro2} can be used in determining the inner diameter of the output bearing.

The maximum wobble gear bore diameter is given by the following equation.

$$d_{wb} = k \left(d_{w2} - \frac{7.9}{P_d} \right)$$

Eqn. 97

These bore and rim diameters are consistent with AGMA standards (for involute teeth) and are chosen to ensure adequate thickness behind the teeth to prevent deformation of the gear rim. The k factors are included for the designer to manually adjust these settings for circular arc teeth based on the needs of the application.

Using the overall length as L_g , the width of one stage of the wobble gear can be computed from the following equation.

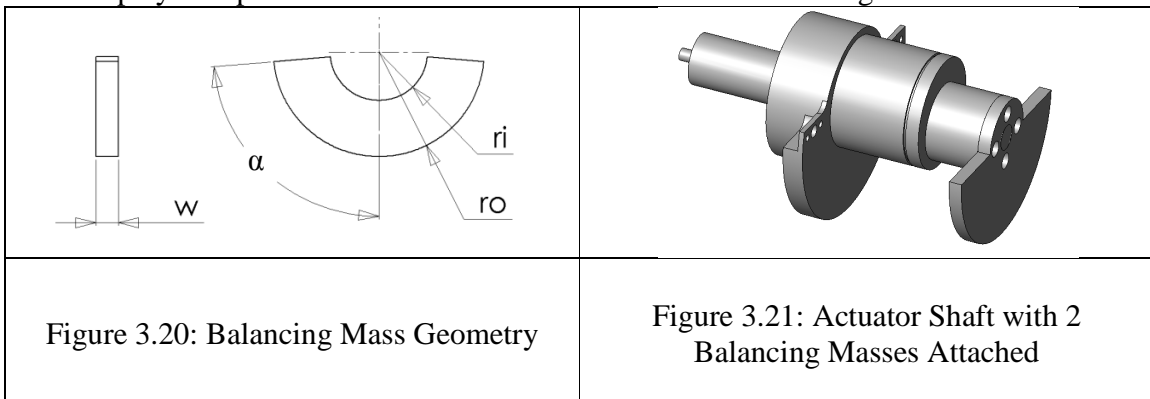
$$L_w = kL_g$$

Eqn. 98

The factor k in this equation is typically between 0.25 and 0.40, depending upon the desired geometry of the design (i.e., more cylindrical or more pancake) and the width of the balancing masses.

3.9.4 Balancing Mass Model

Because the wobble gear, wobble gear bearing, and eccentric shaft are offset from the centerline of the gear train, balancing masses are necessary to ensure static and dynamic balance of the rotating components. Appendix A3 details the balancing mass model used to determine the required balancing mass sizes and compute their weight (W_{bm}) and inertia (I_{bm}). Figure 3.20 details the general shape of the balancing masses used to balance the eccentrically mounted shaft, bearings, and wobble gear, and Figure 3.21 displays a representative eccentric shaft on which the balancing masses are mounted.



3.9.5 Weight and Inertia Computations

Since all of the HGT components can be modeled as either hollow or solid cylinders, their weight and inertia can be computed simply using the general modeling equations developed at the beginning of this chapter. For a detailed listing of the specific equations for each component, the reader is referred to the computer code discussed in Appendix A1.

3.9.6 Total Weight

The weight of the HGT (W_{hgt}) can be defined as the sum of the weights of its components.

$$W_{hgt} = W_w + W_{es} + W_o + W_{sh} + W_{bm1} + W_{bm2} + W_{bearings} \quad \text{Eqn. 99}$$

For a quick estimate of the HGT weight knowing only the overall diameter D_g and length L_g , the following equation can be used.

$$W_{hgt_app} = k \frac{\rho \pi D_g^2 L_g}{4} \quad \text{Eqn. 100}$$

Here, k is generally from 70 to 80%. This approximate weight calculation is accurate enough for the preliminary design stage.

3.9.7 Total Inertia

The inertia of the HGT reflected to the input shaft (I_{hgt}) can be defined as the sum of the inertias of its components, using the appropriate gear ratios (g , g_1) to reflect some of the inertias to the input.

$$I_{hgt} = I_{es} + \frac{I_w}{g_1^2} + W_w e^2 + \frac{I_o}{g^2} + I_{bm1} + I_{bm2} + I_{bearings} \quad \text{Eqn. 101}$$

3.10 PARALLEL ECCENTRIC GEAR TRAIN (PEGT)

The parallel eccentric gear train is similar in form to the Nabtesco gear train [Nabtesco, 2008] but employs circular arc gear teeth meshes between the PE gear and output gear, while Nabtesco utilizes pins in place of gear teeth on the output gear. The reference PEGT designs used for this report are shown in Figure 3.22 and Figure 3.23, depending upon whether a star (Figure 3.24) or star compound gear train (Figure 3.25) is used for the first stage (front end) of the gear train. Table 3.12 provides a listing of the design parameters (classified by component) that can be used to completely specify the geometry of these reference designs (Appendix A1).

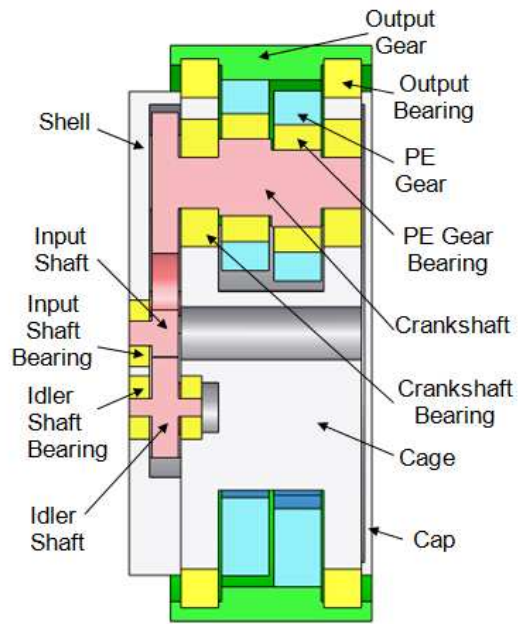


Figure 3.22: Star+PEGT Reference Design

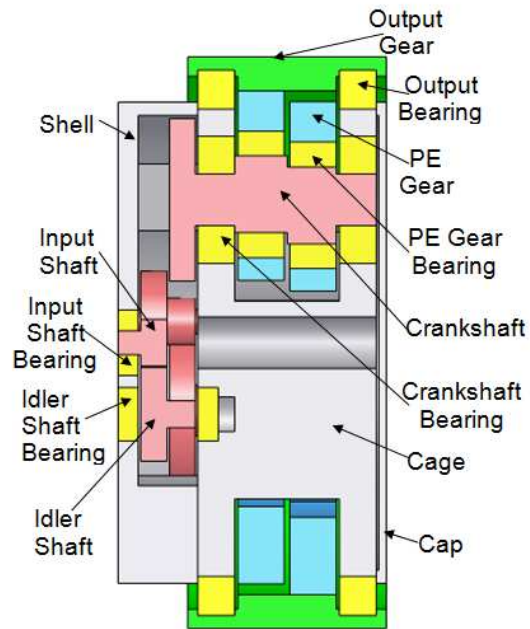


Figure 3.23: Star Compound+PEGT Reference Design

Table 3.12: PEGT Design Parameters Classified by Component (for generating reference design)

Component	Design Parameters
PE gear	$d_{pe}, L_{pe}, d_{peb}, c_c, d_{pec}, r_{pec}, L_{pec1}, L_{pec2}$
Cage	$L_{c1}, L_{c2}, L_{c4}, c_c, c_i, d_{c1}, d_{c2}, d_{c3}, d_{c4}, d_{ci}, d_{cc}, r_{cc}, L_{cc1}, L_{cc2}, \theta$
Output gear	$L_{o1}, L_{o2}, L_{o3}, c, d_{o1}, d_{o2}, d_{o3}(d_r), d_{o4}$
Input shaft	$L_{ms1}, L_{ms2}, d_{ms1}, d_{ms2}(d_{sun})$
Idler shaft (Star)	$L_{is1}, L_{is2}, d_{is1}, d_{is2}(d_p)$
Idler shaft (Star Compound)	$L_{is1}, L_{is2}, L_{is3}, d_{is1}, d_{is2}(d_{p1}), d_{is3}(d_{p2})$
Crank shaft	$L_{cs1}, L_{cs2}, L_{cs3}, L_{cs4}, L_{cs5}, d_{cs1}(d_{o2}), d_{cs2}, d_{cs3}, d_{cs4}, d_{cs5}, e$
Output bearing	ID_output_bearing, OD_output_bearing, W_output_bearing
PE gear bearing	ID_PE_gear_bearing, OD_PE_gear_bearing, W_PE_gear_bearing
Crank shaft bearing	ID_crank_shaft_bearing, OD_crank_shaft_bearing, W_crank_shaft_bearing
Idler shaft bearing	ID_idler_shaft_bearing, OD_idler_shaft_bearing, W_idler_shaft_bearing
Input shaft bearing	ID_input_shaft_bearing, OD_input_shaft_bearing, W_input_shaft_bearing
Shell	$L_{s1}, L_{s2}, L_{s3}, L_{s4}, d_{s1}, d_{s2}, d_{s4}, d_{s5}, d_{si}, c_i, r_{sm}, \theta$
Cap	$L_{cp1}, L_{cp2}, d_{cp1}, d_{cp2}$

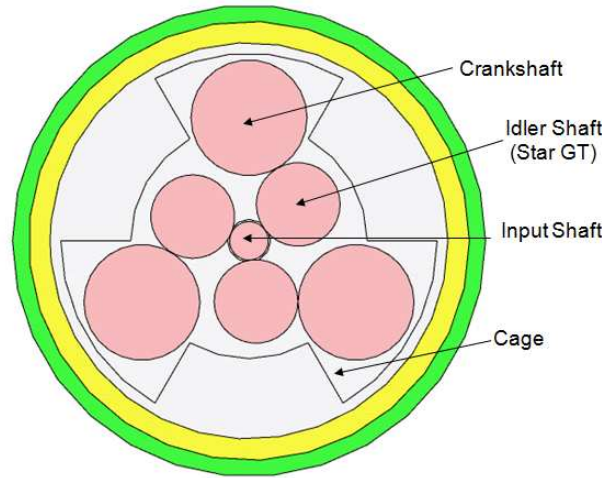


Figure 3.24: Star Gear Train (1st Stage) for PEGT

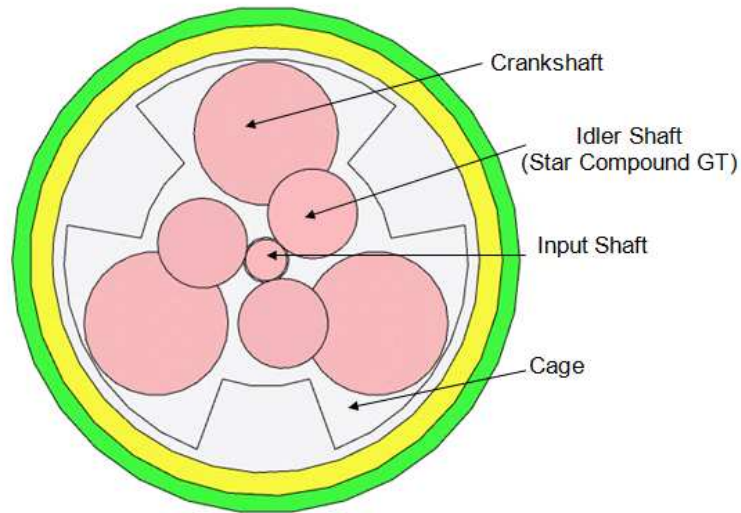


Figure 3.25: Star Compound Gear Train (1st Stage) for PEGT

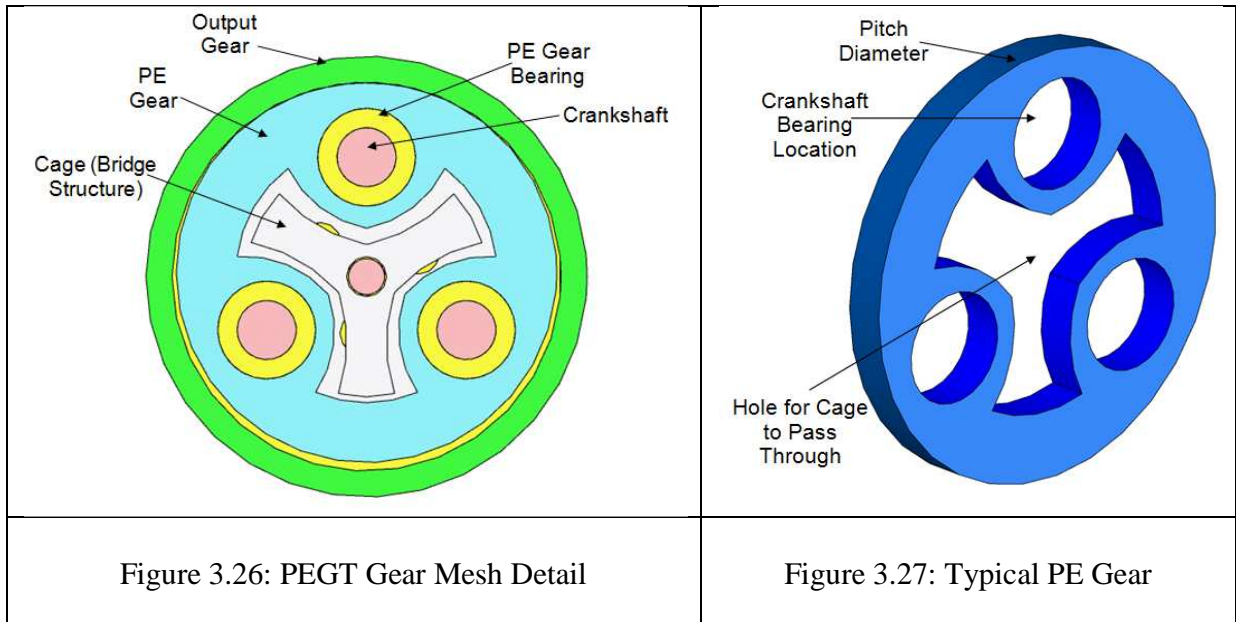
The input torque from the motor drives the input shaft (on which the sun gear is mounted), which meshes with the planet gear on the idler shaft. This planet gear (or additional smaller diameter planet for the star compound gear train) meshes with the crankshaft gear mounted on the crankshaft. Two PE gears are eccentrically mounted on the 3 crankshafts and drive the output ring gear, which provides the desired output torque and speed from the actuator.

The geometric foundation for this model comes from Sigwald and Tesar [2008] and has been under development in the RRG for over 2 years. A prototype based on the PEGT (Figure 3.22) is currently under development [Tesar et al., 2008].

Figure 3.26 illustrates the PEGT gear mesh detail, and Figure 3.27 displays the PE gear. Table 3.13 lists the internal design, intermediate, and performance parameters discussed in this section.

Table 3.13: PEGT Parameters (Discussed in this section)

Key Internal Design Parameters	Intermediate Parameters	Performance Parameters
Gear pitch diameters d_r ring gear d_{pe} PE gear d_s sun (Star and SC) d_p planet (Star) d_o crankshaft gear (Star) d_{p1} planet 1 (SC) d_{p2} planet 2 (SC) d_{o2} crankshaft gear (SC) Gear face widths L_{pe} PE gear face L_1 SC 1 st stage L_2 SC 2 nd stage (or Star) e Eccentricity Diametral pitch P_{d_min} Minimum P_{d_max} Maximum θ Offset angle for idler shaft Numbers of teeth (PE Gear) N_r ring N_{pe} PE gear Numbers of teeth (Front End) N_s sun (Star and SC) N_p planet (Star) N_o crankshaft/output (Star) N_{p1} sun (SC) N_{p2} planet (SC) N_{o2} crankshaft/output (SC) Gear ratios g_1 Front end g_{pe} PEGT g Overall ϕ Pressure angle S_b Bending strength S_c Contact strength	Rim diameters d_{ro} output gear stage rim d_{perim} PE gear Weights W_{pe} PE gear W_o output gear W_{cs} crankshaft W_{is} idler shaft W_{ms} input (motor) shaft W_{sh} shell W_c cage W_{cp} cap $W_{bearings}$ bearings Inertias I_{pe} PE gear I_o output gear I_{cs} crankshaft I_{is} idler shaft I_{ms} input (motor) shaft $I_{bearings}$ bearings	T_{pegt} Torque capacity W_{pegt} Weight (total) I_{pegt} Inertia (total)



There are a total of 84 design parameters needed to completely describe the geometry of the reference PEGT in Figure 3.23. Considering the constraints that come from matching the dimensions of mating components and some other common assumptions (e.g., same face widths for both PE gears, same face widths for both 1st stage gears), the number of independent design parameters is approximately 50 to 60. The designer must choose or search through these remaining independent design parameters to meet a desired set of performance requirements. This relatively large number of parameters is difficult to deal with at one time, and this difficulty usually results in a gear train design that meets the requirements but is less than optimal. Overcoming this difficulty is one of the primary motivations for this research and justifies the need for the design rules (Chapters 5 and 6) that illustrate the effect of parameter choices.

3.10.1 Key PEGT Design Parameters

All of the intermediate and performance parameters can be written as functions the key internal design parameters listed in Table 3.13. Unless otherwise specified, the

following values (Table 3.14) will be held fixed and can be considered to be the assumptions for all of the PEGT designs in this report.

Table 3.14: PEGT Assumptions

Parameter	Value
Pressure angle	$\phi=25$
Minimum tooth number difference	$N_{\min}=3$
Number of teeth in contact	3 (nominal load condition)
Diametral pitch range	$5 < P_d < 25$
Bending strength	$S_b=100$ ksi
Contact strength	$S_c=250$ ksi
Efficiency	100%
Axial clearance	$c = 0.005D_g$
Density	$\rho = 0.284$ lbm/in ³
Bearing Life	5000 hours

The following sections provide analytical equations to compute the intermediate and performance parameters of the PEGT. As a preview, Table 3.15 details the gear ratio, torque, weight, and inertia written as functions of the design and intermediate parameters. These equations are suitable for direct implementation into a computer environment.

The load capacities of the 1st stage star and star compound gear train portions of this system are typically limited by the bending and contact stresses in the gear teeth (usually based on using involute teeth). However, since the PE gear-output gear mesh and supporting bearings usually limit the overall torque capacity of the design, the 1st stage gear train must always meet the geometric constraints imposed by PE gear and its supporting components before it is designed to meet any material stress limits. In most cases, this means that the 1st stage is oversized and has a larger safety factor than the PE-output gear mesh.

Table 3.15: Summary of PEGT Design and Performance Parameter Relationships

Parameter	Equation
Gear Ratio	$g = g_1 g_{pe} = \frac{N_o}{N_s} \frac{N_r}{(N_r - N_{pe})} = \frac{d_o}{d_s} \frac{d_r}{(d_r - d_{pe})} \text{ (Star)}$ $g = g_1 g_{pe} = \frac{N_{o2} N_{p1}}{N_{p2} N_s} \frac{N_r}{(N_r - N_{pe})} = \frac{d_{o2} d_{p1}}{d_{p2} d_s} \frac{d_r}{(d_r - d_{pe})} \text{ (SC)}$
Torque	$T_{\text{pegt}} = \frac{S_b d_{pe} L_{pe} J}{2 P_d K_v K_s K_o K_m K_b S} \text{ (bending stress-limited)}$
Weight	$W_{\text{pegt}} = 2W_{pe} + W_o + 3W_{cs} + 3W_{is} + 3W_{ms} + W_{sh} + W_c + W_{cp} + W_{\text{bearing}}$ $W_{\text{pegt_app}} = k \frac{\rho \pi D_g^2 L_g}{4}$
Inertia	$I_{\text{pegt}} = \frac{I_o}{g^2} + \frac{2I_{pe} + 2W_{pe} e^2 + I_{cs}}{g_1^2} + I_{is} \left(\frac{d_{\text{sun}}}{d_p} \right)^2 + I_{ms} + I_{\text{bearings}} \text{ (Star)}$ $I_{\text{pegt}} = \frac{I_o}{g^2} + \frac{2I_{pe} + 2W_{pe} e^2 + I_{cs}}{g_1^2} + I_{is} \left(\frac{d_{\text{sun}}}{d_{p1}} \right)^2 + I_{ms} + I_{\text{bearings}} \text{ (SC)}$

While the HGT torque capacity is limited by the gear teeth stresses, the PEGT torque capacity is also sometimes limited by the load capacity of the crankshaft and PE gear bearings. The detailed derivation of the forces on these bearings as a function of the output torque capacity has been documented by Sigwald and Tesar [2008] and implemented in the computer code described in Appendix A1. Once these forces are known, they can be used with the standard (industry-accepted) bearing life equation to compute the required bearing load capacity that achieves a desired torque value. A more detailed discussion of bearing life will be provided later in this chapter, but as a preview, designating the known radial force on the bearing as P, the required load capacity C for life L (hours) and speed ω (rpm) is as follows.

$$C = P \left(\frac{60L\omega}{10^6} \right)^{1/n} \quad \text{Eqn. 102}$$

Here, n is a function of the bearing type with $n=3$ for ball bearings and $n=10/3$ for roller bearings. The constants in this equation are used for unit consistency. Note that because the speed is included in this relationship, the operating speed of the PEGT must be known in order to accurately quantify its torque capacity. For this reason, some of the PEGT torque specifications in this report (Section 5.2.3.1) will have an output speed attached to it.

There is a desire to increase the bearing-limited torque capacity and bring it up to the gear-tooth limited load capacity level. Given this desire, the approach taken in this research will report (Sections 5.2.3, 5.2.4, 6.5.2, and 6.5.3) the tooth limited load capacity (T_{pegt}) and then compute the required bearing load capacities (C) to achieve this torque capacity. Then, a designer can use the results of this research to search among available bearings that the meet the given load capacity and space requirements.

3.10.2 1st Stage Geometry and Gear Ratio

Referring to Figure 3.28 and Figure 3.29, the 1st stage gear ratios for the star and star compound options, respectively, are as follows.

$$g_1 = \frac{N_o}{N_s} = \frac{d_o}{d_s} \text{ (Star)} \quad \text{Eqn. 103}$$

$$g_1 = \frac{N_{o2}N_{p1}}{N_{p2}N_s} = \frac{d_{o2}d_{p1}}{d_{p2}d_s} \text{ (StarCompound)} \quad \text{Eqn. 104}$$

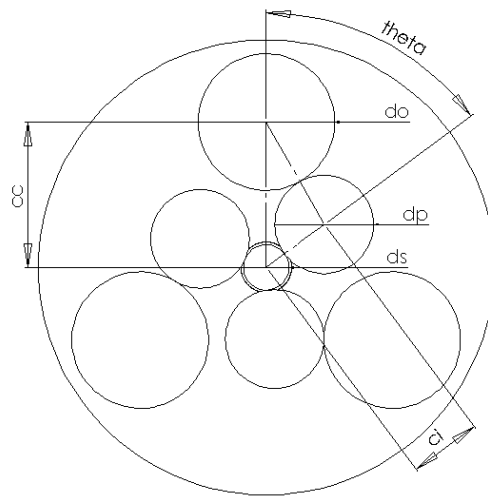


Figure 3.28: 1st Stage Star Gear Train for PEGT with Labeled Gear Sizes

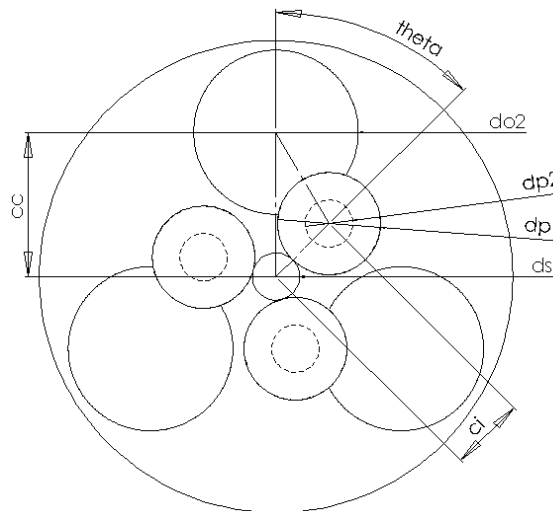


Figure 3.29: 1st Stage Star Compound Gear Train for PEGT with Labeled Gear Sizes

The offset angle (θ) can be modified to achieve the desired 1st stage gear ratio. Offset angles between 45 and 55 degrees typically result in the highest gear ratios while still ensuring adequate spacing between the three idler gears.

3.10.3 PEGT Eccentricity and Gear Ratio

The eccentricity (e), defined graphically in Figure 3.30 as the distance between the crankshaft centerline and the eccentric lobe centerline (also shown in Figure 3.26), is a key design parameter in the PEGT. It determines the achievable gear ratio of the system and also affects the geometry of the crankshaft, crankshaft and PE gear bearings, and PE gear.

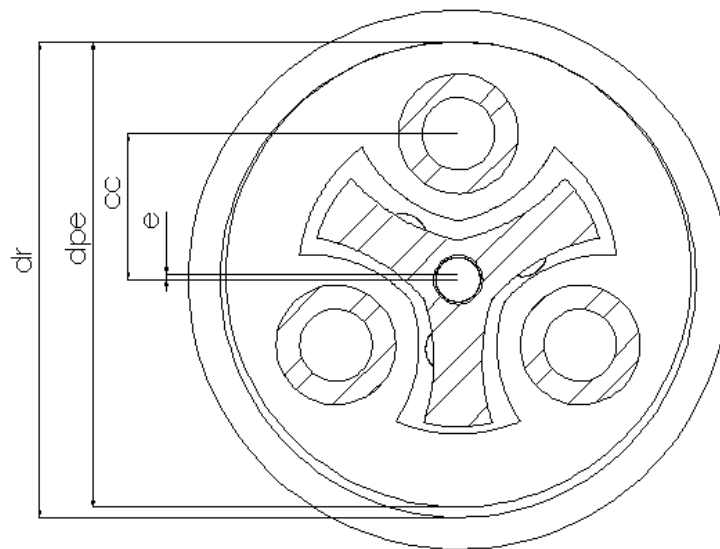


Figure 3.30: Eccentricity (e) of the PEGT

The following relationship must hold for the PE gear and output gear to mesh properly and perform as designed:

$$2e = d_r - d_{pe} \quad \text{Eqn. 105}$$

The PEGT gear ratio (not including the 1st stage gear train) is given by the following equation.

$$g_{pe} = \frac{N_r}{(N_r - N_{pe})} = \frac{d_r}{(d_r - d_{pe})} \quad \text{Eqn. 106}$$

Like the HGT, the minimum tooth number differences between the PE gear and output ring gear ($N_r - N_{pe}$) is 2 or 3 because the relative motions between the mating circular arc gears in the HGT and PEGT are identical.

The overall gear ratio can be written as the product of the 1st stage and PE gear mesh ratios.

$$g = g_1 g_{pe} \quad \text{Eqn. 107}$$

3.10.4 Geometry Relationships

Figure 3.31 shows the overall length (L_g) and diameter (D_g) of the reference PEGT design.

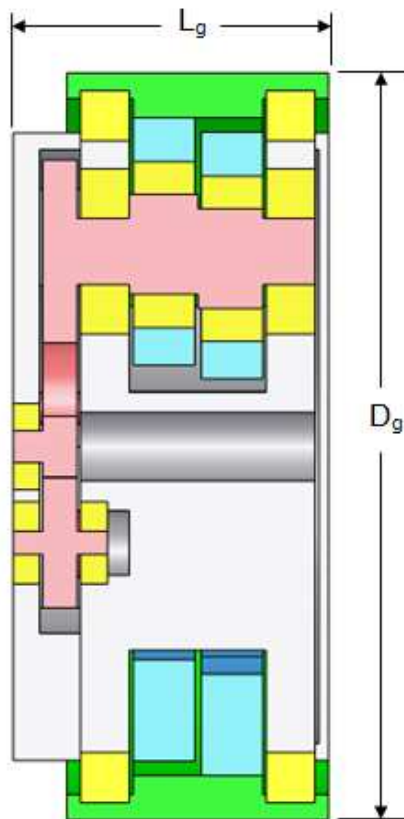


Figure 3.31: PEGT Overall Length and Diameter Parameters

Using the overall diameter D_g , the output ring gear diameter can be obtained from the following.

$$d_r = kD_g \quad \text{Eqn. 108}$$

The factor k in this equation is typically between 0.80 and 0.90 for the standard PEGT design (in which the output bearings are located as shown in Figure 3.22). This proportion is chosen in order to maximize the torque capacity of the gear train while trying to ensure adequate space and ease of assembly for the output bearings.

Following the development in the general gear train modeling Sections 3.5.6-3.5.8, the minimum ring gear outer diameter is given by the following equation.

$$d_{ro} = k \left(d_r + \frac{7.9}{P_d} \right) \quad \text{Eqn. 109}$$

The diameter d_{ro} should be checked against the outer diameter D_g .

The maximum PE gear bore diameter is given by the following.

$$d_{perim} = k \left(d_r - \frac{7.9}{P_d} \right) \quad \text{Eqn. 110}$$

The k factors are included for the designer to manually adjust these settings based on the needs of the application.

The center distance (c_c) between the gear train centerline and the crankshaft centerline (Figure 3.28) should be maximized in order to provide the largest moment arm for the bearings mounted on the crankshaft and therefore the highest possible torque capacity. However, there is also a need for large diameter bearings (which decreases the center distance) to ensure the bearings have adequate load capacity. This conflict has been considered for a variety of different sizes of PEGT designs, with the following suggested relationship between the center distance and overall diameter (D_g).

$$c_c = kD_g \quad \text{Eqn. 111}$$

Typical values of k used have been between 0.25 and 0.35 for past designs, and these have simultaneously provided a large moment arm c_c and also adequate space for the bearings on the crankshaft.

Designating the overall gear train length as L_g , the width of the PE gear (L_{pe}) can be estimated from the following equation.

$$L_{pe} = kL_g \quad \text{Eqn. 112}$$

The factor k in this equation is typically between 0.20 and 0.25, allowing adequate space for the 1st stage gear train, cage structure, and 2 PE gears and depending upon the desired geometry of the design (i.e., more cylindrical or more pancake). In past designs, the 1st stage gear face widths (L_1, L_2) have typically been required to be from 40 to 60% of L_{pe} in order to stay within bending and contact stress limits, and these proportions will also be used in this research.

The center distance (c_i) between the gear train centerline and the idler shaft centerline (Figure 3.28) is also an important designer choice. In general, this parameter should be maximized to provide adequate spacing between the input shaft and idler shaft bearing mounting locations in the PEGT shell (Figure 3.22).

In order to compute the gear ratio of the 1st stage, reasonable values of the input shaft diameter need to be specified by the designer. In general, a lower sun gear (i.e., input gear for the PEGT) pitch diameter limit of 1 inch can be assumed because gear manufacturing becomes more difficult and non-standard as the gear sizes becomes less than this. This suggests that the input shaft diameter range anywhere from 0.50 inches up to an unspecified upper limit that depends on the application. The designer should note that the input shaft diameter also dictates the input shaft bearing sizes.

3.10.5 Weight and Inertia Computations

Since all of the PEGT components can be modeled as either hollow or solid cylinders, their weight and inertia can be computed simply using the general modeling equations developed at the beginning of this chapter. For a detailed listing of the specific equations for each component, the reader is referred to the computer code in Appendix A1.

3.10.6 Total Weight

The weight of the PEGT (W_{pegt}) can be defined as the sum of the weights of its components (assuming 2 PE gears and 3 crankshafts).

$$W_{\text{pegt}} = 2W_{pe} + W_o + 3W_{cs} + 3W_{is} + 3W_{ms} + W_{sh} + W_c + W_{cp} + W_{bearing} \quad \text{Eqn. 113}$$

For a quick estimate of the PEGT weight knowing only the overall diameter D_g and length (L_g), the following equation can be used.

$$W_{\text{pegt_app}} = k \frac{\rho \pi D_g^2 L_g}{4} \quad \text{Eqn. 114}$$

Here, k is generally from 70 to 80%. This approximate weight calculation is accurate enough to develop preliminary gear train designs.

3.10.7 Total Inertia

The inertia of the PEGT reflected to the input shaft (I_{pegt}) can be defined as the sum of the following terms, grouped according to the gear ratios used to reflect it to the input shaft.

$$I_{\text{pegt}} = \frac{I_o}{g^2} + \frac{2I_{pe} + 2W_{pe}e^2 + I_{cs}}{g_1^2} + I_{is} \left(\frac{d_{\text{sun}}}{d_p} \right)^2 + I_{ms} + I_{bearings} \quad \text{(Star)} \quad \text{Eqn. 115}$$

$$I_{\text{pegt}} = \frac{I_o}{g^2} + \frac{2I_{pe} + 2W_{pe}e^2 + I_{cs}}{g_1^2} + I_{is} \left(\frac{d_{\text{sun}}}{d_{p1}} \right)^2 + I_{ms} + I_{bearings} \quad \text{(SC)}$$

3.11 SRM+HGT

The reference SRM+HGT actuator design used for this report is shown in Figure 3.32. Table 3.16 provides a listing of the design parameters (classified by component) that can be used to completely specify the geometry of this reference design (Appendix A1). The individual SRM and HGT model development above can be used to compute the torque, weight, inertia, and other parameters of this design.

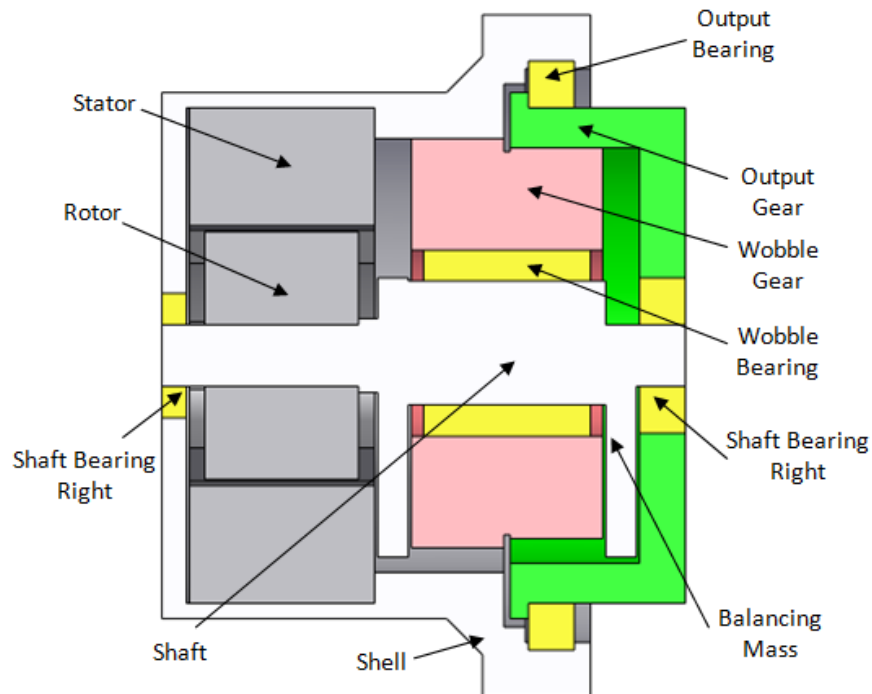


Figure 3.32: SRM+HGT Reference Design

Table 3.16: SRM+HGT Design Parameters Classified by Component (for generating reference design)

Component	Design Parameters
Rotor	$d_r, d_{rb}, d_b, \theta_r, t_r, h_r, L_s$
Stator	$d_s, d_{sb}, d_{si}, \theta_s, t_s, h_s, L_m$
Wobble gear	$d_{w1}, d_{w2}, d_{wb}, d_{wo}, L_w$
Output gear	$d_{r2}, L_{o1}, L_{o2}, L_{o3}, d_{o1}, d_{o2}, d_{o3}$
Shaft (including balance masses)	$L_1, L_2, L_3, L_4, L_5, d_1, d_2, d_3, d_4, d_5, e, r_{o1}, r_{o2}, w$
Output bearing	ID_output_bearing, OD_output_bearing, W_output_bearing
Wobble bearing	ID_wobble_bearing, OD_wobble_bearing, W_wobble_bearing
Shaft bearing right	ID_shaft_bearing_right, OD_shaft_bearing_right, W_shaft_bearing_right
Shaft bearing left	ID_shaft_bearing_left, OD_shaft_bearing_left, W_shaft_bearing_left
Shell	$d_{r1}, L_{s1}, L_{s2}, L_{s3}, L_{s4}, L_{s5}, L_{s6}, L_{s7}, d_{s1}, d_{s2}, d_{s4}, d_{s5}, d_{s6}, d_{s7}, d_{s8}, d_{s9}$

3.12 SRM+PEGT

The reference SRM+PEGT designs used for this report are shown in Figure 3.33 and Figure 3.34, depending upon whether a star or star compound gear train are used for the first stage of the gear train. Table 3.17 provides a listing of the design parameters (classified by component) that can be used to completely specify the geometry of these reference designs (Appendix A1). The individual SRM and PEGT model sections can be used to compute the torque, weight, inertia, and other parameters of this design.

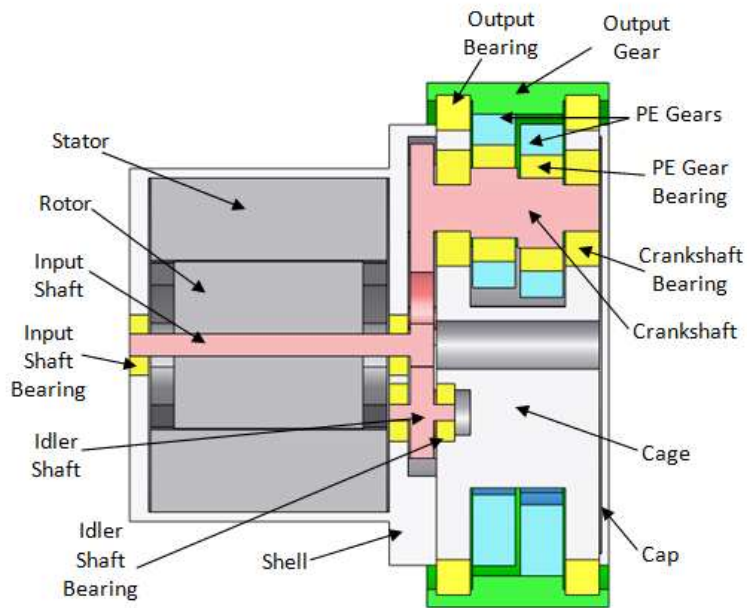


Figure 3.33: SRM+Star+PEGT Reference Design

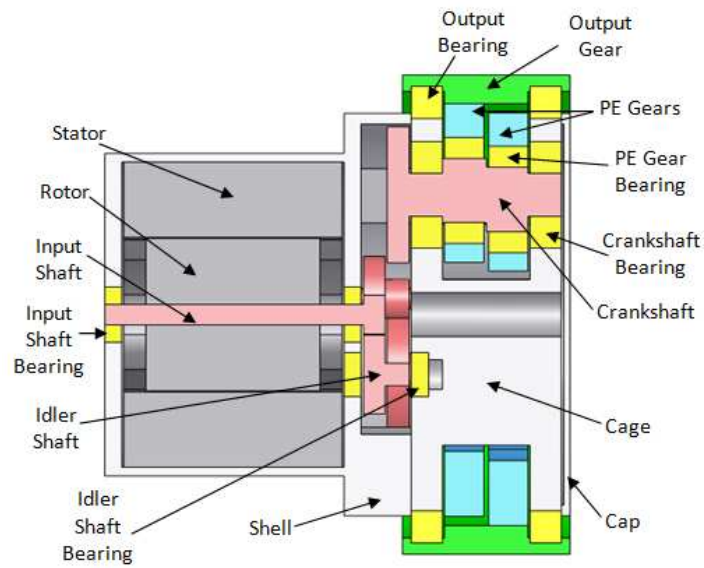


Figure 3.34: SRM+Star Compound+PEGT Reference Design

Table 3.17: SRM+PEGT Design Parameters Classified by Component (for generating reference design)

Component	Design Parameters
Rotor	$d_r, d_{rb}, d_b, \theta_r, t_r, h_r, L_s$
Stator	$d_s, d_{sb}, d_{si}, \theta_s, t_s, h_s, L_m$
PE gear	$d_{pe}, L_{pe}, d_{peb}, c_c, d_{pec}, r_{pec}, L_{pec1}, L_{pec2}$
Cage	$L_{c1}, L_{c2}, L_{c4}, c_c, c_i, d_{c1}, d_{c2}, d_{c3}, d_{c4}, d_{ci}, d_{cc}, r_{cc}, L_{cc1}, L_{cc2}, \theta$
Output gear	$L_{o1}, L_{o2}, L_{o3}, c, d_{o1}, d_{o2}, d_{o3}(d_r), d_{o4}$
Input shaft	$L_{ms1}, L_{ms2}, d_{ms1}, d_{ms2}(d_{sun})$
Idler shaft (Star)	$L_{is1}, L_{is2}, d_{is1}, d_{is2}(d_p)$
Idler shaft (Star Compound)	$L_{is1}, L_{is2}, L_{is3}, d_{is1}, d_{is2}(d_{p1}), d_{is3}(d_{p2})$
Crank shaft	$L_{cs1}, L_{cs2}, L_{cs3}, L_{cs4}, L_{cs5}, d_{cs1}(d_{o2}), d_{cs2}, d_{cs3}, d_{cs4}, d_{cs5}, e$
Output bearing	ID_output_bearing, OD_output_bearing, W_output_bearing
PE gear bearing	ID_PE_gear_bearing, OD_PE_gear_bearing, W_PE_gear_bearing
Crank shaft bearing	ID_crank_shaft_bearing, OD_crank_shaft_bearing, W_crank_shaft_bearing
Idler shaft bearing	ID_idler_shaft_bearing, OD_idler_shaft_bearing, W_idler_shaft_bearing
Input shaft bearing	ID_input_shaft_bearing, OD_input_shaft_bearing, W_input_shaft_bearing
Shell	$L_{s1}, L_{s2}, L_{s3}, L_{s4}, d_{s1}, d_{s2}, d_{s4}, d_{s5}, d_{si}, c_i, r_{sm}, \theta$
Cap	$L_{cp1}, L_{cp2}, d_{cp1}, d_{cp2}$

3.13 GEAR RATIO RANGES

Tesar [2006] discussed the fundamental importance of the gear ratio choice when coupling a motor and a gear train into an integrated actuator. The typical gear ratio range from the HGT is from 75 to 1 up to 500 to 1, depending upon the size (diameter) of the gear train. As the size of the HGT decreases, the suggested upper limit decreases because higher teeth numbers (and thus smaller teeth) are required, and these smaller teeth reduce the torque capacity of the gear mesh. Below the lower limit of approximately 75 to 1, the two distinct diameters on the wobble gear tend to become very different, and the wobble gear geometry becomes difficult to integrate with the eccentric shaft.

The typical gear ratio range from the PE gear-output gear mesh in the PEGT is from 15 to 1 up to 35 to 1, again depending upon the size of the gear train. The typical gear ratio range for star gear train (used as the 1st stage of the PEGT) is up to 4 to 1, while

star compound gear train (also used as the 1st stage of the PEGT) is up to 15 to 1. In general, higher gear ratios are possible for larger designs. Combining these individual limits, the PEGT can operate comfortably in gear ratios from 15 to 1 up to 500 to 1.

Chapter 5 and 6 will make objective comparisons between the PEGT and HGT with the same size and gear ratios in an attempt to provide some more concrete justification for these gear ratio ranges.

3.14 BEARING DESIGN AND SELECTION ISSUES

3.14.1 Bearing Life

The standard equation used to define the life (L) of a bearing (expressed in hours) is as follows.

$$L = \left(\frac{C}{P} \right)^n \frac{1}{\omega} 10^6 \quad \text{Eqn. 116}$$

In this relationship, C is the bearing dynamic load capacity (lbf), P is the equivalent radial load (lbf) on the bearing, and ω is the speed (rpm). The exponent n is a function of the bearing type with n=3 for ball bearings and n=10/3 for roller bearings. This equation applies for any bearing type and any loading combination if the designer combines radial, axial (thrust), and moment loads into an effective applied load (P). The load capacity (C) is the load which, if applied to the bearing, will result in failure of 10% of a group of identical bearings at 10^6 revolutions. The bearing speed used for life calculations is the relative rotational speed between the inner and outer races of the bearing.

This life relationship is based purely on experimental testing and is statistical in nature. For an identical group of bearings (i.e., same designed load capacity C) subjected to the same load, speed, and duty cycle, only 90% of the bearings will reach and exceed

the life determined by the relationship above. This fact must be kept in mind when specifying bearings for a given application.

For electromechanical actuator design (and in most cases), the applied loads (P), speed (ω), and duty cycle often follow directly from the design requirements and are usually fixed for a given actuator task. Given this observation, the only remaining design parameter is the bearing load capacity (C). Thus, the task of bearing selection/design is simply searching for a bearing that 1) has adequate load capacity to meet the desired life requirements and 2) meets the geometrical constraints of the system.

Because the bearing life computation requires the use of a single equivalent applied load value (P), any time-varying bearing loads need to be converted to an equivalent load. The root-mean cube is commonly used to compute the equivalent bearing load (P_m) as follows.

$$P_m = \sqrt[3]{\frac{P_1^3 t_1 + P_2^3 t_2 + \dots}{t}} \quad \text{Eqn. 117}$$

Here, load P_1 is the load applied to the bearing for time duration t_1 , P_2 for duration t_2 , etc., and t is the total length of time of interest. The PE gear and crankshaft bearing loads in the PEGT vary as a function of the location of the PE gear-output gear mesh (see Sigwald and Tesar [2008]), so this equivalent load relationship must be used to estimate their life.

For the purposes of calculating the life of a bearing with loads in the x and y directions, the resultant load (P_{res}) for a bearing can simply be calculated from its x (P_x) and y (P_y) components as follows.

$$P_{res} = \sqrt{P_x^2 + P_y^2} \quad \text{Eqn. 118}$$

The bearing life equation will be utilized to compute the required HGT and PEGT bearing load capacities to meet a designer-specified operating life in Sections 5.2 and 6.5.

The following few sections discuss bearing topics that will not be dealt with further because they are not critical in the preliminary design stage, the focus of the present research. However, future actuator design researchers should keep these concepts in mind.

3.14.2 Bearing Friction (Approximation)

The three types of friction present in bearings are lubricant friction, rolling friction, and sliding friction, and a detailed description of each can be found in Brandlein et al. [1999]. A simple expression that can be used to estimate the friction torque (M) in a given bearing arrangement with applied load P , coefficient of friction μ , and mean diameter (d_m) is:

$$M = \mu P d_m \quad \text{Eqn. 119}$$

The diameter (d_m) is the roller pitch diameter or mean diameter of a bearing and is defined as follows.

$$d_m = \frac{ID + OD}{2} \quad \text{Eqn. 120}$$

Here, OD and ID are the outer diameter and inner diameter of the bearing, respectively.

This equation can only be used if the following assumptions hold true for the bearing in question.

- The loading condition is such that $P/C < 0.1$.
- There is no additional stressing from tilting and/or radial/axial preload.
- Good lubrication/viscosity conditions exist, with a mean speed range from 0.3 to 0.7 times the kinematically permissible speed.
- The bearing does not have rubbing seals.

The first assumption ensures that the applied bearing load P is not too high relative to the bearing load capacity C . Despite the fact that this friction torque equation

is rarely used in practice, it still provides a useful qualitative relationship between friction, load, and diameter that can be used as a starting point for the design rules of this and future researches.

3.14.3 Bearing Friction

A more accurate estimate of bearing friction can be achieved if it is divided into two separate components: the load-independent moment (M_0) and the load-dependent moment (M_1) [Brandlein et al., 1999].

$$\begin{aligned} M_0 &= 10^{-7} f_0 (v\omega)^{2/3} d_m \\ M_1 &= f_1 P d_m \end{aligned} \quad \text{Eqn. 121}$$

In these expressions, f_0 and f_1 are friction factors based on the bearing type and loading condition, v is the viscosity, and ω is the bearing speed. The total friction torque (M) is then the sum of the two individual types.

$$M = M_0 + M_1 \quad \text{Eqn. 122}$$

If the bearing friction is relatively large compared to the output torque (i.e., greater than 10%) of the actuator, then means to reduce it should be taken by modifying the parameters in the above relationships.

3.14.4 Friction Power Loss

Using the frictional moment (M), the power loss (P_{loss}) due to bearing friction is as follows.

$$P_{\text{loss}} = M \omega \quad \text{Eqn. 123}$$

If the power lost due to bearing friction is significant compared to the total power output of the actuator, then means to reduce it (e.g., by reducing speed or modifying the design parameters that govern friction) should be taken.

3.15 SPEED AND LIFE LIMITS

It is important for the actuator designer to understand the phenomena that limit the speed and life of the three fundamental components in an EMA: the motor, gear train, and bearings.

3.15.1 Motors

In general, the motor speed is limited by a few factors. First, hoop stresses result in the rotor during operation, and these must remain well below the yield strength of the rotor material. Second, higher speeds mean higher switching frequencies for the stator windings (for a given size), and these higher switching frequencies lead to higher core losses and higher temperatures. Third, a given speed can only be achieved if the heat generated in the stator windings can be dissipated through the motor structure. Finally, a given motor has a well-defined torque-speed curve, and different points on the curve have different operating efficiencies. When an actuator designer is choosing the gear ratio (for a fixed gear train/output torque and speed), he/she is changing the motor torque and speed requirements and thus the available efficiency, and care must be taken to ensure that the desired speeds and efficiencies are achievable. Unlike bearings, there are no life ratings or life calculations suggested for motors. Ashok and Tesar [2002] provide a more detailed discussion of these issues, and the actuator designer should keep these in mind when choosing motor speeds.

3.15.2 Gear Trains

As discussed previously, the gear teeth bending and contact stresses are proportional to their operating speed through the effect of the velocity factor (K_v) and the pitch line velocity in the AGMA stress formulas (Sections 3.5.1 and 3.5.4). In addition, the bending and contact material fatigue strengths are proportional to number of cycles of

operation (see Norton [2000] or any standard machine design text). A given material used in a particular application will begin to fatigue at a fixed number of cycles. If the designer chooses to run a gear train at a higher speed (i.e., higher pitch line velocities), the bending and contact stresses will be increased (due to K_v), and the fixed number of cycles to failure will be reached sooner, both of which are undesirable. This conclusion is based on the use of involute teeth, and Park and Tesar [2005] discuss how the circular arc teeth can mitigate some of these undesirable effects.

3.15.3 Bearings

Referring to the standard bearing life formula in Section 3.14.1, and assuming that the load capacity (C) and applied load (P) are known, the life of a bearing is directly proportional to the desired number of cycles of operation. If the designer chooses to operate a given bearing at a higher speed, the bearing will reach a given number of cycles sooner in its lifetime.

The lubrication method chosen directly affects the maximum permissible linear (peripheral) velocity (V_{\max}) of a bearing. Figure 3.35 provides suggested maximum velocities for different lubrication methods.

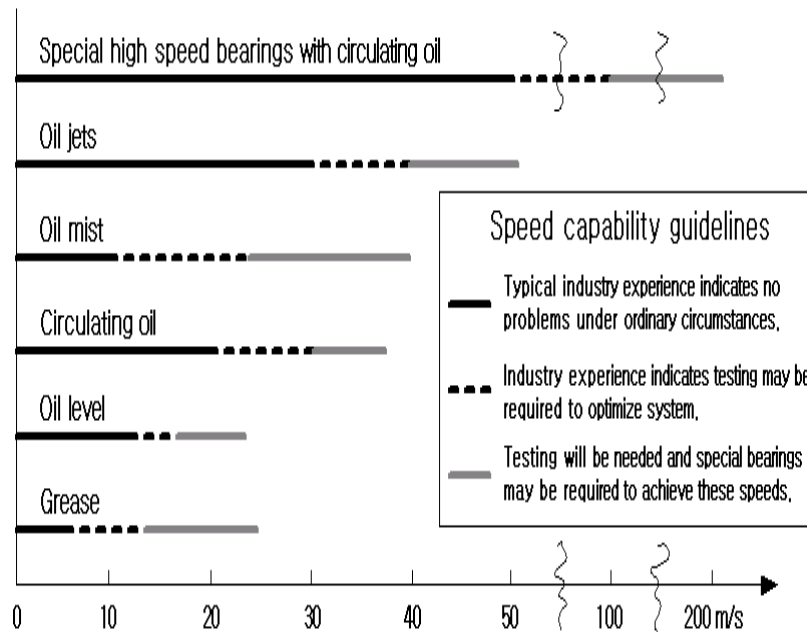


Figure 3.35: Maximum Bearing Linear Speeds for Different Lubrication Methods, from Timken [2004]

These recommended values are based on industry experience and testing, while the actual values in practice are based on many other factors (e.g., amount of preload, quality of fit, support structure, temperature, and load variability) that are not explicitly included. For the preliminary design efforts of this research, these values provide sufficient accuracy. Given these values for maximum linear velocity, the maximum rotational velocity (ω_{\max}) can be determined from the following equation.

$$\omega_{\max} = \frac{2V_{\max}}{d_m} \quad \text{Eqn. 124}$$

The maximum speed for a given lubrication method and bearing diameter will usually be slightly different than what the equation provides, and the exact value cannot be known without testing due to the variability in the factors described above. Manufacturers

sometimes provide maximum rotational speeds for their bearings, and when available, these should be used instead of the values based on Figure 3.35.

3.16 SUMMARY

This chapter has summarized the parametric modeling equations needed to design the SRM, HGT, and PEGT in isolation and to design integrated actuators that couple an SRM to a HGT or PEGT. Appendix A1 discusses the implementation of these models into the computational software MatLab, which provides more details regarding the weight and inertia computations for these systems. This appendix should be read along with this chapter. The remainder of this report will detail how these component models can be used to develop scaling rules (Chapter 5), balanced actuator designs (Chapter 6), direct drive and geared actuators (Chapter 7), and minimum sets of actuators (Chapter 8).

Chapter 4 Actuator Design Procedures

Chapter 3 presented the parametric models for the SRM, HGT, and PEGT, and this chapter will describe how the parametric models will be used in the context of a formal actuator design procedure. First, the high-level actuator development process will be provided to illustrate where this research fits into the RRG actuator development work. Then, the current RRG actuator design procedure and a new, augmented procedure will be detailed. The features of both the current and proposed design procedures will be discussed, with an emphasis on the advantages of the proposed procedure (visualization to enhance the designer's ability to manage major objectives such as performance levels, torque capacity, parametric balance, etc.). A brief description of each of the embedded design tasks in the procedure will be provided. Then, the lower level motor and gear train design procedures will illustrate how the models of Chapter 3 can be used to generate motor, gear train, and actuator designs. Since the models of Chapter 3 and procedures of Chapter 4 were embedded into a computational environment (to allow efficient generation of actuator designs and their corresponding design rules), some notes on the implementation will be provided. This chapter serves as a roadmap for the rest of the report in that each of the remaining chapters either use the proposed procedure or fit into a specific part of the procedure.

4.1 HIGH LEVEL ACTUATOR DESIGN DEVELOPMENT PROCESS

Figure 4.1 illustrates the high level actuator development process the RRG follows. It shows the relevant steps a design team uses to move from a set of application requirements to a working prototype. As discussed in the literature review in Section 2.1, Gloria and Tesar [2004] suggested how to map a set of application requirements to a specific class of actuator (high torque, fault tolerant, low noise, etc.) and then choose the

most promising gear train type for that class. Gloria and Tesar considered only the star compound and HGT in their work and the current research adds the PEGT as another option. This research will assume that the high-level application requirements have been translated into a set of concrete requirements for an actuator design (torque, speed, weight, volume constraints, etc.) and that a preliminary gear train type has been selected for the application. Thus, the focus of the current research is on the “Design Actuator” and “Determine Minimum Set” blocks in the process, and the remainder of this chapter discusses the former in detail. Chapter 8 details the minimum set concept.

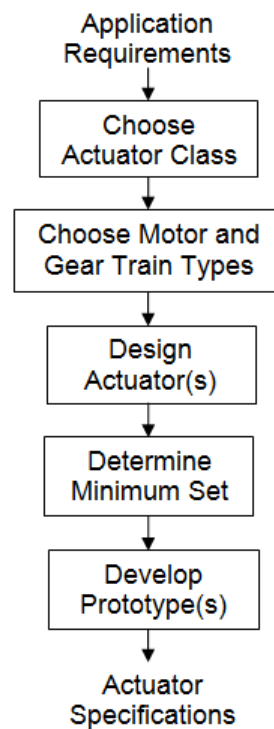


Figure 4.1: High Level Actuator Development Process

The following two sections detail the “Design Actuator(s)” block from Figure 4.1 by explaining the current actuator design procedure and then proposing an augmented

procedure that incorporates the two central concepts of this research, scaling and balancing parameters.

4.2 CURRENT ACTUATOR DESIGN PROCEDURE

Figure 4.2 details the design procedure currently used by the RRG to develop actuators for a variety of applications. The procedure begins when the designer inputs his/her design parameter choices (D_p) and performance parameter targets (P_p) for a particular application. Designing the gear train and motor are the two critical tasks in the procedure. Unless the application dictates otherwise, the gear train is always designed before the motor for a number of reasons. First, the gear train is typically the larger of the two and thus dominates the weight of the design. Second, the gear ratio must be known before the required motor torque can be computed. Finally, the gear train is the technology being studied in depth at the RRG and often times off-the-shelf motor designs are used in place of the custom SRM designs available from the models in Chapter 3. The “Iteration” that occurs between the motor and gear train design typically involves modifying the gear ratio, motor aspect ratio, gear train aspect ratio, number of gear train stages, and other parameters to meet the application requirements and to achieve a balanced design. The design selection task involves choosing the most promising alternative from among a set of potential actuator geometries. The outputs of the procedure are the design and performance parameter specifications and solid models either in a preliminary or detailed design state, with the level of complexity depending on whether a prototype is being built.

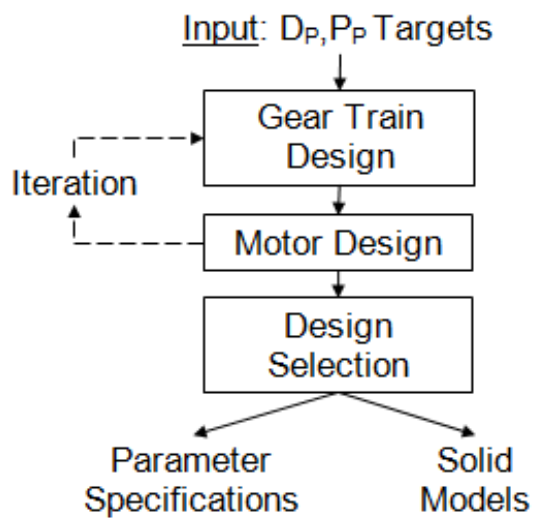


Figure 4.2: Current RRG Actuator Design Procedure

While this procedure has proven very effective for developing actuators, it has the following features that could be potentially improved.

- Only a single actuator design can be completed per solution run.
- Comparisons among multiple actuators require multiple runs and/or multiple designers.
- Different designers manage the motor and gear train design efforts.
- No formal model reduction and solution tools are included.
- It is somewhat difficult to compare past and current designs objectively due to conflicting parameter assumptions.
- There is often substantial effort in generating component solid model and drawing documentation for reporting purposes.

The primary challenge with the current procedure is the difficulty in generating sets of actuator designs for an application in which multiple actuators are needed, which has important implications for product line design and actuator commercialization.

4.3 PROPOSED ACTUATOR DESIGN PROCEDURE

This research will augment the current RRG actuator design procedure above with the two central concepts of this research: balancing the motor and gear train and developing scaling rules (Figure 4.3). It will also make minor additions relating to design selection, design map generation, and faster generation of solid models. The designer inputs are the same as for the current procedure, with the key difference being that parameter information for more than one design at a time can be considered. This procedure allows the designer to control which parameters are fixed and which vary for a set of actuator designs, which is critical for the utility of the scaling and balancing rules developed in Chapters 5 and 6 of this report.

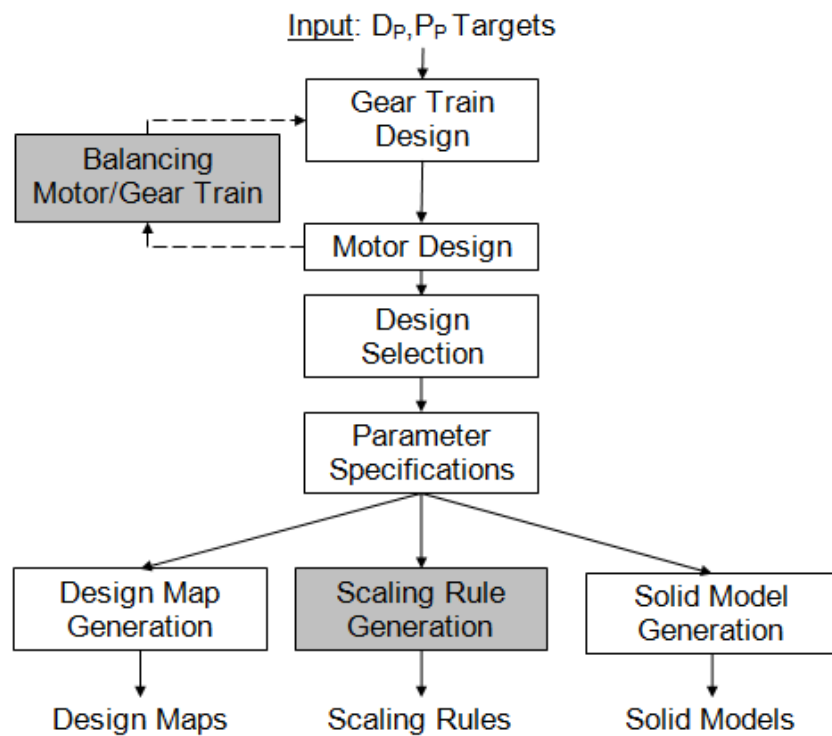


Figure 4.3: Proposed Actuator Design Procedure (D_P -design parameter, P_P -performance parameters)

The primary difference between the current procedure (Figure 4.2) and the proposed procedure (Figure 4.3) will be that as much of the procedure will be automated as possible. This will allow efficient generation of motor, gear train, and actuator designs. Automation of these tasks is possible for the following reasons: 1) RRG's and the present designer's experience in quickly responding to customer requests by developing preliminary actuator designs and 2) the availability of analytical models for the SRM, HGT, and PEGT that can be implemented in a computational environment.

The proposed procedure has the following features that improve upon the current procedure.

- Multiple actuator designs can be completed per solution run.

- Comparisons among alternative actuators for an application are easier to manage.
- A single designer can manage the gear train and motor designs.
- The procedure is suitable for formal model reduction and solution tools because it is embedded into a computational environment.
- Comparisons between past and future designs (often created by different designers) are easier to manage because the designer can control his/her assumptions.

All of the additional steps (i.e., the new blocks in Figure 4.3) in the proposed procedure are certainly addressed in the current procedure but they have not been formalized or considered in detail by past RRG researchers. In particular, many decisions are made not by the individual actuator designer but based on the experience of the RRG management team. This research has attempted to embed the lessons learned from past actuator designs and expert knowledge of the RRG management team into the parametric models of Chapter 3 and the procedures of this chapter.

4.3.1 Actuator Design Procedure Tasks

Table 4.1 summarizes the input and output information for each of the actuator design tasks in Figure 4.3, and this section provides a basic description of each of the tasks.

Table 4.1: Proposed Actuator Design Procedure Tasks

Tasks	Input	Output
Gear Train Design	Design and performance parameter targets/constraints	Gear ratio, torque, weight, inertia
Motor Design	Gear ratio, motor geometry preference	Motor torque, weight, inertia
Balancing Motor and Gear Train	Aggregate actuator performance parameters	Modified gear ratio, motor geometry, gear train geometry to balance the designs
Design Selection	Parameter data for viable, alternative actuator designs	Design(s) selected as the best alternative(s)
Parameter Specifications	Complete design and performance parameter data for the selected design(s)	Standard summary of design and performance parameter information
Design Map Generation	Standard summary of design and performance parameter information	2-D and 3-D maps (P_p vs. D_p)
Scaling Rule Generation	Standard summary and design and performance parameter information	Power law and low order polynomial scaling rule representations
Solid Model Generation	Design parameter data written to SolidWorks design tables	Solid models and drawings of all components and assemblies

The input design and performance parameter data (single values or ranges) can either be in an unstructured, random arrangement or in the form suggested by some of the different experimental designs listed in the literature review in Section 2.7.3. In this research, only uniform experimental designs will be used because there is little computational savings in using some of the more complex designs.

The gear train design task (discussed in detail later in this chapter in Section 4.3.3) includes computation of the gear ratio, torque capacity, weight, and inertia of the chosen gear train. The motor design task (discussed in detail later in this chapter in Section 4.3.2) will balance the motor torque with the gear ratio and gear train torque capacity (so that neither the motor nor the gear train limits the overall torque capacity more than the other) and also computes the motor weight and inertia. The balancing

motor and gear train task will include involve the choice of the gear ratio, ratio of motor length to overall length, and ratio of motor diameter to gear train diameter and will be discussed in detail in Chapter 6.

The design selection task sorts through all the designs and outputs all of the designs that meet the desired performance parameter targets. The selection task is currently based on an exhaustive search of a small number of the design parameters in the motor and gear train models and selects the “best” designs among the candidates given the designer’s preference for the most important objective. In this research, the objectives are limited to maximizing torque, torque density, and responsiveness and minimizing weight and inertia. If more than one of these objectives is important for an application, then multi-objective design techniques can be used to select a design that balances competing objectives. Marler and Arora [2004] provide a summary of the different ways to formulate the objective function for a multi-objective design problem (Table 4.2 includes a few) and discuss the relative merits of the different formulations. The simplest and most common formulation is a weighted sum of the multiple objectives, where the designer is free to specify the weights (i.e., relative importance) for the different objectives.

Table 4.2: Different Methods Used to Formulate the Objective Function

Formulation	Objective Function (F)	Parameter Description
Weighted Sum (Simplest)	$F = \frac{w_1 f_1(x)}{f_{1norm}} + \frac{w_2 f_2(x)}{f_{2norm}} + \dots$	w_1, w_2 – weights $f_1, f_2(x)$ – objectives f_{1norm}, f_{2norm} – normalization factors
Compromise Programming (General)	$F = \left\{ \sum_{i=1}^m \left[w_i (f_i(x) - f_i^*) \right]^p \right\}^{1/p}$	w_i – weights $f_i(x)$ – objectives f_i^* – ideal value
Compromise Programming (Euclidean, $p=1$)	$F = \sum_{i=1}^m \left[w_i (f_i(x) - f_i^*) \right]$	w_i – weights $f_i(x)$ – objectives f_i^* – ideal value
Compromise Programming (Min-Max, $p=\infty$)	$F = \min \left\{ \max_{i=1..m} \left[w_i (f_i(x) - f_i^*) \right] \right\}$	w_i – weights $f_i(x)$ – objectives f_i^* – ideal value
Goal Programming	$F = \sum_{i=1}^m \left[w_i (d_i^+ + d_i^-) \right]$ <p><u>Additional Constraints</u></p> $f_i(x) + d_i^- - d_i^+ = f_i^T$ $d_i^-, d_i^+ \geq 0, d_i^- * d_i^+ = 0$	w_i – weights $f_i(x)$ – objectives f_i^T – target/goal value d_i^+, d_i^- – deviation variables

Regarding the parameter specification task, Table 4.3 presents the suggested standard ordering and presentation of the design and performance parameter data for an actuator⁵. This is the format that will be used for the remainder of this report and is also the standard input to the design map, scaling rule, and solid model generation blocks in Figure 4.3.

⁵ The dramatic decrease in output responsiveness for this set of actuator designs results from the emphasis on designing for maximum torque density rather than maximum (or constant) output responsiveness. See Section 5.2 and 6.5 for some specific numerical results. Section 7.3.1.5 provides recommendations for achieving near constant output responsiveness for a range of actuator diameters and gear ratios.

Table 4.3: Standard Actuator Design and Performance Parameter Data Summary

Overall Diameter (inches)	Motor Diameter (inches)	Overall Length (inches)	Aspect Ratio	Gear Ratio	Torque (in-lbf)	Weight (lbf)	Inertia (lbm-in ²)	Torque Density (in-lbf/lbf)	Input Responsiveness (rad/sec ²)	Output Responsiveness (rad/sec ²)
5	5.2	4.6	0.91	100	3261	20	3	161	4716	47.1
10	6.5	8.7	0.87	100	14631	73	44	200	1278	12.8
15	9.4	9.2	0.61	102	34923	171	307	204	435	4.2
20	12.5	10.4	0.52	101	63734	346	1273	184	194	1.9
5	5.4	5.6	1.11	100	4348	26	4	170	4668	47.6
10	6.7	10.7	1.07	100	19508	91	58	215	1296	12.9
15	9.4	11.6	0.77	102	46564	211	404	221	441	4.3
20	12.6	13.1	0.65	100	84889	425	1688	200	196	2.0

The design map generation task will involve the generation of 2-D and 3-D plots of design and performance parameter data, with the parameters on the axes chosen by the designer. These plots have been termed “design maps” based on their similarity to the performance maps currently under development at the RRG. The scaling rule generation task will provide a mathematical representation (in power-law or low order polynomial form) of the surfaces in the design maps and will be discussed in detail in Chapter 5. The solid model generation task will use the discrete design parameter data from the parameter specification task to generate the reference SRM, HGT, and PEGT solid designs (shown in Chapter 3) in the SolidWorks solid modeling software.

From a computational point of view, the primary difference between scaling and balancing parameters among a set of actuator designs is which parameters are fixed and which are variable in each. Chapters 5 and 6 will highlight these differences. Both rely on the exercising the parametric models of Chapter 3 and the procedures in this chapter, and the key results in each area will be presented in the form of design maps, mathematical scaling rules, tabular summaries, and solid models.

4.3.2 Motor Design Procedure

The design procedure used to generate SRM designs (Figure 4.4) and embedded in the computational tool is summarized in the following set of steps.

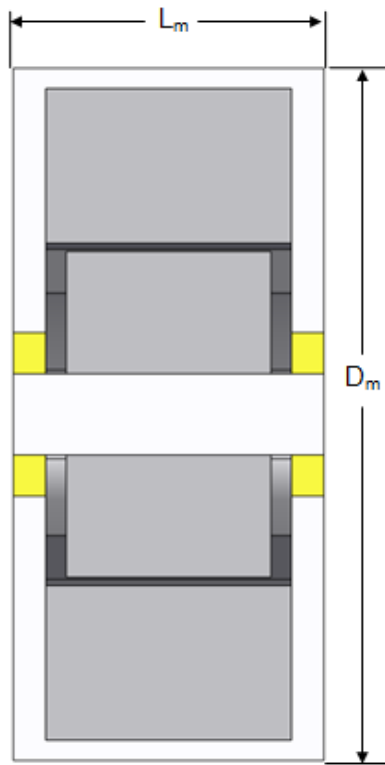


Figure 4.4: SRM Reference Design

1. Input the overall diameter (D_m) and length (L_m)/aspect ratio (A_m).
2. Calculate the standard rotor and stator dimensions using the suggested proportions in Section 3.7.
3. Calculate the space available for windings on the stator using the relationships in Section 3.7.5.
4. Search among the different wire size and number of turn combinations for maximum torque capacity.
5. Calculate the weight and inertia of the chosen geometry in Section 3.7.8.

Considering step 1, note that either the length or aspect ratio may be chosen by the designer but not both. For cases in which a single design is required, the overall

length will likely be known or able to be estimated. However, for cases in which a set of designs is required, the aspect ratio will be a more important parameter and will allow the designer to group the designs more efficiently and draw useful conclusions about the performance parameters from a set of designs.

Table 4.4 summarizes the recommended values of constants and fixed parameters for the SRM. Unless the needs of the particular application or results from ongoing research at RRG dictate otherwise, these values should not be modified when generating rules for scaling and balancing parameters such as those in this research. Keeping these values constant will allow the designer to focus on how changes in the fundamental geometric design parameters (D_m , L_m , A_m) affect the performance parameters.

Table 4.4: SRM Constants and Fixed Parameters

Parameter	Value
Number of stator poles	$N_s=6$
Number of rotor poles	$N_r=4$
Stator pole angle	$\theta_s=30^\circ$
Stator pole angle	$\theta_r=32^\circ$
Saturation flux density	$B_{sat}=1.56$
Axial clearance	$c = 0.005D_m$
Density	$\rho = 0.284 \text{ lbm}/\text{in}^3$

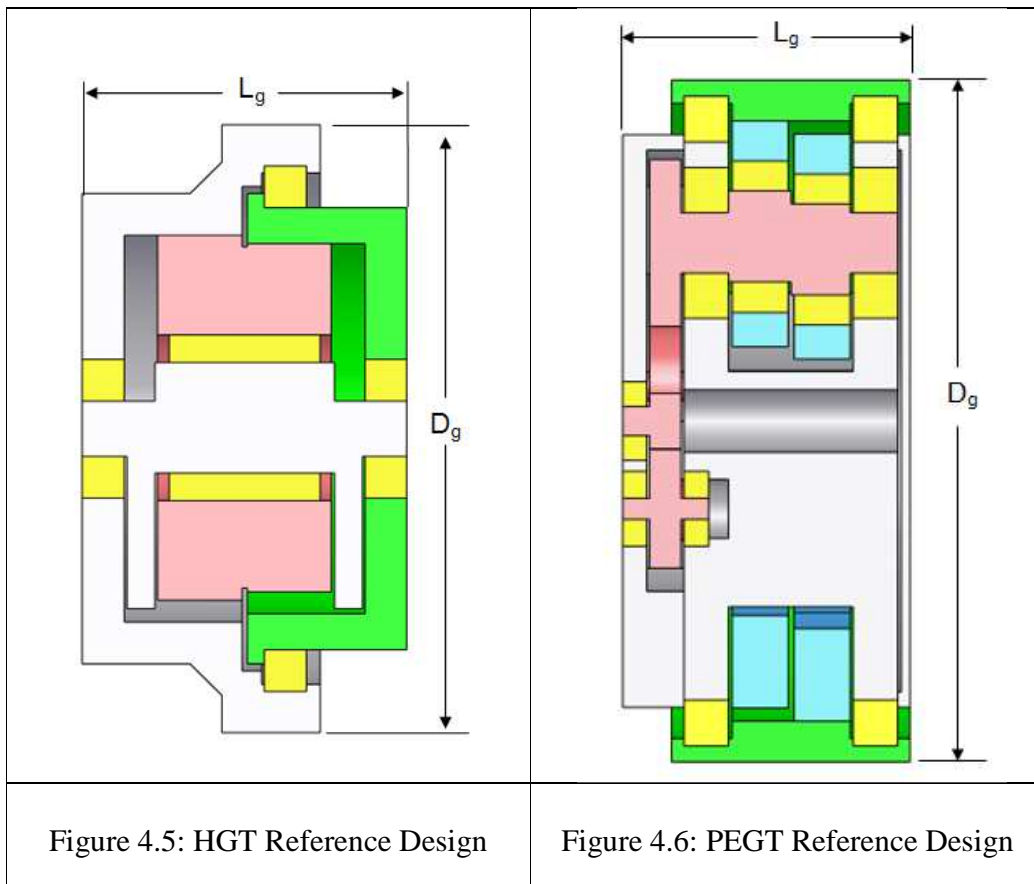
Step 4 of this procedure is best illustrated by an example. Suppose the designer seeks to know the torque capacity of an SRM with $D_m = 5$ inches and $L_m = 3$ inches. Using these overall dimensions and the suggested proportions for the other parameters from Chapter 3, Table 4.5 displays all of the different wire size (d_w), current (I_w), number of turns (N), $N \cdot I$ product, and torque capacity for possible options. Based on this exhaustive search of the winding parameters, the torque capacity can always be maximized.

Table 4.5: Illustration of Searching Winding Parameter to Maximize SRM Torque

Wire Diameter, dw (inches)	Current, Iw (amps)	Number of Turns	N*I Product	Torque Capacity (in-lbf)
0.0119	0.86	2053	1766	14
0.0133	1.2	1624	1949	16
0.0147	1.4	1314	1840	15
0.0164	1.7	1040	1768	15
0.0182	2.2	831	1828	15
0.0203	2.7	656	1771	15
0.0227	3.5	513	1796	15
0.0253	4.7	403	1894	17
0.0281	7	318	2226	20
0.0314	9	247	2223	21
0.0351	11	190	2090	19
0.0391	14	147	2058	19
0.0437	16	112	1792	17
0.0488	19	85	1615	15
0.0545	22	63	1386	12
0.0609	28	47	1316	12
0.0682	32	33	1056	9

4.3.3 Gear Train Design Procedure

The design procedure used to develop HGT (Figure 4.5) and PEGT (Figure 4.6) designs and embedded in the computation tool is summarized in the following set of steps.



1. Input overall diameter (D_g), length (L_g) or aspect ratio (A_g), gear ratio (g), diametral pitch range (P_{dmin} - P_{dmax}), material strength limits (S_b, S_c), output speed, and desired bearing life.
2. Calculate key internal gear train design parameters needed for gear ratio and torque calculations using the suggested proportions in Sections 3.9 and 3.10.
3. Search for gear tooth number combinations that achieve the desired gear ratio.
4. Calculate the remaining design parameters (including approximate bearing dimensions) using reasonable assumptions and rules of thumb.

5. Calculate the torque capacity, weight, inertia, and required bearing load capacities of the chosen geometry.

Step 3 of this procedure is best illustrated by an example. Suppose the designer seeks to achieve a gear ratio of $g = 100$ for the HGT with $D_g = 10$ inches. Using a reasonable diametral pitch range of 5-10, Table 4.6 displays all of the different tooth number combinations that achieve this gear ratio to within $\pm 2\%$. Based on this exhaustive search of the tooth number parameters, numerous options are available to meet the target gear ratio. In order to proceed with the gear train design procedure, one or a subset of these options should be chosen. The current approach is to choose the option that results in the maximum torque capacity for a given gear train diameter, and this translates into selecting the design with the lowest diametral pitch (see Section 3.5.1). However, current research is underway at the RRG to study the contact ratio and interference properties for tooth number and size combinations (and other tooth level parameters not shown) such as those in Table 4.6. As this research progresses, then the tooth number combinations that result in the maximum contact ratio while still avoiding interference can be chosen instead of maximum torque capacity options.

Table 4.6: Illustration of Searching Gear Tooth Parameters to Meet Target Gear Ratio in the HGT

Gear Ratio, g	1st Stage Ring Gear Teeth, Nr1	1st Stage Wobble Gear Teeth, Nw1	2nd Stage Ring Gear Teeth, Nr2	2nd Stage Wobble Gear Teeth, Nw2	Eccentricity, e	Diametral Pitch, Pd
99.2	38	34	35	31	0.37	5.4
101.3	43	38	40	35	0.41	6.2
100.0	44	40	40	36	0.33	6.2
100.2	47	41	44	38	0.44	6.8
99.0	49	44	45	40	0.36	6.9
100.6	51	44	48	41	0.47	7.4
100.0	54	48	50	44	0.39	7.7
100.0	55	50	50	45	0.33	7.7
98.4	58	51	54	47	0.42	8.3
99.0	60	55	54	49	0.30	8.3
99.0	60	54	55	49	0.35	8.5
101.4	63	55	59	51	0.44	9.1
99.4	65	58	60	53	0.38	9.2
100.0	66	60	60	54	0.33	9.2
98.2	66	57	62	53	0.47	9.5
101.5	67	58	63	54	0.46	9.7
99.0	71	65	64	58	0.30	9.8
100.8	70	62	65	57	0.40	10.0
99.0	71	64	65	58	0.35	10.0

4.3.3.1 Internal Design Parameters

Table 4.7 summarizes the recommended values (from Chapter 3) of the internal design parameters for the HGT and PEGT as a function of the overall diameter and length and also lists other relevant parameter choices that affect the overall results. All of the values in this table can be modified based on the particular performance parameter targets of an application. However, when generating a scaled set of gear train or actuator designs, it is recommended that these basic proportions not be changed in order to allow useful conclusions to be drawn from the resulting design maps, scaling rules, and parameter data.

Table 4.7: Suggested Proportions for the HGT and PEGT Internal Design Parameters

	HGT	PEGT (Star 1st Stage)	PEGT (Star Compound 1st Stage)
Output Gear Pitch Diameter	$d_{r2} = 0.65D_g$	$d_r = 0.87D_g$	$d_r = 0.87D_g$
Face Width	$L_w = 0.30L_g$	$L_{pe} = 0.22L_g$	$L_{pe} = 0.20L_g$
Gear Ratio Range (g)	75-500	15-150	15-500
Aspect Ratio Range (A_g)	0.3 to 2	0.3 to 2	0.3 to 2
Balancing Mass Width	$w = 0.10L_g$	-	-
Center Distance to Crankshaft	-	$c_c = 0.27D_g$	$c_c = 0.27D_g$
1 st Stage Face Width		$L_1 = 0.11L_g$	$L_1 = 0.10L_g$

4.3.3.2 Constants and Fixed Parameters

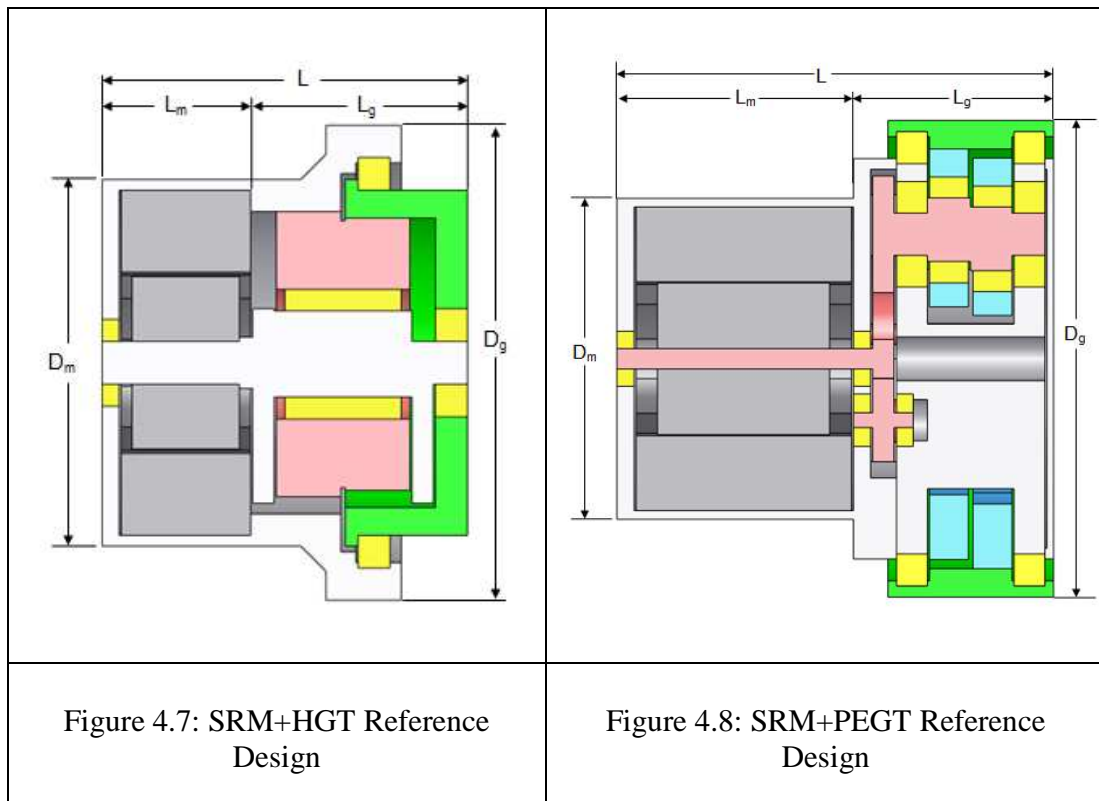
Table 4.8 summarizes the recommended values of constants and fixed parameters for the HGT and PEGT. Again, unless the needs of the particular application or results from ongoing research at RRG dictate otherwise, these values should not be modified when generating rules for scaling and balancing parameters such as those in this research. Keeping these values constant will allow the designer to focus on how changes in the fundamental geometric design parameters (D_g , L_g , g , A_g) affect the performance parameters.

Table 4.8: Constants/Fixed Parameters for the HGT and PEGT

Parameter	Value
Pressure angle	$\phi=25^\circ$
Minimum tooth number difference	$N_{\min}=3$
Number of teeth in contact	3 (nominal load condition)
Efficiency	100%
Axial clearance	$c = 0.005D_g$
Diametral pitch range	$5 < P_d < 25$
Bending strength	$S_b=100$ ksi
Contact strength	$S_c=250$ ksi
Density	$\rho = 0.284$ lbm/in ³
Velocity Factor (K_v)	1.1
Load Distribution Factor (K_m)	1.3
Geometry Factor (J)	0.5
Output Speed (rpm)	1
Bearing Life	5000 hours

4.3.4 Actuator Design Procedure (Textual Description)

The design procedure used to obtain design and performance parameter information for the SRM+HGT (Figure 4.7) and SRM+PEGT (Figure 4.8) designs was summarized graphically in Figure 4.3 and involves the following set of steps (up to the “Parameter Specification” block).



1. Input overall diameter (D_g), length (L) or aspect ratio (A), gear ratio (g), diametral pitch range ($P_{dmin}-P_{dmax}$), material strength limits (S_b, S_c), motor diameter to gear train diameter ratio (K_d), motor length to overall length ratio (K_l), output speed, and desired bearing life.
2. Utilize the gear train design procedure above to compute the gear ratio, torque, weight, and inertia of the gear train.
3. Utilize the motor design procedure above to design a balanced motor and compute its torque, weight, and inertia.
4. Utilize the balancing parameters concepts from Chapter 6 to achieve the desired level of balance between the motor and gear train.
5. Compute the torque, weight, inertia, torque to weight ratio, torque to inertia ratio for the combined motor and gear train design.

The torque, weight, inertia, and torque to weight ratio computations are straightforward and were detailed in Chapter 3. Building upon Section 2.4 in Chapter 2, the torque to inertia ratio (or responsiveness) at the input (R_i) for a combined motor and gear train design can be obtained by dividing the motor torque (T_m) by the total inertia reflected to the motor (I_{in}).

$$R_i = \frac{T_m}{I_{in}} = \frac{T_m}{I_m + I_g + \frac{I_{load}}{g^2}} \quad \text{Eqn. 125}$$

Using the same notation from Chapter 3, the parameters are as follows.

- T_m = motor torque
- I_m = motor inertia
- I_g = gear train inertia, reflected to the input
- I_{load} = load inertia
- g = gear ratio between motor shaft and output link of the gear train

For the purpose of calculating the torque to inertia ratio of an actuator without specific information about the load inertia and geometry, it is useful to define the load inertia (I_{load}) as a multiple of some reasonable reference inertia (I_{ref}).

$$I_{load} = KI_{ref} \quad \text{Eqn. 126}$$

In this report, for stand-alone HGT and PEGT designs and for integrated actuator designs, the reference inertia will always be defined as the inertia of the gear train reflected to its input shaft. For stand-alone SRM designs (important for comparisons between direct drive systems and geared systems in Chapter 7), the reference inertia will be defined as the inertia of a direct drive SRM. Deviations from these assumptions will be made for the comparison between direct drive and geared systems in Chapter 7, so the specific values for the reference and load inertia will be reported there.

In some applications, particularly where a numerical acceleration requirement is known, the torque to inertia ratio at the output (R_o) will be important and can be obtained by dividing the output/gear train torque (T_g) by the inertia at the output (I_{out}).

$$R_o = \frac{T_g}{I_{out}} = \frac{T_g}{I_m g^2 + I_g g^2 + I_{load}} \quad \text{Eqn. 127}$$

Comparing the input and output responsiveness (acceleration values), the following relationship always holds for the motor/gear train combinations being considered in this research.

$$R_o = \frac{R_i}{g} \quad \text{Eqn. 128}$$

For a design in which the motor torque and gear train are compatible (i.e., balanced), the following relationship holds.

$$T_g = g T_m \quad \text{Eqn. 129}$$

Unless otherwise specified, all of the actuator designs in this report will satisfy this relationship. Also, all gear train inertias will be specified at the input shaft of the gear train. Then, if a motor is coupled with the gear train's input shaft, this gear train inertia can be simply added to the motor inertia. Most gear train manufacturers list inertia values at the input shaft.

4.4 COMPUTATIONAL TOOL

The parametric models for each of the SRM, HGT, PEGT, and integrated actuators and the proposed actuator design procedure (Figure 4.3) discussed above were embedded into the MatLab computational environment. This was done to allow efficient generation of motor, gear train, and actuator designs. Currently, a simple exhaustive search of the design space is used to 1) search the gear train design parameters to match the desired gear ratio in the gear train design task and 2) search different wire sizes to

maximize torque in the motor design task. This is reasonable for the limited problem sizes being considered in the preliminary design stage. The computer code mirrors the proposed design procedure has been separated into modules based on the actuator component and the function it provides. At a minimum, there is at least one separate file for each block shown in Figure 4.3 and each step in the motor, gear train, and actuator design procedures listed above. The code has been built into a modular format to assimilate future lessons learned, particularly for the load capacity and interference calculations for the HGT and PEGT. Currently, the computations involve only the solution of nonlinear algebraic equations. For full documentation of the MatLab implementation, refer to Appendix A1. The software link between MatLab, Excel, and SolidWorks (used for quick generation of solid models) is discussed in Appendix A2.

4.5 SUMMARY

This chapter has illustrated how the parametric models of Chapter 3 can be used in the context of a formal actuator design procedure that includes the concepts of scaling and balancing parameters. It also showed how the lower level motor and gear train design procedures can be used to obtain these individual component designs. The actuator and lower level design procedures and their implementation in MatLab will be used to develop all of the motor, gear train, and integrated actuator design information reported in Chapters 5-8.

Chapter 5 Scaling Rules and Design Maps

This chapter documents the details behind the “Scaling Rule Generation” and “Design Map Generation” blocks in the proposed actuator design procedure (Figure 4.3) of Chapter 4, and the results provided are most useful when the designer seeks to develop a set of motor, gear train, or actuator designs rather than a single point design.

Scaling rules will be defined as analytical relationships between performance parameters and design parameters that are based on a relatively small number of carefully chosen motor, gear train, and actuator designs. Scaling rules will be represented in simple power-law form, the standard low-order polynomial form used in the Response Surface Methodology (RSM), two-dimensional plots, and three-dimensional surfaces (termed “design maps”). The scaling rules will be developed using the regression techniques in Chapter 2 in conjunction with the actuator design procedure in Chapter 4. Rios and Tesar [2007] used rules similar to those developed in this chapter to determine the distribution of actuators and their parameters in a robotic manipulator in order to satisfy the force and speed requirements for a particular application.

Because each scaling rule will involve pre-specified design and performance parameters ranges, justification for these ranges will be briefly discussed. Collectively, the scaling rules and design maps provided can be considered as a database from which a designer can efficiently select the appropriate tools and/or the specific design and performance parameters of interest for a given application domain. Since scaling rules and design maps will then be available for the HGT and PEGT, an objective comparison will be made between these two gear trains in terms of their basic performance parameters of interest: torque capacity, weight, inertia, torque density, and responsiveness.

The relevant background material for this chapter is discussed in the following sections from the literature review of Chapter 2.

- Section 2.5: Scaling
- Section 2.6: Product Family Design
- Section 2.7: Regression, Metamodeling, and Response Surface Methodology
- Section 2.8: Design Space Visualization

The reader is encouraged to review these sections to understand why the results of this chapter are presented as they are.

5.1 REPRESENTATION

In the context of this research, scaling rules will be defined as analytical relationships between the performance parameters (P_p) and design parameters (D_p). This definition is consistent with the rules developed in the general scaling and scale-based product family literature, with the exception that the literature emphasis is on the development of the products rather than the rules generated from products as is being considered here.

The basic result from exercising the actuator design procedure of Chapter 4 is a tabular summary of the design and performance parameters. Both low-order polynomial and simple power-law mathematical representations will be used to fit this discrete parameter data. The two primary reasons for fitting the discrete data with analytical expressions are as follows.

1. To learn how the performance parameters vary as a function of the design parameters.

2. To interpolate accurately to obtain intermediate designs, with implications for product family design.

In order for a designer to effectively learn from the scaling rules based on a set of designs, it is important for him/her to know which parameters are variable and which are fixed in the given set. For this reason, this distinction will be made clear for all of the quantitative results in this and later chapters.

5.1.1 Three-Dimensional Surfaces (Design Maps)

A three-dimensional plot of the design and performance parameter data will be termed a design map (Figure 5.1). The map will include a plot of the surface suggested by the scaling rules obtained via regression (described in the next section). This terminology is based on an analogy between this report's design maps and the performance maps currently being developed at the RRG. Both types of maps represent dependent parameters on a vertical axis as a function of two independent parameters on the other two axes. The important difference between these two types of maps is that design maps typically involve geometric design parameters and performance parameters that can be analytically modeled during the design of an actuator (parameters discussed in Chapter 3). Performance maps typically involve operational parameters (such as voltage, current, efficiency, and noise) that are dealt with the operation of an as-designed actuator and often must be measured to be accurately quantified. The design maps are most useful in a formal graphical user interface or visualization-based software environment as opposed for use as a simple-look up table.

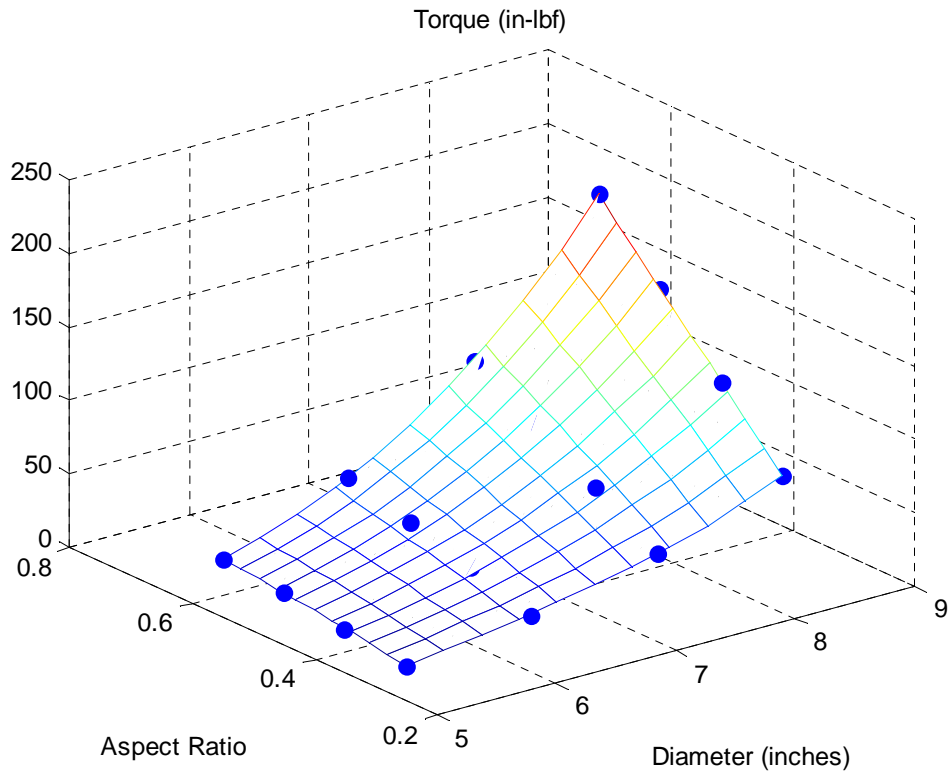


Figure 5.1: Three-Dimensional Representation of a Scaling Rule (Design Map)

5.1.2 Low Order Polynomial Scaling Rules

Using the RSM and metamodeling literature background discussed in Section 2.7, these scaling rules will be written using the standard regression equation of the following form.

$$P_p = n^T u(D_p) \quad \text{Eqn. 130}$$

where

$$D_p = (D_{p1}, D_{p2}, \dots, D_{pm})$$

$$n = (n_0 \ n_1 \ \dots \ n_{k-1})^T$$

$$u = (u_0 \ u_1 \ \dots \ u_{k-1})^T$$

The notation $u(D_P)$ means that each term in u is a function of the design parameters in D_P . In this model, P_P is the vector of fitted values of the performance parameter of interest (rather than the original data), there are m design parameters (denoted by D_P) and k terms (denoted by u with coefficients n).

For example, suppose the designer wishes to describe the torque (T) as a function of the gear train diameter (D_g) and the aspect ratio (A_g). A full quadratic polynomial model would have the following form.

$$T = n_0 + n_1 D_g + n_2 A_g + n_3 D_g^2 + n_4 A_g^2 + n_5 D_g A_g \quad \text{Eqn. 131}$$

Each term in this equation is a function of the design parameters D_g and A_g . The coefficients (n_0 - n_5) can be determined using the least squares minimization techniques discussed in Section 2.7.1.1. Like this example, the polynomial scaling rules presented in this chapter will all involve two (independent) design parameters and a single (dependent) performance parameter and will all use second and third order polynomials. The primary reason for considering no more than two design parameters (and three total parameters) is that the human is limited to visualizing in three dimensions. Including more than two parameters may increase the accuracy of the computations based on the resulting polynomial model, but if a designer cannot see effect of the design parameters, the model may be of limited use. If necessary, the general regression equation and approach used here can be extended to include more parameters and higher order polynomials. Finally, it should be noted that, in general, the coefficients in these polynomial equations do not have physical meaning that can be traced directly back to an analytical relationship.

To assess how well these chosen regression models fit the parameter data (i.e., the quality of the fit), a number of standard error metrics can be used. These metrics are a

function of the error e_i (distance) between a fitted value \hat{y}_i and a data point y_i , defined as follows.

$$e_i = \frac{\hat{y}_i - y_i}{y_i} \quad \text{Eqn. 132}$$

These metrics are the average error (E_{avg}), maximum error (E_{max}), and root mean square error (E_{rms}). [Wang and Shan, 2007 and Jin, Chen, and Simpson, 2001].

$$E_{avg} = \frac{\sum_{i=1}^n e_i}{n} \quad \text{Eqn. 133}$$

$$E_{max} = \text{maximum}(e_1, e_2, \dots, e_n) \quad \text{Eqn. 134}$$

$$E_{rms} = \sqrt{\frac{\sum_{i=1}^n e_i^2}{n}} \quad \text{Eqn. 135}$$

Though the correlation coefficient (usually termed R^2) is often used in standard regression analyses, it has little value in the current research because the data sets are deterministic and therefore have zero variance. Future research that incorporates uncertainty into the design maps and the design process will allow the use of this common statistical metric. Collectively, the correlation coefficient, standard deviation, and other statistical measures of a set of data may become more useful when the designer realizes that all of the design parameters are not sharply defined by the designer and may be bounded by small variations.

5.1.3 Two-Dimensional Plots

Two-dimensional plots (Figure 5.2) of the design and performance parameter data will also be used to present results in this chapter. These plots are most useful for quickly determining preliminary sizes of motors, gear trains, and actuators.

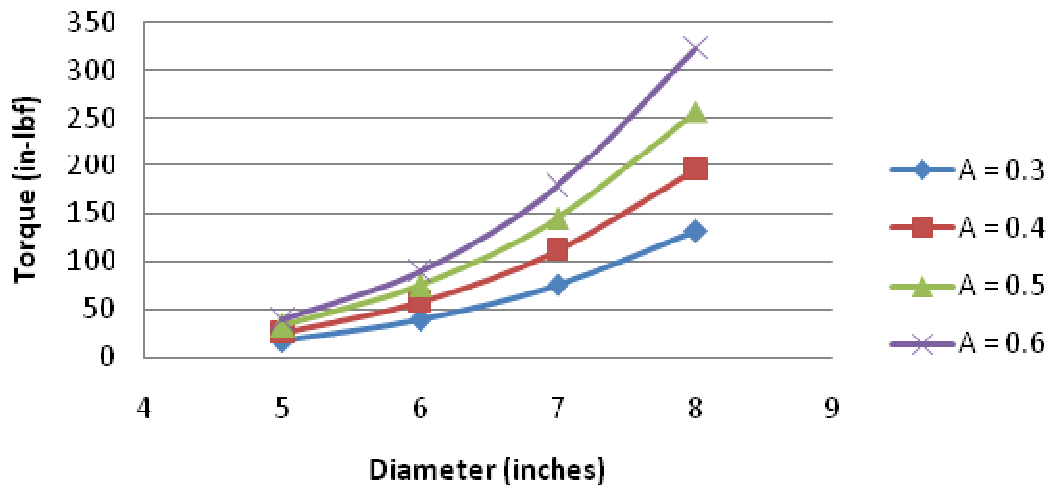


Figure 5.2: Two-Dimensional Representation of a Scaling Rule

5.1.4 Simple Power Law Scaling Rules

These scaling rules will be obtained from the two-dimensional plots of the design and performance parameter data and will be written in the following power law form.

$$P_p = kD_p^b \quad \text{Eqn. 136}$$

Here, k and b are constants that are obtained using the built-in curve-fitting tools in Excel and most statistical software packages and are based on least-squares minimization of the fitting error.

Though other possibilities exist, all of the power law scaling rules in this chapter will be written as a function of the gear train diameter (D_g) as follows.

$$P_p = kD_g^b \quad \text{Eqn. 137}$$

Also, all of the performance parameters considered in this research have an exact linear dependence on the length parameter (L_g for the gear train and L_m for the motor). Using this fact and the definition of the gear train aspect ratio (A_g) as the ratio of the gear train length to diameter (defined in Section 3.3), the power law scaling rule above can also be written as follows.

$$P_p = kD_g^{b-1}D_g = kD_g^{b-1} \frac{L_g}{A_g} \quad \text{Eqn. 138}$$

Finally, if the aspect ratio is constant for a particular set of data being fitted, it can be lumped into the constant k to yield the following.

$$P_p = kD_g^{b-1}L_g \quad \text{Eqn. 139}$$

Unlike the low-order polynomial rules discussed in the Section 5.1.2, the coefficients and exponents in these power-law equations often have physical meaning that can be traced back to the original analytical relationship. This can be done by comparing this chapter's scaling rule results for torque, weight, and inertia to the more complex analytical relationships summarized in Chapter 3.

5.1.5 Summary of Representations

Table 5.1 provides a listing of the different representations that will be used to present scaling information in this chapter and the relative benefits of each based on criteria such as accuracy, visualization, quick estimation, and learning. As the table shows, the most appropriate representation to use depends on the particular design task.

Table 5.1: Scaling Rule Representations and Their Relative Benefits (“1” means the best and “5” means the worst)

Representation	Accuracy Relative to the Analytical Relationship	Visualization Capability	Quick Estimation of Performance	Learning Parameter Relationships
Original Analytical Relationship	1	5	3	4
3-D Design Maps	3	1	5	3
Low-Order Polynomial Equations (RSM)	2	4	4	5
2-D Plots	5	2	1	2
Simple Power Law Equations	4	3	2	1

5.2 COMPONENT SCALING RULES

This section presents design maps and scaling rules for the SRM, HGT, and PEGT as stand-alone component designs. They are particularly useful when only the motor or gear train is required for an application but can also be easily combined to obtain integrated actuators.

5.2.1 SRM Scaling Rules

The SRM scaling rules are based on the reference design (Figure 5.3) and the standard set of assumptions (repeated in Table 5.2) discussed in Chapter 3. The reference load inertia multiplier used for the responsiveness computation was taken as the inertia of the SRM.

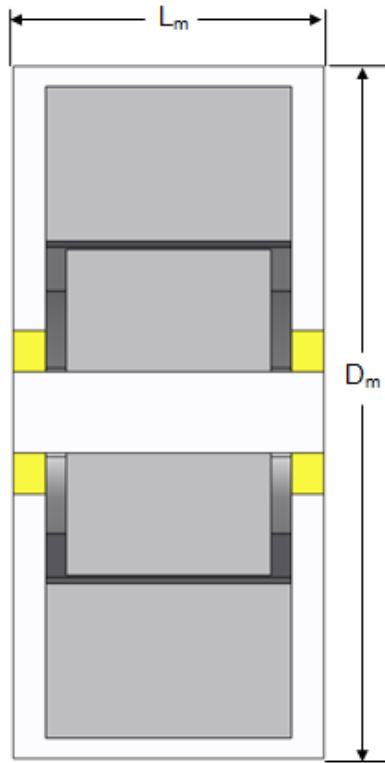


Figure 5.3: SRM Reference Design

Table 5.2: SRM Assumptions

Parameter	Value
Number of stator poles	$N_s=6$
Number of rotor poles	$N_r=4$
Stator pole angle	$\theta_s = 30^\circ$
Rotor pole angle	$\theta_r = 32^\circ$
Saturation flux density	$B_{sat}=1.56$
Axial clearance	$c = 0.005D_m$
Density	$\rho = 0.284 \text{ lbm/in}^3$

Figure 5.4-Figure 5.8 provide design maps (3-D plots) of the torque, weight, inertia, torque density, and responsiveness as a function of the diameter and aspect ratio, and Table 5.3 summarizes the data used to generate the maps. Table 5.4 lists the scaling rule coefficients for the low order polynomial surfaces in the 3-D plots, and Table 5.5 summarizes the values of the three error metrics (E_{avg} , E_{max} , and E_{rms}) for the polynomial fits. The reader should not be alarmed at the relatively high fitting error E_{max} for some of the performance parameters because these typically only occur for the smallest data points in a set, for which the magnitudes of the parameters are relatively small. The largest fitting error throughout this chapter occurs for the inertia, and these occur due to the large changes in the magnitude and the D^4 (4th power of diameter) term in the inertia equations provided in Chapter 3. These maps and rules are of sufficient accuracy to quickly obtain scaled sets of motor designs. Figure 5.9-Figure 5.13 provide all the same design and performance parameter information in the form of 2-D plots, and Table 5.6 lists the constants for the simple power law scaling rules obtained from the 2-D plots.

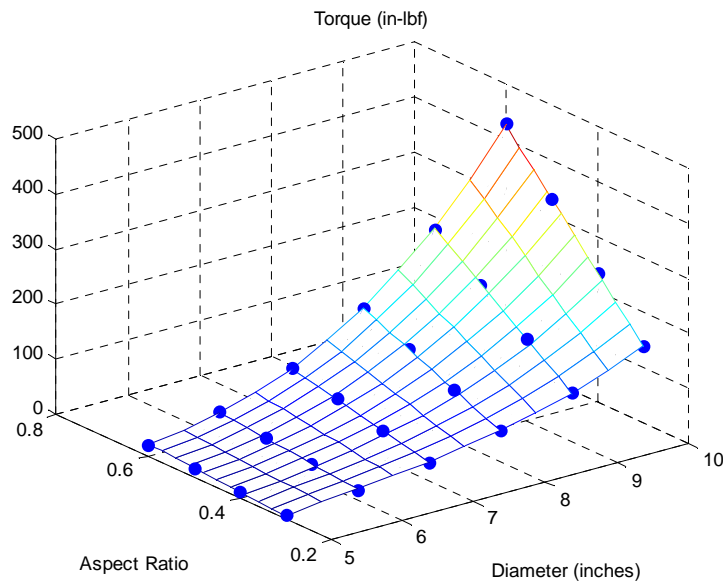


Figure 5.4: SRM Torque Design Map

This torque map is based on the nominal current ratings of the wiring. If the duty cycle of an application is low and there is a need to achieve higher torques than the rated torque, then it is possible to achieve 2-3 times the torque capacity by supplying 2-3 times the current into the windings. In addition, the torque map is shown for a specific value of the saturation flux density of the material (B_{sat}). According to the torque relationships presented in Section 3.7.7, the torque capacity of the SRM is linearly proportional to this material strength limit. For example, doubling B_{sat} (using higher strength, more costly material) will double the torque capacity.

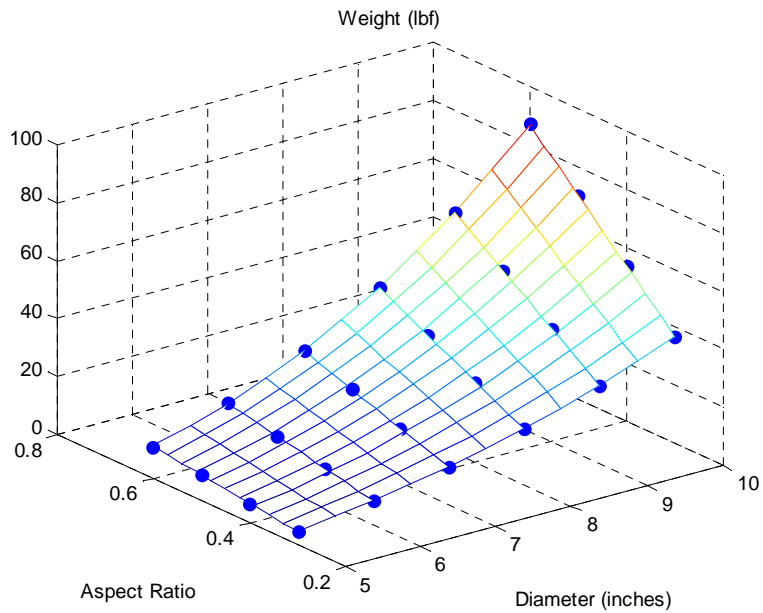


Figure 5.5: SRM Weight Design Map

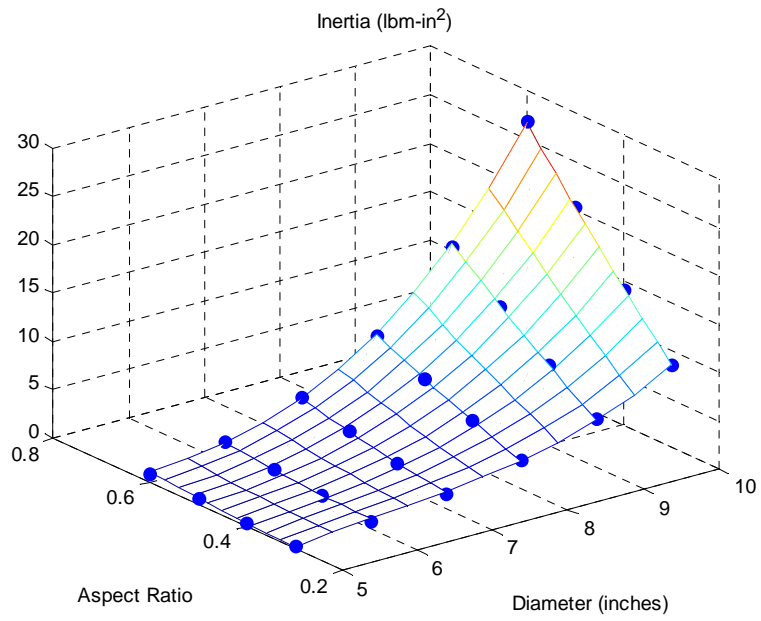


Figure 5.6: SRM Inertia Design Map

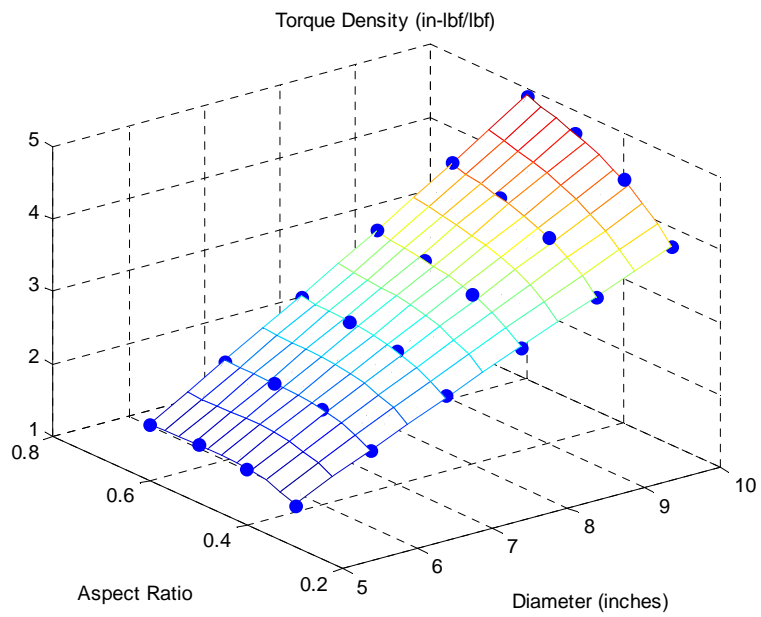


Figure 5.7: SRM Torque Density Design Map

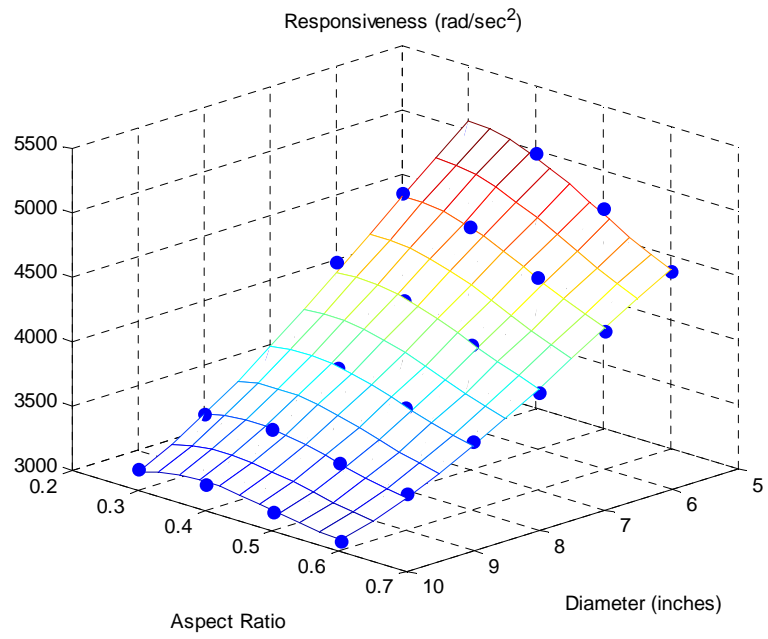


Figure 5.8: SRM Responsiveness Design Map

Table 5.3: SRM Design and Performance Parameter Data

Diameter (inches)	Length (inches)	Aspect Ratio	Torque (in-lbf)	Weight (lbf)	Inertia (lbm-in ²)	Torque Density (in-lbf/lbf)	Responsiveness (rad/sec ²)
5	1.4	0.3	8	5	0.3	1.6	5007
6	1.7	0.3	17	8	0.7	2.1	4677
7	2.0	0.3	32	13	1.5	2.5	4295
8	2.3	0.3	56	19	2.9	2.9	3732
9	2.6	0.3	90	27	5.1	3.3	3436
10	2.9	0.3	138	37	8.4	3.7	3169
5	1.9	0.4	12	7	0.5	1.8	4985
6	2.3	0.4	27	12	1.2	2.3	4573
7	2.7	0.4	53	19	2.5	2.8	4157
8	3.0	0.4	93	28	4.7	3.3	3795
9	3.4	0.4	151	39	8.4	3.9	3475
10	3.8	0.4	233	53	14.1	4.4	3206
5	2.4	0.5	16	9	0.7	1.8	4706
6	2.9	0.5	37	15	1.6	2.4	4335
7	3.3	0.5	72	24	3.5	2.9	3973
8	3.8	0.5	127	36	6.8	3.5	3635
9	4.3	0.5	210	51	12.1	4.1	3370
10	4.8	0.5	330	70	20.3	4.7	3146
5	2.9	0.6	20	11	0.9	1.8	4378
6	3.4	0.6	45	19	2.2	2.4	4068
7	4.0	0.6	90	30	4.6	3.0	3752
8	4.6	0.6	163	45	8.9	3.6	3528
9	5.1	0.6	272	64	16.0	4.3	3292
10	5.7	0.6	428	87	26.9	4.9	3073

Table 5.4: SRM Design Map Coefficients, n_i

$$(P_P = n_0 + n_1 D_m + n_2 A_m + n_3 D_m A_m + n_4 D_m^2 + n_5 A_m^2 + n_6 D_m A_m^2 + n_7 D_m^2 A_m + n_8 D_m^3 + n_9 A_m^3)$$

Parameter	Constant	D_m	A_m	$D_m A_m$	D_m^2	A_m^2	$D_m A_m^2$	$D_m^2 A_m$	D_m^3	A_m^3
Torque	-580	234	1070	-396	-29	0	1	38	1	0
Weight	-28	12	65	-27	-2	0	0	4	0	0
Inertia	-51	21	83	-31	-3	0	1	3	0	0
Torque Density	-4	1	18	1	0	-40	-1	0	0	29
Responsivness	4680	33	13060	420	-93	-36005	0	0	5	23741

Table 5.5: SRM Error Metrics

Parameter	E_{\max} (%)	E_{avg} (%)	E_{rms} (%)
Torque	18.2	3.4	6.1
Weight	1.9	0.5	0.7
Inertia	43.8	7.8	14.1
Torque Density	1.0	0.4	0.4
Responsivness	1.9	0.6	0.8

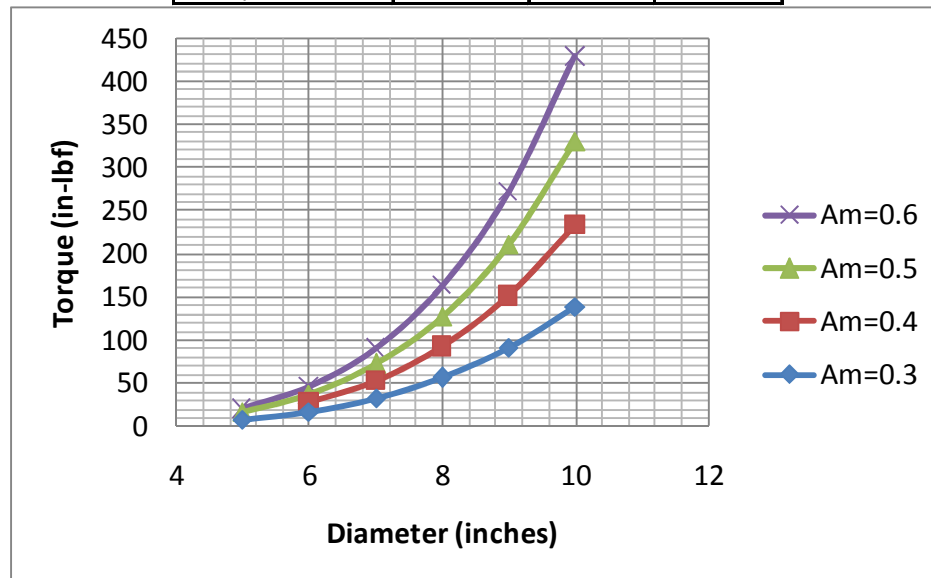


Figure 5.9: SRM Torque Design Map (2-D)

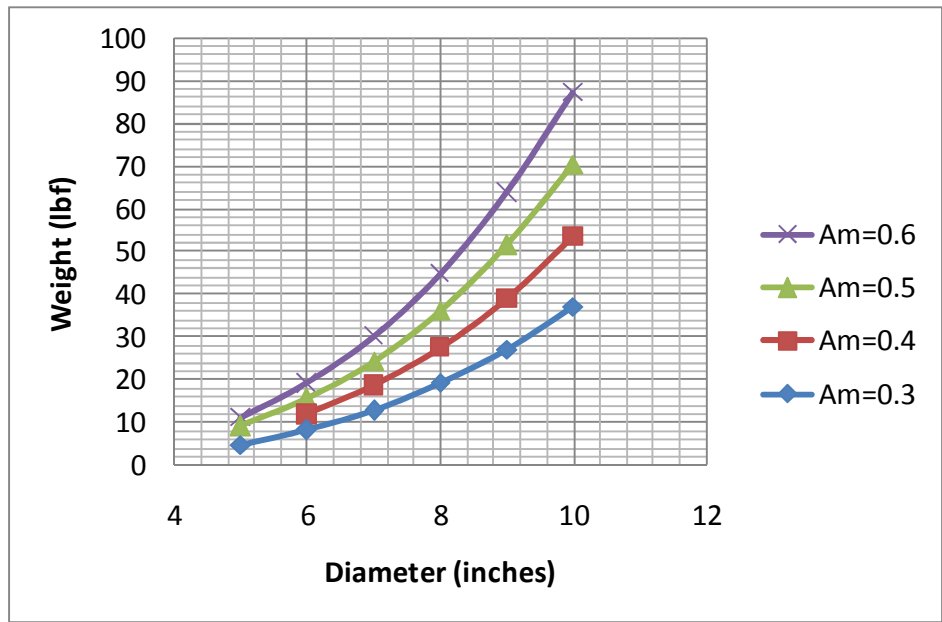


Figure 5.10: SRM Weight Design Map (2-D)

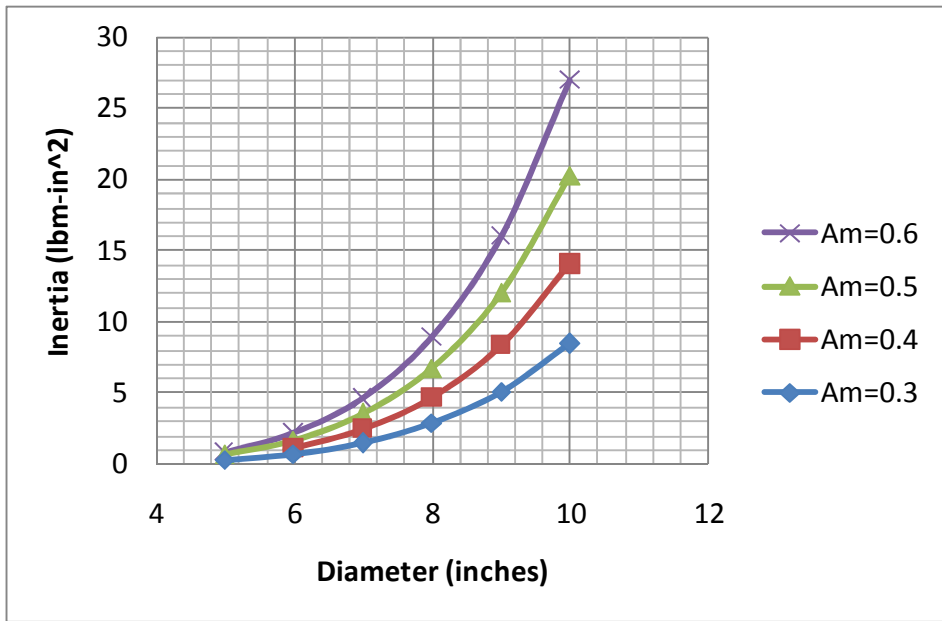


Figure 5.11: SRM Inertia Design Map (2-D)

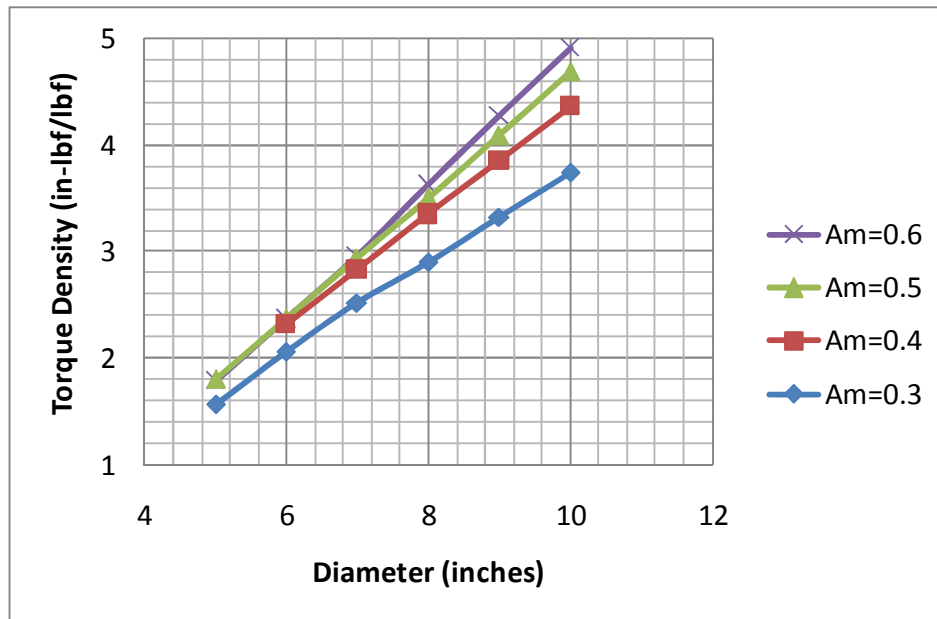


Figure 5.12: SRM Torque Density Design Map (2-D)

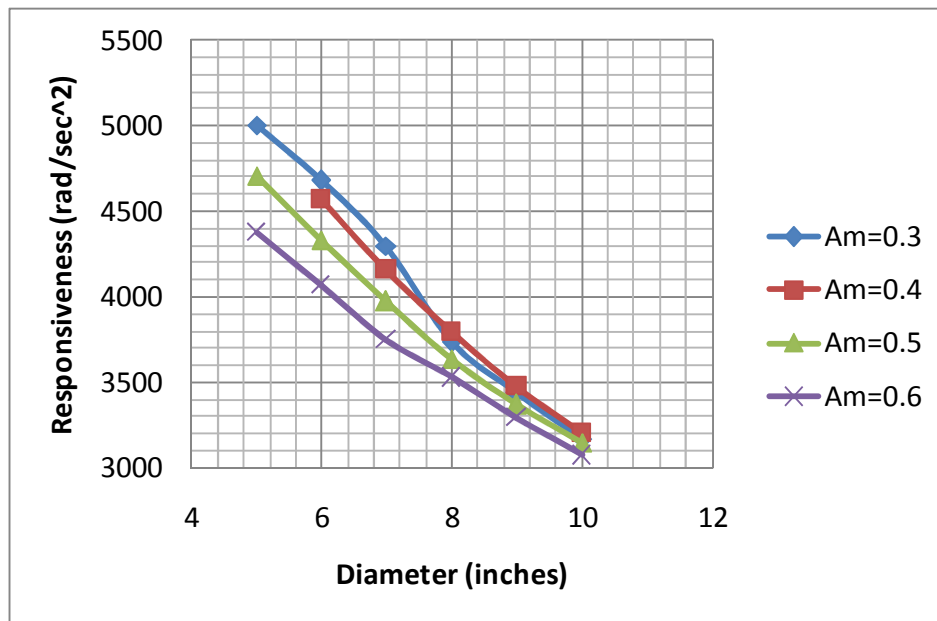


Figure 5.13: SRM Responsiveness Design Map (2-D)

The decrease in output responsiveness (the torque to inertia ratio) with increasing diameter (Figure 5.13) was expected based on the dependence of torque and inertia on the motor diameter in Table 5.6 (approximately D_m^4 for torque and D_m^5 for inertia). Similar responsiveness trends were observed for off-the-shelf motors (see Section 7.2.1).

Table 5.6: SRM Power-Law Scaling Rules ($P_p = kD_m^b = kD_m^{b-1}L_m$)

	Aspect Ratio	Constant (k)	Power (b)
Torque	0.3	0.009	4.18
	0.4	0.015	4.19
	0.5	0.015	4.32
	0.6	0.016	4.43
Weight	0.3	0.041	2.95
	0.4	0.059	2.95
	0.5	0.077	2.96
	0.6	0.094	2.97
Inertia	0.3	0.00012	4.87
	0.4	0.00018	4.88
	0.5	0.00025	4.91
	0.6	0.00031	4.93
Torque Density	0.3	0.428	1.0
	0.4	0.512	1.0
	0.5	0.574	1.0
	0.6	0.626	1.0
Responsiveness	0.3	-385	1.0
	0.4	-342	1.0
	0.5	-315	1.0
	0.6	-259	1.0

5.2.2 HGT Scaling Rules

The HGT scaling rules are based on the reference design (Figure 5.14) and the standard set of assumptions (Table 5.7) discussed in Chapter 3. Table 5.8 provides the proportions used to determine the internal design parameters of the HGT as a function of

the overall diameter and length. The reference load inertia multiplier used for the responsiveness computation was taken as the inertia of the HGT.

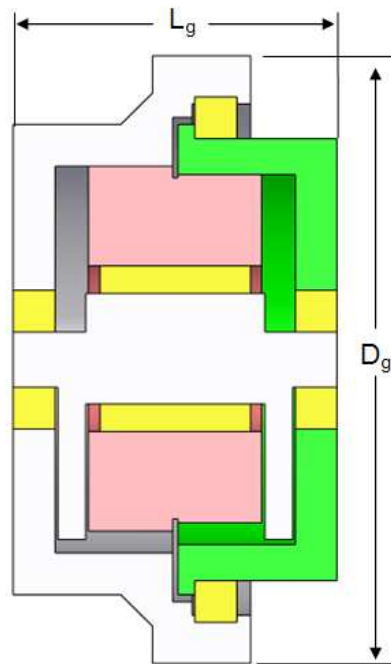


Figure 5.14: HGT Reference Design

Table 5.7: HGT and PEGT Constants and Fixed Parameters

Parameter	Value
Pressure angle	$\phi=25$
Minimum tooth number difference	$N_{\min}=3$
Number of teeth in contact	3 (nominal load condition)
Efficiency	100%
Axial clearance	$c = 0.005D_g$
Diametral pitch range	$5 < P_d < 25$
Bending strength	$S_b=100$ ksi
Contact strength	$S_c=250$ ksi
Density	$\rho = 0.284 \text{ lbm/in}^3$
Velocity Factor (K_v)	1.1
Load Distribution Factor (K_m)	1.3
Geometry Factor (J)	0.5
Output Speed (rpm)	1

Table 5.8: Suggested Proportions for the HGT Internal Design Parameters

Parameter	HGT
Output Gear Pitch Diameter	$d_{r2} = 0.65D_g$
Wobble Gear Face Width (1 stage)	$L_w = 0.30L_g$
Gear Ratio Range (g)	75-500
Aspect Ratio Range (A_g)	0.4 to 1.0
Balancing Mass Width	$w=0.10L_g$

Building upon the gear tooth bending stress discussion in Chapter 3, it is important for the reader to take note of the values of the stress modification factors used to compute the torque capacity of the HGT and PEGT in this report (Table 5.7). According to Juvinal and Marshek [2000], the velocity factor K_v ranges between 1.0 and 1.4 (depending on the pitch line velocity) for very accurate gearing (highest precision, shaved and ground). According to Shigley and Mischke [1989] and Juvinal and Marshek [2000], the load distribution factor K_m can be as low as 1.3 if the following

conditions are achieved: accurate mounting, low bearing clearances, minimum deflections, and precision gears. The values of the J factor range between 0.2 and 0.6 in standard AGMA look-up tables for involute gear teeth, and Appendix A4 provides a simple derivation to justify the meaning behind these J factor values.

The values of these three factors (K_v , K_m , and J) will be held constant for of the HGT and PEGT gear mesh designs in this report for a few reasons. First, the HGT and PEGT utilize circular arc gear teeth, and there are no suggested values for these factors for circular arc teeth. Ongoing research at the RRG and future prototype tests should provide more guidance on the selection of these factors. It is expected that circular arc gear teeth will provide superior load carrying capability when compared to standard involute teeth, and this expectation has been reflected in this research by being somewhat aggressive in the choice of the values for these three factors. Second, keeping these factor values fixed will allow the designs generated in this report to be used as a baseline for comparison with future gear train designs. Finally, it will also allow a focus on how changes in the geometric design parameters (and not subjectively chosen stress modification factors) affect the performance parameters.

This section will provide design maps and scaling rules for small diameter gear train designs (6, 8, 10, and 12 inches) and a constant gear ratio of 100 to 1. The primary reason for this smaller range of diameters is that the resulting scaling rules and design maps are more accurate (i.e., lower fitting errors) and are more useful for smaller ranges. For large diameter ranges, the torque, weight, and inertia can vary by multiple orders of magnitude, and this can result in large fitting errors when using regression techniques to obtain the design maps and scaling rules. For similar results for larger diameter gear train designs, the reader is referred to the integrated actuator designs in Section 6.5.

Figure 5.15-Figure 5.20 provide design maps (3-D plots) of the torque, weight, inertia, torque density, and responsiveness as a function of the diameter and aspect ratio, and Table 5.9 summarizes the data used to generate the maps. Table 5.10 lists the scaling rule coefficients for the low order polynomial surfaces in the 3-D plots, and Table 5.11 summarizes the values of the three error metrics (E_{avg} , E_{max} , and E_{rms}) for the polynomial fits. Again, the reader should not be alarmed at the relatively high fitting error E_{max} for some of the performance parameters because these typically only occur for the smallest data points in a set, for which the magnitudes of the parameters are relatively small. These maps and rules are of sufficient accuracy to quickly obtain scaled sets of HGT designs. Figure 5.21-Figure 5.26 provide all the same design and performance parameter information in the form of 2-D plots, and Table 5.12 lists the constants for the simple power law scaling rules obtained from the 2-D plots. Table 5.13 provides the estimated bearing load capacity requirements for the assumed operating life of 5,000 hours (based on the standard bearing life relationship in Section 3.14.1).

In this and the remaining gear train sections of this chapter, both the input responsiveness (R_i) and output responsiveness (R_o) maps are shown for completeness. However, they do exhibit identical trends, with the input responsiveness value being scaled by a factor of the gear ratio (g) with respect to the other, according to the relationship derived in Section 4.3.4.

$$R_i = gR_o \quad \text{Eqn. 140}$$

Building upon the discussion of the contact ratio and load sharing characteristics of circular arc teeth in Section 3.5.5, the primary reason for the decrease in torque density for increasing diameter is the fact that a contact ratio of 3 was used for designs of different diameters. Ongoing research at the RRG suggests that the contact ratio may increase as the gear mesh diameter increases. Thus, rather than considering the number

of teeth in contact, it may be reasonable to assume that all of the teeth in a given angular region of potential contact (say, 30 degrees) share the load. If more teeth share the load, then the maximum load on the central tooth will see lower loads, and the torque capacity for a given diameter will then increase.

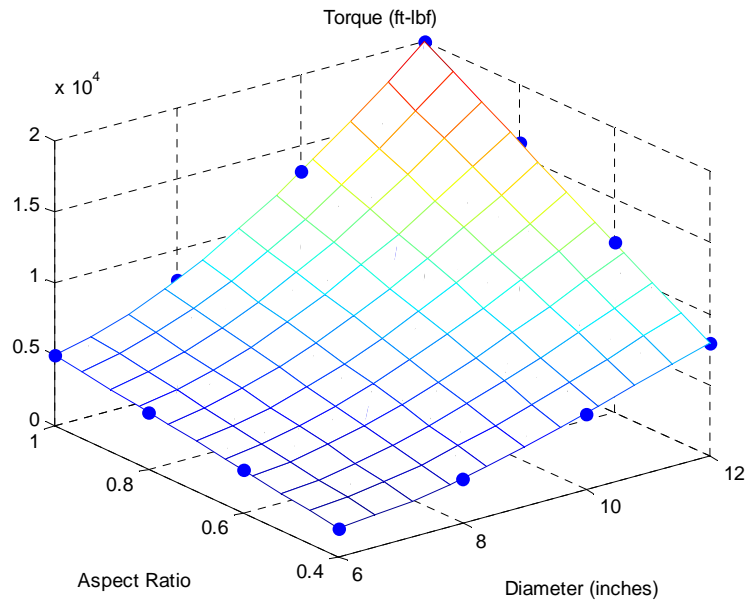


Figure 5.15: HGT Torque Design Map

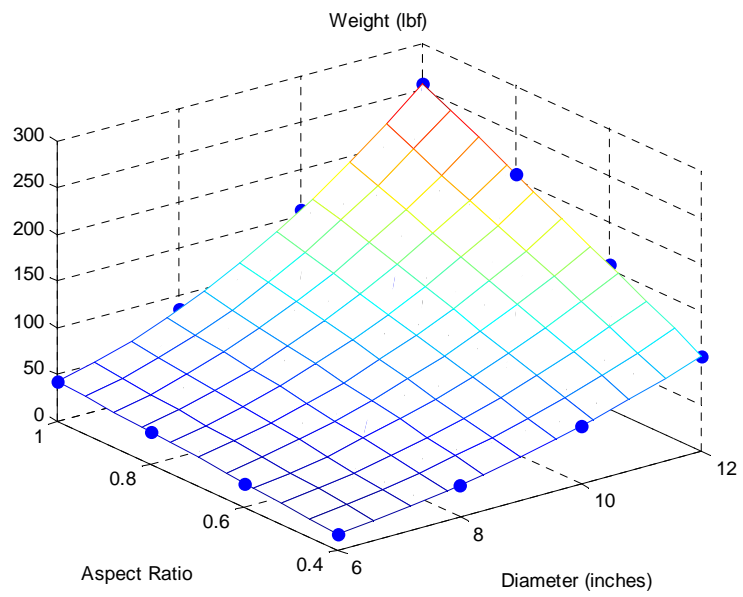


Figure 5.16: HGT Weight Design Map

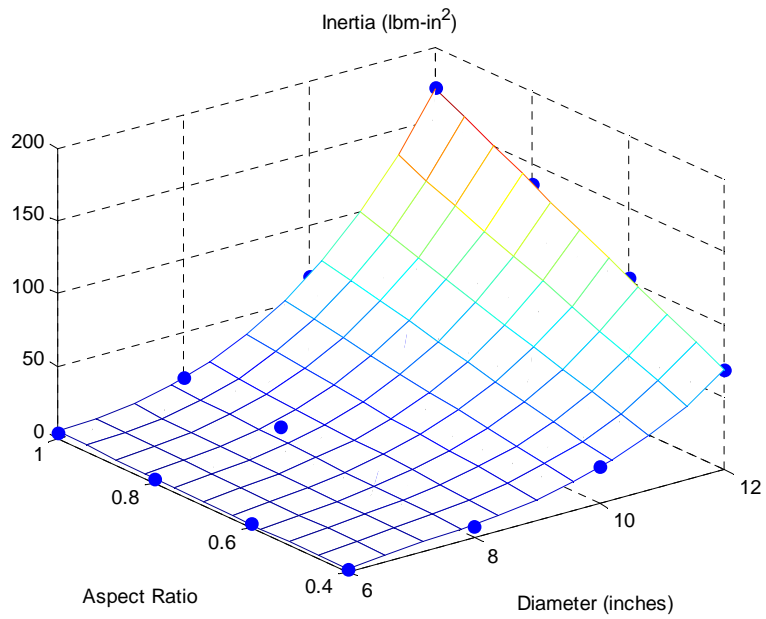


Figure 5.17: HGT Inertia Design Map

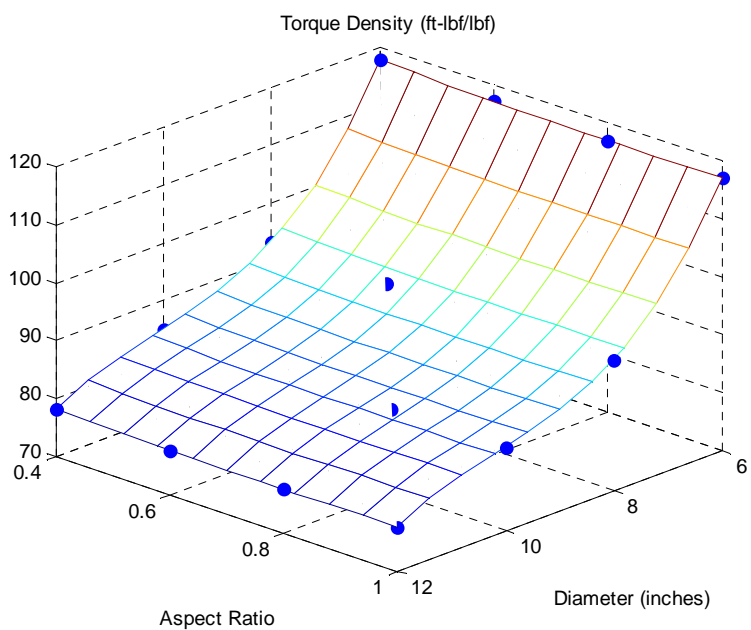


Figure 5.18: HGT Torque Density Design Map

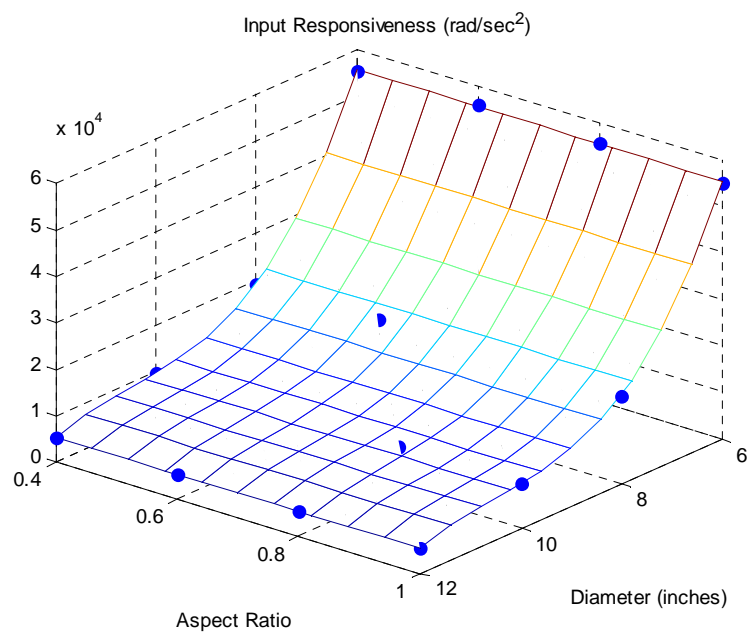


Figure 5.19: HGT Input Responsiveness Design Map

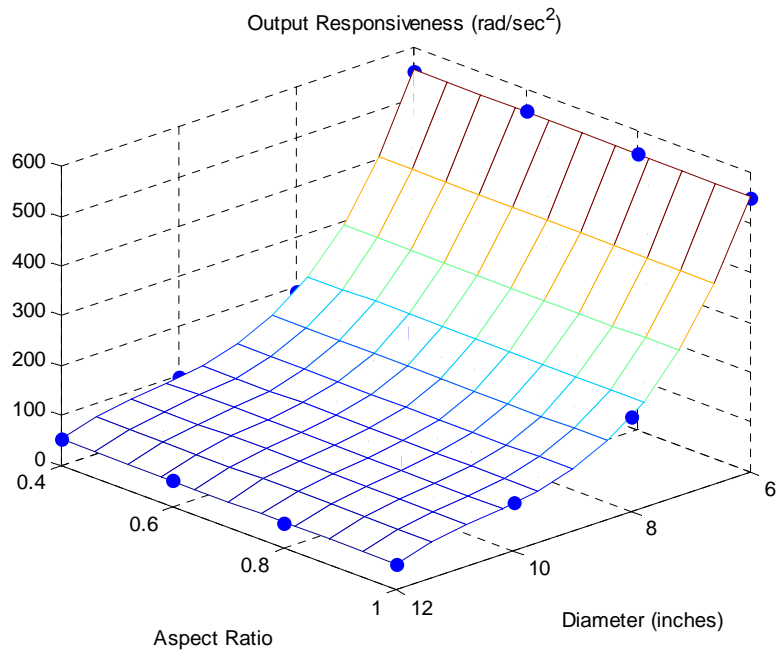


Figure 5.20: HGT Output Responsiveness Design Map

Table 5.9: HGT Design and Performance Parameter Data

Overall Diameter (inches)	Shell Diameter (inches)	Length (inches)	Aspect Ratio	Gear Ratio	Torque (ft-lbf)	Weight (lbf)	Inertia (lbm-in ²)	Torque Density (ft-lbf/lbf)	Input Responsiveness (rad/sec ²)	Output Responsiveness (rad/sec ²)	Diametral Pitch, Pd
6	6.1	2.4	0.4	100	1994	17	2	118	55340	553	5.1
8	7.4	3.2	0.4	100	3152	34	8	93	19071	191	5.8
10	9.0	4.0	0.4	99	5276	62	26	85	9602	97	5.4
12	10.4	4.8	0.4	101	7977	102	68	78	5337	53	5.1
6	6.1	3.6	0.6	100	2991	26	2	117	55795	558	5.1
8	7.4	4.8	0.6	100	4727	51	11	93	19231	192	5.8
10	9.0	6.0	0.6	99	7914	94	38	85	9681	98	5.4
12	10.4	7.2	0.6	101	11966	154	102	78	5380	53	5.1
6	6.1	4.8	0.8	100	3989	34	3	117	55665	557	5.1
8	7.4	6.4	0.8	100	6303	68	15	92	19155	192	5.8
10	9.0	8.0	0.8	99	10552	125	51	84	9646	97	5.4
12	10.4	9.6	0.8	101	15955	206	136	78	5361	53	5.1
6	6.1	6.0	1	100	4986	43	4	117	55073	551	5.1
8	7.4	8.0	1	100	7879	85	19	93	18899	189	5.8
10	9.0	10.0	1	99	13190	156	65	85	9523	96	5.4
12	10.4	12.0	1	101	19943	257	172	78	5295	52	5.1

Table 5.10: HGT Design Map Coefficients, n_i

$$(P_P = n_0 + n_1 D_g + n_2 A_g + n_3 D_g A_g + n_4 D_g^2 + n_5 A_g^2 + n_6 D_g A_g^2 + n_7 D_g^2 A_g + n_8 D_g^3 + n_9 A_g^3)$$

Parameter	Constant	D_g	A_g	$D_g A_g$	D_g^2	A_g^2	$D_g A_g^2$	$D_g^2 A_g$	D_g^3	A_g^3
Torque	9326	-3342	7253	-1834	384	0	0	241	-14	0
Weight	-12	4	86	-28	-1	0	-1	4	0	2
Inertia	-303	109	256	-77	-12	-5	0	6	0	6
Torque Density	448	-101	-19	0	10	20	0	0	0	-6
Input Responsiveness	543933	-150379	-1343	185	14216	0	0	-7	-452	0
Output Responsiveness	5475	-1517	-13	2	144	0	0	0	-5	0

Table 5.11: HGT Error Metrics

Parameter	E_{max} (%)	E_{avg} (%)	E_{rms} (%)
Torque	1.4	0.4	0.5
Weight	0.1	0.1	0.1
Inertia	21.0	6.1	9.1
Torque Density	0.0	0.0	0.0
Input Responsiveness	0.6	0.5	0.5
Output Responsiveness	0.6	0.5	0.5

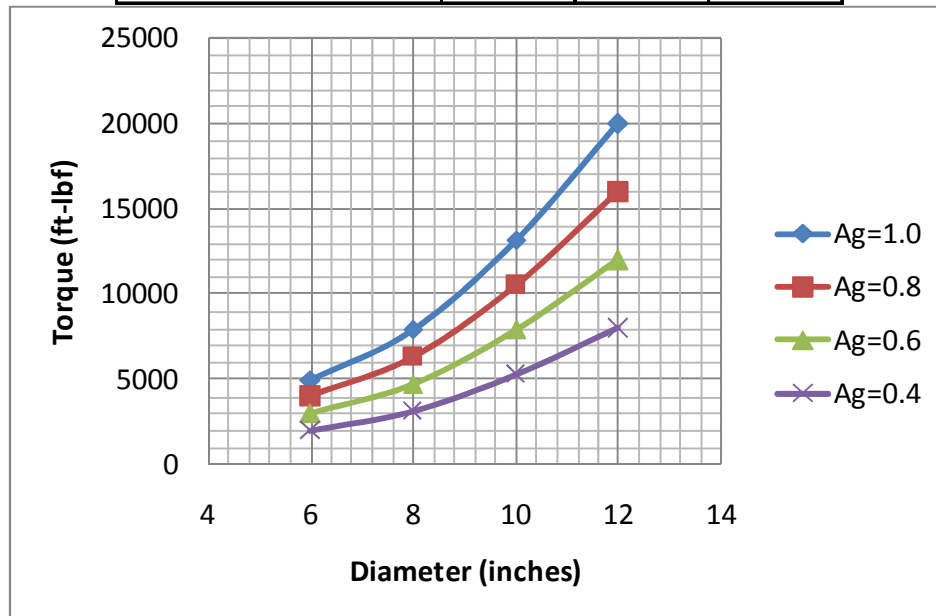


Figure 5.21: HGT Torque Design Map (2-D)

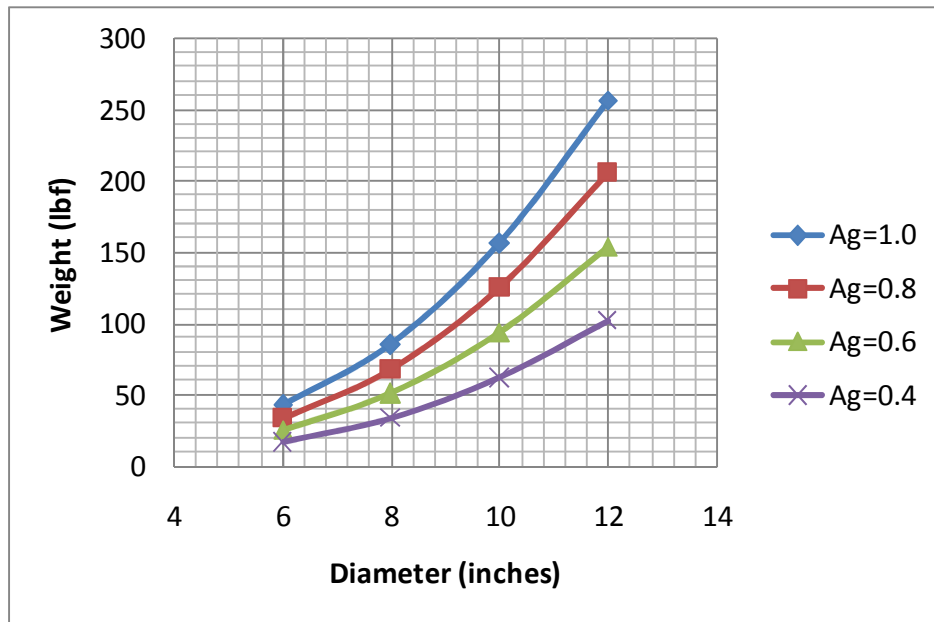


Figure 5.22: HGT Weight Design Map (2-D)

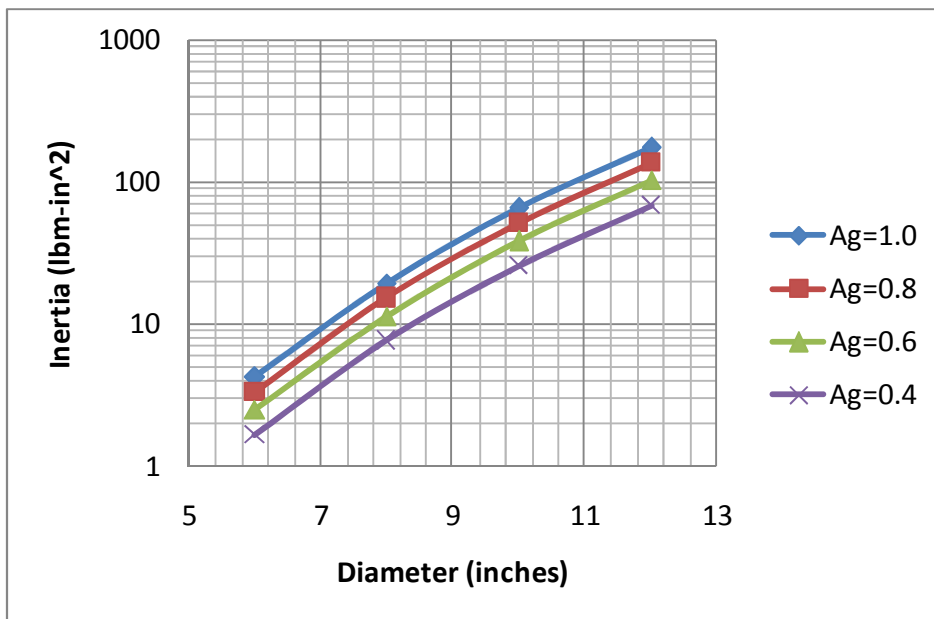


Figure 5.23: HGT Inertia Design Map (2-D)

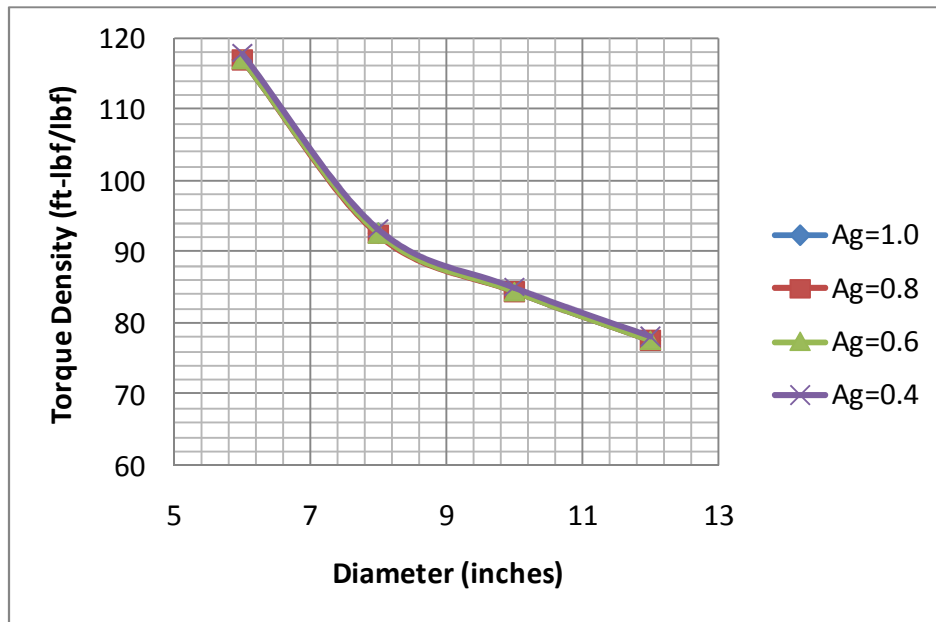


Figure 5.24: HGT Torque Density Design Map (2-D)

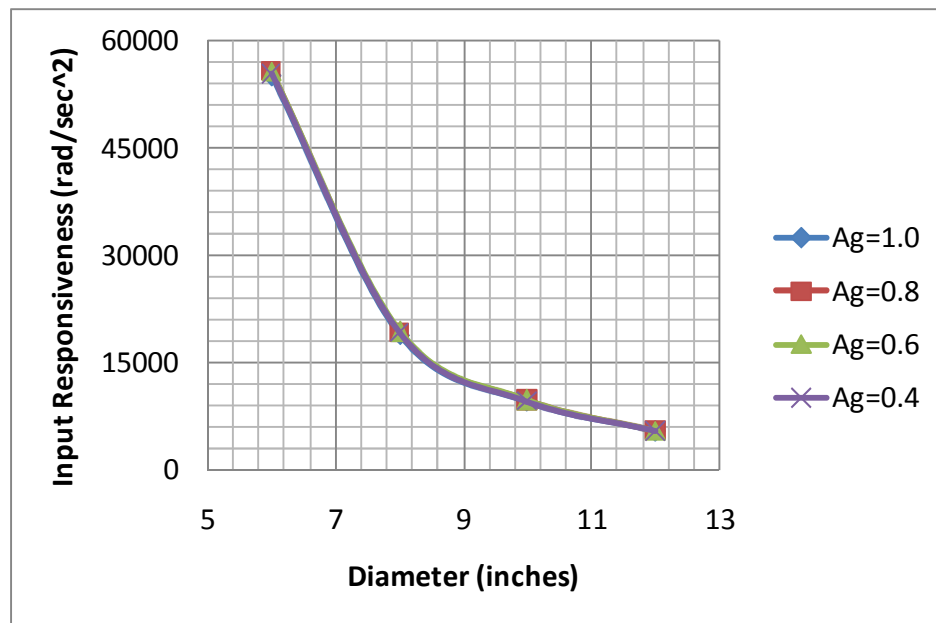


Figure 5.25: HGT Input Responsiveness Design Map (2-D)

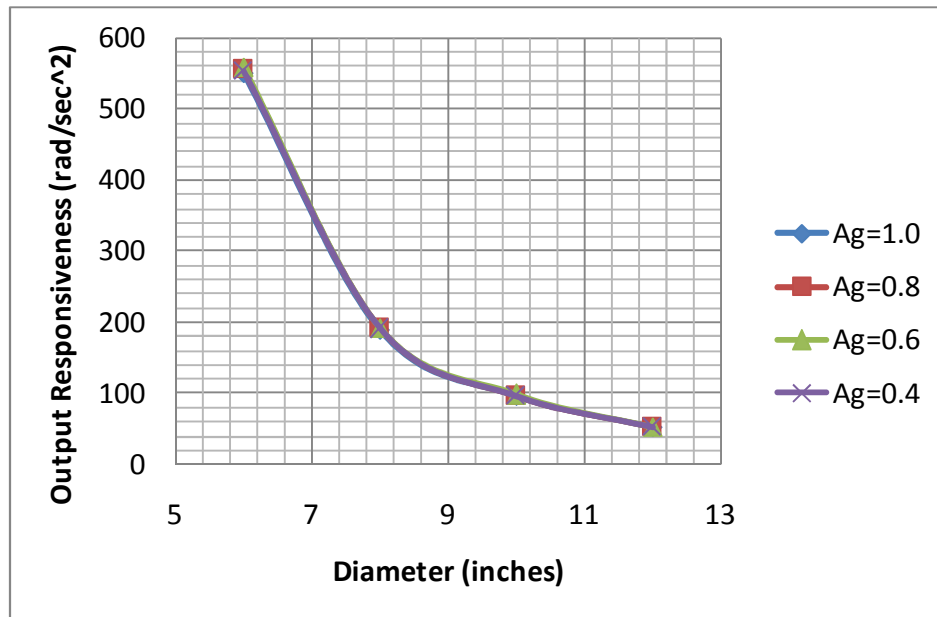


Figure 5.26: HGT Output Responsiveness Design Map (2-D)

The decrease in output responsiveness (the torque to inertia ratio) with increasing diameter (Figure 5.26) was expected based on the dependence of torque and inertia on the gear train diameter in Table 5.12 (approximately D_g^2 for torque and D_m^5 for inertia).

Table 5.12: HGT Power-Law Scaling Rules ($P_p = kD_g^b = kD_g^{b-1}L_g$)

	Aspect Ratio	Constant (k)	Power (b)
Torque	0.4	51.7	2.012
	0.6	77.6	2.012
	0.8	103.4	2.012
	1.0	129.3	2.012
Weight	0.4	0.158	2.596
	0.6	0.238	2.596
	0.8	0.318	2.596
	1.0	0.398	2.596
Inertia	0.4	0.00011	5.360
	0.6	0.00017	5.360
	0.8	0.00022	5.361
	1.0	0.00028	5.363
Torque Density	0.4	324.7	-0.58
	0.6	324.7	-0.58
	0.8	324.7	-0.58
	1.0	324.7	-0.58
Output Responsivenss	0.4	22459	-3.37
	0.6	22459	-3.37
	0.8	22459	-3.37
	1.0	22459	-3.37

Table 5.13: HGT Bearing Load Capacity Requirements (lbf)

Output Bearing	Wobble Bearing	Shaft Bearing Right	Shaft Bearing Left
36797	61144	24398	24471
44580	72467	28916	29003
60212	96460	38392	38509
76369	121981	48458	48602
43290	91716	36596	36707
52700	108700	43373	43504
71312	144690	57588	57763
90579	182972	72686	72903
49479	122288	48795	48943
60425	144933	57831	58006
81866	192920	76784	77018
104084	243963	96915	97204
55465	152859	60994	61178
67875	181167	72289	72507
92039	241151	95980	96272
117093	304954	121144	121505

5.2.3 PEGT Scaling Rules (1st Stage Star Gear Train)

This section will detail design maps and scaling rules for PEGT that utilizes a star gear train as the 1st stage. The first set of scaled PEGT designs is based on a recent prototype design for a submarine water vane application, in which the rated torque capacity is limited by the bearings rather than the gear teeth.

The second set of designs uses the same diameters and aspect ratios as used above for the HGT to facilitate later comparisons between the two (Section 5.3). The rated torque capacity of the second set of designs is limited by the gear teeth. The key assumption for the second set of designs is that bearings of adequate load capacity can be found to match the bearing-limited torque capacity to the tooth-limited torque capacity. To allow a quick feasibility check, the required bearing load capacities that result in an

operating life of 5,000 hours at the stated tooth-limited torque capacity will also be provided.

5.2.3.1 *Bearing-Limited PEGT Designs*

Figure 5.27 displays a current prototype PEGT design (with motor included) for a submarine water vane application [Tesar et al., 2008]. The results in this section are based on the geometry of this reference design and do not include the motor.

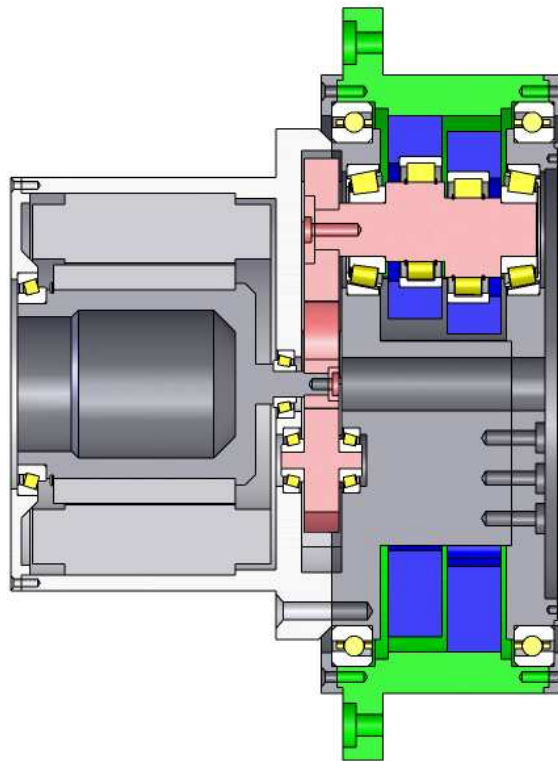


Figure 5.27: PEGT Design (Reference Geometry for Bearing-Limited PEGT Design, Diameter = 11 inches)

Utilizing the design parameter designations in Section 3.10, Table 5.14 summarizes the set of design parameters (in terms of the overall diameter and length) and important assumptions used in these PEGT designs. Then, Table 5.15 summarizes the

design and performance parameter results for PEGT designs that were generated based on these parameters and assumptions.

Table 5.14: PEGT Design Parameters and Assumptions

Parameter	Value
Output Gear Pitch Diameter	$d_r = 0.87D_g$
PE Gear Face Width	$L_{pe} = 0.22L_g$
1 st Stage Face Width	$L_1 = 0.11L_g$
Overall Aspect Ratio	$A_g = 0.40$
Center Distance to Crankshaft	$c_c = 0.25D_g$
Bearing Life	6000 hours
Output Speed	1 rpm
PEGT Gear Ratio	35 to 1
1 st Stage (Star) Gear Ratio	3 to 1
Overall Gear Ratio	105 to 1
Density	$\rho = 0.284 \text{ lbm/in}^3$

Table 5.15: PEGT Design and Performance Parameter Summary⁶

Diameter (inch)	Length (inch)	Nominal Torque Capacity* (ft-lbf)	Peak Torque Capacity** (ft-lbf)	Weight (lbf)	Torque Density (ft-lbf/lbf)	PE Gear Bearing (SKF Part #)
5	2.0	715	1250	8	85	RNU 202 ECP
7	2.8	2008	3750	23	87	RNU 204 ECP
8	3.2	3121	6670	34	91	RNU 2205 ECP
10	4.0	5030	8900	67	75	RNU 206 ECP
11	4.4	6938	13100	89	78	RNU 307 ECP
12	4.8	10315	18500	116	89	RNU 2206 ECP
18	7.2	35431	91000	390	91	RNU 1011 ECP
24	9.6	79470	168000	925	86	RNU 211 ECP
30	12.0	130314	295000	1807	72	RNU 217 ECP
36	14.4	263670	585000	3122	84	RNU 216 ECP
48	19.2	571300	1750000	7400	77	RNU 1038 ML

In Table 5.15, the nominal torque capacity is the applied torque which results in a calculated operating life of 6,000 hours for the PE gear bearing and is based on the bearing's dynamic load capacity. The PE gear bearing or left crankshaft bearing (Figure 3.22 from Chapter 3) are typically the limiting bearings in this design, and all of the other bearings (right crankshaft, idler shaft, motor shaft, and output) should have a longer operating life. The peak load capacity is the applied torque which loads the PE gear bearing up to its static load capacity (which is typically 2 to 3 times its dynamic load capacity).

Specific bearings were selected for each design in this set, and detailed solid models were generated for two of the designs in the set (diameters of 11 inches and 30 inches). Cylindrical roller bearings were found to have the highest load capacity available among bearing types that fit into the available PE gear and crankshaft geometry. Further, cylindrical roller bearings without an inner race (Figure 5.28) were found to have

⁶ No responsiveness computations were made for this set of designs because the application involved a very low output speed of 1 rpm. Emphasis was placed on maximizing torque density rather than responsiveness. For numerical values of the responsiveness for similar sizes, see section 5.2.3.3.

higher load capacities than full complement cylindrical roller bearings of the same size. These bearings will be utilized in the current PEGT prototype.

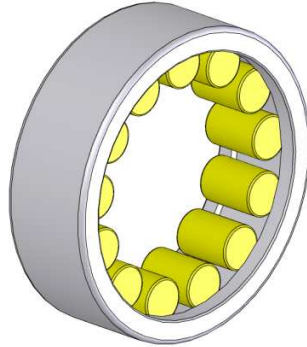


Figure 5.28: SKF Cylindrical Roller Bearings Selected for PE Gear (cage that retains rollers not shown)

Figure 5.29 and Figure 5.30 detail design maps (2-D) for these PEGT designs and illustrate how the bearing-limited torque varies as a function of diameter. Scaling rules in simple power law form are provided in the caption of each figure.

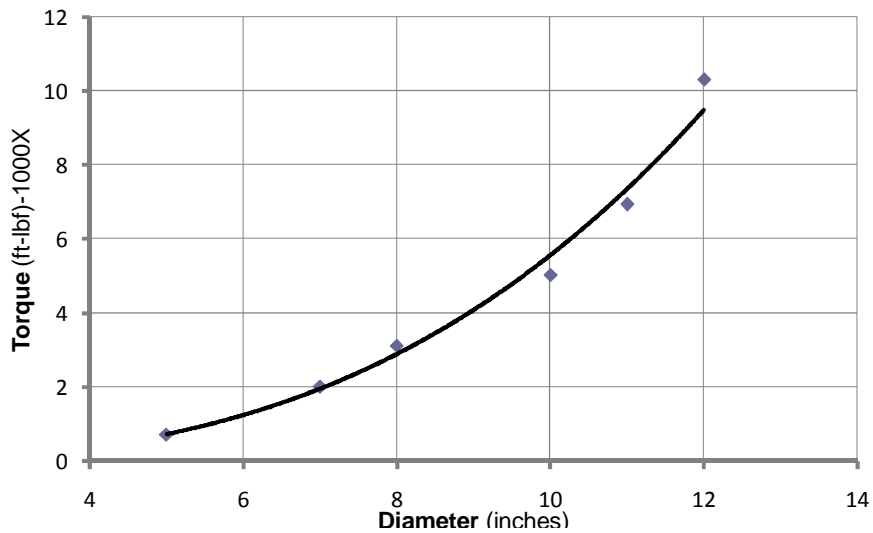


Figure 5.29: PEGT Torque Scaling Rule (Diameters 5-12 inches)

$$\left(T = 0.006\mathcal{D}_g^{2.93} = 0.006\mathcal{D}_g^{1.93}L_g\right)$$

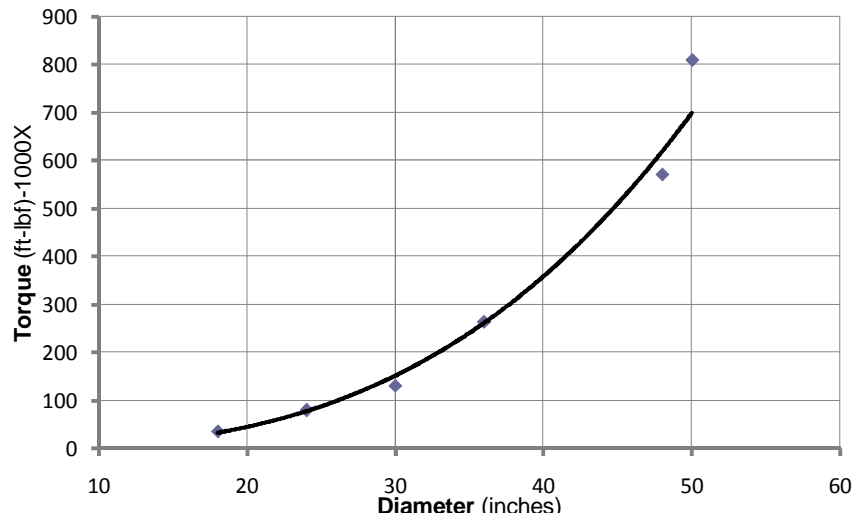


Figure 5.30: PEGT Torque Scaling Rule (Diameters 18-48 inches)

$$\left(T = 0.005 \mathcal{D}_g^{2.99} = 0.005 \mathcal{D}_g^{1.99} L_g \right)$$

All of these gear train designs have an output speed of 1 rpm to match the needs of the submarine application, and all of the torque capacity ratings listed above are based on this reference speed. If the output speed changes, these torque ratings will also change, and the standard bearing life relationship (detailed in Section 3.14.1) can be used to study the effect of a speed change on torque capacity.

$$L = \left(\frac{C}{P} \right)^n \frac{1}{\omega} 10^6 \quad \text{Eqn. 141}$$

In this relationship, C is the bearing dynamic load capacity (lbf), P is the equivalent radial load (lbf) on the bearing, ω is the speed (rpm), and n is a constant based on the bearing type (n = 10/3 for roller bearings).

In the PEGT design, since the PE gear or crankshaft bearings limit the design, each of parameters in this bearing life relationship is specific to these bearings of interest. The load on the bearing (P) is directly proportional to the torque (T) according to the

derivation by Sigwald and Tesar [2008]. Substituting T for P and solving for T yields the following important relationship.

$$T \propto C(L\omega)^{-3/10} \quad \text{Eqn. 142}$$

For the purposes of this section, the bearing load capacity C can be assumed to be constant if the designer has selected the largest bearing available that will fit on the crankshaft and still allow for adequate strength of the crankshaft and supporting components. The desired operating life L can also be assumed to be constant if the life requirement for the application is known. Using these assumptions, this relationship reduces to the following.

$$T \propto \omega^{-3/10} \quad \text{Eqn. 143}$$

Using this simple but physically meaningful relationship, Table 5.16 and Figure 5.31 illustrate the effect of the PEGT output speed choice on the bearing-limited torque capacity for a range of output speeds. The figure plots the data on a log-log scale, so the true relationship is non-linear when plotting this relationship on untransformed axes. For example, changing the output speed from 1 rpm to 0.1 rpm increases the torque capacity by a factor of 2 (i.e., the torque rating for a speed of 0.1 rpm is double the torque rating for a speed of 1 rpm).

Table 5.16: Effect of Output Speed on PEGT Torque Capacity (fixed bearing life and load capacity)

Change in Speed Relative to Reference Speed ($\omega = 1$ rpm)	Absolute Output Speed (rpm)	Change in Torque Relative to Torque Capacity at Reference Speed ($\omega = 1$ rpm)
0.01	0.01	3.98
0.05	0.05	2.46
0.1	0.1	2.00
0.25	0.25	1.52
0.5	0.5	1.23
1	1	1.00
1.5	1.5	0.89
2	2	0.81
5	5	0.62
10	10	0.50
20	20	0.41
50	50	0.31

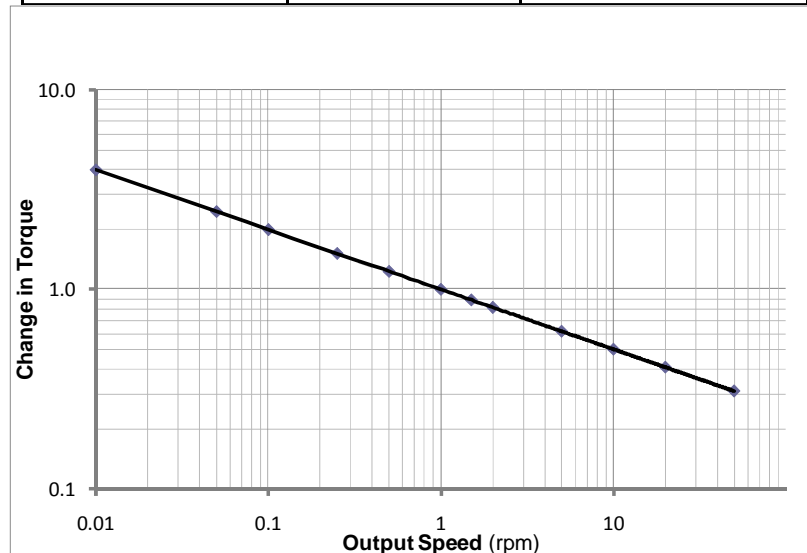


Figure 5.31: Effect of Output Speed on PEGT Torque Capacity⁷

All of the above torque capacity values are limited by the bearings and not the gear teeth. However, it is helpful to compare the bearing-limited torque capacities

⁷ This figure shows how the bearing-limited torque capacity varies as a function of output speed and is independent of any particular PEGT geometry, gear ratio, or other gear train assumptions. It is simply a plot of the approximately inverse cubic relationship between torque T and speed ω that results from the bearing life relationship. The anticipated increase or decrease in the torque capacity for any change in output speed can be considered.

detailed above with the gear tooth-limited torque capacity (shown in Table 5.17) for every design in this set and determine how these two values vary as a function of diameter. The tooth limited load capacities in this set are based on the assumptions listed previously in Table 5.7. Table 5.17 illustrates that the bearing-limited capacity is approximately 10 to 40% larger than the gear tooth limited capacity for the range of diameters considered, with an average of near 25% (i.e., a factor of 1.25 larger). Because both the bearing-limited torque capacities and tooth-limited load capacities are known to increase linearly with an increase in length (based on the fundamental governing equations for these phenomenon), these percentages should not vary significantly for larger or smaller aspect ratios. The largest two designs from the set (diameters of 36 and 48 inches) have been excluded in this comparison because designs of this size have not been considered in great detail. The diametral pitch (P_d) for each gear train design has also been listed for future reference because it can significantly affect the gear-tooth limited torque capacity. Note that these results depend on the output speed of the gear train, and any change in operating speed will change the bearing-limited torque according to the torque-speed relationship plotted above in Figure 5.31.

Table 5.17: Comparison of Bearing and Tooth-Limited Load Capacities of the PEGT

Diameter (inch)	Length (inch)	Bearing-Limited Torque Capacity (ft-lbf)	Gear Tooth-Limited Torque Capacity (ft-lbf)	Diametral Pitch (P_d) for Tooth-Limited Designs	Ratio of Bearing-Tooth Torque Capacity
5	2.0	715	583	23.9	1.2
7	2.8	2008	1600	17.1	1.3
8	3.2	3121	2389	14.9	1.3
10	4.0	5030	4665	12.0	1.1
11	4.4	6938	6210	10.9	1.1
12	4.8	10315	8062	10.0	1.3
18	7.2	35431	27208	6.6	1.3
24	9.6	79470	63879	5.0	1.2
30	12.0	130314	92909	5.4	1.4

5.2.3.2 Strategies for Balancing the Bearing and Gear-Tooth Limited Torque Capacities in the PEGT

Though the bearing-limited torque capacities appear to be superior to the tooth-limited load capacities in Table 5.17, it is important to note that all of the PEGT designs are based on an output speed of 1 rpm. If the operating speed is increased (and the same overall gear is used), the gear tooth limited capacity will decrease slightly, and the bearing-limited capacity will change according to the torque-speed relationship plotted above in Figure 5.31. For example, if the output speed is increased to 10 rpm, the bearing limited torque capacity will decrease by a factor of 2.

Because it appears that the bearing or the tooth-limited capacities may dominate for a given application, this section will provide some useful strategies for improving each one and/or matching the two.

For a fixed gear mesh diameter, the gear-tooth torque capacity (of a fixed diameter) can be most easily modified by changing the diametral pitch (width of the

tooth) and the face width. The reader is referred to the general gear train modeling Section 3.5 of Chapter 3 for documentation of these parameters. In general, for a fixed gear pitch diameter, decreasing the diametral pitch (increasing the width of the tooth) and increasing the face width will increase gear-tooth torque capacity.

The bearing limited torque capacity can be modified by referring to the bearing life equation discussed above.

$$T \propto C(L\omega)^{-3/10} \quad \text{Eqn. 144}$$

Two strategies to increase this bearing limited capacity are illustrated by Figure 5.32.

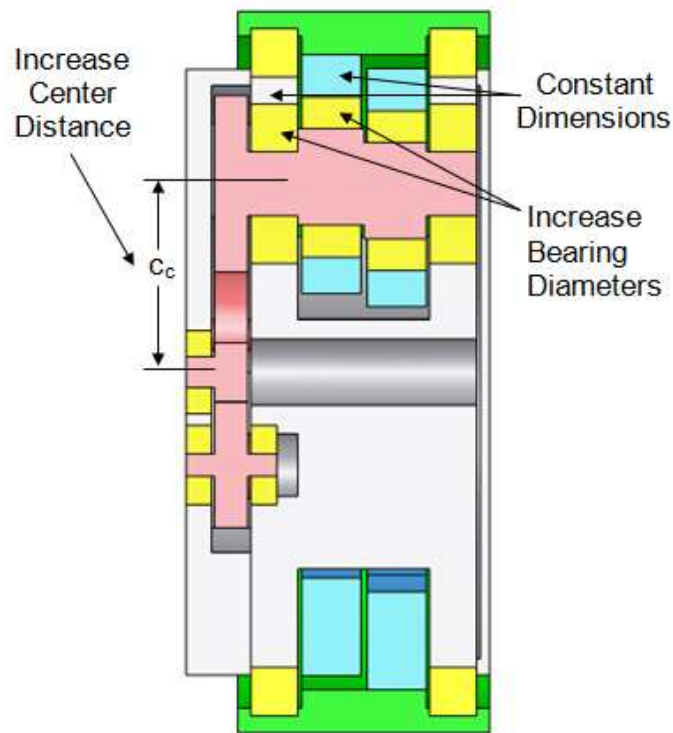


Figure 5.32: Strategies for Increasing the PEGT Bearing-Limited Load Capacity

The first strategy is to increase the center distance c_c , which increases the moment arm available for the crankshaft and PE gear bearings to apply the load that resists the output torque. This linearly decreases the applied load on the crankshaft and PE gear bearings for a given output torque capacity, or if the bearing load remains constant, the torque capacity increases. Figure 5.33 illustrates how the PEGT bearing-limited torque capacity (for the 11 inch diameter current prototype discussed above) varies as a function of the center distance with the bearing load capacity, gear mesh dimensions, and all other parameters held constant.

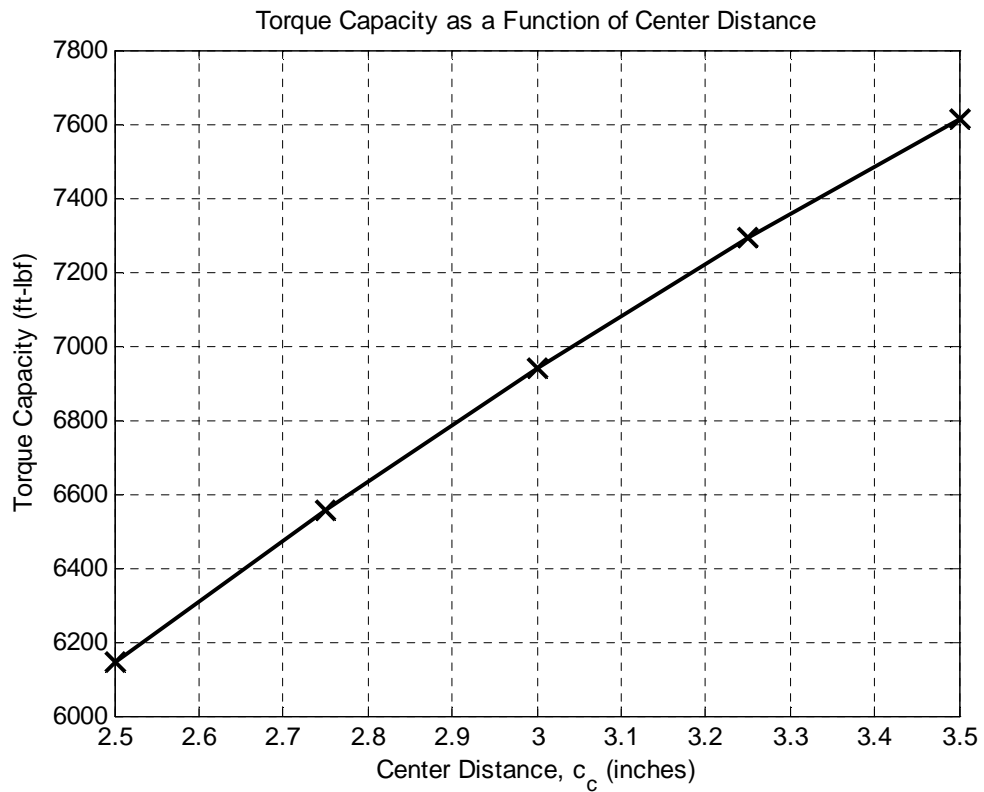


Figure 5.33: Bearing-Limited Torque Capacity as a Function of Center Distance for the PEGT (based on the 11 inch diameter prototype design, with fixed bearing load capacity and gear mesh dimensions)

If the constant dimensions noted in Figure 5.32 are maintained, then increasing the center distance requires that the crankshaft and PE gear bearing diameters be reduced. This decreases their load capacity C in the bearing life equation, and the bearing-limited torque capacity is linearly proportional to C . In order to determine how the bearing load capacity (C) varies as a function of the bearing diameter, the designer may consult theoretical relationships such as Faires [1965] or Brandlein et al. [1999] or may simply tabulate bearing load capacity as a function of diameter for the specific diameters of interest.

The second strategy is to increase the crankshaft and PE gear bearing diameters, which increases the load capacity C . According to the bearing life relationship, the torque increases linearly with an increase in the load capacity C . If the constant dimensions are maintained as shown in the figure, then increasing the bearing diameters requires that the center distance be reduced, which decreases the torque capacity.

The important point here is that both of these strategies are in conflict if the constant dimensions noted in Figure 5.32 must be maintained, and it is difficult to determine which will result in the highest torque capacity in the general case. The best strategy will depend on the specific center distances, bearing diameters, desired torque output, and overall diameter for a given application.

A final, simpler strategy is to use bearings with higher quality steel, which gives higher bearing load capacities C without changing the bearing roller and race sizes. The benefit of this strategy is that it will not disturb any of the other dimensions in the gear train, while the drawback is that it will usually increase the cost of the design.

The results of this section suggest that a designer can compute the gear tooth torque capacity (a straightforward task) for a given geometry and then use this information to confidently estimate the bearing-limited torque capacity (without selecting

specific bearing sizes). Then, the designer can then select specific bearings that will fit into the chosen PEGT geometry and verify an initial estimate.

5.2.3.3 Gear Tooth-Limited PEGT Designs

The maps and rules of this section assume that PE gear and crankshaft bearings of adequate load capacities can be found so that the bearing and tooth-limited torque capacities can be balanced. Specific bearings were not selected for the designs in this section due to the large number of designs being considered. However, the key result from the bearing-limited PEGT designs in the previous section relating the percentage of bearing-limited to tooth-limited torque capacities can be used as evidence that the former is typically near 125% of the latter.

These PEGT design maps and scaling rules are based on the reference design (Figure 5.34) and the standard set of assumptions (Table 5.7) discussed in Chapter 3. Table 5.18 provides the proportions used to determine the internal design parameters of the PEGT as a function of the overall diameter and length. The reader should note that the same assumptions and set of design parameter inputs used here for the PEGT were also used for HGT to facilitate later comparisons between the two. The reference load inertia multiplier used for the responsiveness computation was taken as the inertia of the PEGT. All of the PEGT designs in this section have an overall gear ratio of 100 to 1, a PE gear-output gear mesh ratio of 35 to 1, and a 1st stage gear ratio of 2.86 to 1.

This section will provide PEGT design maps and scaling rules for small diameter designs (diameters of 6, 8, 10, and 12 inches). For large diameter ranges, the torque, weight, and inertia can vary by orders of magnitude, and this can result in large errors when using regression techniques to obtain the design maps and scaling rules. For

similar results for larger diameter designs, the reader is referred to the integrated actuator designs in Section 6.5.

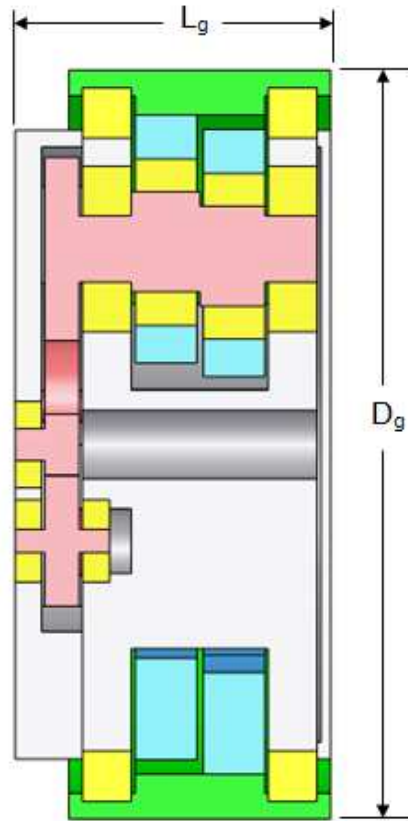


Figure 5.34: Star+PEGT Reference Design

Table 5.18: Suggested Proportions for the PEGT Internal Design Parameters

	PEGT (Star 1st Stage)	PEGT (Star Compound 1st Stage)
Output Gear Pitch Diameter	$d_r = 0.87D_g$	$d_r = 0.87D_g$
Face Width	$L_{pe} = 0.22L_g$	$L_{pe} = 0.20L_g$
Gear Ratio Range (g)	15-150	15-500
Aspect Ratio Range (A_g)	0.4 to 1	0.4 to 1
Center Distance to Crankshaft	$c_c = 0.27D_g$	$c_c = 0.27D_g$
1 st Stage Face Width	$L_1 = 0.11L_g$	$L_1 = 0.10L_g$

Figure 5.35-Figure 5.40 provide design maps (3-D plots) of the torque, weight, inertia, torque density, and responsiveness as a function of the diameter and aspect ratio, and Table 5.19 summarizes the data used to generate the maps. Table 5.20 lists the scaling rule coefficients for the low order polynomial surfaces in the 3-D plots, and Table 5.21 summarizes the values of the three error metrics (E_{avg} , E_{max} , and E_{rms}) for the polynomial fits. Again, the reader should not be alarmed at the relatively high fitting error E_{max} for some of the performance parameters because these typically only occur for the smallest data points in a set, for which the magnitudes of the parameters are relatively small. These maps and rules are of sufficient accuracy to quickly obtain scaled sets of PEGT designs. Figure 5.41-Figure 5.46 provide all the same design and performance parameter information in the form of 2-D plots, and Table 5.22 lists the constants for the simple power law scaling rules obtained from the 2-D plots. In order to verify if bearings of adequate load capacity are available for the given PEGT geometry, Table 5.23 summarizes the bearing load capacities required to achieve the reported gear-tooth torque capacity for the assumed operating life of 5,000 hours.

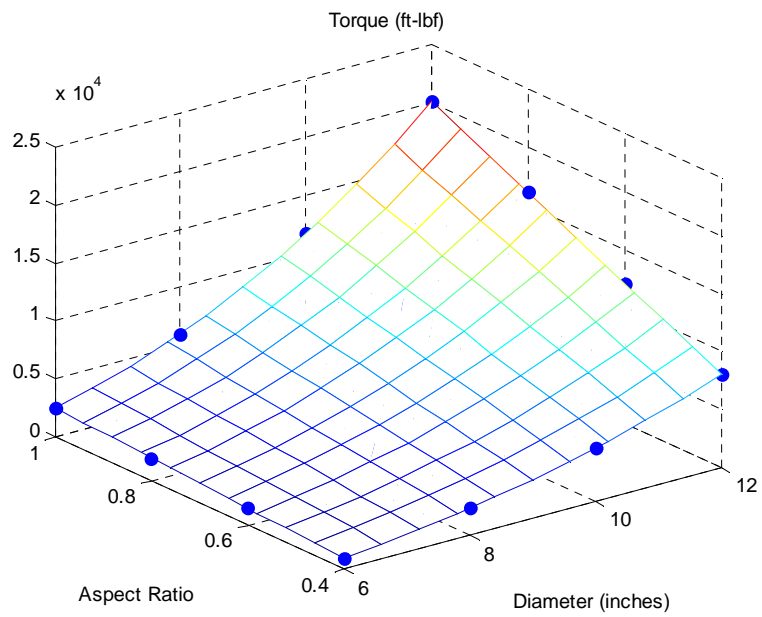


Figure 5.35: Star+PEGT Torque Design Map

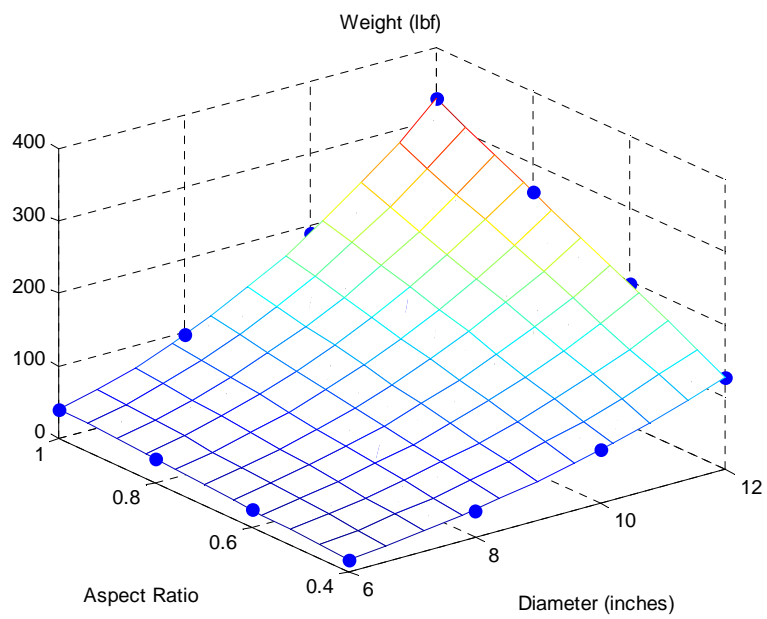


Figure 5.36: Star+PEGT Weight Design Map

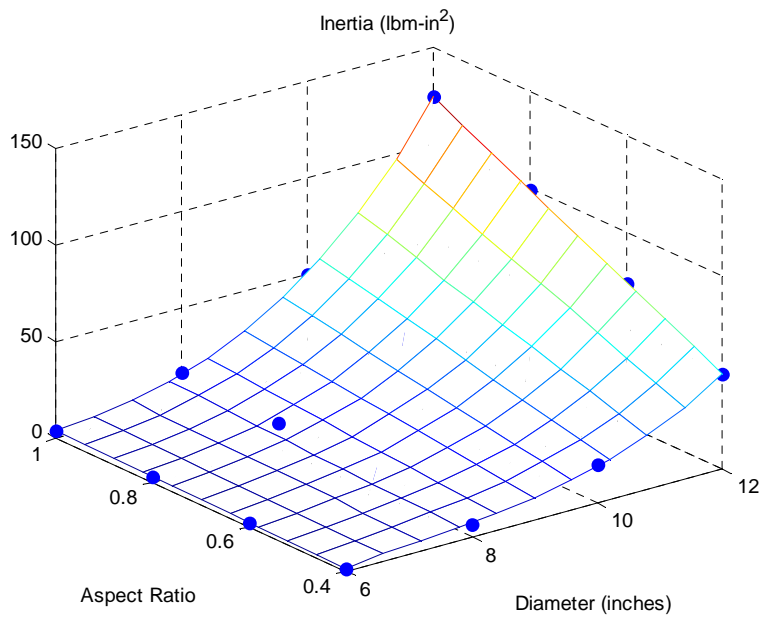


Figure 5.37: Star+PEGT Inertia Design Map

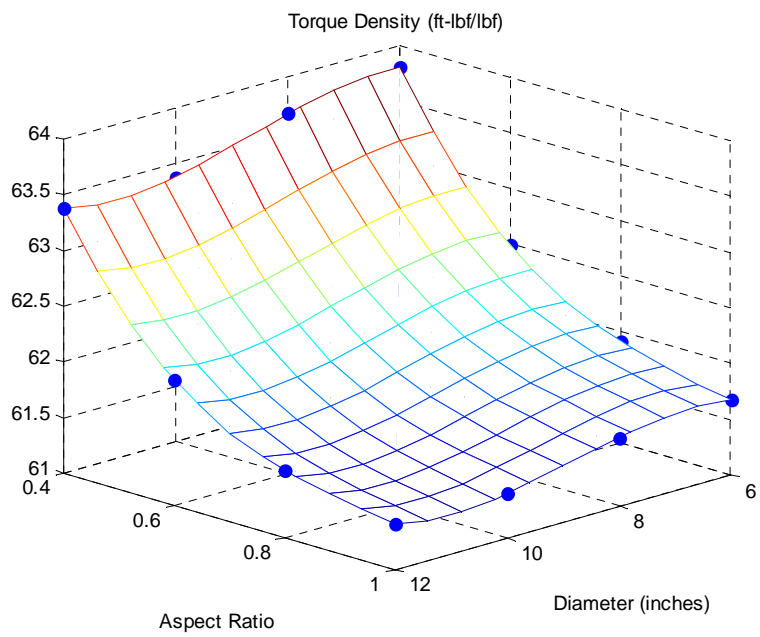


Figure 5.38: Star+PEGT Torque Density Design Map

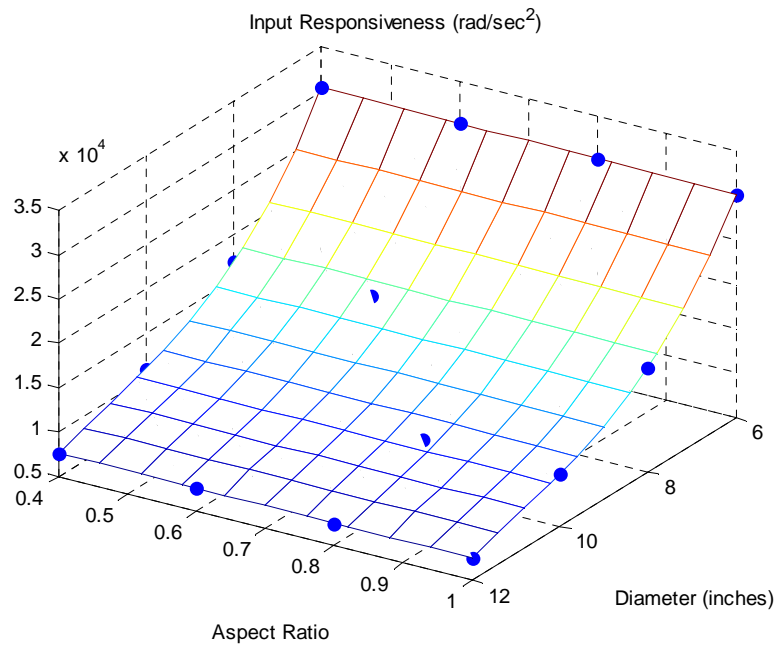


Figure 5.39: Star+PEGT Input Responsiveness Design Map

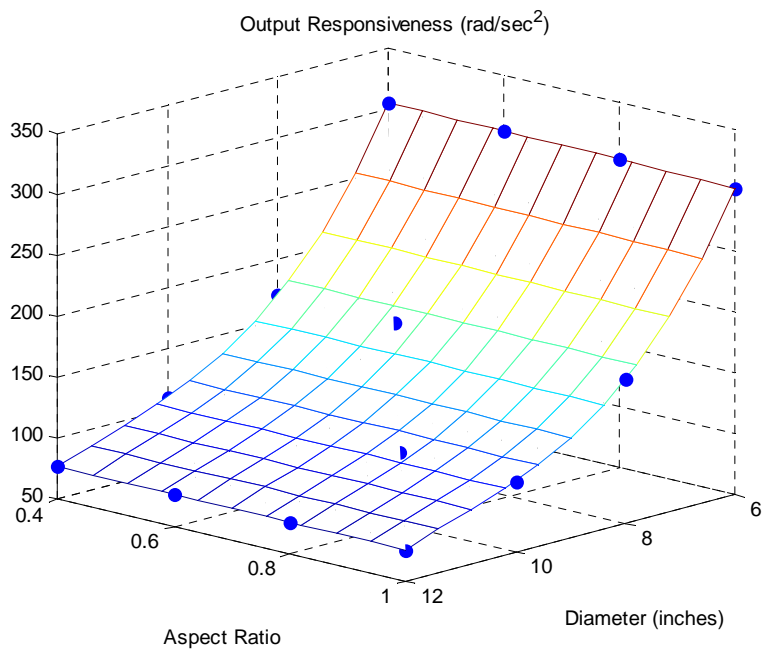


Figure 5.40: Star+PEGT Output Responsiveness Design Map

Table 5.19: Star+PEGT Design and Performance Parameter Data

Overall Diameter (inches)	Shell Diameter (inches)	Length (inches)	Aspect Ratio	Gear Ratio	Torque (ft-lbf)	Weight (lbf)	Inertia (lbm-in ²)	Torque Density (ft-lbf/lbf)	Input Responsiveness (rad/sec ²)	Output Responsiveness (rad/sec ²)	Diametral Pitch, Pd
6	5.2	2.4	0.4	100	1008	16	2	64	30441	305	20
8	6.9	3.2	0.4	100	2389	38	7	64	17039	171	15
10	8.6	4	0.4	100	4665	74	20	63	11018	110	12
12	10.3	4.8	0.4	100	8062	127	49	63	7651	77	10
6	5.2	3.6	0.6	100	1512	24	2	62	30380	304	20
8	6.9	4.8	0.6	100	3583	57	10	62	16996	170	15
10	8.6	6	0.6	100	6998	113	30	62	10982	110	12
12	10.3	7.2	0.6	100	12092	195	74	62	7626	76	10
6	5.2	4.8	0.8	100	2015	33	3	62	30281	303	20
8	6.9	6.4	0.8	100	4777	77	13	62	16924	169	15
10	8.6	8	0.8	100	9331	151	40	62	10923	109	12
12	10.3	9.6	0.8	100	16123	262	99	62	7585	76	10
6	5.2	6	1.0	100	2519	41	4	62	30119	301	20
8	6.9	8	1.0	100	5972	97	16	62	16807	168	15
10	8.6	10	1.0	100	11663	190	50	61	10827	108	12
12	10.3	12.0	1.0	100	20154	328	124	61	7519	75	10

Table 5.20: Star+PEGT Design Map Coefficients, n_i

$$(P_P = n_0 + n_1 D_g + n_2 A_g + n_3 D_g A_g + n_4 D_g^2 + n_5 A_g^2 + n_6 D_g A_g^2 + n_7 D_g^2 A_g + n_8 D_g^3 + n_9 A_g^3)$$

Parameter	Constant	D_g	A_g	$D_g A_g$	D_g^2	A_g^2	$D_g A_g^2$	$D_g^2 A_g$	D_g^3	A_g^3
Torque	-5349	1917	7642	-2739	-220	0	0	315	8	0
Weight	-79	28	124	-44	-3	0	-1	5	0	2
Inertia	-192	69	166	-50	-8	-3	0	4	0	3
Torque Density	66	2	-26	0	0	25	0	0	0	-9
Input Responsiveness	0	-38010	-351	26	3271	0	58	-3	-98	-457
Output Responsiveness	0	-380	-4	0	33	0	1	0	-1	-5

Table 5.21: Star+PEGT Error Metrics

Parameter	E_{max} (%)	E_{avg} (%)	E_{rms} (%)
Torque	1.1	0.3	0.4
Weight	1.0	0.3	0.4
Inertia	15.0	4.2	6.4
Torque Density	0.011	0.004	0.005
Input Responsiveness	0.042	0.020	0.024
Output Responsiveness	0.042	0.020	0.024

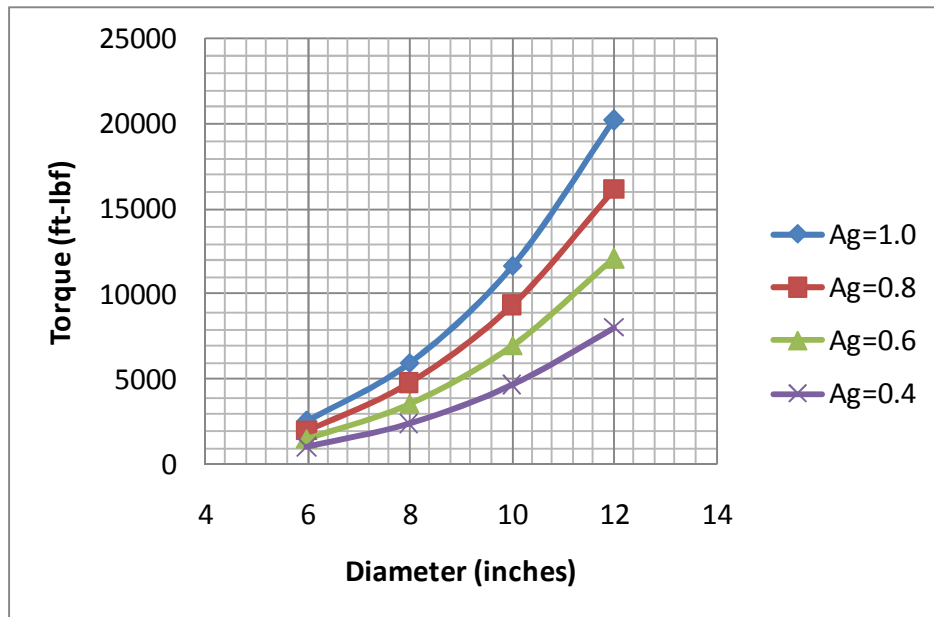


Figure 5.41: Star+PEGT Torque Design Map (2-D)

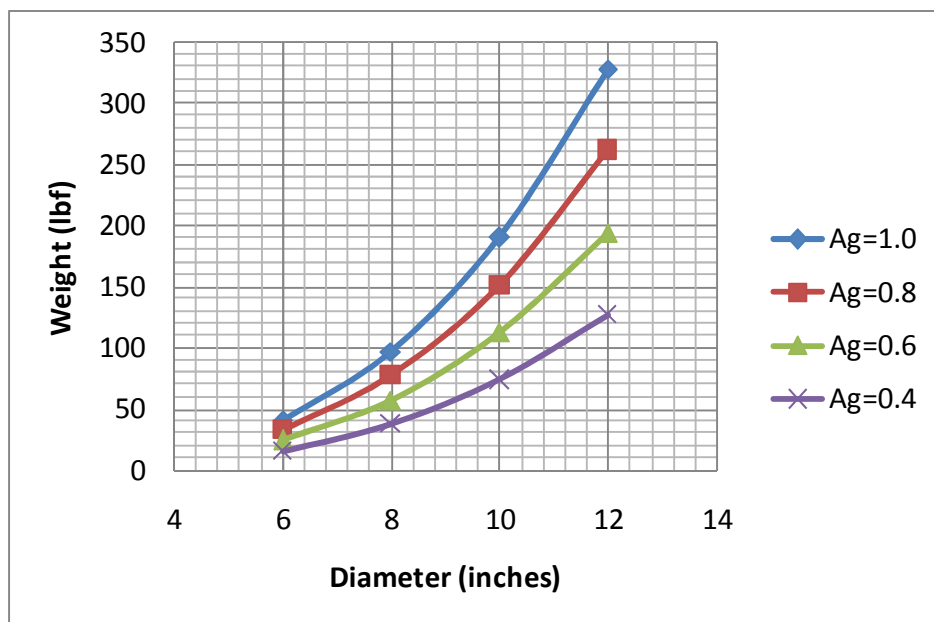


Figure 5.42: Star+PEGT Weight Design Map (2-D)

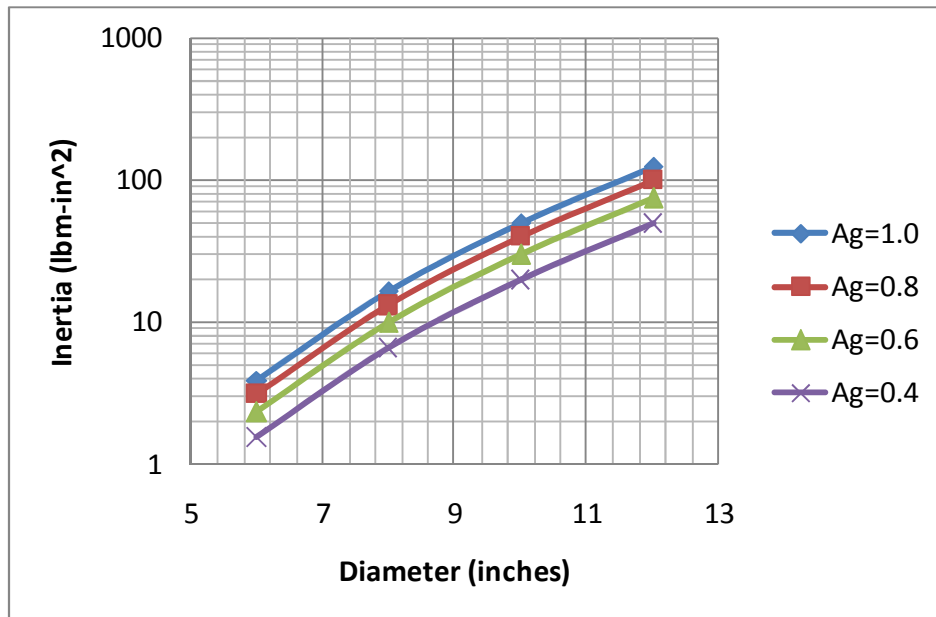


Figure 5.43: Star+PEGT Inertia Design Map (2-D)

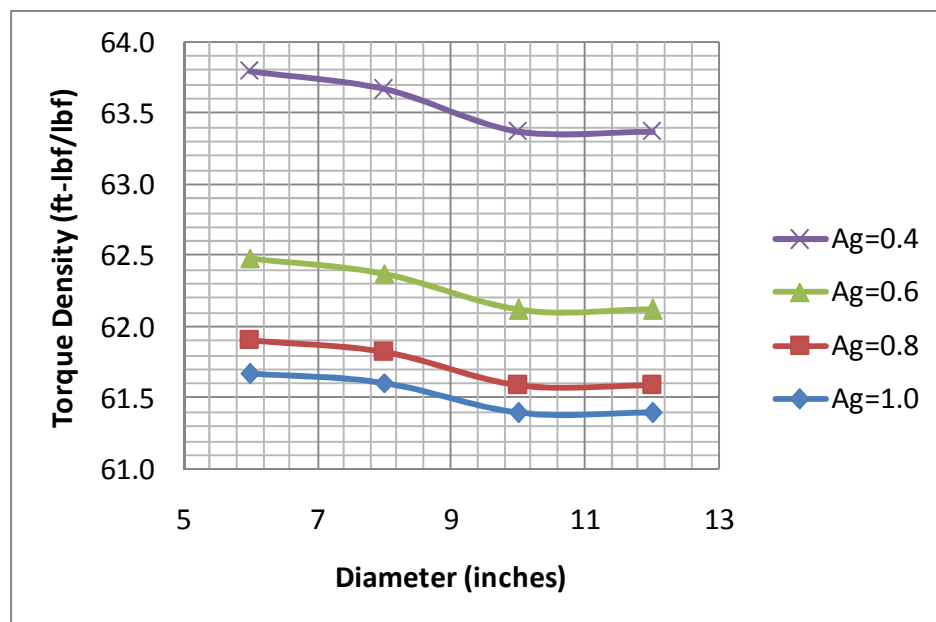


Figure 5.44: Star+PEGT Torque Density Design Map (2-D)

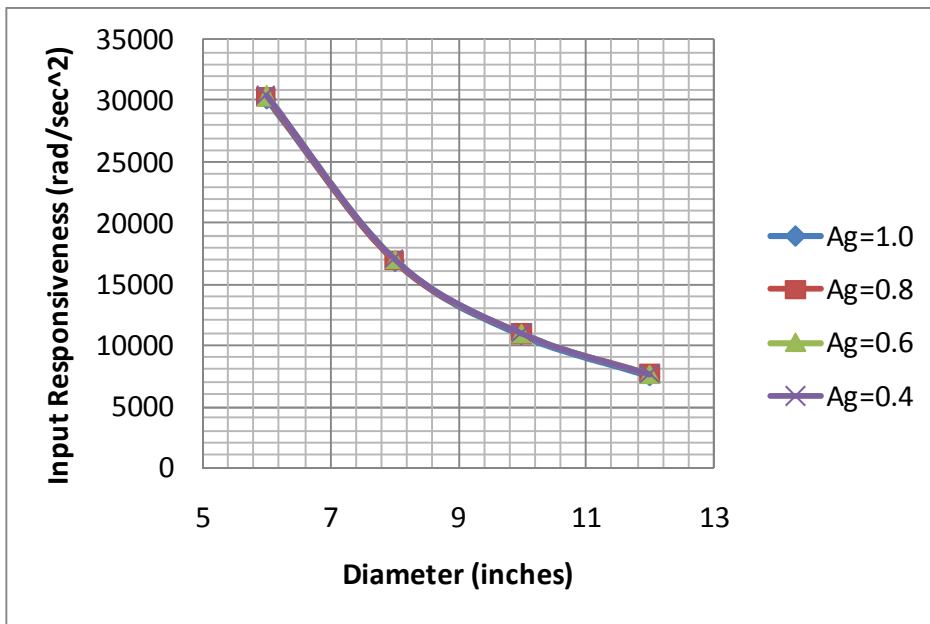


Figure 5.45: Star+PEGT Input Responsiveness Design Map (2-D)

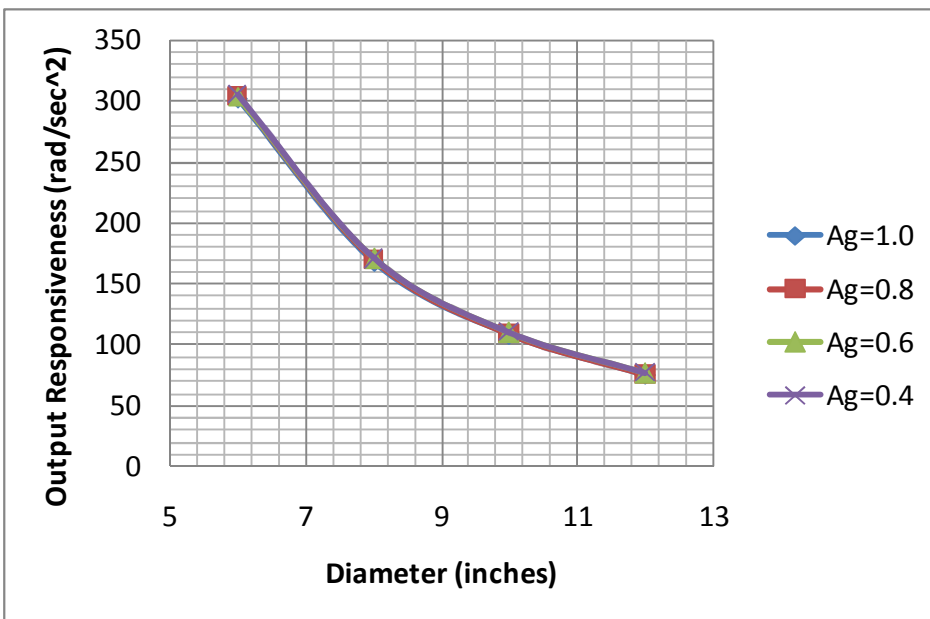


Figure 5.46: Star+PEGT Output Responsiveness Design Map (2-D)

Similar to the results for the individual SRM and HGT designs earlier in this chapter, the decrease in output responsiveness (the torque to inertia ratio) with increasing diameter (Figure 5.46) was expected based on the dependence of torque and inertia on the gear train diameter in Table 5.22 (approximately D_g^3 for torque and D_m^5 for inertia).

Table 5.22: Star+PEGT Power-Law Scaling Rules ($P_p = kD_g^b = kD_g^{b-1}L_g$)

	Aspect Ratio	Constant (k)	Power (b)
Torque	0.4	4.7	3.0
	0.6	7.0	3.0
	0.8	9.3	3.0
	1.0	11.7	3.0
Weight	0.4	0.071	3.010
	0.6	0.110	3.009
	0.8	0.148	3.008
	1.0	0.186	3.007
Inertia	0.4	0.00020	4.989
	0.6	0.00030	4.991
	0.8	0.00040	4.995
	1.0	0.00050	4.999
Torque Density	0.4	65.1	-0.011
	0.6	63.6	-0.009
	0.8	62.8	-0.008
	1.0	62.5	-0.007
Output Responsiveness	0.4	10821	-2.00
	0.6	10821	-2.00
	0.8	10821	-2.00
	1.0	10821	-2.00

Table 5.23: Star+PEGT Bearing Load Capacity Requirements (lbf)

Output Bearing	PE Gear Bearing	Crankshaft Bearing	Idler Shaft Bearing	Input Shaft Bearing
1080	3240	4590	454	744
1920	5737	7824	765	1174
3001	9065	12121	1180	1718
4321	13054	17455	1699	2474
1620	4860	6940	680	1117
2881	8605	11826	1147	1763
4501	13598	18322	1770	2581
6481	19581	26384	2549	3717
2160	6480	9290	907	1490
3841	11473	15830	1530	2352
6001	18130	24526	2360	3444
8642	26108	35318	3398	4960
2701	8100	11641	1134	1863
4801	14341	19835	1912	2942
7502	22663	30732	2950	4308
10802	32635	44253	4248	6203

Different combinations of the pinion, idler, and crankshaft gear tooth numbers/sizes and angular offset of the idler gear (see Figure 3.28 from Chapter 3) will affect all of the performance parameters shown above (weight, inertia, torque density, and responsiveness) slightly, with the exception of torque.

5.2.4 PEGT Scaling Rules (1st Stage Star Compound Gear Train)

The gear train designs discussed in this section replace the 1st stage star gear train from the previous section with a star compound gear train (Figure 5.47) and also use the same overall length and diameter parameters and assumptions from the previous section. The only difference between the two sets is that the PE gear and 1st stage gear face widths are slightly less (see Table 5.18) for the star compound 1st stage gear train option in order to fit into the same overall length dimension as the star gear train option. All of the

PEGT designs in this section have an overall gear ratio of 250 to 1, a PE gear-output gear mesh ratio of 35 to 1, and a 1st stage gear ratio of 7.14 to 1.

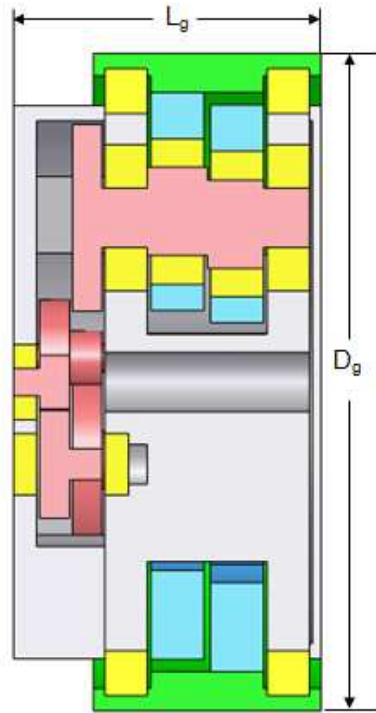


Figure 5.47: Star Compound+PEGT Reference Design

Figure 5.48-Figure 5.53 provide design maps (3-D plots) of the torque, weight, inertia, torque density, and responsiveness as a function of the diameter and aspect ratio, and Table 5.24 summarizes the data used to generate the maps.

Table 5.25 lists the scaling rule coefficients for the low order polynomial surfaces in the 3-D plots, and Table 5.26 summarizes the values of the three error metrics (E_{avg} , E_{max} , and E_{rms}) for the polynomial fits. Again, the reader should not be alarmed at the relatively high fitting error E_{max} for some of the performance parameters because these typically only occur for the smallest data points in a set, for which the magnitudes of the parameters are relatively small. These maps and rules are of sufficient accuracy to

quickly obtain scaled sets of PEGT designs. Figure 5.54-Figure 5.59 provide all the same design and performance parameter information in the form of 2-D plots, and Table 5.27 lists the constants for the simple power law scaling rules obtained from the 2-D plots. In order to verify if bearings of adequate load capacity are available for the given PEGT geometry, Table 5.28 summarizes the bearing load capacities required to achieve the reported gear-tooth torque capacity for the assumed operating life of 5,000 hours.

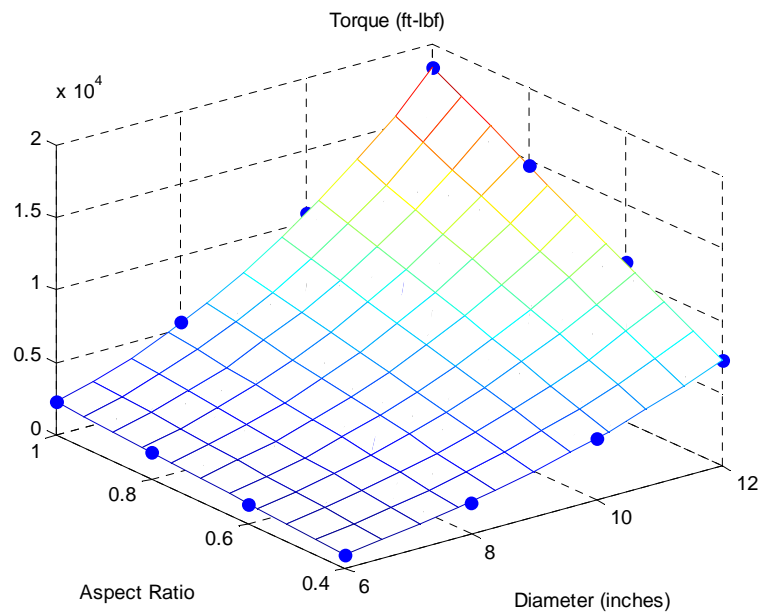


Figure 5.48: Star Compound+PEGT Torque Design Map

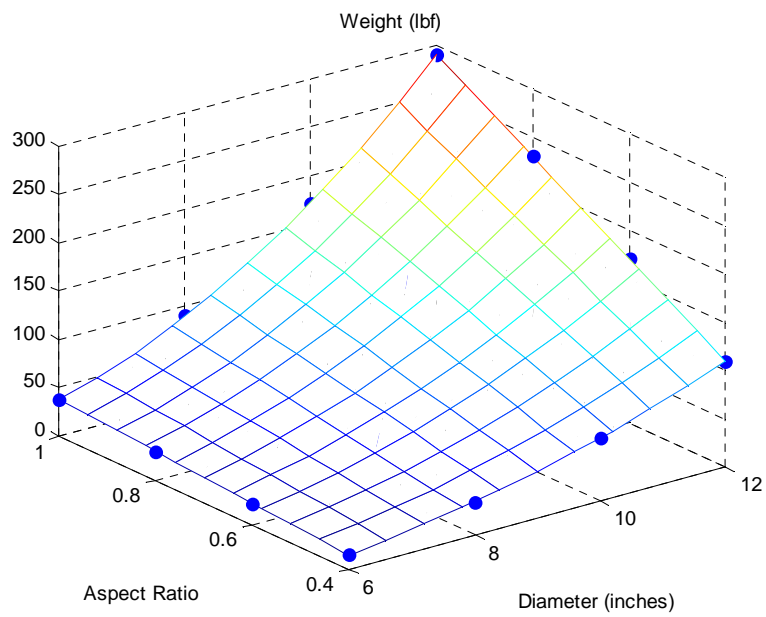


Figure 5.49: Star Compound+PEGT Weight Design Map

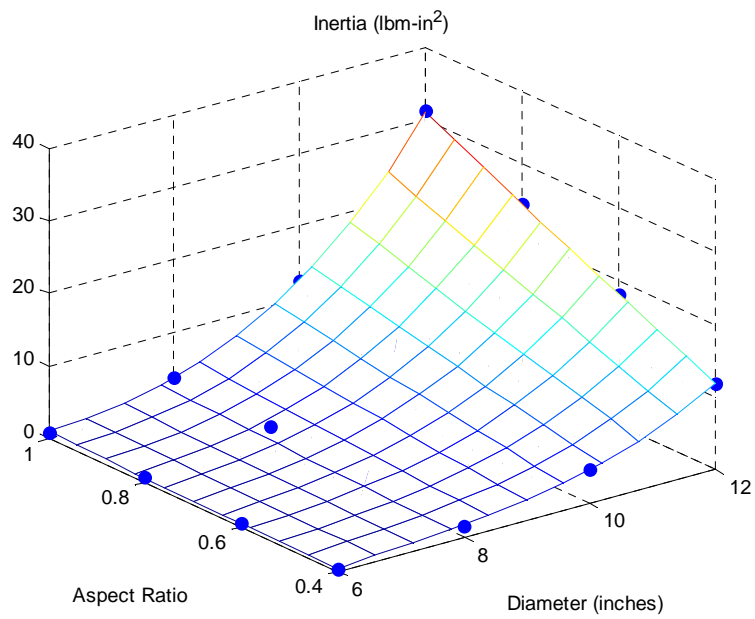


Figure 5.50: Star Compound+PEGT Inertia Design Map

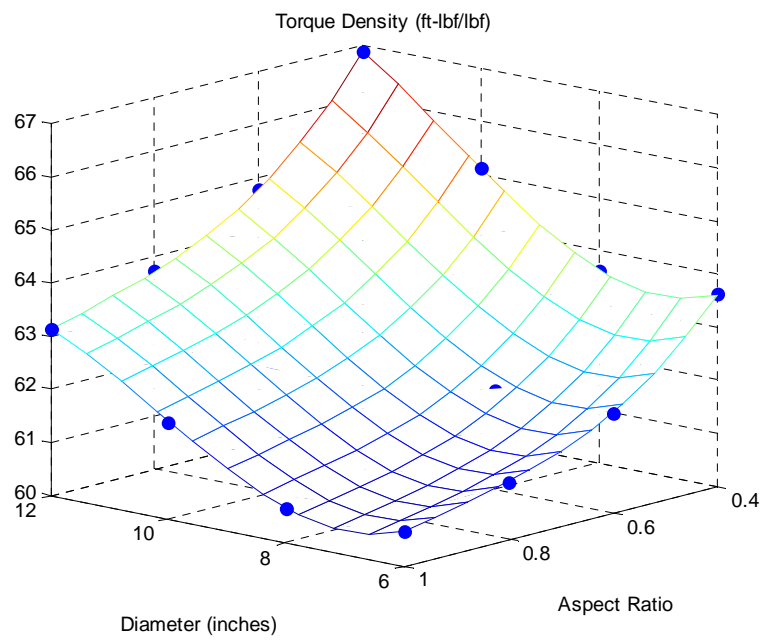


Figure 5.51: Star Compound+PEGT Torque Density Design Map

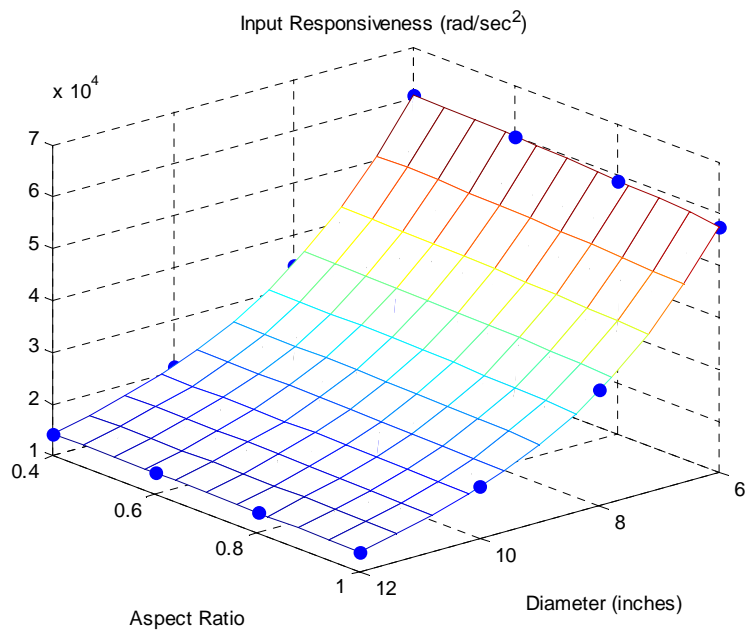


Figure 5.52: Star Compound+PEGT Input Responsiveness Design Map

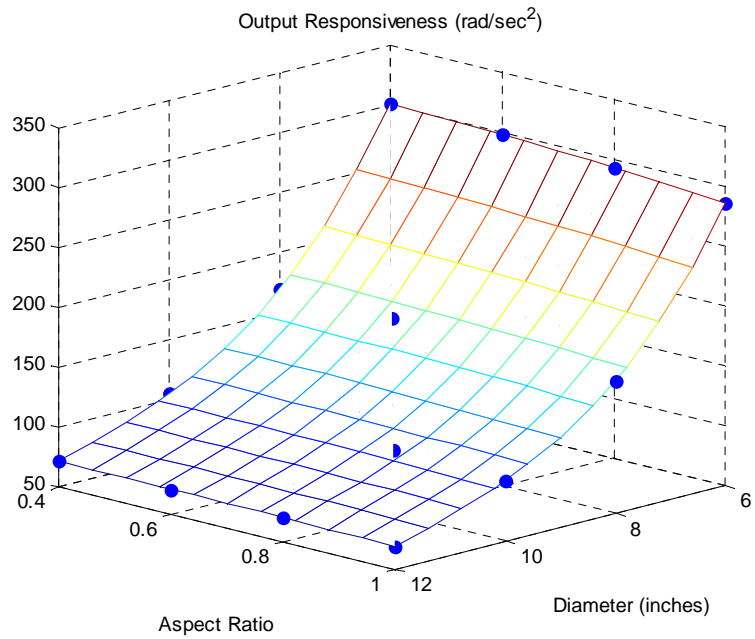


Figure 5.53: Star Compound+PEGT Output Responsiveness Design Map

Table 5.24: Star Compound+PEGT Design and Performance Parameter Data

Overall Diameter (inches)	Shell Diameter (inches)	Length (inches)	Aspect Ratio	Gear Ratio	Torque (ft-lbf)	Weight (lbf)	Inertia (lbm-in ²)	Torque Density (ft-lbf/lbf)	Input Responsiveness (rad/sec ²)	Output Responsiveness (rad/sec ²)	Diametral Pitch, Pd
6	5.2	2.4	0.4	202	916	14	0	64	60634	301	20
8	6.9	3.2	0.4	202	2171	34	1	64	34107	169	15
10	8.6	4	0.4	199	4241	65	5	65	20957	105	12
12	10.3	4.8	0.4	200	7329	110	12	67	14297	72	10
6	5.2	3.6	0.6	202	1374	22	1	62	60041	298	20
8	6.9	4.8	0.6	202	3257	53	2	62	33773	168	15
10	8.6	6	0.6	199	6362	101	7	63	20773	105	12
12	10.3	7.2	0.6	200	10993	170	18	65	14175	71	10
6	5.2	4.8	0.8	202	1832	30	1	61	59063	293	20
8	6.9	6.4	0.8	202	4343	71	3	61	33223	165	15
10	8.6	8	0.8	199	8482	136	10	62	20472	103	12
12	10.3	9.6	0.8	200	14658	230	24	64	13976	70	10
6	5.2	6	1.0	202	2290	38	1	61	57564	286	20
8	6.9	8	1.0	202	5429	90	4	61	32380	161	15
10	8.6	10	1.0	199	10603	172	12	62	20012	101	12
12	10.3	12.0	1.0	200	18322	290	31	63	13675	69	10

Table 5.25: Star Compound+PEGT Design Map Coefficients, n_i

$$(P_P = n_0 + n_1 D_g + n_2 A_g + n_3 D_g A_g + n_4 D_g^2 + n_5 A_g^2 + n_6 D_g A_g^2 + n_7 D_g^2 A_g + n_8 D_g^3 + n_9 A_g^3)$$

Parameter	Constant	D_g	A_g	$D_g A_g$	D_g^2	A_g^2	$D_g A_g^2$	$D_g^2 A_g$	D_g^3	A_g^3
Torque	-4863	1743	6947	-2490	-200	0	0	286	7	0
Weight	-5	2	106	-39	0	0	0	5	0	0
Inertia	-34	12	28	-8	-1	-1	0	1	0	1
Torque Density	47	11	-38	0	-1	35	0	0	0	-12
Input Responsiveness	385599	-92376	-12010	1938	8018	0	855	-129	-242	0
Output Responsiveness	1556	-375	-48	8	33	0	3	-1	-1	0

Table 5.26: Star Compound+PEGT Error Metrics

Parameter	E_{\max} (%)	E_{avg} (%)	E_{rms} (%)
Torque	1.1	0.3	0.4
Weight	0.9	0.2	0.4
Inertia	17.5	4.8	7.3
Torque Density	0.045	0.017	0.021
Input Responsiveness	0.164	0.077	0.090
Output Responsiveness	0.163	0.075	0.089

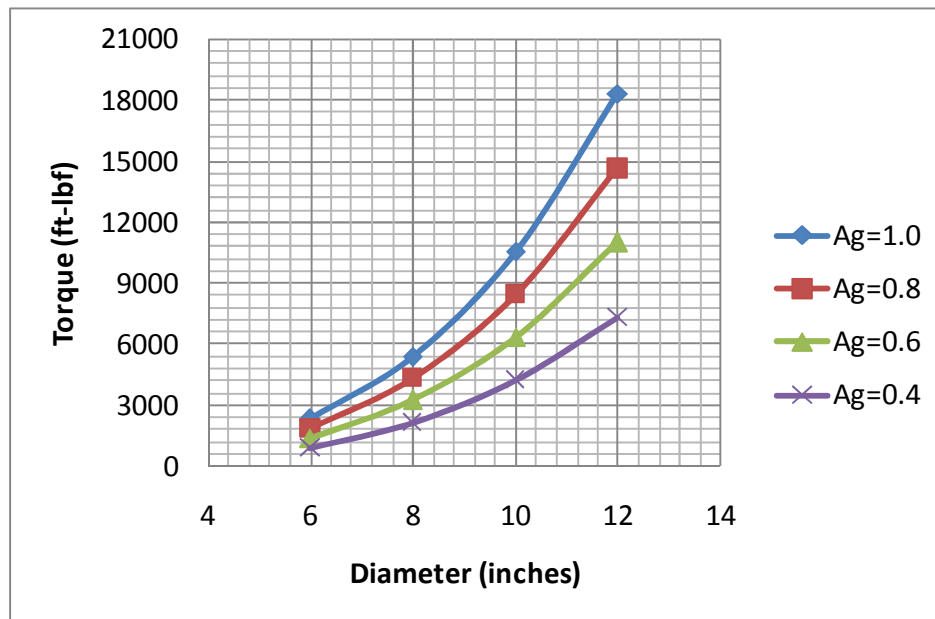


Figure 5.54: Star Compound+PEGT Torque Design Map (2-D)

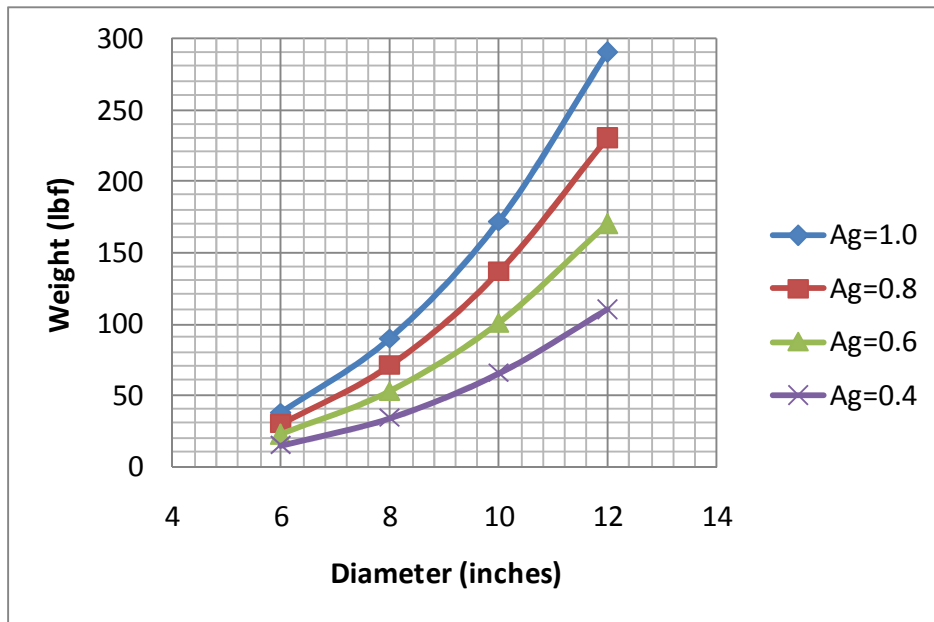


Figure 5.55: Star Compound+PEGT Weight Design Map (2-D)

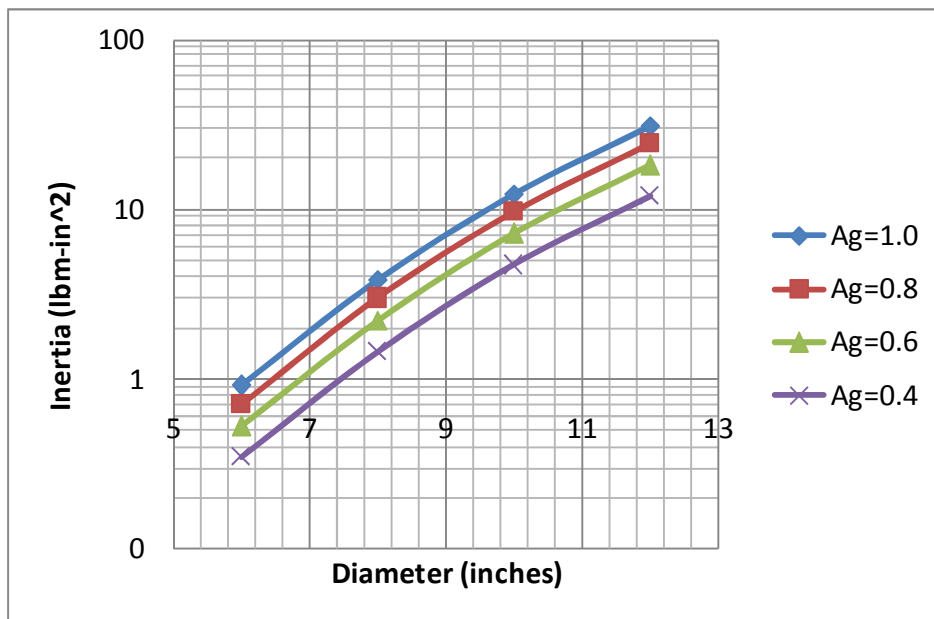


Figure 5.56: Star Compound+PEGT Inertia Design Map (2-D)

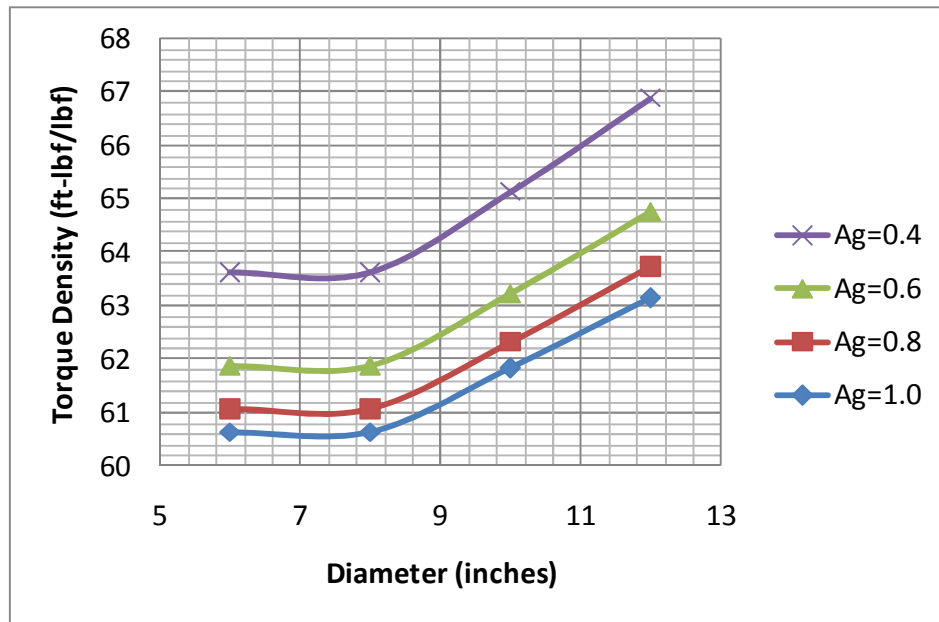


Figure 5.57: Star Compound+PEGT Torque Density Design Map (2-D)

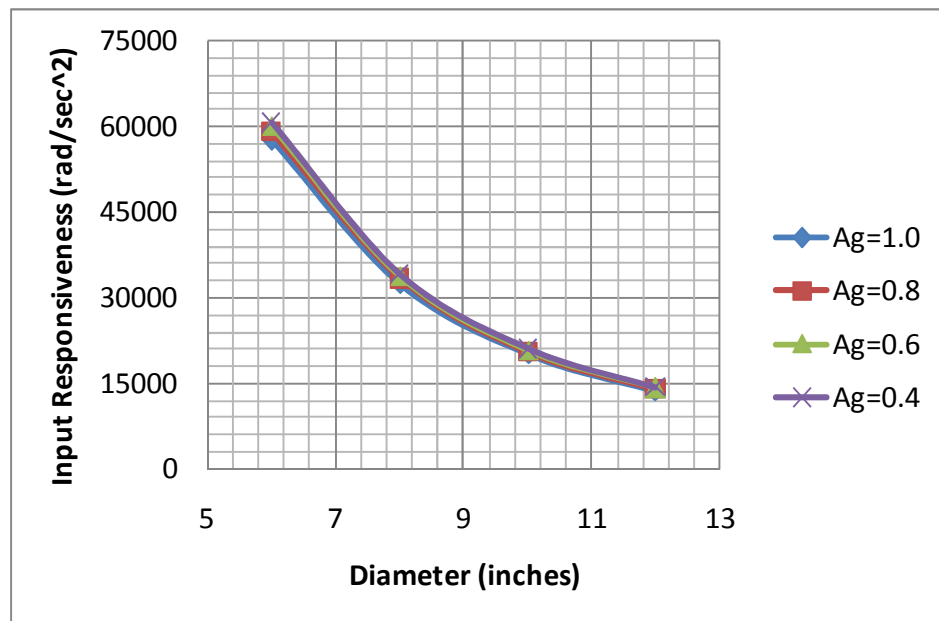


Figure 5.58: Star Compound+PEGT Input Responsiveness Design Map (2-D)

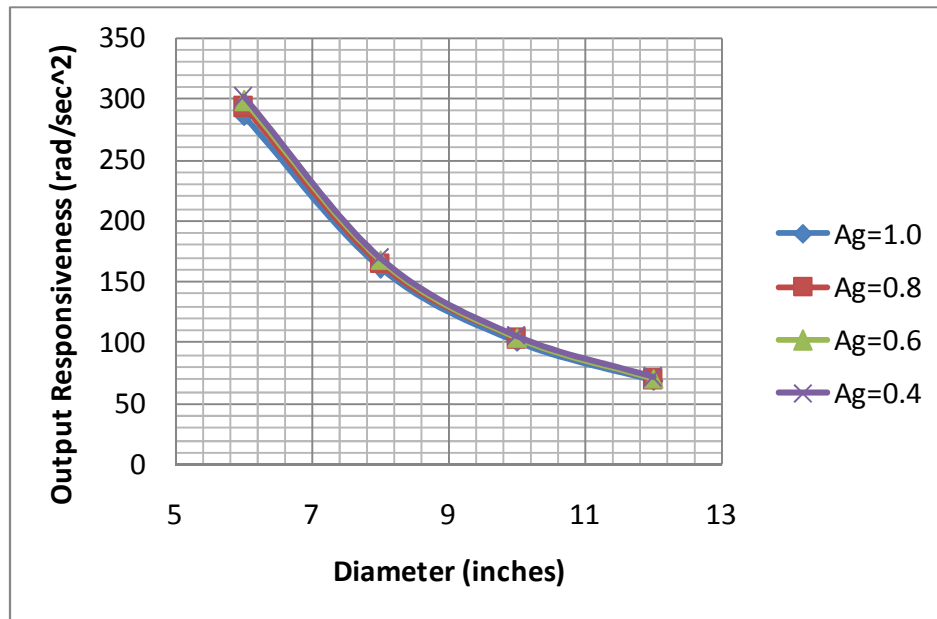


Figure 5.59: Star Compound+PEGT Output Responsiveness Design Map (2-D)

Table 5.27: Star Compound+PEGT Power-Law Scaling Rules ($P_p = kD_g^b = kD_g^{b-1}L_g$)

	Aspect Ratio	Constant (k)	Power (b)
Torque	0.4	4.2	3.0
	0.6	6.4	3.0
	0.8	8.5	3.0
	1.0	10.6	3.0
Weight	0.4	0.076	2.928
	0.6	0.116	2.934
	0.8	0.156	2.938
	1.0	0.195	2.942
Inertia	0.4	0.00004	5.110
	0.6	0.00006	5.108
	0.8	0.00008	5.104
	1.0	0.00010	5.098
Torque Density	0.4	49.3	0.122
	0.6	49.0	0.112
	0.8	49.1	0.104
	1.0	49.4	0.098
Output Responsiveness	0.4	11532	-2.06
	0.6	11532	-2.06
	0.8	11532	-2.06
	1.0	11532	-2.06

Table 5.28: Star Compound+PEGT Bearing Load Capacity Requirements (lbf)

Output Bearing	PE Gear Bearing	Crankshaft Bearing	Idler Shaft Bearing	Input Shaft Bearing
982	2957	4142	348	295
1746	5257	7363	618	524
2728	8044	11570	980	778
3928	11452	16567	1380	1045
1473	4436	6272	522	433
2619	7886	11151	927	770
4092	12066	17509	1471	1142
5892	17178	25042	2070	1533
1964	5914	8404	696	572
3492	10514	14940	1237	1016
5456	16088	23450	1962	1506
7856	22904	33522	2761	2020
2455	7393	10536	870	710
4365	13143	18731	1546	1262
6820	20109	29392	2453	1870
9820	28630	42003	3452	2508

5.2.5 Notes on the Gear Train Scaling Rules

5.2.5.1 Torque Capacity Modification

Utilizing the standard bending stress formula presented in Section 3.5.1, load sharing factor (s), and assumptions about some of the modification factors, the torque capacity (T) of the HGT or PEGT can be written as follows.

$$T = \frac{S_b DLJ}{sP_d K_v K_m} \quad \text{Eqn. 145}$$

For discussion purposes, designate the torque rating of a point in a 2-D or 3-D torque design map (such as those in Figure 5.15 and Figure 5.21) with a subscript “1” and the torque rating of a design with a different set of parameters and assumptions with a subscript “2”.

$$T_1 = \frac{S_{b1} D_1 L_1 J_1}{s_1 P_{d1} K_{v1} K_{m1}} \quad \text{Eqn. 146}$$

$$T_2 = \frac{S_{b2} D_2 L_2 J_2}{s_2 P_{d2} K_{v2} K_{m2}} \quad \text{Eqn. 147}$$

The designer is often interested in how the torque capacity of a design changes as a function of as the parameters in this torque capacity relationship. Designating the ratio of the torque capacities of design #2 to design #1 as ΔT , the following expression results.

$$\Delta T = \frac{T_2}{T_1} = \frac{\Delta S_b \Delta D \Delta L \Delta J}{\Delta s \Delta P_d \Delta K_v \Delta K_m} \quad \text{Eqn. 148}$$

For the purposes of this discussion, the diameter (D) and face width (L) can be considered fixed parameters if the designer is interested how the given geometry can be pushed to meet the specific torque needs of an application. Further, the load distribution factor K_m is a function of L, so it is also constant. The velocity factor K_v is a function of D, so it is also constant if the operating speeds are unchanged. Then, the torque ratio reduces to the following.

$$\Delta T = \frac{T_2}{T_1} = \frac{\Delta S_b \Delta J}{\Delta s \Delta P_d} \quad \text{Eqn. 149}$$

This torque ratio is useful for understanding how changes in the bending strength (S_b), geometry factor (J), load sharing factor (s), and diametral pitch (P_d) modify the HGT and PEGT torque ratings in this chapter. Recalling the discussion in Section 3.5, J, s, and P_d are all a function of the number of teeth on the mating gears, with P_d having the most significant affect on the torque capacity.

A key result from this relationship is that the torque capacity is linearly proportional to the bending strength of the material. Doubling the material strength doubles the torque capacity. This has implications with respect to the upgradability and downgradability of a given gear train size. All other parameters being equal, using low

strength, standard strength, and high strength steels will allow a given gear train size to meet the torque demands of a variety of applications.

The collective set of design maps and scaling rules for HGT and PEGT presented in this chapter allow the designer to choose an appropriate size (diameter, length, aspect ratio, etc.) to meet the torque, weight, inertia, torque density, and/or responsiveness requirements of the application. Then, once a preliminary set of diameter and length parameters have been obtained from the scaling rules, this simplified torque ratio relationship helps the designer answer the question of how he/she can maximize the torque capacity of a given size.

5.2.5.2 *Choosing the Diametral Pitch*

Because lower diametral pitches increase the torque capacity (for a given gear mesh diameter), the approach in this research was to always choose designs with lower diametral pitches because this will result in the highest torque density. The lower limit of the diametral pitch will be governed by ongoing RRG research on the circular arc tooth clearance/interference properties. For a fixed gear pitch diameter, lower diametral pitches result in lower numbers of teeth, larger teeth, higher torque capacities (i.e., lower stresses for a given geometry), fewer teeth in contact, and in general, more potential for interference, while higher diametral pitches result in the opposite.

5.2.5.3 *Relationship Between Bending and Contact Stresses*

As noted in Section 3.5.3 and proven true for past gear train designs based on circular arc gear teeth with small tooth number differences between mating gears (see the HGT stress results in Park and Tesar, 2005), the bending stress typically limits the size of the gear train rather than the contact stress. In other words, the bending stresses exhibited in the gear teeth are relatively closer to typical material bending strength limits than the

contact stresses are to their material contact stress limits. As an example, Table 5.29 lists the values of the bending and contact stresses in the HGT for the range of sizes considered in Section 5.2.2. A bending stress limit of 100 ksi was used for all of the HGT and PEGT designs in this report in order to allow for easy scaling based on the stress limits for a particular application.

Table 5.29: Relative Values of the Bending and Contact Stresses in the HGT

Overall Diameter (inches)	Aspect Ratio	Bending Stress (ksi)	Contact Stress (ksi)	Ratio of Bending to Contact Stress
6	0.4	100	88	1.1
8	0.4	100	72	1.4
10	0.4	100	71	1.4
12	0.4	100	70	1.4
6	0.6	100	88	1.1
8	0.6	100	72	1.4
10	0.6	100	71	1.4
12	0.6	100	70	1.4
6	0.8	100	88	1.1
8	0.8	100	72	1.4
10	0.8	100	71	1.4
12	0.8	100	70	1.4
6	1	100	88	1.1
8	1	100	72	1.4
10	1	100	71	1.4
12	1	100	70	1.4

A key result from the table is that bending stresses are a factor of 1.1 to 1.4 times the contact stresses. Though not shown here, similar results were achieved for the PEGT. Considering typical values of 75 ksi for bending strength and 225 ksi for contact strength [Norton, 2000], it is reasonable to conclude that the bending stresses will be closer to their material strength limit than the contact stresses. Ongoing research at RRG is

underway to consider the choices of the height and width of the gear tooth and how these choices can be used to balance the bending and contact stresses.

5.3 COMPARISONS BETWEEN THE HGT AND THE STAR+PEGT ALTERNATIVES

Based on the results presented earlier in this chapter, it is useful to make a few general comparisons between the PEGT (with the star 1st stage, Section 5.2.3) and the HGT (Section 5.2.2), where each has a 100 to 1 gear ratio. Table 5.30 computes the percent difference between the performance parameters for these two alternatives, with positive numbers indicating that the HGT has larger values for the performance parameter under consideration. The percent difference between the performance parameters (P_p) of the HGT and Star+PEGT was computed as follows.

$$\% \text{ Difference} = 100 \times \left(\frac{P_{P,HGT} - P_{P,PEGT}}{P_{P,HGT}} \right) \quad \text{Eqn. 150}$$

Figure 5.60 presents the same information as Table 5.30 in a graphical representation, and only the average values of the percent difference between the performance parameters (from all the values in a particular column) are plotted.

Table 5.30: Comparison Between the HGT and the Star+PEGT (Gear-Tooth Limited Torque Capacities for both gear trains)⁸

Overall Diameter (inches)	Length (inches)	Torque (% Difference)	Weight (% Difference)	Inertia (% Difference)	Torque Density (% Difference)	Input Responsiveness (% Difference)	Output Responsiveness (% Difference)
6	2.4	49	7	8	46	45	45
8	3.2	24	-11	15	32	11	11
10	4	12	-19	24	26	-15	-14
12	4.8	-1	-25	29	19	-43	-45
6	3.6	49	5	7	47	46	46
8	4.8	24	-12	14	33	12	12
10	6	12	-20	23	26	-13	-13
12	7.2	-1	-26	28	20	-42	-44
6	4.8	49	5	7	47	46	46
8	6.4	24	-13	14	33	12	12
10	8	12	-21	23	27	-13	-12
12	9.6	-1	-27	28	21	-41	-43
6	6	49	4	8	47	45	45
8	8	24	-14	15	33	11	11
10	10	12	-22	23	27	-14	-13
12	12.0	-1	-28	28	21	-42	-44
Averages (%)		21	-14	18	32	0.2	-0.1

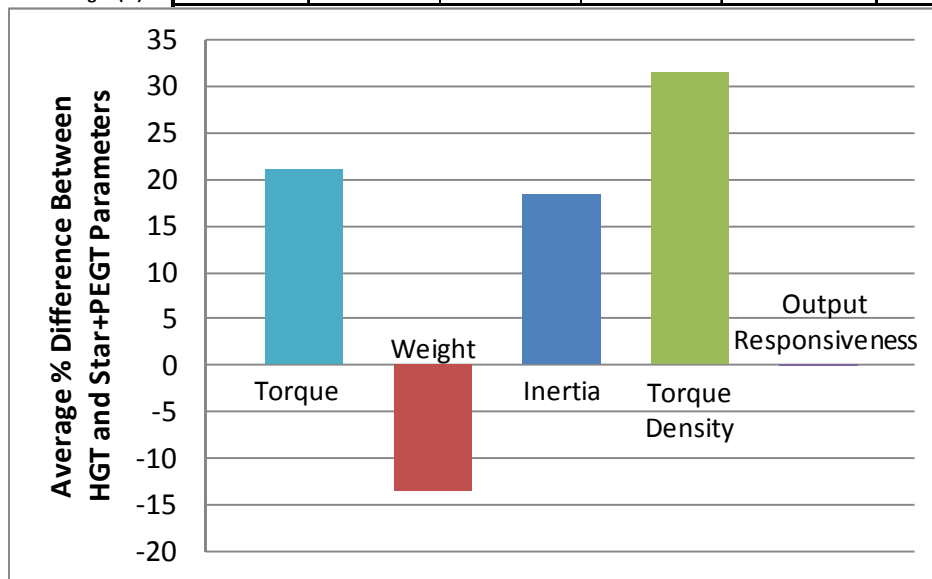


Figure 5.60: Percent Difference Between the Performance Parameters of the HGT and Star+PEGT Alternatives (Only average values of the percent difference are plotted for each performance parameter.)

⁸ Positive (negative) percentages indicate that for the same overall diameter and length, the HGT has a larger (smaller) value for the performance parameter being considered. For torque, torque density, and responsiveness, positive percentages indicate that the HGT is superior to the PEGT. For weight and inertia, positive percentages indicate that the PEGT is superior to the HGT.

According to Table 5.30, the HGT has superior torque capacity for the diameter of 6 inches, but this benefit decreases to the point where the torque capacities are comparable for the largest diameter of 12 inches. This trend occurs because every HGT design in the set has a diametral pitch value of approximately 5 (Table 5.9) while the PEGT has decreasing diametral pitch values of 20, 15, 12, and 10 for diameters of 6, 8, 10, and 12 inches, respectively (Table 5.19).

The differences between the HGT and PEGT torque capacities can be understood in detail by referring to the equation (presented in section 3.5.1) used to compute them.

$$T = \frac{S_b DLJ}{sP_d K_v K_m} \quad \text{Eqn. 151}$$

Designating the ratio of the torque capacities of the HGT (subscript “2”) to the PEGT (subscript “1”) as ΔT , the following expression results.

$$\Delta T = \frac{T_2}{T_1} = \frac{\Delta S_b \Delta D \Delta L \Delta J}{\Delta s \Delta P_d \Delta K_v \Delta K_m} \quad \text{Eqn. 152}$$

When the standard assumptions for the s (load sharing), J , K_v , and K_m factors and the bending strength limit (S_b) are used (Table 5.7), only differences in the pitch diameter (D), face width (L), and diametral pitch (P_d) affect the differences in torque capacity. Then, the torque ratio reduces to the following.

$$\Delta T = \frac{T_2}{T_1} = \frac{\Delta D \Delta L}{\Delta P_d} \quad \text{Eqn. 153}$$

Using the common proportions for the face width and pitch diameter as a function of the overall length and diameter (Table 4.7), the following ratios result.

$$\Delta D = \frac{D_2}{D_1} = \frac{0.65 D_g}{0.87 D_g} = 0.747 \quad \text{Eqn. 154}$$

$$\Delta L = \frac{L_2}{L_1} = \frac{0.30 L_g}{2(0.22) D_g} = 0.682 \quad \text{Eqn. 155}$$

The additional factor of 2 in the denominator of the length ratio calculation is to account for the fact that 2 PE gears carry the load in the PEGT while only 1 stage of the wobble gear carries the load in the PEGT. Physically, these ratios mean that for the same outer diameter, the HGT must have a lower mesh diameter and face width in order to allow for adequate strength of the supporting components and to allow space for bearings. Substituting these ratios into the torque ratio expression and rounding yields the following important result.

$$\Delta T = \frac{0.5}{\Delta P_d} \quad \text{Eqn. 156}$$

This relationship suggests that if the same diametral pitch (essentially the tooth width) is used for the HGT and the PEGT, then the torque capacity of the PEGT will be two times that of the HGT.

However, for most of the PEGT and HGT diameters considered in this comparison, the PEGT torque capacity is less than or comparable to the HGT torque capacity. The primary reason for this is that larger diametral pitches are required for the PEGT.⁹ To achieve the overall 100 to 1 gear ratio in the HGT, a gear ratio of near 10 to 1 in both stages is required. However, to achieve the same 100 to 1 gear ratio in the PEGT, a gear ratio of near 30 to 1 (in the PE gear-output gear mesh) is required due to the limited gear ratio range of the 1st stage star gear train in the PEGT (up to 4 to 1). This higher gear ratio in the PEGT requires nearly 3 times more teeth (because the gear ratio

⁹ These larger diametral pitches for the PEGT can be explained by referring to the HGT and PEGT gear ratio expressions in Sections 3.9.2 and 3.10.3, respectively. Note that the HGT gear ratio involves products of tooth numbers, while the PEGT does not. The relevant figures from Chapter 3 are Figure 3.16 and Figure 3.18 for the HGT and Figure 3.26 and Figure 3.30 for the PEGT. These figures illustrate that the HGT benefits from having two large diameter gear meshes to achieve a given gear ratio, while the PEGT only has a single gear mesh. For this reason and based on the explanation in the text above, each of the two stages in the HGT can have a lower gear ratio relative to the gear ratio in the only stage of the PEGT. The higher gear ratio in the PEGT requires more teeth than the same size (diameter) output gear in the HGT, and this leads to higher diametral pitches for the PEGT.

of 30 is 3 times higher than 10) on the output gear of the PEGT when compared to the output gear of the HGT (assuming the same minimum tooth number difference between mating gears of 3 and same output ring gear diameters for the HGT and PEGT). These higher teeth numbers correspond to higher diametral pitches. If it can be assumed that more teeth are in the contact region for the PEGT, more teeth share the load, and the load sharing factor (Section 3.5.5) then needs to be reintroduced back into the torque equation. Ongoing research at the RRG should yield insight into how the load sharing factor (i.e., contact ratio) changes as more teeth are added to a gear of a fixed diameter. The key conclusion here is that the choice of the diametral pitch, which indirectly accounts for the width of the tooth, significantly affects its torque capacity.

Referring back to Table 5.30, the HGT generally weighs less and has larger torque density than the PEGT because of the stepped down diameter of the HGT behind the fixed gear mesh (see Figure 5.14). The PEGT generally has lower inertia than the HGT because the dominant inertias in the PEGT (primarily the PE gear) are reflected by the square of the gear ratio to the input. The dominant inertia in the HGT is the crankshaft, and because it is directly connected to the input shaft, it is not reduced by the square of the gear ratio when reflected to the input. As the diameter increases from 6 to 12 inches, the relatively large changes in the responsiveness values (both input and output) occur due to the inertia growing faster than the torque as the diameter increases.

Based upon this comparison, as the diameter increases, the Star+PEGT becomes comparable or superior to the HGT for all of the performance parameters except weight. While the results stated here provided a good starting point for comparison, there are other, less quantitative performance parameters such as number of parts, number of bearings, complexity, gear mesh stiffness, etc. that need to be considered in detail before one of these alternatives is selected for a specific application.

5.4 COMPARISONS BETWEEN THE STAR AND STAR COMPOUND 1ST STAGE PEGT ALTERNATIVES

Based on the results presented earlier in this chapter, it is useful to make a few general comparisons between the PEGT with the star (Section 5.2.3) and star compound (Section 5.2.4) 1st stage alternatives. The reader should recall that the overall gear ratio was 100 to 1 for the star 1st stage alternative and 250 to 1 for the star compound 1st stage alternative. Table 5.31 computes the percent difference between the performance parameters for these two alternatives, with positive numbers indicating that the PEGT with the star compound 1st stage option has larger values for the performance parameter under consideration. The percent difference between the performance parameters (P_p) of the Star Compound+PEGT and Star+PEGT was computed as follows.

$$\% \text{ Difference} = 100 \times \left(\frac{P_{P,SC+PEGT} - P_{P,Star+PEGT}}{P_{P,SC+PEGT}} \right) \quad \text{Eqn. 157}$$

Figure 5.61 presents the same information as Table 5.31 in a graphical representation, and only the average values of the percent difference between the performance parameters are plotted.

Table 5.31: Comparison Between the Star Compound and Star 1st Stage Gear Train Options for the PEGT¹⁰

Overall Diameter (inches)	Length (inches)	Torque (% Difference)	Weight (% Difference)	Inertia (% Difference)	Torque Density (% Difference)	Input Responsiveness (% Difference)	Output Responsiveness (% Difference)
6	2.4	-10	-10	-342	0	50	-1
8	3.2	-10	-10	-344	0	50	-1
10	4	-10	-13	-316	3	47	-5
12	4.8	-10	-16	-311	5	46	-7
6	3.6	-10	-9	-338	-1	49	-2
8	4.8	-10	-9	-341	-1	50	-1
10	6	-10	-12	-314	2	47	-5
12	7.2	-10	-15	-308	4	46	-7
6	4.8	-10	-9	-333	-1	49	-3
8	6.4	-10	-9	-335	-1	49	-3
10	8	-10	-11	-310	1	47	-6
12	9.6	-10	-14	-305	3	46	-8
6	6	-10	-8	-324	-2	48	-6
8	8	-10	-8	-327	-2	48	-5
10	10	-10	-11	-304	1	46	-8
12	12.0	-10	-13	-300	3	45	-10
Averages (%)		-10	-11	-322	1	48	-5

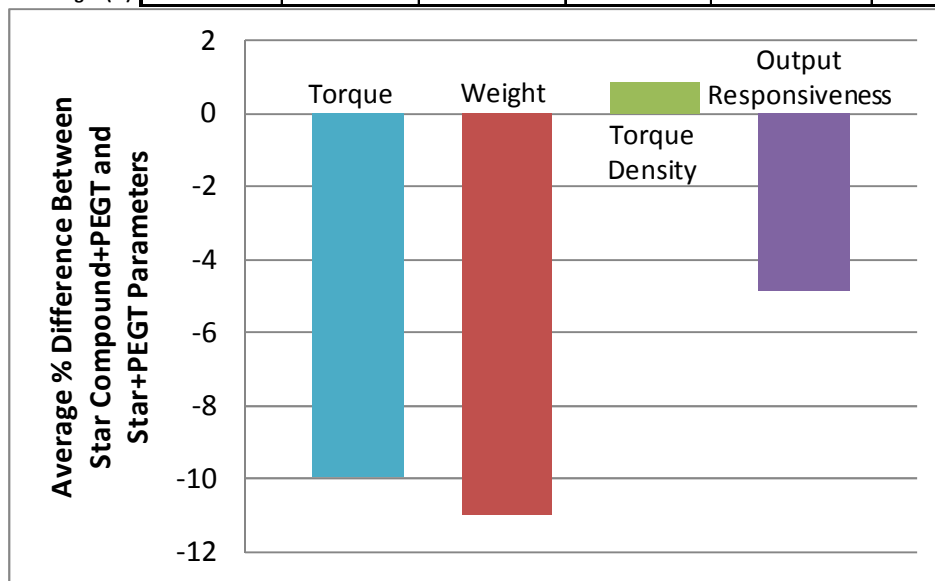


Figure 5.61: Percent Difference Between the Performance Parameters of the Star Compound+PEGT and Star+PEGT Alternatives (Only average values of the percent difference are plotted for each performance parameter.)

¹⁰ Positive (negative) percentages indicate that for the same overall diameter and length, the PEGT with the star compound front end has a larger (smaller) value for the performance parameter being considered. For torque, torque density, and responsiveness, positive percentages indicate that the Star Compound+PEGT is superior to the Star+PEGT. For weight and inertia, positive percentages indicate that the Star+PEGT is superior to the Star Compound+PEGT.

According to Table 5.31, the benefits of replacing the star with the star compound gear train include an 11% reduction in weight, 322% reduction in input inertia, and 48% increase in input responsiveness. The drawbacks include a 10% reduction in torque capacity a 5% decrease in output responsiveness. As expected, the torque capacity changes only slightly due to the slightly smaller PE gear face widths used for the star compound option. Most importantly, the inertia reflected to the input is reduced significantly due to the higher gear ratios available for the star compound gear train. Since both the torque and weight increase by a similar percentage, the change in torque density is not significant.

Based upon this comparison, the Star Compound+PEGT combination is superior to the Star+PEGT combination when considering weight, inertia, and input responsiveness. Unlike the previous comparison between the PEGT and HGT (in which the HGT was by far the less complex design with fewer parts and fewer bearings), the two systems of interest in this section are nearly identical. Both have the same number of parts and bearings, with the star compound option simply having an additional gear stage added to its idler shaft.

The comparisons in the previous two sections do not include a motor but incorporating the motor torque, weight, and inertia is straightforward. While this chapter focuses solely on stand-alone motor and gear train designs, similar comparisons (with a motor included) will be made in Sections 6.5.4 and 6.5.5.

5.5 ACTUATOR DESIGN MAPS AND SCALING RULES

The motors and gear train designs described in the previous sections can be combined to obtain integrated actuator designs. In general, the overall diameter and torque capacity values for potential integrated actuator designs are the same as those for

the stand-alone gear train designs, assuming that the motor (T_m) and gear train torque capacities (T_g) and gear ratio (g) are balanced according the following equation.

$$T_m = \frac{T_g}{g} \quad \text{Eqn. 158}$$

The overall actuator weight, inertia, torque density, and responsiveness parameters should then include the effect of the motor's weight and inertia. Chapter 6 will define this integration of motor and gear train as “balancing parameters”, and the concept of different types of balance will be addressed before actuator scaling rules and design maps can be summarized in a way that is meaningful to the designer. Specifically, Chapter 6 will provide these actuator design maps and scaling rules based on sizing an SRM to fit with many of the stand-alone HGT and PEGT designs generated in this chapter.

5.6 DISCUSSION OF RESULTS

The following discussion will highlight some of the general results with respect to the SRM, HGT, and PEGT designs generated in this chapter that the designer should keep in mind when developing actuator designs based on them.

5.6.1 3-D Maps and Polynomial Scaling Rules

The 3-D design maps were generated with the intent of future use in a visualization-based actuator design (software) environment and are meant to give the designer an understanding of the fundamental design and performance parameter relationships and the dominant parameters in the SRM, HGT, and PEGT. All of the maps and rules use the diameter and aspect ratio as the variable design parameters because these represent the most basic, high level choices when designing a motor or gear train. The low-order polynomial based scaling rules are useful for quickly obtaining the values

of the performance parameters in the 3-D design maps and are more accurate than the simple power law scaling rules.

5.6.2 2-D Maps and Power-Law Scaling Rules

The 2-D maps present the same information as the 3-D maps and were generated for use as a “look-up” table type tool in which quick estimation of performance for given values of the design parameters can be done. The power law scaling rules are useful for quickly obtaining the values of the performance parameters in the 2-D design maps and are obviously less accurate than the more complex polynomial rules. However, these simpler power law rules are arguably more useful for the educating a designer and for comparison with the original analytical relationships used to generate the data.

5.6.3 Curve-Fitting Errors

The largest curve-fitting errors occurred for inertia (typically less than or equal to 20%) and usually only occur for the smallest data points in a set. These relatively large errors occur primarily due to the large order of magnitude changes in inertia for relatively small changes in diameter. The reader is instructed to rely on the original data points for accurate prediction of inertia (rather than the curve fit of the data) and use caution when estimating the inertia. The errors for all of the other performance parameters are typically 1% or less, which is more than sufficient for quickly obtaining the performance of a design with reasonable accuracy. To improve upon the accuracy, some of the more advanced curve fitting techniques listed in Section 2.7.2 can be used in place of regression and/or more data points could be considered. However, every data point requires a given amount of computational effort that must be balanced with the quality of information obtained from its addition.

5.6.4 Diameter and Aspect Ratio Parameters

While the aspect ratio parameter (A) is useful for classifying a motor or gear train design as cylindrical (high A), square ($A \sim 1$), or pancake (low A), all of the performance parameters considered here (torque, weight, inertia, torque density, and responsiveness) are a stronger function of diameter than aspect ratio.

Many of the trends in the 2-D and 3-D plots observed with respect to aspect ratio are identical (though with different units) if the overall length parameter (L_m for the SRM and L_g for the two gear train types) replaces the aspect ratio parameter. The primary value of plotting the results versus aspect ratio rather than length is that the use of the aspect ratio allows more compact 2-D and 3-D plots. It specifically allows the designer to compare designs of different diameters with the same aspect ratio.

5.6.5 Torque, Weight, and Inertia

The simple power law scaling rules obtained for the torque, weight, and inertia of the SRM (Table 5.6), HGT (Table 5.12), Star+PEGT (Table 5.22), and Star Compound+PEGT (Table 5.27) generally agree with their known dependence on diameter and aspect ratio/length (documented in Chapter 3), with some minor deviations. In particular, the deviations in the weight and inertia computations occur because they are based on a complex model with many parameters when compared to the weight and inertia of simple cylindrical shapes. Torque, weight, and inertia each generally increase linearly with an increase in aspect ratio.

For all of the individual motor and gear train design sizes considered in this chapter, the weight was generally from 70 to 80% of the weight of a solid cylinder of the same dimensions. This result is useful because it allows the designer to quickly estimate the weight of a motor or gear train given only its overall dimensions and without doing

any detailed analysis to determine the internal design parameters. It is anticipated that this approximation will hold true for all future designs.

Considering material properties, both the SRM and gear train torque capacities are each linearly proportional to their respective material strength limits (saturation flux density for the SRM and bending strength for HGT and PEGT). This has implications for balancing the torque capacities between the motor and gear train (see Section 6.3.1). In particular, if a motor and gear train geometry are incompatible and all efforts to balance them based on changes in only the geometric design parameters have been made, then using different materials should be considered.

5.6.6 Torque Density and Responsiveness

For the SRM, HGT, and PEGT, the torque density and responsiveness were shown to be essentially independent of the aspect ratio (length). This is consistent with the fact that these parameters are computed from ratios of torque, weight, and inertia, which are each linearly proportional to length.

While both the PEGT and HGT have higher absolute torque density than the SRM for the same diameter, the SRM torque and torque density increase at a faster rate than for the gear train. This important result will affect the relative sizes (i.e., weight and inertial content) of the motor and gear train as the diameter of an actuator is increased. Examples that use this result will be presented in Sections 6.5 and 6.6.

The output responsiveness (a measure of the acceleration capability at the output) always decreases with increasing diameter for the SRM, HGT, and PEGT. This result is in agreement with the computed dependence of torque and inertia on diameter (in the power law scaling rules) and is also consistent with intuition because larger systems usually run at slower speeds and have lower acceleration capabilities.

The responsiveness values for the stand-alone SRM can be used to determine the acceleration capability of a direct drive system based on the particular size being considered. However, for the responsiveness values of the stand-alone gear trains, while valuable for comparative purposes, is not as valuable in an absolute sense. When these gear trains are coupled with a motor (as will be done in Chapters 6 and 7), this information becomes more valuable.

5.7 USING THE DESIGN MAPS AND SCALING RULES

If a designer is generating a single component design for an application, then the rules and maps presented in this chapter are useful for quickly estimating the performance of a design of a particular size. Then, the designer can use this ballpark estimate of performance as a starting point for a detailed design effort. The designer can then modify some of the standard assumptions and lower level parameters (that were often held constant to develop the rules of this chapter) to meet the needs of the particular application. On the other hand, if a designer is generating a set of component designs, the results in this chapter could possibly be used as-is if the designer ensures that the present assumptions are compatible with those pertinent to the application.

The design parameter ranges for diameter, aspect ratio, and other parameters used in this chapter are meant to give the reader a global view of how the performance parameters vary as a function of the key design parameters. They were chosen to simultaneously 1) obtain accurate and useful design maps and scaling rules and 2) meet the performance needs of a large variety of applications. Meeting the accuracy goal required smaller ranges of the parameters, while meeting the second goal required larger ranges for the parameters. If the performance needs of an application are not covered by the maps and rules in this chapter, the reader is referred to Chapters 6 and 7 for larger

ranges of motor and gear train sizes. These chapters will present the larger ranges of sizes to meet a greater range of performance needs and will not put as much emphasis on maximizing the accuracy of the analytically-obtained scaling rules.

5.8 SUMMARY

The scaling rules and design maps of this chapter were obtained by exercising the design procedure in Chapter 4 for a finite set of design parameter inputs. The maps and rules provide a database that can be used by future designers when developing preliminary motor, gear train, and integrated actuator designs, and they can be used without reference to the procedure that generated them if the assumptions listed in this chapter are understood. These maps and rules are intended to give the designer an understanding of the trends in the motor and gear train performance parameters as the basic design parameters of diameter and aspect ratio are modified, and they should allow a designer to quickly estimate performance parameters with a reasonable level of accuracy for preliminary design purposes.

Chapter 6 Balancing Parameters

The integration of motor and gear train in a single housing allows for high torque and power density in a minimum weight/volume envelope and a reduced number of parts. However, this integration presents the challenge of balancing the parameters between the motor and gear train to achieve the overall performance objectives of the actuator. In this report, *balancing parameters* has been defined as the allocation of torque, weight, inertia, torque density (torque to weight ratio), and responsiveness (torque to inertia ratio) between the motor and gear train and specifically determining the actuator design parameters that achieve the desired allocation.

This chapter documents the details behind the “Balancing Motor and Gear Train” block in the proposed actuator design procedure (Figure 4.3) of Chapter 4. It will first motivate the need for balancing parameters between a motor and a gear train and then discuss the actuator design parameters (including the gear ratio, motor and gear train aspect ratios, and other relationships between the motor and gear train geometry) that can be used to achieve that balance. Then, four specific levels of balance between a motor and a gear train will be considered: 1) balance between gear tooth-limited and motor-limited torque capacity (essential), 2) balance between the weight/inertia of the motor and gear train (not essential but highly desirable), 3) balance between the tooth-limited and bearing-limited torque capacity in the parallel eccentric gear train (desirable but not always possible), and 4) balance between the bearing lives of multiple bearings (important for maintenance purposes). Examples will be presented to illustrate the first two types of balance, and strategies for achieving the third type of balance will also be discussed. The examples will provide quantitative guidelines (in the form of plots of

design rules and tabular summaries (similar to the presentation in Chapter 5) for choosing the actuator design parameters to achieve balance.

6.1 NEED FOR BALANCING PARAMETERS

A common scenario illustrating the need for balancing the parameters between the motor and gear train is presented in this section. It will be discussed in the context of the selection of off-the-shelf motors and gear trains, but the same issues are present when utilizing the parametric models in Chapter 3 to design motors and gear trains.

Given the torque, speed, and volume requirements for a particular actuator application, the designer is tasked with selecting a motor and gear train combination that meets these requirements. Since only a few companies offer integrated motor-gear train combinations (Section 2.2), the designer is often forced to select the motor and gear train from different manufacturers. The gear train is often selected first because it must meet the torque requirement for the application. Along with the gear train selection, the designer must choose a gear ratio in order to determine the torque and speed requirements for the motor. Armed with these motor torque and speed requirements, the designer can then select an appropriate motor from a catalog. A typical process involves choosing different candidate motors, checking how well each motor-gear train combination meets the requirements, and then selecting the best option from among the candidates. Geometric compatibility of the motor output shaft and gear train input shaft dimensions must be ensured for every candidate motor. Also, if a different gear ratio is considered for the gear train, then the process must be repeated to find motors that match the new torque and speed requirements.

The scenario just described is a trial and error procedure for coupling a motor and a gear train, and it is not guaranteed to produce an optimal balance of the torque, weight,

inertia, and other parameters between the motor and gear train. Further, the designer has likely not considered all of the possible design parameter combinations that meet the torque and speed requirements of the application.

This example scenario has been repeated many times in developing actuators for a variety of applications, and this was the motivation behind the development of the step-by-step actuator design procedure presented in Chapter 4. This chapter will provide guidance in choosing the key actuator design parameters with the aim of improving upon this commonly used trial and error process to couple a motor and a gear train. The concepts apply equally well to coupling off-the-shelf motors and gear trains, but the numerical results presented below apply to the following systems within the scope of this research: the SRM, HGT, PEGT, and integrated actuators built from these systems.

6.2 KEY ACTUATOR DESIGN PARAMETER CHOICES

Given an overall length (L) and diameter (D_g) for an actuator such as those in Figure 6.1 and Figure 6.2 (typically sized for the torque and speed requirements of the application), the six basic parameters that the designer can choose to balance the motor and gear train are as follows:

- gear ratio (g),
- gear train aspect ratio (A_g),
- motor aspect ratio (A_m),
- overall aspect ratio (A),
- ratio of motor length to overall length (K_l), and
- ratio of motor diameter to gear train diameter (K_d).

Section 3.3 introduced these parameters, and the following sections will discuss them in more detail.

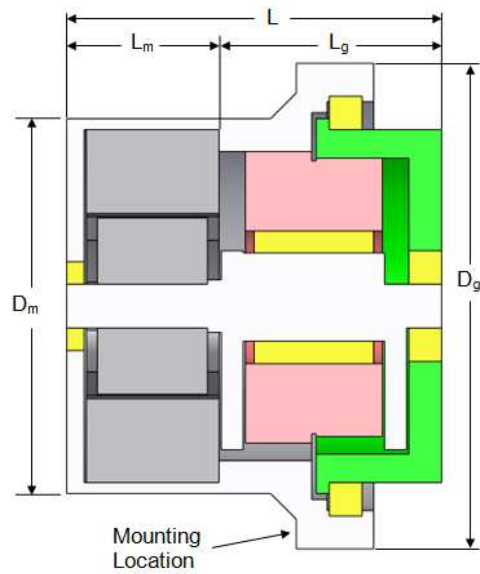


Figure 6.1: SRM+HGT Reference Design Illustrating Important Design Parameter Choices

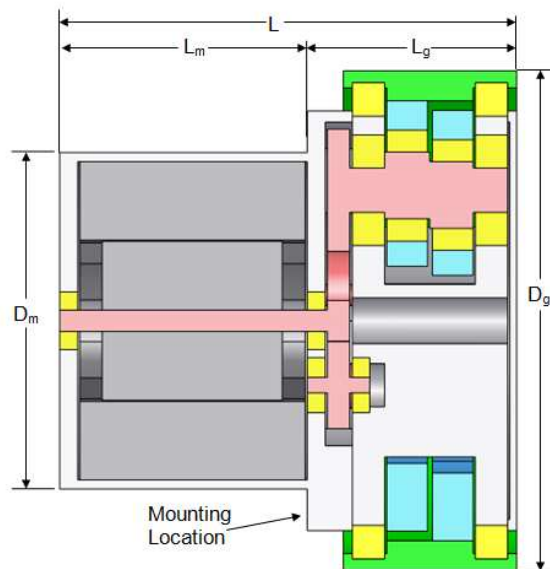


Figure 6.2: SRM+Star+PEGT Reference Design Illustrating Important Design Parameter Choices

6.2.1 Choice of Gear Ratio

Tesar [2006] described the fundamental choice of the gear ratio (g) when coupling a motor and a gear train into an integrated actuator and suggests the most suitable gear train types (including the star, star compound, HGT, and PEGT) for different gear ratio ranges. The literature review in Section 2.4 also suggested that the gear ratio is the most influential parameter choice when coupling a motor and gear train. For a fixed torque capacity, gear train diameter (D_g), and gear train length (L_g), the gear ratio can be used to control the volume, weight, and inertia of the motor relative to the gear train. In general, increasing the gear ratio reduces the torque requirement of the motor, which in turn reduces its individual weight and inertia and the overall actuator weight and inertia. The suggested gear ratio ranges for the HGT (from 75-500) and PEGT (from 15-500) were discussed in Section 3.13.

6.2.2 Choice of Gear Train Aspect Ratio

The gear train aspect ratio (A_g) is defined by the following equation.

$$A_g = \frac{L_g}{D_g} \quad \text{Eqn. 159}$$

This ratio can be used to classify a gear train geometry as “pancake” for a low aspect ratio or “cylindrical” for a high aspect ratio. The value of A_g is typically between 0.3 and 2 for the HGT and PEGT designs considered in this research. In general, pancake designs have higher torque density than cylindrical designs (of the same weight) because torque is a stronger function of diameter than it is of length, as illustrated by the HGT and PEGT scaling rules in Chapter 5. For example, doubling the diameter of a gear train design increases the gear train torque capacity at a faster rate than doubling the length.

6.2.3 Choice of Motor Aspect Ratio

The motor train aspect ratio (A_g) is defined by the following equation.

$$A_m = \frac{L_m}{D_m} \quad \text{Eqn. 160}$$

This parameter is analogous to the gear train aspect ratio and has the same physical meaning. The value of A_m is typically between 0.3 and 2.0 for the SRM designs considered in this research.

6.2.4 Choice of Overall Aspect Ratio

The overall aspect ratio (A) is defined by the following equation.

$$A = \frac{L_m + L_g}{D_g} = \frac{L}{D_g} \quad \text{Eqn. 161}$$

This parameter is analogous to the motor and gear train aspect ratios but includes the motor and the gear train length and assumes that the motor diameter (D_m) is less than the gear train diameter (D_g), which is typically the case for the actuator designs of this research. The value of A can vary widely and is typically between 0.5 and 2.0 for the motor-gear train combinations designs considered in this research.

6.2.5 Choice of Motor to Overall Length Ratio (K_l)

The motor length to overall length ratio (K_l) is given by the following equation.

$$K_l = \frac{L_m}{L} = \frac{L_m}{L_m + L_g} \quad \text{Eqn. 162}$$

The value of K_l is typically between 0.3 and 0.7 for the motor-gear train combinations in this research, and a reasonable starting point is $K_l = 0.5$, which gives equal length to the motor and gear train. As the gear ratio is increased (for a fixed gear train size), K_l decreases because of the reduced motor torque demand.

6.2.6 Choice of Motor to Gear Train Diameter Ratio (K_d)

The motor diameter to gear train diameter ratio (K_d) is given by the following equation.

$$K_d = \frac{D_m}{D_g} \quad \text{Eqn. 163}$$

The value of K_d is typically between 0.3 and 1.0 for the motor-gear train combinations in this research. Referring back to Figure 6.1 and Figure 6.2, the maximum value of K_d is typically limited by the constraint that space must be provided on the actuator for mounting to an external structure, with the specific location depending heavily on the application. The minimum value prevents large diameter changes in the crankshaft in the HGT and makes the input and idler shaft geometries compatible in the PEGT.

K_l and K_d (along with the gear ratio g) generally reveal to the designer which component (motor or gear train) will provide the dominant weight and inertia in the actuator. Reducing the values of K_l and K_d physically result in the motor becoming smaller relative to the gear train. It will be shown in this chapter that the gear train often contains a larger percentage of the weight and inertia than the motor. If there is a need to reduce the weight and inertia of the actuator design, the designer should generally concentrate on the component with the largest weight and inertia.

Given the above parameters, the following relationships between the parameters can be derived.

$$A_g = A(1 - K_l) \quad \text{Eqn. 164}$$

$$A = \frac{A_m K_d}{K_l} = A_g + \frac{L_m}{D_g} \quad \text{Eqn. 165}$$

Though somewhat complex, these relationships have been verified and were used indirectly in this chapter to enforce constraints between the parameters for the sets of designs developed in the examples to follow. They could become more valuable in future research.

6.2.7 Importance of These Design Parameters

The basic design parameter choices discussed above should be tracked as an actuator design is in progress, and the effects of changes in these parameters on the performance parameters of torque, weight, inertia, torque density, and responsiveness should be analyzed.

These are the most basic, high level design parameter choices to consider when designing an actuator. For example, when designing a single actuator, the designer is advised to track the values of these parameters and understand their physical meaning. When designing a set (family) of actuators with the intent of using the results for learning purposes and for future reference, considering the values of these parameters is critical. Specifically, it is important for the designer to understand which of these are fixed and which are variable for a set of actuator designs, and this chapter will make this distinction clear. Designing a family of actuators for an application can be a daunting task, but grouping the designs based on these basic parameter choices can make the task easier. The scaling rules and design maps of Chapter 5 would have little value if the values of these basic parameters (and other assumptions) were not controlled, and there would be little justification for fitting the data with curves and surfaces and using them for prediction of intermediate designs. If these parameters ever deviate outside of the approximate ranges suggested above, the designer should justify their use based on the needs of the application.

6.3 TYPES OF BALANCE

This section will further define the concept of balancing parameters by illustration of the different types of balance that are sought for the EMAs of this research. These types of balance are:

- balance between the motor and gear-tooth limited torque capacities,

- balance between the weight and inertia of the motor and gear train,
- balance between the bearing and tooth-limited torque capacities in the PEGT, and
- balance between the operating lives of multiple bearings.

6.3.1 Balance Between the Motor and Gear Train-Limited Torque Capacities

The basic idea behind balancing the motor and gear train limited torque capacities is that neither the motor nor the gear train limits the overall rated torque capacity of the actuator. Using the gear train torque capacity (T_g) and gear ratio (g), the required motor torque capacity (T_m) for achieving this balance is as follows.

$$T_m = \frac{T_g}{g} \quad \text{Eqn. 166}$$

Satisfying this relationship is the most common and challenging design task when coupling a motor or gear train, whether the motor and gear train are integrated into a single housing (as in this research) or whether they are separated by shafts, couplings, and are contained in their own, individual housings (as is more common in practice). This type of balance is considered essential for any design, and, if not achieved, will result in either the motor or the gear train having larger weight and inertia than necessary. Figure 6.3 displays an actuator with an inside stator and outside rotor, both contained within the HGT, in which the choice of the gear ratio was critical for matching the motor and gear-tooth limited torque capacities.

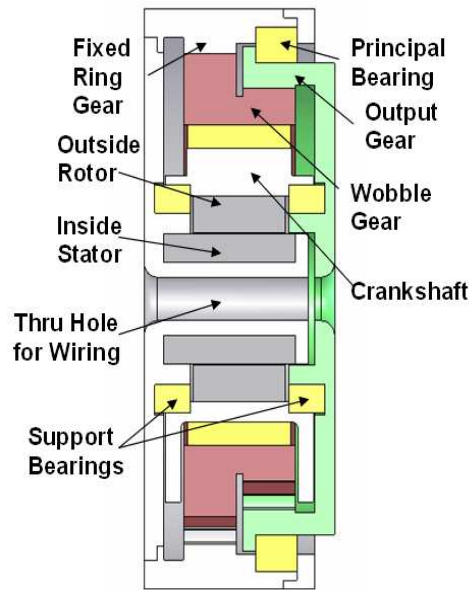


Figure 6.3: SRM+HGT Design (with Inside Stator and Outside Rotor)

This balance can be accomplished using the following process. First, a gear train is designed to match the performance requirements of the application, after which the preliminary values of the gear train length (L_g) and diameter (D_g) would be known. Then, using the gear train torque capacity (T_g) and gear ratio (g), the required motor torque capacity is computed using the relationship above. Then, based on the designer-specified values of K_l and K_d , a preliminary motor length (L_m) and diameter (D_m) can be computed via the following equations.

$$L_m = \frac{K_l}{1 - K_l} L_g \quad \text{Eqn. 167}$$

$$D_m = K_d D_g \quad \text{Eqn. 168}$$

Then, the torque capacity of a motor with dimensions L_m and D_m is determined and checked against the required torque capacity. Finally, the values of K_l and K_d are modified until a balanced design is achieved. These steps have been automated in the actuator design procedure of Chapter 4 (i.e., the “Balancing Motor and Gear Train” block

in Figure 4.3) and in the computational tool used to design integrated actuators (Appendix A1). This type of balance will be illustrated for a range of actuator diameters in Example 1 (Section 6.5) of this chapter.

6.3.2 Balance Between the Weight/Inertia of the Motor and Gear Train

The basic idea behind this type of balance is that the weight and inertial content of the motor and gear train can be “moved” between the two components primarily by the choice of the gear ratio and, to a lesser extent, the other design parameter choices discussed above. The percentage of weight in the motor (W_{mp}) and gear train (W_{gp}) as a function of the total weight can be written as a function of the motor weight (W_m) and gear train weight (W_g) using the following equations.

$$W_{mp}(\%) = 100 \frac{W_m}{W_m + W_g} \quad \text{Eqn. 169}$$

$$W_{gp}(\%) = 100 \frac{W_g}{W_m + W_g} \quad \text{Eqn. 170}$$

The following analogous relationships will be used for the percentage of inertia in the motor (I_{mp}) and the gear train (I_{gp}).

$$I_{mp}(\%) = 100 \frac{I_m}{I_m + I_g} \quad \text{Eqn. 171}$$

$$I_{gp}(\%) = 100 \frac{I_g}{I_m + I_g} \quad \text{Eqn. 172}$$

The reader should note that no load inertia is included in these expressions because the size of the load inertia depends on the specific application in question. If the load inertia is known, then the load inertia should be compared to the individual motor and gear train inertias to determine which is dominant. Though not included in these weight and inertia ratios, a reference load inertia equal to inertia of the gear train (as defined in Section 3.4.1) is included in the responsiveness computations of this chapter.

In some cases, the application requirements (maximum torque density, maximum responsiveness, minimum weight, etc.) might dictate specific values for these weight and inertia percentages, but they are usually left to the discretion of the designer. This type of balance is not essential but highly desirable, especially where responsiveness/acceleration is an important requirement for an application. Example 2 (Section 6.6) of this chapter will report the distribution of weight and inertia as a function of the diameter and gear ratio parameters.

6.3.3 Balance Between the Tooth-Limited and Bearing-Limited Torque Capacity in the PEGT

Chapter 5 (Section 5.2.3.2) identified the need to balance the bearing and gear tooth limited torque capacities in the PEGT and identified strategies to match the two based on a current PEGT prototype design. The important strategies discussed involved modifying the center distance from the actuator centerline to the crankshaft centerline and modifying the size of the crankshaft and PE gear bearings (see Figure 5.32). This type of balance is not essential but highly desirable for ensuring that neither the bearings nor the gear teeth are overdesigned with respect to the other. This type of balance will be discussed briefly in the context of Example 2 (Section 6.6).

6.3.4 Balancing Bearing Life Between Multiple Bearings

The basic idea behind this type of balance is that the estimated bearing lives of the multiple bearings in an actuator should be matched. This type of balance is not essential but desirable for scheduling bearing replacement and maintenance times. If two bearings have the same estimated life, then they can be replaced and/or serviced at the same time, reducing maintenance costs. If this cannot be achieved, then it is desirable to have the bearing lives as multiples of each other, so maintenance can be done on multiple bearings

at one time. Achieving matched bearing lives is generally very difficult because bearings are usually chosen based on the space constraints of an actuator design (after a motor and gear train have already been sized) and are sometimes oversized for their specific loads and operating speeds.

To facilitate this type of balance, the computational tool (Appendix A1) used to generate actuator designs also computes the bearing load capacities for a designer-specified operating life (using 5,000 hours as a reference life) and estimates the dimensions available for each bearing (given the gear train and motor approximate dimensions). This information gives the designer the opportunity to efficiently select bearings that meet the load, speed, and space requirements; estimate their operating lives; and then attempt to balance their lives if possible. Bearing load capacities are reported for the actuator designs generated in Example 1 (Section 6.5).

6.4 BALANCING PARAMETERS EXAMPLES

The following sections will provide examples that illustrate how the basic design parameter choices described above affect the performance parameters of the SRM+HGT and SRM+PEGT actuator combinations. In the examples to follow, different combinations of these parameters can be constant or variable for the actuator designs presented in each set. Though this provides many possible design scenarios, only the possibilities that have been encountered in common RRG design practice will be presented. The computational tool used to generate these results is discussed in Appendix A1 so that future actuator designers can utilize it to explore other design scenarios. Unless otherwise specified, the following set of assumptions were used for the SRM (Table 6.1) and gear train designs (Table 6.2) in this chapter. All of the graphical results will be presented in the form of 2-D plots because these are more useful for

observing trends and quickly obtaining parameter information than their 3-D alternatives. All of the parameter data used to generate the plots is provided so that future researchers can present it in 3-D format if necessary.

Table 6.1: SRM Design Assumptions

Parameter	Value
Number of stator poles	$N_s=6$
Number of rotor poles	$N_r=4$
Stator pole angle	$\theta_s=30^\circ$
Rotor pole angle	$\theta_r=32^\circ$
Saturation flux density	$B_{sat}=1.56$
Axial clearance	$c = 0.005D_m$
Density	$\rho = 0.284 \text{ lbm}/\text{in}^3$

Table 6.2: Gear Train Design Constant Parameters and Assumptions

Parameter	Value
Pressure angle	$\phi=25^\circ$
Minimum tooth number difference	$N_{min}=3$
Number of teeth in contact	3 (nominal load condition)
Efficiency	100%
Axial clearance	$c = 0.005D_g$
Diametral pitch range	$5 < P_d < 25$
Bending strength	$S_b=100 \text{ ksi}$
Contact strength	$S_c=250 \text{ ksi}$
Density	$\rho = 0.284 \text{ lbm}/\text{in}^3$
Velocity Factor (K_v)	1.1
Load Distribution Factor (K_m)	1.3
Geometry Factor (J)	0.5
Output Speed (rpm)	1

Finally, it should be noted that the value of the load inertia multiplier K (introduced in Section 3.4.1) was set equal to 1 for all of the responsiveness computations

in this chapter. This corresponds to a relatively low load inertia and physically implies that the dominant load torque is due to an external load (running at relatively low speed) rather than an inertial torque (required to accelerate the load). For this reason, responsiveness results are reported and only discussed briefly in this chapter. Chapter 7 will devote its entirety to considering different values of load inertia and how to choose the design parameters to maximize responsiveness.

6.5 EXAMPLE 1: BALANCING THE MOTOR AND GEAR-TOOTH LIMITED TORQUE CAPACITIES

This example presents scaled sets of actuator designs that illustrate how the motor length to overall length ratio (K_l), gear train aspect ratio (A_g), and motor diameter to gear train diameter ratio (K_d) can be varied to balance the motor and gear train torque capacities as the gear train diameter increases. The following three actuator combinations were considered: SRM+HGT, SRM+Star+PEGT, and SRM+Star Compound+PEGT. For each combination, gear train diameters (D_g) ranging from 10 to 50 inches (with increments of 5 inches) and a constant overall aspect ratio (A) of 1.0 were considered. Given a feasible range for K_d from (approximately) 0.25 to 1.0, the approach in this example was to adjust the value of K_l for each diameter so that the motor and gear train torque capacities were balanced while maintaining the same overall and motor aspect ratios. The reader should note that all of the results presented in this and the following two sections are for constant overall aspect ratio, gear ratio, and motor aspect ratio. If any of these parameter assumptions are relaxed, the above results would require adjustment.

6.5.1 SRM+HGT

Table 6.3 summarizes the settings of the basic parameter choices (including whether they are constant or variable) and their corresponding values for the SRM+HGT actuator combination, and Table 6.4 summarizes the values of the key design and performance parameters based on these design parameter settings. Figure 6.4-Figure 6.7 illustrate how the torque, weight, torque density, and output responsiveness vary as a function of diameter. Table 6.5 provides the simple power law scaling rules that were obtained from these figures.

Table 6.3: Actuator Parameter Choices for Example 1 (SRM+HGT)

Parameter	Description	Value
Gear Ratio	Constant	$g = 100$ to 1
Overall Aspect Ratio	Constant	$A = 1.0$
Motor Aspect Ratio	Constant	$A_m = 0.6$
Gear Train Aspect Ratio	Variable	$0.4 < A_g < 0.7$
Motor to Overall Length Ratio	Variable	$0.3 < K_l < 0.6$
Motor to Gear Train Diameter Ratio	Variable	$0.5 < K_d < 1.0$

Table 6.4: SRM+HGT Design and Performance Parameter Data¹¹

Overall Diameter (inches)	Motor Diameter (inches)	Length (inches)	Aspect Ratio	Gear Ratio	Torque (ft-lbf)	Weight (lbf)	Inertia (lbm-in ²)	Torque Density (ft-lbf/lbf)	Input Responsiveness (rad/sec ²)	Output Responsiveness (rad/sec ²)	Diametral Pitch, Pd
10	10.0	10	1.0	99	5276	165	73	32	3323	34	5.4
15	12.9	15	1.0	100	15113	460	453	33	1555	15	5.1
20	15.3	20	1.0	99	30682	986	1817	31	784	8	5.0
25	17.3	25	1.0	101	50235	1788	5997	28	393	4	5.2
30	19.4	30	1.0	98	77431	3045	15001	25	247	2	5.1
35	21.1	35	1.0	99	111119	4739	33634	23	156	2	5.0
40	22.7	40	1.0	100	150000	6952	68531	22	103	1	5.0
45	24.0	45	1.0	102	194599	9744	129646	20	69	1	5.0
50	25.6	50	1.0	98	244985	13406	224201	18	52	1	5.0

¹¹ The motor diameter in this and similar tables in this chapter refer to the diameter of the shell outside the motor.

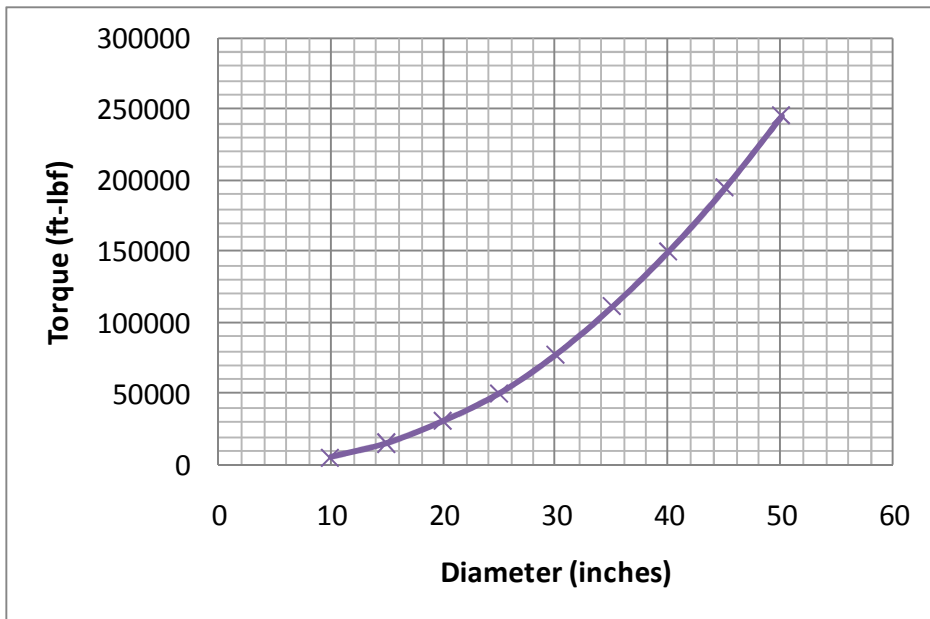


Figure 6.4: SRM+HGT Torque as a Function of Diameter

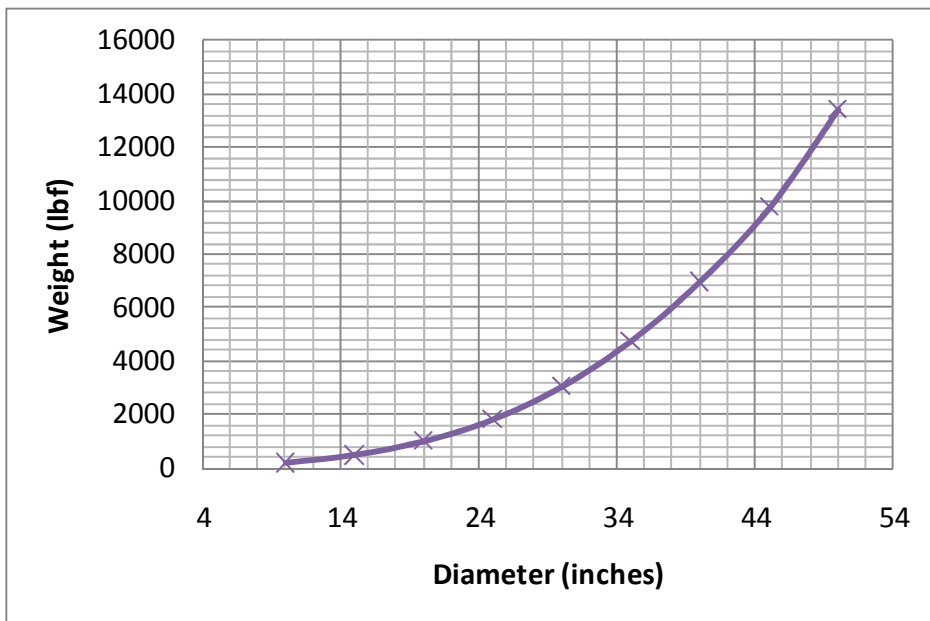


Figure 6.5: SRM+HGT Weight as a Function of Diameter

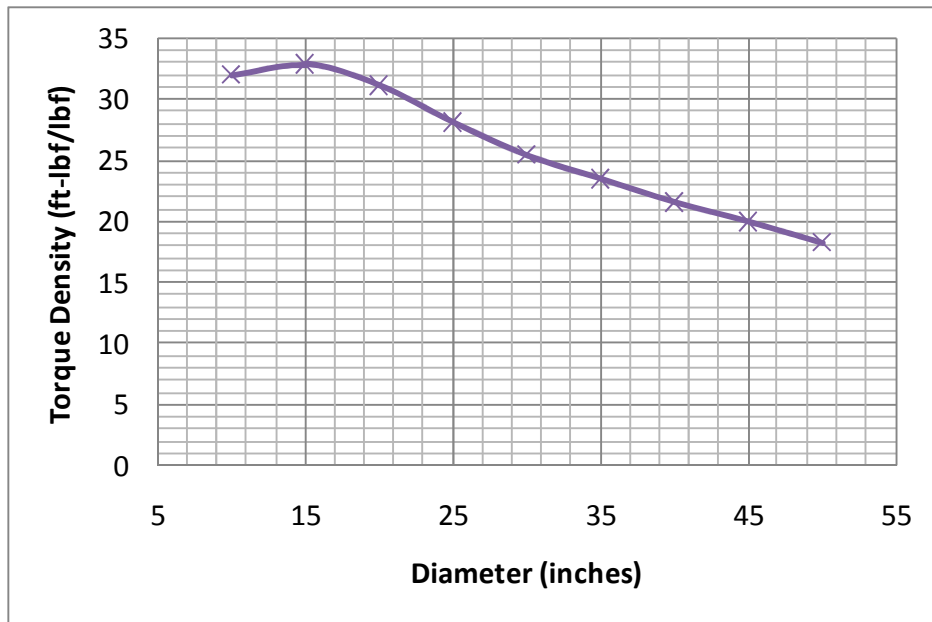


Figure 6.6: SRM+HGT Torque Density as a Function of Diameter

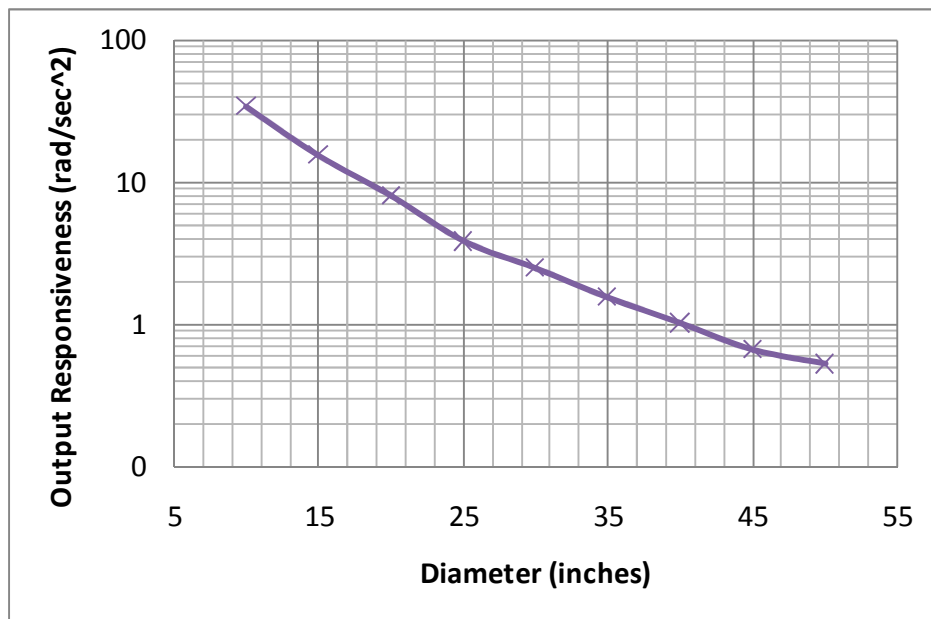


Figure 6.7: SRM+HGT Output Responsiveness as a Function of Diameter

Table 6.5: SRM+HGT Power-Law Scaling Rules ($P_p = kD_g^b$)

Parameter	Constant (k)	Power (b)
Torque	24.0	2.37
Weight	0.28	2.74
Inertia	0.0006	5.04
Torque Density	86	-0.37
Input Responsivness	2.00E+06	-2.65
Output Responsiveness	19725	-2.67

The primary reason for the decrease in torque density of the HGT is the fact that a contact ratio of 3 was used for designs of different diameters, with the reasoning behind this discussed in Section 5.2.2.

The decrease in output responsiveness (the torque to inertia ratio) with increasing diameter (Figure 6.7) was expected based on the dependence of torque and inertia on the diameter in Table 6.5 (approximately D_g^2 for torque and D_g^5 for inertia). Similar trends were observed for the stand-alone HGT designs presented in Section 5.2.2.

Table 6.6 uses the relationships derived in Section 6.3.2 and lists the distribution of weight and inertia in the motor and gear train as a function of diameter. The basic conclusion is that as the diameter increases (at constant gear ratio), the dominant weight and inertia moves from the motor to the gear train. Thus, if the designer is concerned about reducing weight and inertial content, he/she should concentrate on the gear train. Figure 6.8 and Figure 6.9 graphically display the information in Table 6.6.

Table 6.6: Distribution of Weight and Inertia (as a % of the total) in the Motor and Gear Train as a Function of Diameter (for the SRM+HGT Actuator)

Overall Diameter (inches)	Motor Weight (%)	Gear Train Weight (%)	Motor Inertia (%)	Gear Train Inertia (%)
10	43	57	59	41
15	33	67	34	66
20	25	75	20	80
25	20	80	11	89
30	16	84	8	92
35	14	86	5	95
40	12	88	4	96
45	10	90	3	97
50	9	91	2	98

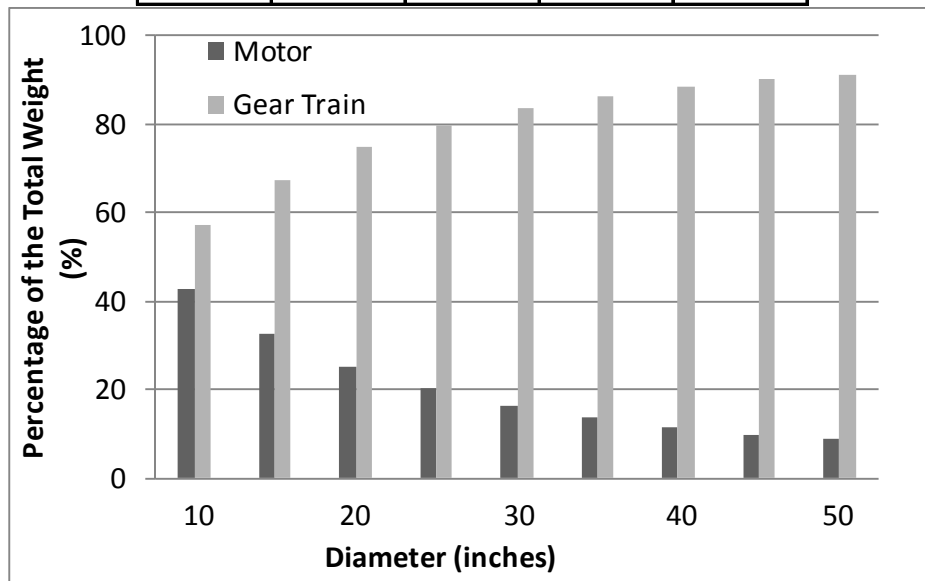


Figure 6.8: Percentage of Weight in the Motor and Gear Train as a Function of Diameter (for the SRM+HGT Actuator)

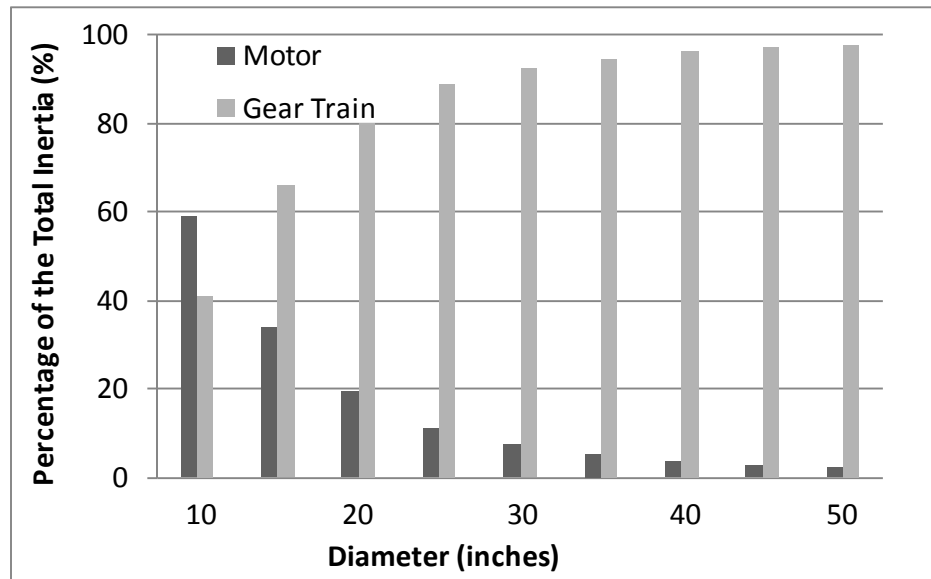


Figure 6.9: Percentage of Inertia in the Motor and Gear Train as a Function of Diameter (for the SRM+HGT Actuator)

Based on the results of Chapter 5 (Section 5.6.6), as the diameter of the motor or gear train increases, the motor torque density (though lower in an absolute sense) increases at a faster rate than the gear train. Given this important result, the motor diameter to gear train diameter (K_d) and motor length to overall length ratios (K_l) decrease and the gear train aspect ratio (A_g) increases as the overall gear train diameter increases, as illustrated in Figure 6.10 for this set of designs. Physically, this means the motor takes up less space than the gear train as the diameter increases, which mirrors the results in Table 6.6. The variation in these parameters gives the designer a preliminary idea of the relative sizes of the motor and the gear train for a large set of diameters for this particular gear ratio of 100 to 1. Similar plots could be generated for different gear ratios, but analogous results would be produced. Table 6.7 provides the same information as Figure 6.10 in tabular form.

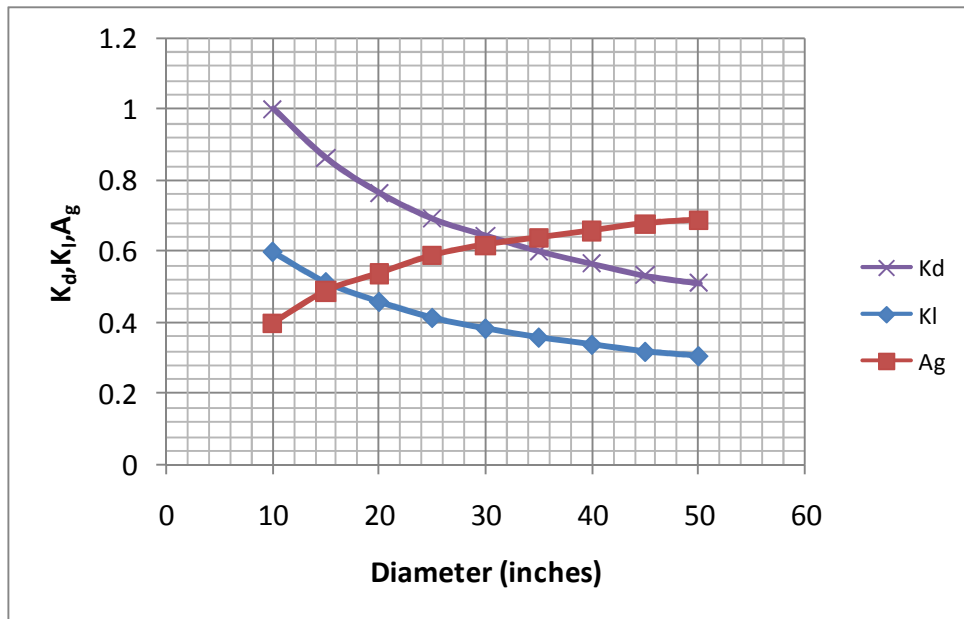


Figure 6.10: Variation of K_d , K_I , and A_g as a Function of Diameter (for the SRM+HGT Actuator)

Table 6.7: Variation of Basic Design Parameters as a Function of Diameter (for the SRM+HGT Actuator)

D_g (inches)	g	K_d	K_I	A	A_g	A_m
10	99	1.00	0.60	1.01	0.40	0.6
15	100	0.86	0.52	1.00	0.49	0.6
20	99	0.77	0.46	1.00	0.54	0.6
25	101	0.69	0.42	1.00	0.59	0.6
30	98	0.65	0.39	1.00	0.62	0.6
35	99	0.60	0.36	1.00	0.64	0.6
40	100	0.57	0.34	1.00	0.66	0.6
45	102	0.53	0.32	1.00	0.68	0.6
50	98	0.51	0.31	1.00	0.69	0.6

For a quick feasibility check on the bearings, Table 6.8 provides the estimated bearing load capacities (as a function of diameter) required for a life of 5,000 hours.

Table 6.8: SRM+HGT Bearing Load Capacity Requirements (lbf)

Output Bearing	Wobble Bearing	Shaft Bearing Right	Shaft Bearing Left
51731	96460	60430	16404
90017	184394	108412	38336
130801	280852	158714	65310
167182	367675	199662	92414
210009	472253	251560	125626
254961	583790	304751	161908
298825	689827	353761	197343
342498	796906	400969	234716
385287	898040	447879	269832

6.5.2 SRM+Star+PEGT

Table 6.9 summarizes the settings of the basic parameter choices (including whether they are constant or variable) and their corresponding values for the SRM+Star+PEGT actuator combination, and Table 6.10 summarizes the values of the key design and performance parameters based on these design parameter settings. Figure 6.11-Figure 6.14 illustrate how the torque, weight, torque density, and output responsiveness vary as a function of diameter. Table 6.11 provides the simple power law scaling rules that were obtained from these figures.

Table 6.9: Actuator Parameter Choices for Example 1 (SRM+Star+PEGT)

Parameter	Description	Value
Gear Ratio (1 st Stage Star)	Constant	$g_1 = 2.86$ to 1
Gear Ratio (PE-Output Gear)	Constant	$g_{pe} = 35$ to 1
Gear Ratio (Overall)	Constant	$g = 100$ to 1
Overall Aspect Ratio	Constant	$A = 1.0$
Motor Aspect Ratio	Constant	$A_m = 0.6$
Gear Train Aspect Ratio	Variable	$0.4 < A_g < 0.65$
Motor to Overall Length Ratio	Variable	$0.35 < K_l < 0.6$
Motor to Gear Train Diameter Ratio	Variable	$0.55 < K_d < 0.95$

Table 6.10: SRM+Star+PEGT Design and Performance Parameter Data

Overall Diameter (inches)	Motor Diameter (inches)	Length (inches)	Aspect Ratio	Gear Ratio	Torque (ft-lbf)	Weight (lbf)	Inertia (lbm-in ²)	Torque Density (ft-lbf/lbf)	Input Responsiveness (rad/sec ²)	Output Responsiveness (rad/sec ²)	Diametral Pitch, Pd
10	10.0	10	1.0	100	4724	166	58	29	3784	38	12.0
15	13.7	15	1.0	100	17910	517	353	35	2325	24	8.0
20	17.2	20	1.0	100	45254	1178	1333	38	1566	16	6.0
25	19.5	25	1.0	100	71913	2199	3781	33	889	9	6.5
30	22.4	30	1.0	100	128215	3761	9168	34	651	7	5.4
35	24.2	35	1.0	101	170920	5865	19160	29	413	4	5.8
40	26.8	40	1.0	101	259496	8752	37227	30	323	3	5.1
45	28.7	45	1.0	99	318746	12475	69435	26	219	2	5.5
50	30.0	50	1.0	100	385073	17081	117828	23	152	2	5.8

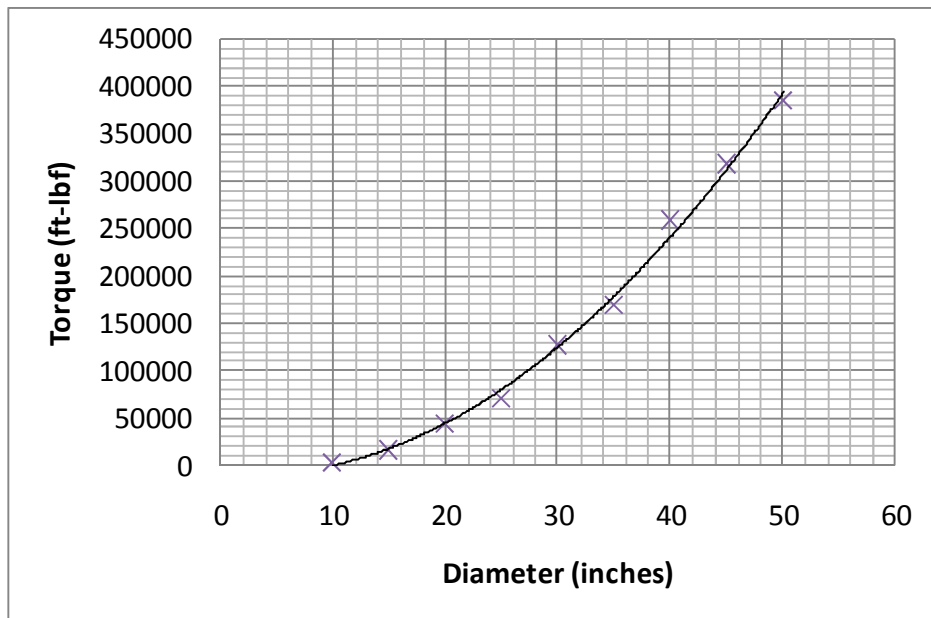


Figure 6.11: SRM+Star+PEGT Torque as a Function of Diameter

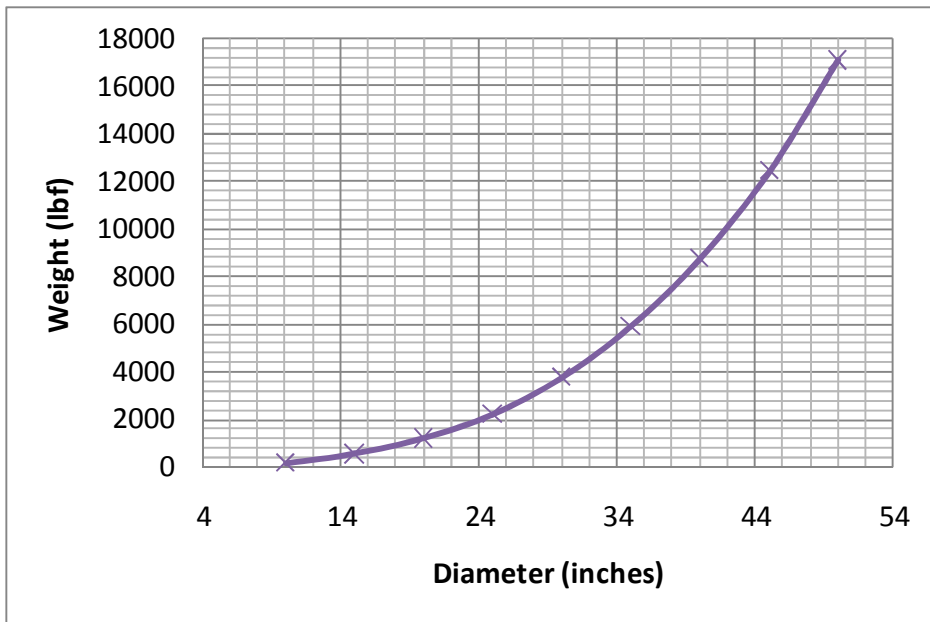


Figure 6.12: SRM+Star+PEGT Weight as a Function of Diameter

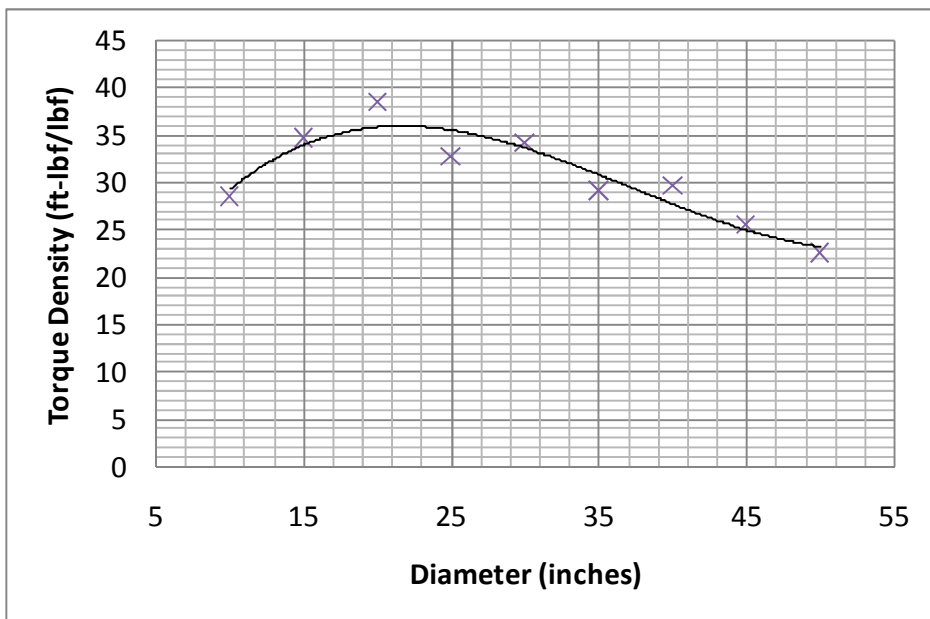


Figure 6.13: SRM+Star+PEGT Torque Density as a Function of Diameter



Figure 6.14: SRM+Star+PEGT Output Responsiveness as a Function of Diameter

Table 6.11: SRM+Star+PEGT Power-Law Scaling Rules ($P_p = kD_g^b$)

Parameter	Constant (k)	Power (b)
Torque	10.92	2.72
Weight	0.21	2.88
Inertia	0.0010	4.74
Torque Density	NA	NA
Input Responsivness	5.12E+04	-2.01
Output Responsiveness	5264	-2.01

Unlike the HGT, the PEGT torque density (Figure 6.13) increases for the lower range of designs because of a decrease in diametral pitch (i.e., wider, bigger teeth) and then begins to decrease after that due to the fact that a contact ratio of 3 was used for designs of different diameters. The torque density could increase (with increasing diameter) if more teeth are in contact, using the same reasoning as discussed in the previous section for the HGT. The torque density line not being smooth is a consequence of the diametral pitch not decreasing as a smooth function as the overall diameter

increases and results to due to the specific tooth number combinations required to achieve the desired gear ratio.

Table 6.12 provides the distribution of weight and inertia in the motor and gear train as a function of diameter. The basic conclusion, similar to that for the HGT in the previous section, is that as the diameter increases, the dominant weight and inertia moves from the motor to the gear train. Figure 6.15 and Figure 6.16 graphically display the information in Table 6.12.

Table 6.12: Distribution of Weight and Inertia (as a % of the total) in the Motor and Gear Train as a Function of Diameter (for the SRM+Star+PEGT Actuator)

Overall Diameter (inches)	Motor Weight (%)	Gear Train Weight (%)	Motor Inertia (%)	Gear Train Inertia (%)
10	40	60	64	36
15	33	67	50	50
20	28	72	41	59
25	21	79	26	74
30	19	81	22	78
35	15	85	15	85
40	14	86	13	87
45	11	89	9	91
50	9	91	7	93

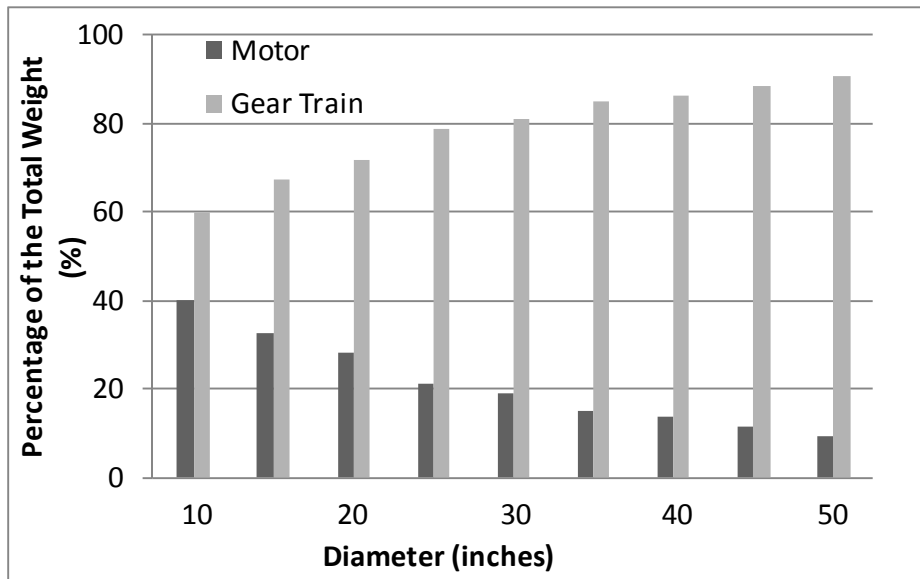


Figure 6.15: Percentage of Weight in the Motor and Gear Train as a Function of Diameter (for the SRM+Star+PEGT Actuator)

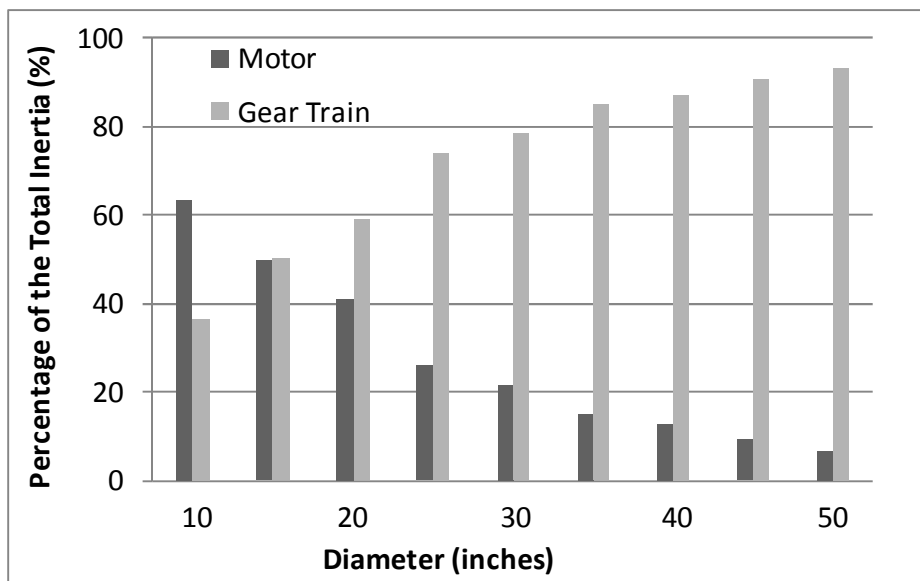


Figure 6.16: Percentage of Inertia in the Motor and Gear Train as a Function of Diameter (for the SRM+Star+PEGT Actuator)

Given the fact that the motor torque density increases (with increasing diameter) at a faster rate than the gear train, the motor diameter to gear train diameter (K_d) and motor length to overall length ratios (K_l) decrease and the gear train aspect ratio (A_g) increases as the overall gear train diameter increases, as illustrated in Figure 6.17 (analogous to Figure 6.10 for the SRM+HGT actuator). Table 6.13 provides the same information as Figure 6.17 in tabular form.

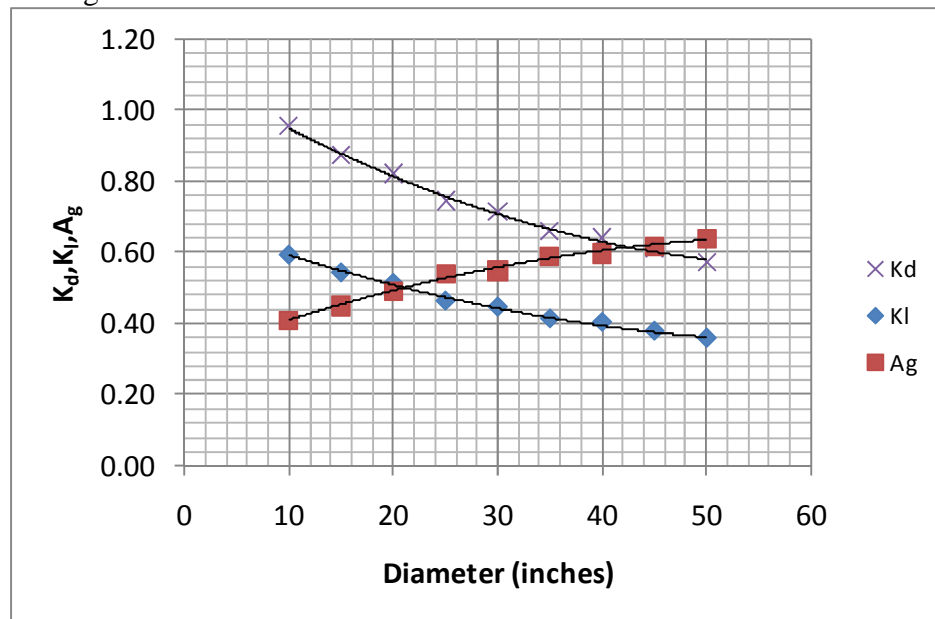


Figure 6.17: Variation of K_d , K_l , and A_g as a Function of Diameter (for the SRM+Star+PEGT Actuator)

Table 6.13: Variation of Basic Design Parameters as a Function of Diameter (for the SRM+Star+PEGT Actuator)

D_g (inches)	g	K_d	K_l	A	A_g	A_m
10	100	0.95	0.60	1.00	0.41	0.60
15	100	0.87	0.55	1.00	0.45	0.60
20	100	0.82	0.52	1.00	0.49	0.60
25	100	0.74	0.47	1.00	0.54	0.60
30	100	0.71	0.45	1.00	0.55	0.60
35	101	0.66	0.42	1.00	0.59	0.60
40	101	0.64	0.41	1.00	0.60	0.60
45	99	0.61	0.38	1.00	0.62	0.60
50	100	0.57	0.36	1.00	0.64	0.60

For a quick feasibility check on the bearings, Table 6.14 provides the estimated bearing load capacities (as a function of diameter) required for a life of 5,000 hours. Unlike the bearings in the HGT, the bearings in these PEGT designs can be the torque-limiting component, so these numerical results are potentially more useful in this case. The reader should recall that the PE gear and crankshaft bearings are typically the limiting components in the design (recall Figure 3.33 from Chapter 3), so the bearings for these particular locations should be considered first.

Table 6.14: SRM+Star+PEGT Bearing Load Capacity Requirements

Output Bearing	PE Gear Bearing	Crankshaft Bearing	Idler Shaft Bearing	Input Shaft Bearing
3038	9178	11164	1195	1799
7680	23201	27694	3020	4608
14553	43966	51970	5722	8811
18501	55001	64897	7209	11912
27488	81699	94823	10541	17097
31409	93735	112168	12757	23011
41726	124405	142462	15890	26278
45558	136861	161142	18377	33089
49535	149061	179205	20900	40368

6.5.3 SRM+Star Compound+PEGT

Table 6.15 summarizes the settings of the basic parameter choices (including whether they are constant or variable) and their corresponding values for the SRM+Star Compound+PEGT actuator combination, and Table 6.16 summarizes the values of the key design and performance parameters based on these design parameter settings. Figure 6.18-Figure 6.21 illustrate how the torque, weight, torque density, and output responsiveness vary as a function of diameter. Table 6.17 provides the simple power law scaling rules that were obtained from these figures. Because many of the results and conclusions are similar for the star and star compound 1st stage gear train options, only a brief discussion of these results will be provided. A comparison between these two alternatives will be made in Section 6.5.5.

Table 6.15: Actuator Parameter Choices for Example 1 (SRM+Star Compound+PEGT)

Parameter	Description	Value
Gear Ratio (1 st Stage Star Compound)	Constant	$g_1 = 5.71$ to 1
Gear Ratio (PE-Output Gear)	Constant	$g_{pe} = 35$ to 1
Gear Ratio (Overall)	Constant	$g = 250$ to 1
Overall Aspect Ratio	Constant	$A = 1.0$
Motor Aspect Ratio	Constant	$A_m = 0.6$
Gear Train Aspect Ratio	Variable	$0.5 < A_g < 0.7$
Motor to Overall Length Ratio	Variable	$0.3 < K_l < 0.5$
Motor to Gear Train Diameter Ratio	Variable	$0.45 < K_d < 0.8$

Table 6.16: SRM+Star Compound+PEGT Design and Performance Parameter Data

Overall Diameter (inches)	Motor Diameter (inches)	Length (inches)	Aspect Ratio	Gear Ratio	Torque (ft-lbf)	Weight (lbf)	Inertia (lbm-in ²)	Torque Density (ft-lbf/lbf)	Input Responsiveness (rad/sec ²)	Output Responsiveness (rad/sec ²)	Diametral Pitch, Pd
10	8.3	10	1.0	250	5301	127	19	42	5114	21	12.0
15	11.3	15	1.0	248	19503	417	101	47	3562	14	8.0
20	14.2	20	1.0	250	48774	962	356	51	2562	10	6.0
25	15.9	25	1.0	251	75762	1880	845	40	1657	7	6.5
30	18.4	30	1.0	248	133451	3127	2045	43	1228	5	5.4
35	19.8	35	1.0	251	175303	5218	3840	34	859	3	5.8
40	21.9	40	1.0	248	265642	7904	7333	34	679	3	5.1
45	23.2	45	1.0	252	323887	10840	13100	30	458	2	5.5
50	24.3	50	1.0	250	386714	15509	21163	25	338	1	5.8

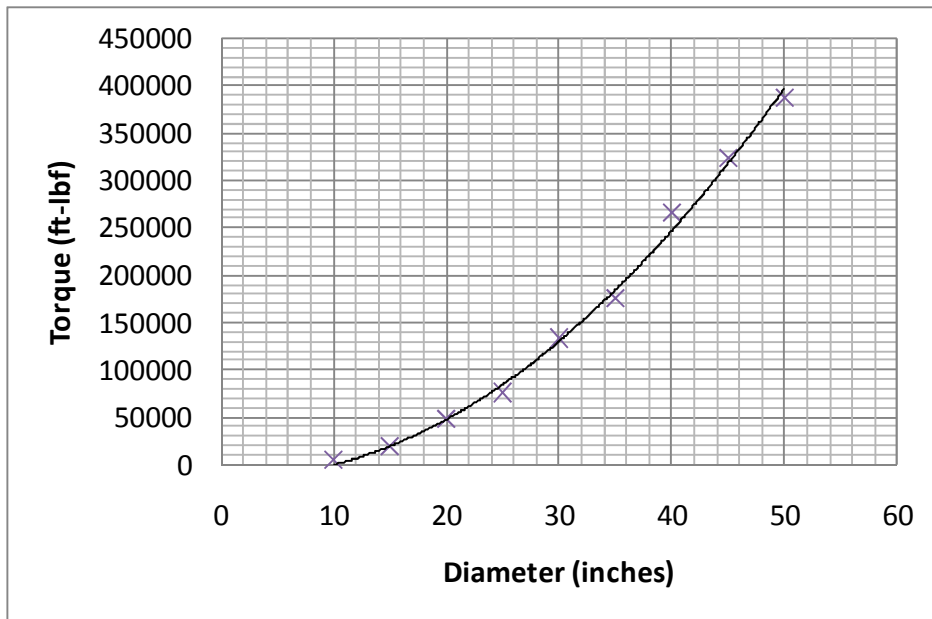


Figure 6.18: SRM+Star Compound+PEGT Torque as a Function of Diameter

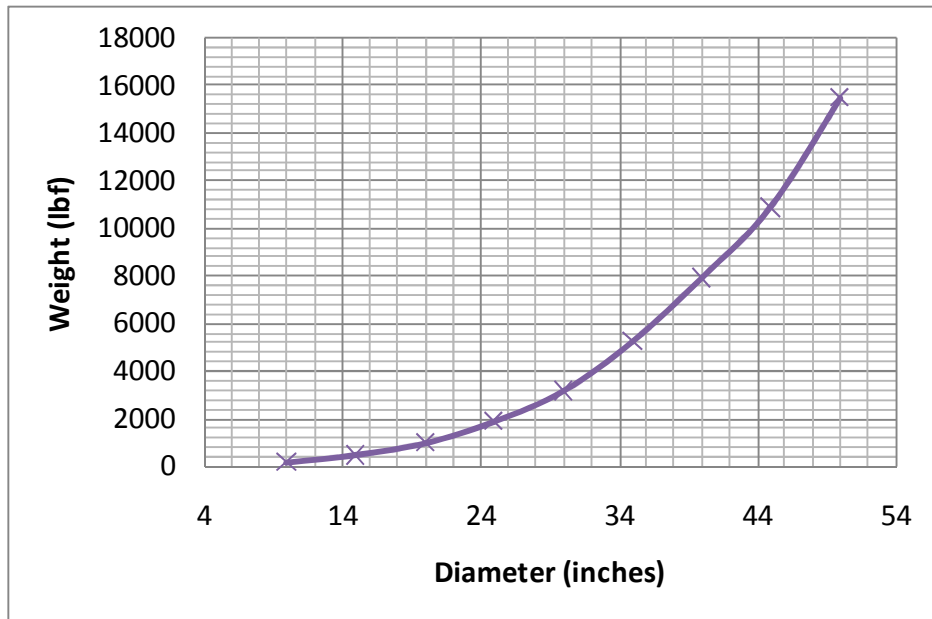


Figure 6.19: SRM+Star Compound+PEGT Weight as a Function of Diameter



Figure 6.20: SRM+Star Compound+PEGT Torque Density as a Function of Diameter



Figure 6.21: SRM+Star Compound+PEGT Output Responsiveness as a Function of Diameter

Table 6.17: SRM+Star Compound+PEGT Power-Law Scaling Rules ($P_p = kD_g^b$)

Parameter	Constant (k)	Power (b)
Torque	14.35	2.65
Weight	0.13	2.98
Inertia	0.0008	4.36
Torque Density	NA	NA
Input Responsivness	3.38E+04	-1.69
Output Responsiveness	1405	-1.71

Table 6.18 provides the distribution of weight and inertia in the motor and gear train as a function of diameter. The basic conclusion is that as the diameter increases, the dominant weight and inertia moves from the motor to the gear train. Figure 6.22 and Figure 6.23 graphically display the information in Table 6.18.

Table 6.18: Distribution of Weight and Inertia (as a % of the total) in the Motor and Gear Train as a Function of Diameter (for the SRM+Star Compound+PEGT Actuator)

Overall Diameter (inches)	Motor Weight (%)	Gear Train Weight (%)	Motor Inertia (%)	Gear Train Inertia (%)
10	30	70	77	23
15	22	78	66	34
20	19	81	57	43
25	13	87	41	59
30	12	88	35	65
35	9	91	26	74
40	8	92	23	77
45	7	93	16	84
50	5	95	13	87

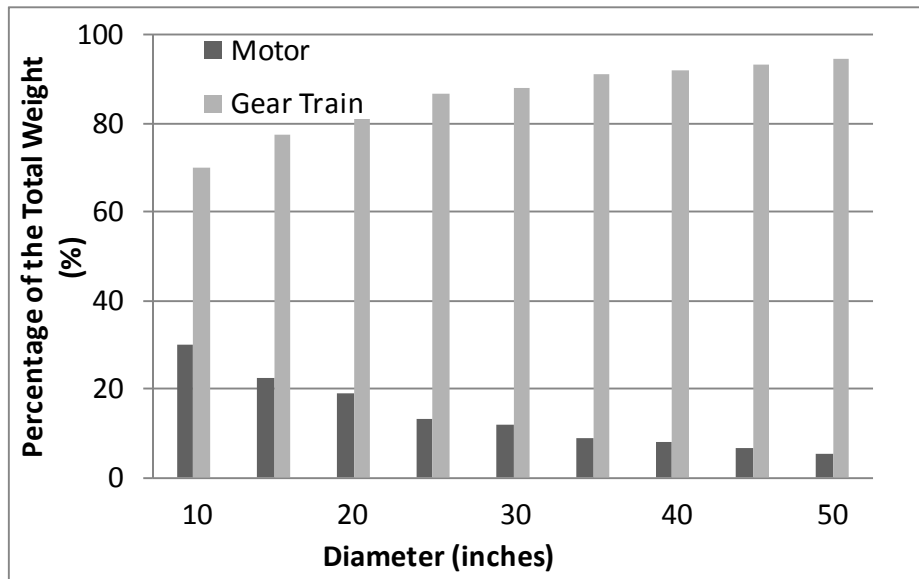


Figure 6.22: Percentage of Weight in the Motor and Gear Train as a Function of Diameter (for the SRM+Star Compound+PEGT Actuator)

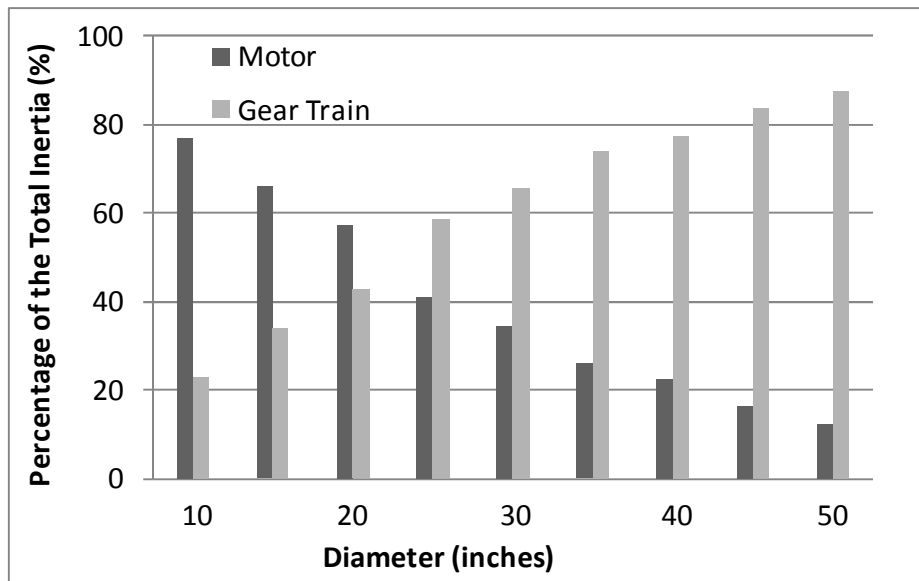


Figure 6.23: Percentage of Inertia in the Motor and Gear Train as a Function of Diameter (for the SRM+Star Compound+PEGT Actuator)

Figure 6.24 for star compound 1st stage gear train option is analogous to Figure 6.17 for the star 1st stage gear train option. Figure 6.24 reveals that the values of K_I and K_d are smaller and A_g is larger for the star compound 1st stage option (relative to the same parameters for the star 1st stage option in Figure 6.17). Physically, this means that the motor for the star compound 1st stage option is relatively smaller, and this occurs due to the higher gear ratio setting of 250 to 1 (relative to the gear ratio of 100 to 1 for the star 1st stage option). Table 6.19 provides the same information as Figure 6.24. Table 6.20 provides the estimated bearing load capacities (as a function of diameter) required for a life of 5,000 hours.

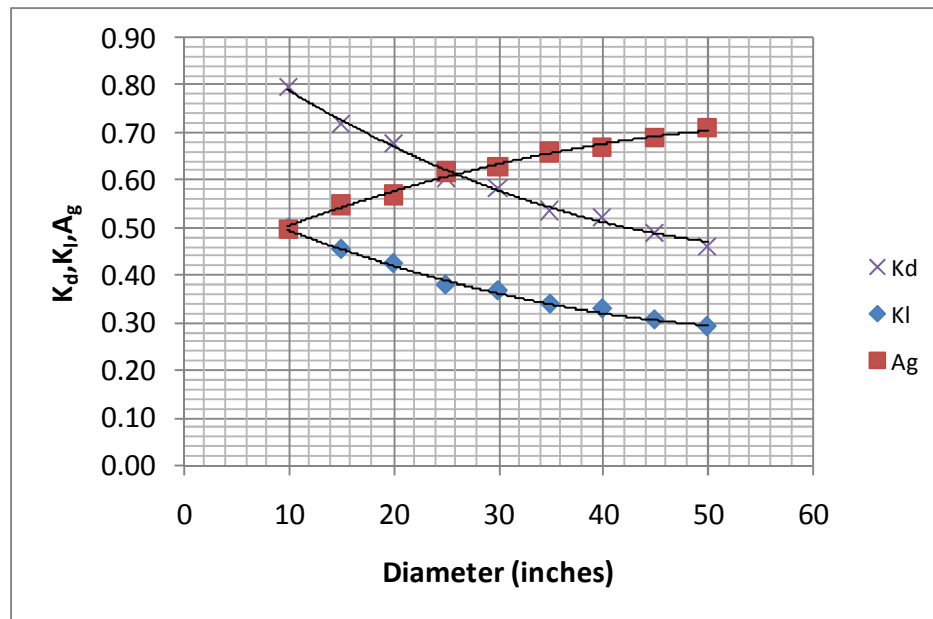


Figure 6.24: Variation of K_d , K_I , and A_g as a Function of Diameter (for the SRM+Star Compound+PEGT Actuator)

Table 6.19: Variation of Basic Design Parameters as a Function of Diameter (for the SRM+Star Compound+PEGT Actuator)

D_g (inches)	g	K_d	K_l	A	A_g	A_m
10	250	0.80	0.50	1.00	0.50	0.60
15	248	0.72	0.46	1.00	0.55	0.60
20	250	0.68	0.43	1.00	0.57	0.60
25	251	0.61	0.38	1.00	0.62	0.60
30	248	0.58	0.37	1.00	0.63	0.60
35	251	0.54	0.34	1.00	0.66	0.60
40	248	0.52	0.33	1.00	0.67	0.60
45	252	0.49	0.31	1.00	0.69	0.60
50	250	0.46	0.29	1.00	0.71	0.60

Table 6.20: SRM+Star Compound+PEGT Bearing Load Capacity Requirements

Output Bearing	PE Gear Bearing	Crankshaft Bearing	Idler Shaft Bearing	Input Shaft Bearing
3410	10142	12183	1299	947
8363	25233	29331	3140	2489
15685	46654	54855	5942	4507
19492	58404	66774	7076	5724
28611	84135	96501	10178	7724
32215	97054	110075	11726	10196
42714	129502	145010	15352	14013
46293	136845	154294	16205	12972
49746	150007	169026	18055	15694

6.5.4 Comparisons Between the SRM+HGT and SRM+Star+PEGT Alternatives

Based on the results presented earlier in this chapter, it is useful to make a few general comparisons between the SRM+Star+PEGT (with the star 1st stage, Section 6.5.2) and the SRM+HGT (Section 6.5.1), where each has a 100 to 1 gear ratio. Table 6.21 computes the percent difference between the performance parameters for these two alternatives, with positive numbers indicating that the SRM+HGT combination has larger values for the performance parameter under consideration. An analogous comparison

was made in Chapter 5 (Section 5.3) with only the gear trains, but the results in this section include the SRM. Figure 6.25 presents the same information as Table 6.21 in a graphical representation, and only the average values of the percent difference between the performance parameters (from all the values in a particular column) are plotted.

Table 6.21: Comparison Between the SRM+HGT and the SRM+Star+PEGT (Gear-Tooth Limited Torque Capacities for both gear trains)¹²

Overall Diameter (inches)	Length (inches)	Torque (% Difference)	Weight (% Difference)	Inertia (% Difference)	Torque Density (% Difference)	Input Responsiveness (% Difference)	Output Responsiveness (% Difference)
10	10	10	0	21	11	-14	-11
15	15	-19	-12	22	-5	-49	-52
20	20	-47	-19	27	-23	-100	-98
25	25	-43	-23	37	-16	-126	-132
30	30	-66	-24	39	-34	-163	-163
35	35	-54	-24	43	-24	-165	-164
40	40	-73	-26	46	-37	-212	-215
45	45	-64	-28	46	-28	-217	-223
50	50	-57	-27	47	-23	-193	-192
Averages (%)		-46	-20	36	-20	-138	-139

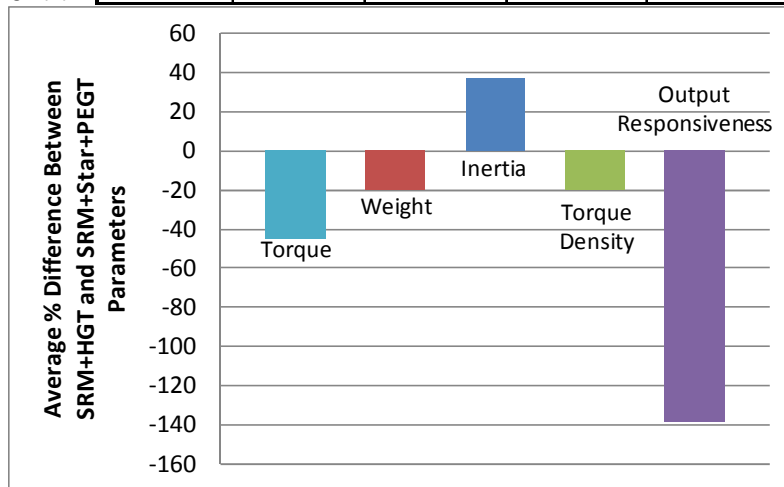


Figure 6.25: Percent Difference Between the Performance Parameters of the SRM+HGT and SRM+Star+PEGT Alternatives (Only average values of the percent difference are plotted for each performance parameter.)

¹² Positive (negative) percentages indicate that for the same overall diameter and length, the SRM+HGT has a larger (smaller) value for the performance parameter being considered. For torque, torque density, and responsiveness, positive percentages indicate that the SRM+HGT is superior to the SRM+Star+PEGT. For weight and inertia, positive percentages indicate that the SRM+Star+PEGT is superior to the SRM+HGT.

According to Table 6.21, the SRM+HGT combination has an average of 46% lower torque capacity than the SRM+PEGT combination for the same diameter. The differences between the HGT and PEGT torque capacities can be understood by referring to the torque capacity derivation provided in Section 5.3 and occurs due to the differences in diametral pitch (tooth size) required to achieve the gear ratio of 100 to 1. Considering the weight, the HGT weighs 20% less than the PEGT because of the stepped down diameter of the HGT behind the fixed gear mesh (see Figure 3.32 in Chapter 5) that is not present for the PEGT. The HGT has an average of 36% higher inertia than the PEGT. This is the case because the dominant inertia in the HGT (the crankshaft) is directly connected to the motor input shaft and does not benefit from reflection by square of the gear ratio. In contrast, the dominant inertias in the PEGT (the PE gear, 3 crankshafts, and output gear) benefit from the reflection by the gear ratio. The HGT has 20% lower torque density than the PEGT, which is consistent with the individual torque and weight comparisons. Finally, considering the input and output responsiveness values (both input and output), the HGT has significantly lower acceleration capabilities than the PEGT, especially as the diameter increases.

Based upon this comparison, the SRM+Star+PEGT combination is superior to the SRM+HGT combination for all the performance parameters considered except weight. While the results stated here provided a good starting point for comparison, there are other, less quantitative performance parameters such as number of parts, number of bearings, complexity, gear mesh stiffness, etc. that need to be considered in detail before one of these alternatives is selected for a specific application.

6.5.5 Comparisons Between the Star and Star Compound 1st Stage PEGT Alternatives

Based on the results presented earlier in this chapter, it is useful to make a few general comparisons between the PEGT with the star (Section 6.5.2) and star compound (Section 6.5.3) 1st stage alternatives (both include a motor). The reader should recall that a gear ratio of 100 to 1 was used for the SRM+Star+PEGT combination, and a gear ratio of 250 to 1 was used for the SRM+Star Compound+PEGT combination. For both, the PE gear-output gear mesh gear ratio was held constant at 35 to 1 for each of the different diameters considered. Table 6.22 computes the percent difference between the performance parameters for these two alternatives, with positive numbers indicating that the PEGT with the star compound 1st stage option has larger values for the performance parameter under consideration. An analogous comparison was made in Chapter 5 (Section 5.4) with only the gear trains, but the results in this section include the SRM. Figure 6.26 presents the same information as Table 6.22 in a graphical representation, and only the average values of the percent difference between the performance parameters are plotted

Table 6.22: Comparison Between the Star Compound and Star 1st Stage Gear Train Options for the PEGT¹³

Overall Diameter (inches)	Length (inches)	Torque (% Difference)	Weight (% Difference)	Inertia (% Difference)	Torque Density (% Difference)	Input Responsiveness (% Difference)	Output Responsiveness (% Difference)
10	10	11	-31	-203	32	26	-83
15	15	8	-24	-248	26	35	-63
20	20	7	-22	-274	24	39	-54
25	25	5	-17	-348	19	46	-35
30	30	4	-20	-348	20	47	-33
35	35	2	-12	-399	13	52	-22
40	40	2	-11	-408	12	52	-17
45	45	2	-15	-430	14	52	-20
50	50	0	-10	-457	10	55	-13
Averages (%)		5	-18	-346	19	45	-38

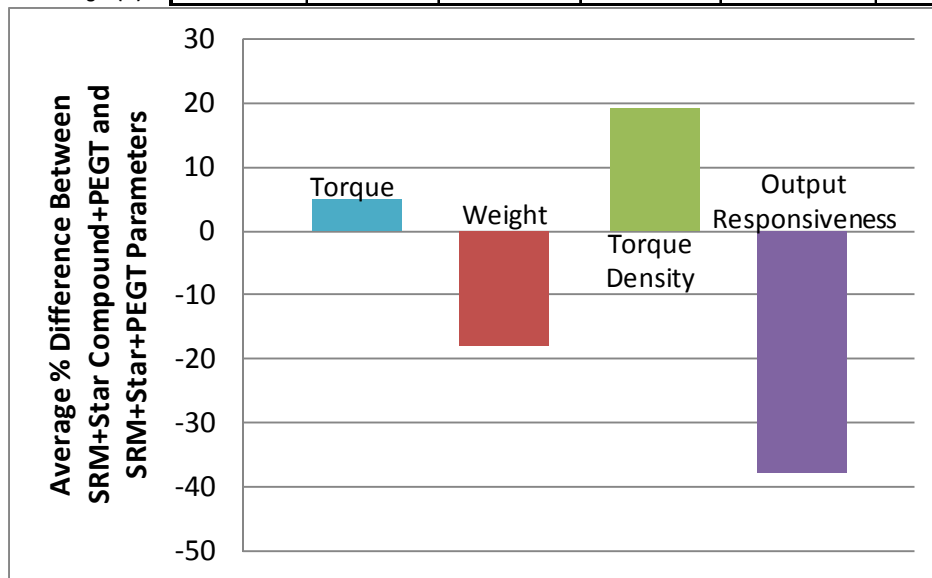


Figure 6.26: Percent Difference Between the Performance Parameters of the SRM+Star Compound+PEGT and SRM+Star+PEGT Alternatives (Only average values of the percent difference are plotted for each performance parameter.)

According to Table 6.22, the noteworthy benefits of replacing the star with the star compound gear train include an average 5% increase in torque, 18% reduction in

¹³ Positive (negative) percentages indicate that for the same overall diameter and length, the SRM+Star Compound+PEGT has a larger (smaller) value for the performance parameter being considered. For torque, torque density, and responsiveness, positive percentages indicate that the SRM+Star Compound+PEGT is superior to the SRM+Star+PEGT. For weight and inertia, positive percentages indicate that the SRM+Star+PEGT is superior to the SRM+Star Compound+PEGT.

weight, 346% reduction in input inertia, 19% increase in torque density, and a 45% increase in input responsiveness. The only drawback is a 38% decrease in output responsiveness. According to the table, the benefits in torque, weight, and torque density appear to decrease as the diameter increases, while the benefits in inertia and input responsiveness increase as the diameter increases. As expected, the torque capacity changes only slightly due to the fact that the larger gear ratio requires a smaller motor and thus more space for the gear train. Most importantly, the inertia reflected to the input is reduced significantly due to the higher gear ratios available for the star compound gear train.

Based upon this comparison, the SRM+Star Compound+PEGT combination is superior to the SRM+Star+PEGT combination for all the performance parameters considered except output responsiveness. However, the superiority of the SRM+Star+PEGT in output responsiveness diminishes as the diameter increases. Unlike the previous comparison between the PEGT and HGT (in which the HGT was by far the less complex design with fewer parts and fewer bearings), the two systems of interest in this section are nearly identical. Both have the same number of parts and bearings, with the star compound option simply having an additional gear stage added to its idler shaft.

The reader should recall that all of the results presented in Example 1 (and the two comparisons based upon those results) were for constant overall aspect ratio, gear ratio, and motor aspect ratio. If any of these parameter assumptions are relaxed, the above results and comparisons would require adjustment.

6.6 EXAMPLE 2: EFFECT OF GEAR RATIO ON BALANCE BETWEEN WEIGHT/INERTIA IN THE MOTOR AND GEAR TRAIN

This example illustrates how the diameter and gear ratio affect the distribution of weight and inertia between the motor and the gear train. The results will help the

designer to identify the dominant weight and inertia in designs of different diameters and gear ratios. To allow for objective comparisons, gear train diameters (D_g) of 8, 12, 16, and 20 inches were considered for both the HGT and PEGT. The reader should note that all of the results presented in this section are for constant overall aspect ratio, gear train aspect ratio, and motor to overall length ratio. If any of these parameter assumptions are relaxed, the above results and comparisons would require adjustment.

6.6.1 SRM+HGT

Table 6.23 summarizes the settings of the basic parameter choices (including whether they are constant or variable) and their corresponding values for the SRM+HGT actuator combination, and Table 6.24 summarizes the values of the key design and performance parameters based on these design parameter settings. The gear ratio range from 100 to 400 was chosen based on the currently accepted range for the HGT, which is subject to current RRG research on the clearance and load-carrying properties of the circular arc teeth. It is important to note that torque is essentially constant for a given diameter (size), with minor variations due to the slight differences in the diametral pitch (essentially the width of the tooth) needed to achieve the different gear ratios. Figure 6.27-Figure 6.29 illustrate how the weight, torque density, and output responsiveness vary as a function of gear ratio for multiple diameters. Note that some of the diameters have been omitted from the plots to better illustrate the trends without large changes in magnitude.

Table 6.23: Actuator Design Parameter Choices for Example 2 (SRM+HGT)

Parameter	Description	Value or Range
Gear Ratio	Variable	$100 < g < 400$
Overall Aspect Ratio	Constant	$A = 1.0$
Motor Aspect Ratio	Variable	$0.35 < A_m < 1.1$
Gear Train Aspect Ratio	Constant	$A_g = 0.55$
Motor to Overall Length Ratio	Constant	$K_l = 0.45$
Motor to Gear Train Diameter Ratio	Variable	$0.40 < K_d < 1.25$

Table 6.24: SRM+HGT Design and Performance Parameter Data

Overall Diameter (inches)	Motor Diameter (inches)	Length (inches)	Aspect Ratio	Gear Ratio	Torque (ft-lbf)	Weight (lbf)	Inertia (lbm-in ²)	Torque Density (ft-lbf/lbf)	Input Responsiveness (rad/sec ²)	Output Responsiveness (rad/sec ²)	Diametral Pitch, Pd
8	10.0	8	1.0	100	2600	102	41	26	2891	29	10
8	7.8	8	1.0	200	2549	77	24	33	2434	12	10
8	6.9	8	1.0	301	2653	69	21	38	1924	6	9
8	6.1	8	1.0	400	2321	62	18	37	1436	4	11
12	11.1	12	1.0	99	6010	244	188	25	1504	15	9
12	8.7	12	1.0	201	6094	202	139	30	998	5	9
12	7.6	12	1.0	299	5698	183	130	31	678	2	10
12	6.8	12	1.0	399	5286	173	122	31	498	1	11
16	12.0	16	1.0	99	11064	491	634	23	816	8	9
16	9.4	16	1.0	198	10722	414	559	26	447	2	9
16	8.3	16	1.0	301	10612	384	561	28	294	1	9
16	7.5	16	1.0	399	10097	371	531	27	223	1	10
20	12.8	20	1.0	99	17214	857	1835	20	448	4	9
20	10.1	20	1.0	199	17361	753	1647	23	247	1	9
20	8.8	20	1.0	298	16650	702	1673	24	156	1	9
20	8.1	20.0	1.0	400	17069	692	1570	25	127	0	9

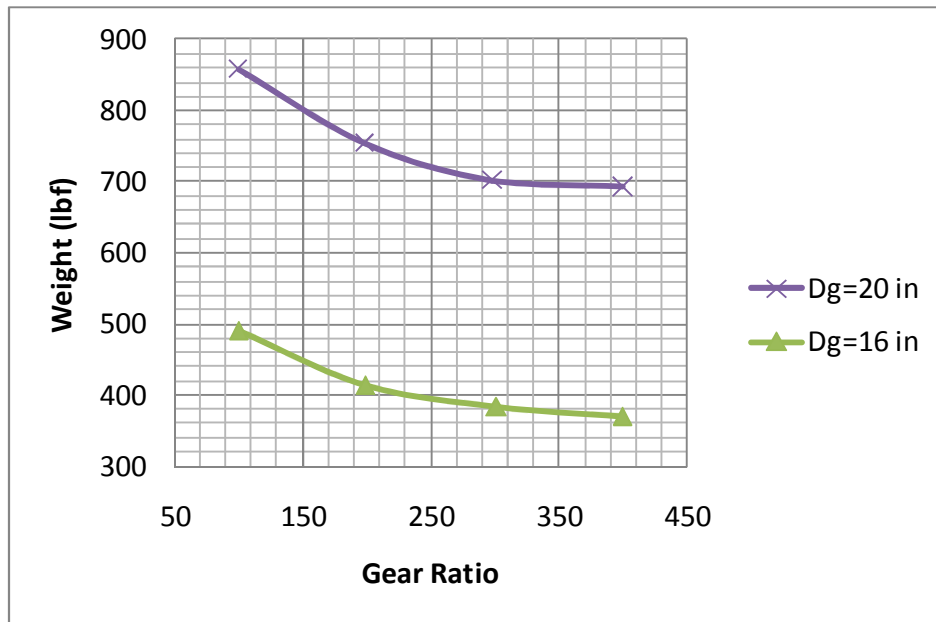


Figure 6.27: SRM+HGT Weight as a Function of Gear Ratio and Diameter

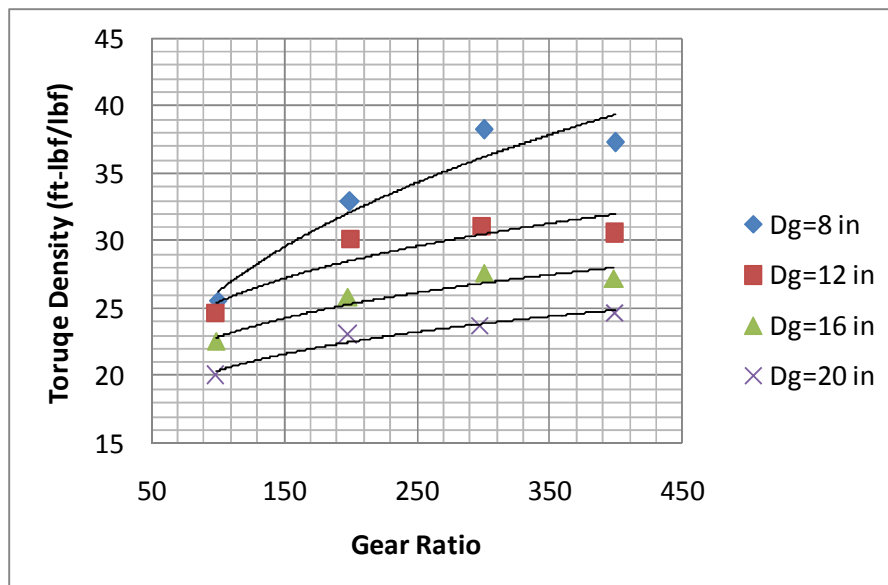


Figure 6.28: SRM+HGT Torque Density as a Function of Gear Ratio and Diameter

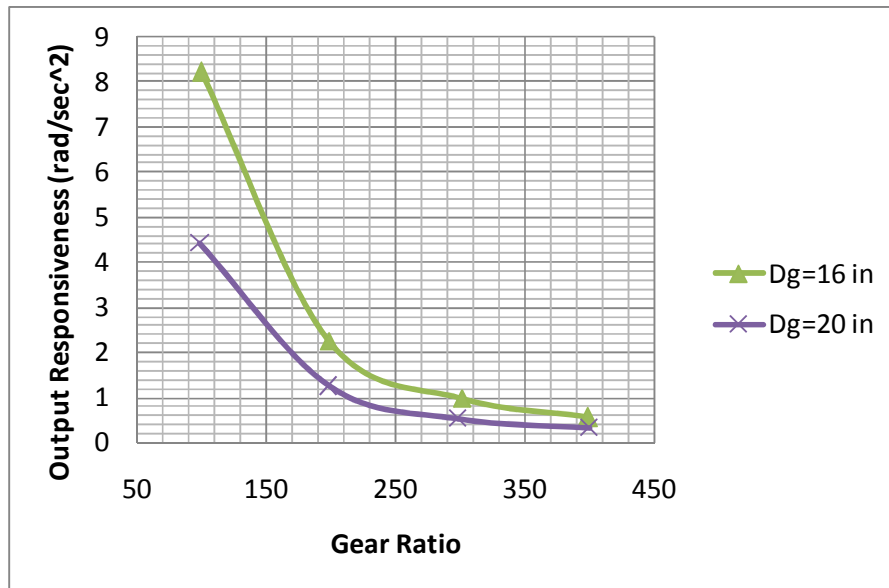


Figure 6.29: SRM+HGT Output Responsiveness as a Function of Gear Ratio and Diameter¹⁴

There was some difficulty in finding a motor of suitable torque for the smallest diameter/gear ratio combination (diameter of 8 inches and gear ratio of 100), and the diameter of the motor was actually required to be slightly larger than the gear train diameter for this case. This does not occur in general, but it can be remedied by increasing the diametral pitch (i.e., a larger number of smaller teeth) and consulting the values of the design parameter choices (K_1 and K_d in particular) from Example 1 in this chapter. Increasing the diametral pitch will decrease the torque capacity of the gear train (5.2.5.2) and should allow the matching of gear and motor-limited torque capacities.

Table 6.25 lists the percentage change in each of the performance parameters as the difference between the value of the performance parameter for the highest gear ratio

¹⁴ The variation in output responsiveness due to changes in gear ratio and diameter will be discussed in detail throughout Chapter 7. The trends in this figure are consistent with the stand-alone HGT responsiveness results reported in Section 5.2.2.

of 400 to 1 and the value of the parameter for the lowest gear ratio of 100 to 1. This percentage variation between the performance parameters (P_p) was computed as follows.

$$\% \text{ Variation} = 100 \times \left(\frac{P_{P,g=400} - P_{P,g=100}}{P_{P,g=100}} \right) \quad \text{Eqn. 173}$$

Thus, a positive number in the table indicates an increase in the parameter due to increasing the gear ratio. The key result from the table is that increasing the gear ratio from 100 to 400 provides the benefits of reduced weight and inertia and increased torque density without any added complexity (same number of parts and bearings). One drawback of increasing the gear ratio is the reduction in both the input and output responsiveness, which suggests that lower gear ratios might be more favorable for applications in which achieving high acceleration is important. Section 7.3.1.1 discusses this result in more detail. Figure 6.30 presents the same information as Table 6.25 in a graphical representation, and only the average values of the percentage change of the performance parameters are plotted.

Table 6.25: Percentage Change of the SRM+HGT Performance Parameters as the Gear Ratio is Varied from 100 to 400 for Different Diameters

Overall Diameter (inches)	Torque (ft-lbf)	Weight (lbf)	Inertia (lbm-in ²)	Torque Density (ft-lbf/lbf)	Input Responsiveness (rad/sec ²)	Output Responsiveness (rad/sec ²)
8	-11%	-39%	-55%	46%	-50%	-88%
12	-12%	-29%	-35%	24%	-67%	-92%
16	-9%	-24%	-16%	21%	-73%	-93%
20	-1%	-19%	-14%	23%	-72%	-93%
Average % Change	-8%	-28%	-30%	28%	-65%	-91%

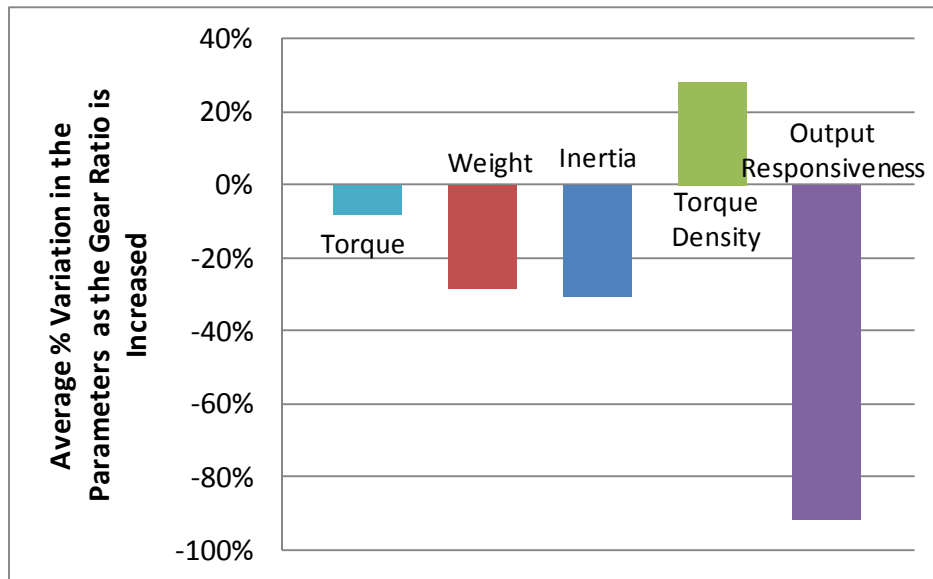


Figure 6.30: Percentage Change of the SRM+HGT Performance Parameters as the Gear Ratio is Varied from 100 to 400 (Only average values of the percentage change are plotted for each performance parameter.)

Table 6.26 provides the distribution of weight and inertia in the motor and gear train as a function of diameter and gear ratio. The basic conclusion is that as the gear ratio increases for a given diameter, the weight and inertia content moves from the motor to the gear train. Thus, if the designer is concerned about reducing weight and inertial content, he/she should generally concentrate on the gear train if higher gear ratios and larger diameters are used. Figure 6.31 and Figure 6.32 graphically display the information in Table 6.26 for the 12 inch diameter design.

Table 6.26: Distribution of Weight and Inertia (as a % of the total) in the Motor and Gear Train as a Function of Diameter and Gear Ratio (for the SRM+HGT Actuator)

Overall Diameter (inches)	Gear Ratio	Motor Weight (%)	Gear Train Weight (%)	Motor Inertia (%)	Gear Train Inertia (%)
8	100	41	59	61	39
	200	32	68	39	61
	301	29	71	27	73
	400	25	75	19	81
12	99	31	69	31	69
	201	24	76	16	84
	299	20	80	10	90
	399	17	83	7	93
16	99	24	76	17	83
	198	18	82	7	93
	301	15	85	4	96
	399	13	87	3	97
20	99	20	80	9	91
	199	14	86	4	96
	298	12	88	2	98
	400	10	90	2	98

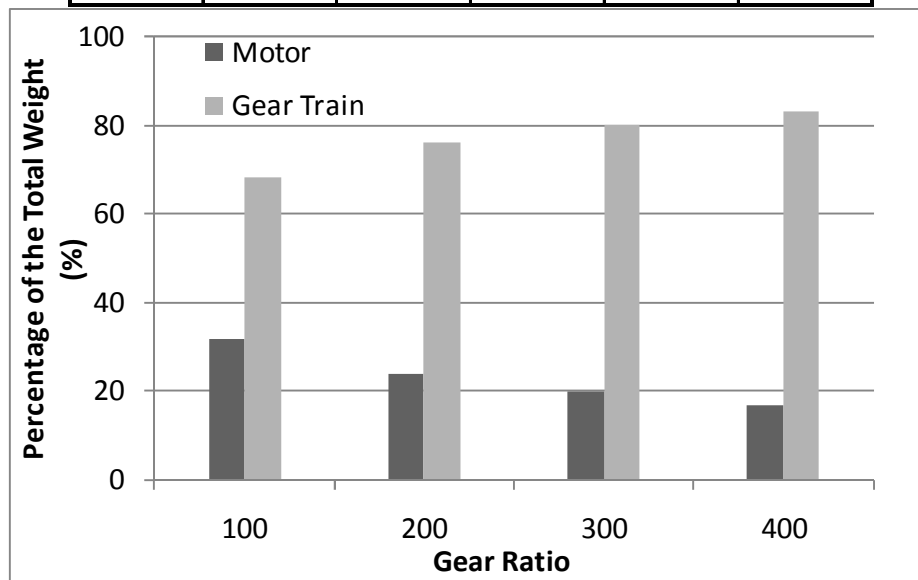


Figure 6.31: Percentage of Weight in the Motor and Gear Train as a Function of Gear Ratio for the Overall Diameter of 12 inches (for the SRM+HGT Actuator)

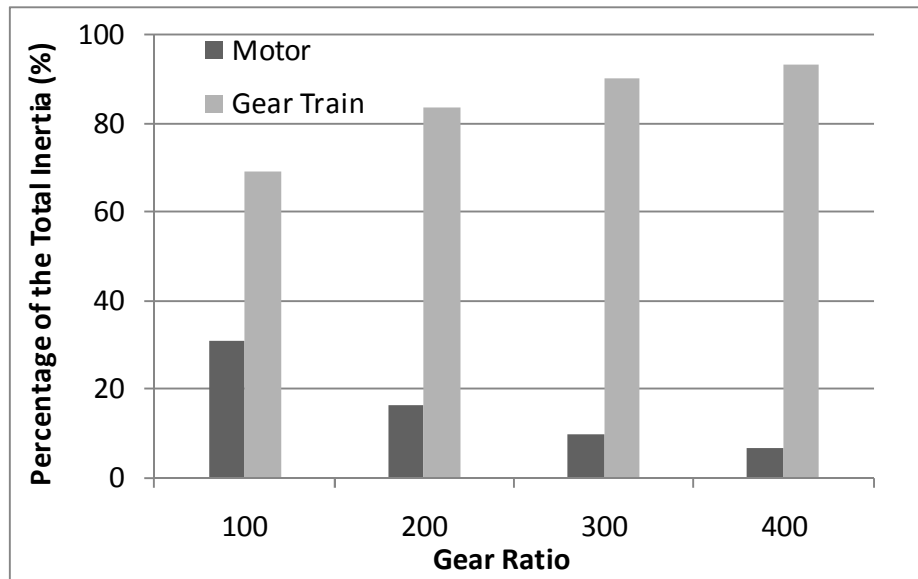


Figure 6.32: Percentage of Inertia in the Motor and Gear Train as a Function of Gear Ratio for the Overall Diameter of 12 inches (for the SRM+HGT Actuator)

Figure 6.33 illustrates how the motor diameter to gear train diameter ratio (K_d) and motor aspect ratio (A_m) vary as a function of gear ratio for the 8 inch diameter design. Both lines change the way they do because the motor diameter is getting smaller relative to the gear train diameter (K_d) and motor length (A_m) and as the gear ratio increases. The motor diameter decreases due to the lower motor torque demand as the gear ratio increases and also due to the constraint of a fixed aspect ratio (length) for the different gear ratio options. Keeping the motor length fixed and decreasing only the motor diameter gives the most favorable benefit in terms of reduced weight and inertia. Table 6.27 provides the same information as Figure 6.33 in tabular form and also includes the 12, 16, and 20 inch diameter designs.

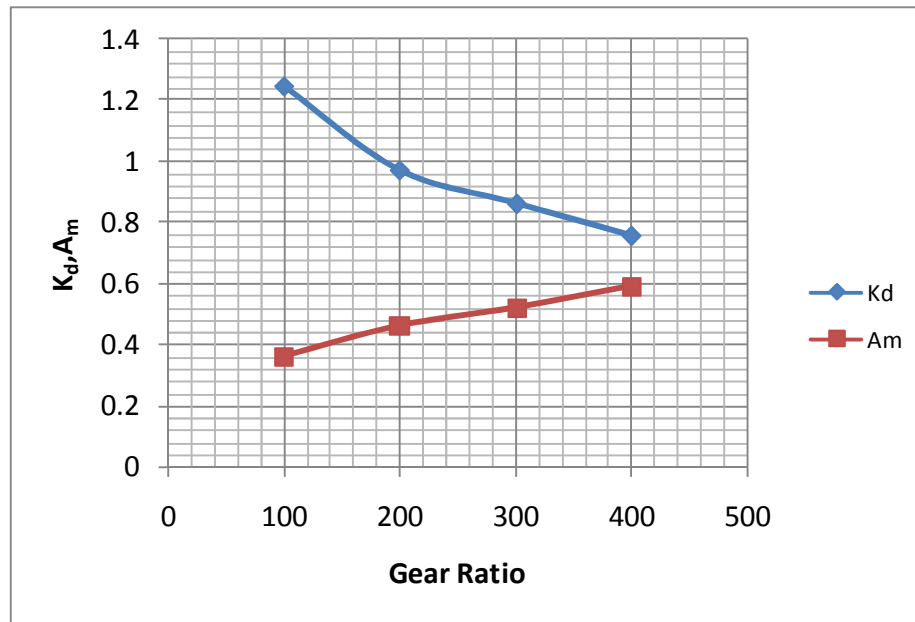


Figure 6.33: Variation of K_d and A_m as a Function of Gear Ratio (8 inch diameter SRM+HGT actuator)

Table 6.27: Variation of Basic Design Parameters as a Function of Diameter and Gear Ratio (for the SRM+HGT Actuator)

D_g (inches)	g	K_d	K_l	A	A_g	A_m
8	100	1.25	0.45	1.00	0.55	0.36
8	200	0.97	0.45	1.00	0.55	0.46
8	301	0.86	0.45	1.00	0.55	0.52
8	400	0.76	0.45	1.00	0.55	0.59
12	99	0.92	0.45	1.00	0.55	0.49
12	201	0.73	0.45	1.00	0.55	0.62
12	299	0.63	0.45	1.00	0.55	0.71
12	399	0.57	0.45	1.00	0.55	0.79
16	99	0.75	0.45	1.00	0.55	0.60
16	198	0.59	0.45	1.00	0.55	0.76
16	301	0.52	0.45	1.00	0.55	0.87
16	399	0.47	0.45	1.00	0.55	0.96
20	99	0.64	0.45	1.00	0.55	0.70
20	199	0.51	0.45	1.00	0.55	0.89
20	298	0.44	0.45	1.00	0.55	1.02
20	400	0.41	0.45	1.00	0.55	1.11

6.6.2 SRM+Star+PEGT (Effect of Variation of 1st Stage Gear Ratio)

6.6.2.1 Background

The stand-alone PEGT designs reported in Section 5.2.3.3 were based on a 100 ksi bending stress limit. This stress limit is a somewhat aggressive value considering standard practice bending stress limits of near 65 ksi [Norton, 2000] but is justified if advanced materials are used. However, a recent PEGT prototype effort (introduced in Chapter 5, Section 5.2.3.1) suggests that using the gear train torque capacities based on this stress limit makes it difficult to find a motor capable of producing the required torque capacity in a diameter that is compatible with the PEGT. Table 6.28 lists the motor, bearing, and gear-tooth limited torque capacities of the current PEGT prototype. All of the values in the table can be considered nominal values in that each component was designed based on its nominal material strength limits.

Table 6.28: Motor, Bearing, and Gear-Tooth Limited Torque Capacities for a recent PEGT Prototype Effort

Component	Nominal Torque Capacity (ft-lbf)
Gear Teeth (bending strength, $S_b=100$ ksi)	6210
Bearings (life of 6,000 hours)	6938
Motor (flux density, $B_{sat}=1.56$)	2000

Based on the discussion in Chapter 5 (Section 5.2.3.2), it is reasonable to assume that the bearing and gear-tooth limited capacities can be balanced if the bearing and gear train design parameters (gear ratio, output speed, crankshaft and PE gear bearing sizes, etc.) are properly managed. However, the motor was clearly limiting this design and will continue to limit future designs of this diameter. Considering a fixed overall length and diameter of the actuator, a few things could have been done to fix this imbalance between the motor and gear train limited torque capacities.

- Allow more axial length for the motor and less for the gear train (i.e., increase K_l).
- Increase the maximum allowable diameter available for the motor while still providing means for mounting to an external structure (i.e., increase K_d).

The second option will be implemented here, and physically this means that the motor diameter will sometimes approach the gear train outer diameter and an external rib must be added for mounting to an external structure.

6.6.2.2 Results

Given this important background, the results of this section can now be presented. Table 6.29 summarizes the settings of the basic parameter choices (including whether they are constant or variable) and their corresponding values for the SRM+Star+PEGT actuator combination, and Table 6.30 summarizes the values of the key design and performance parameters based on these design parameter settings.

Though the PEGT can achieve gear ratios as low as 15 to 1 (pending current research at the RRG), a lower limit of 100 to 1 was used here because below this value, it was difficult to find a motor with adequate torque capacity and with a diameter less than or equal to the gear train diameter. The upper limit of 175 to 1 was chosen because maximum gear ratios of near 5 to 1 and 35 to 1 were achievable with the 1st stage star and 2nd stage PE-output gear meshes, respectively.

It is important to note that, just as for the HGT in Section 6.6.1, the torque is essentially constant for a given diameter, because the PE gear-output gear mesh ratio was held constant at 35 to 1 and thus the pitch diameters and tooth numbers were identical. Figure 6.34-Figure 6.36 illustrate how the weight, torque density, and output

responsiveness vary as a function of gear ratio for multiple diameters. Note that some of the diameters have been omitted from the plots to better illustrate the trends without large changes in magnitude.

Table 6.29: Actuator Design Parameter Choices for Example 2 (SRM+Star+PEGT)

Parameter	Description	Value or Range
Gear Ratio (1 st Stage Star)	Variable	$2.8 < g_1 < 5$
Gear Ratio (PE-Output Gear)	Constant	$g_{pe} = 35$ to 1
Gear Ratio (Overall)	Variable	$100 < g < 175$
Overall Aspect Ratio	Constant	$A = 1.0$
Motor Aspect Ratio	Variable	$0.55 < A_m < 1.0$
Gear Train Aspect Ratio	Constant	$A_g = 0.4$
Motor to Overall Length Ratio	Constant	$K_l = 0.6$
Motor to Gear Train Diameter Ratio	Variable	$0.60 < K_d < 1.05$

Table 6.30: SRM+Star+PEGT Design and Performance Parameter Data

Overall Diameter (inches)	Motor Diameter (inches)	Length (inches)	Aspect Ratio	Gear Ratio	Torque (ft-lbf)	Weight (lbf)	Inertia (lbm-in ²)	Torque Density (ft-lbf/lbf)	Input Responsiveness (rad/sec ²)	Output Responsiveness (rad/sec ²)	Diametral Pitch, Pd
8	8.7	8	1.0	100	2389	94	24	25	4543	45	15
8	8.1	8	1.0	124	2389	86	18	28	5013	40	15
8	7.7	8	1.0	149	2389	81	14	30	5362	37	15
8	7.4	8	1.0	173	2389	78	11	31	5676	33	15
12	11.0	12	1.0	100	8062	257	116	31	3182	32	10
12	10.2	12	1.0	124	8062	239	83	34	3595	29	10
12	9.7	12	1.0	149	8062	227	64	36	3991	27	10
12	9.2	12	1.0	173	8062	218	50	37	4317	25	10
16	13.1	16	1.0	100	19109	542	390	35	2287	23	7
16	12.1	16	1.0	124	19109	504	267	38	2618	21	7
16	11.5	16	1.0	149	19109	481	202	40	2971	20	7
16	10.9	16	1.0	173	19109	464	157	41	3265	19	7
20	15.0	20	1.0	100	37322	973	1016	38	1702	17	6
20	13.9	20	1.0	124	37322	918	703	41	1993	16	6
20	13.1	20	1.0	149	37322	873	514	43	2271	15	6
20	12.5	20.0	1.0	173	37322	842	399	44	2504	14	6

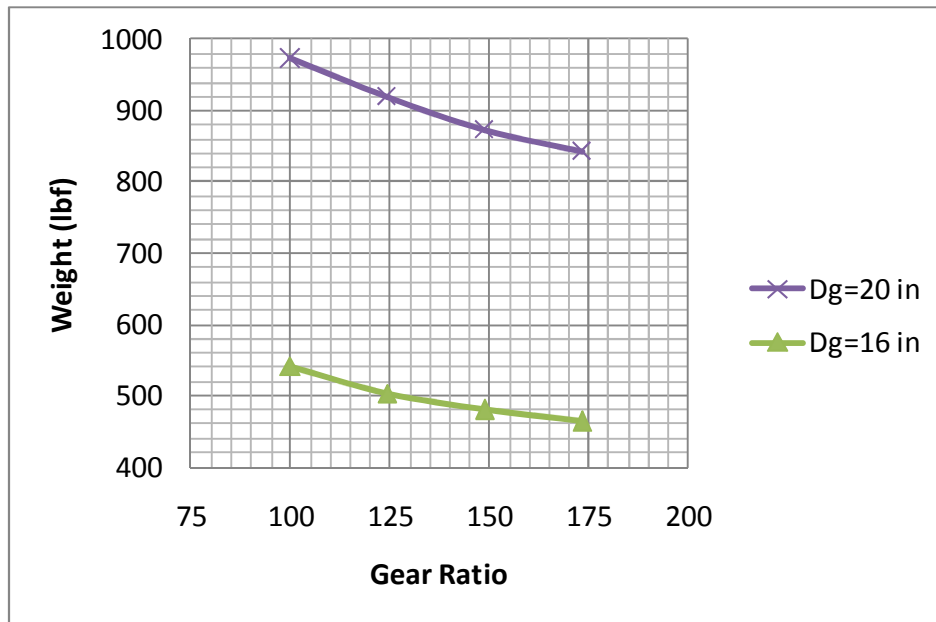


Figure 6.34: SRM+Star+PEGT Weight as a Function of Gear Ratio and Diameter

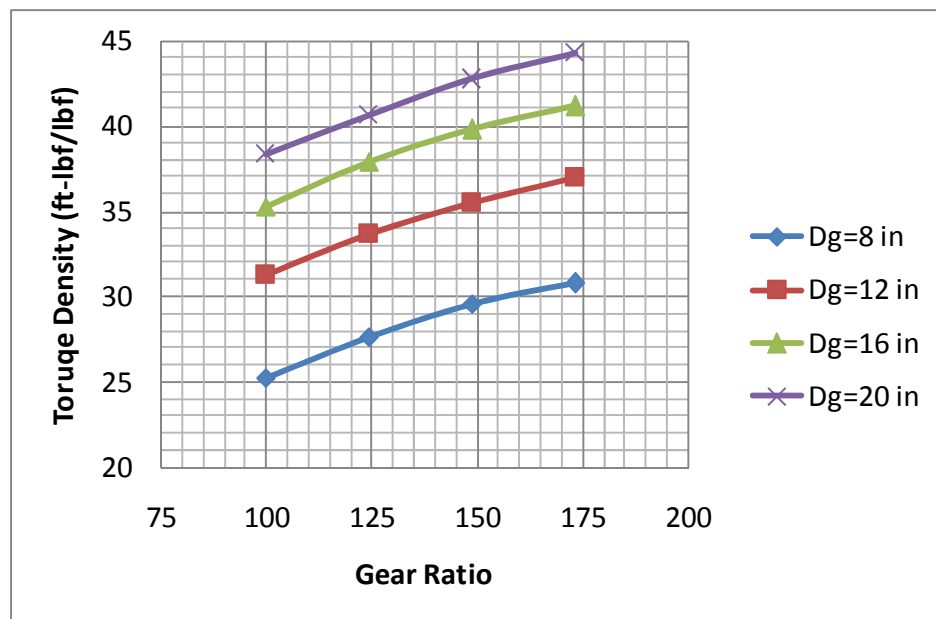


Figure 6.35: SRM+Star+PEGT Torque Density as a Function of Gear Ratio and Diameter

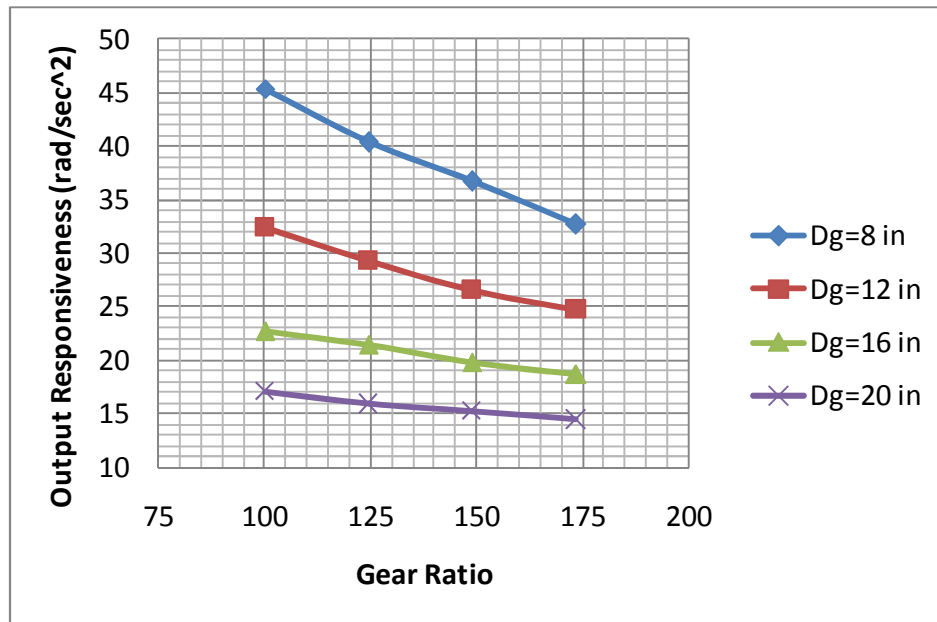


Figure 6.36: SRM+Star+PEGT Output Responsiveness as a Function of Gear Ratio and Diameter

Table 6.31 lists the percentage change in each of the performance parameters as the difference between the value of the performance parameter for the highest gear ratio of 175 to 1 and the value of the parameter for the lowest gear ratio of 100 to 1. Thus, a positive number in the table indicates an increase in the parameter due to increasing the gear ratio. The key result from the table is that increasing the gear ratio from 100 to 175 provides the benefits of reduced weight and inertia and increased torque density and input responsiveness without any added complexity (same number of parts and bearings). One drawback of increasing the gear ratio is the reduction in the output responsiveness, which suggests that lower gear ratios might be more favorable for applications in which achieving high acceleration is important. Similar qualitative results were found for the SRM+HGT combination in the previous section. A noteworthy difference here is that increasing the gear ratio in the HGT decreased the input responsiveness while doing the

same for the Star+PEGT increased the input responsiveness. Figure 6.37 presents the same information as Table 6.31 in a graphical representation, and only the average values of the percentage change of the performance parameters are plotted.

Table 6.31: Percentage Change of the SRM+Star+PEGT Performance Parameters as the Gear Ratio is Varied from 100 to 175 for Different Diameters

Overall Diameter (inches)	Torque (ft-lbf)	Weight (lbf)	Inertia (lbm-in ²)	Torque Density (ft-lbf/lbf)	Input Responsiveness (rad/sec ²)	Output Responsiveness (rad/sec ²)
8	0%	-18%	-54%	22%	25%	-28%
12	0%	-15%	-57%	18%	36%	-24%
16	0%	-14%	-60%	17%	43%	-18%
20	0%	-13%	-61%	15%	47%	-15%
Average % Change	0%	-15%	-58%	18%	38%	-21%

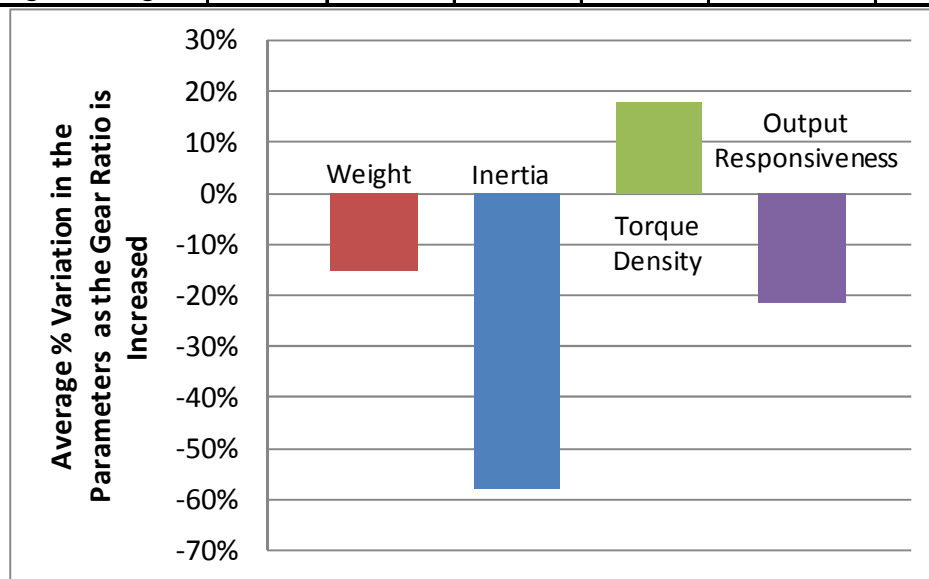


Figure 6.37: Percentage Change of the SRM+Star+PEGT Performance Parameters as the Gear Ratio is Varied from 100 to 175 (Only average values of the percentage change are plotted for each performance parameter.)

Table 6.32 provides the distribution of weight and inertia in the motor and gear train as a function of diameter. The basic conclusion is that as the gear ratio increases for

a given diameter, the dominant weight moves to the gear train and the dominant inertia moves to the motor. This shifting of the inertia from the gear train to the motor is contrary to the result found the SRM+HGT combination in the previous section and occurs due to the relatively low inertial content of the PEGT in comparison to the HGT (see Section 5.3 for a comparison of these gear trains). Figure 6.38 and Figure 6.39 graphically display the information in Table 6.32 for the 12 inch diameter design.

Table 6.32: Distribution of Weight and Inertia (as a % of the total) in the Motor and Gear Train as a Function of Diameter and Gear Ratio (for the SRM+Star+PEGT actuator)

Overall Diameter (inches)	Gear Ratio	Motor Weight (%)	Gear Train Weight (%)	Motor Inertia (%)	Gear Train Inertia (%)
8	100	43	57	71	29
	124	41	59	74	26
	149	39	61	76	24
	173	38	62	78	22
12	100	38	62	56	44
	124	35	65	59	41
	149	34	66	63	37
	173	32	68	65	35
16	100	34	66	45	55
	124	31	69	48	52
	149	30	70	52	48
	173	28	72	54	46
20	100	31	69	37	63
	124	28	72	40	60
	149	27	73	43	57
	173	25	75	46	54

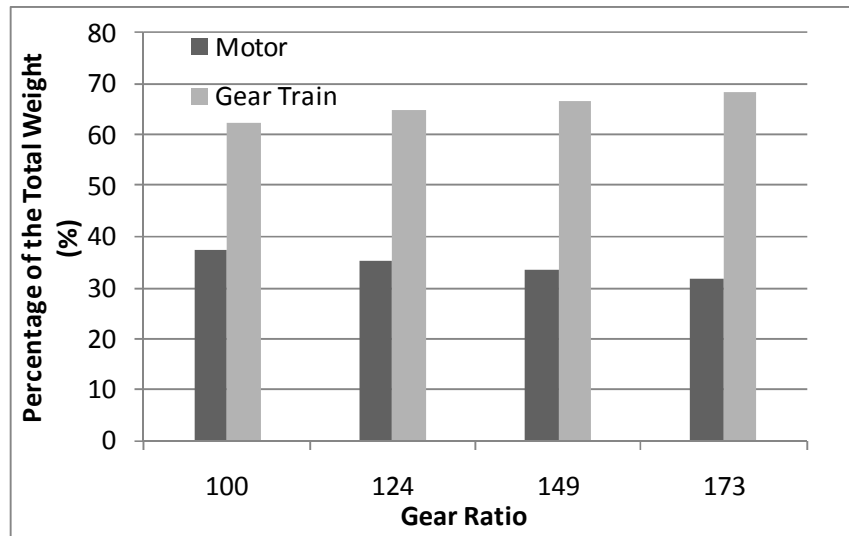


Figure 6.38: Percentage of Weight in the Motor and Gear Train as a Function of Gear Ratio for the Overall Diameter of 12 inches (for the SRM+Star+PEGT actuator)

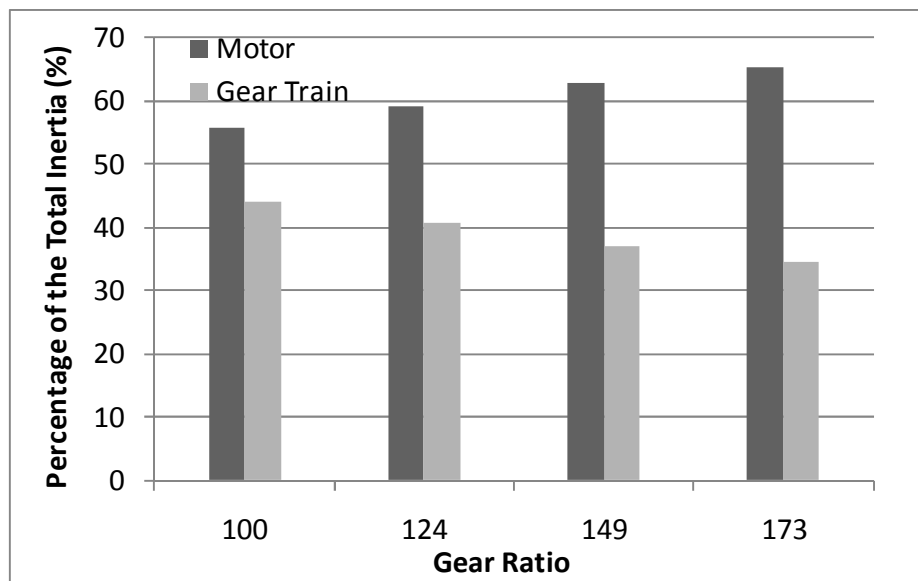


Figure 6.39: Percentage of Inertia in the Motor and Gear Train as a Function of Gear Ratio for the Overall Diameter of 12 inches (for the SRM+Star+PEGT actuator)

Figure 6.40 illustrates how the motor diameter to gear train diameter ratio (K_d) and motor aspect ratio (A_m) vary as a function of gear ratio for the 8 inch diameter design

and is analogous to Figure 6.33 in the previous section. The value of K_d near 1 suggests that that motor and gear train outside diameters are similar for this particular size. Table 6.33 provides the same information as Figure 6.40 in tabular form and also includes the 12, 16, and 20 inch diameter designs.

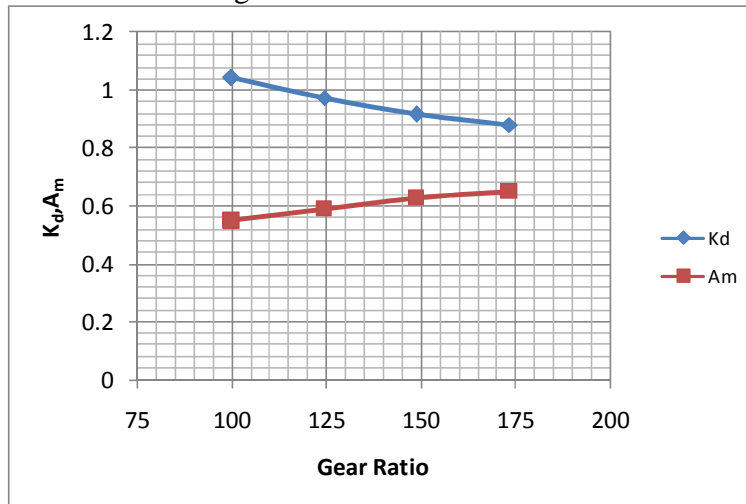


Figure 6.40: Variation of K_d and A_m as a Function of Gear Ratio (8 inch diameter SRM+Star+PEGT actuator)

Table 6.33: Variation of Basic Design Parameters as a Function of Diameter and Gear Ratio (for the SRM+Star+PEGT actuator)

D_g (inches)	g	K_d	K_l	A	A_g	A_m
8	100	1.04	0.60	1.00	0.40	0.55
8	124	0.97	0.60	1.00	0.40	0.59
8	149	0.92	0.60	1.00	0.40	0.63
8	173	0.88	0.60	1.00	0.40	0.65
12	100	0.87	0.60	1.00	0.40	0.66
12	124	0.81	0.60	1.00	0.40	0.70
12	149	0.77	0.60	1.00	0.40	0.74
12	173	0.74	0.60	1.00	0.40	0.78
16	100	0.78	0.60	1.00	0.40	0.73
16	124	0.72	0.60	1.00	0.40	0.79
16	149	0.69	0.60	1.00	0.40	0.83
16	173	0.65	0.60	1.00	0.40	0.88
20	100	0.71	0.60	1.00	0.40	0.80
20	124	0.67	0.60	1.00	0.40	0.86
20	149	0.63	0.60	1.00	0.40	0.91
20	173	0.60	0.60	1.00	0.40	0.96

6.6.3 SRM+Star Compound+PEGT (Effect of Variation of 1st Stage Gear Ratio)

Table 6.34 summarizes the settings of the basic parameter choices (including whether they are constant or variable) and their corresponding values for the SRM+Star Compound+PEGT actuator combination, and Table 6.35 summarizes the values of the key design and performance parameters based on these design parameter settings. Though the PEGT can achieve gear ratios as low as 15 to 1 (pending current research at the RRG), a lower limit of 150 to 1 was used here because below this value, the same gear ratio can be achieved with a relatively simpler star gear train in place of the star compound. The upper limit of 450 to 1 was chosen because maximum gear ratios of near 13 to 1 and 35 to 1 were achievable with the 1st stage star compound and 2nd stage PE-output gear meshes, respectively.

Again, it is important to note that torque is constant for a given diameter, because the PE gear-output gear mesh ratio was held constant at 35 to 1 and thus the pitch diameters and tooth numbers were identical. Figure 6.41-Figure 6.43 illustrate how the weight, torque density, and output responsiveness vary as a function of gear ratio for multiple diameters. Note that some of the diameters have been omitted from the plots to better illustrate the trends without large changes in magnitude.

Table 6.34: Actuator Design Parameter Choices for Example 2 (SRM+Star Compound+PEGT)

Parameter	Description	Value or Range
Gear Ratio (1 st Stage Star Compound)	Variable	$4.3 < g_1 < 12.9$
Gear Ratio (PEGT)	Constant	$g_{pe} = 35 \text{ to } 1$
Gear Ratio (Overall)	Variable	$150 < g < 450$
Overall Aspect Ratio	Constant	$A = 1.0$
Motor Aspect Ratio	Variable	$0.65 < A_m < 1.35$
Gear Train Aspect Ratio	Constant	$A_g = 0.4$
Motor to Overall Length Ratio	Constant	$K_l = 0.6$
Motor to Gear Train Diameter Ratio	Variable	$0.45 < K_d < 0.9$

Table 6.35: SRM+Star Compound+PEGT Design and Performance Parameter Data

Overall Diameter (inches)	Motor Diameter (inches)	Length (inches)	Aspect Ratio	Gear Ratio	Torque (ft-lbf)	Weight (lbf)	Inertia (lbm-in ²)	Torque Density (ft-lbf/lbf)	Input Responsiveness (rad/sec ²)	Output Responsiveness (rad/sec ²)	Diametral Pitch, Pd
8	7.4	8	1.0	149	2171	68	12	32	5385	37	15
8	6.4	8	1.0	251	2171	57	6	38	6288	25	15
8	5.9	8	1.0	348	2171	53	4	41	6767	19	15
8	5.5	8	1.0	450	2171	49	3	44	6903	15	15
12	9.3	12	1.0	151	7329	187	56	39	4031	27	10
12	8.0	12	1.0	251	7329	157	27	47	5065	20	10
12	7.3	12	1.0	353	7329	141	17	52	5702	16	10
12	6.8	12	1.0	447	7329	136	12	54	6128	14	10
16	11.2	16	1.0	149	17372	389	186	45	2955	20	7
16	9.4	16	1.0	251	17372	330	82	53	3928	16	7
16	8.5	16	1.0	351	17372	310	49	56	4669	13	7
16	7.9	16	1.0	450	17372	299	35	58	5197	11	7
20	12.7	20	1.0	149	33930	695	479	49	2236	15	6
20	10.7	20	1.0	250	33930	607	201	56	3122	13	6
20	9.7	20	1.0	348	33930	579	119	59	3811	11	6
20	9.0	20.0	1.0	447	33930	534	84	64	4179	9	6

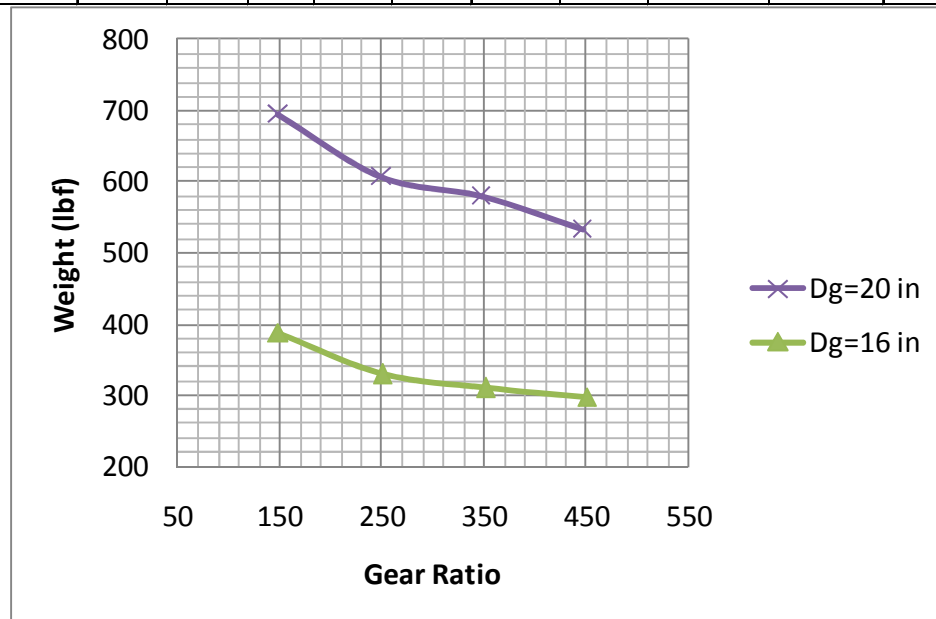


Figure 6.41: SRM+Star Compound+PEGT Weight as a Function of Gear Ratio and Diameter

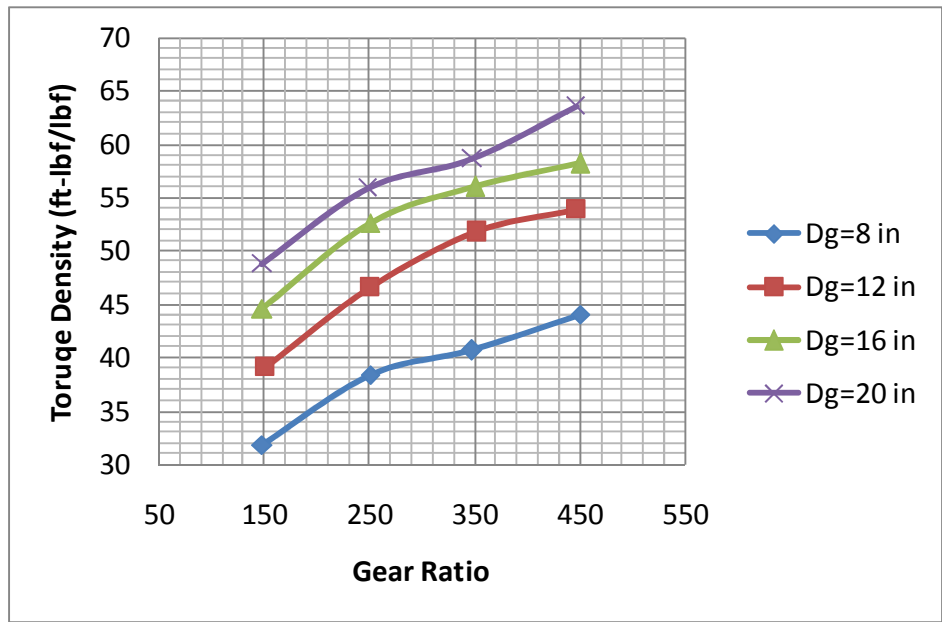


Figure 6.42: SRM+Star Compound+PEGT Torque Density as a Function of Gear Ratio and Diameter

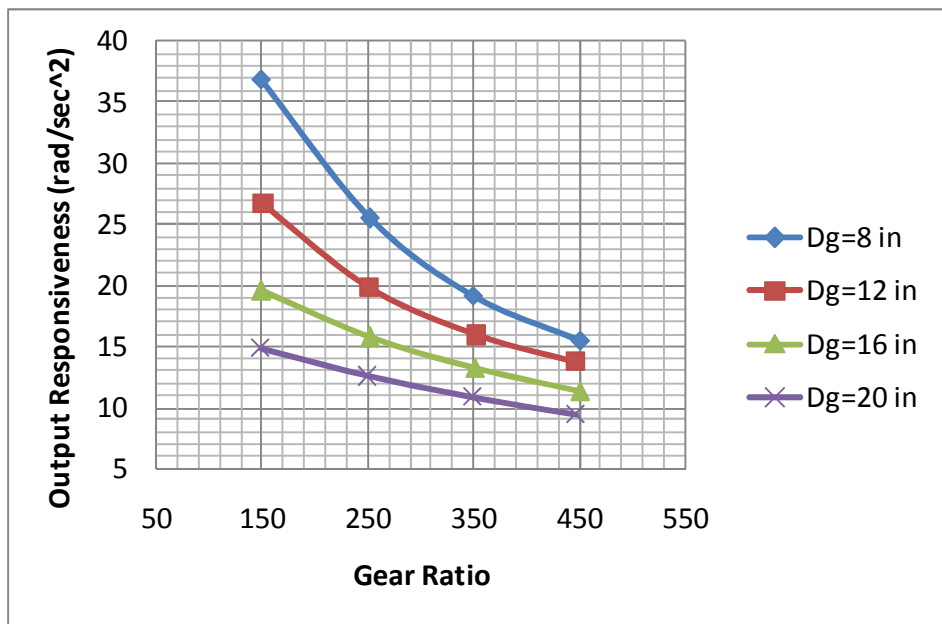


Figure 6.43: SRM+Star Compound+PEGT Output Responsiveness as a Function of Gear Ratio and Diameter

Table 6.36 lists the percentage change in each of the performance parameters as the difference between the value of the performance parameter for the highest gear ratio of 450 to 1 and the value of the parameter for the lowest gear ratio of 150 to 1. Thus, a positive number in the table indicates an increase in the parameter due to increasing the gear ratio. The key result from the table is that increasing the gear ratio from 150 to 450 provides the benefits of reduced weight and inertia and increased torque density and input responsiveness without any added complexity (same number of parts and bearings). One drawback of increasing the gear ratio is the reduction in the output responsiveness, which suggests that lower gear ratios might be more favorable for applications in which achieving high acceleration is important. When comparing the 1st stage star (Table 6.30 and Table 6.31) and star compound alternatives (Table 6.35 and Table 6.36) of the same diameter and aspect ratio, the star compound option provides superior benefits in terms of weight, inertia, torque density, and input responsiveness while the star option provides higher output responsiveness. Figure 6.44 presents the same information as Table 6.36 in a graphical representation, and only the average values of the percentage change of the performance parameters are plotted.

Table 6.36: Percentage Change of the SRM+Star Compound+PEGT Performance Parameters as the Gear Ratio is Varied from 150 to 450 for Different Diameters

Overall Diameter (inches)	Torque (ft-lbf)	Weight (lbf)	Inertia (lbm-in ²)	Torque Density (ft-lbf/lbf)	Input Responsiveness (rad/sec ²)	Output Responsiveness (rad/sec ²)
8	0%	-28%	-74%	39%	28%	-58%
12	0%	-28%	-78%	38%	52%	-49%
16	0%	-23%	-81%	30%	76%	-42%
20	0%	-23%	-83%	30%	87%	-36%
Average % Change	0%	-25%	-79%	34%	61%	-46%

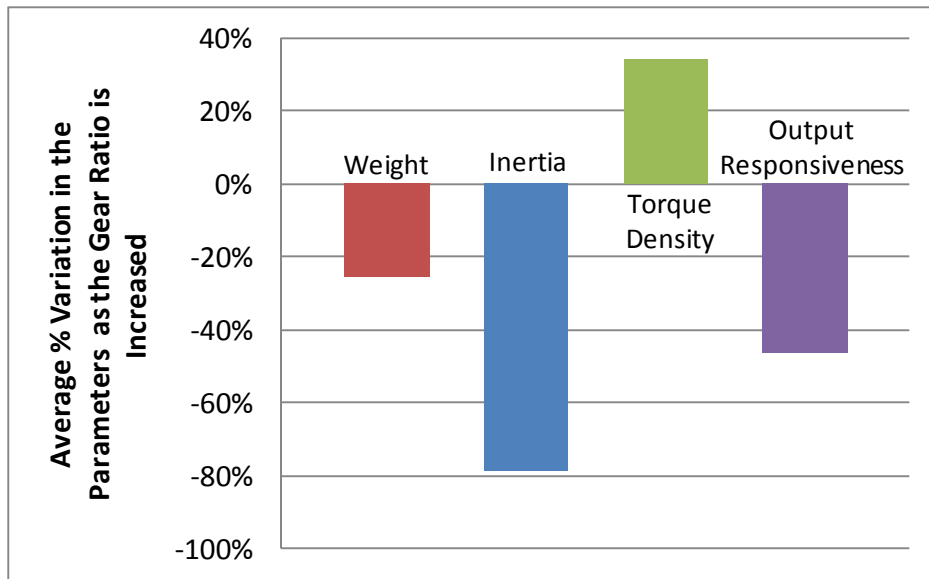


Figure 6.44: Percentage Change of the SRM+Star Compound+PEGT Performance Parameters as the Gear Ratio is Varied from 150 to 450 (Only average values of the percentage change are plotted for each performance parameter.)

Table 6.37 provides the distribution of weight and inertia in the motor and gear train as a function of diameter. The basic conclusion is that as the diameter increases, the dominant weight moves to the gear train and the dominant inertia moves to the motor. A similar conclusion was reached for the star 1st stage option in the previous section. Figure 6.45 and Figure 6.46 graphically display the information in Table 6.37 for the 12 inch diameter design.

Table 6.37: Distribution of Weight and Inertia (as a % of the total) in the Motor and Gear Train as a Function of Diameter and Gear Ratio (for the SRM+Star Compound+PEGT actuator)

Overall Diameter (inches)	Gear Ratio	Motor Weight (%)	Gear Train Weight (%)	Motor Inertia (%)	Gear Train Inertia (%)
8	149	44	56	75	25
	251	39	61	81	19
	348	35	65	86	14
	450	33	67	87	13
12	151	38	62	61	39
	251	33	67	69	31
	353	30	70	73	27
	447	27	73	77	23
16	149	35	65	50	50
	251	29	71	58	42
	351	25	75	64	36
	450	23	77	68	32
20	149	32	68	41	59
	250	26	74	50	50
	348	22	78	56	44
	447	20	80	58	42

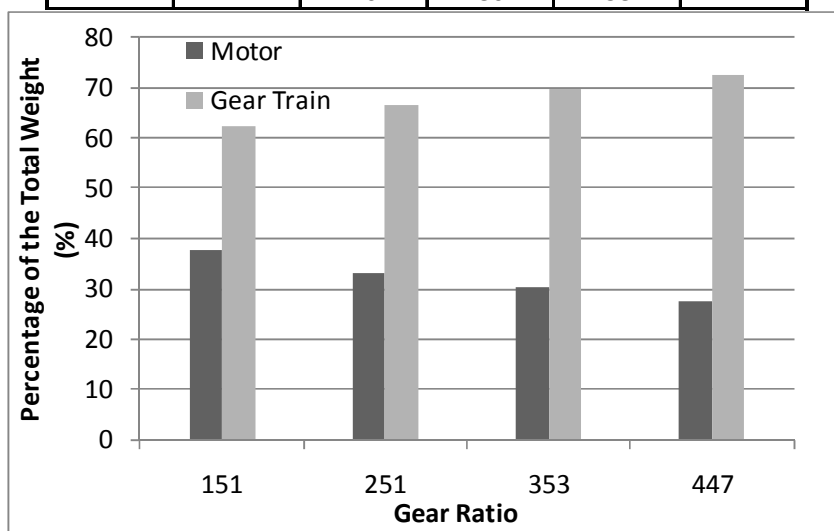


Figure 6.45: Percentage of Weight in the Motor and Gear Train as a Function of Gear Ratio for the Overall Diameter of 12 inches (for the SRM+Star Compound+PEGT actuator)

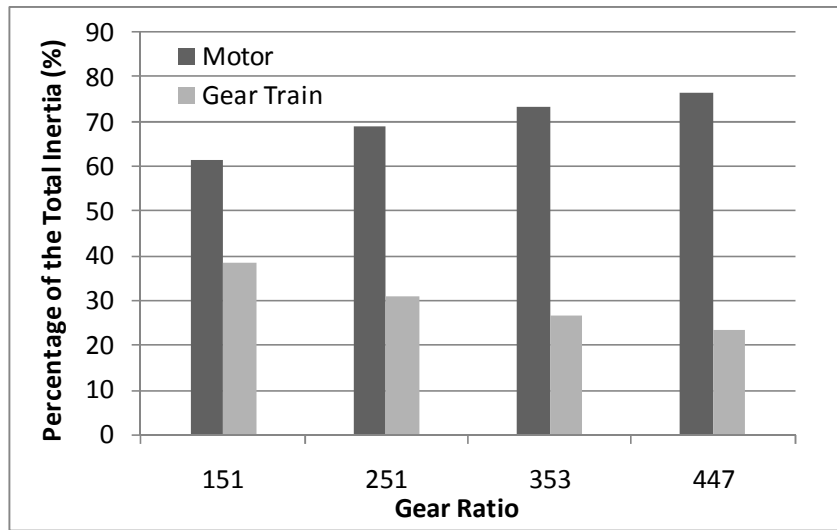


Figure 6.46: Percentage of Inertia in the Motor and Gear Train as a Function of Gear Ratio for the Overall Diameter of 12 inches (for the SRM+Star Compound+PEGT actuator)

Figure 6.47 illustrates how the motor diameter to gear train diameter ratio (K_d) and motor aspect ratio (A_m) vary as a function of gear ratio for the 8 inch diameter design, and is analogous to Figure 6.40. Table 6.38 provides the same information as Figure 6.47 in tabular form and also includes the 12, 16, and 20 inch diameter designs.

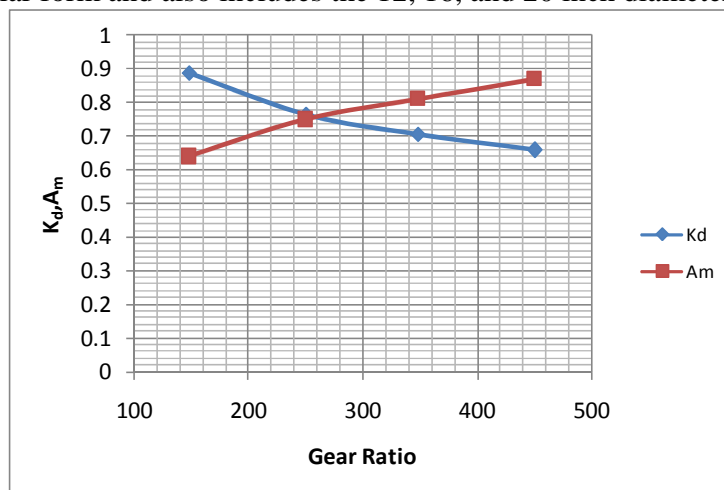


Figure 6.47: Variation of K_d and A_m as a Function of Gear Ratio (8 inch diameter SRM+Star Compound+PEGT actuator)

Table 6.38: Variation of Basic Design Parameters as a Function of Diameter and Gear Ratio (for the SRM+Star Compound+PEGT actuator)

D_g (inches)	g	K_d	K_l	A	A_g	A_m
8	149	0.89	0.60	1.00	0.40	0.64
8	251	0.77	0.60	1.00	0.40	0.75
8	348	0.71	0.60	1.00	0.40	0.81
8	450	0.66	0.60	1.00	0.40	0.87
12	151	0.74	0.60	1.00	0.40	0.77
12	251	0.64	0.60	1.00	0.40	0.90
12	353	0.58	0.60	1.00	0.40	0.99
12	447	0.54	0.60	1.00	0.40	1.06
16	149	0.67	0.60	1.00	0.40	0.86
16	251	0.56	0.60	1.00	0.40	1.02
16	351	0.51	0.60	1.00	0.40	1.13
16	450	0.47	0.60	1.00	0.40	1.21
20	149	0.61	0.60	1.00	0.40	0.94
20	250	0.51	0.60	1.00	0.40	1.12
20	348	0.46	0.60	1.00	0.40	1.24
20	447	0.43	0.60	1.00	0.40	1.34

6.7 DISCUSSION OF RESULTS

The following section will highlight and summarize some of the specific results already discussed in the context of Examples 1 and 2. The designer should keep these points in mind when developing actuator designs for a specific application.

6.7.1 Diameter, Gear Ratio, and Aspect Ratio Parameters

While the aspect ratio parameter (A) is useful for classifying a motor or gear train design as cylindrical (high A), square ($A \sim 1$), or pancake (low A), all of the performance parameters considered in this chapter (torque, weight, inertia, torque density, and responsiveness) are a stronger function of diameter (typically squared or higher) and gear ratio than aspect ratio. A similar conclusion was reached from the results in Chapter 5. Because of this result, only the variation in the diameter and gear ratio parameters (with constant overall aspect ratios) was considered in the examples of this chapter.

6.7.2 Balancing Motor and Gear Tooth Limited Torque Capacities

For small HGT and PEGT gear train diameters (less than 10 inches for the examples presented here), it is sometimes difficult to find motors with suitable torque capacity that have a diameter and length that are compatible with the gear train. For these smaller designs, the motor may provide the dominant weight and inertia in the actuator. This incompatibility occurs because while both the PEGT and HGT have higher absolute torque density than the SRM for the same diameter, the SRM torque and torque density increase at a faster rate than for the gear train. This important result was discussed in Chapter 5 (Section 5.6.6) in the context of stand-alone SRM, HGT, and PEGT designs. To fix this imbalance between the motor and the gear train, it is suggested to use the maximum gear ratios possible for the HGT and PEGT (while still preventing interference) for these smaller designs, which will reduce the torque and size requirements of the motor.

6.7.3 Distribution of Weight and Inertia

As the diameter is increased for a fixed gear ratio (Example 1) and as the gear ratio is increased for a fixed diameter (Example 2), the weight and inertial content generally moves from the motor to the gear train. Considering the weight parameter, this result physically means that motor is becoming smaller relative to the gear train for these two design scenarios (see the decrease in K_d and K_l in Figure 6.10, Figure 6.17, Figure 6.24, Figure 6.33, Figure 6.40, and Figure 6.47). The exception to this result occurs for the SRM coupled with the star or star compound 1st stage gear trains, in which the dominant inertia shifts from the gear train to the motor as the gear ratio increases for a fixed diameter (see Sections 6.6.2.2 and 6.6.3).

When using the suggested gear ratio ranges for the HGT and PEGT, the gear train will usually dominate the weight in the actuator, except for the designs of smaller

diameter where the motor and gear train weights may be comparable. The dominant inertial component in the actuator can be generally be shifted between the motor and gear train by suitable choice of the gear ratio and diameter, and the results of this chapter should be consulted for specific guidance.

6.7.4 Torque Density

As the diameter is increased for a fixed gear ratio (Example 1), the slightly decreasing trends in torque density mirror the results from Chapter 5 for the individual HGT and PEGT designs. The reader should recall that the choice of diametral pitch (essentially the tooth width and indirectly, the tooth height) and the anticipated contact ratio for a given gear mesh greatly affect its torque capacity. Ongoing research at the RRG combining gear tooth shape, tolerances, and deformations should allow for a constant and possibly increasing torque density as a function of diameter.

As the gear ratio is increased for a fixed diameter (Example 2), the torque density generally increases and the weight decreases due to the reduced motor torque demands and the ability to use a smaller motor. However, the relative benefits in weight reduction and increased torque density diminish as the gear ratio is increased to near its maximum limit.

6.7.5 Responsiveness

As the diameter is increased for a fixed gear ratio (Example 1) and as the gear ratio is increased for a fixed diameter (Example 2), the output responsiveness (i.e., the ability to accelerate the load) always decreases. However, the effect on the input responsiveness (i.e., the motor's acceleration capability) depends on the location of the dominant weight and inertia in the actuator, and the reader is instructed to consult the specific results in this chapter.

6.7.6 Power-Law Scaling Rules

The simple power law scaling rules (provided in Example 1) obtained for the torque, weight, and inertia of each of the three actuator combinations considered generally agree with their known dependencies on diameter (presented in Chapter 3). However, unlike the rules of Chapter 5, the rules in this example accounted for the combined effect of the motor and the gear train, with the motor and gear train aspect ratios varying as the gear train diameter is increased to achieve a balanced design. Thus, the designer is instructed to use the rules as they are presented for quick estimation of the performance parameters as a function of diameter and to use caution when comparing these rules with the original governing equations presented in Chapter 3.

6.7.7 Design Parameter Ranges

The reader should recall that the design parameter ranges of Chapter 5 were chosen to result in accurate design maps and useful rules, with less of an emphasis on the specific numerical results. However, the design parameter ranges for this chapter were chosen to illustrate how to balance the parameters between the motor and the gear train and make specific numerical comparisons between alternative designs. Practically, this meant larger ranges for the motor and gear train diameters and gear ratios in this chapter. Larger ranges of data are generally more difficult to fit with the standard regression (curve-fitting) techniques utilized in Chapter 5, so there was less emphasis on these techniques in this chapter. Though not presented in Example 2, 3-D design maps of the parameter data can be easily generated (using the raw data provided) to view the results in a different representation.

6.8 SUMMARY

The concepts in this chapter apply to the balance between the motor and gear train for a single actuator design, and each actuator in a set can be balanced by choosing appropriate values for the key actuator design parameters defined in this chapter. All of the results of this chapter were obtained by exercising the design procedure of Chapter 4 for a finite set of design and performance parameter inputs from the user. Now that these results have been developed, they represent a database of rules and numerical results that can be used by future designers when developing actuators.

Chapter 7 Comparisons Between Direct Drive and Geared Actuators

This chapter will use the actuator design procedure presented in Chapter 4 to answer the question: “Why use a gear train?” by making multiple comparisons between direct drive and geared actuators. In this chapter, the “direct drive” designation refers to a system that includes a motor directly connected to an inertial load and does not include a gear train. The “geared” designation refers to a system in which a motor-gear train combination (i.e., an integrated actuator) is connected to an inertial load. The direct drive systems considered in this chapter are based on the SRM, and the geared systems are the SRM+HGT, SRM+Star+PEGT, and SRM+Star Compound+PEGT actuators.

Before presenting numerical results for these systems, typical values of the torque density (torque to weight ratio) and responsiveness (torque to inertia ratio) for off-the-shelf motors will be provided to give the designer insight into these performance criteria. The results of a brief comparison between a direct drive and geared system (involving off-the-shelf motors and gear trains) will also be presented. Then, the geared and direct drive systems specific to this report will be compared based on their relative torque density and responsiveness values, using the motor and gear train parametric models presented in Chapter 3.

The results will illustrate the trade-offs between designing for high torque density and high responsiveness encountered when comparing direct drive and geared systems. To parallel the analytical argument for using a gear train, other practical considerations involved when using a gear train including backlash/lost motion, increased complexity, and increased number of parts/bearings will be briefly discussed. The relevant background for this chapter was discussed in detail in Section 2.4.1 (“Designing for Inertial Loads) in the literature review presented in Chapter 2.

One of the motivations for studying the responsiveness of an actuator comes from the following quote taken from a manufacturer's catalog [Kollmorgen, 2008]. "A direct drive motor provides the highest practical torque-to-inertia ratio where it counts—at the load. In a geared system, reflected output torque is proportional to the gear reduction while reflected output inertia is proportional to the square of the gear reduction. Thus, the torque-to-inertia ratio in a geared system is less than that of a direct drive system by a factor equal to the gear-train ratio. The higher torque-to-inertia ratio of direct drive motors makes them ideally suited for high acceleration applications with rapid starts and stops." It is the aim of this chapter to explore the validity of this statement for the specific motor and gear train types being considered in this research.

Another motivation for this chapter stems from the need to design actuators for vehicle suspension applications. These applications typically require high torque density (to save weight) and also high responsiveness/acceleration (to quickly respond to variable terrain and ensure that the vehicle wheel maintains contact with the road).

7.1 RESPONSIVENESS RELATIONSHIPS

Chapters 5 and 6 have reported results for actuator torque, weight, inertia, torque density, and responsiveness and have used the numerical results to make important comparisons. This chapter will focus on only the torque density (T_w) and responsiveness (R) performance parameters because they include the effect of the individual torque, weight, and inertia information. The responsiveness relationships for geared and direct drive systems will be detailed in this section.

Continuing the discussion on designing for dominant inertial loads from Chapter 2 (Section 2.4.1), Table 7.1 summarizes the important torque, weight, inertia, and other parameters needed to compare the responsiveness of direct drive and geared systems in

this chapter. All of these parameters have been defined and used in previous chapters but are provided here for easy reference. Unless otherwise noted, all of the actuator inertia values reported in this chapter have been reflected to the motor/input shaft of the systems being considered.

Table 7.1: Motor, Gear Train, and Load Parameters

Component	Parameter	Symbol	Description
Motor	Torque	T_m	torque capacity of the motor
	Inertia	I_m	inertia reflected to the motor (input) shaft
Gear Train	Torque	T_g	torque capacity of the gear train
	Inertia	I_g	inertia reflected to the input gear or shaft of the gear train
	Gear Ratio	g	gear ratio between motor/input shaft and output shaft/gear of the gear train
Load	Torque	T_l	load torque given by the application requirements
	Inertia	I_l	load inertia attached to the output shaft
	Load to Reference (Motor) Inertia Ratio	K	factor used to specify the load inertia as a multiple of a specified reference inertia
	Reference Inertia	I_{ref}	reference inertia (typically that of the direct drive SRM) used to define the load inertia
Geared System (Motor+Gear Train)	Input Responsiveness	R_{gi}	acceleration of the motor shaft in a motor-gear train system
	Output Responsiveness	R_{go}	acceleration of the output shaft/load in a motor-gear train system
Direct Drive System (Motor Only)	Responsiveness	R_d	acceleration of the motor shaft and load in a motor only system

7.1.1 Geared System Responsiveness

The fundamental governing equation of an integrated motor and gear train system can be written as follows.

$$T_m - T_f - T_{loss} - \frac{T_l}{g} = \left(I_m + I_g + \frac{I_l}{g^2} \right) R_{gi} \quad \text{Eqn. 174}$$

For the purposes of this discussion, the friction torque (T_f) and motor iron and copper losses (T_{loss}) can be neglected. Then, this equation can be solved for the motor torque as follows.

$$T_m = \left(I_m + I_g + \frac{I_l}{g^2} \right) R_{gi} + \frac{T_l}{g} \quad \text{Eqn. 175}$$

This form of the equation is useful because it expresses the motor torque required to overcome inertial/acceleration loads (given by the first term) and external loads (given by the second term), with the dominant load term depending on the particular application. Solving for the input responsiveness (R_{gi}), the previous equation becomes the following.

$$R_{gi} = \frac{T_m - \frac{T_l}{g}}{\left(I_m + I_g + \frac{I_l}{g^2} \right)} \quad \text{Eqn. 176}$$

If the designer can assume that the load torque term is insignificant in comparison to the inertial term (an assumption that should always be justified), the responsiveness reduces to the following.

$$R_{gi} = \frac{T_m}{\left(I_m + I_g + \frac{I_l}{g^2} \right)} \quad \text{Eqn. 177}$$

This equation defines the input responsiveness (i.e., the acceleration of the motor shaft) as a function of the motor, gear train, and load parameters defined in Table 7.1. For a geared system, a distinction needs to be made between the input (R_{gi}) and output

(R_{go}) responsiveness. The latter can be obtained by dividing the output/gear train torque (T_g) by the inertia reflected to the output.

$$R_{go} = \frac{T_g}{I_m g^2 + I_g g^2 + I_l} \quad \text{Eqn. 178}$$

Comparing the input and output responsiveness, the following relationship always holds for the motor/gear train combinations being considered in this research.

$$R_{go} = \frac{R_{gi}}{g} \quad \text{Eqn. 179}$$

For a design in which the motor torque and gear train are compatible (i.e., balanced), the following relationship holds.

$$T_g = g T_m \quad \text{Eqn. 180}$$

For the purpose of calculating responsiveness of an actuator without specific information about the load inertia and geometry (i.e., without a specific application in mind), it is necessary to define a load inertia (I_l) that is a multiple of a reasonable reference inertia (I_{ref}).

$$I_l = K I_{ref} \quad \text{Eqn. 181}$$

In the examples presented in this chapter, the reference inertia will be defined as the inertia of the direct drive system (i.e., only the motor inertia) of interest. Given this designation, K can be referred to as the load (inertia) to motor inertia ratio. This load inertia multiplier K can be physically interpreted as an inertial disturbance being added to the system.

In Chapters 5 and 6, the value of K was held constant to focus on the performance parameters of torque, weight, inertia, and torque density. However, K will be an important variable in this chapter to illustrate how the responsiveness of a system changes as the load inertia is varied. The specific ranges of K used (typically from 1 to

2,000) will depend on the systems in question and are documented in the examples presented later in the chapter.

7.1.2 Direct Drive System Responsiveness

Removing the gear train inertia term from the relationships above, the responsiveness of a direct drive system (R_d) can be defined as follows.

$$R_d = \frac{T_m}{I_m + I_l} \quad \text{Eqn. 182}$$

No distinction is necessary between the input and output responsiveness of a direct drive system because the motor and load run at the same speed.

7.2 OFF-THE-SHELF COMPONENT CHARACTERISTICS AND COMPARISONS

Before discussing the examples illustrating comparisons based on the SRM, HGT, and PEGT, it is important for the designer to understand how the torque density and responsiveness vary for off-the-shelf motors and motor-gear train combinations. For this reason, this section will present torque density and responsiveness information for some commercially available motors, representative of motors that could be used in a direct drive system. Then, a brief comparison between the responsiveness of a direct drive and geared system (again based on off-the-shelf motors and gear trains) will be made to provide a model for the types of comparisons to be made later in the chapter. All of the parameter information is taken directly from the referenced manufacturers' websites and catalogs.

7.2.1 Off-The-Shelf Motor Characteristics

Emoteq [2008] offers different lines of brushless DC (BLDC) motors with "High Torque", "High Speed", and/or "MegaFlux" designations, and their design and performance parameter data will be used in this section. Figure 7.1 and Figure 7.2

illustrate how the responsiveness (R_d) and torque density (T_w) of their “High Torque” motors vary as a function of the overall diameter (D_m). The caption titles include the simple power-law scaling rules based on curve fits of the data. Figure 7.3 and Figure 7.4 provide the same information for their “MegaFlux” motors. In all four plots, there are multiple data points for a given diameter, and these represent motors of different stack lengths with the same diameter. The plots illustrate that torque density and responsiveness are a strong function of diameter and are practically independent of the stack length.

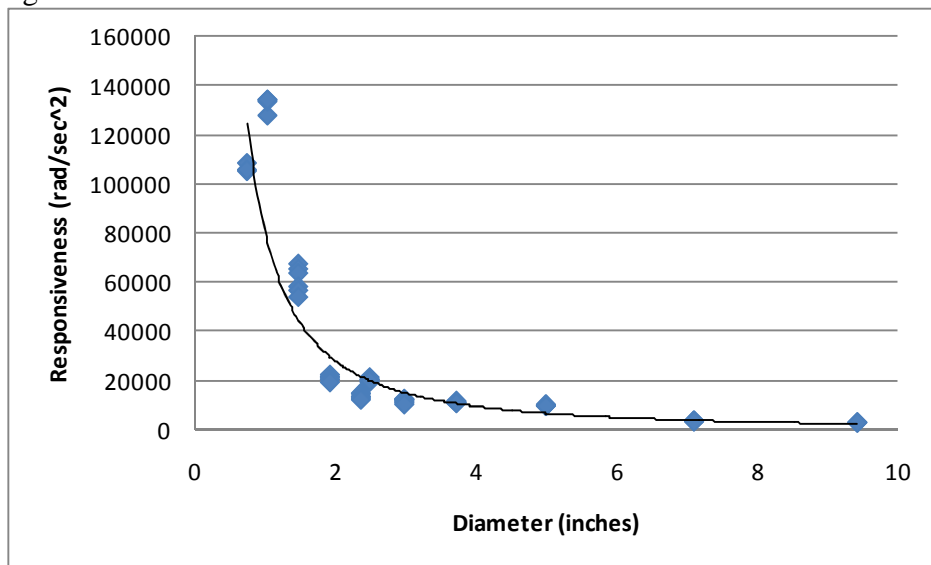


Figure 7.1: Responsiveness as a Function of Diameter for Emoteq Brushless DC Motors- High Torque Series ($R_d = 8170D_m^{-1.53}$)

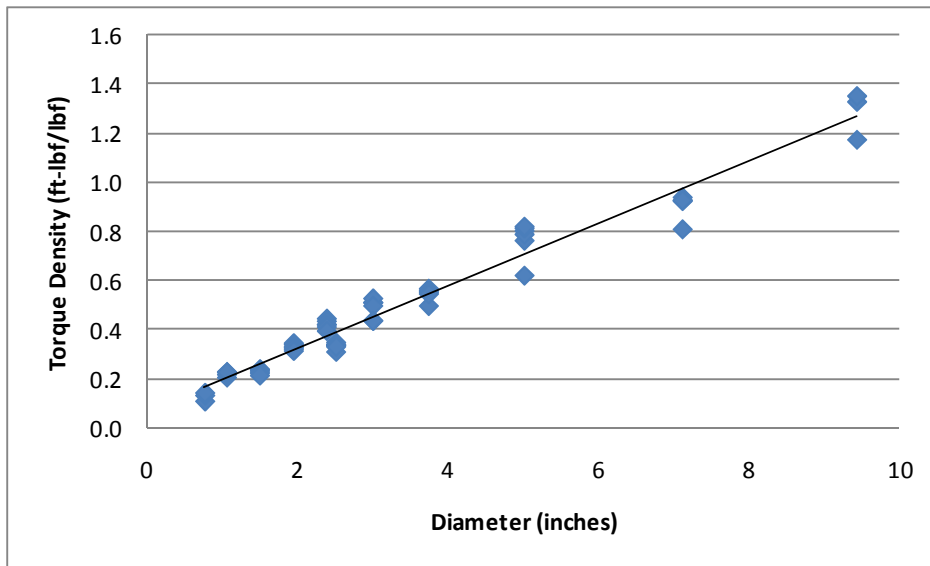


Figure 7.2: Torque Density as a Function of Diameter for Emoteq Brushless DC Motors-
High Torque Series ($T_w = 0.127D_m$)

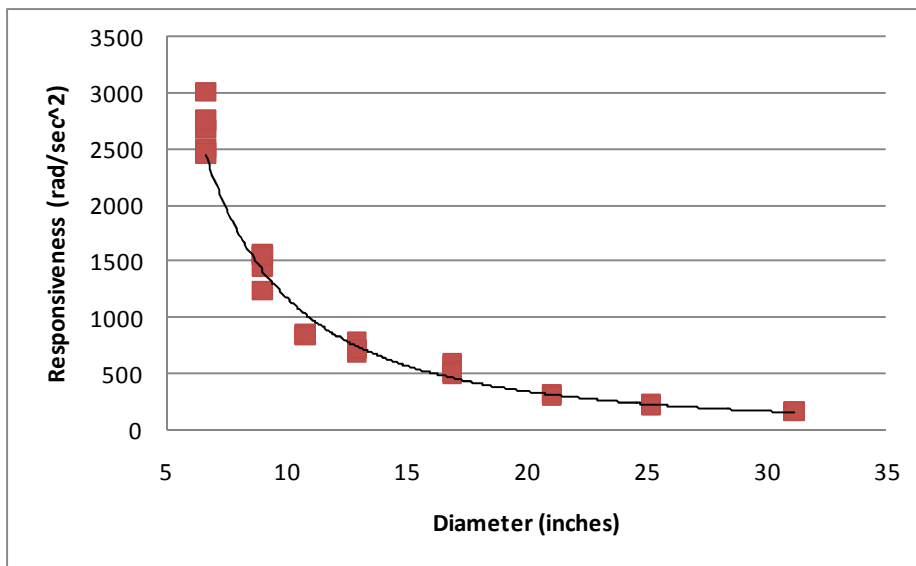


Figure 7.3: Responsiveness as a Function of Diameter for Emoteq Brushless DC Motors-
Megaflux Thin Ring Series ($R_d = 7456D_m^{-1.79}$)

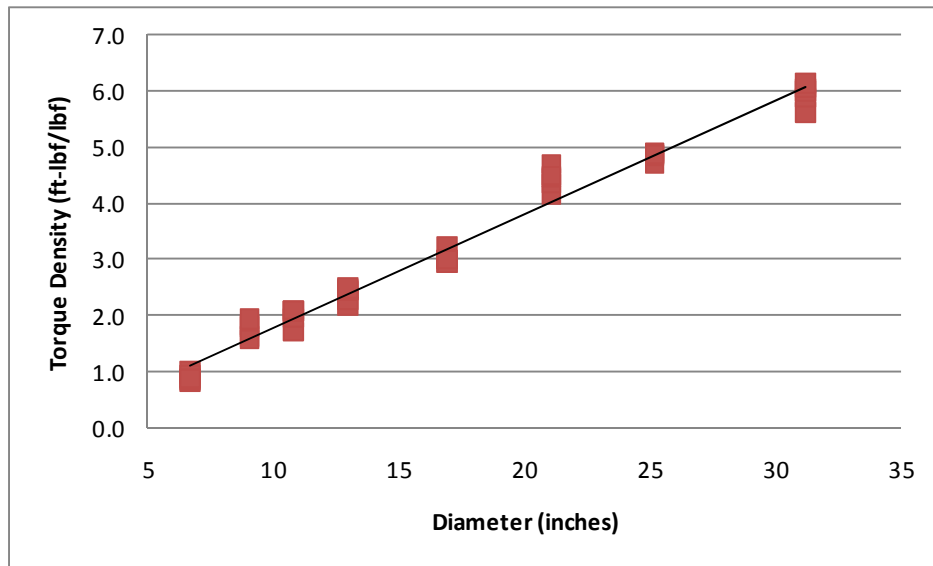


Figure 7.4: Torque Density as a Function of Diameter for Emoteq Brushless DC Motors-Megaflux Thin Ring Series ($T_w = 0.203D_m$)

For comparison purposes, Figure 7.5 plots the torque density of an off-the-shelf SRM from Rocky Mountain Technologies [2008]. A preliminary comparison of Figure 7.2 (BLDC) and Figure 7.5 (SRM) suggests that the BLDC is approximately 4 to 6 times more torque dense than an SRM for these particular diameters. Note that this result is based on comparisons from different motor manufacturers, who each utilize their own models and test procedures. Off-the-shelf BLDC motors will be utilized for the comparisons in Section 7.2.2, and SRM designs based upon the analytical SRM model in Chapter 3 will be utilized for the comparisons in Section 7.3. The superior torque density of the BLDC (as indicated by this preliminary comparison) should be kept in mind throughout the examples presented in this chapter.

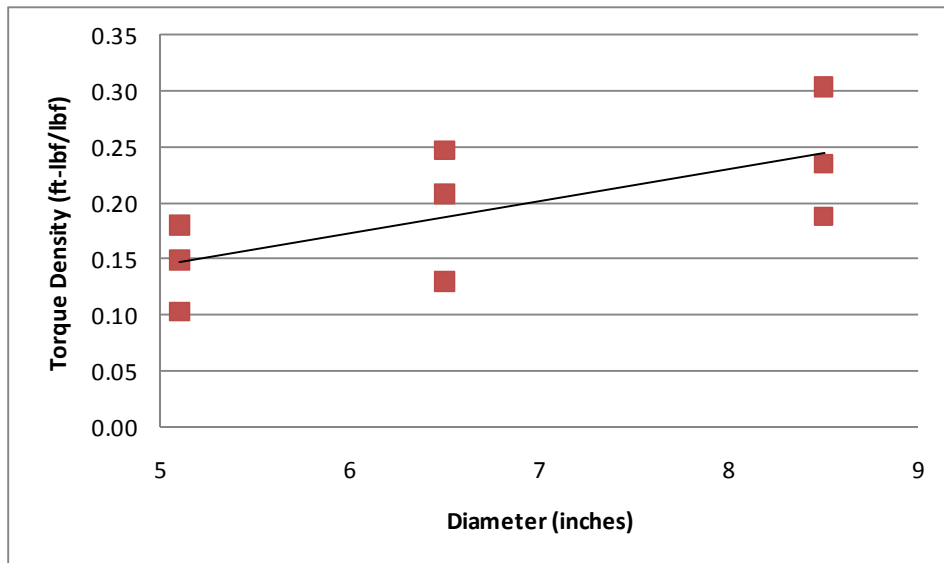


Figure 7.5: Torque Density as a Function of Diameter for Rocky Mountain Technologies SRM ($T_w = 0.028D_m$)

The reader should note that these torque density and responsiveness plots for off-the-shelf motors exhibit similar trends to the corresponding plots for the SRM model used in this research (see the stand alone SRM 2-D design maps in Section 5.2.1 and the tabular results in Examples 1 and 2 of this chapter).

7.2.2 Comparisons of Direct Drive and Geared Systems Using Off-the-Shelf Components

This section will use brushless DC motors from Kollmorgen [2008] and Emoteq [2008] and gear trains from Nabtesco [2008] to make two distinct comparisons between direct drive systems (based on the Kollmorgen motors) and geared systems (based on Emoteq motors coupled with Nabtesco gear trains).

The first comparison (illustrated by Figure 7.6) will involve systems of the same size (diameter, length, aspect ratio, etc.). This comparison is important when there is a fixed volume (diameter and length) in which a system can fit, and the designer is seeking

to maximize the performance of the system that fits into the space. Since both the direct drive and geared systems are the same size and the geared system generally has a much higher torque density than the direct drive system (a result to be proven in this chapter), the geared system will have higher torque capacity.

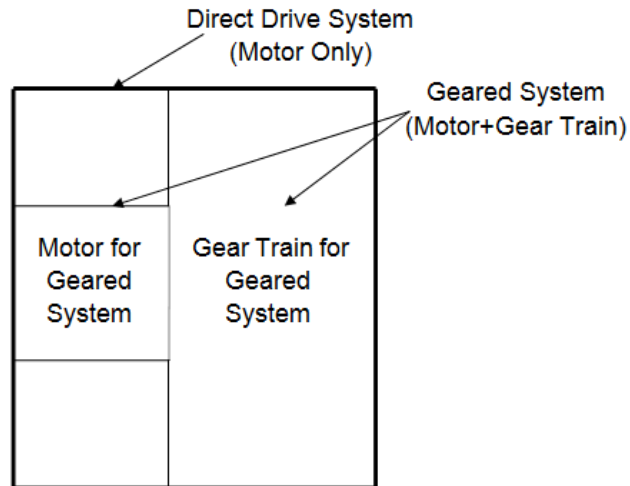


Figure 7.6: Illustration of Geared and Direct Drive Systems of the Same Size (The geared system will always have a larger torque capacity.)

The second comparison (illustrated by Figure 7.7) will involve systems of the same torque capacity. This comparison is important when there is a specific torque requirement that must be met, and the designer is seeking to determine the size of the system that meets the requirement. Since both the direct drive and geared systems have the same torque capacity and the geared system has a much higher torque density, the geared system will be much smaller than the direct drive system.

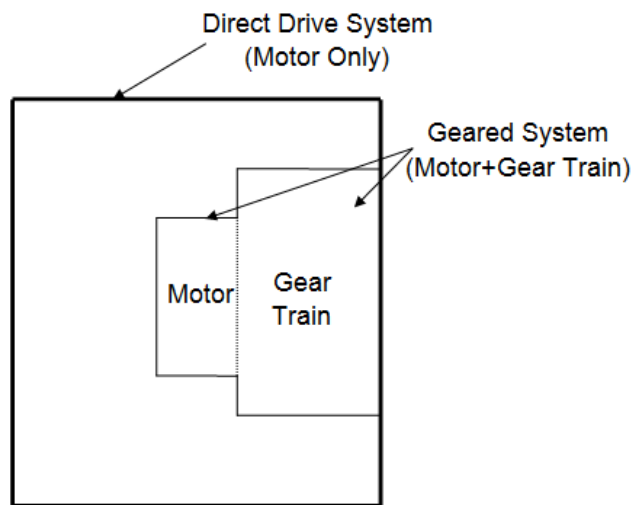


Figure 7.7: Illustration of Geared and Direct Drive Systems of the Same Torque Capacity (The geared system will always be smaller than the direct drive system.)

7.2.2.1 Comparing Systems of the Same Size

Table 7.2 summarizes the values of the design and performance parameters of the direct drive system (Kollmorgen QT-9704 motor) used for this comparison. The inertia values listed in the table do not include any load inertia and will be used as the reference inertia (designated by I_{ref} in Table 7.1 above) for all of the responsiveness computations in this example.

Table 7.2: Direct Drive System (Kollmorgen QT-9704 Motor) Design and Performance Parameter Data Used for Comparison with Geared Systems ($K=0$)

Overall Diameter (inches)	Length (inches)	Aspect Ratio	Torque (ft-lbf)	Weight (lbf)	Inertia (lbm-in ²)	Torque Density (ft-lbf/lbf)	Responsiveness (rad/sec ²)
11	2	0.14	13	11	116	1.15	507

Table 7.3 summarizes the values of the design and performance parameters of the geared system (Emoteq 7000 series motors of different lengths coupled with the Nabtesco RV-320E gear train) used for this comparison. The inertia values listed in the table have

been reflected to the input motor shaft and do not include any load inertia. Note that different values of the gear ratio were considered, and motors of a fixed diameter and various lengths were selected to balance the motor and gear train torque capacities for each gear ratio. Both the geared and direct drive systems have a similar overall diameter of 11 inches, which justifies this “same size” comparison. Figure 7.8 compares the torque density values in Table 7.2 and Table 7.3 and illustrates that the torque density of the geared system is approximately 13 to 14 times that of the torque density of the direct drive system. This benefit ratio can be obtained from the plot as the torque density for the geared system divided by the torque density for the direct drive system.

Table 7.3: Geared System (Emoteq 7000 Series Motor + Nabtesco RV-320E Gear Train)
Design and Performance Parameter Data (K=0)

Overall Diameter (inches)	Length (inches)	Aspect Ratio	Gear Ratio	Torque (ft-lbf)	Weight (lbf)	Inertia (lbm-in ²)	Torque Density (ft-lbf/lbf)	Output Responsiveness (rad/sec ²)
11.2	9.6	0.86	81	1881	128	27	14.7	49
11.2	8.9	0.80	101	1881	123	22	15.2	40
11.2	8.5	0.76	118.5	1881	121	18	15.6	34
11.2	8.2	0.74	129	1881	119	17	15.8	31
11.2	8.0	0.72	141	1881	118	15	16.0	29
11.2	7.7	0.69	171	1881	115	13	16.3	24
11.2	7.5	0.67	185	1881	115	12	16.4	22

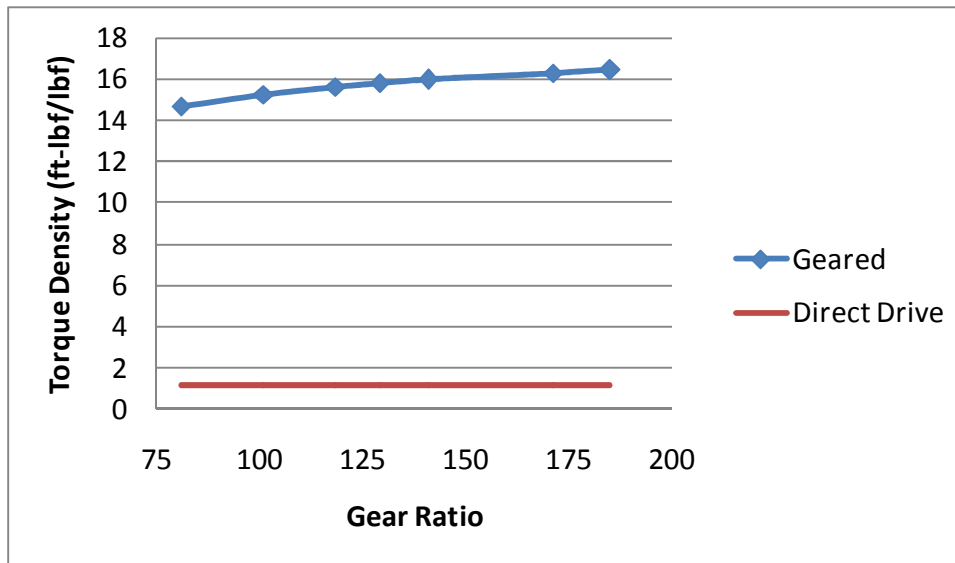


Figure 7.8: Comparison of Torque Density Between the Geared and Direct Drive Systems

Figure 7.9 compares the output responsiveness of the direct drive and geared systems as a function of the load to motor inertia ratio K for different values of the gear ratio. One important result here is that the lowest value of the gear ratio results in the highest output responsiveness. Another key result is that either the direct drive or the geared system can have higher responsiveness, depending upon the specific gear ratio and values of K (i.e., load inertia) considered. The value of K for which the geared system becomes superior to the direct drive system depends upon the gear ratio. Yet another result is that the output responsiveness of the geared system is nearly constant (i.e., insensitive to the load) for the values of K considered.

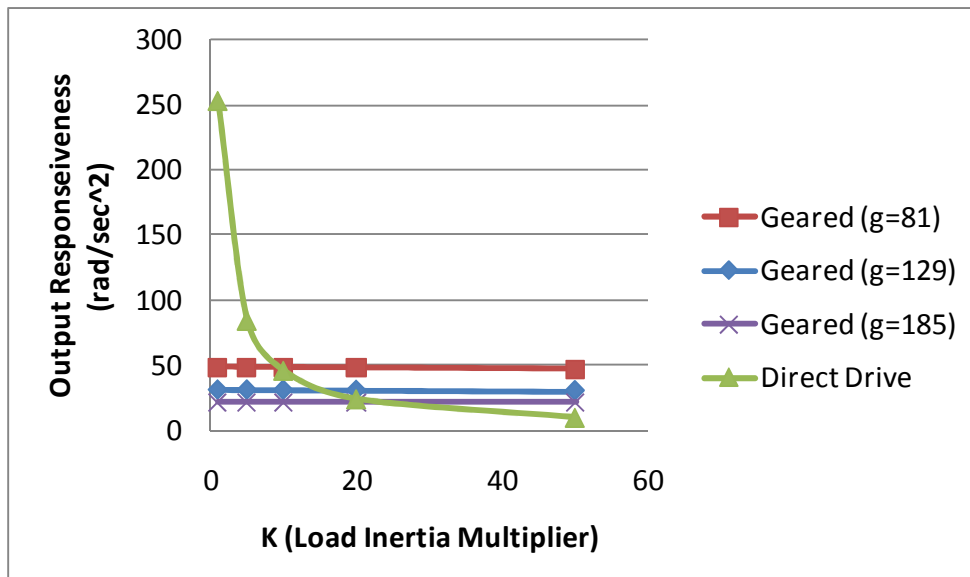


Figure 7.9: Geared and Direct Drive Output Responsiveness as a Function of K and Gear Ratio

7.2.2.2 Comparing Systems of the Same Torque Capacity

Table 7.4 summarizes the values of the design and performance parameters of the direct drive system (Kollmorgen T-10020 motor) used for this comparison. The inertia values listed in the table do not include any load inertia and will be used as the reference inertia for all of the responsiveness computations in this example.

Table 7.4: Direct Drive System (Kollmorgen T-10020 Motor) Design and Performance Parameter Data Used for Comparison with Geared Systems (K=0)

Overall Diameter (inches)	Length (inches)	Aspect Ratio	Torque (ft-lbf)	Weight (lbf)	Inertia (lbm-in ²)	Torque Density (ft-lbf/lbf)	Responsiveness (rad/sec ²)
14	6	0.45	40	110	818	0.37	228

Table 7.5 summarizes the values of the design and performance parameters of the geared system (Emoteq 3000 series motors of different lengths coupled with the Nabtesco RV-6E gear train) used for this comparison. Note that both systems have a torque

capacity of 40 ft-lbf, which justifies this “same torque capacity” comparison. Figure 7.12 compares the torque density values in Table 7.4 and Table 7.5 and illustrates that the torque density of the geared system varies from approximately 13 to 17 times the torque density of the direct drive system.

Table 7.5: Geared System (Emoteq 3000 Series Motor + Nabtesco RV-6E Gear Train)
Design and Performance Parameter Data (K=0)

Overall Diameter (inches)	Length (inches)	Aspect Ratio	Gear Ratio	Torque (ft-lbf)	Weight (lbf)	Inertia (lbf-in ²)	Torque Density (ft-lbf/lbf)	Output Responsiveness (rad/sec ²)
4.8	4.5	0.94	31	40	8.2	0.54	4.9	356
4.8	4.0	0.82	43	40	7.4	0.38	5.4	263
4.8	3.7	0.76	53	40	7.0	0.30	5.7	219
4.8	3.6	0.74	59	40	6.9	0.27	5.8	196
4.8	3.3	0.68	79	40	6.5	0.19	6.2	154
4.8	3.1	0.64	103	40	6.2	0.14	6.4	125

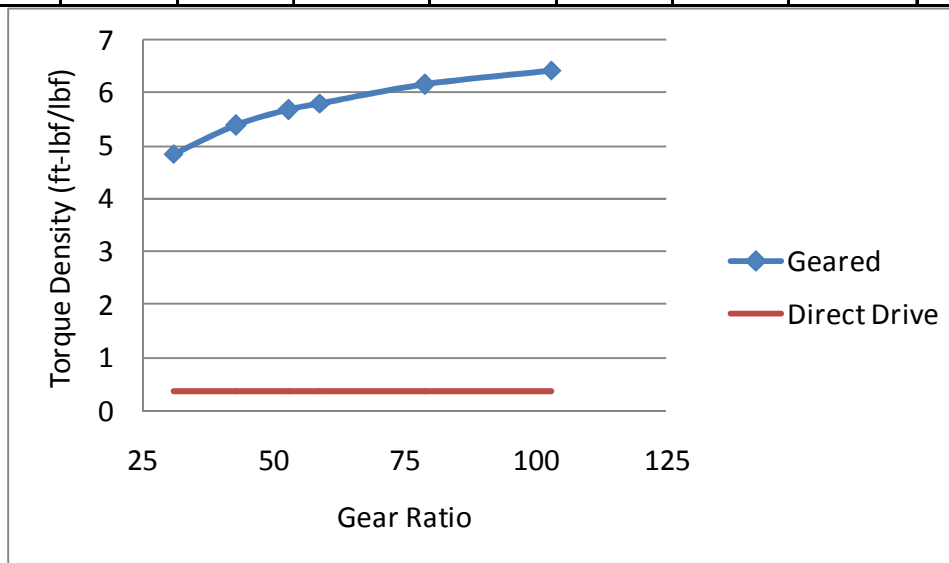


Figure 7.10: Comparison of Torque Density Between the Geared and Direct Drive Systems

Figure 7.11 compares the output responsiveness of the direct drive and geared systems as a function of the load to motor inertia ratio K for different values of the gear ratio. The results here based on the same torque comparison are similar to the results for the same size comparison in the previous section. The lowest value of the gear ratio result in the highest output responsiveness, and the direct drive or the geared system can have higher responsiveness, depending upon the specific gear ratio and values of K considered. However, relative magnitudes of the output responsiveness values in Figure 7.9 (from the same size comparison) and Figure 7.11 (from the same torque comparison) are somewhat different. For the same torque comparison here, in the limit as K becomes large, the load inertia dominates any motor or gear train reflected inertia, and both the geared and direct drive systems have practically the same inertia. Then, since both systems have the same torque accelerating the same inertia (see the responsiveness relationships in Section 7.1), the responsiveness of both systems become identical, and the lines in the figure approach each other.

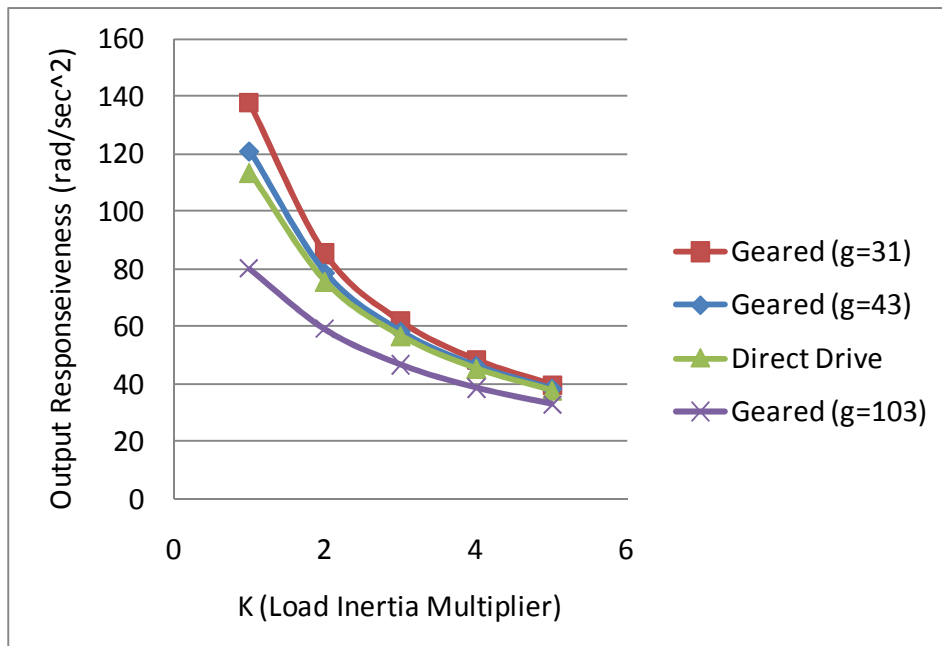


Figure 7.11: Geared and Direct Drive Output Responsiveness as a Function of K and Gear Ratio

7.2.3 Off-the-Shelf Comparison Summary

The results in this section are typical of what an engineer who commonly specifies motors and gear trains might obtain when selecting off-the-shelf motors and gear trains for an application. The reader should note that these torque density and responsiveness plots for off-the-shelf motor-gear train combinations exhibit similar trends to the corresponding plots for the integrated actuators in Examples 1 and 2 presented in the following sections of this chapter. The differences between the values of K for these off-the-shelf comparisons and the values of K used in Examples 1 and 2 below can be attributed to the relatively smaller sample of systems used for the off-the-shelf systems. Also, the results in Examples 1 and 2 are completely based on the motor and gear train parametric models in Chapter 3, while the off-the-shelf comparison results are based on the models and testing procedures of the noted manufacturers.

7.3 COMPARISONS BASED ON THE SRM, HGT, AND PEGT

With the comparison in Section 7.2.2 based on off-the-shelf components as a baseline, this section will compare a direct drive system (based on a stand-alone SRM design) with the following integrated actuator options (SRM+HGT, SRM+Star+PEGT, and SRM+Star Compound+PEGT). The performance parameters of torque, weight, inertia, torque density, and responsiveness will be computed using the parametric models documented in Chapter 3 and embedded in the computational tool developed for this research (described in Chapter 4 and Appendix A1). Unless otherwise specified, the following set of assumptions were used for the SRM (Table 7.6) and HGT/ PEGT designs (Table 7.7) in this chapter. Like the off-the-shelf comparison presented in the previous section, geared and direct drive systems of the same size (Example 1 below) and the same torque capacity (Example 2 below) will be compared. For each example, the raw design and performance parameter data has been provided so that results for a specific actuator size can be computed and for future reproduction of the graphics.

Table 7.6: SRM Design Constant Parameters and Assumptions

Parameter	Value
Number of stator poles	$N_s=6$
Number of rotor poles	$N_r=4$
Stator pole angle	$\theta_s = 30^\circ$
Rotor pole angle	$\theta_r = 32^\circ$
Saturation flux density	$B_{sat}=1.56$
Axial clearance	$c = 0.005D_m$
Density	$\rho = 0.284 \text{ lbm/in}^3$

Table 7.7: HGT and PEGT Constant Parameters and Assumptions

Parameter	Value
Pressure angle	$\phi=25^\circ$
Minimum tooth number difference	$N_{\min}=3$
Number of teeth in contact	3 (nominal load condition)
Efficiency	100%
Axial clearance	$c = 0.005D_g$
Diametral pitch range	$5 < P_d < 25$
Bending strength	$S_b=100$ ksi
Contact strength	$S_c=250$ ksi
Density	$\rho = 0.284$ lbm/in ³
Velocity Factor (K_v)	1.1
Load Distribution Factor (K_m)	1.3
Geometry Factor (J)	0.5
Output Speed (rpm)	1

All of the comparisons in Examples 1 and 2 will be with respect to the direct drive system based on the SRM. Chapters 5 and 6 made useful comparisons between only geared system alternatives and highlighted the variation of the performance parameters with respect to changes in diameter for a fixed gear ratio (Sections 5.3 and 5.4). Chapter 6 (Section 6.6) had a brief example discussing the variation in the performance parameters with respect to changes in gear ratio for a fixed diameter, and Example 1 will provide additional insight into this design scenario.

7.3.1 Example 1: Comparing Systems of the Same Size

This example presents scaled sets of actuator designs that illustrate how the performance parameters of torque density and responsiveness vary for geared and direct drive systems of the same size. The following systems were considered: SRM, SRM+HGT, SRM+Star+PEGT, and SRM+Star Compound+PEGT, and Table 7.8 lists the gear ratios considered for each gear train type. For each system, diameters ranging

from 10 to 30 inches (with increments of 5 inches) and a constant overall aspect ratio (A) of 1.0 were considered. For each of the three geared systems, a constant motor aspect ratio (A_m) of 0.6 was used.

Table 7.8: Gear Ratios for Geared Systems

Gear Train Type	Gear Ratios
HGT	100,200,300,400
Star+PEGT	100,125,150,175
Star Compound+PEGT	100,200,300,400

Recalling the notation from Chapter 6 (Section 6.2), given a feasible range for motor to gear train diameter ratio (K_d) from 0.25 to 1.0, the approach in this example was to adjust the value of the motor to overall length ratio (K_l) (and thus, the gear train aspect ratio A_g) for each diameter so that the motor and gear train torque capacities are balanced.

7.3.1.1 SRM (Direct Drive Reference Designs)

Table 7.9 summarizes the values of the design and performance parameters of the direct drive SRM based on the assumptions stated above. The inertia values listed in the table include the inertia of the SRM shaft, rotor, and bearings and do not include any load inertia. These inertia values will be used as the reference inertia (designated by I_{ref} in Table 7.1) for all of the responsiveness computations in this example. The responsiveness values in the table do not include any load inertia so that the specific values of the load inertia can be added to each at the designer's discretion. Table 7.10 gives the direct drive responsiveness as a function of diameter and the load to motor inertia ratio K .

Table 7.9: Direct Drive (SRM) Design and Performance Parameter Data Used for Comparison with Different Geared Systems (K=0)

Overall Diameter (inches)	Length (inches)	Aspect Ratio	Torque (ft-lbf)	Weight (lbf)	Inertia (lbm-in ²)	Torque Density (ft-lbf/lbf)	Responsiveness (rad/sec ²)
10	10.0	1.0	73	164	67	0.4	5005
15	15.0	1.0	400	551	508	0.7	3651
20	20.0	1.0	1309	1304	2136	1.0	2841
25	25.0	1.0	3253	2544	6505	1.3	2319
30	30.0	1.0	6820	4392	16166	1.6	1956

Table 7.10: Direct Drive (SRM) Responsiveness (rad/sec²) as a Function of K

Overall Diameter (inches)	Reference Inertia (lbm-in ²)	K (Load to Direct Drive Motor Inertia Ratio)					
		1	10	50	100	500	1000
10	67	2502	455	98	50	10	5
15	508	1826	332	72	36	7	4
20	2136	1421	258	56	28	6	3
25	6505	1159	211	45	23	5	2
30	16166	978	178	38	19	4	2

For a given motor size, a value of K=1000 suggests a load inertia equivalent to a solid cylinder that has a diameter about 5.5 times (and the same length) as that of the corresponding motor. The value of K can also be interpreted by determining an equivalent point load at a distance away from the axis of rotation (i.e., a radius of gyration). Designating the motor weight as W and the motor diameter as D, the load inertia (I_l) can be written as a function of the direct drive motor inertia (I_m) as follows.

$$I_l = KI_m = K \frac{WD^2}{8} \quad \text{Eqn. 183}$$

This load inertia can be equated to the inertia (I_{eq}) of a point weight W located at a distance R away from the axis of rotation via the following.

$$I_l = I_{eq}$$

$$K \frac{WD^2}{8} = WR^2 \quad \text{Eqn. 184}$$

Simplifying the second equation and solving for R gives the following important result.

$$R = D \sqrt{\frac{K}{8}} \quad \text{Eqn. 185}$$

Thus, for a given value of the motor diameter D, the value of K indicates the radius of the moment arm R where a weight equal to that of the motor is located. For example, considering the diameter of 10 inches and K=1000, the load inertia is equivalent to a point weight W of 164 pounds located at a distance R equal to 112 inches away from the axis of rotation. Though this may seem somewhat large, the particular values of the load inertia and the load to motor inertia ratio K should always be interpreted in the context of a specific application. If the exact load inertia is known, it should be used in place of the analytical relationships for the load inertia discussed in this chapter.

The particular ranges of K for each of the geared systems in Example 1 were chosen because they included values for which the geared systems begin to exhibit higher output responsiveness than the direct drive system, as discussed in the following sections.

7.3.1.2 SRM (Direct Drive) vs. SRM+HGT (Geared)

Table 7.11 summarizes the values of the design and performance parameters of the SRM+HGT geared combination. Figure 7.12 compares the torque density values in Table 7.9 and Table 7.11 and illustrates that the torque density of the geared system varies from approximately 19 to 87 times the torque density of the direct drive system (see the exact benefit ratios shown in Table 7.12). The benefit ratio can be obtained from these plots as the torque density for the geared system divided by the torque density for the direct drive system. This result is consistent with the dominance of the individual

gear train torque density values over the motor torque density values reported in Chapter 5 (see Sections 5.2.1 and 5.2.2).

Table 7.11: SRM+HGT Design and Performance Parameter Data (K=0)^{15,16}

Overall Diameter (inches)	Shell Diameter (inches)	Length (inches)	Aspect Ratio	Gear Ratio	Torque (ft-lbf)	Weight (lbf)	Inertia (lbm-in ²)	Torque Density (ft-lbf/lbf)	Input Responsiveness (rad/sec ²)	Output Responsiveness (rad/sec ²)
10	10.0	10	1.0	99	5210	164	73	32	3347	33.8
10	8.6	10	1.0	200	5461	138	54	39	2364	11.8
10	7.9	10	1.0	300	5437	127	54	43	1547	5.2
10	7.1	10	1.0	400	4740	118	55	40	1008	2.5
15	12.9	15	1.0	100	15113	460	453	33	1549	15.5
15	11.3	15	1.0	200	16864	415	398	41	983	4.9
15	10.0	15	1.0	300	15078	389	392	39	595	2.0
15	9.6	15	1.0	400	17111	384	405	45	490	1.2
20	15.3	20	1.0	99	30682	986	1817	31	790	8.0
20	13.2	20	1.0	201	33184	914	1723	36	444	2.2
20	11.8	20	1.0	299	30936	876	1856	35	258	0.9
20	11.0	20	1.0	399	29901	871	1862	34	186	0.5
25	17.3	25	1.0	101	50235	1788	5997	28	386	3.8
25	15.1	25	1.0	200	56299	1731	5598	33	233	1.2
25	13.6	25	1.0	301	56616	1681	6083	34	143	0.5
25	12.9	25	1.0	399	59966	1698	5778	35	120	0.3
30	19.4	30	1.0	98	77431	3045	15001	25	244	2.5
30	16.5	30	1.0	200	81875	2892	15476	28	123	0.6
30	14.8	30	1.0	298	77765	2858	16184	27	75	0.3
30	14.0	30	1.0	399	86767	2866	16091	30	63	0.2

¹⁵ The shell diameter in this and similar tables in this chapter refer to the diameter of the shell outside the motor.

¹⁶ Recommendations for achieving constant (or near constant) responsiveness for a range of diameters are provided in the discussion at the conclusion of this example in Section 7.3.1.5.

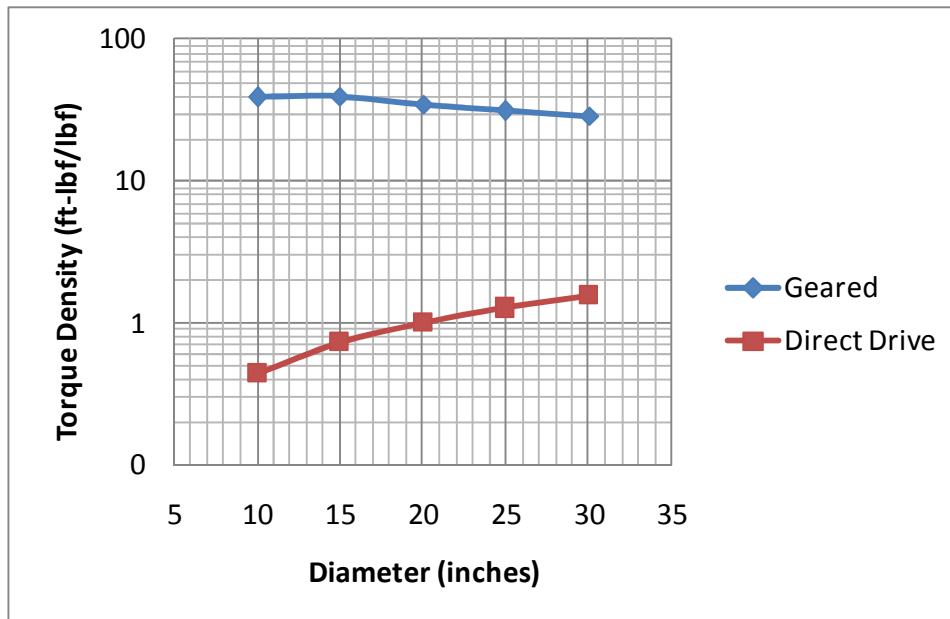


Figure 7.12: Comparison of Torque Density Between the Geared (SRM+HGT) and Direct Drive (SRM) Systems (Geared torque densities are an average for the 4 different gear ratio choices for each diameter.)

Table 7.12: Comparison of Torque Density Between the Geared (SRM+HGT) and Direct Drive (SRM) Systems

Overall Diameter (inches)	Direct Drive Torque Density (ft-lbf/lbf)	Average Geared Torque Density (ft-lbf/lbf)	Torque Density Benefit Ratio
10	0.4	39	87
15	0.7	39	54
20	1.0	34	34
25	1.3	31	24
30	1.6	29	19

Figure 7.13 and Figure 7.14 provide design maps of the output and input responsiveness of the geared system as a function of diameter and gear ratio. The important result here is that the lowest values of the diameter and gear ratio result in the highest input and output responsiveness. Also, these responsiveness values are

practically independent of the load to motor inertia ratio K up to the value of K where the geared system becomes superior to the direct drive system. Figure 7.15 provides the same output responsiveness information in a 2-D representation.

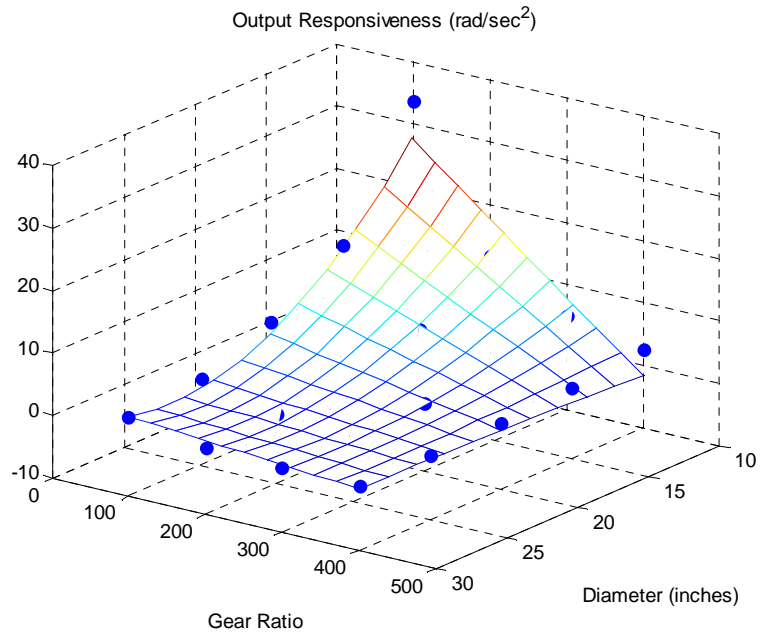


Figure 7.13: SRM+HGT Output Responsiveness as a Function of Diameter and Gear Ratio (practically independent of K)

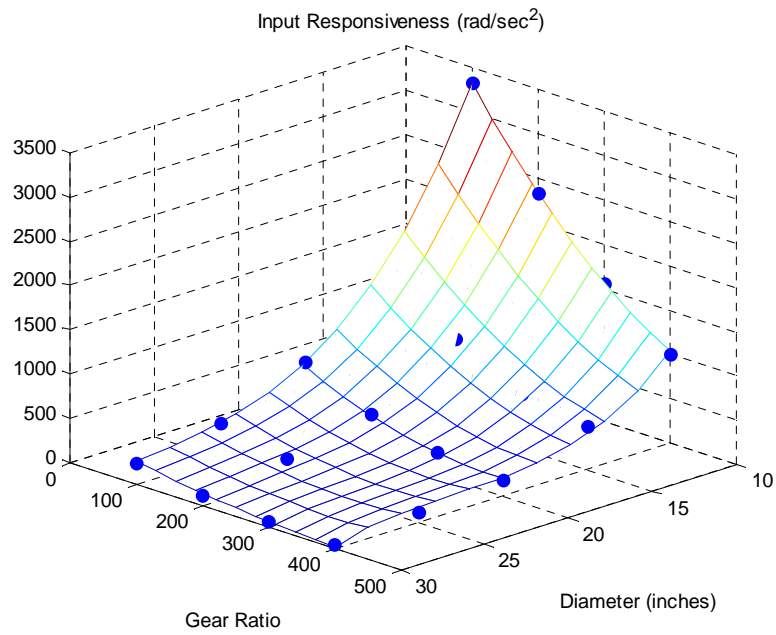


Figure 7.14: SRM+HGT Input Responsiveness as a Function of Diameter and Gear Ratio (practically independent of K)

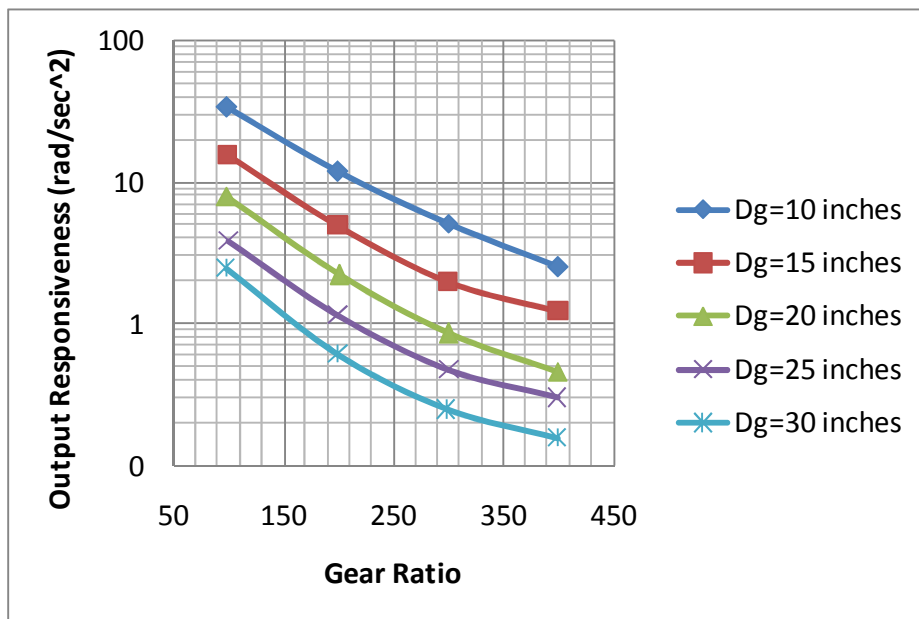


Figure 7.15: Geared (SRM+HGT) Output Responsiveness as a Function of Diameter and Gear Ratio (practically independent of K)

Figure 7.16 compares the output responsiveness of the direct drive and geared systems as a function of the load to motor inertia ratio K for different values of the gear ratio and the diameter of 10 inches. The key result is that the direct drive system is more responsive than the geared system until K reaches values of near 150 and greater for the gear ratio of 100 to 1. Using the equivalent load inertia relationships discussed in the previous section, this value of K gives a load inertia equivalent to a point weight of 164 pounds (equal to the direct drive motor weight) located at a distance of 43 inches away from the axis of rotation. Above this value of K , the geared system is more responsive than the direct drive system. Whether $K=150$ is a reasonable value for the load inertia depends on the particular application being considered. Table 7.13 provides the values of the ratio of the geared responsiveness to the direct drive responsiveness as a function of the diameter and the K value (the same information as in Figure 7.16).

Figure 7.17 and Table 7.14 provide analogous information for the input responsiveness. While these results suggest that geared system responsiveness is far superior to the direct drive system, the output responsiveness comparison is usually the most relevant when a specific output responsiveness (acceleration) is known or sought for a specific application. This input responsiveness comparison does suggest that the acceleration of the input motor for the geared system is practically unaffected by the increasing values of the load inertia.

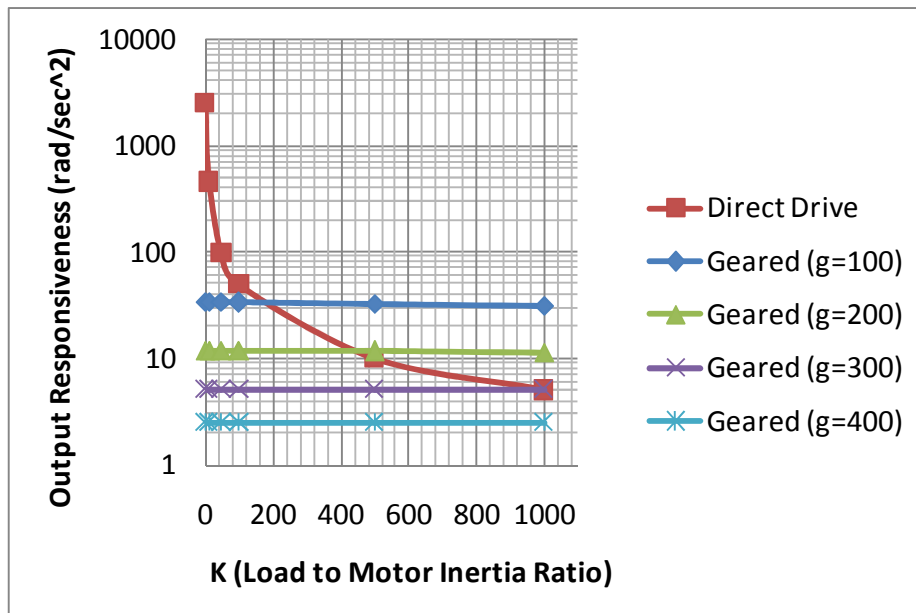


Figure 7.16: Geared (SRM+HGT) and Direct Drive (SRM) Output Responsiveness as a Function of K and Gear Ratio (for diameter = 10 inches)

Table 7.13: Geared (SRM+HGT) Output Responsiveness Benefit Ratio as a Function of Diameter and K (Gear ratio = 100 to 1)

Overall Diameter (inches)	K=1	K=10	K=50	K=100	K=500	K=1000
10	0.01	0.07	0.34	0.67	3.23	6.17
15	0.01	0.05	0.22	0.42	2.01	3.82
20	0.01	0.03	0.14	0.28	1.33	2.51
25	0.00	0.02	0.08	0.17	0.79	1.50
30	0.00	0.01	0.06	0.13	0.60	1.15

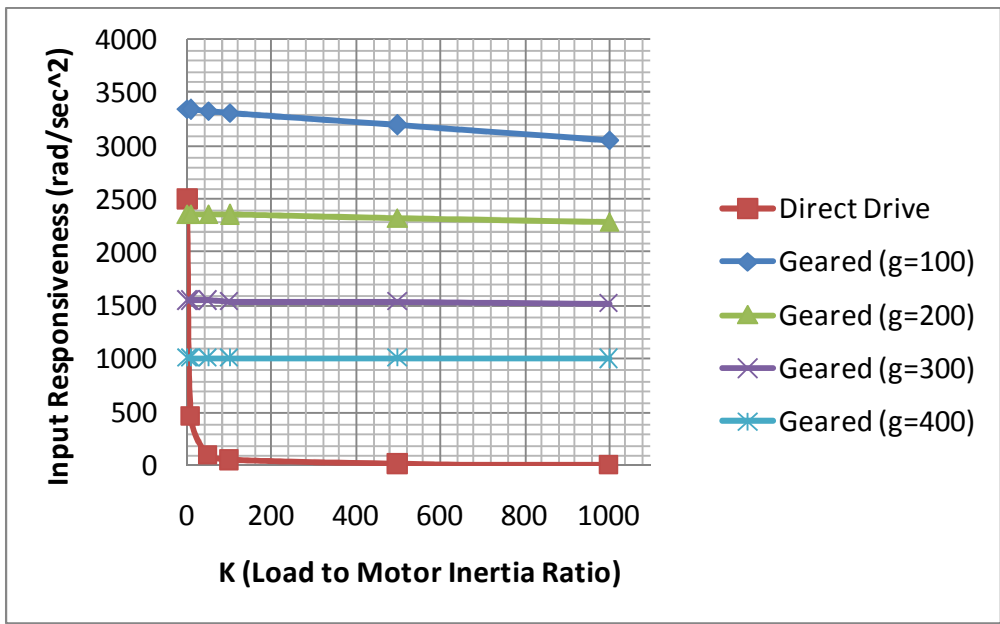


Figure 7.17: Geared (SRM+HGT) and Direct Drive (SRM) Input Responsiveness as a Function of K and Gear Ratio (for diameter = 10 inches)

Table 7.14: Geared (SRM+HGT) Input Responsiveness Benefit Ratio as a Function of Diameter and K (Gear ratio = 100 to 1)

Overall Diameter (inches)	K=1	K=10	K=50	K=100	K=500	K=1000
10	1.3	7.3	33.9	67	320	612
15	0.8	4.7	21.5	42	201	382
20	0.6	3.1	14.1	28	132	249
25	0.3	1.8	8.5	17	79	151
30	0.2	1.4	6.3	12	59	112

To allow a deeper understanding of these results, Table 7.15 lists the distribution of inertia in the motor, gear train, and load as a function of diameter and gear ratio. All of the inertia values are reflected to the output of the system. Key results from the table are that the dominant inertia is generally in the gear train, and the load inertia is insignificant even for a relatively large value of K. The load inertias are on the order of

1/10 of 1% of the total output inertia (i.e., extremely small) because of the relatively large gear ratios used. These large gear ratios (when squared) lead to large reflected motor and gear train inertias at the output (see the responsiveness relationships in Section 7.1). Armed with this knowledge of the inertial content, the designer can improve the responsiveness of this geared system by reducing the inertial content in the gear train. Figure 7.18 graphically displays the information in Table 7.15 for the 10 inch diameter design.

Table 7.15: Distribution of Inertia in the Motor, Gear Train, and Load as a Function of Diameter and Gear Ratio (All inertia values are reflected to the output.)

Overall Diameter (inches)	Gear Ratio	Motor Inertia (%)	Gear Inertia (%)	Load Inertia for K=1000 (%)
10	99	59	41	0.09
	200	38	62	0.03
	300	24	76	0.01
	400	14	86	0.01
15	100	34	66	0.11
	200	19	81	0.03
	300	11	89	0.01
	400	9	91	0.01
20	99	20	80	0.12
	201	10	90	0.03
	299	5	95	0.01
	399	4	96	0.01
25	101	11	89	0.11
	200	6	94	0.03
	301	3	97	0.01
	399	3	97	0.01
30	98	8	92	0.11
	200	3	97	0.03
	298	2	98	0.01
	399	1	99	0.01

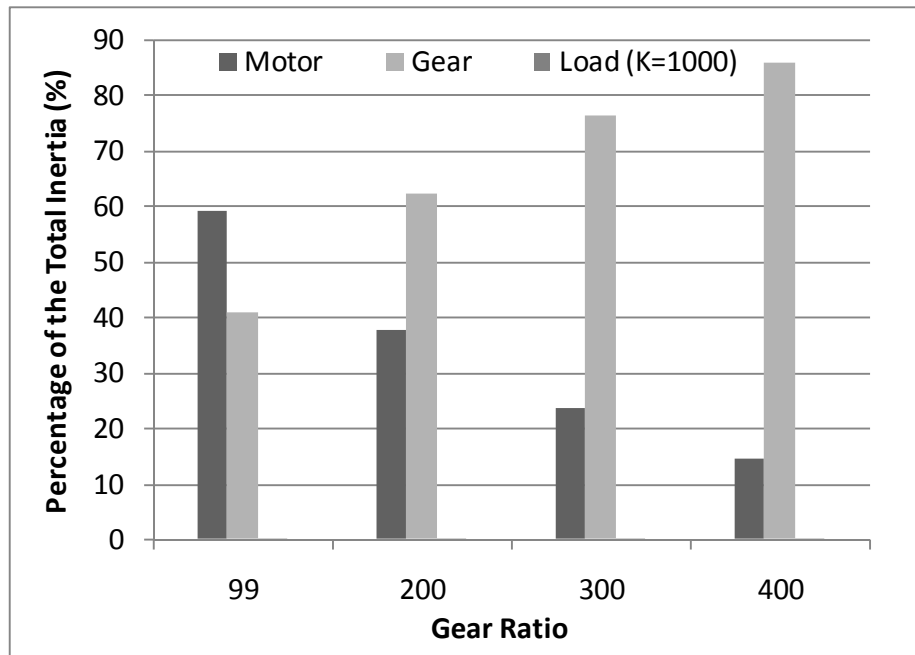


Figure 7.18: Percentage of Inertia in the Motor, Gear Train, and Load as a Function of Gear Ratio for the Overall Diameter of 10 inches (for the SRM+HGT actuator)

7.3.1.3 SRM (Direct Drive) vs. SRM+Star+PEGT (Geared)

Table 7.16 summarizes the values of the design and performance parameters of the SRM+Star+PEGT geared combination. Figure 7.19 compares the torque density values in Table 7.9 and Table 7.16, and illustrates that the torque density of the geared system varies from approximately 24 to 72 times the torque density of the direct drive system, as shown in Table 7.17. Again, this result is consistent with the individual motor and gear train torque density values reported in Chapter 4.

Table 7.16: SRM+Star+PEGT Design and Performance Parameter Data (K=0)

Overall Diameter (inches)	Shell Diameter (inches)	Length (inches)	Aspect Ratio	Gear Ratio	Torque (ft-lbf)	Weight (lbf)	Inertia (lbm-in ²)	Torque Density (ft-lbf/lbf)	Input Responsiveness (rad/sec ²)	Output Responsiveness (rad/sec ²)
10	10.0	10	1.0	100	4724	166	58	29	3770	37.7
10	9.6	10	1.0	124	4957	159	45	31	4132	33.2
10	9.3	10	1.0	149	5190	155	36	33	4442	29.8
10	9.0	10	1.0	173	5307	152	30	35	4655	26.9
15	13.7	15	1.0	100	17910	517	355	35	2342	23.4
15	13.2	15	1.0	124	18698	504	264	37	2637	21.2
15	12.6	15	1.0	151	19367	492	203	39	2925	19.4
15	12.4	15	1.0	173	19879	488	173	41	3081	17.8
20	17.2	20	1.0	100	45254	1177	1343	38	1564	15.6
20	16.5	20	1.0	124	47120	1154	981	41	1790	14.4
20	15.9	20	1.0	151	48519	1136	743	43	2008	13.3
20	15.6	20	1.0	173	49919	1135	624	44	2141	12.4
25	19.5	25	1.0	100	71913	2202	3752	33	893	9.0
25	18.5	25	1.0	124	74198	2173	2594	34	1066	8.6
25	18.0	25	1.0	149	76618	2172	1986	35	1198	8.0
25	17.4	25	1.0	174	77962	2163	1559	36	1331	7.6
30	22.4	30	1.0	100	128215	3768	9073	34	658	6.6
30	21.6	30	1.0	124	132396	3750	6293	35	784	6.3
30	20.7	30	1.0	149	135880	3722	4720	37	894	6.0
30	20.1	30	1.0	174	138202	3712	3679	37	1000	5.7

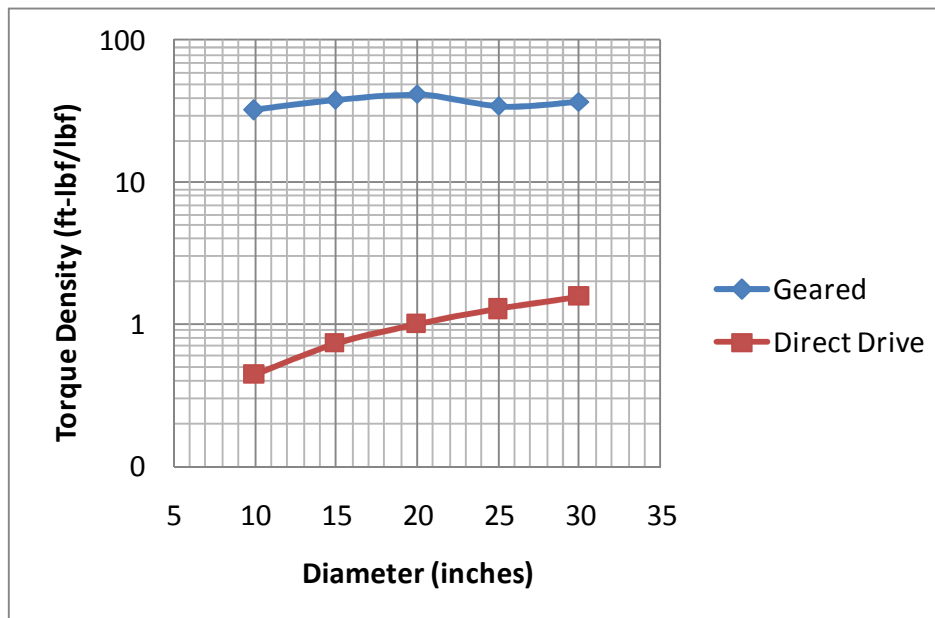


Figure 7.19: Comparison of Torque Density Between the Geared (SRM+Star+PEGT) and Direct Drive (SRM) Systems

Table 7.17: Comparison of Torque Density Between the Geared (SRM+Star+PEGT) and Direct Drive (SRM) Systems

Overall Diameter (inches)	Direct Drive Torque Density (ft-lbf/lbf)	Average Geared Torque Density (ft-lbf/lbf)	Torque Density Benefit Ratio
10	0.4	32	72
15	0.7	38	52
20	1.0	41	41
25	1.3	34	27
30	1.6	37	24

Figure 7.20 and Figure 7.21 provide design maps of the output and input responsiveness of the geared system as a function of diameter and gear ratio. Just as in the previous section, the important result here is that the lowest values of the diameter and gear ratio result in the highest output responsiveness. Figure 7.22 provides the same output responsiveness information in a 2-D representation.

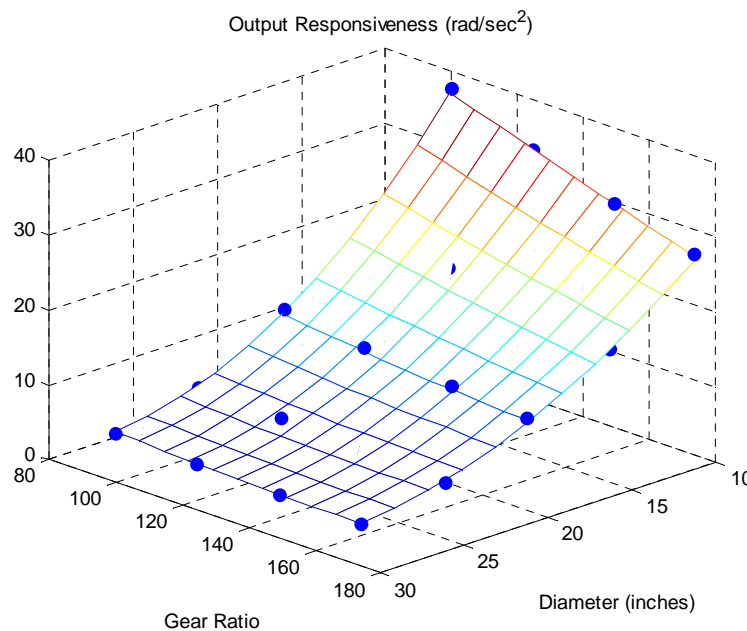


Figure 7.20: SRM+Star+PEGT Output Responsiveness as a Function of Diameter and Gear Ratio (practically independent of K)

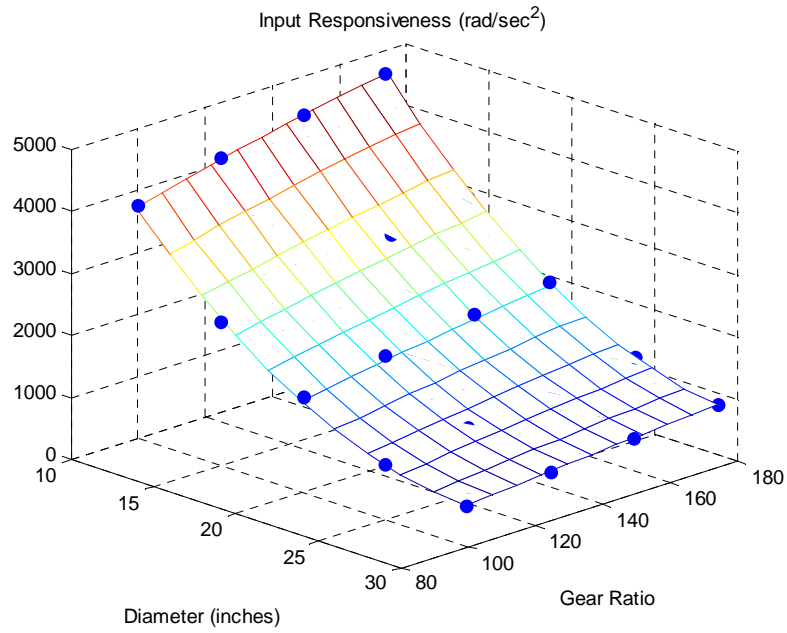


Figure 7.21: SRM+Star+PEGT Input Responsiveness as a Function of Diameter and Gear Ratio (practically independent of K)

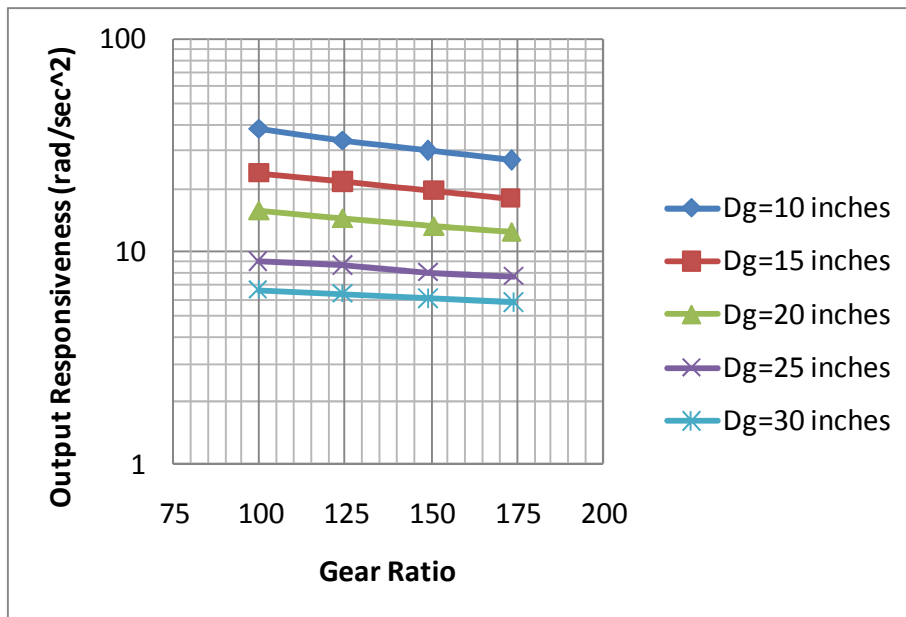


Figure 7.22: Geared (SRM+Star+PEGT) Output Responsiveness as a Function of Diameter and Gear Ratio (practically independent of K)

Figure 7.23 compares the output responsiveness of the direct drive and geared systems as a function of the load to motor inertia ratio K for different values of the gear ratio and the diameter of 10 inches. The key result is that the direct drive system is more responsive than the geared system until K reaches values of near 140 and greater for the gear ratio of 100 to 1. This value of K gives a load inertia equivalent to a point weight of 164 pounds (equal to the direct drive motor weight) located at a distance of 42 inches away from the axis of rotation. Above this value of K , the geared system is more responsive than the direct drive system. Table 7.18 provides the values of the ratio of the geared responsiveness to the direct drive responsiveness as a function of the diameter and the K value (the same information as in Figure 7.23).

Figure 7.24 and Table 7.19 provide analogous information for the input responsiveness. This input responsiveness comparison suggests that the acceleration of the motor for the geared system is practically unaffected by the increasing values of the load inertia.

While the output responsiveness trends with respect to gear ratio are similar for the HGT and Star+PEGT gear train alternatives, the input responsiveness trends are reversed (see Figure 7.17 and Figure 7.24, respectively). Increasing the gear ratio reduced the input responsiveness for the HGT while it increased the input responsiveness for the Star+PEGT. This occurs due to the dominant inertia in the Star+PEGT (the PE gear, crankshafts, and idler shafts) benefiting from reduction in reflected inertia by the square of the gear ratio and the dominant inertia in the HGT (the eccentric crankshaft) not benefiting from this reduction. A similar result was achieved in Example 2 of Chapter 6 (Section 6.6).

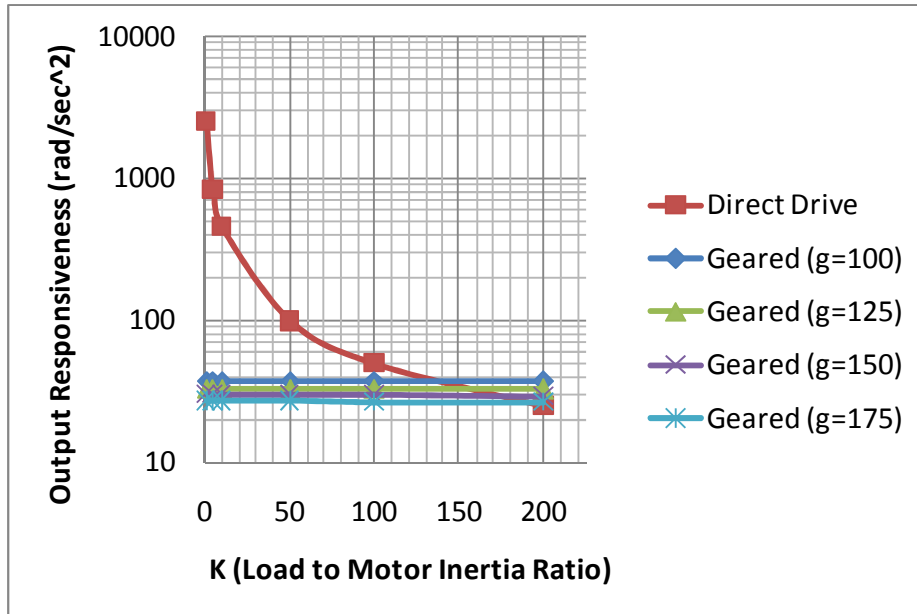


Figure 7.23: Geared (SRM+ Star+PEGT) and Direct Drive (SRM) Output Responsiveness as a Function of K and Gear Ratio (for diameter = 10 inches)

Table 7.18: Geared (SRM+Star+PEGT) Output Responsiveness Benefit Ratio as a Function of Diameter and K (Gear ratio = 100 to 1)

Overall Diameter (inches)	K=1	K=5	K=10	K=50	K=100	K=200
10	0.02	0.05	0.08	0.38	0.75	1.48
15	0.01	0.04	0.07	0.33	0.64	1.25
20	0.01	0.03	0.06	0.28	0.55	1.07
25	0.01	0.02	0.04	0.20	0.38	0.75
30	0.01	0.02	0.04	0.17	0.34	0.66

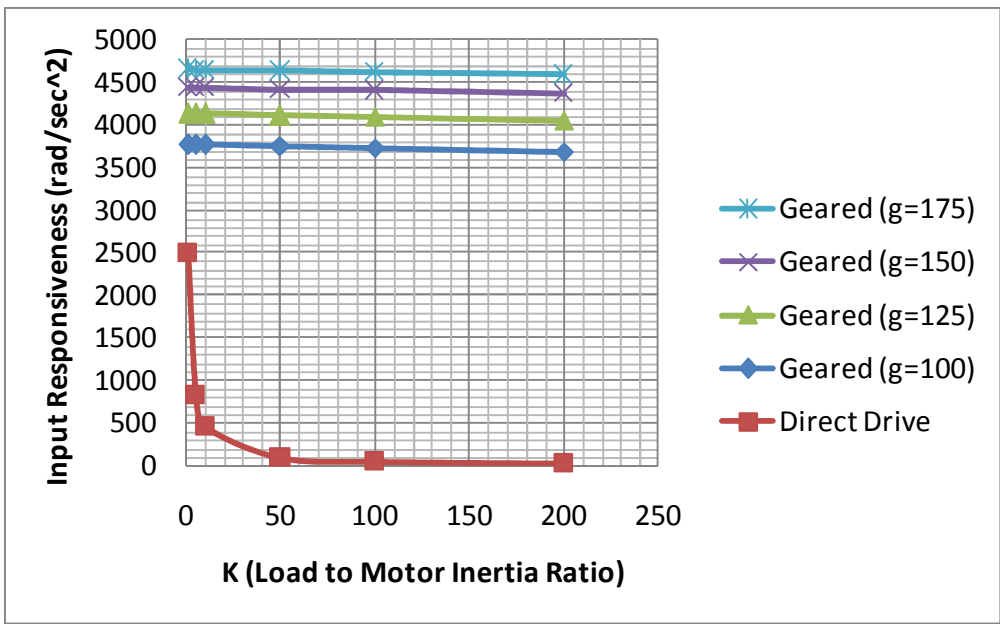


Figure 7.24: Geared (SRM+Star+PEGT) and Direct Drive (SRM) Input Responsiveness as a Function of K and Gear Ratio (for diameter = 10 inches)

Table 7.19: Geared (SRM+Star+PEGT) Input Responsiveness Benefit Ratio as a Function of Diameter and K (Gear ratio = 100 to 1)

Overall Diameter (inches)	K=1	K=5	K=10	K=50	K=100	K=200
10	1.5	4.5	8.3	38	75	148
15	1.3	3.8	7.0	32	64	125
20	1.1	3.3	6.0	28	55	107
25	0.8	2.3	4.2	19	38	75
30	0.7	2.0	3.7	17	33	65

Table 7.20 lists the distribution of inertia in the motor, gear train, and load as a function of diameter and gear ratio. All of the inertia values are reflected to the output of the system. A key result from the table is that the motor and gear train inertia are both significant, with the dominant inertia depending on the specific values of the diameter and gear ratio considered. The reader should recall that the dominant inertia in the

SRM+HGT geared system of the previous section was always in the gear train. Table 7.20 also suggests that the load inertia is insignificant even for a relatively large value of K. Armed with this knowledge, the designer can improve the responsiveness of this geared system by reducing the inertial content in the motor and the gear train. Figure 7.25 graphically displays the information in Table 7.20 for the 10 inch diameter design.

Table 7.20: Distribution of Inertia in the Motor, Gear Train, and Load as a Function of Diameter and Gear Ratio (All inertia values are reflected to the output.)¹⁷

Overall Diameter (inches)	Gear Ratio	Motor Inertia (%)	Gear Inertia (%)	Load Inertia for K=200 (%)
10	100	63	37	0.02
	124	67	33	0.02
	149	70	29	0.02
	173	73	27	0.01
15	100	50	50	0.03
	124	54	46	0.02
	151	58	42	0.02
	173	61	39	0.02
20	100	41	59	0.03
	124	45	55	0.03
	151	49	51	0.03
	173	52	48	0.02
25	100	26	74	0.03
	124	30	70	0.03
	149	33	67	0.03
	174	36	64	0.03
30	100	22	78	0.04
	124	26	74	0.03
	149	28	72	0.03
	174	31	69	0.03

¹⁷ See section 7.3.1.1 for the reason behind these very low load inertia values.

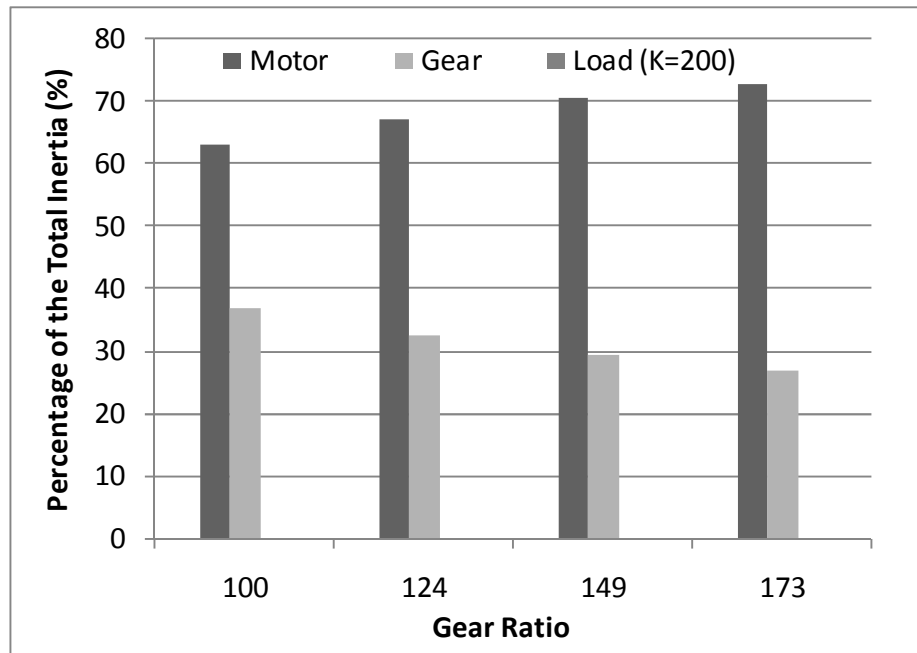


Figure 7.25: Percentage of Inertia in the Motor, Gear Train, and Load as a Function of Gear Ratio for the Overall Diameter of 10 inches (for the SRM+Star+PEGT actuator)

7.3.1.4 SRM (Direct Drive) vs. SRM+Star Compound+PEGT (Geared)

Table 7.21 summarizes the values of the design and performance parameters of the SRM+Star Compound+PEGT geared combination. Figure 7.26 compares the torque density values in Table 7.9 and Table 7.21, and illustrates that the torque density of the geared system varies from approximately 27 to 91 times the torque density of the direct drive system, as shown in Table 7.22. Again, this result is consistent with the individual motor and gear train torque density values reported in Chapter 4.

Table 7.21: SRM+Star Compound+PEGT Design and Performance Parameter Data (K=0)

Overall Diameter (inches)	Shell Diameter (inches)	Length (inches)	Aspect Ratio	Gear Ratio	Torque (ft-lbf)	Weight (lbf)	Inertia (lbm-in ²)	Torque Density (ft-lbf/lbf)	Input Responsiveness (rad/sec ²)	Output Responsiveness (rad/sec ²)
10	9.8	10	1.0	101	4400	140	54	31	3734	37.1
10	8.7	10	1.0	200	5089	128	25	40	4791	24.0
10	8.1	10	1.0	300	5461	127	16	43	5336	17.8
10	7.7	10	1.0	403	5726	122	12	47	5578	13.8
15	13.4	15	1.0	100	16640	445	335	37	2300	23.0
15	11.8	15	1.0	200	18787	407	136	46	3219	16.1
15	11.0	15	1.0	299	20111	402	84	50	3724	12.4
15	10.4	15	1.0	403	20934	402	58	52	4149	10.3
20	16.9	20	1.0	100	41988	1018	1237	41	1572	15.7
20	14.8	20	1.0	202	47247	987	470	48	2314	11.5
20	13.7	20	1.0	300	50046	976	275	51	2808	9.3
20	13.0	20	1.0	403	51912	952	197	55	3031	7.5
25	19.1	25	1.0	100	66598	1892	3528	35	879	8.8
25	16.6	25	1.0	200	73318	1893	1166	39	1457	7.3
25	15.3	25	1.0	299	76984	1917	641	40	1859	6.2
25	14.5	25	1.0	398	79428	1889	444	42	2085	5.2
30	21.8	30	1.0	101	118670	3264	8192	36	667	6.6
30	19.1	30	1.0	201	129862	3111	2831	42	1057	5.3
30	17.6	30	1.0	299	136196	3312	1480	41	1426	4.8
30	16.8	30	1.0	401	140842	3246	1010	43	1611	4.0

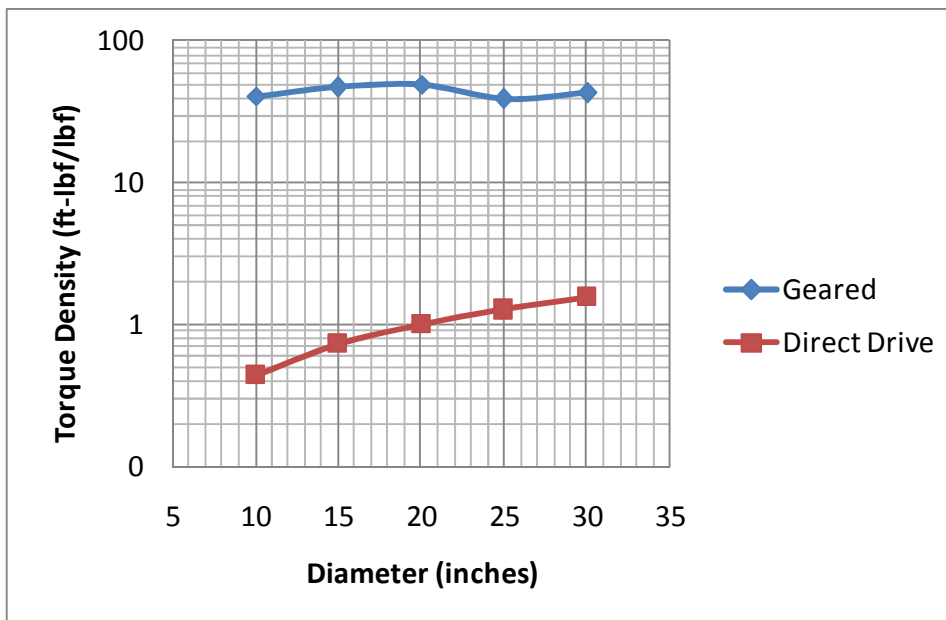


Figure 7.26: Comparison of Torque Density Between the Geared (SRM+Star Compound+PEGT) and Direct Drive (SRM) Systems

Table 7.22: Comparison of Torque Density Between the Geared (SRM+Star Compound+PEGT) and Direct Drive (SRM) Systems

Overall Diameter (inches)	Direct Drive Torque Density (ft-lbf/lbf)	Average Geared Torque Density (ft-lbf/lbf)	Torque Density Benefit Ratio
10	0.4	40	91
15	0.7	46	64
20	1.0	49	49
25	1.3	39	30
30	1.6	42	27

Figure 7.27 and Figure 7.28 provide design maps of the output and input responsiveness of the geared system as a function of diameter and gear ratio. Just as in the previous two sections, the important result here is that the lowest values of the diameter and gear ratio result in the highest output responsiveness. Figure 7.29 provides the same output responsiveness information in a 2-D representation.

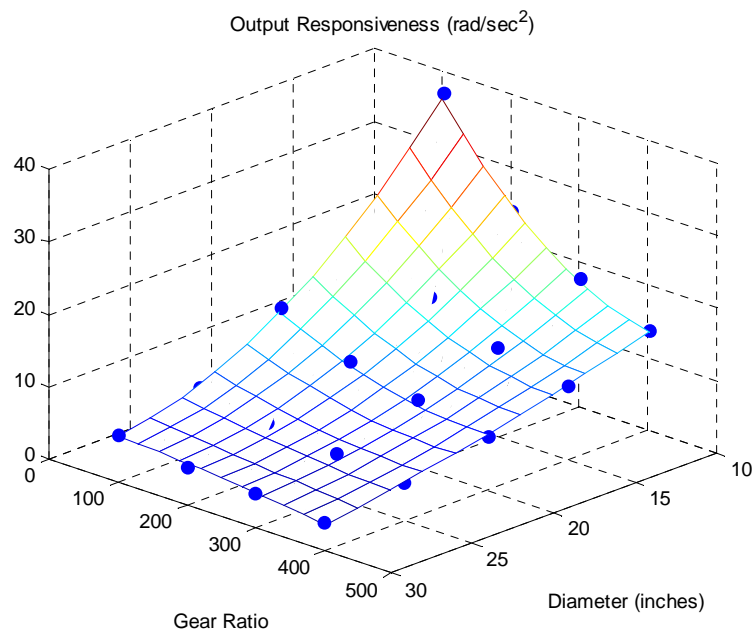


Figure 7.27: SRM+Star Compound+PEGT Output Responsiveness as a Function of Diameter and Gear Ratio (practically independent of K)

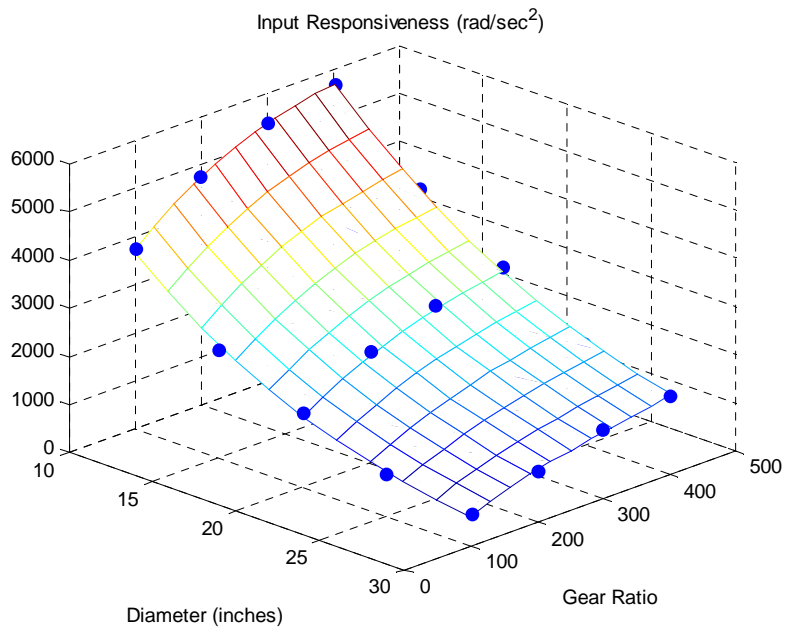


Figure 7.28: SRM+Star Compound+PEGT Input Responsiveness as a Function of Diameter and Gear Ratio (practically independent of K)

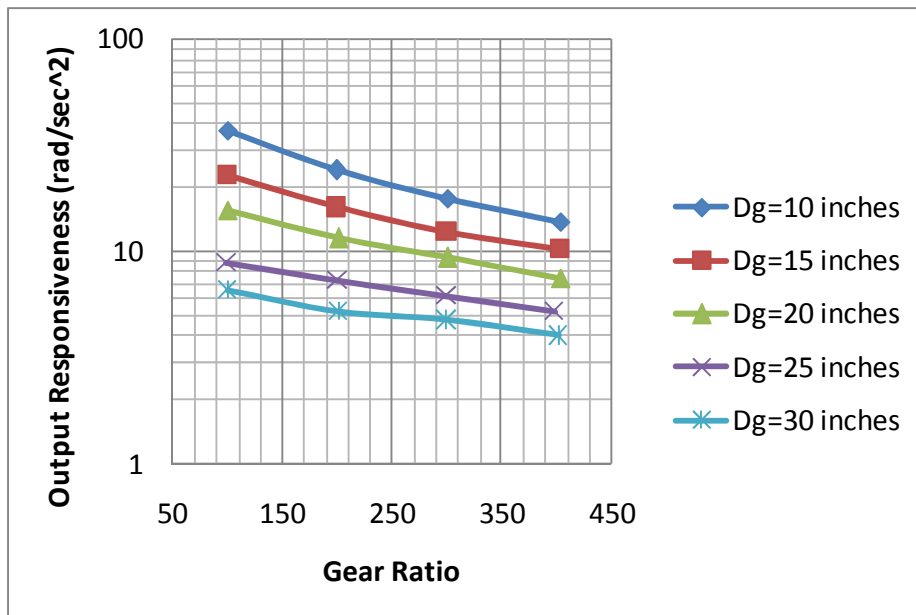


Figure 7.29: Geared (SRM+Star Compound+PEGT) Output Responsiveness as a Function of Diameter and Gear Ratio (practically independent of K)

Figure 7.30 compares the output responsiveness of the direct drive and geared systems as a function of the load to motor inertia ratio K for different values of the gear ratio and the diameter of 10 inches. The key result is that the direct drive system is more responsive than the geared system until K reaches values of near 130 and greater for the gear ratio of 100 to 1. This value of K gives a load inertia equivalent to a point weight of 164 pounds (equal to the direct drive motor weight) located at a distance of 40 inches away from the axis of rotation. Above this value of K , the geared system is more responsive than the direct drive system. A similar result was achieved for the SRM+Star+PEGT actuator discussed in the previous section. Table 7.23 provides the values of the ratio of the geared responsiveness to the direct drive responsiveness as a function of the diameter and the K value (the same information as in Figure 7.30).

Figure 7.31 and Table 7.24 provide analogous information for the input responsiveness. This input responsiveness comparison suggests that the acceleration of the input motor for the geared system is practically unaffected by the increasing values of the load inertia.

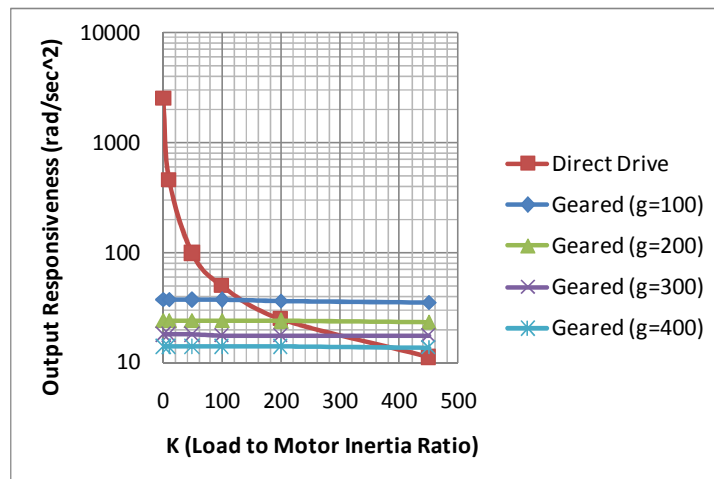


Figure 7.30: Geared (SRM+Star Compound+PEGT) and Direct Drive (SRM) Output Responsiveness as a Function of K and Gear Ratio (for diameter = 10 inches)

Table 7.23: Geared (SRM+Star Compound+PEGT) Output Responsiveness Benefit Ratio as a Function of Diameter and K (Gear ratio = 100 to 1)

Overall Diameter (inches)	K=1	K=10	K=50	K=100	K=200	K=450
10	0.01	0.08	0.38	0.74	1.45	3.17
15	0.01	0.07	0.32	0.63	1.23	2.66
20	0.01	0.06	0.28	0.55	1.07	2.31
25	0.01	0.04	0.19	0.38	0.74	1.59
30	0.01	0.04	0.17	0.34	0.66	1.41

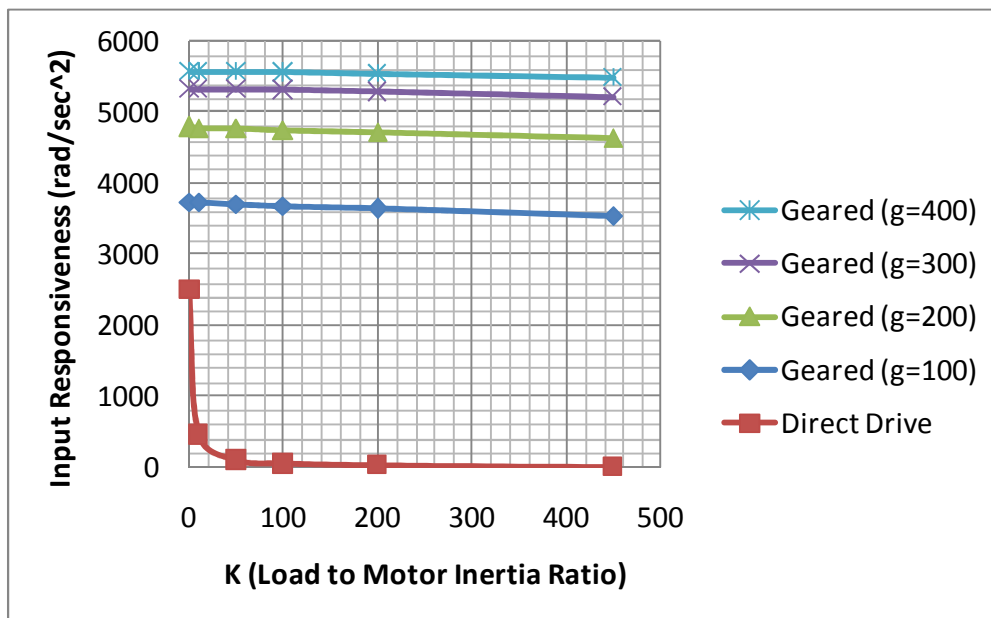


Figure 7.31: Geared (SRM+Star Compound+PEGT) and Direct Drive (SRM) Input Responsiveness as a Function of K and Gear Ratio (for diameter = 10 inches)

Table 7.24: Geared (SRM+Star Compound+PEGT) Input Responsiveness Benefit Ratio as a Function of Diameter and K (Gear ratio = 100 to 1)

Overall Diameter (inches)	K=1	K=10	K=50	K=100	K=200	K=450
10	1.5	8.2	37.8	74	146	319
15	1.3	6.9	31.9	63	123	266
20	1.1	6.1	28.0	55	107	232
25	0.8	4.2	19.2	38	74	158
30	0.7	3.7	17.2	34	66	141

Table 7.25 lists the distribution of inertia in the motor, gear train, and load as a function of diameter and gear ratio. All of the inertia values are reflected to the output of the system. The important results from Table 7.25 for the star compound 1st stage gear train are similar to those from Table 7.20 for the star 1st stage gear train, so they will not be repeated here. Figure 7.32 graphically displays the information in Table 7.25 for the 10 inch diameter design.

Table 7.25: Distribution of Inertia in the Motor, Gear Train, and Load as a Function of Diameter and Gear Ratio (All inertia values are reflected to the output.)¹⁸

Overall Diameter (inches)	Gear Ratio	Motor Inertia (%)	Gear Inertia (%)	Load Inertia for K=450 (%)
10	101	62	38	0.06
	200	73	27	0.03
	300	80	20	0.02
	403	82	18	0.02
15	100	48	52	0.07
	200	61	39	0.04
	299	68	32	0.03
	403	72	28	0.02
20	100	40	60	0.08
	202	54	46	0.05
	300	60	40	0.04
	403	64	36	0.03
25	100	25	75	0.08
	200	37	63	0.06
	299	45	55	0.05
	398	49	51	0.04
30	101	21	79	0.09
	201	31	69	0.06
	299	39	61	0.05
	401	43	57	0.04

¹⁸ See section 7.3.1.1 for the reason behind these very low load inertia values.

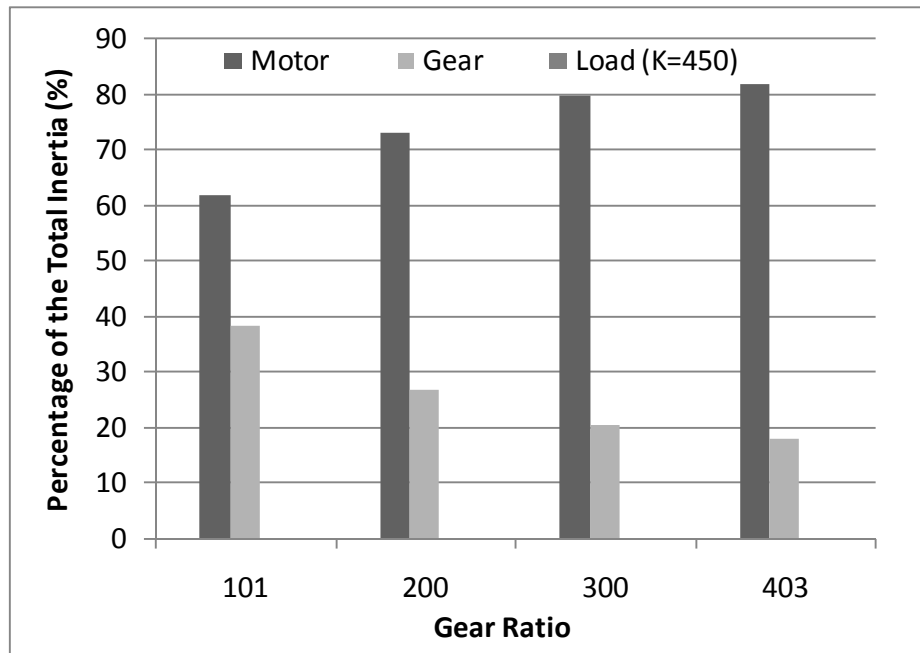


Figure 7.32: Percentage of Inertia in the Motor, Gear Train, and Load as a Function of Gear Ratio for the Overall Diameter of 10 inches (for the SRM+Star Compound+PEGT actuator)

7.3.1.5 Example 1 Discussion of Results

For the range of diameters (10 to 30 inches) and gear ratios (100-400) considered in this example, the geared systems had approximately 20 to 90 times higher torque density than a direct drive system of the same size based on the SRM. This superiority of the torque density for the geared system occurs due the different physical mechanisms that limit the load capacity of the motor and gear train. The motor torque capacity is limited by the safe current capacity of the windings and the flux density of the magnetic material in the rotor and stator (Section 3.7.7), while the gear train torque capacity is limited by the bending and contact stresses occurring in the gear teeth (Section 3.5). Utilizing other motor types (such as the brushless DC (Section 7.2.1), brushed DC, inside-out SRM, etc.) and gear train types (star compound, epicyclic, etc.) may change

this benefit ratio, but any geared system should still remain far superior to the direct drive system in terms of torque density for the same size. This result is independent of the load to motor inertia ratio K and only depends upon the motor and gear train torque and weight relationships provided in Chapter 3.

For all the geared systems considered, the lowest diameter and gear ratio design parameter settings yielded the highest responsiveness values. Smaller systems (i.e., lower diameter settings) having larger responsiveness than larger systems (i.e., higher diameter settings) is consistent with the torque (2^{nd} power) and inertia (4^{th} or 5^{th} power) dependence on diameter determined in Chapter 5 (Section 5.2). The result of lower gear ratios yielding higher responsiveness occurs due to the relative changes in the inertia terms in the denominator of the output responsiveness relationship (as shown in Table 7.15, Table 7.20, and Table 7.25), keeping in the mind the same size comparison assumption in this example. This result is still under investigation and should be more fully explored in future research.

The direct drive system is superior to each of the geared systems in terms of the output responsiveness until K reaches values between approximately 130 and 150 (equivalent to a weight of 164 lbf at an approximately 40 inch moment arm for the 10 inch diameter system). For values of K less than this, the designer is sacrificing acceleration if he/she is using a geared system in place of a direct drive system. For K values larger than this, the geared system becomes superior to the direct drive system by factors equal to the benefit ratios stated in the tables above for each geared system. The particular cutoff value of K occurred for a gear ratio of 100 for all three geared systems considered, with higher gear ratios making the direct drive system superior. In general, the cutoff value of K for which the geared system becomes superior depends on the

relative magnitudes of the terms in the direct drive and geared output responsiveness expressions detailed at the beginning of this chapter in Section 7.1.

Regarding the gear ratio ranges considered in this chapter, both the HGT and PEGT can achieve gear ratios lower than 100. However, values less than 100 were not considered because the results of Chapter 6 (Section 6.7.2) suggested that these lower gear ratios resulted in a motor diameter significantly larger than the gear train diameter (i.e., an imbalance or incompatibility between the motor and gear train).

For the range of diameters (10 to 30 inches) and gear ratios (100-400) considered in this example, the dominant inertia in the SRM+HGT actuator combination was in the gear train, while the dominant inertia in the two actuators based on the PEGT depended on the specific values of the gear ratios and diameters being considered.

Given the results from this example, the designer is advised to use higher gear ratios (i.e., near the maximum for each gear train type) when designing for maximum torque density (because this reduces the size of the motor) and to use lower gear ratios (near 100 for the gear trains here) when designing for maximum output responsiveness (because this provides a lower reflected motor and gear train inertia at the output). This recommendation is justified by the dominance of the motor and gear train inertia (rather than the load inertia) for the ranges of K considered. The specific values of the gear ratio used to balance the torque density and responsiveness will depend on the application torque and acceleration requirements.

Finally, consider the result that the output responsiveness decreases with increasing gear ratio (from this example and from Example 2 of Chapter 6 (Section 6.6)), and assume that the designer desires to achieve near constant responsiveness for a range of actuator diameters. To achieve this, the designer is advised to use relatively higher gear ratios for the smaller designs in a set (to decrease their responsiveness below their

maximum possible values) and lower gear ratios for the larger designs (to increase their responsiveness to the maximum values possible).

7.3.2 Example 2: Comparing Systems of the Same Torque Capacity

This example presents scaled sets of actuator designs that illustrate how the performance parameters of torque density and responsiveness vary for geared and direct drive systems of the same torque capacity. The same systems from Example 1 were considered: direct drive SRM and the SRM+HGT, SRM+Star+PEGT, and SRM+Star Compound+PEGT geared systems. Table 7.26 lists the gear ratios considered for each gear train type. For each of the geared systems, diameters ranging from 10 to 30 inches (with increments of 5 inches), a constant overall aspect ratio (A) of 1.0, and a constant motor aspect ratio (A_m) of 0.6 was used. The geared system parameter data was taken directly from the designs generated for Example 1 above. The direct drive motor aspect ratio was held constant at 0.6.

Table 7.26: Gear Ratios for Geared Systems

Gear Train Type	Gear Ratios
HGT	100 and 400
Star+PEGT	100 and 175
Star Compound+PEGT	100 and 400

The gear ratios in the table are near the approximate upper and lower limits for the gear train types being considered (Section 3.13), and the analysis for this example was done for both gear ratio settings. However, because the results of the off-the-shelf comparisons (Section 7.2) and those of Example 1 (Section 7.3.1.5) suggest that geared systems with lower gear ratios (for a given diameter) achieve the highest responsiveness, only the results for the low gear ratio setting of 100 to 1 are recorded in this section. The particular ranges of K for each of the geared systems in the following sections were

chosen because they included values for which the geared systems begin to exhibit comparable output responsiveness to the direct drive system.

7.3.2.1 SRM (Direct Drive) vs. SRM+HGT (Geared)

Table 7.27 summarizes the values of the design and performance parameters of the direct drive SRM. The inertia values listed in the table include the inertia of the SRM shaft, rotor, and bearings and do not include any load inertia. These inertia values will be used as the reference inertia for all of the responsiveness computations in this comparison. The responsiveness values in the table do not include any load inertia so that the specific values of the load inertia can be added to each at the designer's discretion. Table 7.28 gives the direct drive responsiveness as a function of torque capacity and the load to motor inertia ratio K .

Table 7.27: Direct Drive (SRM) Design and Performance Parameter Data Used for Comparison with Different Geared Systems ($K=0$)

Overall Diameter (inches)	Length (inches)	Aspect Ratio	Torque (ft-lbf)	Weight (lbf)	Inertia (lbm-in ²)	Torque Density (ft-lbf/lbf)	Responsiveness (rad/sec ²)
33	19.8	0.6	5210	3287	11108	1.6	2175
43	25.8	0.6	15113	7247	41461	2.1	1690
51	30.8	0.6	30682	12274	99757	2.5	1426
58	34.8	0.6	50235	17723	183982	2.8	1266
65	38.7	0.6	77431	24488	315381	3.2	1138

Table 7.28: Direct Drive (SRM) Responsiveness (rad/sec²) as a Function of K

Torque (ft-lbf)	Reference Inertia (lbm-in ²)	K (Load to Direct Drive Motor Inertia Ratio)					
		10	50	100	500	1000	2000
5210	11108	198	43	22	4.3	2.2	1.09
15113	41461	154	33	17	3.4	1.7	0.84
30682	99757	130	28	14	2.8	1.4	0.71
50235	183982	115	25	13	2.5	1.3	0.63
77431	315381	103	22	11	2.3	1.1	0.57

Table 7.29 summarizes the values of the design and performance parameters of the SRM+HGT geared combination. A target gear ratio of 100 to 1 was used for all of the designs in the set. Figure 7.33 compares the torque density values in Table 7.27 and Table 7.29 and illustrates that the torque density of the geared system varies from approximately 8 to 20 times the torque density of the direct drive system (see the exact benefit ratios shown in Table 7.30).

Table 7.29: SRM+HGT Design and Performance Parameter Data (K=0)

Overall Diameter (inches)	Shell Diameter (inches)	Length (inches)	Aspect Ratio	Gear Ratio	Torque (ft-lbf)	Weight (lbf)	Inertia (lbm-in ²)	Torque Density (ft-lbf/lbf)	Input Responsiveness (rad/sec ²)	Output Responsiveness (rad/sec ²)
10	10.0	10	1.0	99	5210	164	73	32	3347	33.8
15	12.9	15	1.0	100	15113	460	453	33	1549	15.5
20	15.3	20	1.0	99	30682	986	1817	31	790	8.0
25	17.3	25	1.0	101	50235	1788	5997	28	386	3.8
30	19.4	30	1.0	98	77431	3045	15001	25	244	2.5

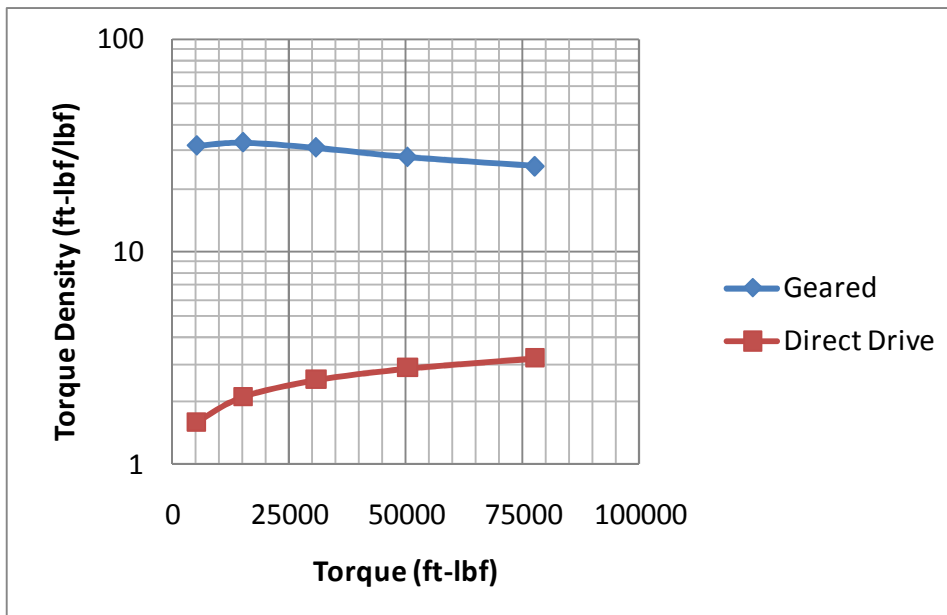


Figure 7.33: Comparison of Torque Density Between the Geared (SRM+HGT) and Direct Drive (SRM) Systems

Table 7.30: Comparison of Torque Density Between the Geared (SRM+HGT) and Direct Drive (SRM) Systems

Torque (ft-lbf)	Direct Drive Torque Density (ft-lbf/lbf)	Geared Torque Density (ft-lbf/lbf)	Torque Density Benefit Ratio
5210	1.6	32	20
15113	2.1	33	16
30682	2.5	31	12
50235	2.8	28	10
77431	3.2	25	8

Based on the data in Table 7.29, Figure 7.34 plots the output responsiveness of the geared system as a function of the weight and load to motor inertia ratio K . Using the relationships in Section 7.3.1.1, the load inertia is expressed as the constant K times the inertia of an equivalent weight W at a moment arm of R away from the axis of rotation. The weight parameter data on the x-axis can be replaced with the torque parameter data

from Table 7.29, and similar trends would be observed. As the weight of the geared system increases (i.e., moving from left to right on the x-axis, the reference load inertia I_{ref} increases. This was done in order to provide a realistic result for the responsiveness based on the assumption that larger systems will typically be used to accelerate larger inertias. For a given actuator size (i.e., weight and torque capacity), this chart gives the designer an idea of the acceleration capability of the system for a given load inertia.

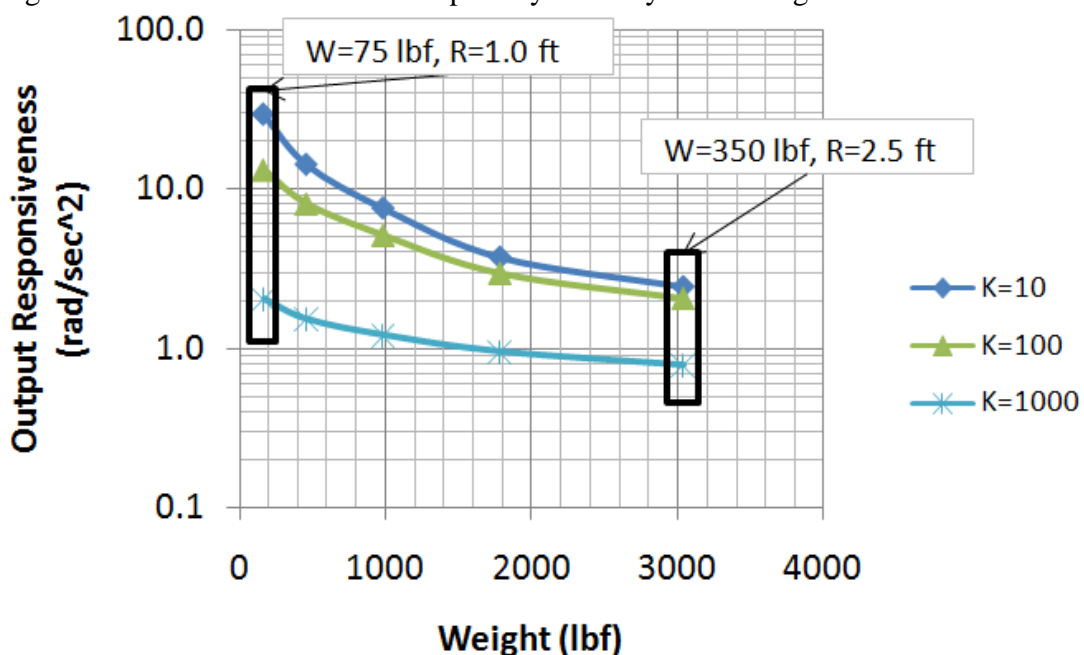


Figure 7.34: Geared (SRM+HGT) Output Responsiveness as a Function of Actuator Weight and Load to Motor Inertia Ratio K (Load Inertia, $I_l = KI_{ref} = KWR^2$)

Figure 7.35 and Figure 7.36 compare the output responsiveness of the direct drive and geared systems as a function of the load to motor inertia ratio K for the highest torque setting of about 77,000 ft-lbf. The first figure gives the responsiveness for values of K up to 500, and the second figure gives results for the full range of K considered.

The key result is that the direct drive system is more responsive than the geared system up to certain values of K . The physical reasoning behind this result can be

explained by referring to the geared output responsiveness (R_{go}) relationship detailed at the beginning of this chapter.

$$R_{go} = \frac{T_g}{I_{out}} = \frac{T_g}{I_m g^2 + I_g g^2 + K I_{ref}} \quad \text{Eqn. 186}$$

Recall that T_g is the output torque capacity, I_m is the motor inertia reflected to the input, I_g is the gear train inertia reflected to the input, g is the gear ratio, and I_{ref} is equal to the inertia of the direct drive motor. In the limit as K becomes large, the load inertia term ($K \cdot I_{ref}$) dominates the motor and gear train reflected inertia in the geared system and the motor inertia in the direct drive system. Then, the geared systems and direct drive systems have the same torque capacity (given the assumption in this example) accelerating practically the same load inertia. Thus, the direct drive system is superior in terms of output responsiveness until a particular value of K is reached. After this particular value of K (discussed below), both systems will accelerate the load at nearly the same rate.

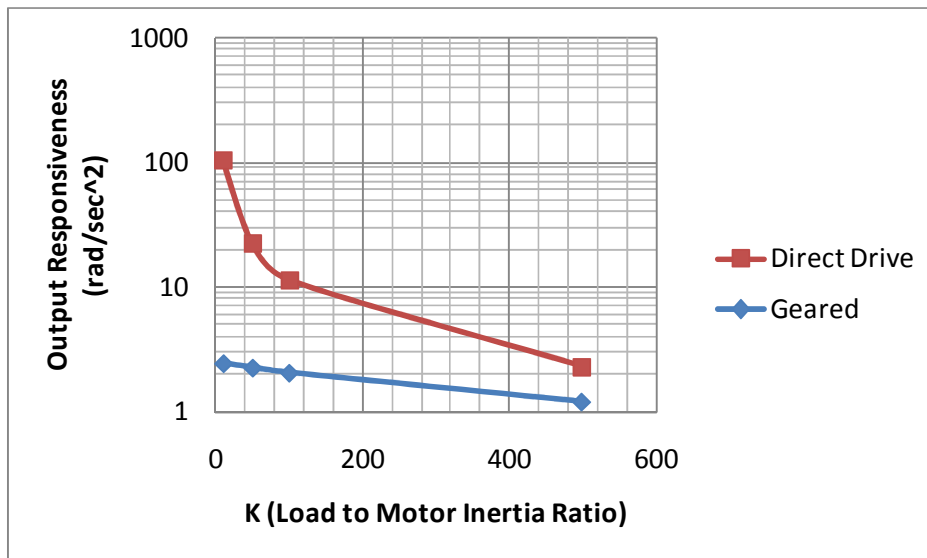


Figure 7.35: Geared (SRM+HGT) and Direct Drive (SRM) Output Responsiveness as a Function of K (for lower range of K and highest torque value)

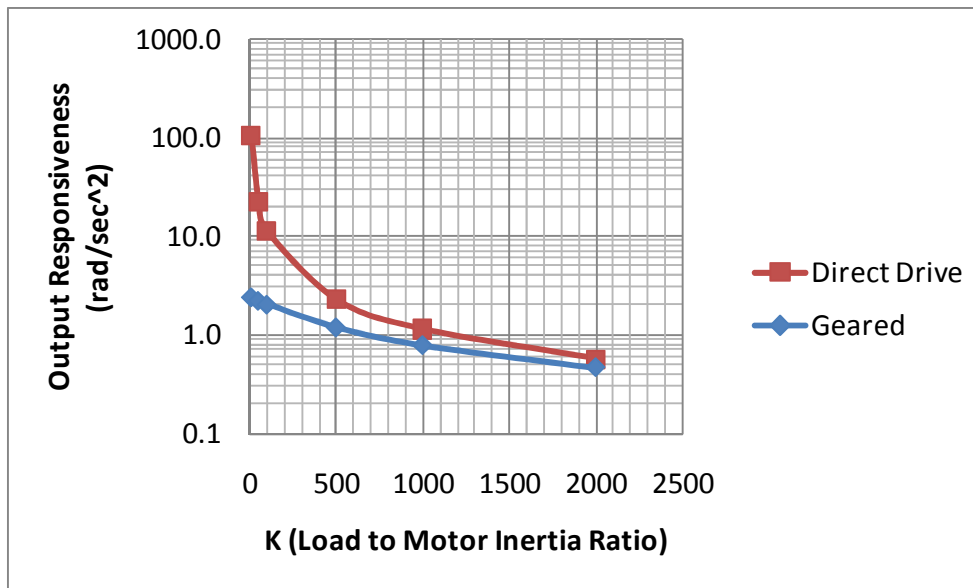


Figure 7.36: Geared (SRM+HGT) and Direct Drive (SRM) Output Responsiveness as a Function of K (for full range of K and highest torque value)

Table 7.31 provides the values of the ratio of the geared responsiveness to the direct drive responsiveness as a function of the torque capacity and the K value (the same information as in Figure 7.36). Considering the lowest torque capacity of 5,210 ft-lbf as an example, the ratio of the geared to direct drive responsiveness reaches approximately 90% (or 0.9) near a K value of 500. This value of K gives a load inertia equivalent to a point weight of 32,870 pounds (10 times the direct drive motor weight) located at a distance of 83 inches (7 feet) away from the axis of rotation. Other equivalent load inertias can be calculated using the load inertia relationships in Example 1 (Section 7.3.1.1). As noted earlier, the specific values of K used (and thus, the load inertia) will always depend on the particular application being considered.

Table 7.31: Geared (SRM+HGT) Output Responsiveness Benefit Ratio as a Function of Torque Capacity and K

Torque (ft-lbf)	K=10	K=50	K=100	K=500	K=1000	K=2000
5210	0.15	0.45	0.61	0.89	0.94	0.97
15113	0.09	0.32	0.48	0.82	0.90	0.95
30682	0.06	0.22	0.36	0.74	0.85	0.92
50235	0.03	0.13	0.24	0.60	0.75	0.86
77431	0.02	0.10	0.18	0.52	0.69	0.81

To allow a deeper understanding of these results, Table 7.32 lists the distribution of inertia in the motor, gear train, and load as a function of torque capacity and using $K=2,000$. All of the inertia values are reflected to the output of the system. Key results from the table are that the dominant inertia depends on the torque capacity (i.e., the size of the system), and the load inertia becomes less significant as the size increases. Comparing the inertial distribution results of Table 7.15 (from the same size comparison) with those in Table 7.32 (same torque capacity comparison), it is evident that the load inertia is a larger percentage of the total geared system inertia when comparing geared and direct drive systems of the same torque capacity. Physically, this occurs due to the fact that, relative to the direct drive system, the geared system for the same torque comparison (Figure 7.7) is much smaller than the geared system for the same size comparison (Figure 7.6). This gives relatively lower absolute values of the motor and gear train reflected inertia (in same torque capacity comparison) and therefore the load inertia becomes more significant. Armed with this knowledge of the inertial content, the designer can improve the responsiveness of this geared system by reducing the inertial content of the dominant component. Figure 7.37 graphically displays the information in Table 7.32.

Table 7.32: Distribution of Inertia in the Motor, Gear Train, and Load as a Function of Torque Capacity (All inertia values are reflected to the output.)

Torque (ft-lbf)	Gear Ratio	Motor Inertia (%)	Gear Inertia (%)	Load Inertia for K=2000 (%)
5210	99	45	31	24
15113	100	29	56	15
30682	99	18	72	10
50235	101	10	84	6
77431	98	7	88	4

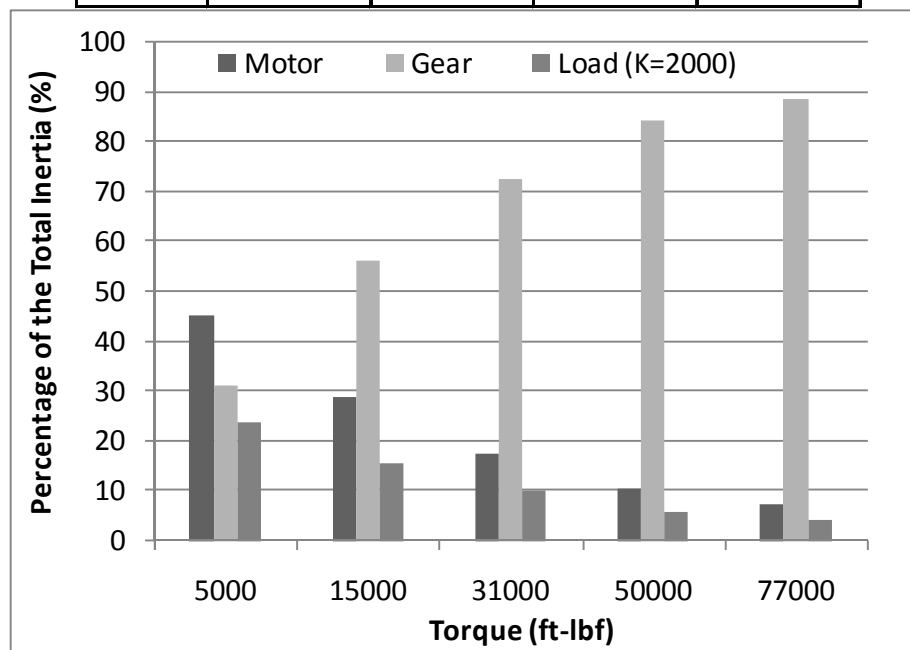


Figure 7.37: Percentage of Inertia in the Motor, Gear Train, and Load as a Function of Torque Capacity (for the SRM+HEGT actuator)

7.3.2.2 SRM (Direct Drive) vs. SRM+Star+PEGT (Geared)

Table 7.33 summarizes the values of the design and performance parameters of the direct drive SRM. The inertia values listed in the table include the inertia of the SRM shaft, rotor, and bearings and do not include any load inertia. These inertia values will be

used as the reference inertia for all of the responsiveness computations in this comparison. Table 7.34 gives the direct drive responsiveness as a function of torque capacity and the load to motor inertia ratio K.

Table 7.33: Direct Drive (SRM) Design and Performance Parameter Data Used for Comparison with Different Geared Systems (K=0)

Overall Diameter (inches)	Length (inches)	Aspect Ratio	Torque (ft-lbf)	Weight (lbf)	Inertia (lbm-in ²)	Torque Density (ft-lbf/lbf)	Responsiveness (rad/sec ²)
32	19.3	0.6	4724	3057	9843	1.5	2225
45	26.9	0.6	17910	8222	51169	2.2	1623
56	33.9	0.6	45254	16396	161603	2.8	1298
63	38.0	0.6	71912	23175	287726	3.1	1159
73	43.9	0.6	128215	35665	590098	3.6	1007

Table 7.34: Direct Drive (SRM) Responsiveness (rad/sec²) as a Function of K

		K (Load to Direct Drive Motor Inertia Ratio)					
Torque (ft-lbf)	Reference Inertia (lbm-in ²)	10	50	100	500	1000	2000
4724	9843	202	44	22	4.4	2.2	1.11
17910	51169	148	32	16	3.2	1.6	0.81
45254	161603	118	25	13	2.6	1.3	0.65
71912	287726	105	23	11	2.3	1.2	0.58
128215	590098	92	20	10	2.0	1.0	0.50

Table 7.35 summarizes the values of the design and performance parameters of the SRM+Star+PEGT geared combination. A target gear ratio of 100 to 1 was used for all of the designs in the set. Figure 7.38 compares the torque density values in Table 7.27 and Table 7.35 and illustrates that the torque density of the geared system varies from approximately 9 to 18 times the torque density of the direct drive system (see the exact benefit ratios shown in Table 7.36).

Table 7.35: SRM+Star+PEGT Design and Performance Parameter Data (K=0)

Overall Diameter (inches)	Shell Diameter (inches)	Length (inches)	Aspect Ratio	Gear Ratio	Torque (ft-lbf)	Weight (lbf)	Inertia (lbm-in ²)	Torque Density (ft-lbf/lbf)	Input Responsiveness (rad/sec ²)	Output Responsiveness (rad/sec ²)
10	10.0	10	1.0	100	4724	166	58	29	3770	37.7
15	13.7	15	1.0	100	17910	517	355	35	2342	23.4
20	17.2	20	1.0	100	45254	1177	1343	38	1564	15.6
25	19.5	25	1.0	100	71913	2202	3752	33	893	9.0
30	22.4	30	1.0	100	128215	3768	9073	34	658	6.6

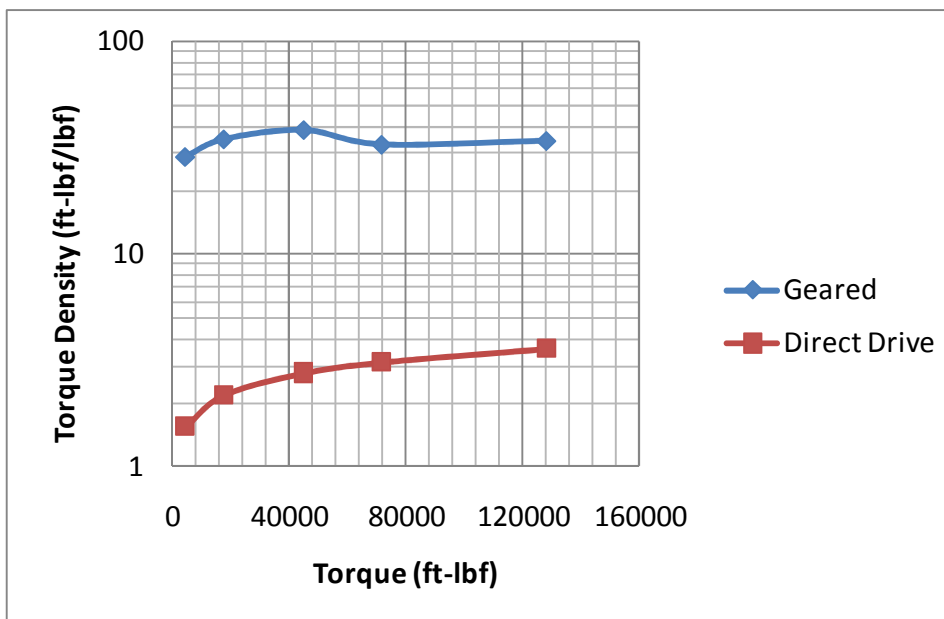


Figure 7.38: Comparison of Torque Density Between the Geared (SRM+Star+PEGT) and Direct Drive (SRM) Systems

Table 7.36: Comparison of Torque Density Between the Geared (SRM+Star+PEGT) and Direct Drive (SRM) Systems

Torque (ft-lbf)	Direct Drive Torque Density (ft-lbf/lbf)	Geared Torque Density (ft-lbf/lbf)	Torque Density Benefit Ratio
4724	1.5	29	18
17910	2.2	35	16
45254	2.8	38	14
71912	3.1	33	11
128215	3.6	34	9

Figure 7.39 and Figure 7.40 compare the output responsiveness of the direct drive and geared systems as a function of the load to motor inertia ratio K for the highest torque setting of about 128,000 ft-lbf. The first figure gives the responsiveness for values of K up to 500, and the second figure gives results for the full range of K considered.

Similar to the results from the SRM+HGT combination, the key result is that the direct drive system is more responsive than the geared system up to a particular value of K . The physical reasoning behind this result was explained in the previous section. In the limit as K becomes large, the load inertia dominates the motor and gear train reflected inertia in the geared system and the motor inertia in the direct drive system. Then, the geared systems and direct drive systems have the same torque capacity (given the assumption in this example) accelerating practically the same inertia. Thus, the direct drive system is superior in terms of output responsiveness until a particular value of K is reached, after which both systems will accelerate the load at the same rate.

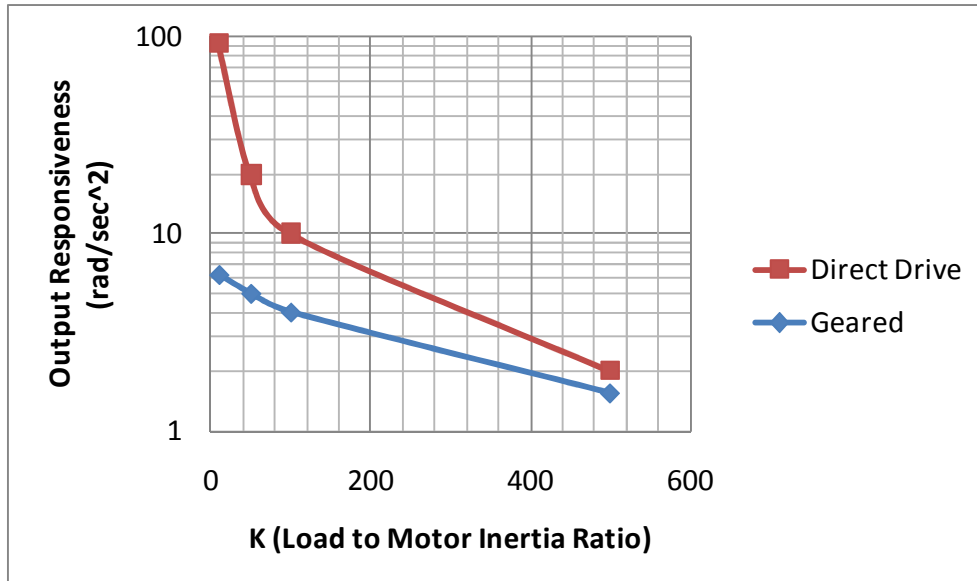


Figure 7.39: Geared (SRM+Star+PEGT) and Direct Drive (SRM) Output Responsiveness as a Function of K (for lower range of K and highest torque value)

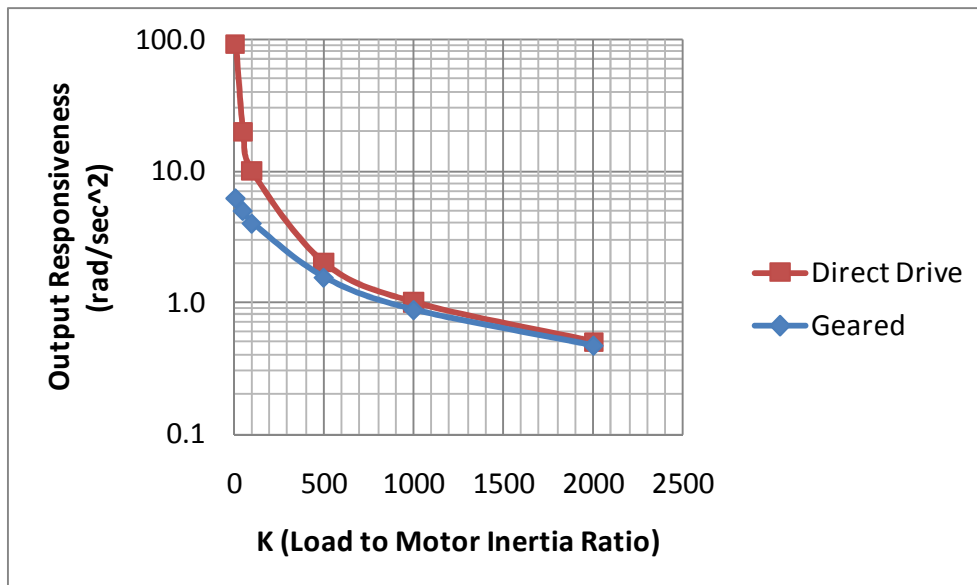


Figure 7.40: Geared (SRM+Star+PEGT) and Direct Drive (SRM) Output Responsiveness as a Function of K (for full range of K and highest torque value)

Table 7.37 provides the values of the ratio of the geared responsiveness to the direct drive responsiveness as a function of the torque capacity and the K value (the same information as in Figure 7.40). Considering the lowest torque capacity of 4,724 ft-lbf as an example, the ratio of the geared to direct drive responsiveness reaches approximately 90% (or 0.9) for a K value near 500. This value of K gives a load inertia equivalent to a point weight of 30,570 pounds (10 times the direct drive motor weight) located at a distance of 80 inches (6.7 feet) away from the axis of rotation.

Table 7.37: Geared (SRM+Star+PEGT) Output Responsiveness Benefit Ratio as a Function of Torque Capacity and K

Torque (ft-lbf)	K=10	K=50	K=100	K=500	K=1000	K=2000
4724	0.16	0.47	0.64	0.90	0.95	0.97
17910	0.14	0.43	0.60	0.88	0.94	0.97
45254	0.12	0.38	0.55	0.86	0.92	0.96
71912	0.08	0.28	0.44	0.80	0.89	0.94
128215	0.07	0.25	0.40	0.77	0.87	0.93

Table 7.38 lists the distribution of inertia in the motor, gear train, and load as a function of torque capacity and using K=2,000. All of the inertia values are reflected to the output of the system. As before, the key results from the table are that the dominant inertia depends on the torque capacity (i.e., the size of the system), and the load inertia becomes less significant as the size increases. When comparing Table 7.38 (for the SRM+Star+PEGT) with Table 7.32 (for the SRM+HGT), the former generally has larger motor and load inertial percentage when compared to the latter. Figure 7.41 graphically displays the information in Table 7.38.

Table 7.38: Distribution of Inertia in the Motor, Gear Train, and Load as a Function of Torque Capacity (All inertia values are reflected to the output.)

Torque (ft-lbf)	Gear Ratio	Motor Inertia (%)	Gear Inertia (%)	Load Inertia for K=2000 (%)
4724	100	47	27	25
17910	100	38	39	22
45254	100	33	48	19
71912	100	23	64	13
128215	100	19	69	12

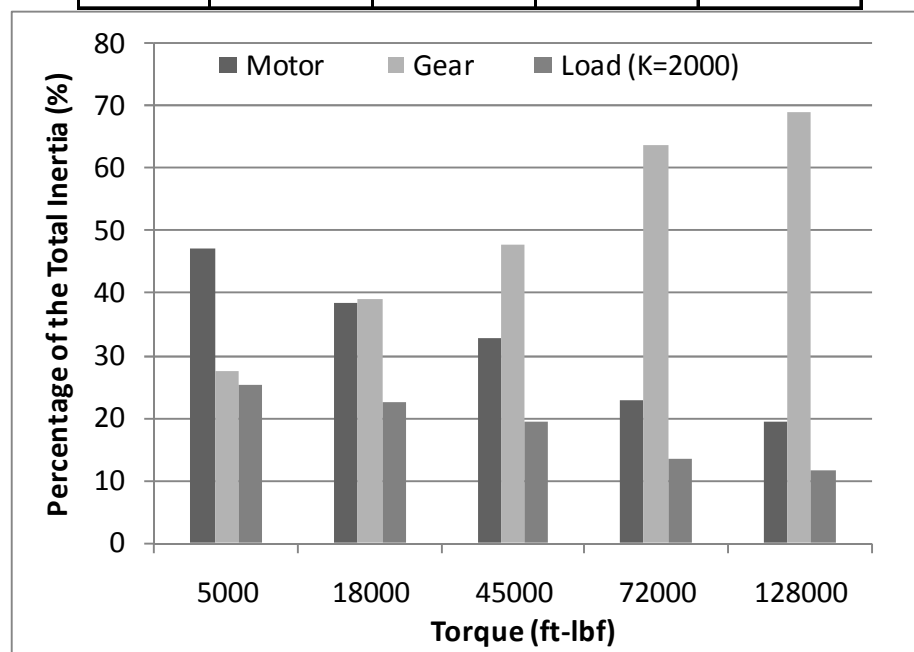


Figure 7.41: Percentage of Inertia in the Motor, Gear Train, and Load as a Function of Torque Capacity (for the SRM+Star+PEGT actuator)

7.3.2.3 SRM (Direct Drive) vs. SRM+Star Compound+PEGT (Geared)

Table 7.39 summarizes the values of the design and performance parameters of the direct drive SRM. The inertia values listed in the table include the inertia of the SRM shaft, rotor, and bearings and do not include any load inertia. These inertia values will be

used as the reference inertia for all of the responsiveness computations in this comparison. Table 7.40 gives the direct drive responsiveness as a function of torque capacity and the load to motor inertia ratio K.

Table 7.39: Direct Drive (SRM) Design and Performance Parameter Data Used for Comparison with Different Geared Systems (K=0)

Overall Diameter (inches)	Length (inches)	Aspect Ratio	Torque (ft-lbf)	Weight (lbf)	Inertia (lbm-in ²)	Torque Density (ft-lbf/lbf)	Responsiveness (rad/sec ²)
32	19.0	0.6	4400	2900	9017	1.5	2262
44	26.4	0.6	16640	7784	46711	2.1	1652
55	33.3	0.6	41988	15506	147251	2.7	1322
62	37.3	0.6	66598	21886	261562	3.0	1181
72	43.1	0.6	118672	33666	536008	3.5	1027

Table 7.40: Direct Drive (SRM) Responsiveness (rad/sec²) as a Function of K

		K (Load to Direct Drive Motor Inertia Ratio)					
Torque (ft-lbf)	Reference Inertia (lbm-in ²)	10	50	100	500	1000	2000
4400	9017	206	44	22	4.5	2.3	1.13
16640	46711	150	32	16	3.3	1.7	0.83
41988	147251	120	26	13	2.6	1.3	0.66
66598	261562	107	23	12	2.4	1.2	0.59
118672	536008	93	20	10	2.0	1.0	0.51

Table 7.41 summarizes the values of the design and performance parameters of the SRM+Star Compound+PEGT geared combination. A target gear ratio of 100 to 1 was used for all of the designs in the set. Figure 7.42 compares the torque density values in Table 7.27 and Table 7.41 and illustrates that the torque density of the geared system varies from approximately 10 to 21 times the torque density of the direct drive system (see the exact benefit ratios shown in Table 7.42).

Table 7.41: SRM+Star Compound+PEGT Design and Performance Parameter Data (K=0)

Overall Diameter (inches)	Shell Diameter (inches)	Length (inches)	Aspect Ratio	Gear Ratio	Torque (ft-lbf)	Weight (lbf)	Inertia (lbm-in ²)	Torque Density (ft-lbf/lbf)	Input Responsiveness (rad/sec ²)	Output Responsiveness (rad/sec ²)
10	9.8	10	1.0	101	4400	140	54	31	3734	37.1
15	13.4	15	1.0	100	16640	445	335	37	2300	23.0
20	16.9	20	1.0	100	41988	1018	1237	41	1572	15.7
25	19.1	25	1.0	100	66598	1892	3528	35	879	8.8
30	21.8	30	1.0	101	118670	3264	8192	36	667	6.6

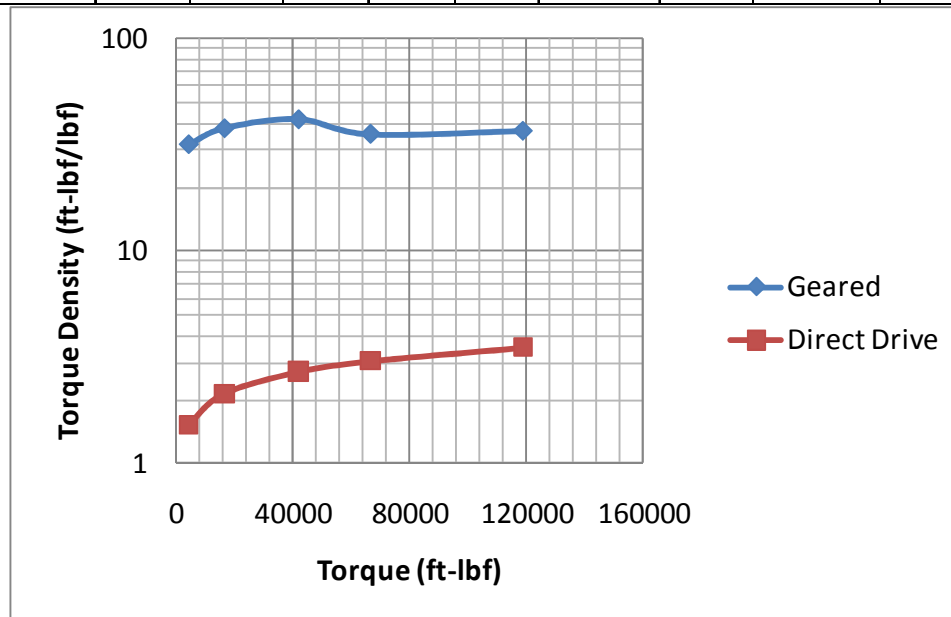


Figure 7.42: Comparison of Torque Density Between the Geared (SRM+Star Compound+PEGT) and Direct Drive (SRM) Systems

Table 7.42: Comparison of Torque Density Between the Geared (SRM+Star Compound+PEGT) and Direct Drive (SRM) Systems

Torque (ft-lbf)	Direct Drive Torque Density (ft-lbf/lbf)	Geared Torque Density (ft-lbf/lbf)	Torque Density Benefit Ratio
4400	1.5	31	21
16640	2.1	37	17
41988	2.7	41	15
66598	3.0	35	12
118672	3.5	36	10

Figure 7.43 and Figure 7.44 compare the output responsiveness of the direct drive and geared systems as a function of the load to motor inertia ratio K for the highest torque setting of about 119,000 ft-lbf. The first figure gives the responsiveness for values of K up to 500, and the second figure gives results for the full range of K considered. Similar to the results from the SRM+HGT and SRM+Star+PEGT combinations in the previous sections, the key result is that the direct drive system is more responsive than the geared system, with the geared system “catching up” as the value of K becomes large.

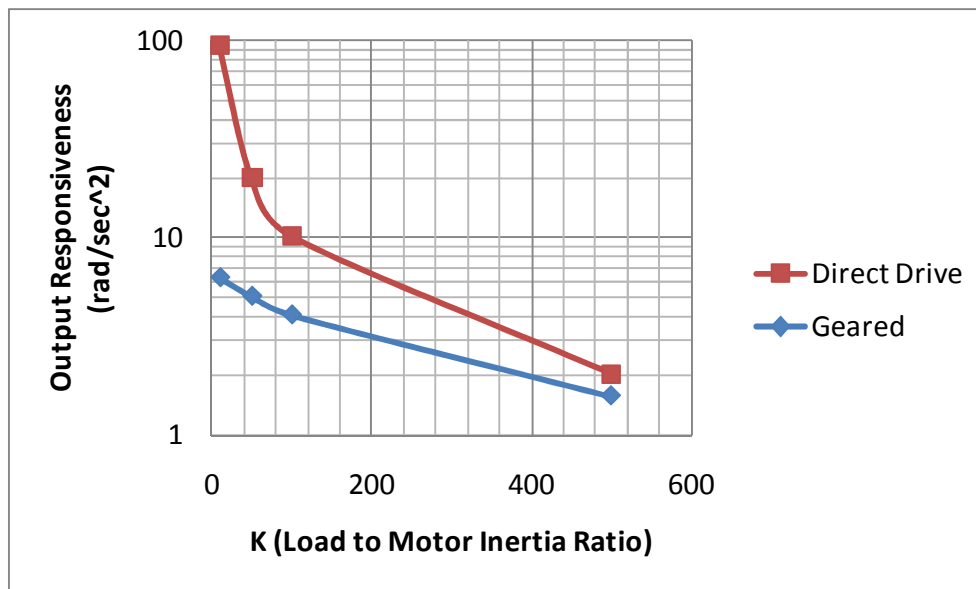


Figure 7.43: Geared (SRM+Star Compound+PEGT) and Direct Drive (SRM) Output Responsiveness as a Function of K and Gear Ratio (for lower range of K and highest torque value)

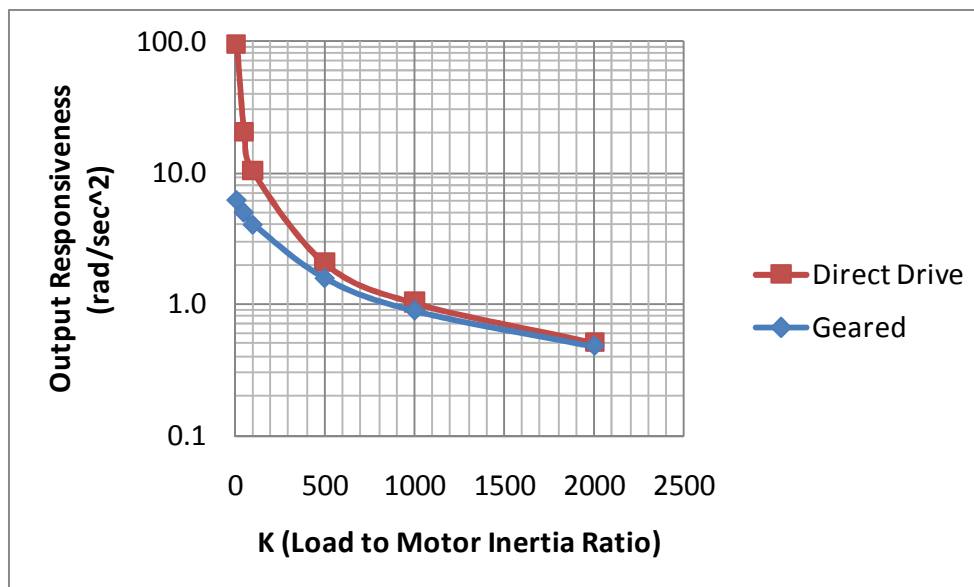


Figure 7.44: Geared (SRM+Star Compound+PEGT) and Direct Drive (SRM) Output Responsiveness as a Function of K and Gear Ratio (for full range of K and highest torque value)

Table 7.43 provides the values of the ratio of the geared responsiveness to the direct drive responsiveness as a function of the torque capacity and the K value (the same information as in Figure 7.44). Considering the lowest torque capacity of 4,400 ft-lbf as an example, the ratio of the geared to direct drive responsiveness reaches approximately 90% (or 0.9) near a K value of 500. This value of K gives a load inertia equivalent to a point weight of 29,000 pounds (10 times the direct drive motor weight) located at a distance of 80 inches (6.7 feet) away from the axis of rotation.

Table 7.43: Geared (SRM+Star Compound+PEGT) Output Responsiveness Benefit Ratio as a Function of Torque Capacity and K

Torque (ft-lbf)	K=10	K=50	K=100	K=500	K=1000	K=2000
4400	0.15	0.46	0.63	0.89	0.94	0.97
16640	0.13	0.42	0.59	0.88	0.93	0.97
41988	0.12	0.38	0.55	0.86	0.92	0.96
66598	0.08	0.28	0.43	0.79	0.88	0.94
118672	0.07	0.25	0.40	0.77	0.87	0.93

Table 7.44 lists the distribution of inertia in the motor, gear train, and load as a function of torque capacity and using K=2,000. All of the inertia values are reflected to the output of the system. As before, the key results from the table are that the dominant inertia depends on the torque capacity (i.e., the size of the system), and the load inertia becomes less significant as the size increases. When comparing Table 7.44 (for the SRM+Star Compound+PEGT) with Table 7.38 (for the SRM+Star+PEGT), both the former and the latter have very similar inertial distributions (as expected due to the identical gear ratios and sizes). Figure 7.45 graphically displays the information in Table 7.44.

Table 7.44: Distribution of Inertia in the Motor, Gear Train, and Load as a Function of Diameter and Gear Ratio (All inertia values are reflected to the output.)

Torque (ft-lbf)	Gear Ratio	Motor Inertia (%)	Gear Inertia (%)	Load Inertia for K=2000 (%)
4400	101	47	29	25
16640	100	37	41	22
41988	100	32	48	19
66598	100	22	65	13
118672	101	19	70	11

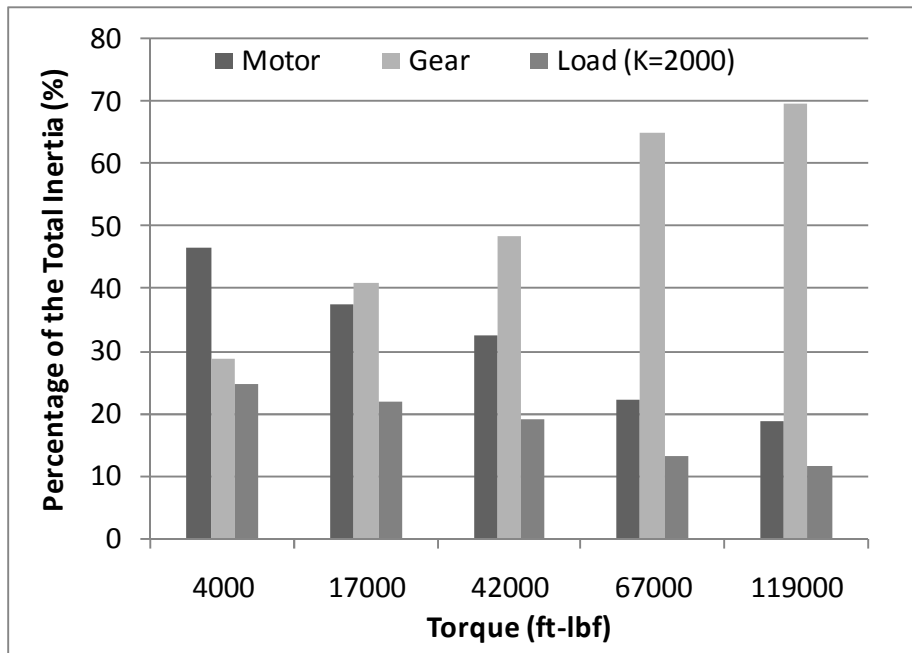


Figure 7.45: Percentage of Inertia in the Motor, Gear Train, and Load as a Function of Torque Capacity (for the SRM+Star Compound+PEGT actuator)

7.3.2.4 Example 2 Discussion of Results

For the range of diameters (10 to 30 inches) and gear ratios considered in this example, the geared systems had approximately 10 to 20 times higher torque density than a direct drive system of the same torque capacity based on the SRM. Just as for example 1, this superiority of the torque density for the geared system occurs due to the different load-carrying means in each system. Collectively, Examples 1 and 2 confirm the intuitive notion that any geared system should be superior to a direct drive system in terms of torque density when comparing systems of the same size or the same torque capacity. This result is independent of the load to motor inertia ratio K and only depends upon the motor and gear train torque and weight relationships provided in Chapter 3.

Example 1 showed that (for a given size) there exists a value of K for which the geared system becomes superior to the direct drive system in terms of output

responsiveness. However, Example 2 has shown that (for a given torque capacity) the direct drive system will generally provide higher output responsiveness than the geared system. In the limit as the load inertia becomes large relative to any motor and gear train reflected inertia (i.e., as K becomes large), both the geared and direct drive systems will have similar output responsiveness. The comparisons in Example 2 are consistent with the stated superiority of direct drive systems discussed in the quote from the motor manufacturer's catalog provided in the introduction to this chapter.

Considering the inertial distribution between motor, gear train, and load for the geared systems, the load inertia was generally a more significant component for Example 2 (same torque assumption) than Example 1 (same size assumption). This occurred because the geared system is much smaller than the direct drive system in Example 2 (recall that the geared and direct drive systems were the same size for Example 1), but both systems were coupled with the same relatively larger direct drive reference inertia.

7.4 OTHER GEARED SYSTEM CONSIDERATIONS

While the examples of this chapter have compared direct drive and geared systems based on their torque density and responsiveness characteristics, other issues should be considered when comparing these systems for a specific application. Using a geared system generally introduces the issues of backlash, lost motion, and clearance due to the gear teeth, but these issues can be managed by controlling the relative height and width of the gear teeth. Geared systems will typically exhibit less lost motion than a direct drive system. Geared systems will typically involve more bearings, shafts, and support structures and could be considered more complex than a direct drive system. The stiffness of a geared system is generally determined by the gear tooth contacts, principal bearings, and support structure, while the stiffness of a direct drive system is dependent

on the air gap forces between the rotor and the stator. The geared system will typically have much higher stiffness than a direct drive system, and numerical comparisons based on finite element analysis are suggested for quantifying this benefit. Considering cost, geared and direct drive systems of the same size should have similar cost if it can be assumed that cost is approximately proportional to weight. While motors are generally considered standard off-the-shelf components with well-established, low cost manufacturing techniques, the cost of manufacturing the unique circular arc gear teeth used in the HGT and PEGT is still under investigation.

7.5 EFFECT OF OUTPUT SPEED ON RESPONSIVENESS

The output speed of all the actuator designs in this chapter was held constant, and the reasoning behind this assumption is explained here. The usual approach when designing a motor or gear train is to maximize its torque density (which results in the minimum weight) and then determine if the desired operating speeds do not violate any material limits for the motor, gear train, bearings, and other components in the actuator. Running motors, gear trains, and bearings at higher speeds typically means higher frictional losses, and these losses are difficult to accurately quantify without physical testing.

Given the emphasis on maximizing the actuator torque density, there is typically a higher margin of safety (based on material strength limits) when comparing the rated speed with the maximum speed than when comparing the rated torque density with the maximum torque density. It is generally difficult to match these margins of safety, and for this reason, the maximum speed was not considered as a limiting criterion in this chapter. However, because the output speed can influence the results in specific applications (e.g., utilizing the PEGT in a relatively high speed application, which puts a

high demand on the bearings, see Section 5.2.3.1), the designer is advised to consider the speed-independent results of this chapter in conjunction with the specific operating speeds of the application in question for future analysis.

7.6 SUMMARY

This chapter has highlighted the important trade-off between torque density and responsiveness when choosing between direct drive and geared systems. Examples were presented in which direct drive and geared systems of the same size and the same torque capacity were compared. The examples presented considered systems built from off-the-shelf motors and gear trains and systems built from the motors and gear trains in the scope of this research. The similarity in the torque density and responsiveness trends observed for both types of systems serves to validate the results based on the SRM, HGT, and PEGT. These specific examples were chosen to cover two common comparison criteria of same size and same torque capacity, and it is anticipated that the Example 1 scenario of a fixed size requirement for the geared and direct drive systems will be the most useful in the future. The results in this chapter illustrate that the geared systems considered in this report should always have higher torque density than a direct drive system, and the specific values of the gear ratio and load inertia (or load to motor inertia ratio K as used here) dictate which of the two systems will provide higher output responsiveness.

Chapter 8 Development of a Minimum Set of Actuators

A primary goal of the RRG is to determine the minimum set of components (motors, gear trains, actuators, etc.) that achieve maximum market penetration for a particular application. It is desirable to enable the assembly of a maximum population of systems from a minimum set of these components. This chapter will define the concept of a minimum set of actuators by example and develop criteria with which to determine if a set of actuators is a minimum set for a given application. The concept will be illustrated with examples in which low cost, minimum sets of actuators based on the SRM+Star+PEGT actuator combination (see Section 3.10) will be developed for a hypothetical set of torque requirements. This chapter will illustrate how using common motor geometry (diameters and lengths) and different gear ratios for a range of different gear train sizes can result in low cost, minimum sets that have minimal performance trade-offs with respect to an optimum set of designs that do not share any common dimensions.

Relevant literature on existing product family design methods and the minimum set concept was discussed in the literature review of Chapter 2 (see Section 2.6), and it provides important background for further understanding the concepts in this chapter. Also, Vaculik and Tesar [2005] discuss how existing product family design methods can be used to develop electromechanical actuator families and measure the performance losses of reducing the size of a family (i.e., achieving a minimum set). Rios and Tesar [2008] discuss how to determine the minimum set of gear ratios and actuator sizes for the joints of a robotic manipulator such that it has sufficient end-effector force to accomplish a task and also exhibits minimum weight. They assumed that they had a finite population of actuators available and assessed the performance capabilities of different combinations

of the actuators (i.e., different minimum sets) from the population. They also solved the same problem with analytical formulations for actuator performance parameters as a function of the design parameters (based on the scaling rules presented in Chapter 5), which results in a practically infinite set of actuators limited by the granularity/tolerance of the numerical computations.

8.1 NEED FOR A MINIMUM SET

Consider an example in which there are 20 known and distinct actuator torque requirements for a particular application. To exactly meet these requirements, a designer would ideally design 20 different actuators with few or no common dimensions among them. Current product family design literature suggests that there are cost benefits if the designer designs only 10 actuators (for example) to meet the needs of the application. While there are marketing and business strategies for addressing this issue, this research aims to address it from a design point of view. Fewer different sizes of actuators means reduced manufacturing and certification costs (for the designer/manufacturer) and generally lower inventory costs and easier maintenance (for the customer/end-user). However, there is a performance loss incurred because the 10 available actuator torque capacities do not exactly match the 20 distinct torque requirements. Borrowing terminology from the product family literature, this concept of a minimum set extends the commonality among products in a family from a limited number of common design parameters settings to the point where the design parameters describing two designs are identical. When this occurs, two distinct designs in the family are effectively merged into one (Figure 8.1). The same trade-off between maximizing commonality (to reduce costs) while minimizing the resulting performance losses evident in the product family design

literature is also important when seeking a minimum set (i.e., minimizing the size of a family) of actuators.

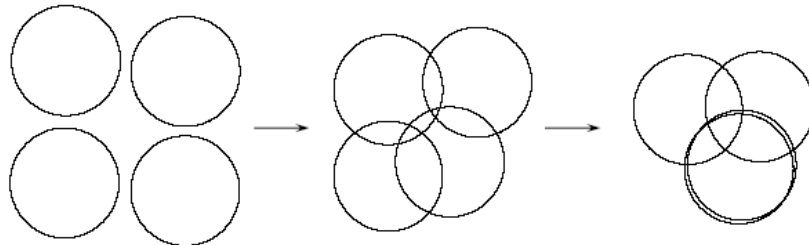


Figure 8.1: Illustration of Reducing the Size of a Family of Products to the Point Where Two Products are Merged into One [Fellini, Kokkolaras, and Papalambros, 2003]

8.2 MINIMUM SET LITERATURE

Product family design literature and its relevance to the current research were discussed in detail in Section 2.6 of the literature review of Chapter 2. This section is an extension of that in Chapter 2 and provides a brief summary of two product family design methods: the Commonality Decision Method (CDM) and an extension of the CDM. The latter provides a framework for reducing the size of a family of products and achieving a minimum set. While many of the product family design methods reviewed in the literature allowed the family size to be varied, the method described below is one of the few that was found that specifically addressed the minimum set problem.

The Commonality Decision Method (CDM) [Fellini et. al., 2005] features the formulation of the commonality decision (constrained optimization) problem extended from Nelson, Parkinson, and Papalambros [2001]. The objective is to maximize commonality among a product family while maintaining a user-defined level of performance loss compared to individually-optimized designs (that have no commonality). Commonality is achieved by attempting to share as many parameters as possible among the products in the family. The commonality decision problem can

mathematically be summarized in the commonly used constrained optimization representation.

$$\text{Maximize } \sum_{p,q} |S_{pq}| - \sum_{p,q} D_{\alpha}(x_i^p - x_i^q)$$

subject to :

$$g^p(x^p) \leq 0$$

$$h^p(x^p) = 0$$

$$f^p(x^p) \geq (1 - L^p(\delta))f^{p^o}$$

where

S_{pq} = set of possible shared variables

x^p = vector of design variables for product p

Eqn. 187

D_{α} = function measuring commonality

$D_{\alpha} = 0$ if variable x_i is shared between products p and q

$D_{\alpha} = 1$ otherwise

p, q = index of current product

g^p = inequality constraints for product p

h^p = equality constraints for product p

f^p = objective function for product p, converted to a constraint

f^{p^o} = optimum value of the objective function for product p

As initially posed, the commonality decision problem is combinatorial due to the presence of both continuous design variables and discrete commonality decision variables, which specify how variables are shared among the products in a family. The combinatorial problem is then relaxed to yield a continuous problem that can be solved with a gradient-based optimization algorithm. The steps of this method are as follows.

1. Determine the optimal (null) platform design for each product by solving individual product optimization problems with no assumed commonality among the products.
2. Identify the variables that could be shared among products.

3. Determine the amount of performance loss that is acceptable for each of the products.
4. Formulate and solve the commonality decision problem.
5. Based on the results of step 4, select the variables to be shared among products in the family.
6. Formulate and solve the multi-objective product family design problem, which combines the individual product design problem from step 1.

This and other works by Fellini are the only ones found in the literature that allow the designer to specify an acceptable performance loss prior to solving a product family optimization problem. Figure 8.2 provides example results from the application of this method and illustrates how performance losses are incurred as more variables are shared among a family of products.

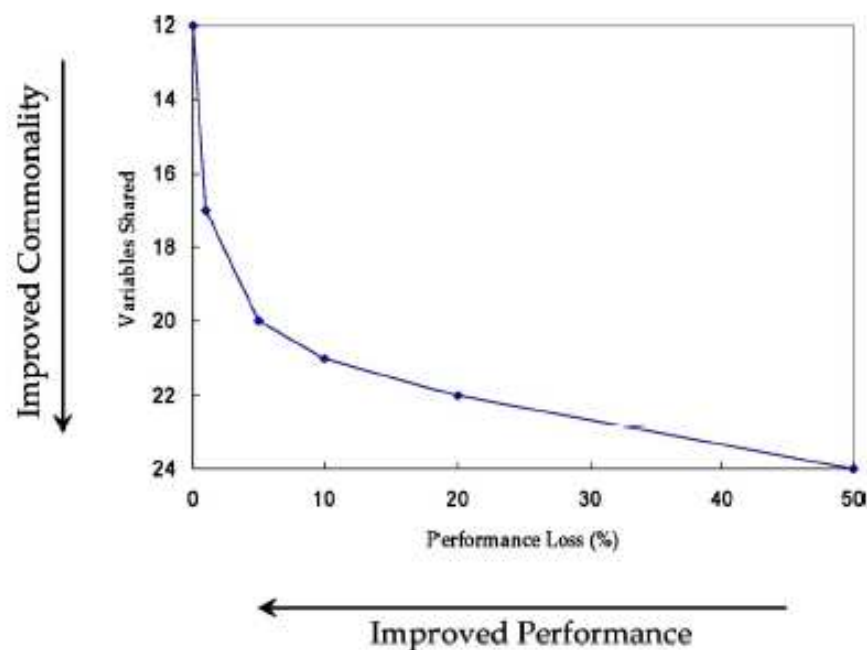


Figure 8.2: Example Results for the CDM, Illustrating the Performance Loss Due to the Sharing of Parameters Between Product Designs in a Family

Fellini, Kokkolaras, and Papalambros [2003] extend the CDM described above with a portfolio reduction problem. The portfolio reduction problem and commonality decision problem are solved in a nested loop so that the product portfolio (number of products) is reduced while attempting to maximize commonality between products in the family and maintain a user-defined performance loss. Example results illustrating how the performance loss (δ) increases as the number of products (P) is reduced are shown in Figure 8.3.

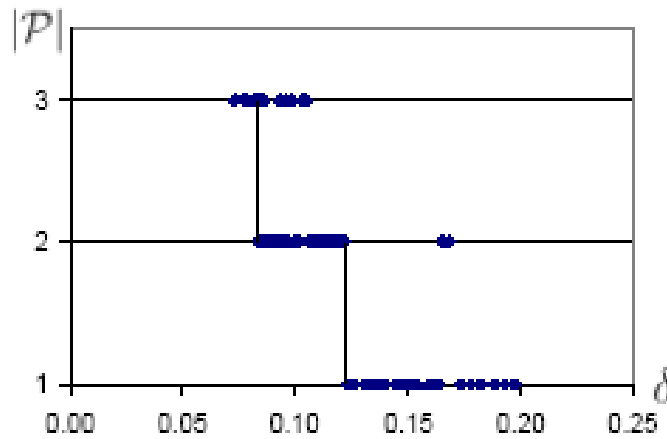


Figure 8.3: Number of Products (P) vs. Performance Loss (δ) due to Sharing Parameters Among Products in a Family

During the design process, the set of products is not reduced in number until the maximum level of sharing is achieved for a given performance loss. This was one of the few product family design methods found in the literature that dealt with efficiently reducing the size of a product family. The designer inputs to the method include the acceptable performance loss for each product in the family, the desired number of products, and the criteria used to determine which variables should be made common. The steps of this method are as follows.

1. Determine the allowable performance loss functions for each of the products.
2. Define the desired reduced portfolio size.
3. Solve the nested loop of the portfolio reduction and commonality decision problems.
4. Based on the results of Step 3, determine the variables to be shared.
5. Optimize the product portfolio, using the platform determined in Step 4.

This particular method and the examples presented in this chapter (Sections 8.5 and 8.6) should be used as a starting point to develop actuators product families (for different applications) and reduce their size with the goal of developing low cost minimum sets. Eventually, a minimum set module should be added to the actuator design procedure (discussed in Chapter 4 and shown in Figure 4.3) and integrated into the actuator design computational tool (Appendix A1).

8.3 MINIMUM SET CRITERIA

In order to determine if a set of actuators is a “minimum” set, criteria must be introduced to evaluate sets of actuators against each other for a given application. Thevenot et al. [2007] suggest the use of both performance and cost criteria in the selection of a product line (i.e., a minimum set) and apply their method to select the best product line of a family of staplers.

The performance parameters that describe each actuator in a set (torque, weight, inertia, torque density, and responsiveness) can be used as performance criteria, and these individual parameters can also be combined in order to define some other useful criteria. A preliminary list of performance-related criteria that can be used to describe a set of actuators includes the following:

- performance deviation/loss,
- combined weight of the actuators,
- number of distinct actuator designs,
- number of distinct gear train designs, and
- number of distinct motor designs.

The performance deviation/loss (P_l) can be defined as the difference between the actual, as-designed performance of an actuator (P_a) and the target performance based on the application requirements or a reference set of requirements (P_r).

$$P_l = P_a - P_r \quad \text{Eqn. 188}$$

It is useful to normalize this loss value and express it as a percentage difference (P_{ln}) using the following relationship.

$$P_{ln} = 100 \times \left(\frac{P_a - P_r}{P_r} \right) \quad \text{Eqn. 189}$$

This performance loss relationship will be used in Sections 8.5 and 8.6 to compare the torque, weight, inertia, torque density, and responsiveness of alternative minimum sets of actuators.

If different actuators in a set are being used in independent locations in a system, then the effectiveness (measured by P_l or P_{ln}) of each individual actuator in the set in meeting its target performance would be an important performance metric. The combined weight of the actuators in a set is a useful metric when the entire family of actuators is used in one system, such as in a robotic manipulator.

In addition to the performance-related criteria listed above, various cost criteria (inventory, materials, manufacturing, assembly, certification, and business/marketing costs) can also be used to distinguish between sets of actuators, but these are often difficult to analytically model. However, some assumptions can be made regarding the

correlation between the performance and cost criteria, and these assumptions will allow the present research to avoid developing any cost models. First, it can be reasonably assumed that minimizing the number of distinct components in a system (motors and gear trains in this actuator context) will generally reduce all of these costs. Second, some past RRG research partners have suggested that weight is a good surrogate (indicator) for cost. That is, if a designer knows the weight of a system and its material composition (primarily steel, plastic, etc.), then its cost can be reasonably estimated without too much regard for the specifications and design details for the system's internal components.

It is anticipated that each application domain will have its own unique minimum set requirements and that the criteria above should be useful to measure the anticipated performance losses. For example, robotic manipulator actuators generally must run at low speeds and have high torque density. Vehicle drive wheel actuators generally must run at higher speeds and have high responsiveness/acceleration capability. There may be some crossover such that actuators designed for one application nearly match the needs of another application. Additional criteria may need to be introduced for this scenario.

8.4 LOW COST MINIMUM SET FEATURES

This chapter will focus on the development of possible low cost, minimum set alternatives based on a hypothetical set of torque requirements. The cost criteria listed above will not be modeled analytically, but it will be assumed that a smaller number of distinct motor, gear train, and actuators designs (and the use of as many common parameters as possible) will generally reduce cost. The proposed minimum sets will be based upon the SRM+Star+PEGT actuator combination (Figure 8.4) used throughout this research. It will be used as an example because it easily illustrates design features that can be used to develop a low cost minimum set.

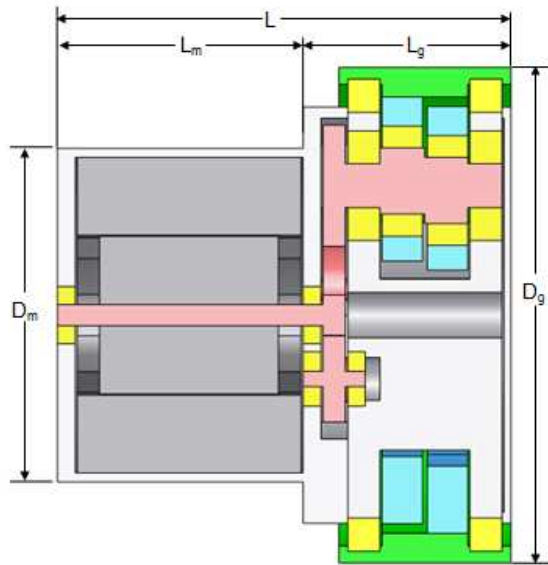


Figure 8.4: SRM+Star+PEGT Actuator

Several design features for achieving a low cost minimum set have been identified and will be elaborated upon in this section. The first two features, the use of common motor diameters and variable 1st stage gear ratios, will be focused on in the examples that follow this section. Collectively, all of these features allow a set of actuator designs to meet the application requirements of a large population of systems with a minimum number of distinct parts and without significantly changing the geometry of the motor and gear train.

8.4.1 Common Motor Diameters

To meet a specific motor torque requirement, the motor designer generally has the choice of the motor diameter and the motor length. Because motor rotor and stators are typically made up of stacks of laminations, once a given diameter lamination is available, a motor of any length can be built by simply using a different number of laminations. Due to this common manufacturing practice, it is generally very cost effective to vary

only the motor length and maintain constant diameter (rather than using a fixed length and variable diameters) when seeking to meet a range of motor torque requirements. Figure 8.5 conceptually illustrates how the motor diameter can be held constant and only the motor length be varied to achieve an increased motor torque capacity. In the figure, the bold lines represent a baseline design, and the dashed lines represent how the gear train and motor sizes change as the gear train/actuator torque capacity increases. If the gear ratio is held constant (as was done for many of the gear train scaling rules in Chapters 5 and 6), the motor torque capacity increases as the gear train torque capacity increases, so the motor must increase in length to meet the higher torque requirement.

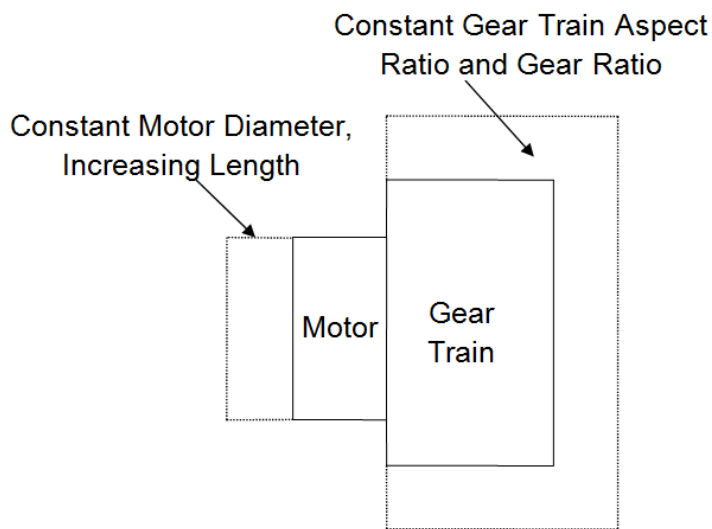


Figure 8.5: Illustration of Motor and Gear Train Size Variation as the Gear Train (Actuator) Torque Capacity is Increased (constant motor diameter and variable motor length)

8.4.2 Variable 1st Stage Gear Ratio

While the PE-output gear mesh in the PEGT utilizes the relatively more expensive circular arc gear teeth, the 1st stage star gear train (Figure 8.6) utilizes standard involute gear teeth. Because involute gears of various sizes can be obtained at a relatively low

cost, the gear ratio can be changed by simply modifying the size of the input shaft, idler shaft, and crankshaft gears. This gear ratio change will remain a low cost option if 1) the center distance between the input shaft and crankshaft centerlines (a parameter that affects the load capacity of the overall gear train, see Section 5.2.3.2) can be maintained as a constant and if 2) the same bearing sizes can be used for the different gear ratio values. As long as the PE-output gear mesh specifications remain constant, the torque capacity, weight, stiffness, and torque density ratings for the collective system will remain essentially constant. Note that for a fixed output speed, increasing (decreasing) the gear ratio will also increase (decrease) the motor speed. Finally, if the star gear train is not capable of reaching the desired gear ratio, it can also be replaced with a star compound gear train (see Section 3.10), which is capable of providing higher gear ratios. This is an additional low cost modification because it only involves one extra gear stage on the idler shaft gear, a longer shell of the same diameter, and no extra parts or bearings.

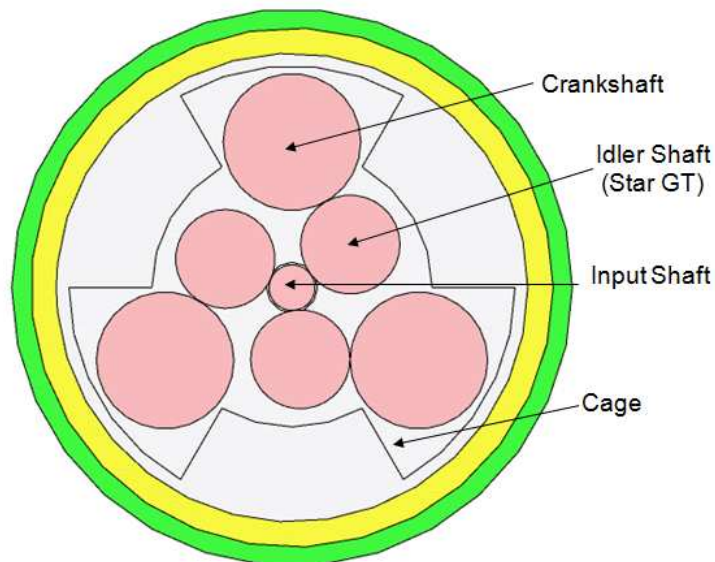


Figure 8.6: Star Gear Train (1st Stage) for PEGT

Similar to Figure 8.5, Figure 8.7 illustrates how the motor diameter and length can be held constant as the gear train torque capacity is increased. If the gear ratio is increased appropriately as the gear train torque capacity and size increases, then it is possible to maintain the motor torque requirement at a constant value for a range of increasing gear train sizes. Numerical results illustrating the conceptual changes in motor and gear train sizes in Figure 8.5 and Figure 8.7 will be provided in the examples in Section 8.5.

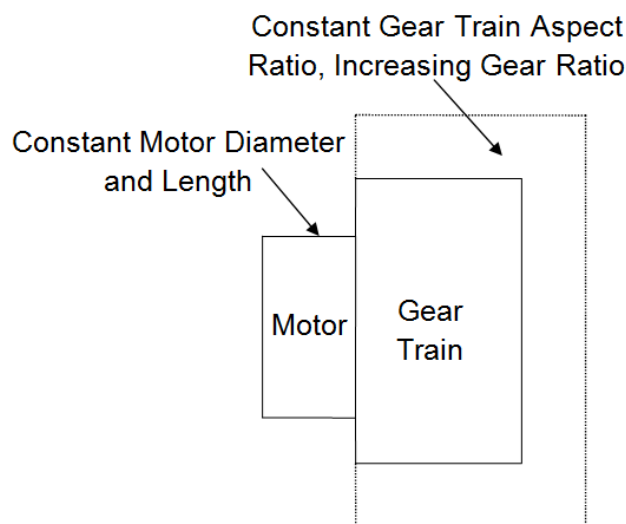


Figure 8.7: Illustration of Motor and Gear Train Size Variation as the Gear Train Torque Capacity is Increased (constant motor diameter and length)

One important assumption associated with changing the 1st stage gear ratio involves the power ratings of the gear train and motor. If the output torque and speed are held constant, then the output power available from the gear train is also constant. Now, if the gear ratio of the 1st stage is increased without changing the size, torque capacity, or speed output of the PE-output gear geometry (as was done in this chapter), then the required motor torque is reduced, and the motor speed is increased. If a smaller motor is

chosen (to balance the motor and gear train torque capacities) and to save weight, then the designer should verify that the motor power rating can remain constant despite a reduction in its size.

8.4.3 Common Gear Train Diameters

Like the motor designer, the gear train designer has the basic choices of the overall gear train diameter and length (which involves the pitch diameters and face widths of the individual gears) when seeking to achieve a torque requirement. Past RRG prototypes have revealed that the manufacturing of the circular arc gear teeth utilized in the HGT and PEGT can be costly. During this manufacturing process, a gear shaping tool is generated based upon the pitch diameters and tooth numbers for the gears being cut. The tool is generally only useful for cutting gears for a single diameter and tooth number specification so that more tools are needed to cut gears with different specifications. However, the single tool can be used to cut gears of any length (i.e., face width) so that gear trains of different length can be achieved simply by utilizing gear blanks of different lengths.

8.4.4 Moving from 3 to 6 Crankshafts

All of the PEGT designs specified in this report utilize 3 crankshafts, but preliminary analysis has shown that bearing-limited torque capacity can be doubled by moving from 3 to 6 crankshafts (Figure 8.8) and maintaining all the other parameters constant. This adds additional bearings (2 more bearing per crankshaft or 6 total) but all are identical to the bearings used for the existing 3 crankshafts. Also note that no additional idler shaft gears are necessary because the 3 idler shafts in the 3 crankshaft design above (Figure 8.6) can be used to drive the 3 additional crankshafts. When the

torque capacity of an existing PEGT design needs to be increased, this modification may be more cost effective than simply using a larger diameter 3 crankshaft design.

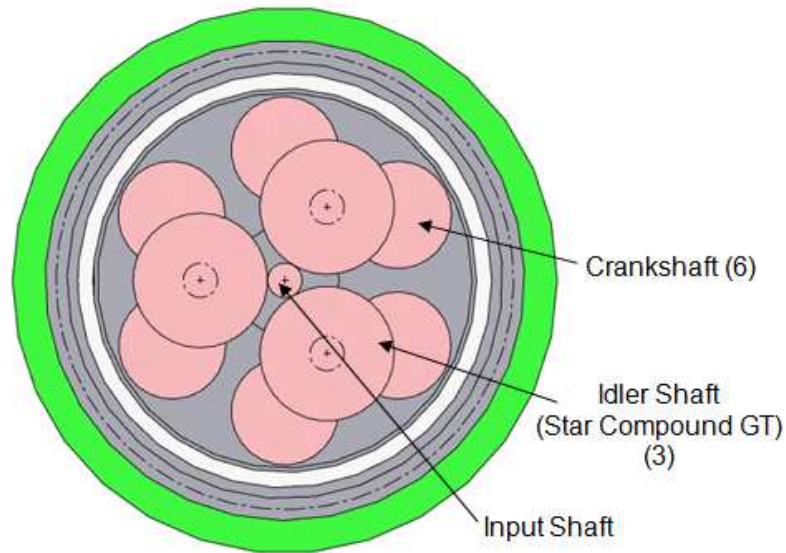


Figure 8.8: Star Compound Gear Train (1st Stage) for PEGT with 6 Crankshafts

8.4.5 Materials

The cost of the motor, gear train, and bearing materials are generally proportional to their strength and other desirable properties. Thus, swapping out motor, gear, and bearing components made of standard quality steel with components of the same size but made of higher quality steel will allow the same geometry to provide higher performance. The higher quality materials will always cost more, but the added benefit of being able to meet a wider variety of performance requirements may outweigh the increased costs. This is the basic notion of direct upgradability and downgradability.

8.5 EXAMPLE 1: ALTERNATIVE MINIMUM SETS

Table 8.1 lists a hypothetical set of torque requirements that will be utilized throughout this example. This and the following example in Section 8.6 will focus on

keeping the overall gear train size fixed (to meet the output torque requirement) and using variable motor geometry and 1st stage gear ratios to achieve low cost minimum sets. An alternative approach is to keep the motor geometry fixed (meaning a fixed motor torque) and vary the gear ratio and gear train size to achieve low cost minimum sets. The former approach based on a fixed gear train size is more representative of the common task of designing actuators to meet a set of known (torque) requirements. This approach allows the standardization of the potentially high cost gears in the PEGT (not including the 1st stage) and takes advantage of the low cost geometry modifications in the motor and 1st stage gear train.

Table 8.1: Actuator Torque Requirements¹⁹

Index	Torque (ft-lbf)
1	2000
2	4000
3	8000
4	12000
5	16000
6	20000
7	24000
8	28000
9	32000
10	36000

8.5.1 Reference Set of Actuator Designs

A reference set of actuators designs with no common motor diameters is needed to provide a baseline for comparison with the proposed minimum sets to be detailed in the following sections. The design parameter settings used to generate the reference set

¹⁹ The effect of output speed on the results presented in this chapter was not considered in detail. This is consistent with the focus on how the geometric parameters in the actuator (diameters, lengths, etc.) rather than the speed parameters affect the performance. For the purposes of this example, the output speed requirement for each of these actuators can be assumed to be identical. Thus, the output power requirement increases linearly with the increase in the torque.

of actuator designs is listed in Table 8.2. Different values of the gear ratio in the suggested range for the Star+PEGT could be considered for meeting the torque capacity requirements in Table 8.1. If the designer is seeking to minimize actuator weight and maximize torque density, he/she might use the maximum possible gear ratio. In this reference set of designs, a gear ratio of 141 to 1 was used for all the designs. This value is near the middle of the suggested range for this gear train (see the example in Section 6.6.2). This particular value was chosen to illustrate (in the minimum set alternatives in the next section) how varying the gear ratio above and below this value will allow a smaller number of distinct motor sizes to be used.

Table 8.2: Design Parameters for Reference Set

Parameter	Description	Value or Range
Gear Ratio (1 st Stage Star)	Constant	$g_1 = 4$ to 1
Gear Ratio (PE-Output Gear)	Constant	$g_{pe} = 35$ to 1
Gear Ratio (Overall)	Constant	$g = 140$ to 1
Overall Aspect Ratio	Constant	$A = 1.0$
Gear Train Aspect Ratio	Constant	$A_g = 0.4$
Motor Aspect Ratio	Variable	$0.5 < A_m < 0.9$
Motor to Overall Length Ratio	Constant	$K_l = 0.6$
Motor to Gear Train Diameter Ratio	Variable	$0.6 < K_d < 1.1$

In this reference set of designs, the motor diameter and length grow in proportion to the gear train diameter and length (Figure 8.9), and the overall aspect ratio is constant for every design in the set²⁰. Table 8.3 summarizes the resulting design and performance parameters for the reference set of actuators and illustrates that the desired torque

²⁰ In this reference set, the overall aspect ratio and gear train aspect ratio of each actuator in the set was held constant as the overall gear train diameter increased to meet the increasing torque requirements. However, the choice of the overall actuator diameter and length to meet the application requirements should in general depend on the needs of the end-user. For example, if the end-user wants to achieve different torque requirements with actuators of different length but the same overall diameter, the reference and minimum sets generated should be designed with this desire in mind. A suggested approach is to use a linear distribution of actuator lengths if length is the basic parameter of interest and a quadratic distribution of diameters if the diameter is the basic parameter.

requirements are met exactly. Since all of the motors have different diameters and lengths, there are a total of 12 distinct motor designs, which is the largest possible number for a set of 12 actuators. This set represents the most expensive set of actuators (in the context of this example) because none of the motor designs have been standardized. This is the set of actuators that might be delivered to the customer if cost was not a primary issue.

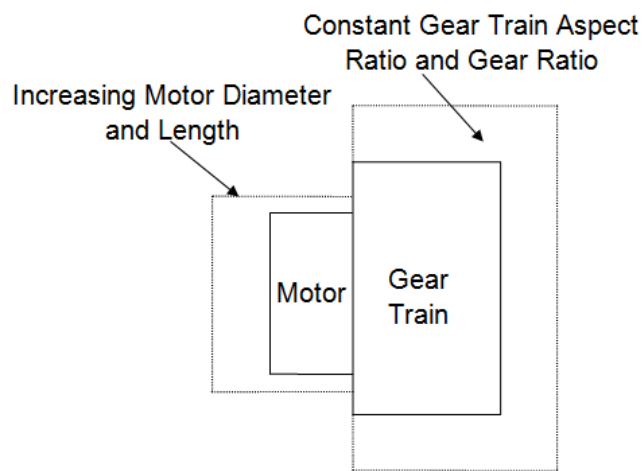


Figure 8.9: Illustration of Motor and Gear Train Size Variation as the Gear Train (Actuator) Torque Capacity is Increased (variable motor diameter and length)

Table 8.3: Design and Performance Parameters for the Reference Set (12 distinct motor diameters and fixed gear ratio and aspect ratio)

Overall Diameter (inches)	Motor Diameter (inches)	Length (inches)	Aspect Ratio	Gear Ratio	Torque (ft-lbf)	Weight (lbf)	Inertia (lbm-in ²)	Torque Density (ft-lbf/lbf)	Input Responsiveness (rad/sec ²)	Output Responsiveness (rad/sec ²)
6.0	6.4	6.0	1.0	141	1000	38	5	26	6236	44
7.5	7.3	7.5	1.0	141	2000	67	12	30	5521	39
9.5	8.2	9.5	1.0	141	4000	120	27	33	4861	35
10.9	8.9	10.9	1.0	141	6000	173	47	35	4231	30
12.0	9.3	12.0	1.0	141	8000	218	66	37	4017	29
13.7	10.2	13.7	1.0	141	12000	314	114	38	3472	25
15.1	10.8	15.1	1.0	141	16000	405	168	40	3141	22
16.2	11.3	16.2	1.0	141	20000	496	229	40	2876	20
17.3	11.7	17.3	1.0	141	24000	582	297	41	2667	19
18.2	12.1	18.2	1.0	141	28000	674	371	42	2487	18
19.0	12.4	19.0	1.0	141	32000	755	444	42	2377	17
19.8	12.6	19.8	1.0	141	36000	833	519	43	2289	16

Table 8.4 lists the SRM stator diameter, length, and other parameters that correspond to each design in Table 8.3. The motor diameter listed in Table 8.7 is the overall motor diameter including its housing.

Table 8.4: SRM Design and Performance Parameters for the Reference Set (12 distinct motor diameters and 12 motors total)

Stator Diameter (inches)	Stator Length (inches)	Aspect Ratio	Torque (ft-lbf)	Weight (lbf)	Inertia (lbm-in ²)	Torque Density (in-lbf/lbf)	Responsiveness (rad/sec ²)
6.1	3.3	0.5	7	18	4	5	7505
6.9	4.2	0.6	14	29	9	6	6999
7.9	5.3	0.7	29	48	20	7	6669
8.5	6.0	0.7	43	64	31	8	6433
9.0	6.7	0.7	58	79	43	9	6248
9.7	7.6	0.8	86	105	66	10	5987
10.3	8.4	0.8	114	129	91	11	5783
10.7	9.0	0.8	142	152	118	11	5619
11.2	9.6	0.9	173	175	147	12	5465
11.5	10.1	0.9	202	196	175	12	5349
11.8	10.6	0.9	229	215	202	13	5260
12.2	11.0	0.9	262	237	236	13	5148

8.5.2 Alternative Minimum Sets

Because it is possible to minimize costs by reducing the number of distinct motor sizes in the reference set, this section will present a series of minimum set options with

reduced numbers of distinct motor sizes. Minimum sets 1-5 will utilize different numbers of common motor diameters and a fixed gear ratio of 141 to 1 for every design in the set. Minimum sets 6-10 will utilize the same motor diameters as minimum sets 1-5 and a different gear ratio for every design in the set.

8.5.2.1 Choice of Common Motor Diameters

Table 8.5 lists the suggested common motor diameters (for minimum sets 1-5) that will be used for each distinct output torque requirement. The particular motor diameters chosen were calculated using average values of the motor diameters from the reference set. For example, considering minimum set #1, the common motor diameter of 6.8 inches for the first two designs comes from average of the 6.4 and 7.3 inch diameter motors of the reference set. Considering set #2, the common motor diameter of 7.3 inches for the first three designs comes from average of the 6.4, 7.3, and 8.2 inch diameter motors of the reference set. These motor diameters are in general free choices of the designer, and the average values used here are a good starting point unless the geometric constraints of an application dictate otherwise. The minimum set alternatives 1-5 are distinguished in the table by the number of distinct motor diameters used in each (from 6 distinct diameters for set 1 down to only 1 distinct diameter for set 5).

Table 8.5: Common Motor Diameter Choices for Minimum Set Alternatives 1-5

Gear Train Diameter (inches)	Output Torque (ft-lbf)	Motor Diameters (inches)					
		Reference Set (12 Motors)	Set 1 (6 Diameters)	Set 2 (4 Diameters)	Set 3 (3 Diameters)	Set 4 (2 Diameters)	Set 5 (1 Diameter)
6.0	1000	6.4	6.8	7.3	7.7	8.4	10.1
7.5	2000	7.3	6.8	7.3	7.7	8.4	10.1
9.5	4000	8.2	8.6	7.3	7.7	8.4	10.1
10.9	6000	8.9	8.6	9.5	7.7	8.4	10.1
12.0	8000	9.3	9.8	9.5	10.4	8.4	10.1
13.7	12000	10.2	9.8	9.5	10.4	8.4	10.1
15.1	16000	10.8	11.0	11.3	10.4	11.8	10.1
16.2	20000	11.3	11.0	11.3	10.4	11.8	10.1
17.3	24000	11.7	11.9	11.3	12.2	11.8	10.1
18.2	28000	12.1	11.9	12.4	12.2	11.8	10.1
19.0	32000	12.4	12.5	12.4	12.2	11.8	10.1
19.8	36000	12.6	12.5	12.4	12.2	11.8	10.1

Given these now common motor diameters, torque balancing between the motor and the gear train (see Section 6.3.1) can in general be achieved by varying the 1st stage gear ratio and motor length while keeping the motor diameter fixed for the range of gear train diameters suggested in Table 8.5.

8.5.2.2 Minimum Sets 1-5(Fixed 1st Stage Gear Ratio)

The gear train design parameter settings used to generate minimum sets 1-5 are listed in Table 8.6. Given these gear train parameters and the motor diameter choices in Table 8.5, the remaining design parameters and performance parameters can be computed.

Table 8.6: Gear Train Design Parameters for Minimum Sets 1-5

Parameter	Value
Gear Ratio (1 st Stage Star)	$g_1 = 4 \text{ to } 1$
Gear Ratio (PE-Output Gear)	$g_{pe} = 35 \text{ to } 1$
Gear Ratio (Overall)	$g = 140 \text{ to } 1$
Gear Train Aspect Ratio	$A_g = 0.4$

As an example, Table 8.7 summarizes the performance parameter results for minimum set #3, which has 3 distinct motor diameters and a fixed gear ratio and also

meets the distinct torque requirements listed in Table 8.1 above. This set of actuators is a potential minimum set because the common motor diameter of 7.7 inches was used for the first four gear train/actuator diameters in the set (i.e., diameters of 6, 8, 10, and 12 inches). Note that the overall aspect ratio of these designs is no longer constant (as it was for the reference set in Table 8.3).

Table 8.7: Design and Performance Parameters for Minimum Set #3 (3 distinct motor diameters and fixed gear ratio)

Gear Train Diameter (inches)	Motor Diameter (inches)	Length (inches)	Aspect Ratio	Gear Ratio	Torque (ft-lbf)	Weight (lbf)	Inertia (lbm-in ²)	Torque Density (ft-lbf/lbf)	Input Responsiveness (rad/sec ²)	Output Responsiveness (rad/sec ²)
6	7.7	4.8	0.8	141	1000	38	7	27	4722	34
8	7.7	7.0	0.9	141	2000	66	13	30	5139	37
10	7.7	10.5	1.1	141	4000	122	26	33	5123	36
11	7.7	13.9	1.3	141	6000	180	41	33	4809	34
12	10.4	10.5	0.9	141	8000	218	75	37	3539	25
14	10.4	13.3	1.0	141	12000	314	117	38	3397	24
15	10.4	15.8	1.1	141	16000	406	162	39	3250	23
16	10.4	18.2	1.1	141	20000	501	215	40	3066	22
17	12.2	16.3	1.0	141	24000	579	306	41	2584	18
18	12.2	18.0	1.0	141	28000	673	374	42	2470	18
19	12.2	19.2	1.0	141	32000	751	435	43	2427	17
20	12.2	20.8	1.1	141	36000	837	507	43	2344	17

Table 8.8 lists the SRM stator diameter, length, and other parameters that correspond to each design in Table 8.7. Each motor diameter listed in Table 8.7 is the overall motor diameter including its housing, while the stator diameter in Table 8.8 does not include the housing. Note that while a common stator diameter of 7.3 inches is used for the first four designs, the stator lengths must increase to achieve the increasing motor torque requirements.

Table 8.8: SRM Design and Performance Parameters for Minimum Set #3 (3 distinct motor diameters and 12 motors total)

Stator Diameter (inches)	Stator Length (inches)	Aspect Ratio	Torque (ft-lbf)	Weight (lbf)	Inertia (lbm-in ²)
7.3	2.1	0.3	7	17	6
7.3	3.6	0.5	14	28	10
7.3	6.3	0.9	28	50	18
7.3	9.1	1.2	42	71	26
9.9	5.2	0.5	58	75	50
9.9	7.2	0.7	86	104	69
9.9	9.1	0.9	112	130	86
9.9	11.0	1.1	139	158	104
11.6	8.7	0.7	174	171	156
11.6	9.9	0.9	203	195	178
11.6	10.8	0.9	223	212	193
11.6	12.0	1.0	253	237	216

Because both the reference set (Table 8.3) and minimum set (Table 8.7) have identical gear train diameter and output torque parameters, they can be compared to assess the relative benefits or sacrifices due to using the minimum set alternative. Table 8.9 computes the percent difference between the minimum set performance parameters (torque, weight, inertia, torque density, and responsiveness) and the reference set parameters using the performance loss/deviation metric defined in Section 8.2. Positive numbers indicate that the minimum set has larger values than the reference set for the performance parameter under consideration. For a specific gear train diameter being considered, the table allows the designer to determine the relative benefit of choosing the minimum set alternative.

Table 8.9: Tabular Comparison of the Performance Parameters Between Minimum Set #3 and the Reference Set

Gear Train Diameter (inches)	Torque (% Difference)	Weight (% Difference)	Inertia (% Difference)	Torque Density (% Difference)	Input Responsiveness (% Difference)	Output Responsiveness (% Difference)
6.0	0	-1.3	32	1.3	-24	-24
7.5	0	-1.0	7	1.0	-7	-7
9.5	0	2.1	-5	-2.1	5	5
10.9	0	4.2	-12	-4.0	14	14
12.0	0	-0.2	14	0.2	-12	-12
13.7	0	-0.1	2	0.1	-2	-2
15.1	0	0.1	-3	-0.1	3	3
16.2	0	1.0	-6	-1.0	7	7
17.3	0	-0.5	3	0.5	-3	-3
18.2	0	-0.1	1	0.1	-1	-1
19.0	0	-0.5	-2	0.5	2	2
19.8	0	0.4	-2	-0.4	2	2
Averages (%)	0.0	0.3	2.3	-0.3	-1.3	-1.3

Figure 8.10 graphically summarizes the tabular information in Table 8.9 by plotting the average percent difference for each of the performance parameters. For example, the average value of 0.3% for weight is the average of all the individual percent difference values for the different gear train diameters in Table 8.9. While there are both positive and negative values in the performance parameters in each column, the average value gives a good one-number indication of the overall difference between this minimum set and the reference set.

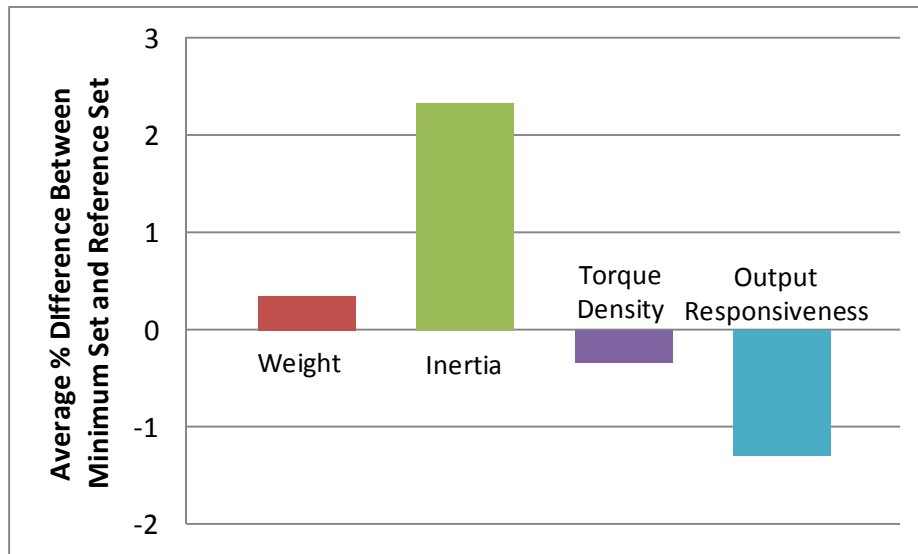


Figure 8.10: Graphical Comparison of the Performance Parameters Between Minimum Set #3 and the Reference Set (Average values from the entire set of actuators are plotted for each performance parameter.)

Figure 8.10 confirms the anticipated performance losses in the weight, inertia, torque density, and output responsiveness parameters due to using this minimum set in place of the reference set. According to the figure, the weight and inertia of the minimum set are larger than the weight (by 0.3%) and inertia (by 2.3%) of the reference set (on average), while the torque density and output responsiveness of the minimum set are smaller than the torque density (by 0.3%) and output responsiveness (by 1.3%) for the reference set.

While the original reference set is superior to the reference set in terms of these parameters, the less than 3% average variation is arguably not significant. The cost benefits of choosing the minimum set should outweigh these slight reductions in the performance parameters, and both the producer and end user of these actuators would probably be willing to tolerate these performance losses. Unless dictated by the

application, a reasonable goal is to stay within 10% of the performance parameters obtainable by the reference set (or in general, some optimum set).

While the results above have only been presented for minimum set 3, complete design and performance parameter information was computed for minimum sets 1-5. Table 8.10 lists the resulting gear ratios, motor diameters, and motor lengths for alternative minimum sets 1-5. As the table and this section have illustrated, a potential minimum set can be achieved when a single motor diameter is used with multiple gear train diameters.

Table 8.10: Minimum Set Options 1-5, Based Upon the Number of Distinct Motor Sizes (common motor diameters for each noted in bold)

Gear Train Diameter (inches)	Output Torque (ft-lbf)	Gear Ratio	Ref. Set (12 Motors)		Set 1 (6 Motors)		Set 2 (4 Motors)		Set 3 (3 Motors)		Set 4 (2 Motors)		Set 5 (1 Motor)	
			Motor Diameter (inches)	Motor Length (inches)	Motor Diameter (inches)	Motor Length (inches)	Motor Diameter (inches)	Motor Length (inches)	Motor Diameter (inches)	Motor Length (inches)	Motor Diameter (inches)	Motor Length (inches)	Motor Diameter (inches)	Motor Length (inches)
6.0	1000	141	6.4	3.3	6.8	2.8	7.3	2.3	7.7	2.1	8.4	1.9	10.1	1.6
7.5	2000	141	7.3	4.2		5.0		4.2		3.6		2.9		2.2
9.5	4000	141	8.2	5.3	8.6	4.8	9.5	7.4	10.4	6.3	11.8	5.1	12.2	3.3
10.9	6000	141	8.9	6.0		6.5		5.1		9.1		7.0		4.5
12.0	8000	141	9.3	6.7	9.8	6.0	11.3	6.5	12.2	5.2	11.8	9.1	10.1	5.6
13.7	12000	141	10.2	7.6		8.3		9.1		7.2		13.0		7.7
15.1	16000	141	10.8	8.4	11.0	8.1	12.4	7.5	12.2	9.1	11.8	6.7	10.1	9.8
16.2	20000	141	11.3	9.0		9.5		8.9		11.0		8.1		12.1
17.3	24000	141	11.7	9.6	11.9	9.2	12.4	10.3	12.2	8.7	11.8	9.4	10.1	14.3
18.2	28000	141	12.1	10.1		10.3		9.4		9.9		10.5		16.5
19.0	32000	141	12.4	10.6	12.5	10.4	12.4	10.5	12.2	10.8	11.8	11.8	10.1	18.6
19.8	36000	141	12.6	11.0		11.2		11.4		12.0		13.1		20.8

Comparisons were made between the other alternative minimum sets (1, 2, 4, and 5) and the reference set, and the similar trade-off of performance losses and potential cost reductions were again evident. Section 8.5.3 later in this chapter provides a summary table (Table 8.17) of the performance losses for each of the other minimum sets.

8.5.2.3 Minimum Sets 6-10 (Variable 1st Stage Gear Ratios)

In minimum sets 1-5 (summarized in Table 8.10), common motor diameters (but not lengths) were used for a range of gear train diameters, and the gear ratio was held constant at 141 to 1 for every design in the set. While minimum sets 1-5 do represent a

cost savings over the reference set, a smaller number of motors can be used if the overall gear ratio of the gear train is varied. Alternative minimum sets 6-10 use the same motor diameters as sets 1-5 (Table 8.5) but allow the 1st stage (and overall) gear ratio to vary in order to use the same motor diameter and length for a range of gear train diameters²¹. Using a motor with same diameter and length practically means that the motors are identical, which is analogous to the “product merging” idea from the literature (Figure 8.1). Since minimum sets 1-5 utilized only common motor diameters and no common lengths, minimum sets 6-10 should provide a relatively higher level of commonality and a smaller minimum set of components.

The gear train design parameter settings used to generate minimum sets 6-10 are listed in Table 8.11. The only difference between these settings and those for minimum sets 1-5 is the variable 1st stage and overall gear ratios. If only the gear ratio of the 1st stage star gear train is varied, then the torque capacity of the gear train will remain constant for a given size. This is because the torque capacity is typically limited by the PE-output gear mesh (rather than the 1st stage gear meshes) and crankshaft bearings (see Section 3.10). Changing the gear ratio of the 1st stage is a relatively low cost change because it only requires modifying the sizes of the gears on the input shaft, idler shaft, and crankshafts (see Figure 8.6) without changing the rest of the gear train geometry. Using the constant output speed assumption given in this example, the different gear ratios for different designs in the set means that the motor inputs speeds are changing in proportion to the change in gear ratio.

²¹ In a computational or conceptual design environment, an infinite number of gear ratio settings are possible. However, in practice, a finite number of gear ratio options is more reasonable and should be considered for most minimum sets.

Table 8.11: Gear Train Design Parameters for Minimum Sets 6-10

Parameter	Description	Value or Range
Gear Ratio (1 st Stage Star)	Variable	$1 < g_1 < 9$
Gear Ratio (PE-Output Gear)	Constant	$g_{pe} = 35 \text{ to } 1$
Gear Ratio (Overall)	Variable	$40 < g < 250$
Gear Train Aspect Ratio	Constant	$A_g = 0.4$

The basic approach to generate minimum sets 6-10 was to vary the 1st stage gear ratio so that the same motor size (not only diameter but also length) could be used for a range of gear train diameters. As an example, Table 8.12 summarizes the results for minimum set #8, which has 3 distinct motor diameters and a variable gear ratio and also meets the distinct torque requirements listed in Table 8.1 above. Table 8.13 lists the SRM stator diameter, length, and other parameters that correspond to each design in Table 8.12. This set of actuators is a potential minimum set because the same motor (with stator diameter of 7.3 inches and length 5.5 inches in Table 8.13) was used for the first four gear train/actuator diameters in the set (i.e., diameters of 6, 8, 10, and 12 inches). This set effectively reduces the total number of motors required from 12 for the reference set to only 3 for this minimum set.

Table 8.12: Design and Performance Parameters for Minimum Set #8 (3 distinct motor diameters and variable gear ratio)

Gear Train Diameter (inches)	Motor Diameter (inches)	Length (inches)	Aspect Ratio	Gear Ratio	Torque (ft-lbf)	Weight (lbf)	Inertia (lbm-in ²)	Torque Density (ft-lbf/lbf)	Input Responsiveness (rad/sec ²)	Output Responsiveness (rad/sec ²)
6	7.7	8.2	1.4	41	1000	69	25	15	4561	112
8	7.7	8.9	1.2	82	2000	85	23	24	4879	60
10	7.7	9.7	1.0	165	4000	115	21	35	5256	32
11	7.7	10.4	1.0	254	6000	144	21	42	5331	21
12	10.4	13.4	1.1	81	8000	264	151	30	3046	38
14	10.4	14.1	1.0	122	12000	327	139	37	3264	27
15	10.4	14.7	1.0	169	16000	389	130	41	3382	20
16	10.4	15.2	0.9	210	20000	454	127	44	3473	17
17	12.2	18.3	1.1	108	24000	619	438	39	2344	22
18	12.2	18.7	1.0	126	28000	685	431	41	2399	19
19	12.2	19.0	1.0	145	32000	744	416	43	2464	17
20	12.2	19.3	1.0	167	36000	809	397	45	2518	15

Table 8.13: SRM Design and Performance Parameters for Minimum Set #8 (3 distinct motor diameters and 3 motors total)

Stator Diameter (inches)	Stator Length (inches)	Aspect Ratio	Torque (ft-lbf)	Weight (lbf)	Inertia (lbm-in ²)	Torque Density (in-lbf/lbf)	Responsiveness (rad/sec ²)
7.3	5.5	0.8	24	43	16	6.7	7089
7.3	5.5	0.8	24	43	16	6.7	7092
7.3	5.5	0.7	24	43	16	6.6	7082
7.3	5.5	0.8	24	43	16	6.7	7088
9.9	8.0	0.8	97	115	76	10.1	5925
9.9	8.0	0.8	97	115	76	10.1	5921
9.9	8.0	0.8	96	114	76	10.1	5917
9.9	8.0	0.8	97	115	76	10.1	5921
11.6	10.6	0.9	219	209	190	12.6	5345
11.6	10.6	0.9	220	209	191	12.6	5346
11.6	10.6	0.9	218	208	190	12.6	5342
11.6	10.6	0.9	218	208	189	12.6	5342

Because both the reference set (Table 8.3) and minimum set (Table 8.12) have identical gear train diameter and output torque parameters, they can be compared to assess the relative benefits or sacrifices due to using the minimum set alternative. Table 8.14 computes the percent difference between the minimum set performance parameters (torque, weight, inertia, torque density, and responsiveness) and the reference set parameters using the performance loss/deviation metric defined in Section 8.2. Positive

numbers indicate that the minimum set has larger values for the performance parameter under consideration.

Table 8.14: Tabular Comparison of the Performance Parameters Between Minimum Set #8 and the Reference Set²²

Overall Diameter (inches)	Torque (% Difference)	Weight (% Difference)	Inertia (% Difference)	Torque Density (% Difference)	Input Responsiveness (% Difference)	Output Responsiveness (% Difference)
6.0	0	81	371	-45	-27	152
7.5	0	27	95	-21	-12	52
9.5	0	-4	-21	4	8	-8
10.9	0	-16	-56	20	26	-30
12.0	0	21	129	-17	-24	32
13.7	0	4	22	-4	-6	8
15.1	0	-4	-23	4	8	-10
16.2	0	-9	-45	9	21	-19
17.3	0	6	48	-6	-12	14
18.2	0	2	16	-2	-4	8
19.0	0	-1	-6	1	4	1
19.8	0	-3	-23	3	10	-7
Averages (%)	0	9	42	-4	-1	16

The table illustrates the performance deviations that occur due to using common motor sizes for a range of gear train diameters. For example, the seemingly large losses in weight (81% increase) and inertia (371% increase) for the 6 inch overall diameter design occur because the common motor diameter of 7.7 inches (Table 8.12) replaced the 6.4 inch motor diameter in the reference set (Table 8.3). Going a step deeper to the lower level motor parameters, the stator dimensions of this particular motor in minimum set 8 (7.3 inch diameter and 5.5 inch length in Table 8.13) are larger than the corresponding motor in the reference set (6.1 inch diameter and 3.3 inch length in Table 8.4). Physically, a larger motor than necessary is being used in the reference set (for this

²² These performance losses are heavily dependent on the choices of the diameters and lengths of the actuator designs in the reference set (section 8.5.1). It is anticipated that the use of different distributions of these parameters (i.e., linear, quadratic, etc.) might improve the individual performance losses of a particular actuator in the set, but the average performance losses should not change significantly.

particular 6 inch design) to achieve a higher level of commonality (and thus cost savings) in the set.

As another example using the 6 inch overall diameter design in Table 8.14, the desirable increase in output responsiveness (by 152%) occurs due to the lower gear ratio used for this 6 inch design in minimum set 8 (gear ratio of 41 in Table 8.12) in comparison to the corresponding design in the reference set (gear ratio of 141 in Table 8.3). This result is consistent with the result of lower gear ratios resulting in higher responsiveness discussed in Sections 7.3.1.5 and 7.3.2.4. In this case, the 6 inch minimum set design outperforms the 6 inch reference set design. Similar arguments can be made for the outstanding performance deviations for the 7.5, 10.9, and 12 inch overall diameter designs in Table 8.14.

Figure 8.11 graphically summarizes the tabular information in Table 8.14 by plotting the average percent difference for each of the performance parameters. For example, the average value of 9% for weight is the average of all the individual percent difference values for the different gear train diameters in Table 8.14.

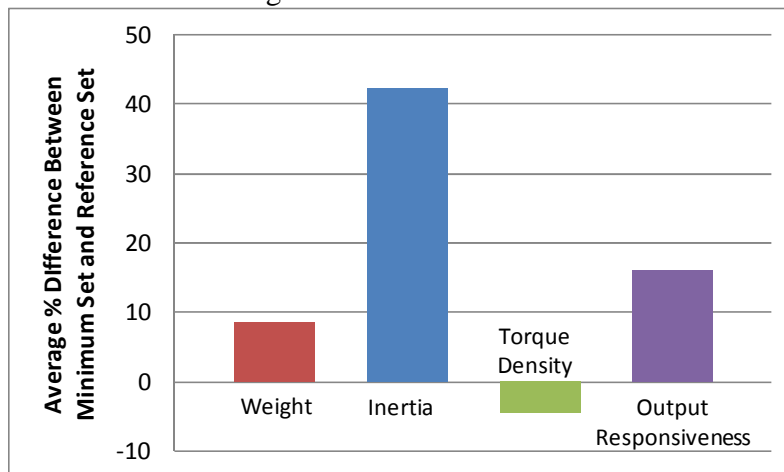


Figure 8.11: Graphical Comparison of the Performance Parameters Between Minimum Set #8 and the Reference Set (Average values from the entire set of actuators are plotted for each performance parameter.)

Like Figure 8.10, Figure 8.11 confirms the anticipated performance losses in the weight, inertia, torque density, and output responsiveness parameters due to using this minimum set in place of the reference set. According to the figure, the weight and inertia of the minimum set are larger than the weight (by 9%) and inertia (by 42%) of the reference set (on average), while the torque density of minimum set is 4% smaller than the corresponding values for the reference set.

One noteworthy difference here for minimum sets 6-10 (compared to sets 1-5 in Figure 8.10) is that these minimum sets provide higher responsiveness (on average) than the designs in the reference set. This occurs due to the relatively lower gear ratios in these minimum sets (see the gear ratios of 41, 82, etc. in Table 8.12 and note that the average gear ratio is less than 141) relative to the constant gear ratio of 141 used for the reference set (Table 8.3). This result is consistent with the results of Section 7.3.1, in which reducing the gear ratio of the SRM+Star+PEGT actuator combination (for a fixed gear train size) increased the responsiveness.

Another noteworthy difference is that the relative magnitudes of the performance losses are larger for minimum set 8 (ranging from 5 to 40% in Figure 8.11) when compared to those for minimum set 3 (less than 3% in Figure 8.10). This suggests that trying to achieve a smaller minimum set (by using the common motor diameters and lengths in this particular minimum set) may increase the performance losses beyond what might be tolerated by a producer or end user. The cost benefits of choosing the minimum set may not outweigh these deviations in the performance parameters.

While the results above have only been presented for minimum set 8, complete design and performance parameter information was computed for minimum sets 6-10. Table 8.15 lists the resulting gear ratio, motor diameters, and motor lengths for alternative minimum sets 6-10, with each row corresponding to the gear train diameter

and torque settings listed in Table 8.10. As the table and illustrates, a potential minimum set can be achieved when an identical motor is used with multiple gear train diameters.

Table 8.15: Minimum Set Options 6-10, Based Upon the Number of Distinct Motor Sizes (common motor diameters for each noted in bold)

Set 6 (6 Diameters)			Set 7 (4 Diameters)			Set 8 (3 Diameters)			Set 9 (2 Diameters)			Set 10 (1 Diameter)		
Gear Ratio	Motor Diameter (inches)	Motor Length (inches)	Gear Ratio	Motor Diameter (inches)	Motor Length (inches)	Gear Ratio	Motor Diameter (inches)	Motor Length (inches)	Gear Ratio	Motor Diameter (inches)	Motor Length (inches)	Gear Ratio	Motor Diameter (inches)	Motor Length (inches)
91	6.8	4.0	50	7.3	5.4	41	7.7	5.5	41	8.4	4.4	41	10.1	3.0
189			100			82			82			82		
108			199			165			167			163		
169	8.6	5.8	90	9.5	7.3	254	10.4	8.0	124	11.8	7.8	243	10.1	9.1
110			120			81			165			165		
168	9.8	7.3	184	11.3	9.4	122	12.2	10.6	249	11.8	10.0	116	10.1	16.9
122			104			169			85			154		
158			130			210			106			193		
126	11.9	9.9	160	12.4	10.5	108	12.2	10.6	128	11.8	10.0	116	10.1	16.9
152			121			126			149			137		
129	12.5	10.9	139	12.4	10.5	145	12.2	10.6	173	11.8	10.0	154	10.1	16.9
150			160			167			197			173		

Comparisons were made between the other alternative minimum sets (6, 7, 9, and 10) and the reference set, and the similar trade-off between performance losses and potential cost reductions were again evident. Section 8.5.3 (Table 8.17) provides a summary table of the average performance losses for each of these minimum sets.

8.5.3 Minimum Sets 1-10: Summary and Additional Results

This section summarizes the design and performance parameter results for minimum sets 1-10 and provides a more general discussion of the results. Table 8.16 summarizes the total number of distinct motor diameters and total number of distinct motor designs (with identical diameter and length) for each of the alternative minimum sets 1-10 considered in this example. Recall that the motor diameter is a free choice of the designer, often subject to the size of the gear train and other application-specific constraints. Since each of these sets have less than 12 distinct motor diameters, a fewer total number of parts is required to build the set of 12 actuators, and each set represents a cost savings both to the producer and the end user.

Table 8.16: Total Number of Distinct Motor Diameters and Distinct Motor Sizes Required for Each Minimum Set

	Minimum Set Alternative	Number of Distinct Motor Diameters	Number of Distinct Motors
Fixed Gear Ratio of 141 to 1	Reference Set	12	12
	1	6	12
	2	4	12
	3	3	12
	4	2	12
	5	1	12
Variable Gear Ratio	6	6	6
	7	4	4
	8	3	3
	9	2	3
	10	1	3

Table 8.17 collects information from all the comparisons between minimum set alternatives 1-10 and the reference set (recall that detailed comparisons were made for set 3 (Figure 8.10) and set 8 (Figure 8.11) in the previous sections). Like Table 8.9 and Table 8.14, Table 8.17 again lists the average percentage change in the performance parameters (relative to the reference set) for each of the alternative minimum sets considered here.

Table 8.17: Tabular Summary of the Average Percent Change in the Performance Parameters for the Different Minimum Set Alternatives

Minimum Set Alternative	Gear Ratio	Average % Change in the Performance Parameters					
		Torque	Weight	Inertia	Torque Density	Input Responsiveness	Output Responsiveness
1 (highest cost)	Fixed Value of 141 to 1	0.0	0.0	0.4	0.0	-0.2	-0.2
2		0.0	0.1	1.4	-0.1	-0.9	-0.9
3		0.0	0.3	2.3	-0.3	-1.3	-1.3
4		0.0	0.9	5.3	-0.9	-2.6	-2.6
5		0.0	3.7	21.9	-3.3	-7.8	-7.8
6	Variable	0.0	2.0	8.3	-1.4	-0.7	3.3
7		0.0	7.6	32.7	-4.9	-1.8	16.1
8		0.0	8.6	42.3	-4.4	-0.7	16.0
9		0.0	8.0	45.3	-4.5	-0.1	14.3
10 (lowest cost)		0.0	10.2	65.9	-6.0	-5.8	7.3

Figure 8.12-Figure 8.15 graphically present the same information given in Table 8.17. For example, Figure 8.12 illustrates the percent different in weight between each minimum set alternative and the reference set, again with positive numbers indicating a larger weight for the minimum set. The figure makes a distinction between minimum sets 1-5, which used a fixed gear ratio of 141 for every actuator in the set, and minimum sets 6-10, which allowed the gear ratio to vary among the actuators in a set. The increases in weight for sets 6-10 are relatively larger when compared to those for sets 1-5. The reader should note that the output power (torque and speed) remained constant as the gear ratio was varied for a given actuator design in each minimum set. Thus, the motor speed increases (decreases) as the gear ratio increases (decreases).

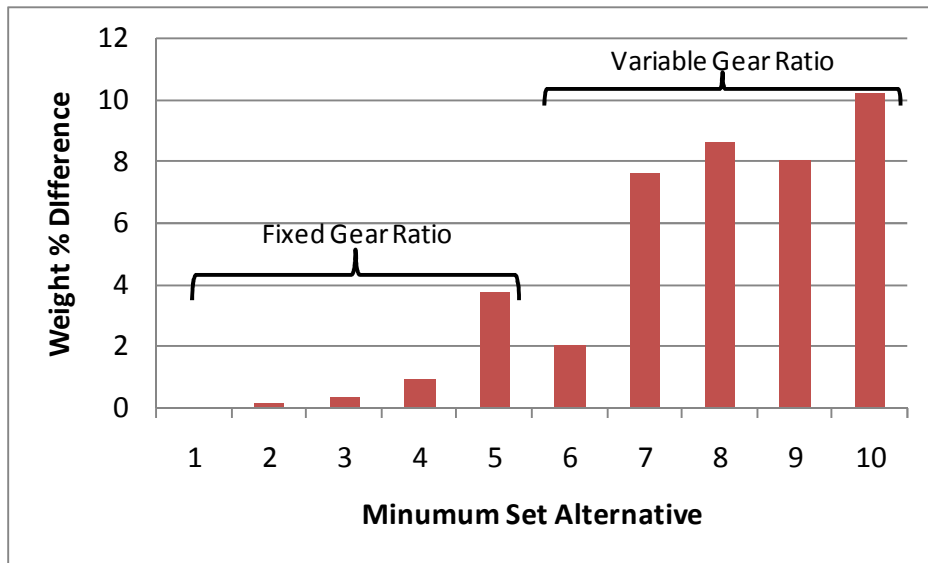


Figure 8.12: Weight Percent Difference Between the Minimum Set Alternatives and the Reference Set (Average values are plotted for each minimum set alternative.)

Considering sets 1-5, these figures collectively suggest that increasing the number of common motor diameters (i.e., moving from set 1 to set 5) increases the weight (Figure 8.12) and inertia (Figure 8.13) and decreases the torque density (Figure 8.14) and responsiveness (Figure 8.15) in comparison to the reference set. All of these deviations can be considered performance losses. A similar conclusion can be drawn when moving from set 6 to set 10, with the exception of the increase in output responsiveness for sets 6-10 (see Section 8.5.2.3 for the justification for this result). The apparent non-linear increases in the losses when moving from set 1 to set 10 (i.e., from a lower level of commonality to a higher level of commonality) is heavily influenced by the choice of common motor diameters discussed in Section 8.5.2.1. Different distributions of these diameters will influence the shape of this trend.

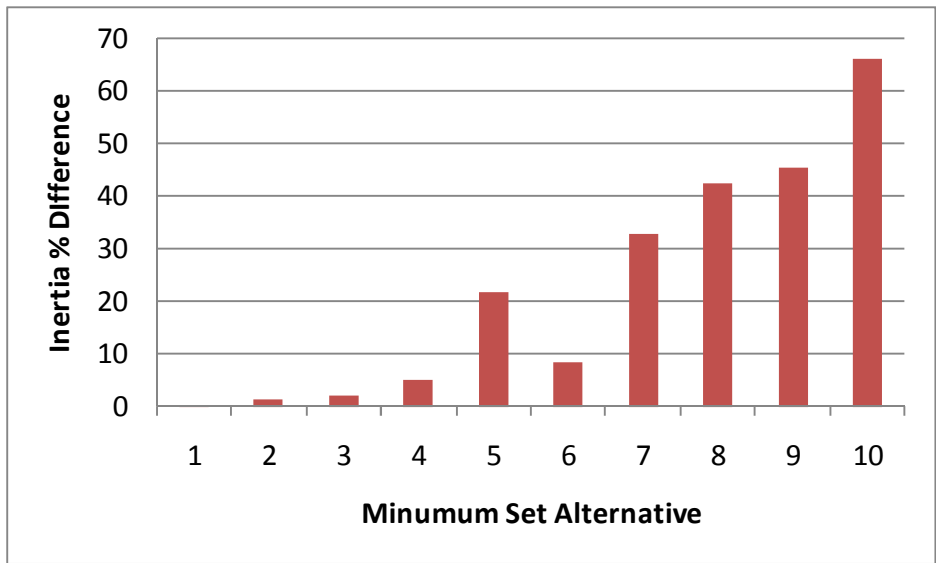


Figure 8.13: Inertia Percent Difference Between the Minimum Set Alternatives and the Reference Set

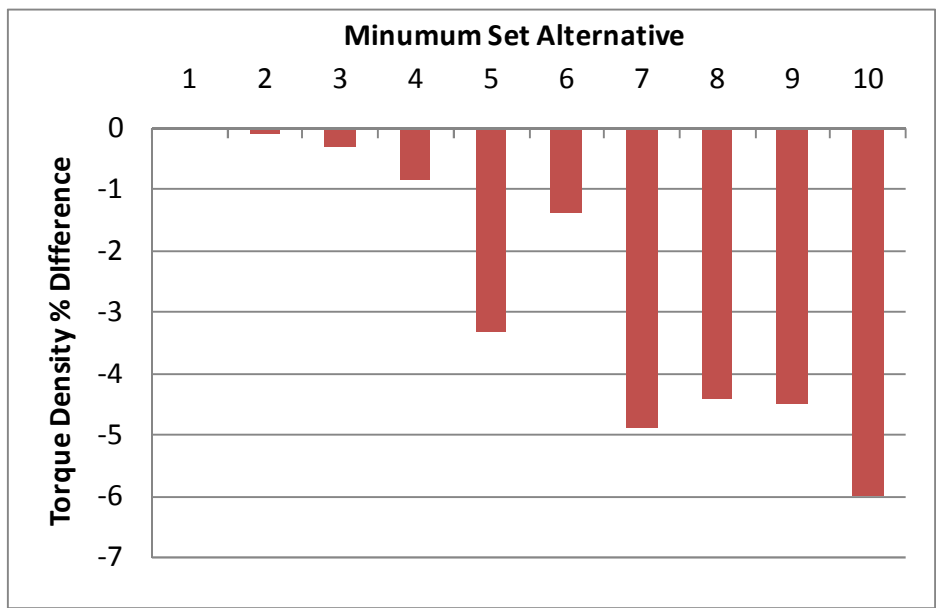


Figure 8.14: Torque Density Percent Difference Between the Minimum Set Alternatives and the Reference Set

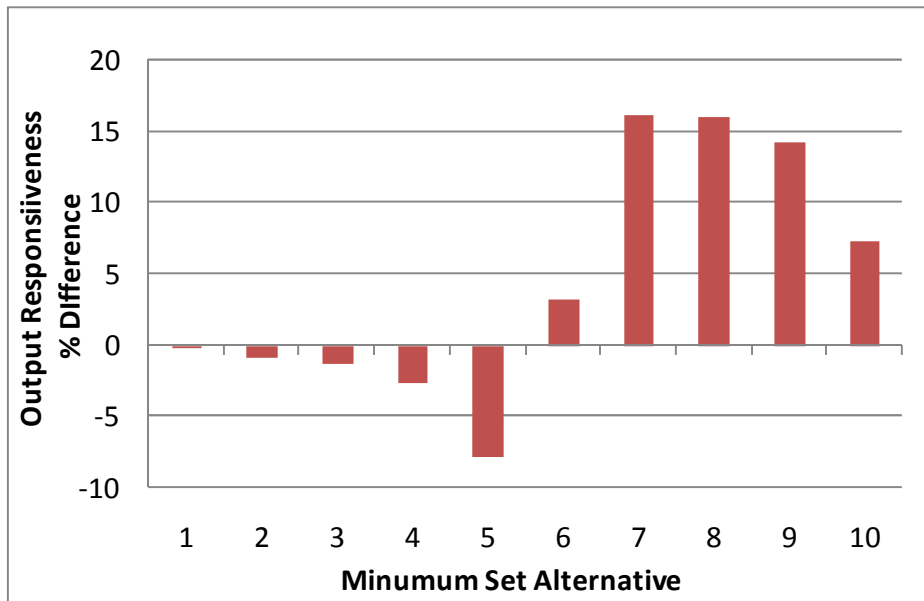


Figure 8.15: Output Responsiveness Percent Difference Between the Minimum Set Alternatives and the Reference Set

In general, set 1 will have the highest cost, lowest level of commonality, and best performance relative to the reference set, while set 10 will have the lowest cost, highest level of commonality, and poorest performance (though still possibly sufficient for the application) relative to the reference set. The cost benefits of each of these sets should be considered relative to these performance losses in order to determine the best set for an application in question. These results illustrate that using common motor diameters and varying the gear ratio allows the use of a relatively small set of motors to cover a large range of actuator torque requirements with potentially minimal performance trade-offs.

Though somewhat obscure, a brief discussion of the motor aspect ratio A_m (i.e., length to diameter ratio) ranges for these minimum sets is warranted. As the number of distinct motor diameters for a fixed total number of actuators is reduced, the motor length must vary over a wider range to meet its torque requirements. If a reasonable aspect ratio range for the motor (e.g., $0.5 < A_m < 2$) is not being met, then the gear ratio can be

changed as it was in minimum sets 6-10 to alleviate this problem. Varying the gear ratio allows a smaller range of motor aspect ratios to meet the torque requirements, which could potentially reduce costs. This advantage is evident when comparing the relatively larger motor aspect ratio ranges for the fixed gear ratio minimum sets 1-5 (Table 8.18) with the relatively smaller ranges for the variable gear ratio minimum sets (Table 8.19). For example, the motor aspect ratio range for minimum set 4 was between 0.25 and 1.62. Minimum set 9 used the same motor diameters as set 4, but the variation of the gear ratio allowed a smaller aspect ratio range of between 0.55 and 1.00. This physically means that a smaller range of motor lengths is required when the 1st stage gear ratio is allowed to vary for different actuator designs in a set.

Table 8.18: Motor Aspect Ratio Range for Minimum Sets 1-5 (Fixed Gear Ratio of 140)

	Reference Set (12 Diameters)	Set 1 (6 Diameters)	Set 2 (4 Diameters)	Set 3 (3 Diameters)	Set 4 (2 Diameters)	Set 5 (1 Diameter)
Minimum Motor Aspect Ratio	0.56	0.45	0.36	0.31	0.25	0.19
Maximum Motor Aspect Ratio	0.94	0.97	1.07	1.24	1.62	2.14

Table 8.19: Motor Aspect Ratio Range for Minimum Sets 6-10 (Variable Gear Ratios)

	Reference Set (12 Diameters)	Set 6 (6 Diameters)	Set 7 (4 Diameters)	Set 8 (3 Diameters)	Set 9 (2 Diameters)	Set 10 (1 Diameter)
Minimum Motor Aspect Ratio	0.56	0.63	0.78	0.75	0.55	0.32
Maximum Motor Aspect Ratio	0.94	0.94	0.91	0.94	1.00	1.77

8.6 EXAMPLE 2: REDUCING THE NUMBER OF ACTUATORS IN A SET

All of the alternative minimum sets discussed above have a total of 12 actuators. Because there are 12 distinct torque requirements that need to be met (Table 8.1), each of the sets above can be designed to meet the requirements exactly. While using these

minimum sets in place of the reference set can result in reduced costs, additional cost savings are possible if the customer is willing to utilize a smaller set of actuators (less than 12) to meet the requirements. This section will compare different reduced sets of actuators based on one of the minimum set alternatives above, with each set containing less than 12 actuators. Because the customer will be using less than 12 actuators, he/she will incur performance losses similar to those shown in Figure 8.10 and Figure 8.11.

For discussion purposes, the term “minimum set” will be used to describe actuator sets 1-10 from the previous sections, with each set containing a total of 12 actuators. The term “reduced set” will be used to describe the actuator sets in the following section, in which there are less than 12 actuators in each set.

8.6.1 Reference Set of Actuators

Table 8.20 and Table 8.21 list the design and performance parameters for the actuators in minimum set #6 from the previous section. This set of designs will be used as a reference for computing the performance losses for the reduced sets in this section. For discussion purposes, the designs in this set will be numbered 1 through 12, with design #1 corresponding to the actuator with torque capacity of 1,000 ft-lbf, design #2 with a torque capacity of 2,000 ft-lbf, and so on up to design #12 with a torque capacity of 36,000 ft-lbf.

Table 8.20: Design and Performance Parameters for Minimum Set #6 (reference designs for this section)

Index	Gear Train Diameter (inches)	Motor Diameter (inches)	Length (inches)	Aspect Ratio	Gear Ratio	Torque (ft-lbf)	Weight (lbf)	Inertia (lbm-in ²)	Torque Density (ft-lbf/lbf)	Input Responsiveness (rad/sec ²)	Output Responsiveness (rad/sec ²)
1	6	6.8	6.6772	1.1	91	1000	46	9	22	5712	63
2	8	6.8	7.335	1.0	189	2000	61	8	33	5863	31
3	10	8.6	9.9947	1.1	108	4000	132	39	30	4385	40
4	11	8.6	10.5786	1.0	169	6000	162	36	37	4543	27
5	12	9.8	12.5923	1.1	110	8000	238	95	34	3564	32
6	14	9.8	13.4013	1.0	168	12000	300	88	40	3757	22
7	15	11.0	15.5074	1.0	122	16000	422	207	38	2932	24
8	16	11.0	15.9766	1.0	158	20000	482	193	42	3042	19
9	17	11.9	17.5527	1.0	126	24000	597	350	40	2532	20
10	18	11.9	17.9719	1.0	152	28000	658	328	43	2612	17
11	19	12.5	19.3193	1.0	129	32000	762	497	42	2313	18
12	20	12.5	19.6511	1.0	150	36000	833	476	43	2344	16

Table 8.21: SRM Design and Performance Parameters for Minimum Set #6 (reference designs for this section)

Index	Stator Diameter (inches)	Stator Length (inches)	Aspect Ratio	Torque (ft-lbf)	Weight (lbf)	Inertia (lbm-in ²)	Torque Density (in-lbf/lbf)	Responsiveness (rad/sec ²)
1	6.5	4.0	0.6	11	25	7	5.3	7232
2	6.5	4.0	0.6	11	24	7	5.3	7223
3	8.2	5.8	0.7	36	57	26	7.7	6573
4	8.2	5.8	0.7	36	56	25	7.7	6567
5	9.3	7.3	0.8	72	93	54	9.3	6140
6	9.3	7.3	0.8	72	93	55	9.3	6145
7	10.5	8.8	0.8	129	141	105	11.0	5719
8	10.5	8.8	0.8	128	140	104	10.9	5714
9	11.3	9.9	0.9	188	185	161	12.1	5412
10	11.3	9.9	0.9	188	186	161	12.1	5414
11	11.9	10.9	0.9	243	225	215	13.0	5242
12	11.9	10.9	0.9	243	225	215	13.0	5242

Though many potential minimum sets of less than 12 distinct actuators can be built from the set of 12 in Table 8.20, only a small number of these will be considered here. The suggested approach to reduce the size of the set is to remove actuators while ensuring that the torque requirements are still met. For example, if the designer removes

actuator 2 from the reference set, then he/she must use actuator 3 (rather than actuator 1) in its place to meet the 2,000 ft-lbf torque requirement. As another example, if the designer removes actuator 11, he/she must use actuator 12 in its place because it is the only one that meets the largest torque requirement of 36,000 ft-lbf. The assumption associated with this approach is that the customer is willing to compromise and accept performance losses with respect to weight, inertia, torque density, and responsiveness (for the potential cost savings of using a smaller set of actuators), but the customer is not willing to accept less than the required torque capacity.

8.6.2 A Potential Reduced Set of Actuators

Table 8.22 lists the design and performance parameters for one potential reduced set of actuators that is built from the reference set in Table 8.20. This set was built by removing actuators 1, 3, 5, 7, 9, and 11 from the reference set, and replacing them with actuators 2, 4, 6, 8, 10, and 12, respectively²³. This reduces the total number of actuators in the set from 12 down to 6, which has obvious cost benefits. This means that the producer and end-user are essentially choosing to specify actuator 2 with 2,000 ft-lbf torque capacity to meet the 1,000 ft-lbf torque requirement (that was originally provided by actuator 1 in the reference set). Likewise, actuator 4 with 6,000 ft-lbf torque capacity would be used to meet 4,000 ft-lbf torque requirement (that was provided by actuator 3 in the reference set).

²³ An alternative reduced set might use the average size of actuators 1 and 2 from the reference set to meet both 1,000 and 2,000 ft-lbf torque requirements, the average of actuators 3 and 4 to meet the 4,000 and 6,000 ft-lbf torque requirements, and so on for the rest of the set. This still results in a total number of 6 actuators to meet the 12 distinct torque requirements. While this set would reduce the individual performance losses in Table 8.23, the average performance losses for the entire set should not change significantly.

Table 8.22: Design and Performance Parameters for a Potential Reduced Set of Actuators

Actuator from Reference Set	Gear Train Diameter (inches)	Motor Diameter (inches)	Length (inches)	Aspect Ratio	Gear Ratio	Torque (ft-lbf)	Weight (lbf)	Inertia (lbm-in ²)	Torque Density (ft-lbf/lbf)	Input Responsiveness (rad/sec ²)	Output Responsiveness (rad/sec ²)
2	8	7	7	1	189	2000	61	8	33	5863	31
2	8	7	7	1	189	2000	61	8	33	5863	31
4	11	9	11	1	169	6000	162	36	37	4543	27
4	11	9	11	1	169	6000	162	36	37	4543	27
6	14	10	13	1	168	12000	300	88	40	3757	22
6	14	10	13	1	168	12000	300	88	40	3757	22
8	16	11	16	1	158	20000	482	193	42	3042	19
8	16	11	16	1	158	20000	482	193	42	3042	19
10	18	12	18	1	152	28000	658	328	43	2612	17
10	18	12	18	1	152	28000	658	328	43	2612	17
12	20	13	20	1	150	36000	833	476	43	2344	16
12	20	13	20	1	150	36000	833	476	43	2344	16

Because both the reference set (Table 8.20) and reduced set (Table 8.22) have identical gear train diameter and output torque parameters, they can be compared to assess the relative benefits or sacrifices due to using the reduced set alternative. Table 8.23 computes the percent difference between the reduced set performance parameters (torque, weight, inertia, torque density, and responsiveness) and the reference set parameters using the performance loss/deviation metric defined in Section 8.2. Positive numbers indicate that the reduced set has larger values for the performance parameter under consideration.

Table 8.23: Tabular Comparison of the Performance Parameters Between Reduced Set and the Reference Set

Overall Diameter (inches)	Torque (% Difference)	Weight (% Difference)	Inertia (% Difference)	Torque Density (% Difference)	Input Responsiveness (% Difference)	Output Responsiveness (% Difference)
6.0	100	33	-6	51	3	-51
7.5	0	0	0	0	0	0
9.5	50	23	-7	22	4	-34
10.9	0	0	0	0	0	0
12.0	50	26	-7	19	5	-31
13.7	0	0	0	0	0	0
15.1	25	14	-7	9	4	-20
16.2	0	0	0	0	0	0
17.3	17	10	-6	6	3	-15
18.2	0	0	0	0	0	0
19.0	12	9	-4	3	1	-13
19.8	0	0	0	0	0	0
Averages (%)	21	10	-3	9	2	-14

Figure 8.16 graphically summarizes the tabular information in Table 8.23 by plotting the average percent difference for each of the performance parameters. For example, the average value of 10% for weight is the average of the all the individual percent difference values for the different gear train diameters in Table 8.23.

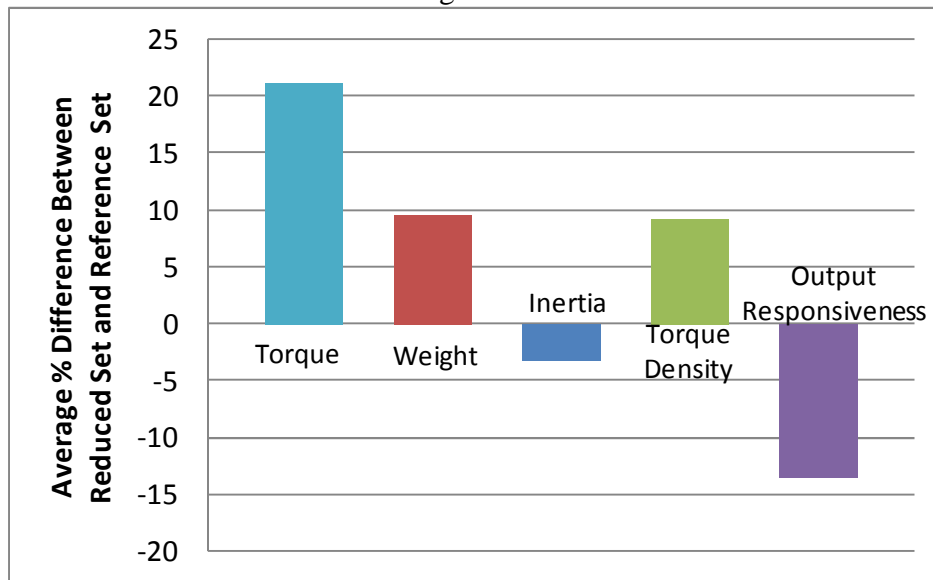


Figure 8.16: Graphical Comparison of the Performance Parameters Between the Reduced Set and the Reference Set (Average values from the entire set of actuators are plotted for each performance parameter.)

Similar to Figure 8.10 and Figure 8.11 for the minimum set alternatives, Figure 8.16 again confirms the anticipated performance deviations in the torque, weight, inertia, torque density, and output responsiveness parameters that occur when using this reduced set in place of the reference set. According to the figure, the torque, weight, and torque density of the reduced set are larger than the torque (by 21%), weight (by 10%), and torque density (by 9%) of the reference set (on average). This occurs due to the producer/end-user using actuators of larger torque capacity (and thus larger weight) than required to meet a specific torque requirement.

The inertia and output responsiveness of the reduced set are smaller than the inertia (by 3%) and output responsiveness (by 14%) of the reference set (on average). These reductions occur due to the relatively higher gear ratios used in the reduced set relative to those used for the reference set. Refer to the gear ratios in Table 8.20 (reference set) and Table 8.22 (reduced set), and note the larger gear ratios for the odd-numbered actuator designs in the reduced set. These higher gear ratios decrease the reflected inertia (see Section 6.6.2 and 6.6.3) and decrease the responsiveness (see Section 7.3.1).

These results suggest that trying to achieve a reduced set (by elimination of actuators from the set) results in modest performance deviations (20% or less), which are possibly beyond what might be tolerated by a producer or end user. The cost benefits of choosing this reduced set may not outweigh these deviations in the performance parameters.

8.6.3 Other Potential Reduced Sets of Actuators

The previous section analyzed one potential reduced set in detail. Table 8.24 lists other possible reduced sets built from the reference set, the actuators included in each set,

the number of distinct motor and gear train designs, and the values of the criteria (focused on weight in this example) used to distinguish among them. The reduced set built of only actuators 2, 4, 6, 8, 10, and 12 (discussed in the previous section) is index #15 in the table. Each of these reduced sets are feasible alternatives if the cost benefits due to the reduced number of gear train and motor designs is sufficient to justify the increases in weight (and other performance deviations). In this example, the number of gear trains in each set is equal to the number of distinct actuators because a distinct gear train diameter and length are used to meet each of the torque requirements. This assumption can be relaxed if, for example, there are cost benefits to standardizing the diameter of the gear train and only varying the length to achieve the different torque requirements.

Table 8.24: Reduced Minimum Sets and Criteria Values for Each

Index	Actuators In the Set	Number of Actuators	Number of Gear Train Designs	Number of Motor Designs	Combined Weight (lbf)	Weight Penalty (lbf)	% Increase in Weight
0	All (1-12)	12	12	6	4693	0	0.0
1	All except 1 (2-12)	11	11	6	4708	15	0.3
2	All except 2 (1,3-12)	11	11	6	4764	71	1.5
3	All except 3 (1-2,4-12)	11	11	6	4723	30	0.6
4	All except 4 (1-3,5-12)	11	11	6	4769	76	1.6
5	All except 5 (1-4,6-12)	11	11	6	4755	62	1.3
6	All except 6 (1-5,7-12)	11	11	6	4816	122	2.6
7	All except 7 (1-6,8-12)	11	11	6	4753	60	1.3
8	All except 8 (1-7,9-12)	11	11	6	4809	116	2.5
9	All except 9 (1-8,10-12)	11	11	6	4754	61	1.3
10	All except 10 (1-9,11-12)	11	11	6	4797	103	2.2
11	All except 11 (1-10,12)	11	11	6	4765	72	1.5
12	3-12	10	10	5	4850	157	3.3
13	4-12	9	9	5	4940	247	5.3
14	5-12	8	8	4	5242	549	11.7
15	2,4,6,8,10,12	6	6	6	4993	299	6.4
16	3,6,9,12	4	4	4	5587	894	19.0
17	4,8,12	3	3	3	5908	1215	25.9
18	6,12	2	2	2	6797	2104	44.8

Referring to the table, the combined weight of the actuators in the set increases as the total number of actuators in the set decreases (relative to the reference weight of 4,693 lbf of all 12 actuators, listed as index #0 in the table). This weight increase was expected and is one measure of the performance losses associated with reducing the size of a set. The weight penalty value listed in the table for each set is the difference between the weight of the actuators in the reduced set and the weight of the actuators in the reference set. Positive values of the weight penalty indicate that the combined weight of the actuators in the reduced set is greater than the combined weight of the actuators in the reference set. Figure 8.17 plots this weight penalty as a function of the number of actuators in the set, and Figure 8.18 illustrates the same information as a percentage increase in weight relative to the reference weight.

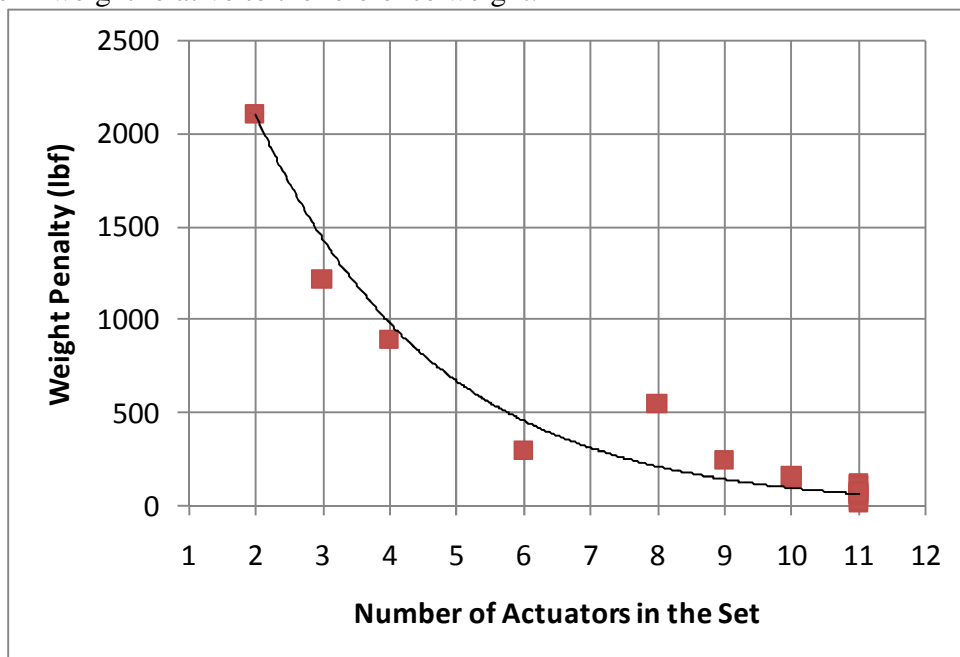


Figure 8.17: Weight Penalty (lbf) as a Function of Number of Actuators in the Set

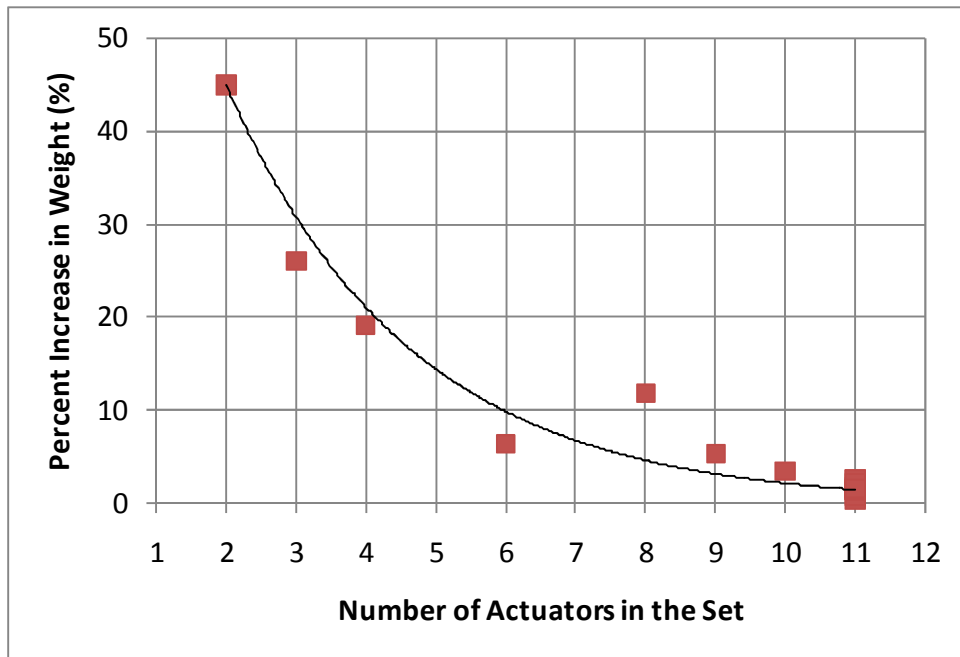


Figure 8.18: Percent Increase in Weight (%) as a Function of Number of Actuators in the Set

As expected, the weight penalty (representative of the performance loss) increases as the total number of actuators decreases. This occurs due to the customer being forced to use actuators with higher torque capacity (and thus higher weight) than needed for a given torque requirement. The specific weight penalty that the producer or end-user can tolerate will depend on the application. Instead of considering the number of actuators in the set as a basic designer choice, the number of distinct motor designs can also be used. In this regard, Figure 8.19 plots the same percent increase in weight information as a function of the number of motor designs in the set.

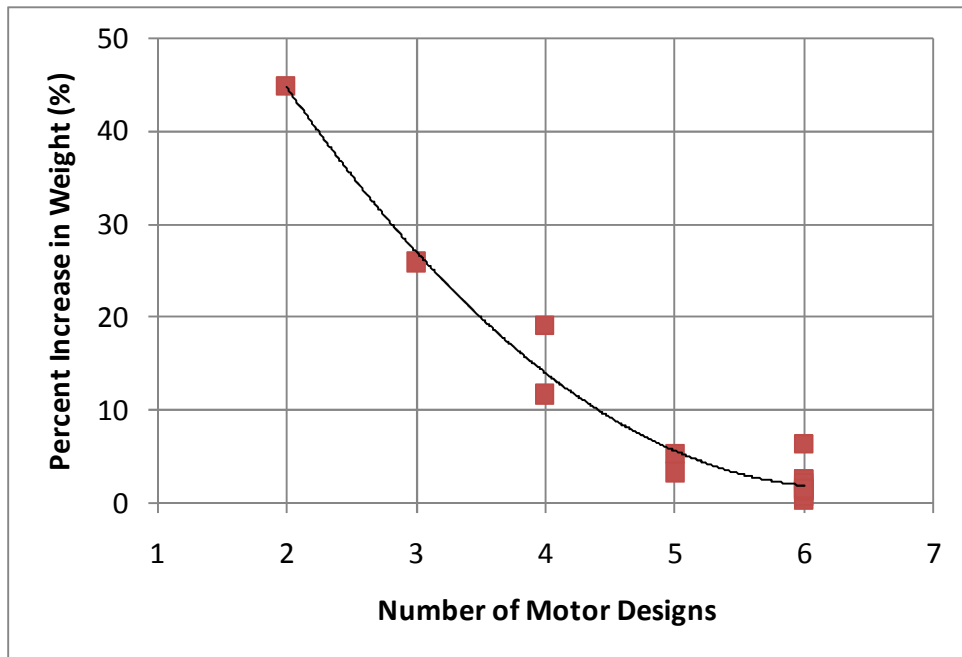


Figure 8.19: Percent Increase in Weight (%) as a Function of Number of Motor Designs in the Set

Though this reduced set comparison was made with respect to minimum set #6 from Section 8.5.2.3, the original reference set from Section 8.5.1, or any set from sets 1-10 could have been used as a reference set, and similar trends illustrating trade-offs between performance deviations and cost savings would result. Also, the other performance parameters of inertia, torque density, and responsiveness can be used as measures of the performance loss if the application suggests their importance. The combined weight and weight penalty criteria were the focus of this example because weight has proven to be important in most actuator applications considered in the RRG program.

8.7 MINIMUM SET DEVELOPMENT PROCEDURE

Based upon the examples in this chapter (Sections 8.5 and 8.6), a process to develop a minimum set of actuators for an application should involve (at a minimum) the following steps.

1. Collect the distinct performance requirements for all the actuators required in the application.
2. Design an actuator to meet each distinct requirement. This set of actuators will serve as a reference for comparison.
3. Design alternative minimum sets of actuators. Alternatives should include sets that range from sharing only a few common parameters (low level of commonality) and sets with less actuators than distinct requirements (high level of commonality).
4. Quantify the performance losses and potential cost benefits for each alternative minimum set.
5. Based on the desired criterion values, choose the best minimum set.

This procedure is similar to the procedure suggested by Fellini, Kokkolaras, and Papalambros [2003], who authored one of the few works on the minimum set concept.

8.8 INVERSION OF THE PRODUCT DEVELOPMENT PROCESS

The minimum set concept discussed in this chapter suggests an inversion of the traditional, one-off product development process. For example, the traditional process involves steps similar to the following.

1. Obtain customer requirements for a product.
2. Design a product to exactly meet the requirements.
3. Build, test, and certify the product.
4. Deliver the product to the customer.

5. Repeat the process when the customer's requirements change.

The primary advantage of this approach is that the customer requirements are always satisfied exactly (if they are willing to wait for a relatively longer development time for custom products). However, this advantage is less important when considering that customers are usually willing to compromise and accept products that have performance "close enough" to their particular requirement.

The inverted product development process (considering the actuator as the product) involves the following steps.

1. Identify (anticipate) the requirements for a distinct application domain.
2. Determine the minimum set of actuators that meets the requirements with minimal performance loss and at minimum cost (i.e., balance profit and cost).
3. Build, test, and certify the minimum set of actuators.
4. Customers will select from the available minimum set of components and actuators to meet their needs.

One advantage of this approach is that both suppliers/manufacturers and customers only have a finite number of different actuators on their shelf, which leads to reduced lead times, manufacturing costs, and maintenance costs. An example of this process in action is the desktop computers of today. Computer manufacturers have a finite number of supply chain components on their shelf (memory, processors, motherboards, disk drives, etc.) with which they can build a large variety of systems to meet customer needs. They typically give the customer only a finite number of choices when building their computer system. Another advantage of this approach is that certification costs are lower because there are far fewer distinct actuator and component

sizes to test and certify. This advantage is particularly important for high-end technologies (e.g., aircraft, ships) where in-depth certification of systems is required.

The product development process of choice (traditional or inverted) will likely depend on the designer/manufacturer's business goals (breaking into the market, becoming more established in the market, etc.) and the level of maturity of the technology.

8.9 SUMMARY

This chapter began by introducing the need for a minimum set of actuators, discussing relevant minimum set literature, listing some criteria that can be used to compare alternative minimum sets of actuators, and suggesting some potential design features of a low cost minimum set. Then, alternative minimum sets based on standardizing the motor size and varying the gear ratio of the SRM+Star+PEGT actuator were developed, and their performance deviations relative to a reference set were computed.

The key result from this chapter is that reducing the number of distinct motor sizes and allowing the gear ratio to vary among an actuator set increases the associated performance losses at the expense of reduced costs. This result was consistent with the noted performance loss-commonality trade-off in the product family design and minimum set literature reviewed for this research effort. When making numerical performance parameter comparisons of the sort in this chapter, the designer is advised to justify the parameter assumptions (including the gear ratio, aspect ratio, motor diameter choices, etc.) associated with both a reference set and a potential minimum set, since these choices will greatly affect the computed performance deviations.

As the number of distinct actuator requirements for a particular application increases, the minimum set concepts introduced in this chapter become increasingly important because the end-user will not likely request a different actuator for each distinct requirement. Both the designer/manufacturer and the customer can reduce their costs if they are willing to use a minimum/reduced set of actuators and accept the anticipated reductions in performance. With this research as a starting point, some natural questions arise. Suppose that there is another related application domain that could be satisfied by an existing minimum set of actuators. Important questions for future research include the following.

- How well does the current set of actuators meet the requirements for this related domain?
- What actuators should be added to (or removed from) the set to make it suitable for this domain?

Finally, though not discussed in this chapter in detail, it is important to note how actuator intelligence (based on the use of performance maps and the associated decision-making framework, see Section 2.8.1) and the concept of upgradability/downgradability of an actuator (primarily based on material and component quality choices) is related to the minimum set question. In particular, both can help bridge the gap between the performance requirements for a particular application. This allows either a smaller minimum set or increased performance capabilities for a given set of actuators, both of which are desirable.

Chapter 9 Summary and Recommendations

9.1 OVERVIEW

One of the Robotics Research Group (RRG) missions is to design an array of Electromechanical Actuators (EMA), which, because of their distinctive features, forms a complete architecture of actuators that are useful as building blocks for intelligent open architecture machines. To fulfill this mission, the RRG is currently developing a science of design for intelligent mechanical systems, which include EMA as one of the key elements. Currently, the RRG focuses on designing EMA for a wide variety of applications including vehicle drive wheels, aircraft control surfaces, submarine control surfaces, robotic manipulators, and many others. An example of a fully integrated actuator previously designed by the RRG for a manipulator shoulder is shown in Figure 9.1, where the locations of some of the basic components are labeled.

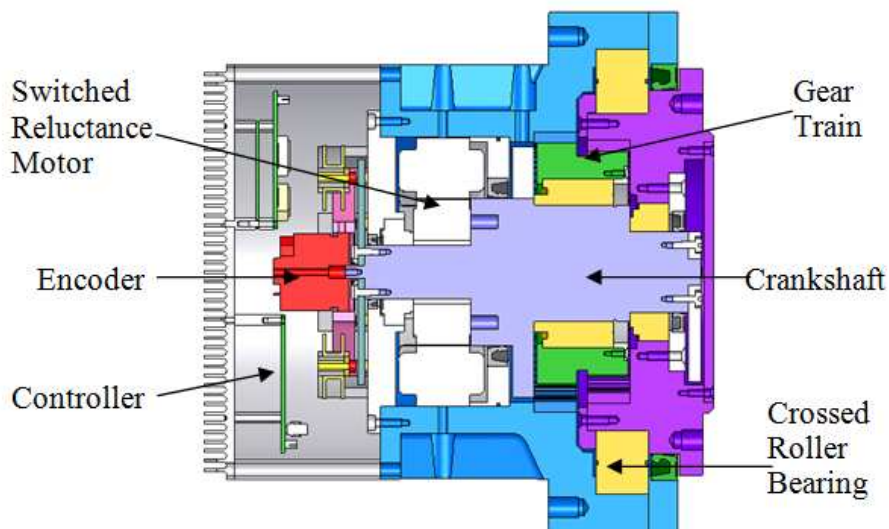


Figure 9.1: Electromechanical Actuator [Tesar et al., March 2004]

9.1.1 Integrating Motors and Gear Trains

The integration of motor and gear train in a single housing allows for high torque and power density in a minimum weight/volume envelope and a reduced number of parts. However, this integration presented the challenge of balancing the parameters between the motor and gear train to achieve the overall performance objectives of the actuator. In this report, *balancing parameters* was defined as the allocation of torque, weight, inertia, torque density (torque to weight ratio), and responsiveness (torque to inertia ratio) between the motor and gear train and specifically determining the actuator design parameters (gear ratio, motor size/inertia, motor speed, aspect ratio, and other geometric dimensions of the motor and gear train) that achieve the desired allocation.

9.1.2 Motivation

Experience has shown that the motor and gear train are the most critical, performance-providing (or limiting) actuator components. The EMA design process currently used by the RRG is based on intuitive rules of thumb and the experience of the designer and often requires multiple design iterations between the motor and gear train.

One of the primary motivations for the present research was to improve this limited process by studying the fundamental design problem of coupling an electric motor to a gear train (see Chapter 2, Section 2.4 and all of Chapter 6) and proposing an actuator design framework (see Chapter 4) to manage it. The proposed framework decreased the amount of time and effort required to obtain preliminary, balanced actuator designs.

Another motivation for the present research stemmed from a desire to develop scaled sets of actuators (i.e., product lines) and understand how the performance of an actuator changes as the basic dimensions (primarily the motor and gear train diameter and aspect ratio and gear ratio) are varied (see Chapters 5 and 6).

9.1.3 Scope

This research specifically focused on the preliminary design of rotary²⁴ electromechanical actuators of the type shown in Figure 9.1. Only the gear train and motor were considered in detail because these are typically the components that dictate the performance capabilities and limits of an actuator. One motor (the Switched Reluctance Motor (SRM)) and three different gear train types (Hypocyclic Gear Train (HGT), star 1st stage gear train coupled with the Parallel Eccentric Gear Train (Star+PEGT), and star compound 1st stage gear train coupled with the Parallel Eccentric Gear Train (Star Compound+PEGT)) were considered. The parametric models (used for the computation of the torque, weight, inertia, torque density, and responsiveness) of the SRM and three gear train types were discussed in detail in Chapter 3.

9.1.4 Research Goals

This research fits within the context of RRG's high level (long-term) actuator development objectives, summarized as follows:

- maximize actuator performance,
- enable/improve human choice of design parameters to achieve target performance,
- minimize weight and development cost, and
- develop minimum sets of actuators for each selected application domain.

To make progress on these high level objectives, the specific goals of the present research were to:

²⁴ This choice is based on the reality that all hydraulic systems were removed from industrial robots by 1980, all linear actuators were removed by 1990, such that today, this cost effective system is durable enough to last 90,000 hours in a high duty cycle task.

1. balance parameters between the motor and gear train for a single-stage actuator configuration (SRM+HGT, Figure 9.1),
2. balance parameters between the motor and gear train for representative two-stage actuator configurations (SRM+Star+PEGT in Figure 9.2 and SRM+Star Compound+PEGT),
3. generate sets of scaled motors, gear trains, and actuators (Figure 9.3) and develop scaling rules that accurately represent the effect of design parameter choices on actuator performance (for the three different motor-gear train combinations listed in goals 1 and 2), and
4. determine a minimum set of actuators based on the standard SRM+Star+PEGT actuator combination for an illustrative application.

A more detailed description of these goals is provided in Section 1.5

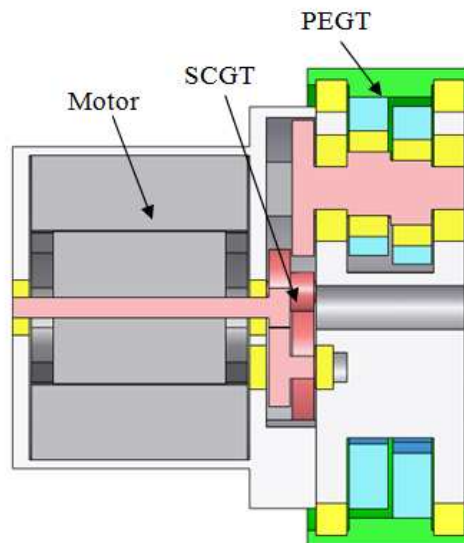


Figure 9.2: Actuator with Two Stage Gear Train (Ship Rudder Control Application)

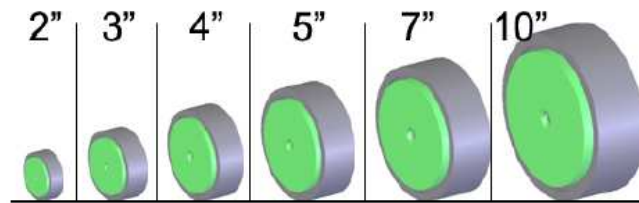


Figure 9.3: Scaled Set of Surgical Manipulator Actuators (Diameters: 2, 3, 4, 5, 7, and 10 inches)

9.2 CHAPTER ROADMAP

This chapter will summarize the key results, recommendations, and contributions of this research and will also recommend the future work needed to build upon this research. Section 9.3 will summarize the key results from the literature review (Chapter 2), parametric model development (Chapter 3), and the actuator design procedure (Chapter 4). These preliminary chapters provided the tools necessary to generate design maps and scaling rules (Chapter 5), obtain rules for balancing parameters (Chapter 6), compare direct drive and geared actuators (Chapter 7), and develop minimum sets of actuators (Chapter 8). Section 9.4 will summarize the key results obtained from Chapters 5-8 of the report, using snapshots from some of the examples developed in each chapter. Section 9.5 will provide recommendations based on these key results. Section 9.6 will outline the specific contributions of this research, and Section 9.7 will discuss the relevant future work.

9.3 BACKGROUND AND PARAMETRIC MODEL DEVELOPMENT

9.3.1 Literature Review (Chapter 2)

The literature review began with a review of electromechanical actuator designs for aircraft and space applications (Section 2.2), where the benefits of electromechanical actuators over traditional hydraulic actuators were well documented. Then, electromechanical actuator designs from the academic community and from industry

were briefly reviewed, with an emphasis on the past RRG integrated actuator research efforts (Section 2.1 and 2.2). Literature on gear train design (Section 2.3) was discussed to provide the necessary background for designing the three gear train types considered in this research. The key section of the literature review emphasized the problem of coupling an electric motor to a gear train (Section 2.4). Scaling literature (Section 2.5) was reviewed because the development of scaling rules for motors, gear trains, and actuators was a key contribution of this research. Product family design methods (to produce the minimal set for a given application domain) were reviewed in detail because of their emphasis on scaling and because the computational tools in the present research are similar (Section 2.6). Each of these subsections contained a brief summary of the findings and also outlined the specific contributions of the present research.

The following two summary tables serve as a roadmap for the literature review. Table 9.1 provides a listing of the most important literature for this research and is classified by topic. Table 9.2 provides a summary of the findings and this research's specific contributions for each of the primary topics: electromechanical actuator design, balancing motors and gear trains, scaling, product family design, and design space visualization. For a more detailed look at each of these topics and results from specific references, the reader is referred to Chapter 2.

Table 9.1: Summary of Key References and Their Relevance to the Current Research

Author (Topic)	Description	Relevance
Ashok and Tesar [2002] (Motor Design)	<ul style="list-style-type: none"> • A comprehensive study on the switched reluctance motor (SRM) • Detailed analytical model, with different SRM configurations noted • Design procedure for computing internal motor design parameters 	<ul style="list-style-type: none"> • Employ their standard outside stator, inside rotor SRM model directly in this research
Park and Tesar [2005] (Gear Trains)	<ul style="list-style-type: none"> • A comprehensive study on the hypocyclic gear train (HGT) • Partitioning design and performance parameters into the system level and the tooth level • Detailed analytical model and design procedure 	<ul style="list-style-type: none"> • Employ their gear train model directly in this research • HGT model also useful for the PEGT because both have circular arc teeth
Sigwald and Tesar [2008] (Gear Trains)	<ul style="list-style-type: none"> • A geometric study on the parallel eccentric gear train (PEGT) • Derivation of crankshaft bearing forces as a function of gear mesh forces • Determination of maximum gear ratio (approximately 35 to 1) to avoid interference 	<ul style="list-style-type: none"> • Employ their gear train model directly in this research • Utilize crankshaft bearing force expressions to determine other bearing forces • Use maximum gear ratio and other parametric guidelines
Roos and Spiegelberg [2004] (Gear Trains)	<ul style="list-style-type: none"> • Comparison of gear train size, weight, and inertia of simple spur and planetary gear trains given the same materials, gear ratio, and set of constraints • Graphical solution process used to illustrate the benefits of planetary gears 	<ul style="list-style-type: none"> • Use of three-dimensional surfaces as a design aid • Models formulated for objective comparison between different gear train types
Bai, Chong, and Kubo [2003] (Gear Trains)	<ul style="list-style-type: none"> • Partitioning of preliminary gear train design into dimensional and configuration design • 4-step procedure to automate the preliminary design of multi-stage gear trains 	<ul style="list-style-type: none"> • Illustrates that gear ratio choice is not trivial and guided search algorithms can be helpful • One of only a few references on multi-stage gear trains
Chiang [1990] (Balancing Motor and Gear Train)	<ul style="list-style-type: none"> • Derivation of expression for the move time of a disk drive system as a function of the gear ratio; motor power, time constant, and inertia; and load inertia • Design objective was to achieve minimum move time by careful choice of these parameters 	<ul style="list-style-type: none"> • Suggests that optimum gear ratio differs for low and high power (speed) motors • Normalization and use of dimensionless parameters simplifies the design process and interpretation of results
Meier and Raider [1976] (Balancing Motor and Gear Train)	<ul style="list-style-type: none"> • Derivation of expression for the motor power required as a function of move time and inertia ratio, where the inertia ratio is defined as the motor inertia divided by the total inertia • Design objective was to minimize the motor power required by choice of the inertia ratio and gear ratio 	<ul style="list-style-type: none"> • Suggests that optimum gear ratio differs when different motor power metrics (rated, peak, and average) are considered • Similar approach and use of graphical results when compared to Chiang

Table 9.1: Summary of Key References and Their Relevance to the Current Research
(Continued)

Author (Topic)	Description	Relevance
Tal and Kahne [1973] (Balancing Motor and Gear Train)	<ul style="list-style-type: none"> • Identification of the critical problem in incremental (start-stop) motion system design as overheating of the motor • Design objective was to minimize the motor temperature by selection of the motor size and gear ratio 	<ul style="list-style-type: none"> • Suggests that the optimum gear ratio differs when different load types (inertial and torque) are dominant • Use of dimensionless, equivalent motor and load parameters
Mendez and Ordonez [2003] (Scaling Rules)	<ul style="list-style-type: none"> • Algorithm combines linear regression and dimensional analysis to obtain scaling laws (rules) in power form from a set of existing data • Algorithm seeks to uncover the simplest scaling rules that still provide a user-specified error level 	<ul style="list-style-type: none"> • Importance of a balance between simplicity and accuracy when fitting • Scaling rules obtained in only one form and for simple systems with a few design parameters
Simpson [2004] (Product Family Design)	<ul style="list-style-type: none"> • Survey paper on product family design methods and associated computational tools • Classification of product families/methods into module and scale-based • Summary of optimization approaches used to solve product family design problems 	<ul style="list-style-type: none"> • Scale-based product families are analogous to the scaled sets of actuators sought here • Classification of product family development efforts using multiple criteria (common parameter specification, # of objectives, # of problem stages, solution algorithm, etc.)
Simpson et. al. [1996] (Product Family Design)	<ul style="list-style-type: none"> • Presentation of the Robust Concept Exploration Method (RCEM), useful for designing product families • Method includes experimental design and model fitting techniques to reduce computational expense 	<ul style="list-style-type: none"> • One of the few comprehensive methods for developing product families • No scaling rules developed
Fellini et. al. [2005] (Product Family Design)	<ul style="list-style-type: none"> • Method to design families of products and control the anticipated performance losses • Illustrates trade-off between maximizing commonality and minimizing performance losses • Only method found that allows designers to pre-specify acceptable performance losses 	<ul style="list-style-type: none"> • One of the few comprehensive methods for developing product families • Method applicable for module and scale-based families • No scaling rules developed
Fellini, Kokkolaras, and Papalambros [2003] (Product Family Design, Minimum Set)	<ul style="list-style-type: none"> • Product portfolio reduction method used to reduce the number of products in a family and measure performance losses. • Extends commonality among products in a family to the point where two products merge 	<ul style="list-style-type: none"> • Only literature found on the minimum set concept • A starting point for developing problem formulation, minimum set objectives, and solution algorithms for reducing the size of a family

Table 9.1: Summary of Key References and Their Relevance to the Current Research
(Continued)

Author (Topic)	Description	Relevance
Cook and Weisberg [1999] (Regression Analysis)	<ul style="list-style-type: none"> • Overview of regression techniques for fitting data • Description of least squares estimation • Summary of assumptions necessary for doing statistical inference 	<ul style="list-style-type: none"> • Utilize regression techniques to fit the actuator design data with low-order polynomials
Simpson et. al. [2001] (Metamodeling)	<ul style="list-style-type: none"> • Survey paper on the use of metamodeling in engineering design • Metamodeling can be used to reduce computational expense if accuracy can be sacrificed. • Identifies the two critical steps of choosing an experimental design and choosing a model-fitting technique 	<ul style="list-style-type: none"> • Discussed pitfalls to avoid when apply metamodeling techniques to deterministic models • Suggested the best experimental design and model-fitting techniques based on ease of use, number of parameters, and model type
Myers and Montgomery [1995] (RSM Techniques)	<ul style="list-style-type: none"> • Overview of experimental design, model choice, and model fitting techniques used in RSM 	<ul style="list-style-type: none"> • Utilize full factorial experimental designs and regression models to curve-fit the actuator design data • Response surfaces become the sought-after design maps
Ashok and Tesar [2007] (Design Space Visualization)	<ul style="list-style-type: none"> • Proposed math-based visualization framework for multi-input, multi-output systems • Provided literature review on design space visualization techniques • Computation of norms from performance maps and decision surfaces 	<ul style="list-style-type: none"> • Reviewed same literature and summarized suggested features of a visual decision-making environment • Illustrate how the math tools can be applied directly to the actuator design maps
Waskow and Tesar [1996] (Model Reduction)	<ul style="list-style-type: none"> • Reviewed the methods used to reduce and solve polynomial systems of equations often encountered in designing mechanical systems • Applied a resultant elimination technique to some example problems 	<ul style="list-style-type: none"> • Suggested which methods are most useful for reducing and solving polynomial equations • Applied these methods to a manipulator design problem
Gloria and Tesar [2004] (Model Reduction)	<ul style="list-style-type: none"> • Used Groebner bases to solve the same problem solved by Waskow and Tesar and illustrated how it required less simplifying assumptions • Applied Groebner bases to an example motor/gear train design problem and uncovered design insights gained from the reduced model 	<ul style="list-style-type: none"> • Identified implementation challenges when increasing the number of parameters • Identified the need to deal with complex coefficients, large number of equations sometimes generated, and impact of term ordering

Table 9.2: Literature Review Findings and This Research’s Contributions (Based on All of the Papers Listed in the References Section)

Topic	Findings	Contributions
Electromechanical Actuators (Industrial and Patent Literature)	<ul style="list-style-type: none"> •Limited off-the-shelf availability •Custom designs •Key parameters: torque, weight, compactness, frequency response 	<ul style="list-style-type: none"> •Formalize the RRG actuator design procedure to move closer to standardization. •Integrate motor and gear train for compact designs. •Include torque to inertia ratio (responsiveness) as a preliminary frequency response metric.
Balancing Motor and Gear Train	<ul style="list-style-type: none"> •Identified critical parameters: gear ratio, motor speed, motor size for motor/gear train integration •Emphasis on inertial loads and maximizing acceleration •Graphical results for optimum parameter values 	<ul style="list-style-type: none"> •Provide guidelines for choosing critical parameters for single and two-stage gear trains. •Include inertial and torque loads. •Generate graphical results (design maps) for decision-making.
Scaling	<ul style="list-style-type: none"> •Scaling rules developed for scale-model testing and for learning. •Rules developed for simple systems. •Determination of scaling limits, constant parameters 	<ul style="list-style-type: none"> •Develop scaling procedure for the more complex actuator model, and use it to obtain scaled sets of actuators and the corresponding scaling rules (design maps). •Determine suitable constant and scaling parameters for the considered motors and gear trains.
Product Family Design	<ul style="list-style-type: none"> •Tools available to design actuator families •No scaling rules developed •Performance losses due to commonality illustrated •Little guidance for reducing family size (obtaining a minimum set) 	<ul style="list-style-type: none"> •Develop scaling rules for existing and future actuator product families. •Use scaling rules for both learning and obtaining intermediate designs. •Determine a minimum set of actuators for a selected application.
Design Space Visualization	<ul style="list-style-type: none"> •Discovered the parallel between the RRG’s current operational visualization framework and future design visualization framework •Identified features of an effective visual design decision-making environment 	<ul style="list-style-type: none"> •Develop design maps with the aim to use them in a future visual actuator design environment. •Illustrate that RRG’s math tools can be used with the developed design maps. •Embody the identified features in the design maps.

9.3.2 Parametric Model Development (Chapter 3)

9.3.2.1 Preliminary and Detailed Design Stages

Prior to discussing any detailed modeling issues for the SRM and three gear train types, an important distinction was made between the preliminary and detailed stages of the actuator design process. Figure 9.4 provides an example of a detailed actuator design that couples an SRM with an HGT. As suggested by the figure, the detailed design of an actuator usually involves the following considerations: bearing mounting (snap rings, shoulders, etc.), seal locations, balancing mass placement (for the HGT), weight reduction, finishing details (chamfers, fillets), assembly modifications, and

manufacturability modifications. Figure 9.5 provides an example of a preliminary actuator design that couples an SRM with an HGT. Developing preliminary designs of this sort does not require the designer to deal with the detailed design issues listed above. Considering these issues during the preliminary design stage can often complicate the design and decision process, especially for novice designers.

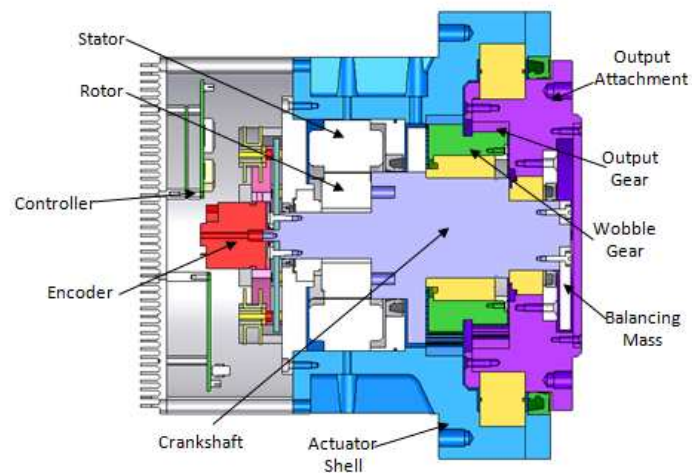


Figure 9.4: Detailed Actuator Design Including an SRM and HGT

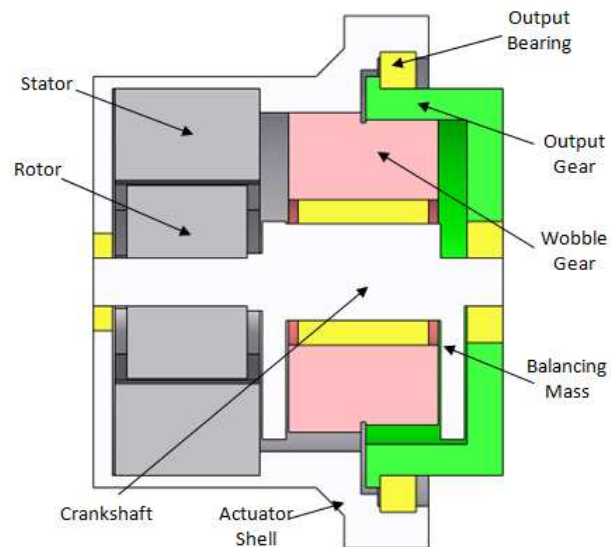


Figure 9.5: Preliminary Actuator Design Including an SRM and HGT

The framework developed in the present research is applicable for the preliminary stages of the actuator design process and provided tools to develop preliminary actuator designs. All of the motor, gear train, and actuator designs were developed to a sufficient level of detail such that a decision could be made whether or not to pursue a detailed design. Making this distinction between the preliminary and detailed design stages should aid the movement toward standardization of the RRG actuator designs (Section 2.2.4), allowing proper allocation of priorities and resources toward each.

9.3.2.2 Motor and Gear Trains Considered

Parametric models for the SRM (Figure 9.6) and three different gear train types (HGT-Figure 9.7, Star+PEGT-Figure 9.8, and Star Compound+PEGT) were documented in Chapter 3. These parametric models were built upon the models of past RRG researchers and augmented when necessary. The parametric models for the SRM [Ashok and Tesar, 2002], HGT [Park and Tesar, 2005], and PEGT [Sigwald and Tesar, 2008] served as the foundation for the present models. Of the three, PEGT was the least mature. Though the star (SGT) and star compound gear trains (SCGT) can be used as stand-alone gear trains in some applications, this research only implemented star and star compound gear trains as the 1st stage of the PEGT.

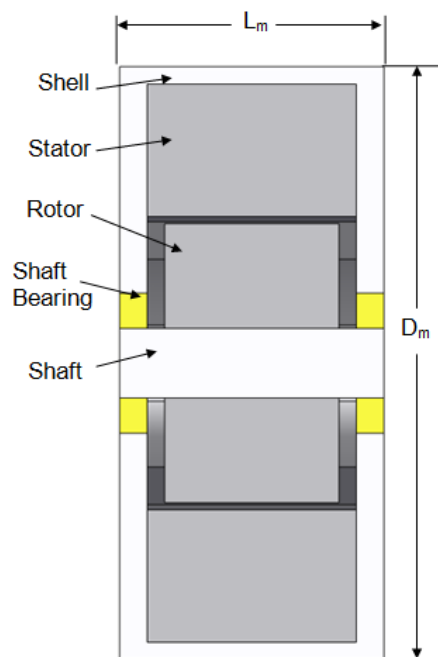


Figure 9.6: SRM Reference Design

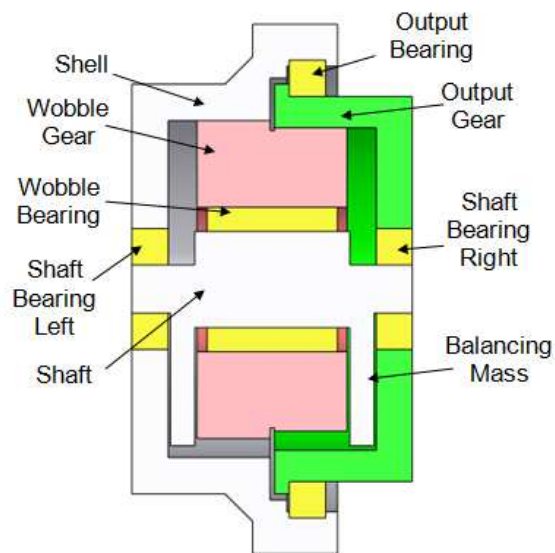


Figure 9.7: HGT Reference Design

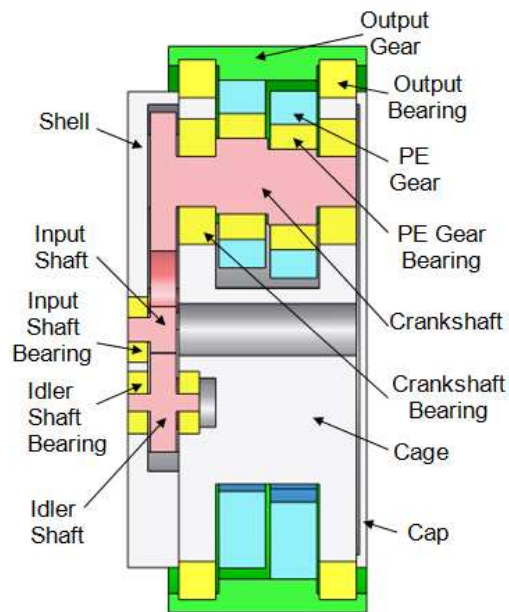


Figure 9.8: Star+PEGT Reference Design

9.3.2.3 Basic Design and Performance Parameters

Table 9.3 lists the fundamental, overall design and performance parameters for the motors and gear trains considered in this research. The design parameters were those that were most often considered and were most relevant during the preliminary stages of design. The performance parameters and metrics were those that could be accurately quantified using an established analytical relationship during the preliminary design stage. Each of these general parameters was discussed in the context of the SRM and three gear train types. For a discussion of the distinction between design and performance parameters, refer to Section 3.1. Figure 9.9 illustrates the diameter and length parameters for the motor, gear train, and integrated actuator.

Table 9.3: Fundamental Design and Performance Parameters

Design Parameters (D_P)	Performance Parameters (P_P)
D_g = gear train diameter L_g = gear train length A_g = gear train aspect ratio D_m = motor diameter L_m = motor length A_m = motor aspect ratio L = overall length A = overall aspect ratio g = gear ratio	T = Torque W = Weight I = Inertia T_w = Torque Density (Torque to Weight Ratio) R = Responsiveness (Torque to Inertia Ratio)

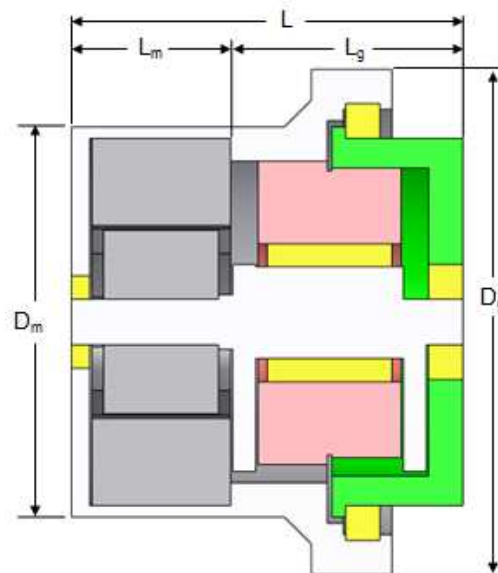


Figure 9.9: Illustration of Motor and Gear Train Design Parameters

The gear train diameter (D_g) was set as the largest outer diameter of the HGT and PEGT. The motor diameter (D_m) was defined as the largest diameter of the SRM, including the shell. The aspect ratio (A) of an actuator was defined as the ratio of its overall length to gear train diameter as follows.

$$A = \frac{L}{D_g} = \frac{L_m + L_g}{D_g} \quad \text{Eqn. 190}$$

The aspect ratio of a motor (A_m) or gear train (A_g) was defined as their length divided by their diameter.

$$A_m = \frac{L_m}{D_m} \quad \text{Eqn. 191}$$

$$A_g = \frac{L_g}{D_g} \quad \text{Eqn. 192}$$

The gear reduction ratio (g) represents the fundamental designer choice for the HGT and PEGT (and any gear train) and was written as functions of numbers of teeth or pitch diameters of the gears in each gear train type. See Sections 3.9 and 3.10 for detailed gear ratio relationships for the HGT and PEGT and Section 3.13 for a discussion of the suggested gear ratio ranges.

9.3.2.4 Torque, Weight, and Inertia Computations

For the SRM and three gear train types shown above, relationships to compute the torque, weight, inertia, torque density and responsiveness were derived in detail. As an example, Table 9.4 summarizes the relationships for the gear ratio, torque, weight, and inertia of the PEGT with the star and star compound (SC) 1st stage gear train options. For the nomenclature of the design parameters used in these relationships and further details, the reader is referred to Section 3.10. Models with similar levels of detail were developed for the SRM (Section 3.7) and HGT (Section 3.9). These models served as the foundation for all of the performance parameter computations in Chapters 5-8.

Table 9.4: Summary of PEGT Design and Performance Parameter Relationships

Parameter	Equation
Gear Ratio	$g = g_1 g_{pe} = \frac{N_o}{N_s} \frac{N_r}{(N_r - N_{pe})} = \frac{d_o}{d_s} \frac{d_r}{(d_r - d_{pe})} \text{ (Star)}$ $g = g_1 g_{pe} = \frac{N_{o2} N_{p1}}{N_{p2} N_s} \frac{N_r}{(N_r - N_{pe})} = \frac{d_{o2} d_{p1}}{d_{p2} d_s} \frac{d_r}{(d_r - d_{pe})} \text{ (SC)}$
Torque	$T_{\text{pegt}} = \frac{S_b d_{pe} L_{pe} J}{2 P_d K_v K_s K_o K_m K_b S} \text{ (bending stress-limited)}$
Weight	$W_{\text{pegt}} = 2W_{pe} + W_o + 3W_{cs} + 3W_{is} + 3W_{ms} + W_{sh} + W_c + W_{cp} + W_{bearing}$ $W_{\text{pegt_app}} = k \frac{\rho \pi D_g^2 L_g}{4}$
Inertia	$I_{\text{pegt}} = \frac{I_o}{g^2} + \frac{2I_{pe} + 2W_{pe} e^2 + I_{cs}}{g_1^2} + I_{is} \left(\frac{d_{sun}}{d_p} \right)^2 + I_{ms} + I_{bearings} \text{ (Star)}$ $I_{\text{pegt}} = \frac{I_o}{g^2} + \frac{2I_{pe} + 2W_{pe} e^2 + I_{cs}}{g_1^2} + I_{is} \left(\frac{d_{sun}}{d_{p1}} \right)^2 + I_{ms} + I_{bearings} \text{ (SC)}$

The torque capacity of each gear train type was derived from the AGMA bending stress relationships discussed in Section 3.5.1 and elaborated on in Section 5.2.2. Of particular importance is the effect of the choice of the diametral pitch (Section 3.5.2 and Section 5.2.5.2) and contact ratio (Section 3.5.5) on the torque capacity. The suggested range for the diametral pitch (number of teeth divided by the pitch diameter of a gear) was between 5 and 25, and a contact ratio of 3 was used for all of the torque capacity calculations in this report. The weight and inertia computations were based on the fact that most of the motor and gear train components could be modeled as either solid or hollow cylinders. The weight and inertia relationships for the SRM were detailed explicitly in Section 3.7.8, and these served as a model for the analogous computations for the HGT and PEGT.

9.3.3 Actuator Design Procedures (Chapter 4)

9.3.3.1 Proposed Actuator Design Procedure

This research augmented the current RRG actuator design procedure (Section 4.2) with the two central concepts of this research: balancing the motor and gear train and developing scaling rules (Figure 9.10). The procedure begins when the designer inputs his/her design parameter choices (D_P) and performance parameter targets (P_P) for a particular application. Designing the gear train and motor are the two critical tasks in the procedure. Unless the application dictates otherwise, the gear train is always designed before the motor for a number of reasons. First, the gear train is typically the larger of the two and often dominates the weight of the design. Second, the gear ratio must be known before the required motor torque can be computed. Finally, the gear train is the technology being studied in depth at the RRG and in some cases, off-the-shelf motor designs are used in place of the custom SRM designs available from the models in Section 3.7. This procedure allowed the designer to control which parameters are fixed and which vary for the set of actuator designs, which is critical for the utility of the scaling and balancing rules developed Chapters 5 and 6.

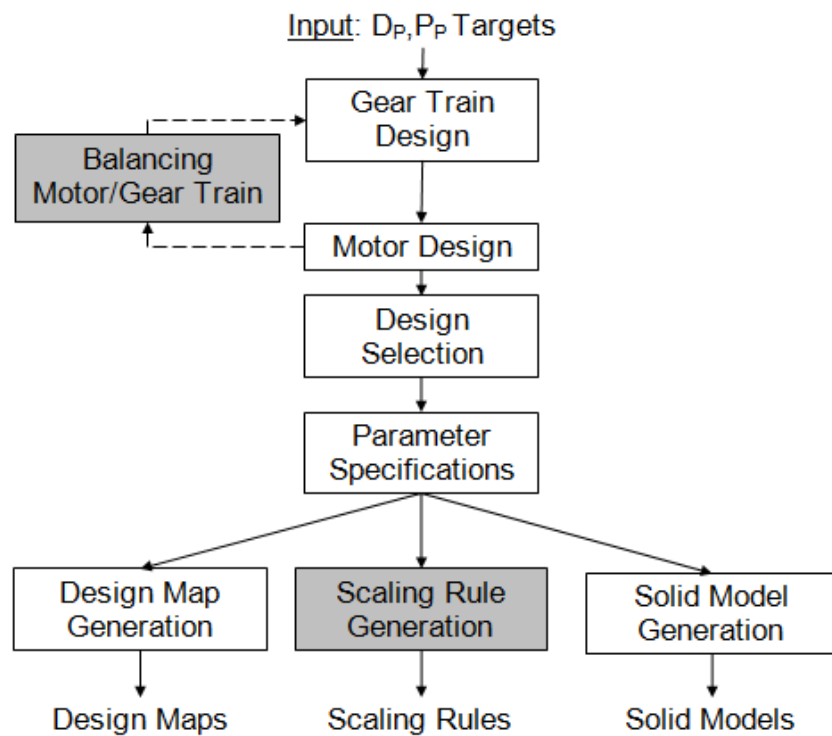


Figure 9.10: Proposed Actuator Design Procedure (D_P -design parameter, P_P -performance parameters)

The primary difference between the current procedure and the proposed procedure (Figure 9.10) is that much of the procedure was automated in a computational environment (Appendix A1). This allowed efficient generation of preliminary motor, gear train, and actuator designs. The proposed procedure had the following features that improved upon the current procedure.

- Multiple actuator designs could be completed per solution run.
- Comparisons among alternative actuators for an application were easier to manage.
- A single designer was able to manage the gear train and motor designs.

- The procedure was suitable for formal model reduction and solution tools because it was embedded into a computational environment.
- Comparisons between past and future designs (often created by different designers) were easier to manage because the designer could control his/her assumptions.

Table 9.5 summarizes the basic input and output information for each of the actuator design tasks in Figure 9.10.

Table 9.5: Input and Output Information (Parameters) for the Actuator Design Procedure Tasks

Tasks	Input	Output
Gear Train Design	Design and performance parameter targets/constraints	Gear ratio, torque, weight, inertia
Motor Design	Gear ratio, motor geometry preference	Motor torque, weight, inertia
Balance Motor and Gear Train	Aggregate actuator performance parameters	Modified gear ratio, motor geometry, gear train geometry to balance the designs
Design Selection	Parameter data for viable, alternative actuator designs	Design(s) selected as the best alternative(s)
Parameter Specifications	Complete design and performance parameter data for the selected design(s)	Standard summary and design and performance parameter information
Design Map Generation	Standard summary and design and performance parameter information	2-D and 3-D maps (P_p vs. D_p)
Scaling Rule Generation	Standard summary and design and performance parameter information	Power law and low order polynomial scaling rule representations
Solid Model Generation	Design parameter data written to SolidWorks design tables	Solid models and drawings of all components and assemblies

9.3.3.2 Motor Design Procedure

The design procedure used to generate SRM designs (Figure 9.6) and embedded in the computational tool (Appendix A1) is summarized in the following set of steps.

1. Input overall diameter (D_m) and length (L_m) or aspect ratio (A_m).
2. Calculate standard rotor and stator dimensions using the suggested proportions in Sections 3.7.2-3.7.4.
3. Calculate the space available for windings on the stator using the relationships in Section 3.7.5.
4. Search among the different wire size and number of turn combinations for maximum torque capacity.
5. Calculate the weight and inertia of the chosen geometry.

Table 9.6 summarizes the values of constants and fixed parameters used for all of the SRM designs in this report. Unless the needs of the particular application or results from ongoing research at RRG dictate otherwise, these values should not be modified when generating rules for scaling and balancing parameters such as those in this research. Keeping these values constant in this report allowed the present researcher to focus on how changes in the fundamental geometric design parameters (D_m , L_m , and A_m) affected the performance parameters.

Table 9.6: SRM Constants and Fixed Parameters

Parameter	Value
Number of stator poles	$N_s=6$
Number of rotor poles	$N_r=4$
Stator pole angle	$\theta_s=30^\circ$
Stator pole angle	$\theta_r=32^\circ$
Saturation flux density	$B_{sat}=1.56$
Axial clearance	$c = 0.005D_m$
Density	$\rho=0.284lbm/in^3$

9.3.3.3 Gear Train Design Procedure

The design procedure used to develop HGT (Figure 9.7) and PEGT (Figure 9.8) designs and embedded in the computation tool (Appendix A1) is summarized in the following set of steps.

1. Input overall diameter (D_g), length (L_g) or aspect ratio (A_g), gear ratio (g), diametral pitch range (P_{dmin} - P_{dmax}), material strength limits (S_b, S_c), output speed, and desired bearing life.
2. Calculate the key internal gear train design parameters needed for the gear ratio and torque calculations using the suggested proportions in Table 9.7.
3. Search for gear tooth number combinations that achieve the desired gear ratio.
4. Calculate the remaining design parameters (including approximate bearing dimensions) using reasonable assumptions, and rules of thumb.
5. Calculate the torque capacity, weight, inertia, and required bearing load capacities of the chosen geometry.

Table 9.7 summarizes the recommended values (from Chapter 3) of the internal design parameters for the HGT and PEGT as a function of the overall diameter (D_g) and length (L_g).

Table 9.7: Suggested Proportions for the HGT and PEGT Internal Design Parameters

	HGT	PEGT (Star 1st Stage)	PEGT (Star Compound 1st Stage)
Output Gear Pitch Diameter	$d_{r2} = 0.65D_g$	$d_r = 0.87D_g$	$d_r = 0.87D_g$
Face Width	$L_w = 0.30L_g$	$L_{pe} = 0.22L_g$	$L_{pe} = 0.20L_g$
Gear Ratio Range (g)	75-500	15-200	15-500
Aspect Ratio Range (A_g)	0.3 to 2	0.3 to 2	0.3 to 2
Balancing Mass Width	$w = 0.10L_g$	-	-
Center Distance to Crankshaft	-	$c_c = 0.27D_g$	$c_c = 0.27D_g$
1 st Stage Face Width		$L_1 = 0.11L_g$	$L_1 = 0.10L_g$

Table 9.8 summarizes the recommended values of constants and fixed parameters for the HGT and PEGT. For a detailed discussion of the bending stress modification factors (K_v , K_m , and J) refer to Section 5.2.2. Just as for the motor, keeping these values constant allowed the present researcher to focus on how changes in the fundamental geometric design parameters (D_g , L_g , g , and A_g) affected the performance parameters. Unless otherwise noted, the values used in Table 9.7 and Table 9.8 were used for all of the gear train designs in this report.

Table 9.8: Constants/Fixed Parameters for the HGT and PEGT

Parameter	Value
Pressure angle	$\phi=25$
Minimum tooth number difference	$N_{\min}=3$
Number of teeth in contact	3 (nominal load condition)
Efficiency	100%
Axial clearance	$c = 0.005D_g$
Diametral pitch range	$5 < P_d < 25$
Bending strength	$S_b=100$ ksi
Contact strength	$S_c=250$ ksi
Density	$\rho=0.284 \text{ lbm/in}^3$
Velocity Factor (K_v)	1.1
Load Distribution Factor (K_m)	1.3
Geometry Factor (J)	0.5
Output Speed (rpm)	1
Bearing Life	5000 hours

9.4 SUMMARY OF KEY RESULTS

9.4.1 Scaling Rules and Design Maps (Chapter 5)

Scaling rules were defined as analytical relationships between performance parameters and design parameters and were based on a relatively small number of carefully chosen motor, gear train, and actuator designs. Scaling rules were presented in simple power-law form, the standard low-order polynomial form used in the Response Surface Methodology (RSM), two-dimensional plots, and three-dimensional surfaces (termed “design maps”). The rules were developed using the regression techniques discussed in Section 2.7.1 in conjunction with the motor, gear train, and actuator design procedures in Chapter 4. Chapter 5 provides detailed scaling rules in the four representations listed above for the stand-alone SRM (Section 5.2.1), HGT (Section

5.2.2), and PEGT (Sections 5.2.3 and 5.2.4) component designs. As an illustrative example, the following section will summarize some of the results for the HGT.

9.4.1.1 HGT Scaling Rules and Design Maps

The HGT scaling rules developed were based on the reference design (Figure 9.7), suggested proportions (Table 9.7), and standard set of assumptions (Table 9.8) given above. Figure 9.11 provides a design map (3-D plot) of the torque as a function of the diameter and aspect ratio, and Figure 9.12 shows the same information in a 2-D representation. Table 9.9 lists the constants for the simple power law scaling rules obtained from the 2-D plots.

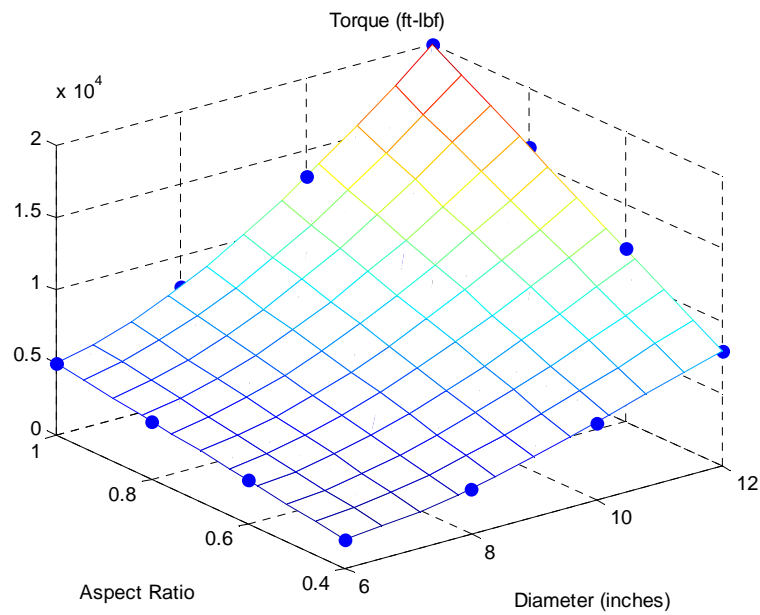


Figure 9.11: HGT Torque Design Map

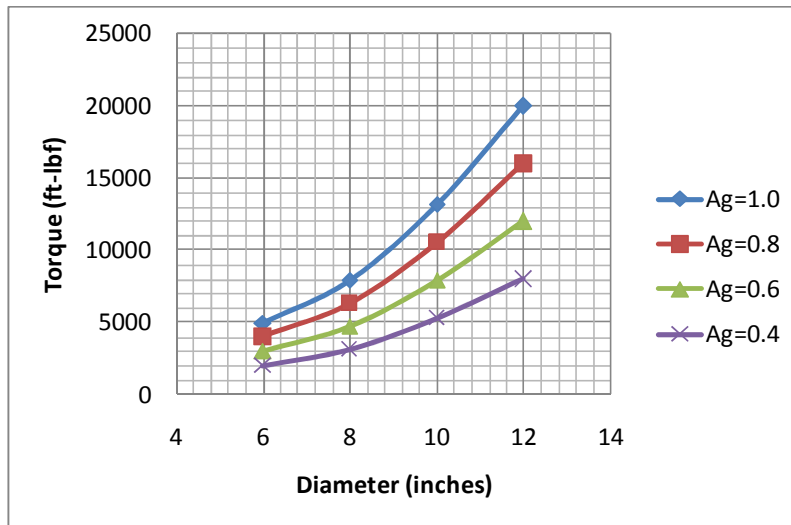


Figure 9.12: HGT Torque Design Map (2-D)

Table 9.9: HGT Power-Law Scaling Rules ($P_p = kD_g^b = kD_g^{b-1}L_g$)

	Aspect Ratio	Constant (k)	Power (b)
Torque	0.4	51.7	2.012
	0.6	77.6	2.012
	0.8	103.4	2.012
	1.0	129.3	2.012
Weight	0.4	0.158	2.596
	0.6	0.238	2.596
	0.8	0.318	2.596
	1.0	0.398	2.596
Inertia	0.4	0.00011	5.360
	0.6	0.00017	5.360
	0.8	0.00022	5.361
	1.0	0.00028	5.363
Torque Density	0.4	324.7	-0.58
	0.6	324.7	-0.58
	0.8	324.7	-0.58
	1.0	324.7	-0.58
Output Responsiveness	0.4	22459	-3.37
	0.6	22459	-3.37
	0.8	22459	-3.37
	1.0	22459	-3.37

9.4.1.2 Torque and Speed Relationship in the PEGT

Section 5.2.3 discussed how the PEGT torque capacity may either be limited by the bearings on the crankshaft or on the bending stresses in the gear teeth. Two key results were developed in that particular section.

First, all of PEGT designs in Section 5.2.3.1 had an output speed of 1 rpm to match the needs of the particular application considered, and all of the torque capacity ratings were based on this reference speed. Since the output speed may change for other applications, Figure 9.13 was used to estimate the effect of the PEGT output speed choice on the bearing-limited torque capacity for a range of output speeds. For example, changing the output speed from 1 rpm to 0.1 rpm increases the torque capacity by a factor of 2 (i.e., the torque rating for a speed of 0.1 rpm is double the torque rating at 1 rpm). This key result is independent of any particular gear train size and modeling assumptions.

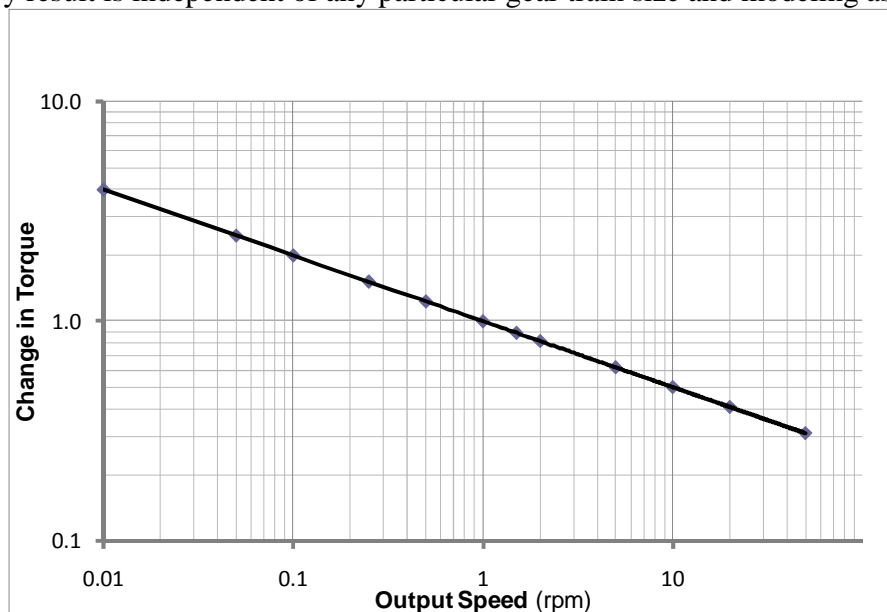


Figure 9.13: Effect of Output Speed on PEGT Torque Capacity²⁵

²⁵ This figure shows how the bearing-limited torque capacity varies as a function of output speed and is independent of any particular PEGT geometry, gear ratio, or other assumptions. It is simply a plot of the

Second, Table 9.10 compares the bearing and gear-tooth limited torque capacities in the PEGT for a range of diameters. The tooth limited load capacities in this set were based on the assumptions listed previously in Table 9.8. Table 9.10 illustrates that the bearing-limited capacity was approximately 10 to 40% larger than the gear tooth limited capacity for the range of diameters considered, with an average of near 25% (i.e., a factor of 1.25 larger). Because both the bearing-limited torque capacities and tooth-limited load capacities are known to increase linearly with an increase in length (based on the fundamental governing equations for these phenomenon in Sections 3.14.1 and 3.5.1, respectively), these percentages should not vary significantly for larger or smaller aspect ratios. The diametral pitch (P_d) for each gear train design has also been listed for future reference because it significantly affects the gear-tooth limited torque capacity (Sections 5.2.5.2 and 5.3). Note that these results depend on the output speed of the gear train, and any change in operating speed will change the bearing-limited torque according to the torque-speed relationship plotted above in Figure 9.13.

approximately inverse cubic bearing life relationship between torque T and speed ω in section 5.2.3.1. The anticipated increase or decrease in the torque capacity for any change in output speed can be considered.

Table 9.10: Comparison of Bearing and Tooth-Limited Torque Capacities of the PEGT

Diameter (inch)	Length (inch)	Bearing- Limited Torque Capacity (ft-lbf)	Gear Tooth- Limited Torque Capacity (ft-lbf)	Diametral Pitch (P_d) for Tooth- Limited Designs	Ratio of Bearing- Tooth Torque Capacity
5	2.0	715	583	23.9	1.2
7	2.8	2008	1600	17.1	1.3
8	3.2	3121	2389	14.9	1.3
10	4.0	5030	4665	12.0	1.1
11	4.4	6938	6210	10.9	1.1
12	4.8	10315	8062	10.0	1.3
18	7.2	35431	27208	6.6	1.3
24	9.6	79470	63879	5.0	1.2
30	12.0	130314	92909	5.4	1.4

9.4.1.3 Relationship Between Bending and Contact Stresses

As discussed in Section 3.5.3 and proven true for past gear train designs based on circular arc gear teeth with small tooth number differences between mating gears (see the HGT stress results in Park and Tesar [2005]), the bending stress typically limits the size of the gear train rather than the contact stress. As an example, Table 9.11 lists the values of the bending and contact stresses in the HGT for the range of sizes considered in Section 5.2.2. A bending stress limit of 100 ksi was used for all of the HGT in this table (and all the gear train designs in this report) in order to allow for easy scaling based on the stress limits for different applications. The key result from the table is that bending stresses were a factor of 1.1 to 1.4 times the contact stresses. Though not shown here, similar results were achieved for the PEGT in Section 5.2.3. Ongoing research at RRG is underway to consider the choices of the height and width of the gear tooth and how these choices can be used to balance the bending and contact stresses.

Table 9.11: Relative Values of the Bending and Contact Stresses in the HGT

Overall Diameter (inches)	Aspect Ratio	Bending Stress (ksi)	Contact Stress (ksi)	Ratio of Bending to Contact Stress
6	0.4	100	88	1.1
8	0.4	100	72	1.4
10	0.4	100	71	1.4
12	0.4	100	70	1.4
6	0.6	100	88	1.1
8	0.6	100	72	1.4
10	0.6	100	71	1.4
12	0.6	100	70	1.4
6	0.8	100	88	1.1
8	0.8	100	72	1.4
10	0.8	100	71	1.4
12	0.8	100	70	1.4
6	1	100	88	1.1
8	1	100	72	1.4
10	1	100	71	1.4
12	1	100	70	1.4

9.4.1.4 Comparisons Between the HGT and the Star+PEGT Alternatives

Based upon their individual scaling rules, a few general comparisons between alternative gear train types (of the same size and gear ratio) can be made. One comparison (Section 5.3) involved the HGT (scaling rules given in Section 5.2.2) and Star+PEGT (Section 5.2.3) alternatives, and another comparison (Section 5.4) involved the Star+PEGT and Star Compound+PEGT (Section 5.2.4) alternatives. As an illustrative example, Figure 9.14 shows the average percent difference between the performance parameters for the former comparison, with positive numbers indicating that the HGT has larger values for the performance parameter (P_p) under consideration. The percent difference between the performance parameters (P_p) of the HGT and Star+PEGT was computed as follows.

$$\% \text{ Difference} = 100 \times \left(\frac{P_{P,HGT} - P_{P,PEGT}}{P_{P,HGT}} \right) \quad \text{Eqn. 193}$$

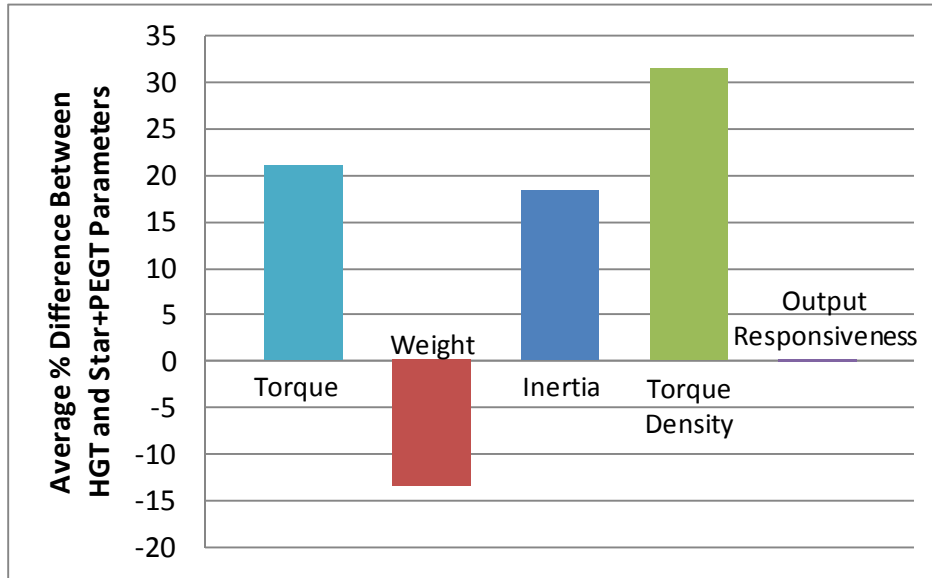


Figure 9.14: Percent Difference Between the Performance Parameters of the HGT and Star+PEGT Alternatives (Only average values of the percent difference are plotted for each performance parameter.)²⁶

Based upon this comparison, as the diameter increases, the Star+PEGT becomes comparable or superior to the HGT for all of the performance parameters except weight (see Section 5.3 for a justification for this result). Diameters only up to 12 inches were considered in this particular comparison, and based upon the trends in the complete results presented in Section 5.3, the Star+PEGT is expected to be the superior choice for diameters larger than 12 inches. While these results provided a good starting point for a comparison, there are other, less quantitative performance parameters such as number of

²⁶ Positive (negative) percentages indicate that for the same overall diameter and length, the HGT has a larger (smaller) value for the performance parameter being considered. For torque, torque density, and responsiveness, positive percentages indicate that the HGT is superior to the PEGT. For weight and inertia, positive percentages indicate that the PEGT is superior to the HGT.

parts, number of bearings, complexity, gear mesh stiffness, etc. that need to be considered in detail before one of these alternatives is selected for a specific application.

9.4.1.5 Key Results from Chapter 5

Table 9.12 summarizes the simple power law scaling rules generated for the SRM, HGT, and Star+PEGT component designs in Chapter 5. This table serves as a quick reference for determining how these performance parameters (P_p) vary with the basic diameter (D) and length (L) choices in the motor and gear train and should be interpreted in the context of the assumptions provided in Table 9.6, Table 9.7, and Table 9.8. The relatively lower exponent for the HGT torque relative (2.0) to the PEGT torque (3.0) occurs due to the relatively lower diametral pitches used for the HGT (near 5) relative to the PEGT (between 10 and 20) for the full range of gear train diameters considered. Also, the constant k is an order of magnitude higher for the HGT (from 50 to 130) relative to the PEGT (from 5 to 12). Refer to Sections 5.2.2 and 5.2.3 specific values of the coefficients k and exponents b for different diameters of the HGT and PEGT. An exact comparison between HGT and PEGT of the same size and gear ratio (Section 5.3) revealed that the absolute HGT torque capacity is approximately 20% higher (on average) than the PEGT for diameters between 6 and 12 inches, but this benefit decreases with increasing diameter.

Table 9.12: Individual Motor and Gear Train Power-Law Scaling Rules
 $(P_p = kD^b = kD^{b-1}L)$

	Power (b)		
	SRM	HGT	Star+PEGT
Torque	4.3	2.0	3.0
Weight	3.0	2.6	3.0
Inertia	4.9	5.4	5.0
Torque Density	1.0	-0.6	0.0
Output Responsiveness	1.0	-3.4	-2.0

Section 5.6 provided a detailed discussion of key results obtained from the scaling rules and design maps generated in Chapter 5. In brief, bulleted form, the key results with respect to the stand-alone SRM, HGT, Star+PEGT, and Star Compound+PEGT component designs were as follows.

- All of the performance parameters considered (torque, weight, inertia, torque density, and responsiveness) were a stronger function of diameter (typically squared or higher) than aspect ratio (typically linear or independent of).
- Torque, weight, and inertia were each proportional to at least the square of the diameter (or higher) and were linearly proportional to the aspect ratio parameter.
- The computed weights of the motor and gear trains considered were generally from 70 to 80% of the weight of a solid cylinder of the same dimensions.
- The torque density and responsiveness were shown to be essentially independent of the aspect ratio (length).

- While both the gear trains had higher absolute torque density than the SRM for the same diameter, the SRM torque and torque density increased (with increasing diameter) at a faster rate than for the gear train.
- The output responsiveness (a measure of the acceleration capability at the output) always decreased with increasing diameter.

9.4.2 Balancing Parameters (Chapter 6)

Chapter 6 defined balancing parameters as the allocation of torque, weight, inertia, torque density, and responsiveness between the motor and gear train and the task of selecting the actuator design parameters that achieve the desired allocation. Section 6.1 described a scenario that illustrated the need to balance the parameters between the motor and gear train. The current approach to balancing parameters is essentially a trial and error procedure for coupling a motor and a gear train, and it is not guaranteed to produce an optimal balance of the torque, weight, inertia, and other parameters between the motor and gear train. This approach has been repeated many times in developing actuators for a variety of applications by the present researcher, and this led to the development of the step-by-step actuator design procedure presented in Chapter 4.

9.4.2.1 Actuator Design Parameter Choices for Balancing Parameters

Given an overall length (L) and diameter (D_g) requirement for an actuator such as those in Figure 9.9, the six basic parameters that the designer can use to balance the motor and gear train are summarized in Table 9.13. For a single actuator design, the designer is advised to use these parameters to control the size of the motor relative to the gear train. For a set/family of actuator designs, the designer is advised to explicitly specify which of these parameters are to be held constant and which are to vary among the set. This particular principle was discussed in more detail in the scaling (Section 2.5)

and product family design (Section 2.6) literature in Chapter 2. Designing a family of actuators for an application can be a daunting task, but grouping the designs based on these basic parameter choices can make the task more tractable. Refer to Section 6.2 for a more detailed explanation of these important parameter choices.

Table 9.13: Key Actuator Design Parameter Choices

Parameter	Description	Typical Range
Gear Ratio (g)	depends on gear train type, see Chapter 3	HGT (from 75-500) PEGT (from 15-500)
Motor Aspect Ratio (A_m)	$A_m = \frac{L_m}{D_m}$	between 0.3 and 2.0
Gear Train Aspect Ratio (A_g)	$A_g = \frac{L_g}{D_g}$	between 0.3 and 2.0
Overall Aspect Ratio (A)	$A = \frac{L_m + L_g}{D_g} = \frac{L}{D_g}$	between 0.5 and 2.0
Ratio of Motor Length to Overall Length (K_l)	$K_l = \frac{L_m}{L} = \frac{L_m}{L_m + L_g}$	between 0.3 and 0.7
Ratio of Motor Diameter to Gear Train Diameter (K_d)	$K_d = \frac{D_m}{D_g}$	between 0.3 and 1.25

9.4.2.2 Types of Balance

Table 9.14 identifies the different types (levels) of balance between the motor and the gear train for the EMAs in the present research. The reader is referred to Section 6.3, where relevant modeling equations are provided for each of type.

Table 9.14: Types of Balance Between the Motor and Gear Train

Type of Balance	Description	Relative Importance and Feasibility
Between the Motor and Gear Train-Limited Torque Capacities	Neither the motor nor the gear train limits the overall rated torque capacity of the actuator more than the other.	This type of balance is essential and always possible if geometric compatibility between the motor and gear train shafts and housings is considered.
Between the Weight/Inertia of the Motor and Gear Train	The weight and inertial content of the motor and gear train can be moved between the two components, primarily by the choice of the gear ratio.	This type of balance is desirable and is particularly important for applications in which high accelerations are required.
Between the Tooth-Limited and Bearing-Limited Torque Capacity in the PEGT	Neither the bearings nor the gear train limits the overall rated torque capacity of the PEGT more than the other.	This type of balance is desirable and whether it can be achieved depends heavily on the running speed of the bearings, which limits their torque capacity for a fixed life (see Section 5.2.3.2)
Bearing Life Between Multiple Bearings	The estimated bearing lives of the multiple bearings in an actuator should be matched or made to be a multiple of the others.	This type of balance is not essential but desirable for scheduling bearing replacement and maintenance times. This balance is generally very difficult because bearings are usually chosen based on the space constraints of an actuator design.

Chapter 6 provided examples that illustrated the first two types of balance, and the following section will summarize some of the key results from Example 1 (Section 6.5) and Example 2 (Section 6.6).

9.4.2.3 *Balancing the Motor and Gear Train Torque Capacities in the SRM+Star+PEGT Actuator*

This example presents scaled sets of actuator designs that illustrate how the motor length to overall length ratio (K_l), gear train aspect ratio (A_g), and motor diameter to gear train diameter ratio (K_d) can be varied to balance the motor and gear train torque capacities as the gear train diameter increases. Gear train diameters (D_g) ranging from 10

to 50 inches (with increments of 5 inches), a constant gear ratio of 100 to 1, and a constant overall aspect ratio (A) of 1.0 were considered. Given a feasible range for K_d from (approximately) 0.25 to 1.0, the approach in this example was to adjust the value of K_l for each gear train diameter so that the motor and gear train torque capacities were balanced while maintaining the same overall and motor aspect ratios.

Figure 9.15-Figure 9.18 illustrate how the torque, weight, torque density, and output responsiveness vary as a function of diameter for the SRM+Star+PEGT actuator combination used in this example. Table 9.15 provides the simple power law scaling rules that were obtained from these 2-D plots.

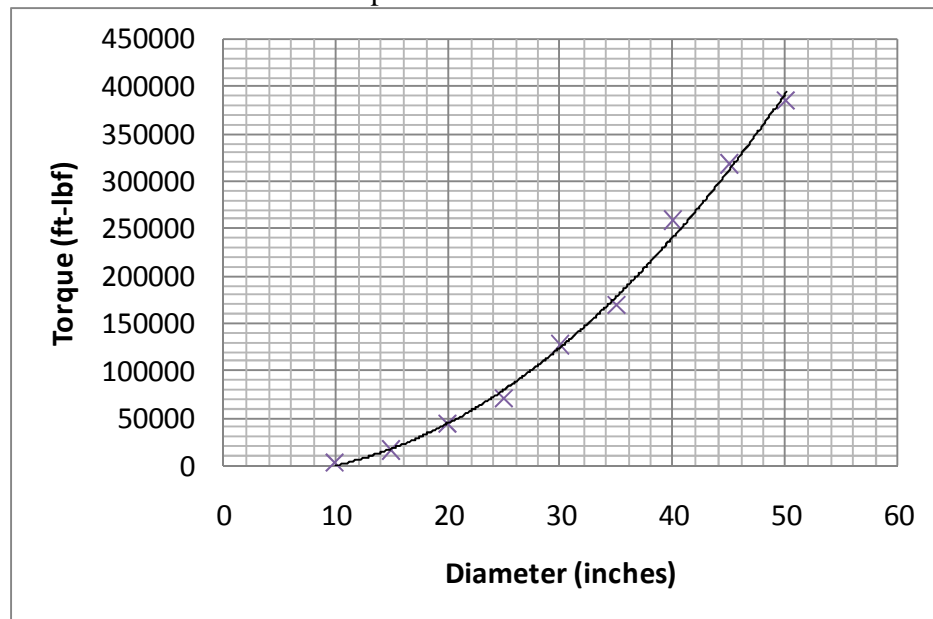


Figure 9.15: SRM+Star+PEGT Torque as a Function of Diameter

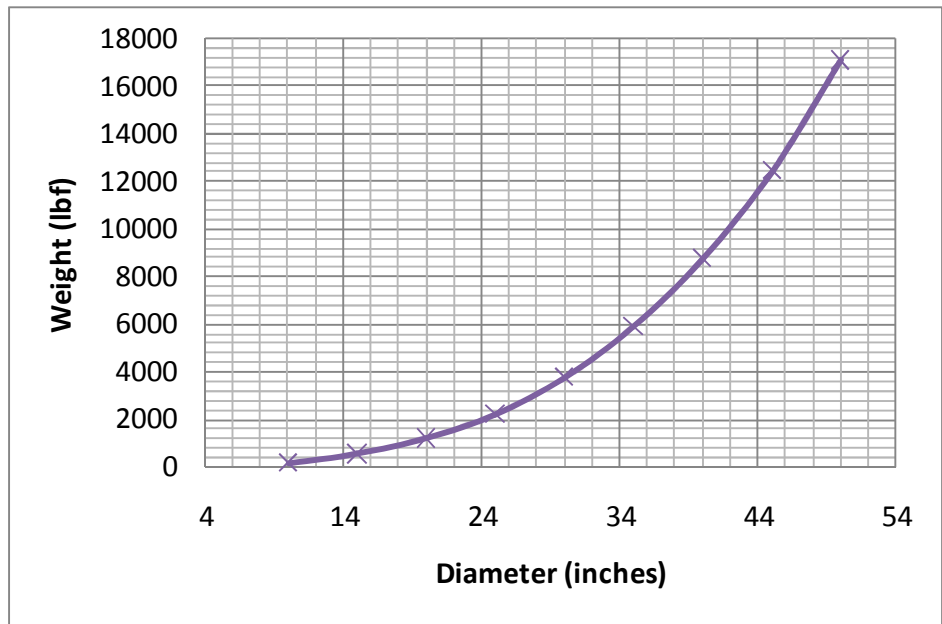


Figure 9.16: SRM+Star+PEGT Weight as a Function of Diameter

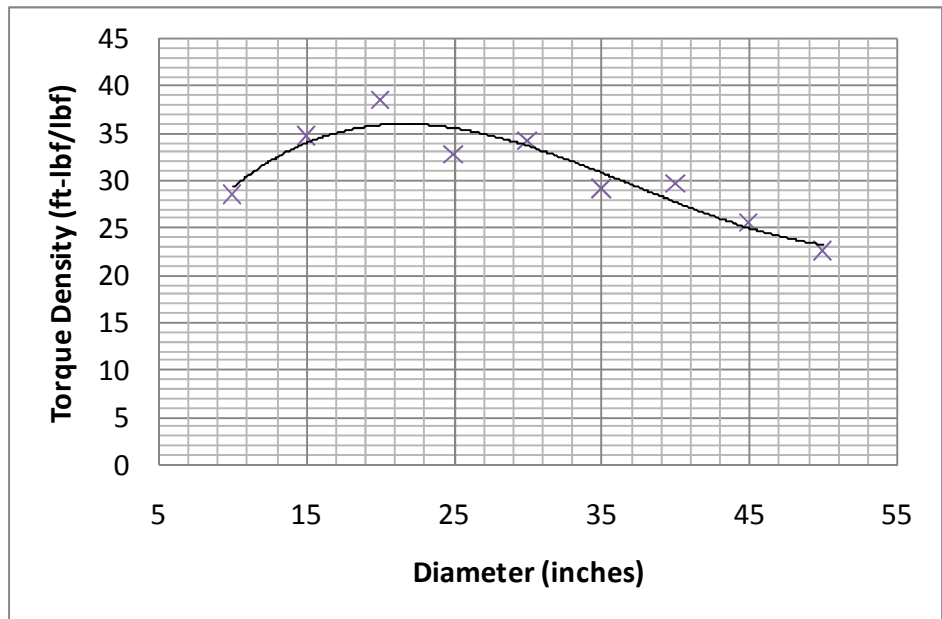


Figure 9.17: SRM+Star+PEGT Torque Density as a Function of Diameter



Figure 9.18: SRM+Star+PEGT Output Responsiveness as a Function of Diameter

Table 9.15: SRM+Star+PEGT Power-Law Scaling Rules ($P_p = kD_g^b$)

Parameter	Constant (k)	Power (b)
Torque	10.92	2.72
Weight	0.21	2.88
Inertia	0.0010	4.74
Torque Density	NA	NA
Input Responsiveness	5.12E+04	-2.01
Output Responsiveness	5264	-2.01

The PEGT torque density increases slightly with increasing diameter for the lower range of diameters because of a decrease in diametral pitch (i.e., wider, bigger teeth) and then begins to decrease slightly after that due to the fact that a contact ratio of 3 was used for designs of different diameters (see Section 6.5.2 for further explanation). Figure 9.19 and Figure 9.20 provide the distribution of weight and inertia in the motor and gear train as a function of diameter. The basic conclusion is that as the diameter increases, the weight and inertial content moves from the motor to the gear train.

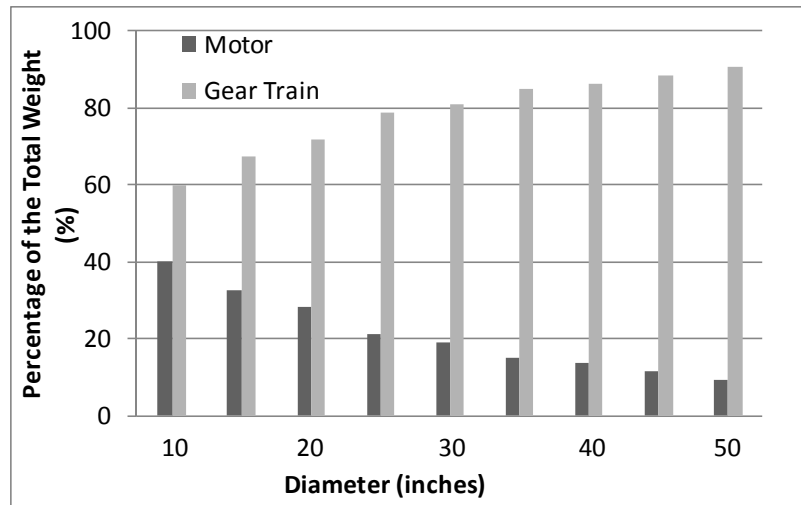


Figure 9.19: Percentage of Weight in the Motor and Gear Train as a Function of Diameter for the SRM+Star+PEGT Actuator

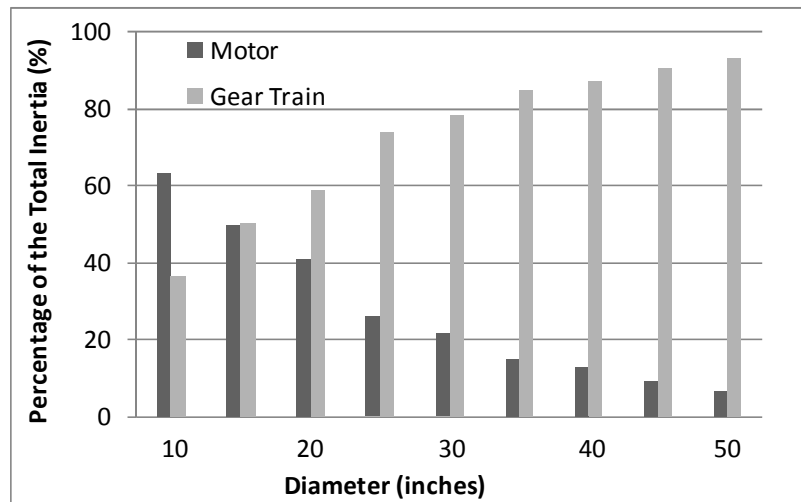


Figure 9.20: Percentage of Inertia in the Motor and Gear Train as a Function of Diameter for the SRM+Star+PEGT Actuator

9.4.2.4 Comparisons Between the SRM+HGT and SRM+Star+PEGT Alternatives

Based upon their similar performance parameter results, it is useful to make a few general comparisons between the SRM+Star+PEGT (Section 6.5.1) and the SRM+HGT (Section 6.5.2), both with a 100 to 1 gear ratio and with the same overall diameter and

length. This comparison is analogous to that provided in Section 9.4.1.4, but the results in this section include the SRM. Figure 9.21 computes the average percent difference between the performance parameters for these two alternatives, with positive numbers indicating that the SRM+HGT combination has larger values for the performance parameter under consideration. The percent difference between the performance parameters (P_p) of the SRM+HGT and SRM+Star+PEGT was computed as follows.

$$\% \text{ Difference} = 100 \times \left(\frac{P_{P,SRM+HGT} - P_{P,SRM+Star+PEGT}}{P_{P,SRM+HGT}} \right) \quad \text{Eqn. 194}$$

Based upon this comparison, the SRM+Star+PEGT combination is superior to the SRM+HGT combination for all the performance parameters considered except weight (see Section 6.5.4 for more details). Note that a similar conclusion was reached when making a comparison between only the gear trains in Section 9.4.1.4.

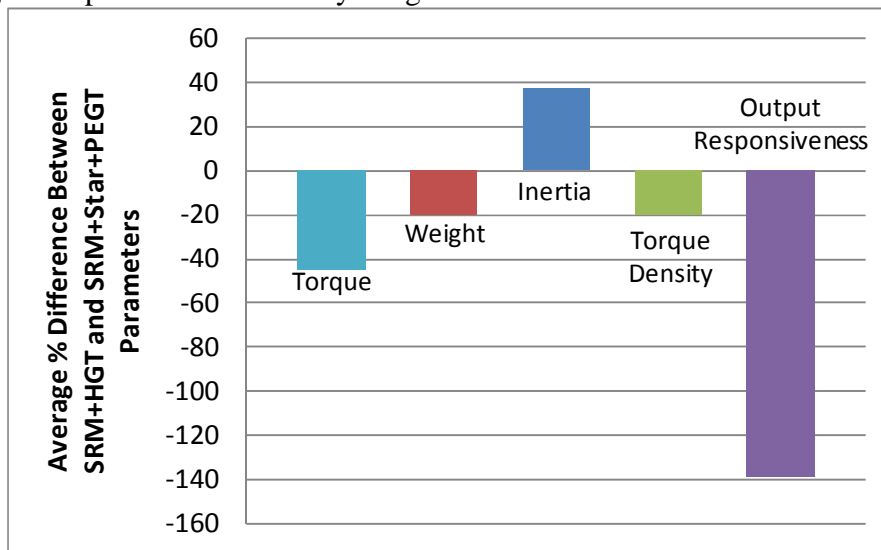


Figure 9.21: Percent Difference Between the Performance Parameters of the SRM+HGT and SRM+Star+PEGT Alternatives (Only average values of the percent difference are plotted for each performance parameter.)²⁷

²⁷ Positive (negative) percentages indicate that for the same overall diameter and length, the SRM+HGT has a larger (smaller) value for the performance parameter being considered. For torque, torque density,

9.4.2.5 Balancing the Weight and Inertia in the SRM+HGT Actuator

This example illustrates how the diameter and gear ratio parameters affect the distribution of weight and inertia between the motor and the gear train. The results will help the designer to identify the dominant weight and inertia in designs of different diameters and gear ratios. Gear train diameters (D_g) of 8, 12, 16, and 20 inches, a constant gear train aspect ratio of 0.55, and gear ratios from 100 to 400 were considered. Figure 9.22-Figure 9.24 illustrate how the weight, torque density, and output responsiveness vary as a function of gear ratio for multiple diameters. Note that some of the diameters have been omitted from the plots to better illustrate the trends without large changes in magnitude.

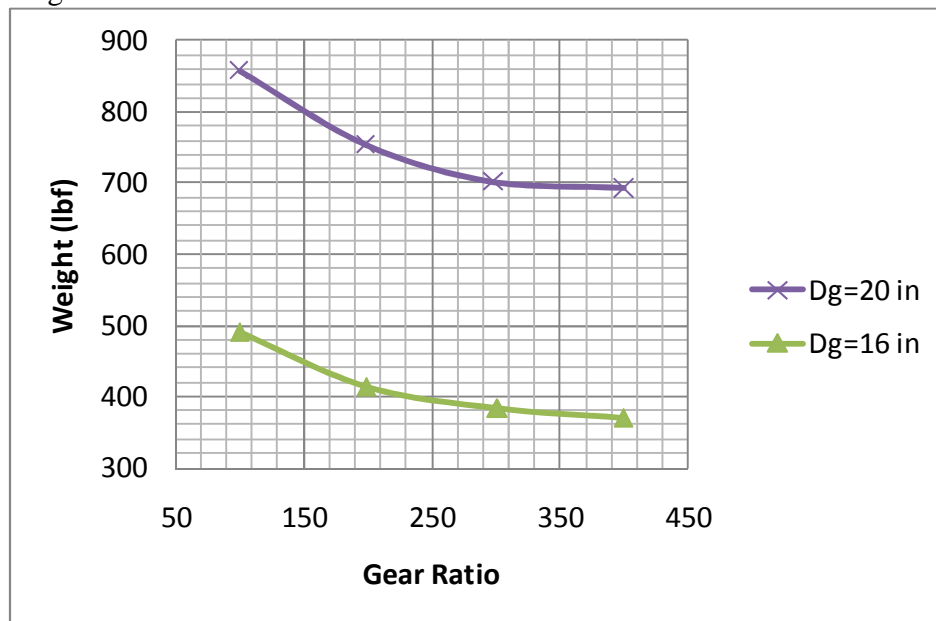


Figure 9.22: SRM+HGT Weight as a Function of Gear Ratio and Diameter

and responsiveness, positive percentages indicate that the SRM+HGT is superior to the SRM+Star+PEGT. For weight and inertia, positive percentages indicate that the SRM+Star+PEGT is superior to the SRM+HGT.

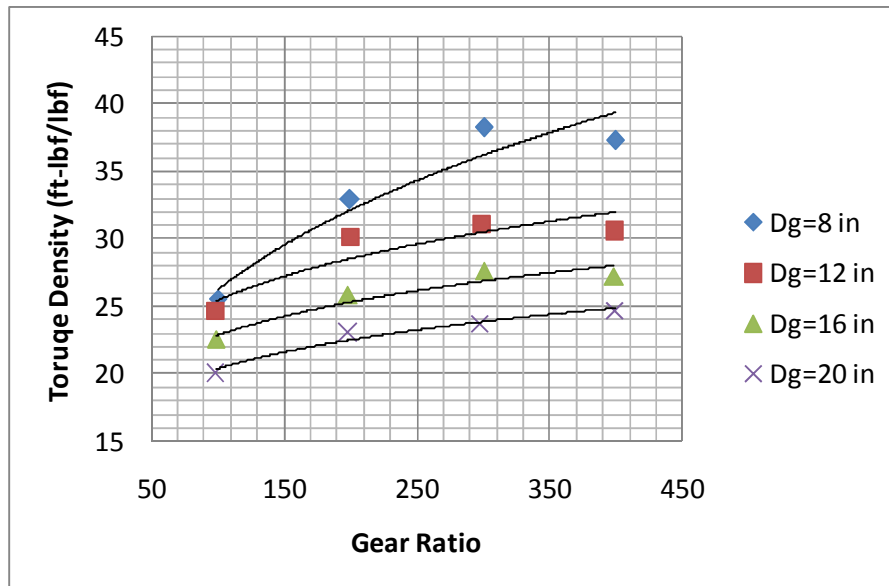


Figure 9.23: SRM+HGT Torque Density as a Function of Gear Ratio and Diameter

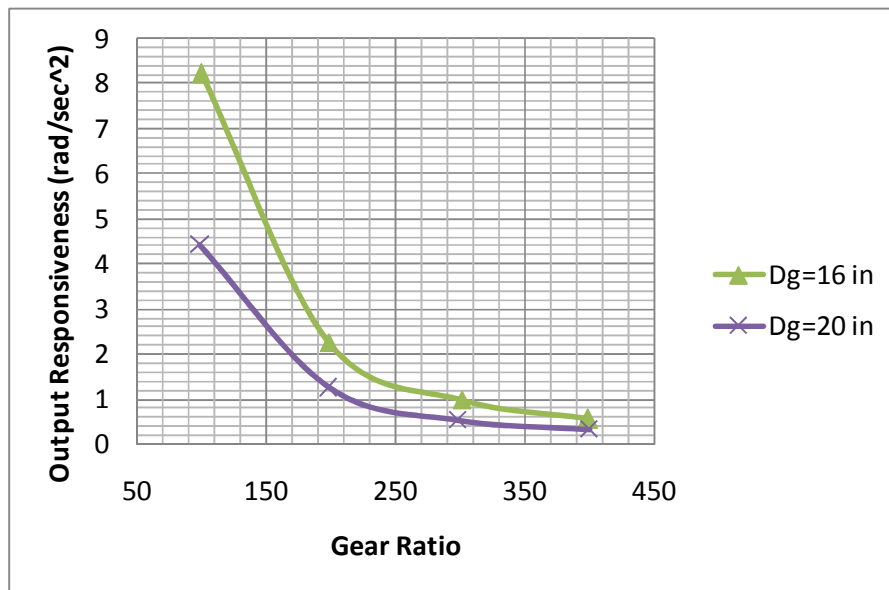


Figure 9.24: SRM+HGT Output Responsiveness as a Function of Gear Ratio and Diameter²⁸

²⁸ The variation in output responsiveness due to changes in gear ratio and diameter was discussed in detail throughout Chapter 7. The trends in this figure are consistent with the stand-alone HGT responsiveness results reported in section 5.2.2.

Table 9.16 lists the percentage change in each of the performance parameters as the difference between the value of the performance parameter for the highest gear ratio of 400 to 1 and the value of the parameter for the lowest gear ratio of 100 to 1. Thus, a positive number in the table indicates an increase in the parameter due to increasing the gear ratio. The key result from the table is that increasing the gear ratio from 100 to 400 provides the benefits of reduced weight and inertia and increased torque density without any added complexity (same number of parts and bearings). One drawback of increasing the gear ratio is the reduction in both the input and output responsiveness, which suggests that lower gear ratios are more favorable for applications in which achieving high acceleration is important. Section 7.3.1.1 discusses this noteworthy result in more detail. Figure 9.25 presents the same information as Table 9.16 in a graphical representation, and only the average values of the percentage change of the performance parameters are plotted.

Table 9.16: Percentage Change of the SRM+HGT Performance Parameters as the Gear Ratio is Varied from 100 to 400 for Different Diameters

Overall Diameter (inches)	Torque (ft-lbf)	Weight (lbf)	Inertia (lbm-in ²)	Torque Density (ft-lbf/lbf)	Input Responsiveness (rad/sec ²)	Output Responsiveness (rad/sec ²)
8	-11%	-39%	-55%	46%	-50%	-88%
12	-12%	-29%	-35%	24%	-67%	-92%
16	-9%	-24%	-16%	21%	-73%	-93%
20	-1%	-19%	-14%	23%	-72%	-93%
Average % Change	-8%	-28%	-30%	28%	-65%	-91%

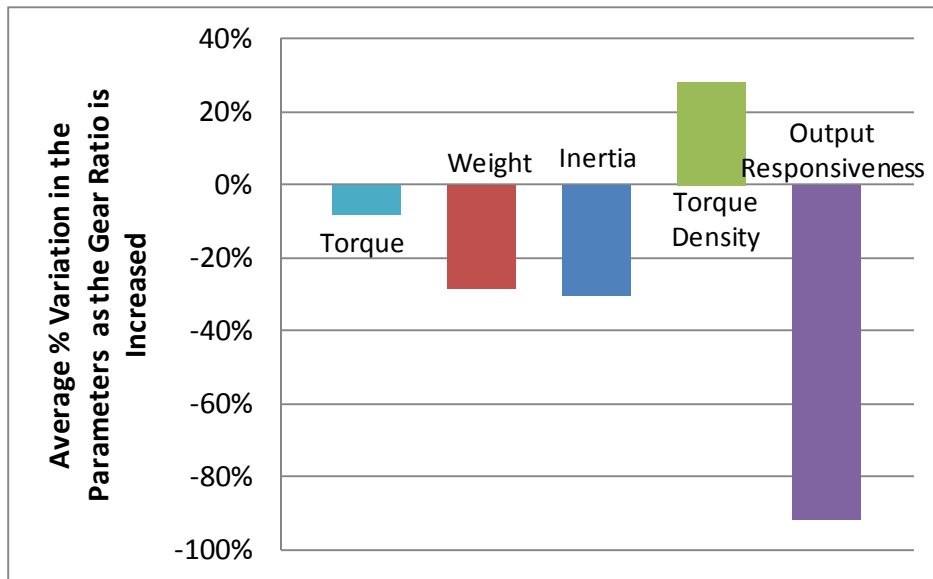


Figure 9.25: Percentage Change of the SRM+HGT Performance Parameters as the Gear Ratio is Varied from 100 to 400 (Only average values of the percentage change are plotted for each performance parameter.)

Table 9.17 provides the distribution of weight and inertia in the motor and gear train as a function of diameter and gear ratio. The basic conclusion is that as the gear ratio increases for a given diameter, the weight and inertial content moves from the motor to the gear train. Figure 9.26 and Figure 9.27 graphically display the information in Table 9.17 for the 12 inch diameter design.

Table 9.17: Distribution of Weight and Inertia (as a % of the total) in the Motor and Gear Train as a Function of Diameter and Gear Ratio (for the SRM+HGT Actuator)

Overall Diameter (inches)	Gear Ratio	Motor Weight (%)	Gear Train Weight (%)	Motor Inertia (%)	Gear Train Inertia (%)
8	100	41	59	61	39
	200	32	68	39	61
	301	29	71	27	73
	400	25	75	19	81
12	99	31	69	31	69
	201	24	76	16	84
	299	20	80	10	90
	399	17	83	7	93
16	99	24	76	17	83
	198	18	82	7	93
	301	15	85	4	96
	399	13	87	3	97
20	99	20	80	9	91
	199	14	86	4	96
	298	12	88	2	98
	400	10	90	2	98

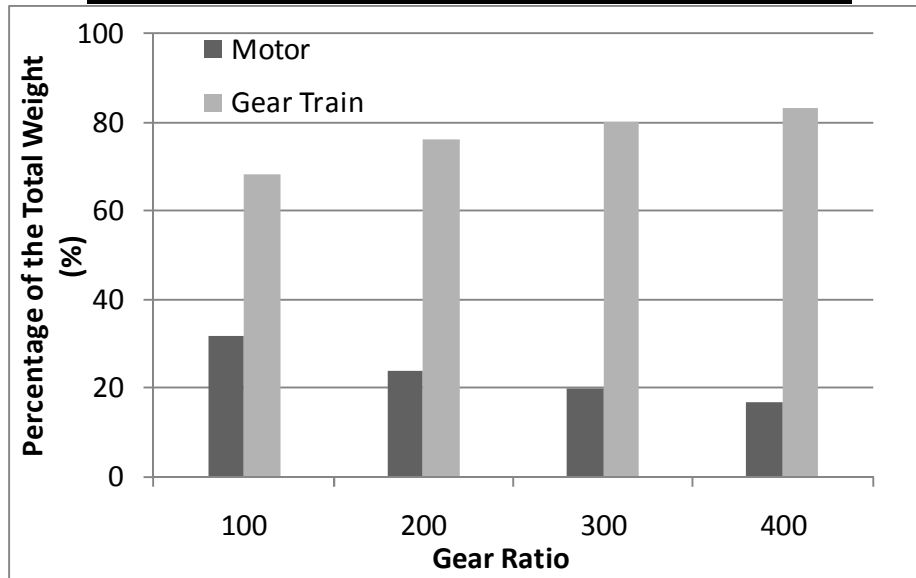


Figure 9.26: Percentage of Weight in the Motor and Gear Train as a Function of Gear Ratio for the Overall Diameter of 12 inches (for the SRM+HGT Actuator)

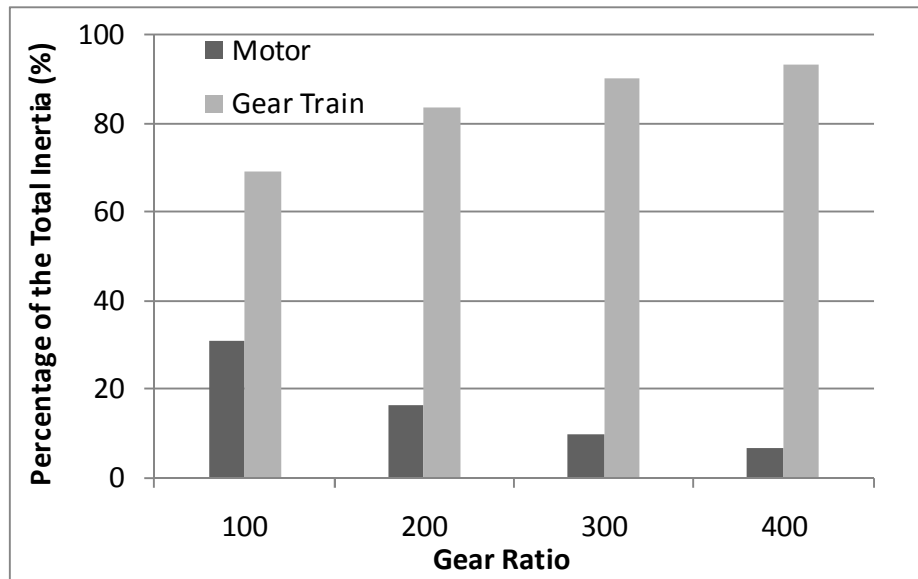


Figure 9.27: Percentage of Inertia in the Motor and Gear Train as a Function of Gear Ratio for the Overall Diameter of 12 inches (for the SRM+HGT Actuator)

9.4.2.6 Key Results from Chapter 6

Table 9.18 summarizes the simple power law scaling rules generated for SRM+HGT, SRM+Star+PEGT, and SRM+Star Compound+PEGT actuator designs in Chapter 6. This table serves as a quick reference for determining how these performance parameters (P_p) vary with the overall diameter (D) choice and should be interpreted in the context of the assumptions provided in Table 9.6, Table 9.7, and Table 9.8. Though less important than the power coefficient (b), refer to Section 6.5 to obtain the values of leading coefficients k for the scaling rules.

Table 9.18: Actuator Power-Law Scaling Rules ($P_p = kD^b$)

	Power (b)		
	SRM+HGT	SRM+Star+PEGT	SRM+Star Compound+PEGT
Torque	2.4	2.7	2.7
Weight	2.7	2.9	3.0
Inertia	5.0	4.7	4.4
Torque Density	-0.4	NA	NA
Output Responsiveness	-2.7	-2.0	-1.7

Section 6.6 provided a detailed discussion of key results obtained from the two examples in Chapter 6. In brief, bulleted form, the key results with respect to the three actuator combinations considered were as follows.

- All of the performance parameters considered (torque, weight, inertia, torque density, and responsiveness) were a stronger function of diameter and gear ratio (typically squared or higher) than aspect ratio (typically linear or independent of).
- For small gear train diameters (less than 10 inches for the examples presented), it was difficult to find motors with suitable torque capacity that have a diameter and length that were compatible with the gear train. To fix this imbalance, the designer was advised to use the largest gear ratios possible for the smaller diameter designs.
- As the diameter was increased for a fixed gear ratio (Example 1, Section 6.5) and as the gear ratio was increased for a fixed diameter (Example 2, Section 6.6), the dominant weight and inertia generally moved from the motor to the gear train. The exception to this result occurred for the SRM coupled with the star or star compound 1st stage gear trains, in which the dominant inertia shifted from the gear train to the motor as the gear ratio increased for a fixed diameter (see Sections 6.6.2.2 and 6.6.3).
- As the diameter was increased for a fixed gear ratio (Example 1), the torque density decreased slightly, mirroring the trends in torque density from Chapter 5 for the individual HGT and PEGT designs.
- As the gear ratio was increased from its minimum to maximum suggested values for a fixed diameter (Example 2), the torque density generally increased (by between 20 and 30%) due to the reduced motor torque

demands and the ability to use a smaller motor. However, the relative benefits in weight reduction and increased torque density diminished as the gear ratio was increased to near its maximum limit.

- As the diameter was increased for a fixed gear ratio (Example 1) and as the gear ratio was increased for a fixed diameter (Example 2), the output responsiveness (i.e., the ability to accelerate the load) always decreased.

9.4.3 Comparison of Direct Drive and Geared Actuators (Chapter 7)

Chapter 7 attempted to answer the question “Why use a gear train?” by making multiple comparisons between direct drive and geared actuators. The “direct drive” designation refers to a system that includes a motor directly connected to an inertial load and does not include a gear train. The “geared” designation refers to a system in which a motor-gear train combination (i.e., an integrated actuator) is connected to an inertial load. The geared systems considered in this chapter were the SRM+HGT, SRM+Star+PEGT, and SRM+Star Compound+PEGT actuators. These geared systems were compared to direct drive systems based on the SRM in terms of their relative torque density and responsiveness values.

One of the motivations for studying the responsiveness of an actuator comes from the following quote taken from a manufacturer’s catalog [Kollmorgen, 2008]. “A direct drive motor provides the highest practical torque-to-inertia ratio where it counts—at the load. In a geared system, reflected output torque is proportional to the gear reduction while reflected output inertia is proportional to the square of the gear reduction. Thus, the torque-to-inertia ratio in a geared system is less than that of a direct drive system by a factor equal to the gear-train ratio. The higher torque-to-inertia ratio of direct drive motors makes them ideally suited for high acceleration applications with rapid starts and

stops.” The aim of Chapter 7 was to explore the validity of this statement for the specific motor and gear train types being considered in this research.

9.4.3.1 Responsiveness Relationships

Continuing the discussion on designing for dominant inertial loads from Chapter 2 (Section 2.4), Table 9.19 summarizes the important torque, weight, inertia, and other parameters needed to compare direct drive and geared systems.

Table 9.19: Motor, Gear Train, and Load Parameters

Component	Parameter	Symbol	Description
Motor	Torque	T_m	torque capacity of the motor
	Inertia	I_m	inertia reflected to the motor (input) shaft
Gear Train	Torque	T_g	torque capacity of the gear train
	Inertia	I_g	inertia reflected to the input gear or shaft of the gear train
	Gear Ratio	g	gear ratio between motor/input shaft and output shaft/gear of the gear train
Load	Torque	T_l	load torque given by the application requirements
	Inertia	I_l	load inertia attached to the output shaft
	Load to Reference (Motor) Inertia Ratio	K	factor used to specify the load inertia as a multiple of a specified reference inertia
	Reference Inertia	I_{ref}	reference inertia (typically that of the direct drive SRM) used to define the load inertia
Geared System (Motor+Gear Train)	Input Responsiveness	R_{gi}	acceleration of the motor shaft in a motor-gear train system
	Output Responsiveness	R_{go}	acceleration of the output shaft/load in a motor-gear train system
Direct Drive System (Motor Only)	Responsiveness	R_d	acceleration of the motor shaft in a motor only system

From Section 2.4.1, the fundamental governing equation of an integrated motor and gear train system was written as follows.

$$T_m - T_f - T_{loss} - \frac{T_l}{g} = \left(I_m + I_g + \frac{I_l}{g^2} \right) R_{gi} \quad \text{Eqn. 195}$$

After some rearrangement and simplifying assumptions (see Section 7.1.1), the input responsiveness of the geared system (R_{gi}) was written as follows.

$$R_{gi} = \frac{T_m}{\left(I_m + I_g + \frac{I_l}{g^2} \right)} \quad \text{Eqn. 196}$$

This equation defined the input responsiveness (i.e., the acceleration of the motor shaft) as a function of the motor, gear train, and load parameters defined in Table 9.19. For a geared system, a distinction was made between the input (R_{gi}) and output (R_{go}) responsiveness. The latter can be obtained by dividing the output/gear train torque (T_g) by the inertia reflected to the output.

$$R_{go} = \frac{T_g}{I_m g^2 + I_g g^2 + I_l} \quad \text{Eqn. 197}$$

For the purpose of calculating responsiveness of an actuator without specific information about the load inertia and geometry (i.e., without a specific application in mind), it was necessary to define a load inertia (I_l) that is a multiple of a reasonable reference inertia (I_{ref}).

$$I_l = KI_{ref} \quad \text{Eqn. 198}$$

In this chapter, the reference inertia was defined as the inertia of the direct drive system (i.e., only the motor inertia) of interest. Given this designation, K was referred to as the load (inertia) to motor inertia ratio and was physically interpreted as an inertial disturbance being added to the system. In previous chapters, the value of K was held constant to focus on the performance parameters of torque, weight, inertia, and torque density. However, in Chapter 7, K was an important variable to illustrate how the responsiveness of a system changes as the load inertia was varied.

Removing the gear train inertia term from the relationships above, the responsiveness of a direct drive system (R_d) was defined as follows.

$$R_d = \frac{T_m}{I_m + I_l} \quad \text{Eqn. 199}$$

9.4.3.2 Comparison Assumptions

Two distinct comparisons were made between direct drive systems and geared systems. The first comparison (illustrated by Figure 9.28) involved systems of the same size (diameter, length, aspect ratio, etc.). This comparison is important when there is a fixed volume (diameter and length) in which the system can fit, and the designer is seeking to maximize the performance of the system that fits into the space.

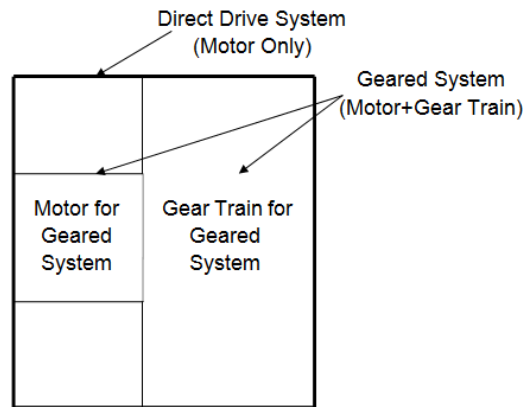


Figure 9.28: Illustration of Geared and Direct Drive Systems of the Same Size (The geared system will always have a larger torque capacity.)

The second comparison (illustrated by Figure 9.29) involved systems of the same torque capacity. This comparison is important when there is a specific torque requirement that must be met, and the designer is seeking to determine the size of the system that meets the requirement.

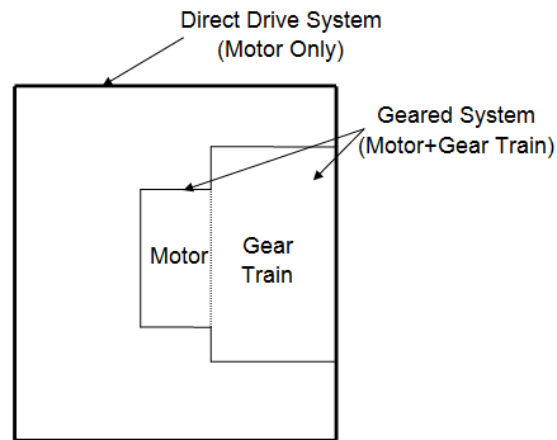


Figure 9.29: Illustration of Geared and Direct Drive Systems of the Same Torque Capacity (The geared system will always be smaller than the direct drive system.)

With the results from an off-the-shelf comparison as a baseline (Section 7.2.2), Example 1 (Section 7.3.1) compared systems of the same size, and Example 2 (Section 7.3.2) compared systems of the same torque capacity. The following section will summarize the results of the same size comparison in Example 1.

9.4.3.3 Comparing Geared and Direct Drive Systems of the Same Size

This example presents scaled sets of actuator designs that illustrate how the performance parameters of torque density and responsiveness vary for geared (based on the SRM+HGT) and direct drive (based on the SRM) systems of the same size. For each system, diameters ranging from 10 to 30 inches (with increments of 5 inches) and a constant overall aspect ratio (A) of 1.0 were considered. For the geared system, a constant motor aspect ratio (A_m) of 0.6 and gear ratios from 100 to 400 were used.

Table 9.20 summarizes the values of the design and performance parameters of the direct drive SRM based on the assumptions in Table 9.6. The inertia values listed in the table include the inertia of the SRM shaft, rotor, and bearings and do not include any load inertia. These inertia values will be used as the reference inertia (designated by I_{ref})

above) for all of the responsiveness computations in this example. The responsiveness values in the table do not include any load inertia so that the specific values of the load inertia can be added to each at the designer's discretion. Table 9.21 gives the direct drive responsiveness as a function of diameter and the load to motor inertia ratio K. The value of K can be used to transform the load inertia to an equivalent point load at a distance away from the axis of rotation (see Section 7.3.1.1).

Table 9.20: Direct Drive (SRM) Design and Performance Parameter Data Used for Comparison with Different Geared Systems (K=0)

Overall Diameter (inches)	Length (inches)	Aspect Ratio	Torque (ft-lbf)	Weight (lbf)	Inertia (lbm-in ²)	Torque Density (ft-lbf/lbf)	Responsiveness (rad/sec ²)
10	10.0	1.0	73	164	67	0.4	5005
15	15.0	1.0	400	551	508	0.7	3651
20	20.0	1.0	1309	1304	2136	1.0	2841
25	25.0	1.0	3253	2544	6505	1.3	2319
30	30.0	1.0	6820	4392	16166	1.6	1956

Table 9.21: Direct Drive (SRM) Responsiveness (rad/sec²) as a Function of K

Overall Diameter (inches)	Reference Inertia (lbm-in ²)	K (Load to Direct Drive Motor Inertia Ratio)					
		1	10	50	100	500	1000
10	67	2502	455	98	50	10	5
15	508	1826	332	72	36	7	4
20	2136	1421	258	56	28	6	3
25	6505	1159	211	45	23	5	2
30	16166	978	178	38	19	4	2

Table 9.22 summarizes the values of the design and performance parameters of the SRM+HGT geared combination. Figure 9.30 compares the torque density values in Table 9.20 and Table 9.22 and illustrates that the torque density of the geared system

varies from approximately 19 to 87 times the torque density of the direct drive system (see the exact benefit ratios shown in Section 7.3.1.2).

Table 9.22: SRM+HGT Design and Performance Parameter Data (K=0)^{29,30}

Overall Diameter (inches)	Shell Diameter (inches)	Length (inches)	Aspect Ratio	Gear Ratio	Torque (ft-lbf)	Weight (lbf)	Inertia (lbm-in ²)	Torque Density (ft-lbf/lbf)	Input Responsiveness (rad/sec ²)	Output Responsiveness (rad/sec ²)
10	10.0	10	1.0	99	5210	164	73	32	3347	33.8
10	8.6	10	1.0	200	5461	138	54	39	2364	11.8
10	7.9	10	1.0	300	5437	127	54	43	1547	5.2
10	7.1	10	1.0	400	4740	118	55	40	1008	2.5
15	12.9	15	1.0	100	15113	460	453	33	1549	15.5
15	11.3	15	1.0	200	16864	415	398	41	983	4.9
15	10.0	15	1.0	300	15078	389	392	39	595	2.0
15	9.6	15	1.0	400	17111	384	405	45	490	1.2
20	15.3	20	1.0	99	30682	986	1817	31	790	8.0
20	13.2	20	1.0	201	33184	914	1723	36	444	2.2
20	11.8	20	1.0	299	30936	876	1856	35	258	0.9
20	11.0	20	1.0	399	29901	871	1862	34	186	0.5
25	17.3	25	1.0	101	50235	1788	5997	28	386	3.8
25	15.1	25	1.0	200	56299	1731	5598	33	233	1.2
25	13.6	25	1.0	301	56616	1681	6083	34	143	0.5
25	12.9	25	1.0	399	59966	1698	5778	35	120	0.3
30	19.4	30	1.0	98	77431	3045	15001	25	244	2.5
30	16.5	30	1.0	200	81875	2892	15476	28	123	0.6
30	14.8	30	1.0	298	77765	2858	16184	27	75	0.3
30	14.0	30	1.0	399	86767	2866	16091	30	63	0.2

²⁹ The shell diameter in this and similar tables in this chapter refer to the diameter of the shell outside the motor.

³⁰ Recommendations for achieving constant (or near constant) responsiveness for a range of diameters are provided in the discussion in Section 7.3.1.5.

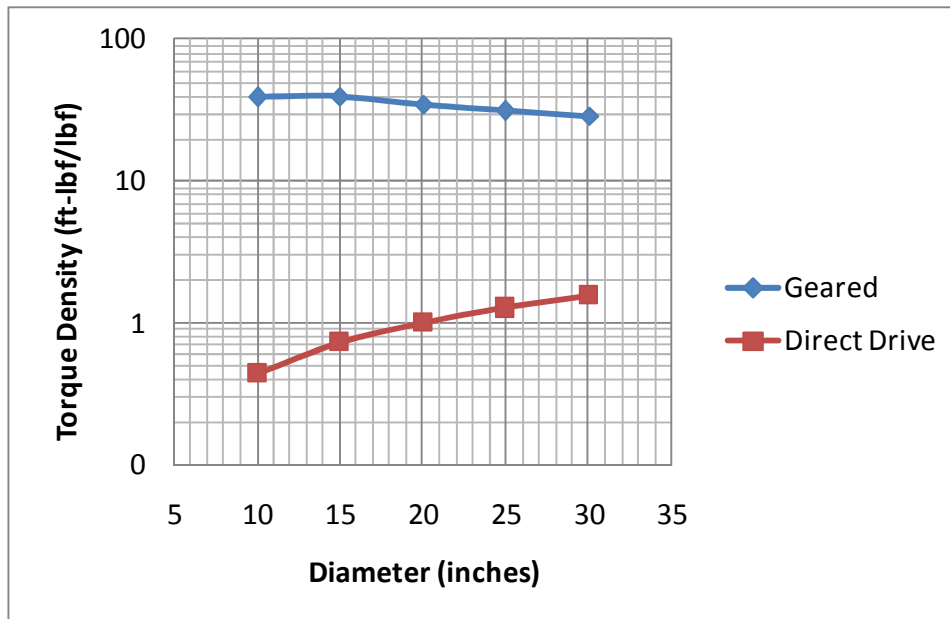


Figure 9.30: Comparison of Torque Density Between the Geared (SRM+HGT) and Direct Drive (SRM) Systems (Geared torque densities are an average for the 4 different gear ratio choices for each diameter.)

Figure 9.31 provides a design map of the output responsiveness of the geared system as a function of diameter and gear ratio. The important result here is that the lowest values of the diameter and gear ratio result in the highest output responsiveness. Figure 9.32 provides the same output responsiveness information in a 2-D representation.

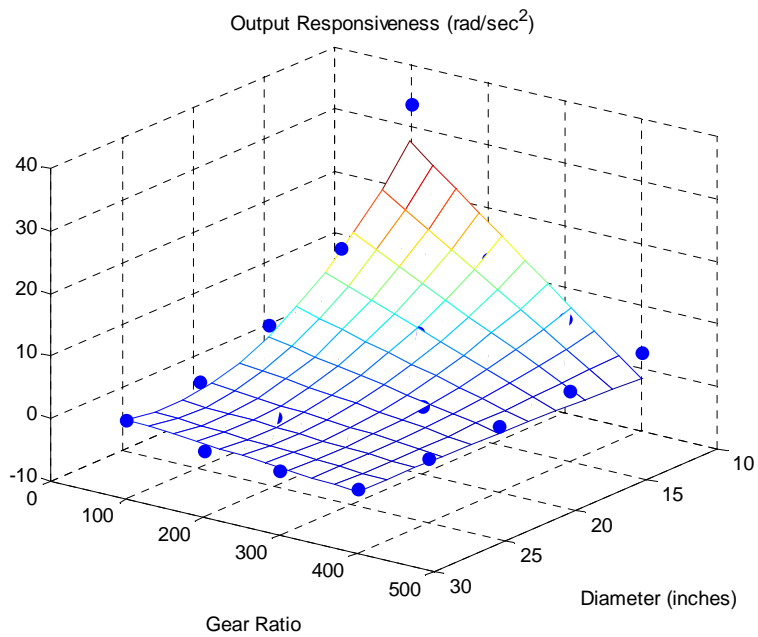


Figure 9.31: SRM+HGT Output Responsiveness as a Function of Diameter and Gear Ratio (practically independent of K)

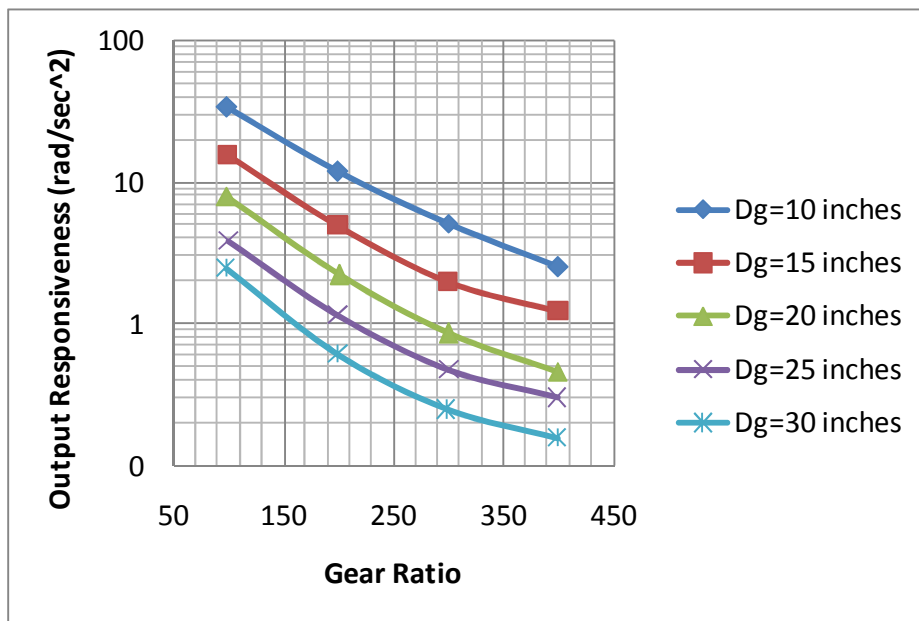


Figure 9.32: Geared (SRM+HGT) Output Responsiveness as a Function of Diameter and Gear Ratio (practically independent of K)

Figure 9.33 compares the output responsiveness of the direct drive and geared systems as a function of the load to motor inertia ratio K for different values of the gear ratio and the diameter of 10 inches. The key result is that the direct drive system is more responsive than the geared system until K reaches values of near 150 and greater for the gear ratio of 100 to 1. Using the equivalent load inertia relationships discussed in Section 7.3.1.1, this value of K gives a load inertia equivalent to a point weight of 164 pounds (equal to the direct drive motor weight) located at a distance of 43 inches away from the axis of rotation. Above this value of K , the geared system is more responsive than the direct drive system. Figure 9.34 illustrates the same result as Figure 9.33 in a 3-D design map. Table 9.23 provides the values of the ratio of the geared responsiveness to the direct drive responsiveness (i.e., a benefit ratio) as a function of the diameter and the K value (the same information as in Figure 9.33).

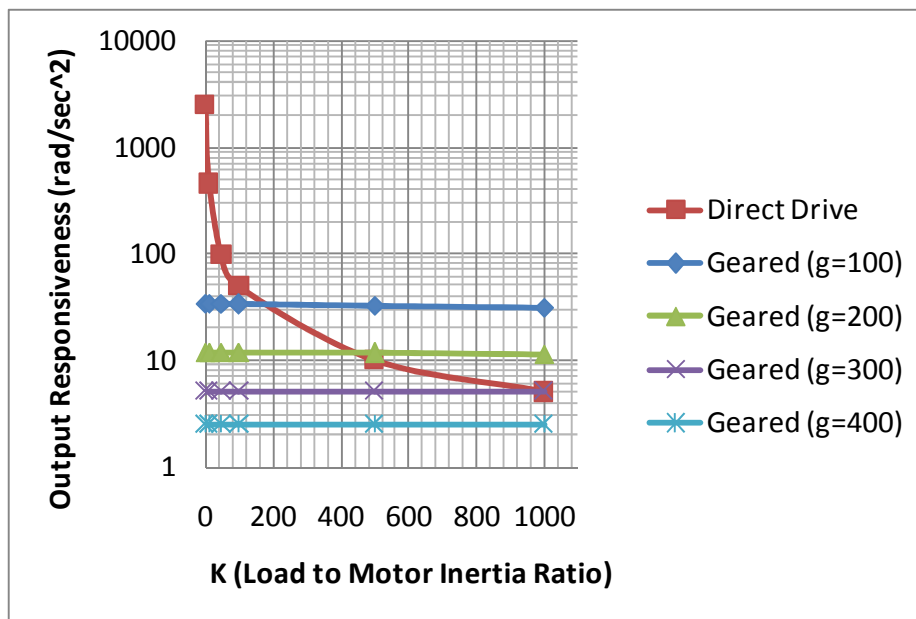


Figure 9.33: Geared (SRM+HGT) and Direct Drive (SRM) Output Responsiveness as a Function of K and Gear Ratio (for diameter = 10 inches)

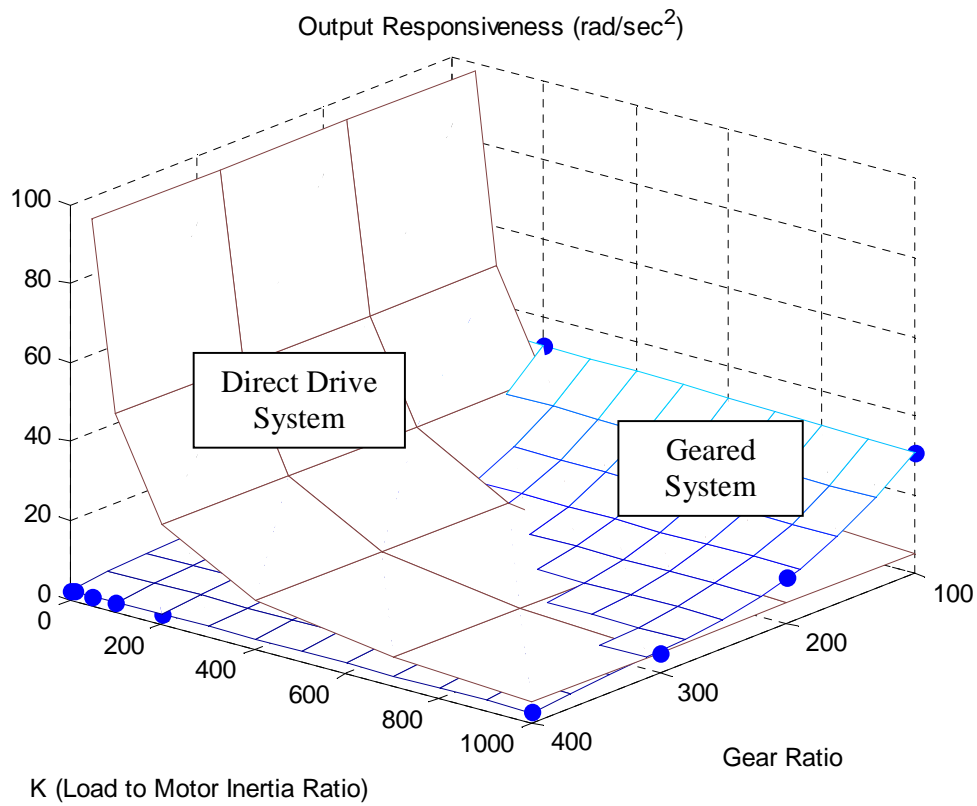


Figure 9.34: 3-D Plot of Geared (SRM+HGT) and Direct Drive (SRM) Output Responsiveness as a Function of K and Gear Ratio (for diameter = 10 inches)

Table 9.23: Geared (SRM+HGT) Output Responsiveness Benefit Ratio as a Function of Diameter and K (Gear ratio = 100 to 1)

Overall Diameter (inches)	K=1	K=10	K=50	K=100	K=500	K=1000
10	0.01	0.07	0.34	0.67	3.23	6.17
15	0.01	0.05	0.22	0.42	2.01	3.82
20	0.01	0.03	0.14	0.28	1.33	2.51
25	0.00	0.02	0.08	0.17	0.79	1.50
30	0.00	0.01	0.06	0.13	0.60	1.15

Figure 9.35 gives the distribution of inertia in the motor, gear train, and load as a function of gear ratio for the 10 inch diameter design. The key result here is that the dominant inertia is generally in the gear train, and the load inertia is insignificant even for a relatively large value of K (as shown by the absence of a bar for the load inertia in the figure). The load inertias are on the order of 1/10 of 1% of the total output inertia (i.e., extremely small) because of the relatively large gear ratios used. These large gear ratios (when squared) lead to large reflected motor and gear train inertias at the output when compared to the load inertia (see the responsiveness relationships in Section 7.1).

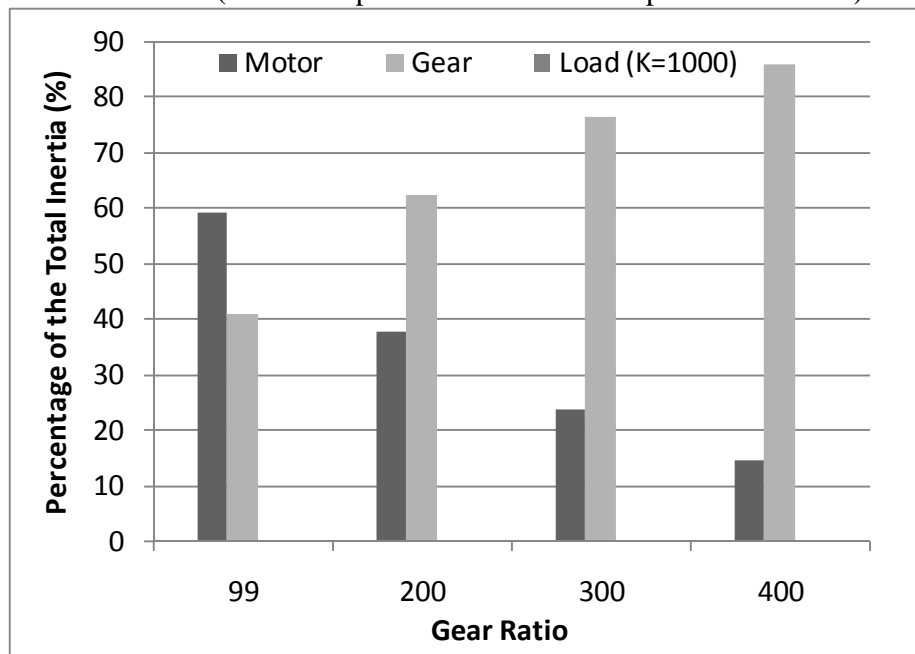


Figure 9.35: Percentage of Inertia in the Motor, Gear Train, and Load as a Function of Gear Ratio for the Overall Diameter of 10 inches (for the SRM+HGT Actuator)

9.4.3.4 Key Results from Chapter 7

Sections 7.3.1.5 (Example 1) and 7.3.2.4 (Example 2) provided a detailed discussion of key results obtained from the two examples in Chapter 7. In brief, bulleted

form, the key results with respect to the three actuator combinations considered were as follows.

- For the range of diameters (10 to 30 inches) and gear ratios (100 to 400) considered (see Section 7.3.1 and 7.3.2, respectively), the geared systems had approximately 10 to 20 times higher torque density than a direct drive of the same torque capacity and 20 to 90 times higher torque density than a direct drive system of the same size.
- The lowest diameter and gear ratio design parameter settings yielded the highest responsiveness values.
- The same size comparison in example 1 showed that the direct drive system is superior to a geared system in terms of the output responsiveness up a value of K between approximately 130 and 150. For K values larger than this, the geared system becomes superior to the direct drive system by factors equal to the benefit ratios stated in the tables in Section 7.3.1 for each geared system. This particular cutoff value of K occurred for a gear ratio of 100 for all three geared systems considered.
- The same torque comparison in example 2 showed that the direct drive system will generally provide higher output responsiveness than the geared system. In the limit as the load inertia becomes large relative to any motor and gear train reflected inertia (i.e., as K becomes large), both the geared and direct drive systems will have similar output responsiveness.
- For the range of diameters (10 to 30 inches) and gear ratios (100 to 400) considered, the dominant inertia in the SRM+HGT actuator combination was in the gear train, while the dominant inertia in the SRM+Star+PEGT

and SRM+Star Compound+PEGT actuators depended on the specific values of the gear ratio and diameter.

- Off-the-shelf comparison results (see Section 7.2.2) yielded similar results as those based on the motor and gear trains of this research and therefore provided some validation.

9.4.4 Minimum Set Development (Chapter 8)

A primary goal of the RRG is to determine the minimum set of components (motors, gear trains, actuators, etc.) that achieve maximum market penetration for a particular application. It is desirable to enable the assembly of a maximum population of systems from a minimum set of these components to take advantage of the potential cost savings. Section 8.1 provided an example design scenario that demonstrated the need for a minimum set and discussed the basic trade-off between achieving a high level of commonality (which reduces costs) and the associated performance deviations/losses among the products in a family.

9.4.4.1 Low Cost Minimum Set Features

Several design features for achieving a low cost minimum set were identified and were discussed in detail in Section 8.4. These features included the following: common motor diameters, variable 1st stage gear ratio, common gear train diameters, moving from 3 to 6 crankshafts in the PEGT, and changing materials. Two of the features, the use of common motor diameters and the use of variable 1st stage gear ratios, were utilized to build the alternative minimum sets in Chapter 8. Collectively, all of the features allow a set of actuator designs to meet the application requirements of a large population of systems with a minimum number of distinct parts and without significantly changing the geometry of the motor and gear train.

All of the minimum sets developed in Chapter 8 were based upon the SRM+Star+PEGT actuator combination (Figure 9.36) used throughout this research. It was used as an example because it easily illustrated these low cost, minimum set design features. Table 9.24 summarizes the alternative minimum sets considered in Chapter 8 and assesses the relative level of commonality and cost of each alternative.

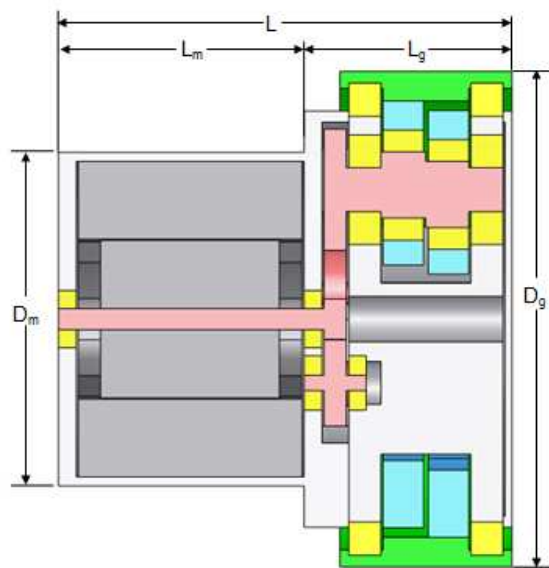


Figure 9.36: SRM+Star+PEGT Actuator Suggested for the Minimum Set Alternatives

Table 9.24: Summary of Alternative Minimum Sets and Relative Commonality and Cost Assessments (Set number references come directly from Chapter 8.)

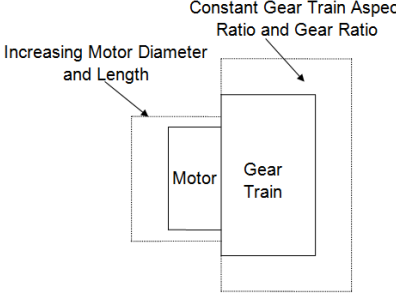
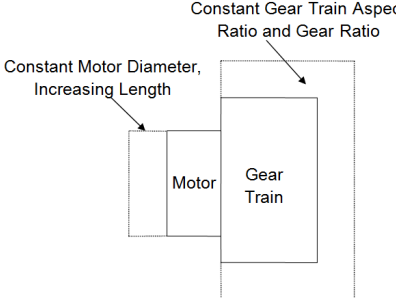
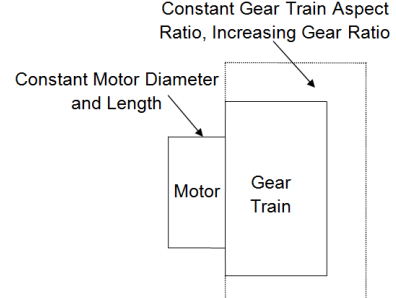
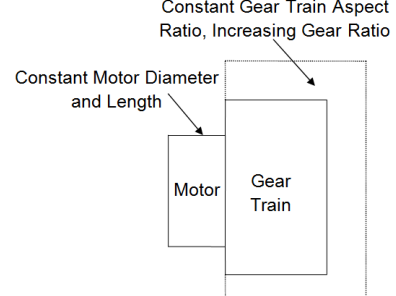
Design Features of a Potential Minimum Set	Illustration	Relative Level of Commonality	Relative Cost
<p>Reference Set (Section 8.5.1)</p> <ul style="list-style-type: none"> • No common motor diameters or lengths • Fixed gear ratio • Same number of actuators as requirements 		Low	High
<p>Sets 1-5 (Section 8.5.2.2)</p> <ul style="list-style-type: none"> • Common motor diameters • Fixed gear ratio • Same number of actuators as requirements 		Medium	Medium
<p>Sets 6-10 (Section 8.5.2.3)</p> <ul style="list-style-type: none"> • Common motor diameters and lengths • Variable gear ratios • Same number of actuators as requirements 		High	Low
<p>Reduced Sets (Section 8.6)</p> <ul style="list-style-type: none"> • Common motor diameters and lengths • Variable gear ratio • Less actuators than requirements 		Highest	Lowest

Table 9.25 lists a hypothetical set of torque requirements that were utilized in the two examples presented in Chapter 8 (see Sections 8.5 and 8.6). These examples focused on keeping the overall gear train size fixed (to meet the output torque requirement) and using variable motor geometry and 1st stage gear ratios to achieve potential low cost minimum sets. This approach based on a fixed gear train size is representative of the common task of designing actuators to meet a set of known (torque) requirements. This approach also allows the standardization of the potentially high cost gears in the PEGT (not including the 1st stage) and takes advantage of the low cost geometry modifications in the motor and 1st stage gear train.

Table 9.25: Actuator Torque Requirements

Index	Torque (ft-lbf)
1	2000
2	4000
3	8000
4	12000
5	16000
6	20000
7	24000
8	28000
9	32000
10	36000

The reference set, minimum sets 1-10, and reduced sets of actuators illustrated in Table 9.24 were designed to meet these torque requirements and are detailed in full in Chapter 8. As an illustrative example, a snapshot of the results for the reference set (Section 8.5.1), minimum set #3 (Section 8.5.2.2), minimum set #8 (Section 8.5.2.3), and potential reduced sets (Section 8.6.3) will be presented here.

9.4.4.2 Reference Set of Designs

In the reference set of designs, the motor diameter and length grow in proportion to the gear train diameter and length, and the overall aspect ratio was held constant for every design in the set. Table 9.26 summarizes the resulting design and performance parameters for the reference set of actuators and illustrates that the desired torque requirements are met exactly. Since all of the motors have different diameters and lengths, there are a total of 12 distinct motor designs, which is the largest possible number for a set of 12 actuators. This set represents the most expensive set of actuators (in the context of this example) because none of the motor designs have been standardized. This is the set of actuators that might be delivered to the customer if cost was not a primary issue.

Table 9.26: Design and Performance Parameters for the Reference Set (12 distinct motor diameters and fixed gear ratio and aspect ratio)

Overall Diameter (inches)	Motor Diameter (inches)	Length (inches)	Aspect Ratio	Gear Ratio	Torque (ft-lbf)	Weight (lbf)	Inertia (lbm-in ²)	Torque Density (ft-lbf/lbf)	Input Responsiveness (rad/sec ²)	Output Responsiveness (rad/sec ²)
6.0	6.4	6.0	1.0	141	1000	38	5	26	6236	44
7.5	7.3	7.5	1.0	141	2000	67	12	30	5521	39
9.5	8.2	9.5	1.0	141	4000	120	27	33	4861	35
10.9	8.9	10.9	1.0	141	6000	173	47	35	4231	30
12.0	9.3	12.0	1.0	141	8000	218	66	37	4017	29
13.7	10.2	13.7	1.0	141	12000	314	114	38	3472	25
15.1	10.8	15.1	1.0	141	16000	405	168	40	3141	22
16.2	11.3	16.2	1.0	141	20000	496	229	40	2876	20
17.3	11.7	17.3	1.0	141	24000	582	297	41	2667	19
18.2	12.1	18.2	1.0	141	28000	674	371	42	2487	18
19.0	12.4	19.0	1.0	141	32000	755	444	42	2377	17
19.8	12.6	19.8	1.0	141	36000	833	519	43	2289	16

9.4.4.3 Choice of Common Motor Diameters

Table 9.27 lists the suggested motor diameters (for minimum sets 1-5) that will be used for each distinct output torque requirement. The particular motor diameters chosen were calculated using average values of the motor diameters from the reference set. For

example, considering minimum set #1, the common motor diameter of 6.8 inches for the first two designs comes from average of the 6.4 and 7.3 inch diameter motors of the reference set. The minimum set alternatives 1-5 are distinguished in the table by the number of distinct motor diameters used in each (from 6 distinct diameters for set 1 down to only 1 distinct diameter for set 5).

Table 9.27: Common Motor Diameter Choices for Minimum Set Alternatives 1-5

Gear Train Diameter (inches)	Output Torque (ft-lbf)	Motor Diameters (inches)					
		Reference Set (12 Motors)	Set 1 (6 Diameters)	Set 2 (4 Diameters)	Set 3 (3 Diameters)	Set 4 (2 Diameters)	Set 5 (1 Diameters)
6.0	1000	6.4	6.8	7.3	7.7	8.4	10.1
7.5	2000	7.3	6.8	7.3	7.7	8.4	10.1
9.5	4000	8.2	8.6	7.3	7.7	8.4	10.1
10.9	6000	8.9	8.6	9.5	7.7	8.4	10.1
12.0	8000	9.3	9.8	9.5	10.4	8.4	10.1
13.7	12000	10.2	9.8	9.5	10.4	8.4	10.1
15.1	16000	10.8	11.0	11.3	10.4	11.8	10.1
16.2	20000	11.3	11.0	11.3	10.4	11.8	10.1
17.3	24000	11.7	11.9	11.3	12.2	11.8	10.1
18.2	28000	12.1	11.9	12.4	12.2	11.8	10.1
19.0	32000	12.4	12.5	12.4	12.2	11.8	10.1
19.8	36000	12.6	12.5	12.4	12.2	11.8	10.1

9.4.4.4 Minimum Set 3 (Fixed 1st Stage Gear Ratio)

Table 9.28 summarizes the performance parameter results for minimum set #3, which has 3 distinct motor diameters and a fixed gear ratio and also meets the distinct torque requirements listed in Table 9.25 above. This set of actuators is a potential minimum set because the common motor diameter of 7.7 inches was used for the first four gear train diameters in the set (i.e., diameters of 6, 8, 10, and 12 inches).

Table 9.28: Design and Performance Parameters for Minimum Set #3 (3 distinct motor diameters and fixed gear ratio)

Gear Train Diameter (inches)	Motor Diameter (inches)	Length (inches)	Aspect Ratio	Gear Ratio	Torque (ft-lbf)	Weight (lbf)	Inertia (lbm-in ²)	Torque Density (ft-lbf/lbf)	Input Responsiveness (rad/sec ²)	Output Responsiveness (rad/sec ²)
6	7.7	4.8	0.8	141	1000	38	7	27	4722	34
8	7.7	7.0	0.9	141	2000	66	13	30	5139	37
10	7.7	10.5	1.1	141	4000	122	26	33	5123	36
11	7.7	13.9	1.3	141	6000	180	41	33	4809	34
12	10.4	10.5	0.9	141	8000	218	75	37	3539	25
14	10.4	13.3	1.0	141	12000	314	117	38	3397	24
15	10.4	15.8	1.1	141	16000	406	162	39	3250	23
16	10.4	18.2	1.1	141	20000	501	215	40	3066	22
17	12.2	16.3	1.0	141	24000	579	306	41	2584	18
18	12.2	18.0	1.0	141	28000	673	374	42	2470	18
19	12.2	19.2	1.0	141	32000	751	435	43	2427	17
20	12.2	20.8	1.1	141	36000	837	507	43	2344	17

Because both the reference set (Table 9.26) and minimum set (Table 9.28) have identical gear train diameter and output torque parameters, they can be compared to assess the relative benefits or sacrifices due to using the minimum set alternative. Table 9.29 computes the percent difference between the minimum set performance parameters (torque, weight, inertia, torque density, and responsiveness) and the reference set parameters using the performance loss/deviation metric defined in Section 8.2. Positive numbers indicate that the minimum set has larger values than the reference set for the performance parameter under consideration.

Table 9.29: Tabular Comparison of the Performance Parameters Between Minimum Set #3 and the Reference Set

Gear Train Diameter (inches)	Torque (% Difference)	Weight (% Difference)	Inertia (% Difference)	Torque Density (% Difference)	Input Responsiveness (% Difference)	Output Responsiveness (% Difference)
6.0	0	-1.3	32	1.3	-24	-24
7.5	0	-1.0	7	1.0	-7	-7
9.5	0	2.1	-5	-2.1	5	5
10.9	0	4.2	-12	-4.0	14	14
12.0	0	-0.2	14	0.2	-12	-12
13.7	0	-0.1	2	0.1	-2	-2
15.1	0	0.1	-3	-0.1	3	3
16.2	0	1.0	-6	-1.0	7	7
17.3	0	-0.5	3	0.5	-3	-3
18.2	0	-0.1	1	0.1	-1	-1
19.0	0	-0.5	-2	0.5	2	2
19.8	0	0.4	-2	-0.4	2	2
Averages (%)	0.0	0.3	2.3	-0.3	-1.3	-1.3

Figure 9.37 graphically summarizes the tabular information in Table 9.29 by plotting the average percent difference for each of the performance parameters. Figure 9.37 confirms the anticipated performance losses in the weight, inertia, torque density, and output responsiveness parameters due to using this minimum set in place of the reference set. The weight and inertia of the minimum set are larger than the weight (by 0.3%) and inertia (by 2.3%) of the reference set (on average), while the torque density and output responsiveness of the minimum set are smaller than the torque density (by 0.3%) and output responsiveness (by 1.3%) for the reference set. The cost benefits of choosing the minimum set should outweigh these slight deviations in the performance parameters, and both the producer and end user of these actuators would probably be willing to tolerate these performance losses.

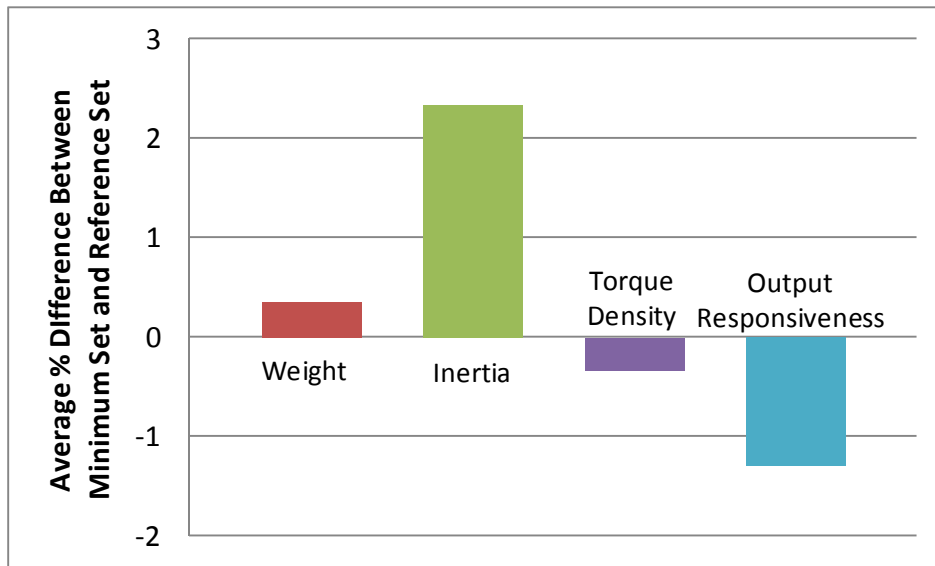


Figure 9.37: Graphical Comparison of the Performance Parameters Between Minimum Set #3 and the Reference Set (Average values from the entire set of actuators are plotted for each performance parameter.)

9.4.4.5 Minimum Set 8 (Variable 1st Stage Gear Ratios)

In minimum set 3, common motor diameters (but not lengths) were used for a range of gear train diameters, and the gear ratio was held constant at 141 to 1 for every design in the set. Minimum set 8 uses the same motor diameters as minimum set 3 but allows the 1st stage gear ratio to vary in order to use the same motor diameter and length for a range of gear train diameters.

Table 9.30 summarizes the performance parameter results for minimum set #8, which has 3 distinct motor diameters and a variable gear ratio and also meets the distinct torque requirements listed in Table 9.25 above. Table 9.31 lists the SRM stator diameter, length, and other parameters that correspond to each design in Table 9.30. This set of actuators is a potential minimum set because the same motor (with stator diameter of 7.3 inches and length 5.5 inches) was used for the first four gear train/actuator diameters in

the set (i.e., diameters of 6, 8, 10, and 12 inches). This set effectively reduces the total number of motors required from 12 for the reference set to only 3 for minimum set 8.

Table 9.30: Design and Performance Parameters for Minimum Set #8 (3 distinct motor diameters and variable gear ratio)

Gear Train Diameter (inches)	Motor Diameter (inches)	Length (inches)	Aspect Ratio	Gear Ratio	Torque (ft-lbf)	Weight (lbf)	Inertia (lbm-in ²)	Torque Density (ft-lbf/lbf)	Input Responsiveness (rad/sec ²)	Output Responsiveness (rad/sec ²)
6	7.7	8.2	1.4	41	1000	69	25	15	4561	112
8	7.7	8.9	1.2	82	2000	85	23	24	4879	60
10	7.7	9.7	1.0	165	4000	115	21	35	5256	32
11	7.7	10.4	1.0	254	6000	144	21	42	5331	21
12	10.4	13.4	1.1	81	8000	264	151	30	3046	38
14	10.4	14.1	1.0	122	12000	327	139	37	3264	27
15	10.4	14.7	1.0	169	16000	389	130	41	3382	20
16	10.4	15.2	0.9	210	20000	454	127	44	3473	17
17	12.2	18.3	1.1	108	24000	619	438	39	2344	22
18	12.2	18.7	1.0	126	28000	685	431	41	2399	19
19	12.2	19.0	1.0	145	32000	744	416	43	2464	17
20	12.2	19.3	1.0	167	36000	809	397	45	2518	15

Table 9.31: SRM Design and Performance Parameters for Minimum Set #8 (3 distinct motor diameters and 3 motors total)

Stator Diameter (inches)	Stator Length (inches)	Aspect Ratio	Torque (ft-lbf)	Weight (lbf)	Inertia (lbm-in ²)	Torque Density (in lbf/lbf)	Responsiveness (rad/sec ²)
7.3	5.5	0.8	24	43	16	6.7	7089
7.3	5.5	0.8	24	43	16	6.7	7092
7.3	5.5	0.7	24	43	16	6.6	7082
7.3	5.5	0.8	24	43	16	6.7	7088
9.9	8.0	0.8	97	115	76	10.1	5925
9.9	8.0	0.8	97	115	76	10.1	5921
9.9	8.0	0.8	96	114	76	10.1	5917
9.9	8.0	0.8	97	115	76	10.1	5921
11.6	10.6	0.9	219	209	190	12.6	5345
11.6	10.6	0.9	220	209	191	12.6	5346
11.6	10.6	0.9	218	208	190	12.6	5342
11.6	10.6	0.9	218	208	189	12.6	5342

Again, because both the reference set (Table 9.26) and minimum set (Table 9.30) have identical gear train diameter and output torque parameters, they can be compared to assess the relative benefits or sacrifices due to using the minimum set alternative. Like Figure 9.37, Figure 9.38 computes the average percent difference between the minimum

set performance parameters (torque, weight, inertia, torque density, and responsiveness) and the reference set parameters using the performance loss/deviation metric defined in Section 8.2. Positive numbers indicate that the minimum set has larger values for the performance parameter under consideration.

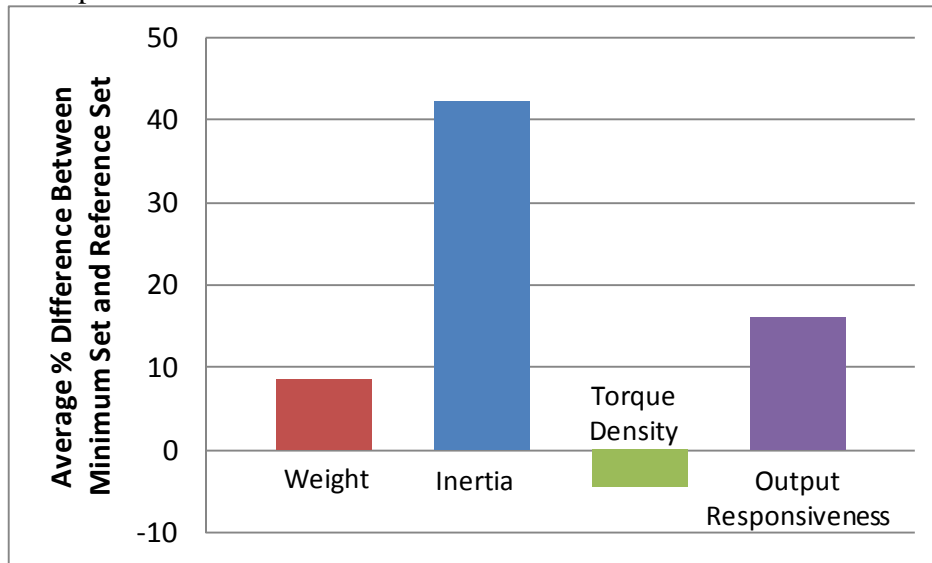


Figure 9.38: Graphical Comparison of the Performance Parameters Between Minimum Set #8 and the Reference Set (Average values from the entire set of actuators are plotted for each performance parameter.)

Like Figure 9.37, Figure 9.38 again confirms the anticipated performance losses in the weight, inertia, torque density, and output responsiveness parameters due to using this minimum set in place of the reference set. One noteworthy difference between these two figures is that the relative magnitudes of the performance losses are larger for minimum set 8 (up to 42% in Figure 9.38) when compared to those for minimum set 3 (less than 3% in Figure 9.37). This suggests that trying to achieve a smaller minimum set (by using common motor diameters and lengths) may increase the performance losses beyond what might be tolerated by a producer or end user. The cost benefits of choosing the minimum set may not outweigh these deviations in the performance parameters.

9.4.4.6 Minimum Sets 1-10 Summary and Additional Results

Table 9.32 collects information from all the comparisons between minimum set alternatives 1-10 and the reference set (recall that detailed comparisons were made for set 3 (Figure 9.37) and set 8 (Figure 9.38) in the previous sections). The table again lists the average percentage change in the performance parameters (relative to the reference set) for each of the alternative minimum sets considered.

Table 9.32: Tabular Summary of the Average Percent Change in the Performance Parameters for the Different Minimum Set Alternatives

Minimum Set Alternative	Gear Ratio	Average % Change in the Performance Parameters					
		Torque	Weight	Inertia	Torque Density	Input Responsiveness	Output Responsiveness
1 (highest cost)	Fixed Value of 141 to 1	0.0	0.0	0.4	0.0	-0.2	-0.2
2		0.0	0.1	1.4	-0.1	-0.9	-0.9
3		0.0	0.3	2.3	-0.3	-1.3	-1.3
4		0.0	0.9	5.3	-0.9	-2.6	-2.6
5		0.0	3.7	21.9	-3.3	-7.8	-7.8
6	Variable	0.0	2.0	8.3	-1.4	-0.7	3.3
7		0.0	7.6	32.7	-4.9	-1.8	16.1
8		0.0	8.6	42.3	-4.4	-0.7	16.0
9		0.0	8.0	45.3	-4.5	-0.1	14.3
10 (lowest cost)		0.0	10.2	65.9	-6.0	-5.8	7.3

The specific results available from Table 9.32 were discussed in detail in Section 8.5.3. As an example, Figure 9.39 illustrates the percent different in weight between each minimum set alternative and the reference set, again with positive numbers indicating a larger weight for the minimum set. The figure makes a distinction between minimum sets 1-5, which used a fixed gear ratio of 141 for every actuator in the set, and minimum sets 6-10, which allowed the gear ratio to vary among the actuators in a set. This figure clearly illustrates the anticipated performance losses (using weight as a metric) that are incurred when seeking a minimum set.

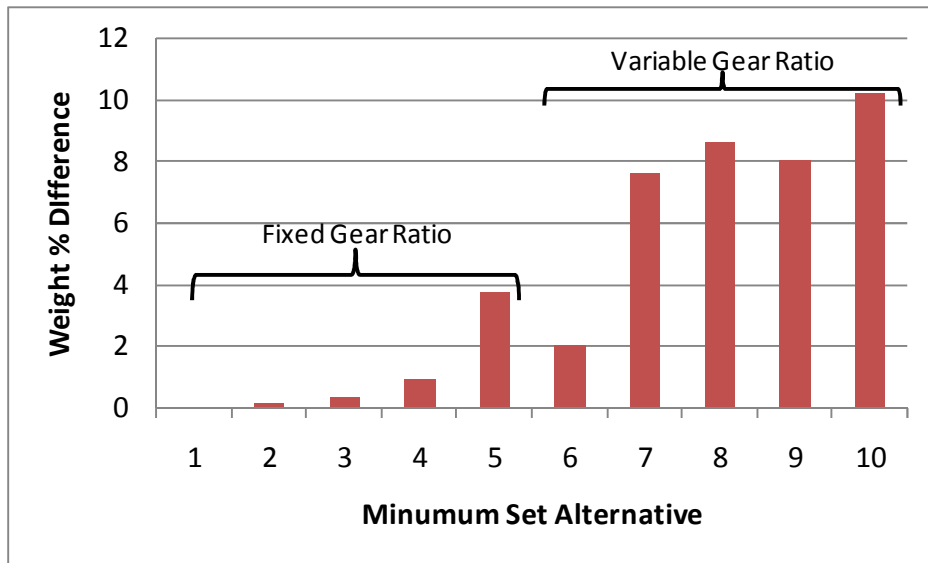


Figure 9.39: Weight Percent Difference Between the Minimum Set Alternatives and the Reference Set

9.4.4.7 Potential Reduced Sets of Actuators

Section 8.6 defines the concept of a reduced set of actuators and suggests multiple reduced set alternatives based on the removal of one or more actuator designs from the reference set. Table 9.33 lists the reduced sets built from a particular reference set (Section 8.6.1), the actuators included in each set, the number of distinct motor and gear train designs, and the values of the criteria (focused on weight in this example) used to distinguish among them. The reduced set built of only actuators 2, 4, 6, 8, 10, and 12 discussed in detail in Section 8.6.2, is index #15 in the table. Each of these reduced sets are feasible alternatives if the cost benefits due to the reduced number of gear train and motor designs is sufficient to justify the increases in weight (and other performance deviations).

Table 9.33: Reduced Minimum Sets and Criteria Values for Each

Index	Actuators In the Set	Number of Actuators	Number of Gear Train Designs	Number of Motor Designs	Combined Weight (lbf)	Weight Penalty (lbf)	% Increase in Weight
0	All (1-12)	12	12	6	4693	0	0.0
1	All except 1 (2-12)	11	11	6	4708	15	0.3
2	All except 2 (1,3-12)	11	11	6	4764	71	1.5
3	All except 3 (1-2,4-12)	11	11	6	4723	30	0.6
4	All except 4 (1-3,5-12)	11	11	6	4769	76	1.6
5	All except 5 (1-4,6-12)	11	11	6	4755	62	1.3
6	All except 6 (1-5,7-12)	11	11	6	4816	122	2.6
7	All except 7 (1-6,8-12)	11	11	6	4753	60	1.3
8	All except 8 (1-7,9-12)	11	11	6	4809	116	2.5
9	All except 9 (1-8,10-12)	11	11	6	4754	61	1.3
10	All except 10 (1-9,11-12)	11	11	6	4797	103	2.2
11	All except 11 (1-10,12)	11	11	6	4765	72	1.5
12	3-12	10	10	5	4850	157	3.3
13	4-12	9	9	5	4940	247	5.3
14	5-12	8	8	4	5242	549	11.7
15	2,4,6,8,10,12	6	6	6	4993	299	6.4
16	3,6,9,12	4	4	4	5587	894	19.0
17	4,8,12	3	3	3	5908	1215	25.9
18	6,12	2	2	2	6797	2104	44.8

Referring to the table, the combined weight of the actuators (relative to the reference weight of 4,693 lbf of all 12 actuators listed as index #0 in the table) increases as the total number of actuators in the set decreases. These increases in weight occur due to the customer being forced to use actuators with higher torque capacity (and thus higher weight) than needed for a given torque requirement and is one measure of the performance losses associated with reducing the size of the set. The weight penalty value listed in the table for each set is the difference between the weight of the actuators in the reduced set and the weight of the actuators in the reference set. Positive values of the weight penalty indicate that the combined weight of the actuators in the reduced set is greater than the combined weight of the actuators in the reference set. Figure 9.40 plots this weight penalty as a function of the number of actuators in the set, and Figure 9.41 illustrates the same information as a percentage increase in weight relative to the

reference weight. The specific weight penalty that the producer or end-user can tolerate will depend on the application.

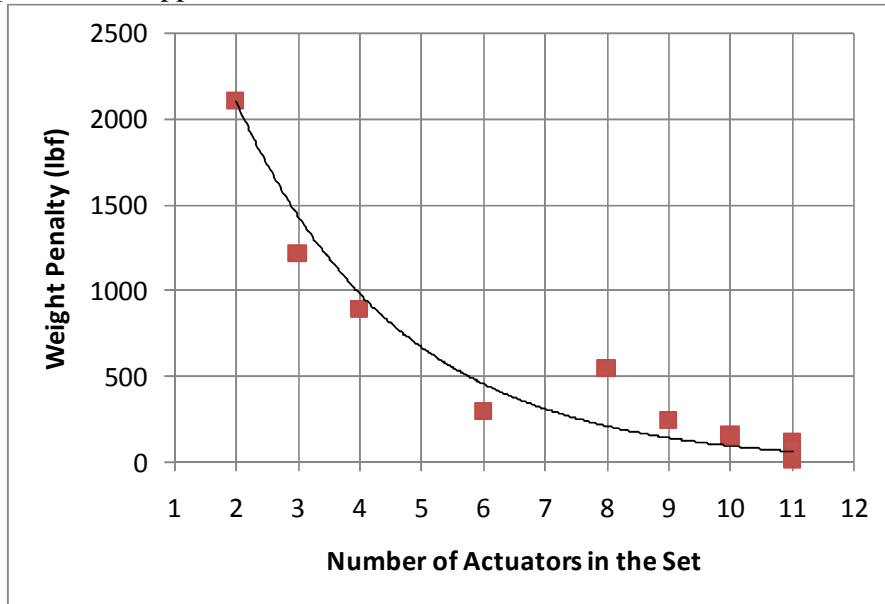


Figure 9.40: Weight Penalty (lbf) as a Function of Number of Actuators in the Set

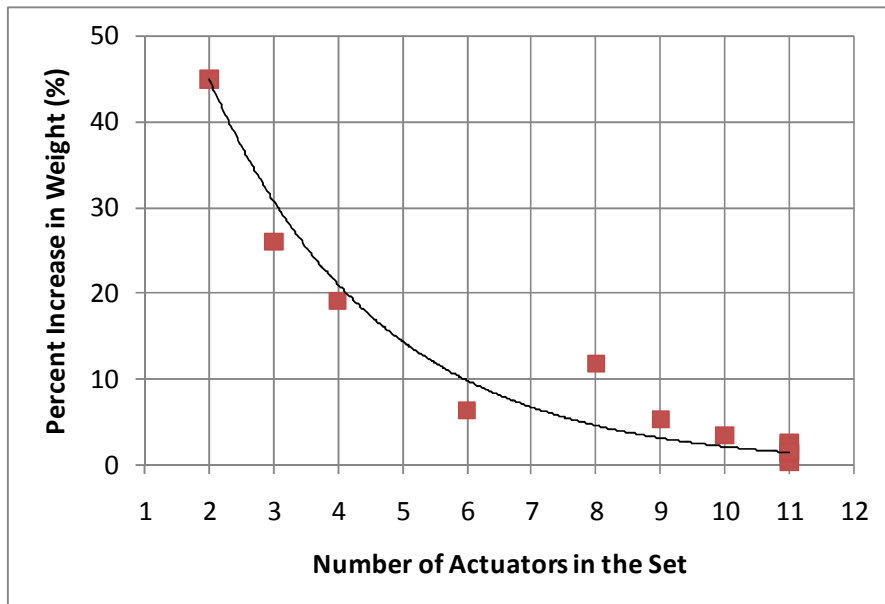


Figure 9.41: Percent Increase in Weight (%) as a Function of Number of Actuators in the Set

9.5 RECOMMENDATIONS

Given the summary of key results in the previous section, this section will make some general recommendations for the development of future actuator designs based on the present research. The reader should note here that all of these recommendations are based on the motor and gear train models developed in Chapter 3. In particular, any changes in the assumptions for the motor and gear train torque capacity relationships would require adjustment of the corresponding design maps and scaling rules in Chapters 5-7.

9.5.1 Model Development and System Comparisons

The torque, weight, and inertia relationships for the SRM, HGT, and PEGT (Chapter 3) were each developed to the same level of detail and with similar assumptions. This parallel development allowed for fair, objective comparisons between alternative actuators and gear trains in Sections 5.3, 5.4, 6.5.4, and 6.5.5. Considering the results from Sections 5.3 and 6.5.4, the designer is advised to use the Star+PEGT in place of the HGT when maximum performance (in terms of torque, weight, etc.) is desired. However, if low complexity and low cost are important objectives for an application, the HGT should be used. The results of the comparisons in these particular sections can be used to draw conclusions about which system is superior with respect to a given performance parameter. The designer is instructed to use these analytical results in conjunction with FEA and physical testing results to continuously refine the important gear tooth stress and torque capacity calculations for the HGT and PEGT. Finally, comparisons between alternative gear trains and actuators should always be based on other practical considerations such as the number of bearings, number of parts, complexity, and balancing issues.

9.5.2 Actuator Design Procedure

The actuator design procedure (Section 4.3) was developed to highlight the specific contributions of the present research: development of scaling rules and guidelines for balancing the motor and gear train. An important distinction was made between the high level, actuator level, and component (motor and gear train) design procedures. Future research can be prioritized by focusing on the specific blocks in the actuator level design procedure. The computational implementation of the actuator design procedure (Appendix A1) was built into a modular format for easy computation and for incorporation into a future visual actuator design environment. The MatLab software was used to do all of the computations in the present research, but future research might show that a C++ implementation of the same models would be more efficient and more appropriate for an actuator design software tool.

9.5.3 Component Scaling Rules

The scaling rules developed in Chapters 5 and 6 were presented in different representations: simple-power law equations, low-order polynomial equations, 2-D plots, 3-D design maps, and tabular summaries. The appropriate representation used should depend on the accuracy and amount of known information for a particular design task. The general shape of trends and surfaces (dependence on diameter and aspect ratio) in the design maps were equally as important as the numerical values generated by the power-law and polynomial scaling rules. If assumptions change (Section 4.3), the absolute values of the performance parameters will change, but the trends will generally stay the same.

The designer is advised to take advantage of the strong dependence of torque, weight, inertia, torque density, and responsiveness on diameter (squared or higher) when

trying to influence these performance objectives (see the simple-power law scaling rules in Sections 5.2 and 6.5).

Though more advanced metamodeling techniques were identified in the literature review (Section 2.7.2), the representations were kept simple (Section 5.1) to focus on understanding how the performance parameters varied as a function of the design parameter choices (rather than focusing on having the most accurate model). The accuracy of rules should always be considered, and this was the reason that the values of the fitting error for all of the low-order polynomial scaling rules were reported in Section 5.2.

9.5.4 Balancing Parameters

Chapter 6 defined different types of balance that should be sought for an actuator, and it is important to recognize what type(s) are needed or achievable for a particular actuator being developed. Any comparison between alternative motors, gear trains, or integrated actuators or any actuator families developed should involve careful selection of the key actuator design parameter choices (gear ratio, motor and gear train aspect ratios, and geometry relationships between the motor and gear train) discussed in Section 6.2. Section 5.2.3.2 discussed strategies for balancing the bearing and gear tooth limited torque capacities in the PEGT and whether this balance is possible depends heavily on the crankshaft bearing speeds and gear ratio choices for the PE-output gear mesh in the PEGT.

9.5.5 Designing for High Torque Density

Based on the collective set of results in Chapters 6 and 7, the designer is advised to use the highest gear ratio settings possible for a given output speed (while still avoiding tooth interference) to maximize the torque density of the actuator combinations

considered in this research³¹. The torque density of the gear trains and integrated actuators were also found to decrease slightly with increasing diameter, but this occurred due to the contact ratio assumptions discussed in Sections 3.5.5 and 5.2.2, which are currently under investigation. Near constant torque density should be achievable (for a range of gear train diameters) if it can be shown that the contact ratio increases as the diameter of the gear train increases. Torque density was found to be practically independent of the aspect ratio/length of the actuator.

9.5.6 Designing for High Responsiveness

Based primarily on the results in Chapter 7, the designer is advised to use the lowest diameter and gear ratio settings possible to maximize the responsiveness of the actuator. Like torque density, the responsiveness was found to be practically independent of the aspect ratio/length of the actuator. Given that the output responsiveness decreases with increasing gear ratio (see Sections 6.6 and 7.3.1), the designer is advised to use relatively higher gear ratios for the smaller design in a set (to decrease their responsiveness below their maximum possible values) and lower gear ratios for the larger designs (to increase their responsiveness to the maximum values possible). This will allow near constant responsiveness to be achieved for a range of actuator diameters.

9.5.7 Gear Ratio Choice

Sections 6.6 and 7.3.1 revealed that (for a given actuator size) increasing the gear ratio increases the torque density and decreases the responsiveness of an actuator of a given size. Decreasing the gear ratio has the opposite effect. An approximate lower limit of the gear ratio of near 100 to 1 was suggested by the actuator designs generated in Section 6.5 and 6.6. In this section, for small gear train diameters (less than 10 inches), it

³¹ This approach is limited by the range of motor speeds that are feasible for a given actuator size.

was difficult to find motors with a suitable torque capacity that had a diameter and length that were compatible with the gear train for gear ratios of 100 to 1. Given this result, the designer is advised to use the highest gear ratios possible (to minimize the required motor torque capacity and size) for smaller diameter gear train designs. Because the torque density of the motor grew at a faster rate with diameter than the torque density of the gear train (see Section 5.6.6), this imbalance between the motor and gear train becomes less of an issue as the diameter is increased.

9.5.8 Motor Speed Choices

The present research did not focus directly on the choice of the motor speed for the actuators considered, but Section 2.4.1 of the literature review listed some relevant relationships between the motor speed and gear ratio. Some researchers suggested that the gear ratio should be chosen so that the maximum desired load speed corresponds to 50-80% of the maximum motor speed, which is typically limited by the hoop stresses in the rotor or the losses due to the higher switching frequencies required at higher speeds. Another researcher suggests selecting the gear ratio so the maximum desired load speed corresponds to the motor's rated speed, which is typically much less than its maximum speed.

9.5.9 Distribution of Weight and Inertia

Sections 6.5, 6.6, and 7.3 illustrated how the distribution of weight and inertia between the motor, gear train, and load is a strong function of the diameter, gear ratio, and load characteristics. When comparing only the motor and gear train (without considering the load), these Sections 6.5 and 6.6 illustrated that the dominant weight is usually in the gear train, but the location of the dominant inertia varies based on the gear train type (HGT, Star+PEGT, or Star Compound+PEGT) and the specific values of the

diameter and gear ratio used. The dominant inertial component in the actuator can generally be shifted between the motor and gear train by suitable choice of the gear ratio and diameter, and the results of Chapters 6 and 7 should be consulted for specific guidance. This distribution information is valuable because it can be used to focus weight and inertial reduction efforts on the dominant components. In comparison, the HGT typically has a much larger inertial content than the PEGT (for the same size and gear ratio, see Sections 7.3.1 and 7.3.2) because of the high rotary inertia of the eccentric shaft that is typically directly connected to the motor input shaft. Finally, the designer should use caution when suggesting that the dominant weight and inertia are usually in a certain component (motor or gear train) for a specific actuator combination. The results were difficult to generalize in the above noted sections.

9.5.10 Choosing Between Direct Drive and Geared Systems

Chapter 7 illustrated that when comparing the responsiveness of two competing actuator alternatives, the same size or same torque capacity assumption is critical. The application in question should dictate which to use. The same size (Section 7.3.1) and same torque capacity (Section 7.3.2) comparison results both suggested that for relatively low load inertias (relative to the motor and gear train reflected inertias), a direct drive system would exhibit higher responsiveness. For relatively high load inertias and geared direct drive and geared systems of the same size, a geared system should achieve the highest responsiveness.

Since geared systems were shown to be more torque dense than direct drive systems for both the same size and same torque capacity assumptions, the designer is advised to always use a geared system when minimizing the weight/volume of the system.

Finally, the input responsiveness results were provided in Chapters 5, 6, and 7 were provided mainly for completeness, and the designer is advised to not use the input responsiveness (i.e., the torque to inertia ratio or acceleration at the motor shaft) as a criteria for comparing direct drive and geared systems (or any two systems in general). The output responsiveness (acceleration at the output shaft) is the only “apples to apples” comparison that should be made for geared and direct drive systems because only the output responsiveness can be compared against a given acceleration requirement.

9.5.11 Minimum Set

The basic principle behind the minimum set concept is to share as many common parameters/dimensions as possible among a set of actuator designs because this will always reduce manufacturing and certification costs. Chapter 8 confirmed the anticipated performance losses incurred when seeking a minimum set of actuators for a particular application. Unless dictated by the application, a reasonable goal is to have the minimum set performance parameters be within 10% of the performance parameters obtainable by a reference set (or in general, some optimum set). To fully justify the use of a minimum set in a particular application, the cost benefits of the suggested minimum set features (common motor diameter, variable 1st stage gear ratio, etc.) need to be quantified.

The choice of the reference set used for making comparisons with alternative minimum and reduced sets is not trivial. In most cases, the reference set can be assumed to be a set of actuator designs with no common dimensions (i.e., no commonality), the set that would likely be delivered if cost was not a primary issue. In the reference set in Chapter 8, the overall aspect ratio and gear train aspect ratio of each actuator in the set was held constant to meet the torque requirements. However, the choice of the overall actuator diameter and length to meet the application requirements should in general

depend on the needs of the end-user. For example, if the end-user wants to achieve different torque requirements with actuators of different length but the same overall diameter, the reference and minimum sets generated should be designed with this desire in mind. A suggested approach is to use a linear distribution of actuator lengths if length is the basic parameter of interest and a quadratic distribution of diameters if the diameter is the basic parameter.

Average values were used to compute the common motor diameters for the alternative minimum sets in Chapter 8, but future research may reveal other more sophisticated ways to choose the common parameters. Rather than pre-specifying these common parameters, the product family design literature (Section 2.6) suggests dealing with this task by using formal optimization techniques to search among all possible values of the parameters and using the optimization results to determine the best set of common and variable parameters that meet the design objectives with minimum performance loss.

In the actuator combinations considered in the present research, the PEGT and HGT will typically be the high cost component relative to the motor, so the designer is advised to use the minimum number of distinct gear train sizes as possible to achieve low cost.

9.6 CONTRIBUTIONS

In light of the two literature review summary tables presented in Chapter 2 (Section 2.1), and the results and recommendations presented in this chapter, the specific contributions of this research can now be summarized.

1. A comprehensive **literature review** on many of the key topics needed to push the actuator technology forward was completed.

2. **Parametric models** of the SRM and three different gear trains have been developed to a similar level of detail (with key assumptions included) such that fair, objective comparisons can be made between alternative gear trains and actuators.
3. An **actuator design procedure** that included the tasks of balancing parameters and generating sets of scaled actuators was formulated and implemented.
4. The parametric models and design procedure were embedded in a **computational tool** that allowed efficient generation of motor, gear train, and actuator designs; scaling rules; design maps; and the necessary data to create a link with a solid modeling program.
5. **Scaling rules and design maps** for the SRM and three different gear types (with diameters ranging from 6 to 50 inches and gear ratios from 100 to 450) were developed and are useful for quickly obtaining intermediate designs and for gaining design insights into parameter choices.
6. Preliminary guidelines for choosing the gear ratios and relative geometries of the motor and gear train to **balance parameters** between the motor and gear train for the three gear train types were provided.
7. Alternative **minimum sets** of actuators were developed and the anticipated performance losses were quantified.

9.7 FUTURE WORK

This section will discuss the future research that is necessary to build upon this research and also to push the electromechanical actuator technology forward.

9.7.1 Actuator Design Process

This is a broad area of future work that is inter-related with many of the other areas discussed. This research has developed a framework that uses the parametric models, design procedures for computation, and computational tool to develop scaling rules, design maps, and rules for balancing parameters. This framework also allowed for efficient comparisons between direct drive and geared actuators and the development of potential minimum sets of actuators.

The next step is the extension of this framework into a more formal design process that will enable RRG to be able to respond quickly to potential actuator applications. As it currently stands, the framework is essentially in the hands of the present researchers. However, the anticipated formal process should allow engineering students with only a bachelor degree in engineering to quickly grasp the concepts in the framework and apply them in the development of actuators. Each step of this design process should present the designer with actuator solid models, design maps, and other graphics that enhance their decision-making capabilities and ultimately lead to better parameter choices.

One way to embody this formal process is in an in-house, proprietary actuator design software. This report has used MatLab for computation, but other, more flexible programming languages such as C++ can be used. Off-the-shelf software should only be used as long as it does not limit the decision-making ability of an actuator designer.

9.7.2 Knowledge Base for EMA Design

One of the aims of this research was to begin developing the knowledge base (parametric models, solid models, scaling rules, design maps, etc.) needed for the future development of a visual decision support system for actuator design (including a graphical user interface, visual display of actuator information, etc.). Future researchers

should utilize the present research's results as the data (information) in the early stages of development. The present results could be easily embedded as simple look-up tables in the software and would be useful for estimating the parameters of potential actuator designs.

Section 2.8.3 identified the features of a good visual decision making software environment, and future researchers should consider incorporating these features. This future actuator design decision-making environment should also incorporate the mathematical framework developed by Ashok and Tesar [2007]. Ashok and Tesar combined operational performance maps to form decision envelopes, and also included the effect of uncertainty in the parameters. Analogously, the design maps presented in Chapter 5 should be combined to create design envelopes and account for uncertainty in the actuator design and performance parameters.

9.7.3 Uncertainty in the Parameters

It is anticipated that future research on the development of a more formal actuator design process will need to include the uncertainty of the parameters (the current research does not). Uncertainty could occur in the process due to the variable tolerances on manufactured parts, due to dealing with only the most dominant parameters at a given time (rather than the complete set of design parameters), and due to the subjective selection of a single option from a set of alternatives. Considering the last point, for example, since many different combinations of tooth numbers and pitch diameters give approximately the same gear ratio in the HGT and PEGT, it is difficult to ensure that different designers will select the same "best" alternative. The uncertainty in the actuator design and performance parameters will show itself as different levels (surfaces) in the design maps of Chapters 5, 6, and 7. Note that uncertainty has already been incorporated

into the decision-making framework of Ashok and Tesar [2007], and perhaps some of their lessons learned will apply to the creation of design maps with uncertainty. Incorporating uncertainty into the current actuator design framework will require a greater understanding of standard regression techniques, and in particular, more in-depth consideration of the variance of the actuator parameter data sets being visualized.

9.7.4 Other Metamodels (Curve-Fitting) Approaches

Though this research generated design maps and scaling rules using standard regression techniques, the literature review identified other more advanced metamodeling techniques (see Section 2.7.2). The reader is referred to the following references [Simpson et al., 2001; Jin, Chen, and Simpson, 2001; Mullur and Messac, 2005; Mullur and Messac, 2006, Simpson, Lin, and Chen, 2001; and Hussain, Barton, and Joshi, 2002]. In each of these works, the authors provide excellent examples for comparing different metamodeling approaches for real data sets, and they also provide useful graphical and tabular summaries of results. These authors also define important criteria for obtaining accurate models, some of which were used as error metrics in the present research. Any future work in this area should begin with a review of these works.

9.7.5 Torque to Inertia Ratio/Responsiveness

Though the acceleration capabilities of the actuator combinations in this research are now reasonably well-understood (from Chapter 7), a more detailed look at the literature dealing with the integration of motor and gear train (Section 2.4) is suggested. Because of the breadth of the present literature review, the specific results of the literature reviewed in this area (i.e., designing for responsiveness) were not tested against the results of this research. Future efforts should also carefully review the results

presented in Chapter 7 of this report and continuously update the present understanding with knowledge gained from real acceleration requirements.

9.7.6 Star Compound Gear Trains

This research has focused on developing parametric models, solid models, scaling rules, design maps, and general guidelines for design of the HGT and PEGT. A similar effort is needed for the star compound gear train (SCGT). The SCGT will be able to meet the needs of applications requiring relatively lower gear ratios than the HGT and PEGT (typically 25 to 1 or less for a single SCGT stage). Based on the results in the present research (i.e., low gear ratios providing the highest acceleration capabilities), the SCGT may prove to be superior to the HGT and PEGT for acceleration-dominant applications. The validity of this hypothesis will depend on whether the unique circular arc gear teeth or standard involute teeth are used in the large diameter output gears in the SCGT. When the SCGT is added to the present framework, the RRG will possess the ability to respond to needs of a larger population of applications.

9.7.7 Bearing Load Capacity

The bearings in the actuator are an essential component that can sometimes limit the speed and torque capacity of the actuator and therefore should not be ignored. All of the bearings used for the actuators designs in this report and for other actuators designed by the current researcher were selected by consulting manufacturer's catalogs and websites. Though this is a necessary process and an invaluable experience for an actuator designer, it would be useful to use an analytical description of bearing load capacity as a function of its dimensions (mean diameter, roller diameter, number of rollers, roller length, ball diameter, etc.). It is likely that bearing manufacturers have not tested every

size available in their catalogs, and they are relying on some basic analytical descriptions to estimate load capacity.

Regarding the analytical model development, Faires [1968] suggests that bearing load capacity is proportional to the square of roller diameter, but this is difficult to verify because bearing roller diameter information is not usually transparent or easily obtained from bearing manufacturers. Also, Brandlein et al. [1999] suggests that roller bearing load capacity is nearly linear with roller diameter, and some success was obtained when attempting to match this relationships with catalog bearings. Future work should pursue both of these suggested avenues simultaneously: analytical models for bearing selection vs. catalog searching. Over time, it is suspected that the catalog searching will be the most promising because of the difficulties in matching theoretical bearing load capacity predictions with those stated by manufacturers and also the discrepancies between published load capacities of bearings of the same size from different manufacturers.

9.7.8 Minimum Set

This research suggested some preliminary minimum set criteria, proposed alternative minimum sets for an illustrative application, and measured their performance losses. Future research should update the current understanding with a review of the product family design literature that focuses on the minimum set concept. This particular area of literature is currently ripe with developments and has served as invaluable learning tool for the present research. Also, a preliminary cost model should be developed with the aim of quantifying some of the claimed cost advantages of the minimum sets of actuators in Chapter 8. Very few researchers model costs when developing product families because of the difficulty in obtaining accurate models in the preliminary/conceptual design stages. Most researchers either only model the technical,

performance-related criteria for a product or the cost-related criteria but not both. As more actuator prototypes are built and the actuator moves closer to commercialization, more accurate cost information should become available.

9.7.9 Parameter Reduction

The actuator parametric models presented in Chapter 3 involved a large number of unknown design parameters and non-linear sets of polynomial equations. These sets of equations were solved by reducing the problem to solving a system of n equations in n unknown parameters. These $n \times n$ systems were achieved by defining reasonable relationships between the unknown internal parameters of the actuator and the external parameters typically specified by the designer (Section 4.3). Essentially, enough design parameter choices and additional constraint equations were specified by the designer to allow this solution approach.

An alternative way of dealing with the large numbers of parameters is to apply some of the model reduction techniques identified in the literature review. Currently, Groebner bases is considered one of the most useful techniques for the non-linear polynomial equations being considered here [Waskow and Tesar, 1996 and Gloria and Tesar, 2004]. The Groebner bases algorithm objectively combines equations and eliminates parameters based on the ordering of the variables by the designer, and the process is automated in the commercially available software MatLab. The aim of these and other reduction techniques (e.g., monotonicity analysis) is to reduce the number of parameters and equations so that the eliminated parameters still affect the design but the designer does not have to deal with them directly. Future work can use the present parametric models to explore the benefits of these parameter reduction techniques. The overall objectives would be to reduce the computational expense of searching through

(manipulating) the relatively large actuator design parameter space, to gain more physical insight into the actuator design problem, and to obtain actuator designs and scaling rules with less effort.

Appendices

APPENDIX A1: COMPUTATIONAL AND SOLID MODELING TOOLS

The parametric models of the SRM, HGT, and PEGT (Chapter 3) and actuator design procedures (Chapter 4) were coded into the MatLab computational software. This implementation was used to efficiently generate performance parameter information, design maps, and scaling rules for the following component/actuators in the scope of the present research.

- SRM (stand alone motor)
- HGT (stand alone gear train)
- Star+PEGT (stand alone gear train)
- Star Compound+PEGT (stand alone gear train)
- SRM+HGT (integrated actuator)
- SRM+Star+PEGT (integrated actuator)
- SRM+Star Compound+PEGT (integrated actuator)

The MatLab files detail the calculation of the torque, weight, inertia, torque density, and responsiveness of these systems using the relationships provided in Chapter 3.

This research required reasonably accurate computation of the torque, weight, and inertia of the reference designs for each of the above systems (to be displayed in the following sections) so that the results such as those in Chapters 5-8 would be useful for future actuator designs. There was also a desire to generate reference designs that could be used as templates for future detailed actuator designs and that could be easily interpreted by future actuator designers. With these aims in mind, the reference designs had the following features.

First, the geometry of many parts was simplified by making some neighboring parts integral and eliminating features such as chamfers, bearing shoulders, snap rings, seals, mounting holes, etc. Using integral parts (e.g. grouping two fixed parts that bolt

together into one part) allows the designer to easily understand which components are fixed and which rotate in a particular design. Elimination of the noted features simplifies the calculation of the weight and inertia while still ensuring reasonable accuracy for the present preliminary design focus. Second, most of the components in the motors, gear trains, and actuators considered were modeled as simple hollow or solid cylinders. This also simplifies the calculation of weight and inertia. Third, gear teeth were not shown for clarity, and all gears in the HGT and PEGT were modeled as solid cylinders with diameters equal to their pitch diameter. Finally, all of the parts were color coded for clarity. For examples, all of the bearings in the HGT and PEGT were the same color to allow a designer to quickly identify the bearing locations.

All of the MatLab (simulation files) and SolidWorks (solid model and drawing) files utilized during the present research can be found in the following location on the RRG network: /Departmental Directories/robotics/historic/Thesis, Dissertations and PhD Proposals/Stewart Vaculik/Dissertation. These files have also been stored on a CD that is included with the original copy of this report in the RRG library. The present author may be contacted with any questions at 512-496-5628 or at sav5470@yahoo.com.

The following sections detail the reference design, design parameter nomenclature for the drawings and solid models, and a listing of MatLab files for each of the 7 systems noted above.

A1.1 SRM

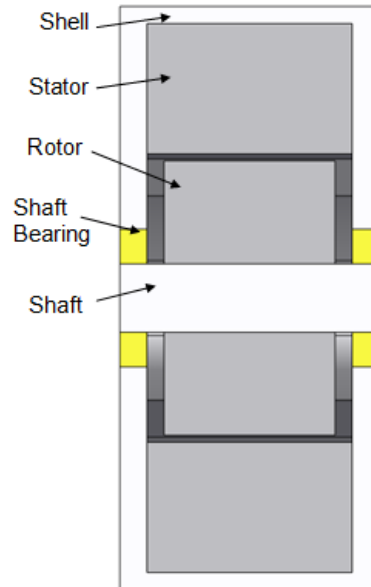


Figure A.1: SRM Reference Design

Table A.1: SRM Design Parameters Classified by Component (for generating reference design)

Component	Design Parameters
Rotor	$d_r, d_{rb}, d_b, \theta_r, t_r, h_r, L_s$
Stator	$d_s, d_{sb}, d_{si}, \theta_s, t_s, h_s, L_m$
Shaft	L_1, d_1
Shaft bearing	ID_shaft_bearing, OD_shaft_bearing, W_shaft_bearing
Shell	$L_{s1}, L_{s2}, L_{s3}, d_{s1}, d_{s2}, d_{s3}, d_{s4}$

Table A.2: MatLab Files for Stand-Alone (Direct Drive) SRM Designs without an SRM (Section 3.7)

File Name	Function
SRM_Design_Main_Direct_Drive.m	Main simulation file for generating performance parameter information, design maps, and scaling rules for the SRM
SRM_Geometry.m	Computation of the internal design parameters of the SRM (back iron diameters, air gap diameter, pole width, pole height, etc.)
SRM_Torque.m	Computation of the available space for windings, number of turns, current capacity, and torque capacity
SRM_Weight_Inertia_Direct_Drive.m	Computation of the total weight and inertia of the SRM

A1.2 HGT

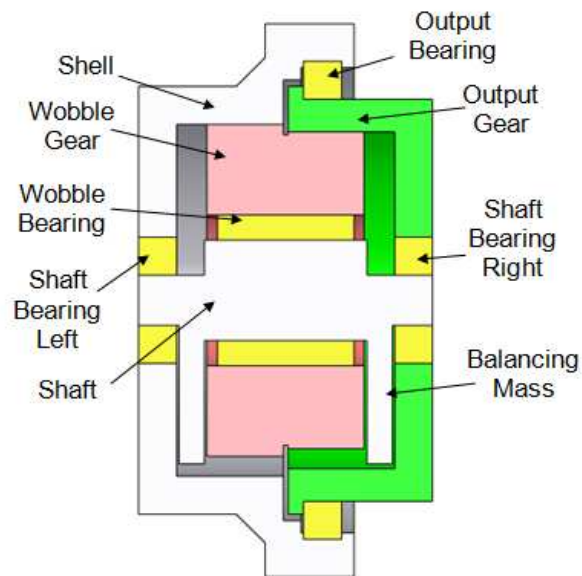


Figure A.2: HGT Reference Design

Table A.3: HGT Design Parameters Classified by Component (for generating reference design)

Component	Design Parameters
Wobble gear	$d_{w1}, d_{w2}, d_{wb}, d_{wo}, L_w$
Output gear	$d_{r2}, L_{o1}, L_{o2}, L_{o3}, d_{o1}, d_{o2}, d_{o3}$
Shaft (including balance masses)	$L_3, L_4, L_5, d_3, d_4, d_5, e, r_{o1}, r_{o2}, W$
Output bearing	ID_output_bearing, OD_output_bearing, W_output_bearing
Wobble bearing	ID_wobble_bearing, OD_wobble_bearing, W_wobble_bearing
Shaft bearing right	ID_shaft_bearing_right, OD_shaft_bearing_right, W_shaft_bearing_right
Shaft bearing left	ID_shaft_bearing_left, OD_shaft_bearing_left, W_shaft_bearing_left
Shell	$d_{r1}, L_{s1}, L_{s3}, L_{s4}, L_{s5}, L_{s6}, L_{s7}, d_{s1}, d_{s4}, d_{s5}, d_{s6}, d_{s7}, d_{s8}, d_{s9}$

Table A.4: MatLab Files for Stand-Alone HGT Designs without an SRM (Section 3.9)

File Name	Function
HGT_SA_Design_Main.m	Main simulation file for generating performance parameter information, design maps, and scaling rules for the HGT
HGT_Gear_Ratio.m	Computation of the HGT gear ratio
HGT_Stress.m	Computation of the gear tooth bending and contact stresses in the HGT
HGT_SA_Weight_Inertia.m	Computation of the total weight and inertia of the HGT
Wobble_Gear_Weight_Inertia.m	Computation of the wobble gear weight and inertia
HGT_SA_Bearing_Weight_Inertia.m	Estimation of the bearing sizes and computation of the bearing weight and inertia
HGT_SA_Eccentric_Shaft_Weight_Inertia.m	Computation of the eccentric shaft weight and inertia
Balancing_Weight_Inertia.m	Computation of the balancing mass dimensions, weight, and inertia
HGT_Output_Gear_Weight_Inertia.m	Computation of the output gear weight and inertia
HGT_SA_Shell_Weight_Inertia.m	Computation of the shell weight and inertia
HGT_SA_Bearing_Load_Capacity.m	Computation of the forces on all the bearings and the bearing load capacity for a desired operating life

A1.3 PEGT (with Star and Star Compound 1st Stage Alternatives)

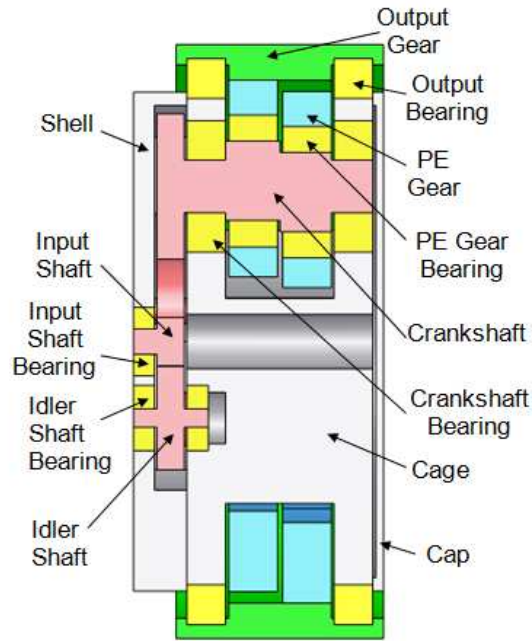


Figure A.3: Star+PEGT Reference Design

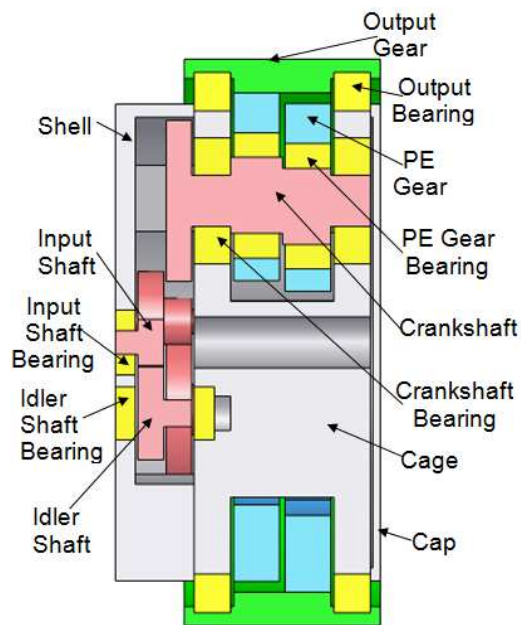


Figure A.4: Star Compound+PEGT Reference Design

Table A.5: PEGT Design Parameters Classified by Component (for generating reference design)

Component	Design Parameters
PE gear	$d_{pe}, L_{pe}, d_{peb}, c_c, d_{pec}, r_{pec}, L_{pec1}, L_{pec2}$
Cage	$L_{c1}, L_{c2}, L_{c4}, c_c, c_i, d_{c1}, d_{c2}, d_{c3}, d_{c4}, d_{ci}, d_{cc}, r_{cc}, L_{cc1}, L_{cc2}, \theta$
Output gear	$L_{o1}, L_{o2}, L_{o3}, c, d_{o1}, d_{o2}, d_{o3}(d_r), d_{o4}$
Input shaft	$L_{ms1}, L_{ms2}, d_{ms1}, d_{ms2}(d_{sun})$
Idler shaft (Star)	$L_{is1}, L_{is2}, d_{is1}, d_{is2}(d_p)$
Idler shaft (Star Compound)	$L_{is1}, L_{is2}, L_{is3}, d_{is1}, d_{is2}(d_{p1}), d_{is3}(d_{p2})$
Crank shaft	$L_{cs1}, L_{cs2}, L_{cs3}, L_{cs4}, L_{cs5}, d_{cs1}(d_{o2}), d_{cs2}, d_{cs3}, d_{cs4}, d_{cs5}, e$
Output bearing	ID_output_bearing, OD_output_bearing, W_output_bearing
PE gear bearing	ID_PE_gear_bearing, OD_PE_gear_bearing, W_PE_gear_bearing
Crank shaft bearing	ID_crank_shaft_bearing, OD_crank_shaft_bearing, W_crank_shaft_bearing
Idler shaft bearing	ID_idler_shaft_bearing, OD_idler_shaft_bearing, W_idler_shaft_bearing
Input shaft bearing	ID_input_shaft_bearing, OD_input_shaft_bearing, W_input_shaft_bearing
Shell	$L_{s1}, L_{s2}, L_{s3}, L_{s4}, d_{s1}, d_{s2}, d_{s4}, d_{s5}, d_{si}, c_i, r_{sm}, \theta$
Cap	$L_{cp1}, L_{cp2}, d_{cp1}, d_{cp2}$

Table A.6: MatLab Files for Stand-Alone PEGT Designs without an SRM (Section 3.10)

File Name	Function
PEGT_SA_Design_Main.m	Main simulation file for generating performance parameter information, design maps, and scaling rules for the PEGT
PEGT_Gear_Ratio.m	Computation of the PEGT gear ratio
Star_for_PEGT_Gear_Ratio.m SC_for_PEGT_Gear_Ratio.m	Computation of the 1 st stage star or star compound gear ratio
PEGT_Stress.m	Computation of the gear tooth bending and contact stresses in the PEGT
S_for_PEGT_Stress SC_for_PEGT_Stress	Computation of the gear tooth bending and contact stresses in the star and star compound 1 st stage alternatives
PEGT_SA_Weight_Inertia.m	Computation of the total weight and inertia of the PEGT
PE_Gear_Weight_Inertia.m	Computation of the parallel eccentric (PE) gear weight and inertia
PEGT_Output_Gear_Weight_Inertia.m	Computation of the output gear weight and inertia
PEGT_SA_Bearing_Weight_Inertia.m	Estimation of the bearing sizes and computation of the bearing weight and inertia
PEGT_Crank_Shaft_Weight_Inertia.m	Computation of the crankshaft weight and inertia
Star_PEGT_Idler_Shaft_Weight_Inertia.m SC_PEGT_Idler_Shaft_Weight_Inertia.m	Computation of the idler shaft weight and inertia, for the star and star compound alternatives
PEGT_SA_Input_Shaft_Weight_Inertia.m	Computation of the input shaft weight and inertia
PEGT_SA_Shell_Weight_Inertia.m	Computation of the shell weight and inertia
PEGT_Cage_Weight_Inertia	Computation of the cage (bridge structure) weight and inertia
PEGT_Cap_Weight_Inertia.m	Computation of the cap weight and inertia
SRM_PEGT_Bearing_Load_Capacity.m	Computation of the forces on all the bearings and the bearing load capacity required for the designer-specified operating life

A1.4 SRM+HGT

Section 3.11 provides the SRM+HGT reference design and the design parameters for each component. Files which have already been listed above for the stand-alone HGT designs are not repeated in the following table.

Table A.7: MatLab Files for SRM+HGT Actuator (Section 3.11)

File Name	Function
SRM_HGT_Design_Main.m	Main simulation file for generating performance parameter information, design maps, and scaling rules for the SRM+HGT
SRM_Design_Main	Computation of the torque, weight, and inertia of the SRM to be coupled with the HGT
SRM_HGT_Weight_Inertia.m	Computation of the total weight and inertia of the SRM+HGT
SRM_HGT_Bearing_Weight_Inertia.m	Estimation of the bearing sizes and computation of the bearing weight and inertia
SRM_HGT_Eccentric_Shaft_Weight_Inertia.m	Computation of the eccentric shaft weight and inertia
SRM_HGT_Shell_Weight_Inertia.m	Computation of the shell weight and inertia
SRM_HGT_Bearing_Load_Capacity.m	Computation of the forces on all the bearings and the bearing load capacity required for the designer-specified operating life

A1.5 SRM+PEGT (with Star and Star Compound 1st Stage Alternatives)

Section 3.12 provides the SRM+PEGT reference design and the design parameters for each component. Files which have already been listed above for the stand-alone PEGT designs are not repeated in the following table.

Table A.8: MatLab Files for SRM+Star+PEGT and SRM+Star Compound+PEGT Actuator Designs (Section 3.12)

File Name	Function
SRM_PEGT_Design_Main.m	Main simulation file for generating performance parameter information, design maps, and scaling rules for the SRM+PEGT
SRM_PEGT_Weight_Inertia.m	Computation of the total weight and inertia of the SRM+PEGT
SRM_PEGT_Bearing_Weight_Inertia.m	Estimation of the bearing sizes and computation of the bearing weight and inertia
SRM_PEGT_Input_Shaft_Weight_Inertia.m	Computation of the input shaft weight and inertia
SRM_PEGT_Shell_Weight_Inertia.m	Computation of the shell weight and inertia

A1.6 General Computation Files

Table A.9 provides a listing of files used with with all of the systems discussed above.

Table A.9: MatLab Files for General Computations

File Name	Function	Section Reference
Design_Rule_Generation.m	Generation of 3-D design maps and computation of scaling rule (polynomial) coefficients	2.7.1, 5.1.2
Weight_Inertia.m	Computation of the volume, weight, and inertia of hollow and solid cylinders, useful for most of the motor and gear train components considered	3.4
Bearing_Equivalent_Load.m	Computation of the equivalent load on a bearing given a load profile that varies as a function of time or position (i.e., a variable duty cycle)	3.14
Bearing_Load_Capacity.m	Computation of the required bearing dynamic load capacity necessary to achieve a desired operating life	3.14
Load_sharing.m	Computation of the load sharing factor (s) given the assumed contact ratio	3.5.5

The design map generation file (Design_Rule_Generation.m) was used to generate 3-D design maps and to compute the polynomial coefficients used for representing the scaling rules. Using the relationships in Sections 2.7.1 and 5.1.2, this file computes the fitting accuracy for all possible polynomial models (built from the different combinations of terms of a third-order polynomial) fitted to a given set of parameter data. The “best” scaling rule/design map is the combination of polynomial terms that results in the lowest fitting error (Section 2.7.1.2).

APPENDIX A2: LINK BETWEEN MATLAB AND SOLIDWORKS

The beginnings of a link between the chosen computational software (MatLab) and solid modeling program (SolidWorks) was generated for this research and is illustrated in Figure A.5.

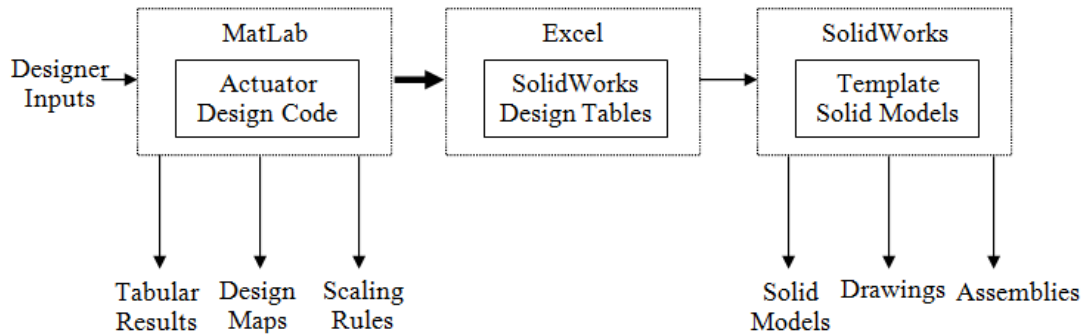


Figure A.5: Actuator Design Information Flow Between MatLab-Excel-SolidWorks

The MatLab files listed in Appendix A1 (Table A.2, Table A.4,

Table A.6-Table A.9) were used to compute the performance parameters (torque, weight, inertia, torque density, and responsiveness) of the SRM, HGT, PEGT, and integrated actuator designs (i.e., all those systems noted in Appendix A1) given a set of inputs from the designer. The design parameters designated for each system in Appendix A1 (Table A.1, Table A.3, and Table A.5) were embedded within SolidWorks Design Tables (Figure A.6) for the components in each system. A similar approach was used by Kendrick and Tesar [2006] to quickly generate solid models of the gear teeth in the HGT. When the designer changes the values in a Design Table for a particular component, the solid model that is linked with the Design Table is updated automatically.

	A	B	C	D	E
1	Design Table for: wobble gear				
2		dw1 @Sketch1	dw2 @Sketch1	d wobble gear bore@Sketch1	Lw1 @Sketch1
3	Default	6.6	6.3	3	1.5
4					

Figure A.6: SolidWorks Design Table in Microsoft Excel for the HGT Wobble Gear

Most of the link was completed during the present research. The only remaining part is to pass the actuator design parameter data from MatLab to Excel, noted by the

bold arrow in Figure A.5. Currently, the parameter data can be entered manually in the Design Table, and what remains is the automation of this particular task. Future research should use the built in MatLab commands that allow for writing to and reading from Excel spreadsheets to complete this link. Completion of the link will allow the designer to programmatically (in MatLab or in another computational software program) change the dimensions in the actuator without opening the SolidWorks solid model files. This linking between these commonly used software tools should reduce the time and effort it takes for a designer to progress from a set of customer requirements to performance specifications (tabular results, design maps, solid models, drawings, etc.).

APPENDIX A3: HGT BALANCING MASS COMPUTATIONS

When a mass is rotating at an eccentric distance away from the axis of rotation of a body, centripetal forces are introduced on that body [Waldron and Kinzel, 2004]. This condition commonly occurs in rotating shafts, which are present in the electromechanical actuators of this research. These centripetal forces add to the applied forces on a system and must be accounted for by the bearings that support the shaft. Mathematically, if an eccentric mass (m) with a given center of mass (r) with respect to the centerline of the shaft is attached to a shaft rotating at a specific angular speed (ω), these centripetal forces (F) are of the form:

$$F = mr \omega^2 \quad \text{Eqn. 200}$$

The HGT designs in this report include an eccentric shaft, wobble bearing, and wobble gear rotating at an eccentric distance away from the actuator centerline, as shown in Figure A.7. This requires that the design be statically and dynamically balanced by adding balancing weights of the appropriate geometry to the rotating shaft [Waldron and Kinzel, 2004]. This section details the geometrical and force and moment balance equations needed to model this system.

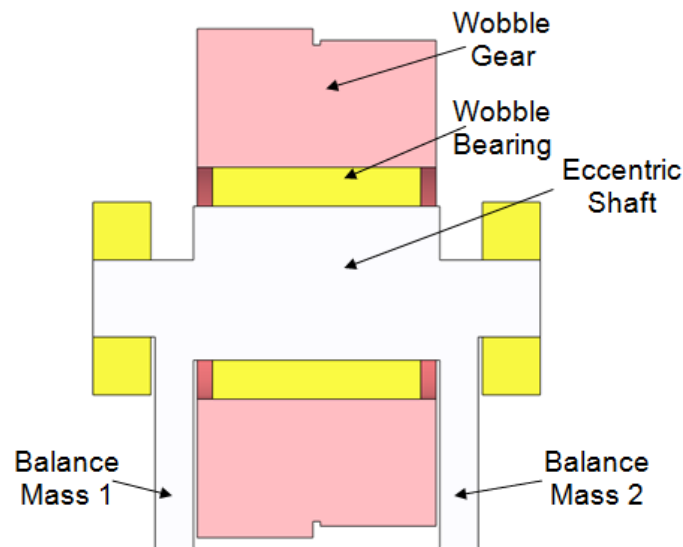
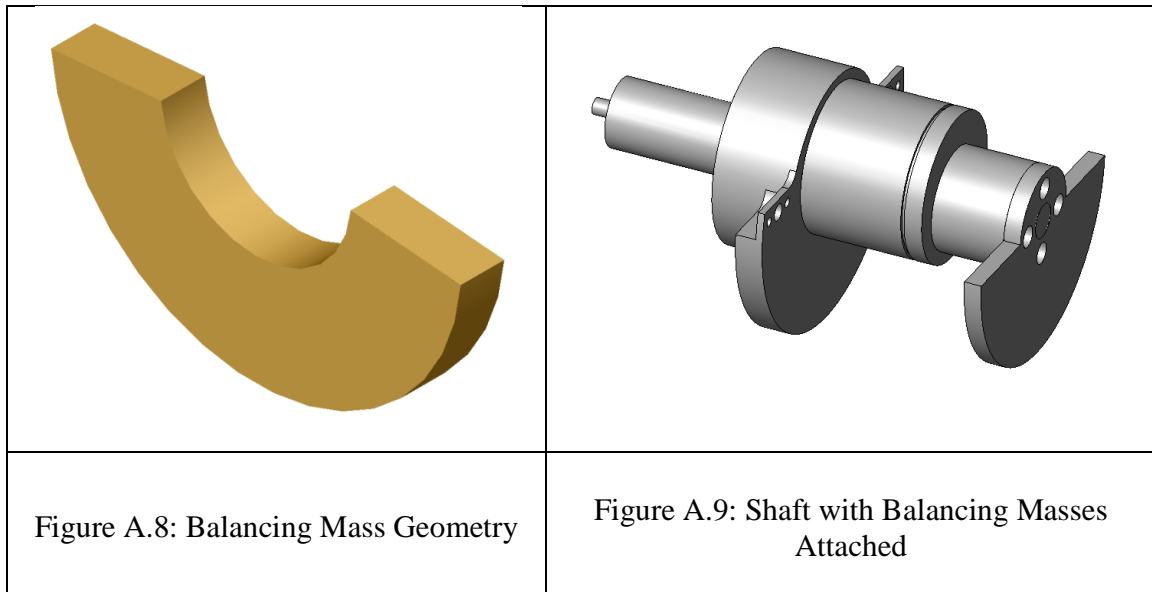


Figure A.7: HGT Shaft Geometry

A3.1 Balancing Mass Geometry

Balancing masses of the semi-circular lobe shape, as shown in Figure A.8 and Figure A.9, are suggested to allow the use of algebraic (rather than integral) equations to determine their center of mass. This shape choice is also simple to manufacture and commonly used in automotive crankshafts. More complex balancing geometries are possible if the relevant modeling equations are derivable or solid modeling software (with the integral weight and center of mass equations built-in) is used. The choice of the number and location of the balancing masses depends on the application, but two masses located on opposite sides of the wobble gear are shown in Figure A.7. This section will present general equations that apply to an individual balancing mass and also specific force and moment balance equations for the two balance mass system suggested for the HGT.



The parameters used in the development of the balancing relationships in this appendix are listed in Table A.10. Figure A.10 provides a drawing of a typical balancing mass with the relevant design parameters labeled. Figure A.11 divides the wobble gear into three sections in order to develop the balancing relationships below.

Table A.10: Balancing Mass Parameters

Constants	Design Parameters	Intermediate Parameters	Performance Parameters
ρ_b Density e Eccentricity c Axial clearance	Outer radii r_{o1} Mass 1 r_{o2} Mass 2 Inner radii r_{i1} Mass 1 r_{i2} Mass 2 α Angle subtended Widths w_1 Mass 1 w_2 Mass 2 Axial locations d_1 Mass 1 d_2 Mass 2 ω Speed	Cross-sectional areas A_1 Mass 1 A_2 Mass 2 Weights W_{es} Eccentric shaft W_{wb} Wobble bearing W_w Wobble gear W_e Total W_{bm1} Mass 1 W_{bm2} Mass 2 Center of mass r_{c1} Mass 1 r_{c2} Mass 2 R Wobble gear (axial) u Balancing product	W_{bal} Weight I_{bal} Inertia

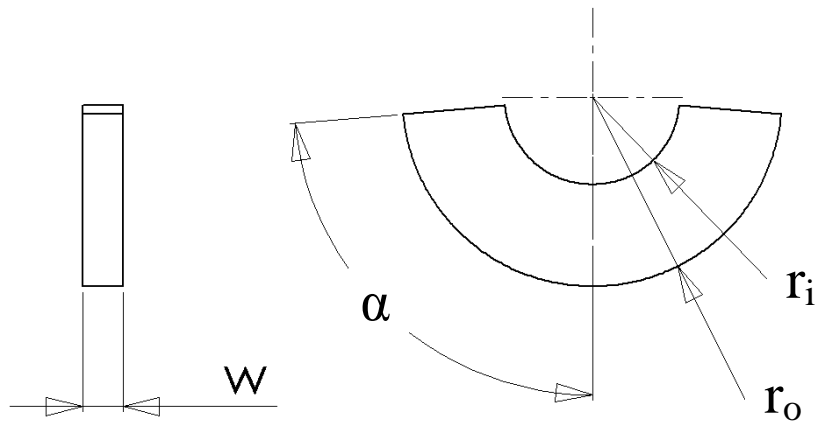


Figure A.10: Balancing Geometry

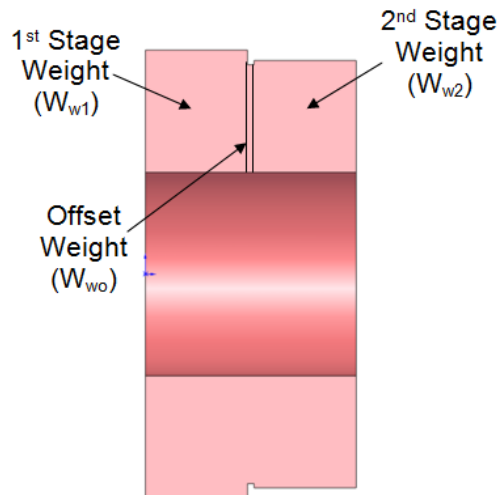


Figure A.11: Wobble Gear and Weights of 3 Individual Sections

A3.2 Cross-Sectional Area of Balancing Mass

The cross-sectional area (A) of the chosen balancing mass geometry in Figure A.10 can be written as follows.

$$A = \alpha (r_o^2 - r_i^2) \quad \text{Eqn. 201}$$

The inner (r_i) and outer (r_o) radius and subtended angle (α) are independent choices of the designer, but they are often constrained by shaft diameters, shell/gear diameters, and weight/inertia limits in the HGT.

A3.3 Balancing Mass Weight

The weight (W_{bm}) of a balancing mass can be determined from its known area (A), width (w), and density (ρ_b) as:

$$W_{bm} = \rho_b A w \quad \text{Eqn. 202}$$

The width of the mass is another independent choice of the designer, but there are minimum widths due to stability and manufacturing constraints and maximum widths based on adequate clearances between rotating internal actuator components and overall actuator length limits.

For the preliminary design purposes of this report, the width of balancing mass (w) was defined as a function of the overall length of the HGT (L_g) using the following relationship.

$$w = k L_g \quad \text{Eqn. 203}$$

The factor k in this equation is typically between 0.05 and 0.15, depending upon the desired shape of the balancing mass (i.e., wider mass with smaller outer radius or thinner mass with larger outer radius).

A3.4 Center of Mass

The center of mass (r_c) of the selected lobe geometry (Figure A.10) can be written as follows [NCEES, 2000].

$$r_c = \frac{2 \sin \alpha (r_o^3 - r_i^3)}{3A} = \frac{2 \sin \alpha (r_o^3 - r_i^3)}{3\alpha (r_o^2 - r_i^2)} \quad \text{Eqn. 204}$$

The product of the mass (m) and its center of mass (r_c) is known as the imbalance or balancing product (u).

$$u = mr_c$$

Eqn. 205

A3.5 Balance of Forces

For a system to be statically and dynamically balanced, a balance of centripetal forces and a balance of moments (due to the centripetal forces) on the shaft must be achieved. A free-body diagram of the HGT shaft with the centripetal forces due to the eccentric mass (W_e) and the added balancing masses (W_{bm1} and W_{bm2}) is shown in Figure A.12. In the figure, e is the HGT eccentricity, r_{c1} and r_{c2} are centers of mass for balancing masses 1 and 2, and ω represents the shaft speed, which will typically be same as the motor speed. Figure A.13 details all of the relevant dimensions for the balancing equations in the following sections.

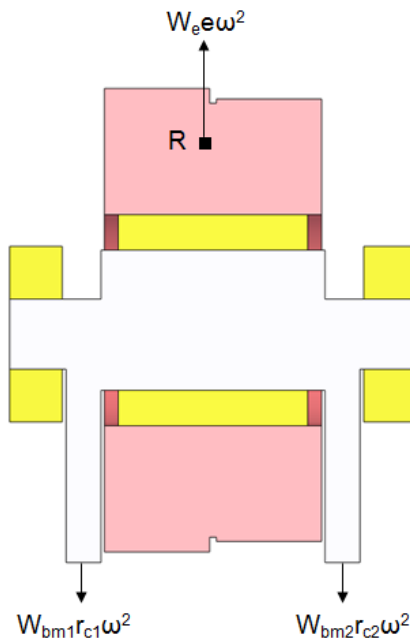


Figure A.12: HGT Balancing Free-Body Diagram

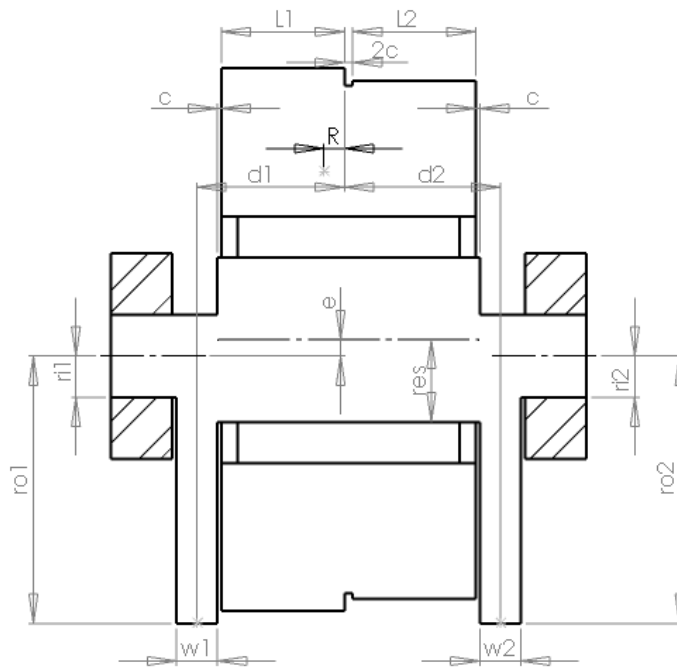


Figure A.13: Relevant HGT Geometry Dimensions for Balancing Relationships

The total eccentric weight (W_e) in Figure A.12 is the sum of the eccentric weights of the wobble gear (W_{w1} , W_{w2} , W_{wo}), wobble gear bearing (W_{wb}), and eccentric shaft (W_{es}).

$$W_e = W_{w1} + W_{w2} + W_{wo} + W_{wb} + W_{es} \quad \text{Eqn. 206}$$

In Figure A.13, R is the axial center of mass of the wobble gear, measured from the right edge of 1st stage.

$$R = \frac{\left[W_{w1} \frac{L_1}{2} - W_{w2} \left(\frac{L_2}{2} + 2c \right) - W_{wo} \frac{2c}{2} \right]}{(W_{w1} + W_{w2} + W_{wo})} \quad \text{Eqn. 207}$$

According to the free-body diagram in Figure A.12, a balance of forces gives the following.

$$W_e \omega^2 = W_{bm1} r_{c1} \omega^2 + W_{bm2} r_{c2} \omega^2 \quad \text{Eqn. 208}$$

Because the eccentric mass and the added balancing masses all rotate at the same speed (ω), the speed squared can be divided out of the equation to yield the simpler equation:

$$W_e e = W_{bm1} r_{c1} + W_{bm2} r_{c2} \quad \text{Eqn. 209}$$

Substituting the weight (W_{bm1} and W_{bm2}) and centers of mass (r_{c1} and r_{c2}) from above into this expression and simplifying yields the following.

$$W_e e = \frac{2\rho_b}{3} [(r_{o1}^3 - r_i^3)w_1 + (r_{o2}^3 - r_i^3)w_2] \quad \text{Eqn. 210}$$

If the balance masses are assumed to be the same width, as is often done for simplicity (i.e., $w_1=w_2=w$), the following is the result.

$$W_e e = \frac{2\rho_b w}{3} (r_{o1}^3 + r_{o2}^3 - 2r_i^3) \quad \text{Eqn. 211}$$

A3.6 Balance of Moments

Summing moments about a line through the wobble gear center of mass R (Figure A.12) results in the following moment balance equation.

$$W_{bm1} r_{c1} \omega^2 d_1 = W_{bm2} r_{c2} \omega^2 d_2 \quad \text{Eqn. 212}$$

Because the two balancing masses rotate at the same speed, the speed squared can be divided out of the equation to yield the following simpler equation.

$$W_{bm1} r_{c1} d_1 = W_{bm2} r_{c2} d_2 \quad \text{Eqn. 213}$$

The two balancing moment arm dimensions (d_1 and d_2) in Figure A.13 can be defined in terms of the labeled design parameters as follows.

$$\begin{aligned} d_1 &= L_1 - R + c + \frac{w}{2} \\ d_2 &= L_2 + R + 3c + \frac{w}{2} \end{aligned} \quad \text{Eqn. 214}$$

To achieve complete static and dynamic balance of an eccentric system, the force and moment balance equations must be simultaneously satisfied. Substituting into the moment balance equation for W_{bm1} , W_{bm2} , r_{c1} , and r_{c2} gives the following result.

$$d_1(r_{o1}^3 - r_i^3) = d_2(r_{o2}^3 - r_i^3) \quad \text{Eqn. 215}$$

Solving the simplified force (Eqn. 211) and moment (Eqn. 215) balance equations (two equations in two unknowns r_{o1} and r_{o2}) yields the following result.

$$r_{o2} = \sqrt[3]{\frac{d_1\left(\frac{3W_e e}{2\rho_b w} + r_i^3\right) + d_2 r_i^3}{d_1 + d_2}} \quad \text{Eqn. 216}$$

$$r_{o1} = \sqrt[3]{\frac{3W_e e}{2\rho_b w} + 2r_i^3 - r_{o2}^3}$$

A3.7 Balancing Weight and Inertia

The total balancing weight (W_{bal}) is simply the sum of the weights of the individual balancing masses.

$$W_{bal} = W_{bm1} + W_{bm2} \quad \text{Eqn. 217}$$

The inertia of a single balance mass about the shaft centerline is as follows

$$I_{bm} = \frac{\rho_b \alpha w (r_o^4 - r_i^4)}{2} \quad \text{Eqn. 218}$$

The inertia of the entire balancing geometry (I_{bal}) is the sum of the inertia of the individual balancing masses.

$$I_{bal} = I_{bm1} + I_{bm2} \quad \text{Eqn. 219}$$

This inertia should be low to maintain the desired acceleration capability of the actuator. Finally, the reader should note that the eccentric weight and inertia due to the wobble gear, wobble bearing, and eccentric shaft are not included in these expressions because they are accounted for elsewhere and cannot be reduced significantly to reduce the size of the balancing masses.

APPENDIX A4: AGMA BENDING STRESS J-FACTOR

In order to understanding the meaning of the geometry factor (J) AGMA in the AGMA bending stress equation, it is useful to model a gear tooth as a simple cantilever beam with an applied load F [Shigley and Mischke, 1989] as shown in Figure A.14.

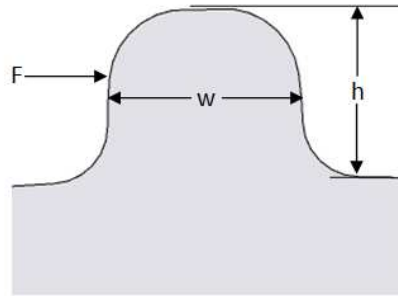


Figure A.14: Modeling a Gear Tooth as a Beam with Applied Load F Near the Pitch Circle

The bending stress at the base of a gear tooth can then be approximated by the following equation.

$$\sigma = \frac{Mc}{I} \quad \text{Eqn. 220}$$

The applied moment (M) is the product of the tangential load (F) and the tooth height (h), temporarily assuming that the load is applied at the tip of the tooth.

$$M = Fh \quad \text{Eqn. 221}$$

In general, h can be replaced by the distance from the point of load application to the base of the tooth, and this will be discussed later in this appendix.

Designating the tooth width as w, c is the distance between the surface of the tooth and neutral axis and is given by the following.

$$c = \frac{w}{2} \quad \text{Eqn. 222}$$

The area moment of inertia (I) of the modeled cantilever beam with tooth face width L (into the page) is as follows.

$$I = \frac{Lw^3}{12} \quad \text{Eqn. 223}$$

Substituting M, c, and I into the bending stress equation and simplifying gives the following.

$$\sigma = \frac{6F}{L} \frac{h}{w^2} \quad \text{Eqn. 224}$$

This equation has been arranged so that the effect of the height and width of the tooth can be considered.

The width of the tooth at the pitch circle (for both circular arc and involute profiles) can be written as a function of the circular pitch (p), number of teeth (N), pitch diameter (d), and diametral pitch (P_d) as follows.

$$w = \frac{p}{2} = \frac{\pi d}{2N} = \frac{\pi}{2P_d} \quad \text{Eqn. 225}$$

For involute teeth, the AGMA recommends that the height of the tooth be written as a function of the diametral pitch as follows.

$$h = \frac{k}{P_d} \quad \text{Eqn. 226}$$

The constant k ranges between 1.8 for stub (short) teeth and 2.25 for standard height teeth.

Thus, the height to width ratio for involute teeth falls into the following range.

$$1.15 < \frac{h}{w} < 1.43 \quad \text{Eqn. 227}$$

Table A.11 summarizes the results of substituting this range of values for the height to width ratio (h/w) into the bending stress equation. The table also includes the approximate lower limit for h/w ratio suggested for the typically shorter circular arc gear teeth.

Table A.11: Bending Stress Relationships for Different Load Conditions and Tooth Height to Width Ratios

	Standard Involute Teeth $\left(\frac{h}{w}=1.43\right)$	Stub (Short) Involute Teeth $\left(\frac{h}{w}=1.15\right)$	Circular Arc Teeth $\left(\frac{h}{w}=1\right)$
Load Applied at Tip of Tooth	$\sigma = \frac{F}{L} \frac{P_d}{0.18}$	$\sigma = \frac{F}{L} \frac{P_d}{0.23}$	$\sigma = \frac{F}{L} \frac{P_d}{0.26}$
Load Applied at Center of Tooth	$\sigma = \frac{F}{L} \frac{P_d}{0.36}$	$\sigma = \frac{F}{L} \frac{P_d}{0.46}$	$\sigma = \frac{F}{L} \frac{P_d}{0.52}$

This equation can be compared to the AGMA bending stress equation (with the stress modification factors removed) for insight into the values of the J factors found in standard AGMA look-up tables.

$$\sigma = \frac{FP_d}{LJ} \quad \text{Eqn. 228}$$

The J factors typically used in this equation are found in the AGMA standard and are typically between 0.2 and 0.6, depending upon the point of load application on the tooth, pressure angle, and numbers of teeth on the mating gears. These standard AGMA J factor values compare very well with those suggested by Table A.11. This result provides an important physical understanding of the J factor and gives the designer a reasonable set of bounds to work within when designing the circular arc gear teeth for the HGT and PEGT. The discrepancy between the J factors in Table A.11 and the AGMA J factors are present due to the current simplifying assumption of modeling the tooth as a cantilever beam of constant cross-section from the root to the tip of the tooth. The AGMA does not use this simplifying assumption when reporting values of the J factor.

Glossary

ElectroMechanical Actuator (EMA)- a motor and gear train integrated into a single housing, also known as “electromagnetic” actuators or “garmotors” in the research and industrial literature

Design parameter (D_P)-parameters that describe the dimensions and overall geometry of a component (e.g., diameter, length, width, numbers of teeth, number of motor poles)

Performance parameter (P_P)-parameters that the describe the performance capabilities of a component (e.g., torque, weight, inertia, torque to weight ratio, torque to inertia ratio)

Design synthesis- the process in which the performance parameters are known and the design parameters are obtained using analytical governing equations

Design analysis- the process in which the design parameters are known and the performance parameters are obtained using finite element analysis, numerical simulation, and/or analytical governing equations

Product family- a group of related products that share common features, components, and subsystems and satisfy a variety of market niches (also called a product line or minimum set in this research)

Scale-based product family- a product family in which features change from product to product with changes in the values of the scaling variables

Common parameters/variables- design parameters that remain constant from product to product within a family and constitute a product platform

Scaling parameters/variables- design parameters that vary from product to product within a family and are used to meet the individual performance requirements of each product in a family

ACRONYMS

EMA-Electromechanical actuator

EMAA-Electromechanical Actuator Architecture

SRM- Switched reluctance motor

BLDCM- Brushless dc motor

HGT- Hypocyclic gear train

SCGT- Star compound gear train

PEGT- Parallel eccentric gear train

FEA- Finite element analysis

RSM- Response surface methodology

References

This section lists all of the references cited in the body of this report and also includes additional references that were reviewed and not specifically cited in the report. The references have been grouped into the same categories used in Chapter 2.

ELECTROMECHANICAL ACTUATORS

- Aghili, F. et al., 2002, "Development of a High-Performance Direct Drive Joint", *Advanced Robotics*, Vol. 16, No. 3, pp. 233-250.
- Ambrose, R. and Tesar, D., 1991, "Design, Construction and Demonstration of Modular, Reconfigurable Robots," Report, Mechanical Engineering, The University of Texas at Austin, Robotics Research Group.
- Bolton, H.R., 1994, "Design Aspects of Electromagnetic Actuators," *IEE Colloquium on Magnetic Materials for Sensors and Actuators*, pp. 6/1-6/5.
- Bonfiglioli, Inc., 2007, "AS Inline Helical Gear Motors", www.bonfiglioli.com/.
- Bozzola, P., 1985, "Electromechanical Actuators for Helicopter Blade Folding Application", *European Rotorcraft Forum*, London, England, Vol. 45, pp. 1-13.
- Brandlein, J. et al., *Ball and Roller Bearings: Theory, Design, and Application*, 3rd Edition, John Wiley and Sons, 1999.
- Carlson-Skalak, S., Maslen, E., and Teng, Y., 1999, "Magnetic Bearing Actuator Design Using Genetic Algorithms," *Journal of Engineering Design*, Vol. 10, No. 2, pp. 143-164.
- Chun, W. and Brunson, P., 1987, "Actuators for a Space Manipulator", NASA, Goddard Space Flight Center, *Proceedings of 1987 Goddard Conference on Space Applications of Artificial Intelligence (AI) and Robotics*, N89-10101.
- Collamore, F.N. and Lister, M., 1990, "A Reliable, Low-Cost Electromechanical Actuator for the ALS Engine Control Effectors", *AIAA/SAE/ASME/ASEE Joint Propulsion Conference*, Orlando, Florida, AIAA-1990-1945.
- Duff-Norton, Inc., 2007, "TracMaster: Electromechanical Linear Actuators," <http://www.duffnorton.com/emact.htm>.
- Fitan, E., Messine, F., and Nogarede, B., 2004, "The Electromagnetic Actuator Design Problem: A General and Rational Approach," *IEEE Transactions on Magnetics*, Vol. 40, No. 3, pp. 1579-1590.

- Messine, F., Nogarede, B., and Lagouanelle, J., 1998, "Optimal Design of Electromechanical Actuators: A New Method Based on Global Optimization," *IEEE Transactions on Magnetics*, Vol. 34, No. 1, pp. 299-308.
- Gloria, C. and Tesar, D., 2004, "Parametric Modeling and Design Synthesis for Electromechanical Actuators," Report, Mechanical Engineering, The University of Texas at Austin, Robotics Research Group.
- Grupinski, S. and Tesar, D., 1996, "Design of Low Cost Robotic Actuators for a Modular, Reconfigurable Six-Degree of Freedom Robotic Manipulator," Report, Mechanical Engineering, The University of Texas at Austin, Robotics Research Group.
- Haskew, T.A. and Schinstock, D.E., 1998, "Optimal Design of Electromechanical Actuators for Active Loads," *IEEE/ASME Transactions on Mechatronics*, Vol. 3, No. 2, pp.129-137.
- HD Systems, Inc., 2007, "Low Profile Actuator (LPA)", <http://www.hdsi.net/>.
- Howe, D., 2000, "Magnetic Actuators," *Sensors and Actuators*, Vol. 81, pp. 268-274.
- Huber, J., 1991, "Lightweight, Direct Drive Electromechanical Actuator," Patent No. 5,041,748.
- Kittock, M., 1993, "High Power Thrust Vector Actuation", AIAA/SAE/ASME/ASEE *Joint Propulsion Conference*, Monterey, California, AIAA-1993-2459.
- McNatt, B. and Tesar, D., 1993, "The Design of an Advanced Actuator Transmission for a Modular Robotic Manipulator," Report, Mechanical Engineering, The University of Texas at Austin, Robotics Research Group.
- Nabtesco, 2008, "AR Series Electromechanical Actuator", <http://www.rd-gear.com/>.
- Nuttall, Inc., 2007, "Moduline Integral GearMotors", <http://www.nuttallgear.com/>.
- Rios, O. and Tesar, D., 2007, "Actuator Gain Distributions to Analytically Meet Specified Performance Capabilities in Serial Robot Manipulators", *Journal of Mechanical Design*, currently in review.
- Smith, S., 1984, "A Compact Electromechanical Actuator" *Proceedings of the National Aerospace and Electronics Conference*, Dayton, Ohio, Vol. 1, pp. 598-605.
- Sumitomo Machinery Corporation of America, 2007, "Sumitomo Drive Technologies," <http://www.smcylo.com/>.
- Swingle, W. and Edge, J., 1981, "The Electric Orbiter", *Proceedings of the National Aerospace and Electronics Conference*, Dayton, Ohio, Vol. 1, pp. 229-240.
- Tesar, D., Aug. 2003, "Human Scale Intelligent Mechanical Systems," *Proceedings of the 11th World Congress in Mechanism and Machine Science*.

- Tesar, D., 2000-2007, "Electromechanical Actuator Architecture (EMAA)," Mechanical Engineering, The University of Texas at Austin, Robotics Research Group.
- Tesar, D. et al., June 2002, "The Design of a High Torque, Fault Tolerant Submarine Actuator," Report, Mechanical Engineering, The University of Texas at Austin, Robotics Research Group.
- Tesar, D. et al., April 2003, "Design of a ¼ Scale Actuator for an Advance Weapons Elevator," Report, Mechanical Engineering, The University of Texas at Austin, Robotics Research Group.
- Tesar, D. et al., Oct. 2003, "Design of a Full-Scale Actuator for an Advanced Weapons Elevator," Report, Mechanical Engineering, The University of Texas at Austin, Robotics Research Group.
- Tesar, D. et al., March 2004, "Design of an Elbow Actuator for a Rugged Manipulator," Report, Mechanical Engineering, The University of Texas at Austin, Robotics Research Group.
- Tesar D. et al., 2008, "Design of an Electro-Mechanical Actuator for Fair Water Planes in Submarines," Report, Mechanical Engineering, The University of Texas at Austin, Robotics Research Group.
- Timken, 2004, "Bearing Speed Capabilities," <http://www.timken.com/products/bearings/fundamen/speed.asp>.
- Vaculik, S. and Tesar, D., 2004, "Advanced Design Methods for Electromechanical Actuators," Master's Thesis, Mechanical Engineering, University of Texas at Austin, Robotics Research Group.
- Waldron, K.J. and Kinzel, G.L., 2004, *Kinematics, Dynamics, and Design of Machinery*, 2nd Edition, John Wiley and Sons, Inc.
- Wallace, R.S., 1993, "Miniature Direct Drive Rotary Actuators," *Robotics and Autonomous Systems*, Vol. 11, pp. 129-133.
- Wallace, R.S., 1994, "Miniature Direct Drive Rotary Actuators II: Eye, Finger, and Leg," *Robotics and Autonomous Systems*. Vol. 13, pp. 97-105.
- Wiese, G. and Tesar, D., 1997, "Low Cost Actuator Design for Modular Robots," Report, Mechanical Engineering, The University of Texas at Austin, Robotics Research Group.
- Zubkow, Z., 1992, "Electromechanical Actuator for Thrust Vector Control", *Proceedings of the 15th Annual AAS Rocky Mountain Conference*, Keystone, CO, AAS 92-043.

GEAR TRAIN DESIGN

- Bai, I., Chong, T., and Kubo, A., 2003, "Development and Application of an Automatic Design System for Multi-Stage Gear Drives", *ASME 2003 Design Engineering Technical Conferences and Computers and Information in Engineering Conference*, Chicago, Illinois, DETC 2003/PTG-48078, pp. 605-614.
- Carrol, R. and Johnson, G., 1998, "Approximate Equations for the AGMA J-factor", *Mechanisms and Machine Theory*, Vol. 23, No. 6, pp. 449-450.
- Donoso, B. and Tesar, D., 1998, "Parametric Modeling and Design of Robot Transmissions Using a New Binary Matrix Solution Methodology," Report, Mechanical Engineering, The University of Texas at Austin.
- Dyson, A., Evans, H., and Snidle, R., 1986, "Wildhaber-Novikov Circular-Arc Gears: Geometry and Kinematics," *Proceedings of the Royal Society of London*, Vol. 403, pp. 313-340.
- Faires, V., 1965, *Design of Machine Elements*, 4th Edition, Macmillan Co.
- Juvinal, R. and Marshek, K., 2000, *Fundamentals of Machine Component Design*, 3rd Edition, John Wiley and Sons, Inc.
- Kendrick, K. and Tesar, D., 2006, "The Design of a Power-Dense Hingeline Electro-Mechanical Actuator Suitable for Primary Flight Surface Control," Report, Mechanical Engineering, The University of Texas at Austin, Robotics Research Group.
- Norton, R., 2000, *Machine Design: An Integrated Approach*, 2nd Edition, Prentice-Hall, New Jersey.
- Park, S. and Tesar, D., 2005, PhD Dissertation, "Fundamental Development of Hypocycloidal Gear Transmissions," Report, Mechanical Engineering, The University of Texas at Austin, Robotics Research Group.
- Sigwald, R. and Tesar, D., 2008, "Geometric Analysis of the Parallel Eccentric Gear Train", Master's Thesis, Mechanical Engineering, University of Texas at Austin, Robotics Research Group.
- Roos, F. and Spiegelberg, C., 2004, "Relations Between Size and Gear Ratio in Spur and Planetary Gear Trains", Royal Institute of Technology, KTH, Stockholm, Sweden.
- Savage, M., Coy, J., and Townsend, D., 1982, "Optimal Tooth Numbers for Compact Standard Spur Gear Sets", *Journal of Mechanical Design*, Vol. 104, pp. 749-757.
- Shigley, J. E. and Mischke, C. R., 1989, *Mechanical Engineering Design*, 5th Edition, McGraw-Hill, Inc.
- Tesar, D., 2006, "Dominance of the Gear Ratio", Internal Report, University of Texas at Austin, Robotics Research Group.

Townsend, D., 1991, *Dudley's Gear Handbook, 2nd Edition*, McGraw-Hill, New York.

MOTOR DESIGN

Ashok, P., 2005, "Comparison of SRM and BLDCM for Aircraft Actuator", Ph. D. Qualifying Exam Research Project, Mechanical Engineering, University of Texas at Austin, Robotics Research Group.

Brisset, S. and Brochet, P., 2005, "Analytical Model for the Optimal Design of a Brushless DC Wheel Motor", *International Journal for Computation and Mathematics in Electrical and Electronic Engineering*, Vol. 24, No. 3, pp. 829-848.

Emoteq Corporation, 2008, <http://www.emoteq.com/>.

Fitan, E., Messine, F., and Nogarede, B., 2003, "A General Analytical Model of Electrical Permanent Magnet Machine Dedicated to Optimal Design", *International Journal for Computation and Mathematics in Electrical and Electronic Engineering*, Vol. 22, No. 4, pp. 1037-1050.

Jones, D., 1995, "Selecting Step Motors vs. Servo Motors", *Electrical Electronics Insulation Conference and Proceedings of the Electrical Manufacturing & Coil Winding Conference*, pp. 355-372.

Kollmorgen, Inc., 2008, "Kollmorgen Motors", <http://kmtg.kollmorgen.com/products/motors/>.

Krishnan, R., 1987, "Selection Criteria for Servo Motor Drives", *IEEE Transactions on Industry Applications*, IA-23, pp. 270-275.

Sergaki, E., Stavrakakis, G., and Pouliezios, A., 2002, "Optimal Robot Speed Trajectory by Minimization of the Actuator Motor Electromechanical Losses", *Journal of Intelligent and Robotics Systems*, Vol. 33, pp. 187-202.

SWITCHED RELUCTANCE MOTOR (SRM) DESIGN

Anwar, M., Husain, I., and Radun, A., 2001, "A Comprehensive Design Methodology for Switched Reluctance Machines", *IEEE Transactions on Industry Applications*, Vol. 37, No. 6, pp. 1684-1692.

Ashok, P. and Tesar, D., 2002, "Design Synthesis Framework for Switched Reluctance Motors," Report, Mechanical Engineering, The University of Texas at Austin, Robotics Research Group.

Krishnan, R., Arumugam, R., and Lindsay, J., 1988, "Design Procedure for Switched Reluctance Motors", *IEEE Transactions on Industry Applications*, Vol. 24, No. 3, pp. 456-461.

Miller, T., 2002, "Optimal Design of Switched Reluctance Motors", *IEEE Transactions on Industrial Electronics*, Vol. 49, No. 1, pp. 15-27.

- Miller, T.J.E., 1993, *Switched Reluctance Motors and Their Control*, Magna Physics Publishing and Clarendon Press.
- Radun, V., 1994, "Design Considerations for the Switched Reluctance Motor", *Industry Applications Society Annual Meeting, 1994, Conference Record of the 1994 IEEE*, Vol. 1, pp. 290-297.
- Richardson, K., Pollock, C., and Flower, J., 1995, "Design of a Switched Reluctance Sector Motor for an Integrated Motor/Propeller Unit", *Seventh International Conference on Electrical Machines and Drives*, Durham, UK, pp. 271-275.
- Rocky Mountain Technologies, Inc., 2008, "SR Motors", <http://www.rockymountaintechnologies.com/>.
- Srinivas, K. and Arumugam, R., 2002, "Finite Element Analysis Combined Circuit Simulation of Dynamic Performances of Switched Reluctance Motors", *Electric Power Components and Systems*, Vol. 30, pp. 1033-1045.

BALANCING MOTOR AND GEAR TRAIN

- Armstrong, R., 1998, "Load to Motor Inertia Mismatch: Unveiling the Truth", *Drives and Controls Conference*, Tedford, England, http://www.motionvillage.com/welcome_center/articles/index.html#Loadtomotorinertia.
- Bullock, T., 2000, "Why Speed Matching?", http://www.control.com/949948993/index_html.
- Brierley, J., Colyer, R., and Trzynadlowski, A., 1989, "The 'Soar' Method for Computer Aided Design of Energy-Optimal Positioning DC Drive Systems", *IEEE Industry Applications Society Annual Meeting*, Vol. 1, pp. 464-467.
- Chiang, W., 1990, "Optimal DC Motor Design for Constant Voltage Seek Motion", *IEEE Transactions on Energy Conversion*, Vol. 5, pp. 195-202.
- Fussell, B. and Taft, C., 1995, "Brushless DC Motor Selection", *Electrical Electronics Insulation Conference and Proceedings of the Electrical Manufacturing & Coil Winding Conference*, pp. 345-353.
- Hamel, W. and Widner, T., 1998, "Control Concepts for Transmission-Based Actuators in Robotics", *Proceedings of the IEEE/RSJ International Conference on Intelligent Robots and Systems*, Victoria, B.C., Canada, pp. 1770-1775.
- Lee, E., 2007, "Getting Torque to Inertia Right", <http://www.electricmotors.machinedesign.com/ArticleDraw.aspx?artid=60138>.
- Meier, J. and Raider, J., 1976, "Electric Motor Requirements for Positioning an Inertial Load", *IBM Journal of Research and Development*, pp. 176-183.
- Ohm, D., 2007, "Selection of Servo Motors and Drives", <http://www.drivetechnic.com/>.

- Saner, C., 2004, "A Design Guideline for Robust High Performance Axes", *Proceedings of the IEEE International Conference on Mechatronics*, pp. 470-475.
- Shuxing, Y. and Ping, Z., 1997, "On the Parametric Design of Electromechanical Actuators", *Journal of Beijing Institute of Technology*, Vol. 6, No. 2, pp. 138-144.
- Tal, J. and Kahne, S., 1973, "Control and Component Selection for Incremental Motion Systems", *Automatica*, Vol. 9, pp. 501-507.
- West, J. and Leonard, J., 1955, "The Necessary Torque Requirements for a Servo-Motor", *Journal of Scientific Instruments*, Vol. 32, pp. 30-32.

SCALING

- Borghini, M., Cantore, G., Milani, M., and Paoluzzi, R., 1998, "Analysis of Hydraulic Components Using Computational Fluid Dynamics Models," *Journal of Mechanical Engineering Science*, Vol. 212, Part C, pp. 619-629.
- Bridgman, P.W., 1963, *Dimensional Analysis*, Yale University Press.
- Buckingham, E., 1914, "On Physically Similar Systems: Illustrations of the Use of Dimensional Equations," *Physical Review*, Vol. 4, Issue 4, pp. 345-376.
- Cheng, Y. and Cheng, C., 1999, "Scaling Relationships in Conical Indentation of Elastic-Perfectly Plastic Solids," *International Journal of Solids and Structures*, Vol. 36, pp. 1231-1243.
- Drexler, K.E., 1992, *Nanosystems*, http://www.amazon.com/gp/reader/0471575186/ref=sib_dp_pt/104-3043079-4315154#reader-page.
- Focken, C.M., 1953, *Dimensional Methods and Their Applications*, Edward Arnold and Co.
- Fox, R.W. and McDonald, A.T., 1998, *Introduction to Fluid Mechanics*, 5th Edition, John Wiley and Sons, Inc..
- Gooch, S.D. and Raine, J.K., 2000, "The Dynamics and Limits on the Scaling of a Flexible Kinetic Sculpture," *Proceedings of the Institution of Mechanical Engineers*, Vol. 214, Part C, pp. 537-548.
- Huntley, H.E., 1955, *Dimensional Analysis*, Rinehart and Company, Inc.
- Langhaar, H., 1951, *Dimensional Analysis and Theory of Models*, John Wiley and Sons, Inc..
- Liang, Q., Xie, Y., and Steven, G., 1999, "Optimal Selection of Topologies for the Minimum-Weight Design of Continuum Structures with Stress Constraints," *Proceedings of the Institution of Mechanical Engineers*, Vol. 213, Part C, pp. 755-762.

- Mendez, P.F. and Ordonez, F., 2003, "Scaling Laws from Statistical Data and Dimensional Analysis," *Journal of Applied Mechanics*, Vol. 72, Issue 5, pp. 648-657.
- Nakajima, N., Ogawa, K., and Fujimasa, I., 1989, "Study on Microengines: Miniaturizing Stirling Engines for Actuators," *Sensors and Actuators*, Vol. 20, pp. 75-82.
- Pahl, G. and Beitz, W., 1991, *Engineering Design: A Systematic Approach*, The Design Council.
- Pankhurst, R.C., 1964, *Dimensional Analysis and Scale Factors*, The Institute of Physics and The Physical Society.
- Pasini, D., Smith, D.J., and Burgess, S.C., 2003, "Selection of Arbitrarily Scaled Cross Sections in Bending Stiffness Design," *Proceedings of the Institution of Mechanical Engineers*, Vol. 217, Part L, pp. 113-125.

PRODUCT FAMILY DESIGN

- Dai, Z. and Scott, M., 2004, "Effective Product Family Design Using Preference Aggregation", *ASME 2004 Design Engineering Technical Conferences and Computers and Information in Engineering Conference*, Salt Lake City, Utah, DETC 2004-57419.
- D'Souza, B. and Simpson, T., 2003, "A Genetic Algorithm Based Method for Product Family Design Optimization," *Engineering Optimization*, Vol. 35, No. 1, pp. 1-18.
- Fellini, R., Kokkolaras, M., Papalambros, P., and Perez-Duarte, A., 2005, "Platform Selection Under Performance Bounds in Optimal Design of Product Families", *Journal of Mechanical Design*, Vol. 127, pp. 524-535.
- Fellini, R. et al., 2002, "A Sensitivity-Based Commonality Strategy for Family Products of Mild Variation, With Application to Automotive Body Structures", *9th AIAA/ISSMO Symposium on Multidisciplinary Analysis and Optimization*, Atlanta, Georgia, AIAA 2002-5610.
- Fellini, R., Kokkolaras, M., and Papalambros, P., 2003, "A Rigorous Framework for Making Commonality and Modularity Decisions in Optimal Design of Product Families", *International Conference on Engineering Design*, Stockholm, Sweden.
- Fellini, R., Kokkolaras, M., and Papalambros, P., 2003, "Efficient Product Portfolio Reduction", *Proceedings of the 5th World Congress on Structural and Multidisciplinary Optimization*, Lido di Jesolo - Venice, Italy.
- Gonzalez-Zugasti, J. et al., 2000, "A Method for Architecting Product Platforms," *Research in Engineering Design*, Vol. 12, No. 2, pp. 61-72.

- Kokkolaras, M., Fellini, R., Kim, H., Michelena, N., and Papalambros, P., 2002, "Extension of the Target Cascading Formulation to the Design of Product Families", *Structural Multidisciplinary Optimization*, Vol. 24, pp. 293-301.
- Messac, A., Martinez, M., and Simpson, T., 2002, "Effective Product Family Design Using Physical Programming", *Engineering Optimization*, Vol. 34, pp. 245-261.
- Messac, A., Martinez, M., and Simpson, T., 2002, "Introduction of a Product Family Penalty Function Using Physical Programming", *Journal of Mechanical Design*, Vol. 124, No. 3, pp. 164-172.
- Mistree, F., Hughes, O., and Bras, B., 1993, "The Compromise Decision Support Problem and the Adaptive Linear Programming Algorithm", *Structural Optimization: Status and Promise*, Washington, D.C., pp. 247-286.
- Nayak, R., Chen, W., and Simpson, T., 2002, "A Variation-Based Method for Product Family Design", *Engineering Optimization*, Vol. 34, No. 1, pp. 65-81.
- Nelson, S., Parkinson, M., and Papalambros, P., 2001, "Multicriteria Optimization in Product Platform Design", *Journal of Mechanical Design*, Vol. 123, pp. 199-204.
- Seepersad, C., Mistree, F., and Allen, J., 2002, "A Quantitative Approach for Designing Multiple Product Platforms for an Evolving Portfolio of Products", *ASME 2002 Design Engineering Technical Conferences and Computers and Information in Engineering Conference*, Montreal, Canada, DETC 2002/DAC-34096, pp. 579-592.
- Simpson, T., 2004, "Product Platform Design and Customization: Status and Promise," *Artificial Intelligence for Engineering Design, Analysis, and Manufacturing*, Vol. 18, pp. 3-20.
- Simpson, T., Allen, J., Chen, W., and Mistree, F., 1996, "Conceptual Design of a Family of Products Through the Use of the Robust Concept Exploration Method", *6th AIAA/USAF/NASA/ISSMO Symposium on Multidisciplinary Analysis and Optimization*, Atlanta, Georgia, Vol. 2, pp. 1535-1545.
- Simpson, T., Maier, J., and Mistree, F., 2001, "Product Platform Design: Method and Application," *Research in Engineering Design*, Vol. 13, pp. 2-22.
- Simpson, T., Seepersad, C., and Mistree, F., 2001, "Balancing Commonality and Performance within the Concurrent Design of Multiple Products in a Family", *Concurrent Engineering: Research and Applications*, Vol. 9, No. 3, pp. 177-190.
- Thevenot et al., 2007, "A Multiattribute Utility Theory-Based Method for Product Line Selection", *Journal of Mechanical Design*, Vol. 129, No. 11, pp. 1179-1184.
- Vaculik, S. and Tesar, D., 2005, "Using Product Family Design Methods to Develop Electromechanical Actuator Families," Ph. D. Qualifying Exam Research Project, University of Texas at Austin, Robotics Research Group.

REGRESSION ANALYSIS

- Cook, R. and Weisberg, S., 1999, *Applied Regression Including Computing and Graphics*, John Wiley & Sons, Inc., New York.
- Lancaster, P. and Salkauskas, K., 1986, *Curve and Surface Fitting: An Introduction*, Academic Press, California.
- Wittnik, D., 1988, *The Application of Regression Analysis*, Allyn and Bacon, Inc., Massachusetts.
- Wu, S., 1964, "Tool Life Testing by Response Surface Methodology-Part 2", *Journal of Engineering for Industry*, pp. 111-113.

METAMODELS AND RESPONSE SURFACE METHODOLOGY

- Barton, R., 1998, "Simulation Metamodels", *Proceedings of the 1998 Winter Simulation Conference*, pp. 167-174.
- Box, G. and Wilson, K., 1951, "On the Experimental Attainment of Optimum Conditions," *Journal of the Royal Statistical Society*, Vol. 13, No. 1, pp. 1-45.
- Carley, K., Kamneva, N., and Reminga, J., 2004, "Response Surface Methodology", Carnegie Mellon University, School of Computer Science, NASA Report.
- Clarke, S., Griebisch, J., and Simpson, T., 2005, "Analysis of Support Vector Regression for Approximation of Complex Engineering Analyses", *Journal of Mechanical Design*, Vol. 127, pp. 1077-1087.
- Currin, C., Mitchell, T., Morris, M., and Ylvisaker, D., 1991, "Bayesian Prediction of Deterministic Functions, with Applications to the Design and Analysis of Computer Experiments", *Journal of the American Statistical Association*, Vol. 86, No. 416, pp. 953-963.
- Friedman, J., 1991, "Multivariate Adaptive Regression Splines", *The Annals of Statistics*, Vol. 19, No. 1, pp. 1-67.
- Hill, W. and Hunter, W., 1966, "A Review of Response Surface Methodology: A Literature Survey", *Technometrics*, Vol. 8, No. 4, pp. 571-590.
- Hussain, M., Barton, R., and Joshi, S., 2002, "Metamodeling: Radial basis functions, versus polynomials", *European Journal of Operational Research*, Vol. 138, pp. 142-154.
- Jin, R., Chen, W. and Simpson, T., "Comparative Studies of Metamodeling Techniques Under Multiple Modeling Criteria", *Structural Multidisciplinary Optimization*, Vol. 23, pp. 1-13.
- Martin, J. and Simpson, T., 2005, "On the Use of Kriging Models to Approximate Deterministic Computer Models", *AIAA JOURNAL*, Vol. 43, No. 4, pp. 853-863.

- Mead, R. and Pike, D., 1975, "A Biometrics Invited Paper. A Review of Response Surface Methodology from a Biometric Viewpoint", *Biometrics*, Vol. 31, No. 4, pp. 803-851.
- Mullur, A. and Messac, A., 2005, "Extended Radial Basis Functions: More Flexible and Effective Metamodeling", *AIAA Journal*, Vol. 43, No. 6, pp. 1306-1315.
- Mullur, A. and Messac, A., 2006, "Metamodeling using extended radial basis functions: a comparative approach", *Engineering with Computers*, Vol. 21, pp. 203-217.
- Myers, R., Khuri, A., and Carter, W., 1989, "Response Surface Methodology: 1966-1988", *Technometrics*, Vol. 31, No. 2, pp. 137-157.
- Myers, R. and Montgomery, D., 1995, *Response Surface Methodology: Process and Product Optimization Using Designed Experiments*, John Wiley & Sons, Inc., New York.
- Osio, I. and Amon, C., 1996, "An Engineering Design Methodology with Multistage Bayesian Surrogates and Optimal Sampling", *Research in Engineering Design*, Vol. 8, pp. 189-206.
- Pacheco, J., Amon, C., and Finger, S., 2003, "Bayesian Surrogates Applied to the Conceptual Stages of the Engineering Design Process", *Journal of Engineering Design*, Vol. 125, pp. 664-672.
- Qian, A., Seepersad, C., Joseph, R., Allen, J., and Wu, J., 2006, "Building Surrogate Models Based on Detailed and Approximate Simulations", *Journal of Mechanical Design*, Vol. 128, No. 4, pp. 668-677.
- Rumelhart, D., Widrow, B., and Lehr, M., 1994, "The Basic Ideas in Neural Networks", *Communications of the ACM*, Vol. 37, No. 3, pp. 87-92.
- Sacks, J., Schiller, S., and Welch, 1989, W., "Designs for Computer Experiments", *Technometrics*, Vol. 31, No. 1, pp. 41-47.
- Sacks, J., Welch, W., Mitchell, T., and Wynn, H., 1989, "Design and Analysis of Computer Experiments", *Statistical Science*, Vol. 4, No. 4, pp. 409-435.
- Simpson, T., Booker, A., Ghosh, D., Giunta, A., Koch, P., and Yang, R., 2004, "Approximation Methods in Multidisciplinary Analysis and Optimization: A Panel Discussion", *Structural Multidisciplinary Optimization*, Vol. 27, pp. 320-313.
- Simpson, T., Lin, D., and Chen, W., 2001, "Sampling Strategies for Computer Experiments: Design and Analysis," *International Journal of Reliability and Application*, Vol. 2, No. 3, pp. 209- 240.
- Simpson, T., Peplinski, J., Koch, P., and Allen, J., 2001, "Metamodels for Computer-Based Engineering Design: Survey and Recommendations", *Engineering with Computers*, Vol. 17, pp. 129-150.

- Wang, G. and Shan S., 2007, "Review of Metamodeling Techniques in Support of Engineering Design Optimization", *Journal of Mechanical Design*, Vol. 129, No. 4, pp. 370-380.
- Welch, W., Buck, R., Sacks, J., Wynn, H., Mitchell, T., and Morris, M., 1992, "Screening, Predicting, and Computer Experiments", *Technometrics*, Vol. 34, No. 1, pp. 15-25.

DESIGN SPACE VISUALIZATION

- Agrawal, G., Lewis, K., Chugh, K., Huang, C., Parashar, S., and Bloebaum, C., 2004, "Intuitive Visualization of Pareto Frontier for Multi-Objective Optimization in n-Dimensional Performance Space", AIAA-2004-4434, 10th AIAA/ISSMO Multidisciplinary Analysis and Optimization Conference, Albany, New York.
- Andrienko, G. and Andrienko, N., 2001, "Interactive Visual Tools to Support Spatial Criteria Decision Making", *IEEE*, pp. 127-131.
- Ashok, P. and Tesar, D., 2007, "A Visualization Framework for Real Time Decision Making in a Multi-Input Multi-Output System," *IEEE Systems Journal*, Vol. 2, No. 1, pp. 129-145.
- Dillon, K., Talbot, P., and Hillis, W., 2005, "Knowledge Visualization: Redesigning the Human-Computer Interface", *Technology Review Journal*, pp. 37-55.
- Eddy, J. and Lewis, K., 2002, "Visualization of Multidimensional Design and Optimization Data Using Cloud Visualization", *Proceedings of the ASME 2002 Design Engineering Technical Conference and Computers and Information in Engineering Conference*, Montreal, Canada.
- Eddy, J. and Lewis, K., 2002, "Multidimensional Design Visualization in Multi-objective Optimization", AIAA-2002-5621, 9th AIAA/ISSMO Symposium on Multidisciplinary Analysis and Optimization, Atlanta, Georgia.
- Hanne, T. and Trinkaus, H., 2005, "KnowCube for MCDM- Visual and Interactive Support for Multicriteria Decision Making", *Computers and Operations Research*, Vol. 32, No. 5, pp. 1289-1309.
- Kanukolanu, D., Lewis, K., and Winer, E., 2006, "A Multidimensional Visualization Interface to Aid in Trade-off Decisions During the Solution of Coupled Systems Under Uncertainty", *Transactions of the ASME*, Vol. 6, pp. 288-299.
- Lohse, G., Biolsi, K., Walker, N., and Rueter, H., 1994, "A Classification of Visual Representations", *Communications of the ACM*, Vol. 37, No. 12, pp. 36-49.
- Messac, A. and Chen, X., 2000, "Visualizing the Optimization Process in Real-Time Using Physical Programming", *Engineering Optimization Journal*, Vol. 32, No. 5, pp. 1-36.

- Simionescu, P. and Beale, D., 2004, "Visualization of Hypersurfaces and Multivariable (Objective) Functions by Partial Global Optimization", *The Visual Computer*, Vol. 20, pp. 665-681.
- Simpson, T., Frecker, M., Barton, R., and Rothrock, L., 2007, "Graphical and Text-Based Design Interfaces for Parameter Design of an I-Beam, Desk Lamp, Aircraft Wing, and Job Shop Manufacturing System", *Engineering with Computers*, Vol. 23, pp. 93-107.
- Winer, E. and Bloebaum, C., 1999, "Development of Visual Design Steering as an Aid in Large-Scale Multidisciplinary Design Optimization. Part I: Method Development", *Structural Multidisciplinary Optimization*, Vol. 23, pp. 412-424.

PATENTS

- Beishline, E. et al., 2004, Electro-mechanical Actuator for an Adjustable Pedal System, U.S. Patent, #6,736,233.
- Bridson, W., 2006, Integrated Selection of Optical Systems, U.S. Patent, #7,149,662.
- Brundrett, R. et al., 2000, Aircraft Brake and Method with Electromechanical Actuator Modules, U.S. Patent, #6,095,293.
- Eric, S. and Gary, F., 2004, Contactless Electro-mechanical Actuator with Coupled Electronic Motor Commutation and Output Position Sensors, U.S. Patent, #6,791,219.
- Griffith, C. and Oliver, K., 1982, Strapdown Multifunction Servoactuator Apparatus for Aircraft, U.S. Patent, #4,345,195.
- Huber, J., 1991, Lightweight, Direct Drive Electromechanical Actuator, U.S. Patent, #5,041,748.
- Meyerdierks, H., 2002, Winch, U.S. Patent, #6,431,103.
- Moskob, F., 2003, Motor-Gear Unit with Integrated Eccentric Wheel Gear, U.S. Patent, #6,661,139.
- Skaggs, R., 1983, Hypocyclic Drive Transmission Apparatus, U.S. Patent, #4,386,540.
- Shube, E., 1986, High Speed, Dual Operated Electromechanical Actuator, U.S. Patent, #4,563,908.
- Szalony, N. and Foukes, J., 2006, Power Transmission with Electromechanical Actuator, U.S. Patent, #7,083,538.

SOLUTION TECHNIQUES: OPTIMIZATION AND MULTI-OBJECTIVE DESIGN

- Marler, R. and Arora, J., 2004, "Survey of Multi-Objective Optimization Methods for Engineering", *Structural Multidisciplinary Optimization*, Vol. 26, pp. 369-395.

- Mester, V., Gillon, F., and Brochet, P., 2005, "Optimal Design of Electric Vehicles Drive Train", *International Journal for Computation and Mathematics in Electrical and Electronic Engineering*, Vol. 24, No. 3, pp. 967-983.
- Michelena, N., Louca, L., Kokkolaras, M., Lin, C., Jung, D., Filipi, Z., Assanis, D., Papalambros, P., Peng, H., Stein, J., and Feury, M., 2001, "Design of an Advanced Heavy Tactical Truck: A Target Cascading Case Study", *Proceedings of the SAE International Truck & Bus Meeting and Exhibition*, Chicago, Illinois, 2001-01-2793.
- Papalambros, P.Y. and Wilde, D.J., 2000, *Principles of Optimal Design: Modeling and Computation*, 2nd Edition, Cambridge University Press.
- Pettersson, M., Krus, P., and Andersson, J., 2005, "On Optimal Drive Train Design in Industrial Robots", *IEEE International Conference on Industrial Technology*, pp. 254-259.
- Simionescu, P., Beale, D., and Dozier, G., 2006, "Teeth-Number Synthesis of a Multispeed Planetary Transmission Using and Estimation of Distribution Algorithm", *Journal of Mechanical Design*, Vol. 128, pp. 108-115.
- Wang, L., 2005, "Hybrid Electric Vehicle Design Based on a Multi-Objective Optimization Evolutionary Algorithm", Texas A&M University, Walter J. Karplus Summer Research Grant Report, pp. 1-16.
- Williams, B.C. and Cagan, J., 1994, "Activity Analysis: The Qualitative Analysis of Stationary Points for Optimal Reasoning," *Proceedings of the Twelfth National Conference on Artificial Intelligence*.
- Zhu, L. and Kazmer, D., 2001, "A Performance-Based Representation for Engineering Design", *Journal of Mechanical Design*, Vol. 123, pp. 486-493.

SOLUTION TECHNIQUES: SOLVING POLYNOMIAL SYSTEMS OF EQUATIONS

- Courtois, N., Klimov, A., Patarain, J., and Shamir, A., 2000, "Efficient Algorithms for Solving Overdefined Systems of Multivariate Polynomial Equations", *Advances in Cryptology - EUROCRYPT 2000: International Conference on the Theory and Application of Cryptographic Techniques, Bruges, Belgium*, pp. 398-413.
- Courtois, N., Goubin, L., Meier, W., and Tacier, J., 2002, "Solving Underdefined Systems of Multivariate Quadratic Equations", *Public Key Cryptography: 5th International Workshop on Practice and Theory in Public Key Cryptosystems, PKC 2002, Paris, France*, pp. 211-227.
- Gad, E. and Nakhla, M., 1999, "Model Reduction for DC Solution of Large Nonlinear Circuits", *IEEE International Conference on Computer-Aided Design (ICCAD '99)*, pp. 376-379.

- Gao, X. and Chou, S., 1998, "Solving geometric constraint systems, II: A symbolic approach and decision of Rc-constructibility", *Computer-Aided Design*, Vol. 30, No. 2, pp. 115-122.
- Gianni, P. and Mora, T., 1987, "Algebraic Solution of Systems of Polynomial Equations Using Groebner Bases", *Proceedings of the 5th international conference, AA ECC-5 on Applied Algebra, Algebraic Algorithms and Error-Correcting Codes*, pp. 247-257.
- Hentenryck, P, Mcallester, D., and Kapur, D., 1997, "Solving Polynomial Systems Using a Branch and Prune Approach", *SIAM Journal of Numerical Analysis*, Vol. 34, No. 2, pp. 797-827.
- Hirschi, N.W. and Frey, D.D., 2002, "Cognition and Complexity: An Experiment on the Effect of Coupling in Parameter Design," *Research in Engineering Design*, Vol. 13, pp. 123-131.
- Manocha, D., 1994, "Solving Systems of Polynomial Equations", *IEEE Computer Graphics and Application*, pp. 46-55.
- Raghavan, M. and Roth, B., 1995, "Solving Polynomial Systems for the Kinematic Analysis and Synthesis of Mechanisms and Robot Manipulators", *Journal of Mechanical Design*, Vol. 117, pp. 71-79.
- Ruiz, O. and Ferreira, P., 1994, "Algebraic Geometry and Group Theory in Geometric Constraint Satisfaction", *International Conference on Symbolic and Algebraic Computation, Proceedings of the international symposium on Symbolic and Algebraic Computation*, pp. 224-233.
- Sawada, H., 1998, "The Algebraic Under Constraint Solver as a Design Tool", *Proceedings of the 1998 IMACS Conference on Applications of Computer Algebra*, pp. 1-11.
- Sawada, H. and Yan. X., 2001, "Applying a Generic Constraint Solving Technique to Engineering Design", *Proceedings of ICED01, Design Methods for Performance and Sustainability*, pp. 123-130.
- Vershelde, J. and Cools, R., 1993, "Symbolic Homotopy Construction", *Applicable Algebra in Engineering, Communication, and Computing*, Vol. 4, pp. 169-183.
- Waskow, T. and Tesar, D., 1996, "Algebraic Elimination Techniques for Design in Mechanical Systems," Report, Mechanical Engineering, The University of Texas at Austin, Robotics Research Group.

Vita

Stewart Andrew Vaculik was born in Weimar, Texas on February 4, 1979, to parents Adolph and Jeanette Vaculik. After graduating from Schulenburg High School in the spring of 1997, Stewart enrolled at Texas A&M University in College Station, Texas. He graduated with a Bachelor of Science degree in Mechanical Engineering in May of 2002. Stewart entered the Graduate School of Engineering at The University of Texas at Austin in September 2002 and earned a Master of Science degree in Engineering in December of 2004. Upon graduation with his Doctor of Philosophy degree in Engineering in May of 2008, Stewart will begin his career as a mechanical engineer at BAE Systems in Austin, Texas.

Permanent Address: 11609 Lansdowne Road, Austin, TX, 78754